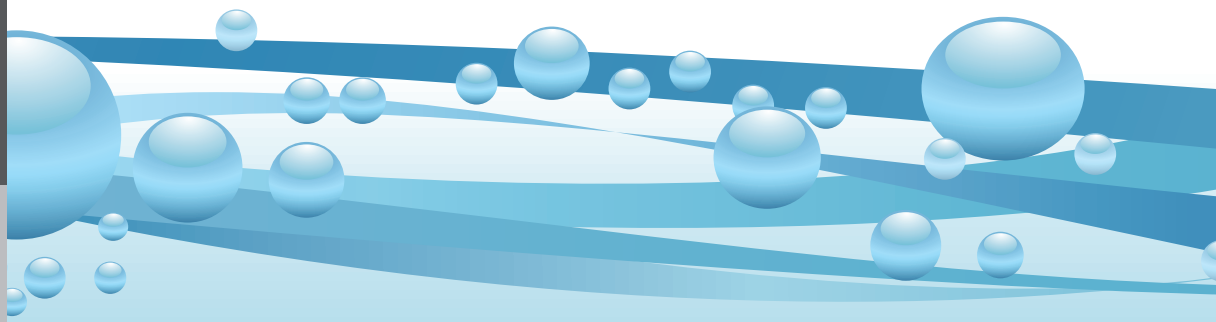

18th World Hydrogen Energy Conference 2010 – WHEC 2010 Proceedings

Parallel Sessions Book 4:
- Storage Systems
- Policy Perspectives, Initiatives and Cooperations

Editors: Detlef Stolten, Thomas Grube

JÜLICH
FORSCHUNGSZENTRUM

Mitglied der Helmholtz-Gemeinschaft

18th World Hydrogen Energy Conference 2010 - WHEC 2010: Parallel Sessions Book 4: Storage Systems / Policy Perspectives, Initiatives and Cooperations

WHEC, May 16.-21. 2010, Essen

Detlef Stolten, Thomas Grube (Eds.)

Institute of Energy Research - Fuel Cells (IEF-3)

Guide to the Online Edition

Forschungszentrum Jülich GmbH, Zentralbibliothek, Verlag

Schriften des Forschungszentrums Jülich / Energy & Environment Vol. 78-4

978-3-89336-654-5 / 1866-1793

HS Storage Systems

HS.1 Physical Hydrogen Storage

Poster

HS.2a Metal Hydrides

Poster

HS.2b Complex Hydrides

Poster

HS.3 Adsorption Technologies

Poster

IP Policy Perspectives, Initiatives and Cooperations

IP.1a National Strategies and Programmes

Poster

IP.1b IEA Hydrogen Implementing Agreement

Poster

IP.2 Renewable Primary Energy Potential for Hydrogen Production

Poster

IP.3 Environmental Impact of Hydrogen Technologies

Poster

Schriften des Forschungszentrums Jülich
Energy & Environment Volume 78-4

Forschungszentrum Jülich GmbH
Institute of Energy Research (IEF)
Fuel Cells (IEF-3)

18th World Hydrogen Energy Conference 2010 – WHEC 2010

Parallel Sessions Book 4:

- Storage Systems

- Policy Perspectives, Initiatives and Cooperations

Editors: Detlef Stolten, Thomas Grube

Schriften des Forschungszentrums Jülich
Energy & Environment Volume 78-4

ISSN 1866-1793 ISBN 978-3-89336-654-5

Bibliographic information published by the Deutsche Nationalbibliothek.
The Deutsche Nationalbibliothek lists this publication in the Deutsche Nationalbibliografie; detailed bibliographic data are available in the Internet at http://dnb.d-nb.de.

Vol. 78 Set (komplett)
ISBN 978-3-89336-657-6
Editors: Detlef Stolten, Thomas Grube, Bernd Emonts

Publisher and Distributor: Forschungszentrum Jülich GmbH
Zentralbibliothek
52425 Jülich
Phone +49 (0) 24 61 61-53 68 · Fax +49 (0) 24 61 61-61 03
e-mail: zb-publikation@fz-juelich.de
Internet: http://www.fz-juelich.de/zb

Cover Design: Grafische Medien, Forschungszentrum Jülich GmbH

Printer: Grafische Medien, Forschungszentrum Jülich GmbH

Schriften des Forschungszentrums Jülich
Reihe Energy & Environment Volume 78-4

ISSN 1866-1793
ISBN 978-3-89336-654-5

The complete volume ist freely available on the Internet on the Jülicher Open Access Server (JUWEL) at http://www.fz-juelich.de/zb/juwel

Book 4: Storage Systems | Policy Perspectives, Initiatives and Cooperations

Contents

HS STORAGE SYSTEMS

Physical Hydrogen Storage Technologies – A Current Overview

Bert Hobein and Roland Krüger

Introduction

The shortage of fossil energy resources demands new energy carriers and energy carrier technologies in the future. Therefore, one of the major challenges currently in the automotive industry and research institutes worldwide is to develop and realize alternative fuel concepts for passenger cars. Physical hydrogen storage systems, that is, compressed and liquid storage, are currently the most mature technology to store hydrogen onboard road vehicles. A combination of compressed and liquid hydrogen storage is so-called cryo-compressed systems, which are currently under development. Since the first hydrogen vehicle generation demonstrated insufficient cruising ranges, new physical storage technologies, such as the 70 MPa technology, can increase vehicles' cruising ranges significantly. This chapter gives an overview of different physical hydrogen storage technologies with regard to their design and their operating and refueling capabilities.

Damage Accumulation and Lifetime Prediction of Carbon Fiber Composite Pressure Vessels

Mathilde Weber, Brian Besancon, Air Liquide R&D, Paris, France
Anthony Bunsell, Hasnae Zejli, Yves Favry, Alain Thionnet, Mines Paris Tech, Paris, France

1 Introduction

The development of hydrogen as a reliable energy vector is strongly connected to the performance and level of safety of the components of the supply chain. In this respect, achieving an efficient storage is crucial to address transition markets and automotive markets.

For near-term markets, high pressure compressed gas storage in carbon fiber composite pressure vessels is currently the most promising technology. These pressure vessels are made of a plastic or metallic liner wrapped with carbon fibers embedded in a polymer matrix. This technology is currently industrialized for working pressures in the range of 200 to 300 bar (self-contained breathing apparatus and compressed natural gas storage for transportation). The feasibility and storage efficiency were demonstrated at higher working pressure (700 bar) in recent developments (European project Storhy for instance [1]).

However, challenges remain to improve performance and reliability of these pressure vessels while still ensuring the safety of cylinders in service over periods of 15 to 20 years. In order to avoid overdesign design and conservative use, a fundamental understanding of damage mechanisms and degradation of carbon fiber composite materials is required. Knowledge of the damage accumulation kinetics permits the assessment of residual lifetimes, which can be used to define design parameters such as the safety factor and during periodic inspections in order to determine whether a cylinder remains fit for service.

The composite structure of a pressure vessel is obtained by filament winding. The fibers are placed on geodesic paths around a mandrel, which later serves as a liner to ensure gas tightness. This means that when the vessel is pressurized the fibers are subjected only to tensile forces and at the level of the fibers an analogy can be made with the behavior of a unidirectional composite loaded in the fiber direction. The fibers support all but one percent of the mechanical stress in the walls of the pressure vessels and their failure is what determines the failure of these composite pressure vessels. As with a unidirectional composite, failure of the material means that the fibers have to break. Carbon fibers are perfectly elastic. In a bundle of fibers, there is a scattering of tensile strength and the tensile strength distribution follow Weibull statistics [2]. Weibull statistics are based on a view of failure processes which concludes that strength is not an intrinsic property of the material but rather a stochastic process governed by the probability of defects occurring within the sample tested [2].

This paper addresses the rate of damage accumulation in carbon fiber composites specimens and pressure vessels and more specifically of carbon fiber breaks accumulation.

In a first part, a model developed in the framework of previous study is described. In a second part, the fiber break accumulation measurement by acoustic emission on samples and pressure vessels is discussed.

2 Carbon Fiber Composites Failure Modeling

The goal of the model discussed here is to simulate the failure of fibers under static load in the fibre direction. A finite element multi-scale approach has been adopted by Bunsell and co. [3, 4]. The micromechanics study considers a three-dimensional analysis of a representative volume element (RVE) comprising all the processes to be considered. These are fiber strength and its stochastic nature, fiber tensile elastic modulus and the properties of the matrix. It is necessary to take into account interfacial debonding of the interface between the broken fiber and the matrix as well as considering the viscoelastic nature of the matrix so that the properties of the composites are time dependent, as are the effects of load transfer between neighboring fibers, which are due to shear of the matrix.

The model has been used in a previous study [4] to predict the failure of unidirectional plate specimens loaded in the fiber direction. It has been shown that the model accurately predicts tensile failure to within ±2% and that the scatter of composite properties also can be simulated [4]. The model reveals that, in the absence of stress concentrations due to the geometry of the composite specimen, fiber breaks initially occur randomly within a unidirectional composite loaded in the fiber direction. These random breaks reflect the random nature of the defects on the fibers. Initially the breaks are isolated in the composite because they are embedded in the matrix material. However, as loading becomes more critical the breaks begin to cluster due to the stress concentrating effects induced by the shear of the matrix around the breaks. This leads to the failure of some neighboring fibers. When the clusters of breaks reach a critical size the composite becomes unstable and this will eventually lead to failure of the composite.

The same reference explores the effects of the viscoelastic properties of the matrix on the long term behavior of the composite under a steady load as shown in figure 1. The model is capable of predicting the scatter of rates of fiber failures when compared to experimental curves obtained by acoustic emission as shown in figure 1 (comparison of 3 samples: 1, 2 and 3 to simulations). Figure 1 also illustrates that fiber breaks will continue to occur, if the composite is held at a constant load, due to the relaxation of the matrix around earlier breaks, but at a decreasing rate. However if eventually several fibers break in the same region this will lead to clustering of the breaks and an acceleration of the damage. A physical instability arises when the density of fiber breaks reaches a critical threshold and the regions of damage begin to interfere. This behavior is predicted by the model [5] and has been observed experimentally [6] both on samples and pressure vessels.

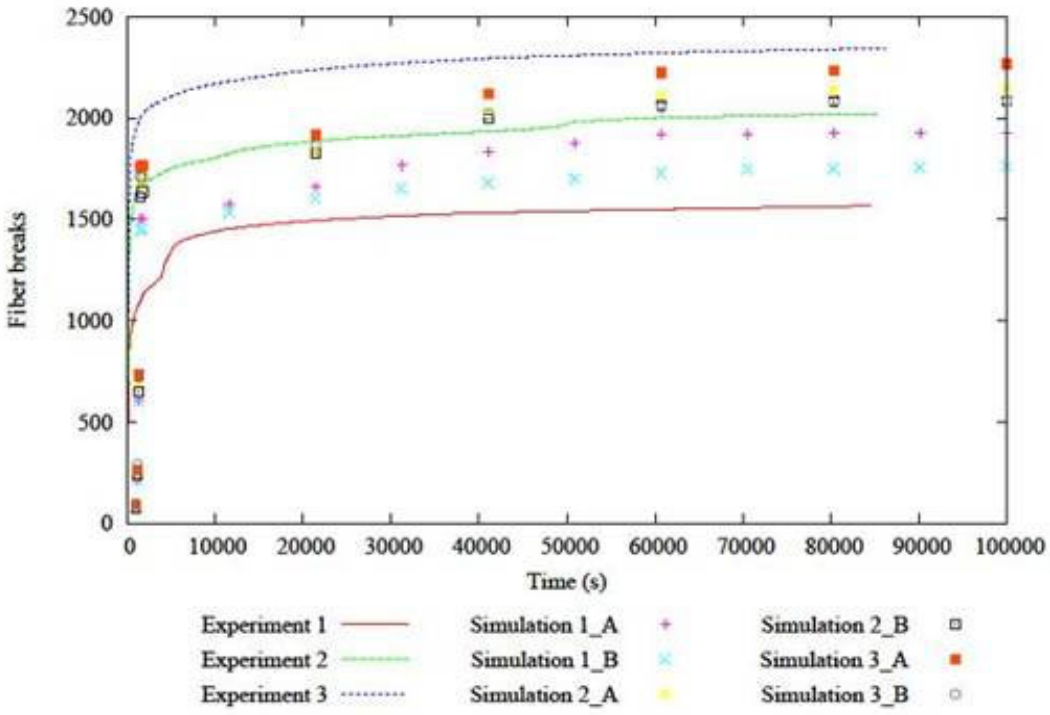

Figure 1: Comparison of simulated and experimental results of constant load tests, at 80% failure stress, with unidirectional CFRP (carbon fiber reinforced polymer) specimens loaded in the fiber direction [4].

3 Damage Detection in Carbon Fiber Composites

To compare experiments to the model, we need an experimental technique that can measure fiber breaks occurrence. In this study, acoustic emission is investigated. When subjected to static or cyclic load, a composite material will exhibit various types of damage mechanisms including fiber breaks as presented in Figure 2. This damages occurrence generates acoustic emissions; the main issue is to be able to discriminate fiber break from other damage mechanisms.

In a first step, plate specimen with various fiber orientations chosen so as to control the failure processes have been studied and the means of discriminating these processes using the acoustic emission technique have been determined. Six types of composite plate samples were investigated including pure epoxy resin, carbon fiber bundles (representative of the one used by cylinder manufacturer, Young modulus=235 GPa), [0°]4 and [90°]4 coupons, [02/902]s and [902/02]s cross-plied coupons.

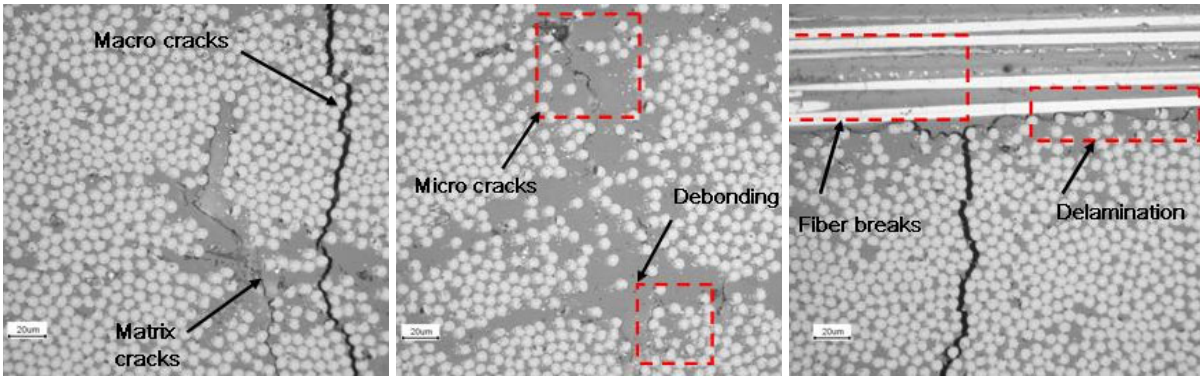

Figure 2: Failure processes in composites that generate acoustic emissions.

Details on the acoustic emission system and measurements are provided elsewhere [6]. A neural type network analysis of several parameters in parallel was carried out so as to better discriminate the types of emissions. It was possible to discriminate fiber breaks from other damages both on samples and on the pressure vessels tested in this study.

The pressure vessels studied were designed to have a burst strength of 115 MPa and were subjected to pressures up to 60 MPa. In order to examine the effects of cyclic pressurization, the pressure vessel was subjected to an initial pressurization up to 60MPa and held at that pressure for twenty four hours; it was then cycled one hundred times from near to zero to 60MPa and again held at the maximum pressure for twenty four hours. This was repeated after a further 1000 cycles, then 5000 cycles and finally 15,000 cycles. During the 20 hours periods at 60 MPa, the acoustic emissions were monitored. The results are displayed in figure 3.

As with the plate specimens, after the first cycle of pressurization, emissions were only recorded near to the maximum pressure. Figure 3 reveals that the major part of the emissions came from fiber breaks and other processes were secondary. It can be seen that the cycles of pressure did not alter the overall curve of damage accumulation which would have been obtained by holding the pressure constant [6, 7, see example figure 1]. The conclusion is that the ageing process in the composite wrap on the pressure vessel is controlled by the viscoelastic nature of the composite, as described in the above model and not significantly affected by cycling the pressure.

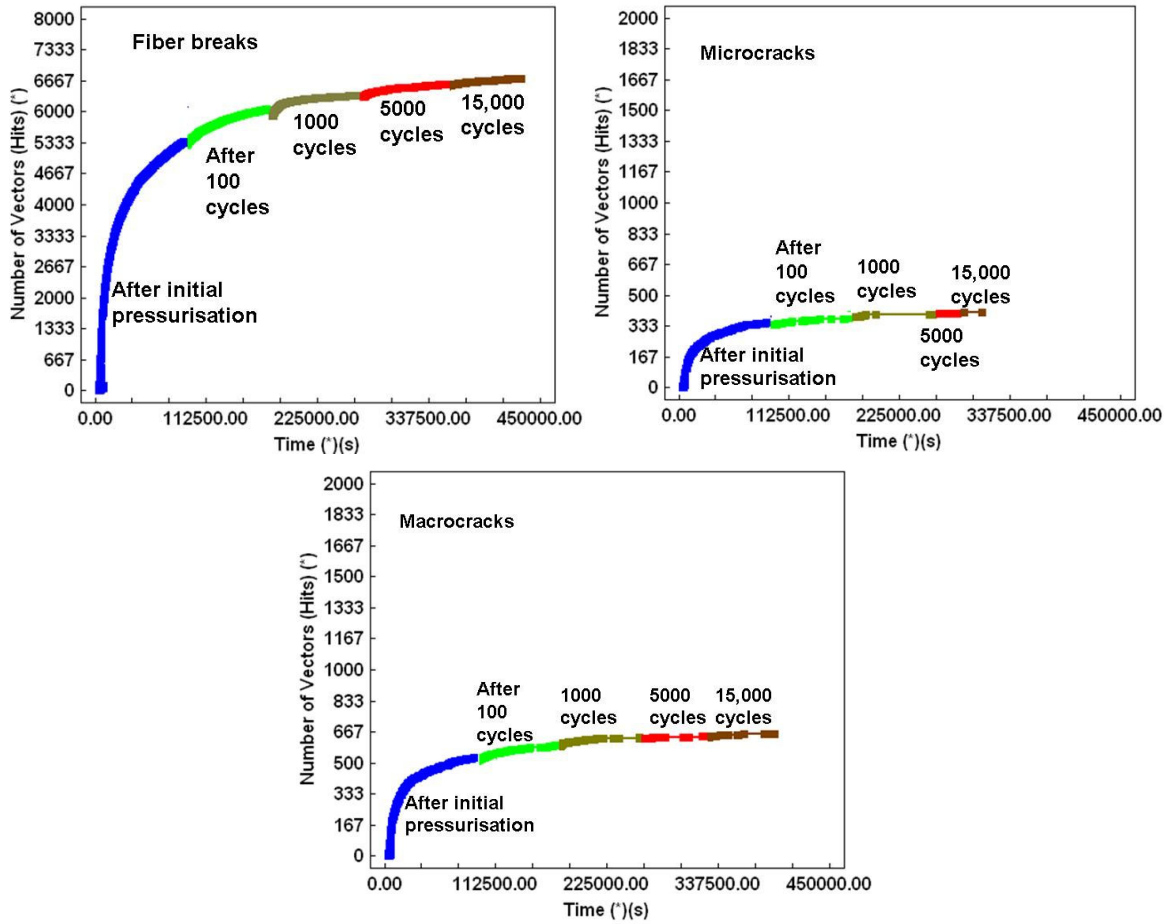

Figure 3: The evolution of damage mechanisms as the pressure vessel was repeatedly subjected to pressure and then held at the maximum pressure of 60MPa for periods of twenty four hours.

4 Conclusion

In this study, the state of damage accumulation in carbon fiber composites specimens and pressure vessels subjected to static and cycling loading has been measured by acoustic emission. Multi-variable analysis of the acoustic emission data has been used to identify the relevant damage mechanisms contributing to composite failure as well as its kinetics.

Failure of the composite pressure vessel is controlled by the progressive failure of the reinforcing fibers which at first is randomly distributed in the composite but if allowed to progress sufficiently will lead to clustering of fiber breaks and instability of the pressure vessel. Fiber breaks occur due to load transfer through the matrix and delayed breaks occur because of the viscoelastic nature of the matrix which leads to its relaxation around earlier breaks and subsequent overloading of intact fibers in regions of fiber breaks. This mechanism is confirmed by finite element modeling. Based on these data, lifetime prediction will be carried out.

References

[1] S Colom, M Weber and F Barbier, Storhy: A European development of composite vessels for 70MPa Hydrogen storage, World Hydrogen Energy Conference (2008)

[2] A.R.Bunsell 'A Handbook of Textile and Technical Fibres' Woodhead Publisher and CRC, Cambridge 2009

[3] S. Blassiau, A. Thionnet and A.R. Bunsell ,Composite structures, 74 (2006) 303-318

[4] S. Blassiau, A. Thionnet and A.R. Bunsell, Composite structures, 83 (2008) 312-323.

[5] S. Camara, A 3D 'Multiscale Finite Element Analysis of Damage Accumulation in Carbon Fiber Unidirectional Composites: *Applied to Pressure Vessels': MS thesis Neb*raska University Lincoln, 2009.

[6] K.Heng-Yi, H.Zejli, A.Thionnet and A.R.Bunsell. To be published.

[7] A.R.Bunsell, Reinforced Plastics February (2006) 39-41.

Effective Structural Design Procedure for Composite Hydrogen Tanks

Jörg B. Multhoff, **Jens Krieger**, ISATEC GmbH, Germany

1 Introduction

On-board storage of hydrogen is a major challenge in the development of future fuel cell based automotive propulsion systems [5]. One standard is the pressurized storage at 700 bar in composite tanks [13]. Several systems including metal or plastic liners are currently under development or in small scale production. However, the conventional technology is unlikely to fulfill the increasing demand for an affordable product in mass production [4]. The expanding market will offer novel opportunities for existing and new suppliers, but any competitive solution will require an optimization of the tanks with respect to both structural efficiency and manufacturing aspects like productivity and reliability.

The key driver for the efficient design of composite pressure tank systems is the understanding of the structural behavior of the complete vessel during the product's life time - including manufacturing. An effective development process will apply adequate modeling and analysis techniques early and integrative to reduce time and cost. The modeling should include the simulation of the manufacturing process to capture decisive factors for product performance and reliability. Evaluation of the structural performance will generate feedback for manufacturing parameters during the optimization loop. Manufacturing and testing of prototypes will generate further feedback necessary for accurate modeling. An effective structural design procedure can only be conceived as integral part of the development process and not as an afterthought to cope with upcoming problems.

The simulation-based design procedure was applied in the H_2 700 NRW project and contributed to the optimization of the developed 700 bar hybrid composite hydrogen tank for automotive applications [7]. Procedural details from this project will be presented together with experiences from similar development projects for composite pressure vessels.

2 Composite Pressure Vessels

The typical composite pressure vessel comprises four main components as shown in Figure 1: Composite hoop windings, composite helical windings, the liner and fittings [6]. The fittings are necessary to connect valves or pipes. The liner is responsible for the gas tightness and may be made of metal or plastic material. From a conceptual point of view the metal liner can be considered to be load carrying or non-load carrying (thin metal liner), the plastic liner is practically never load carrying. In the case of a metal liner the fittings may be an integral part. If they are not, special attention must be paid with respect to the proper connection between fitting and liner.

The composite helical windings cover the entire or most of the surface area of the pressure vessel and have very specific properties due to the nature of the filament winding process [11]. Finally, the hoop windings are only present in the cylindrical part of the pressure vessel

and form a purely circumferential reinforcement. The composite hoop and helical windings together have to take all or a substantial part of the pressure load. A successful design will consider all parts of the pressure vessel – individually and with respect to their interaction. In the following we will focus on the structural design of the composite winding and the metal liner.

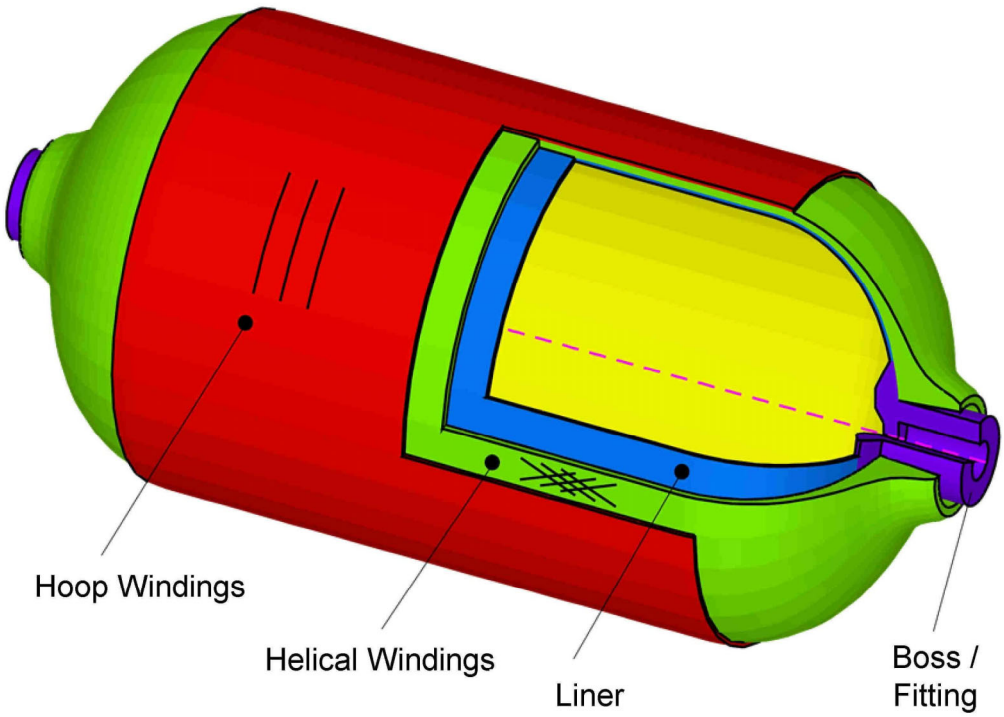

Figure 1: Composite pressure vessel.

3 Structural Behavior

The two overriding concerns with respect to the safety and economy of high pressure vessels are the burst pressure and the number of cycles to fatigue failure. Furthermore, the nature of the respective failure mode is of importance. Typically, both minimum burst pressure and the minimum fatigue life – as well as the circumstances of the related failures – are prescribed in the applicable regulatory codes for pressure vessels (e.g. EIHP [1]). Eventually, conformance of these properties has to be demonstrated by testing to fulfill the safety requirements. From an economic point of view it is necessary not to exceed the safety requirements in any substantial way. Otherwise the resulting product will not be competitive. It is impossible to strike the balance between safety and economy by trial and error alone. The key driver for success is understanding of the structural behavior of the pressure vessel.

4 Modeling Approach

Due to the complicated multilayered, anisotropic composite overwrap and the nonlinear elastic-plastic behavior of the metal liner only detailed modeling and numerical analysis can lead to the required understanding [3,8]. The finite element method is the established and

generally accepted method of analysis for demanding engineering systems. It is therefore obvious to use finite element methods for the analysis of composite and hybrid pressure vessels. However, it is less obvious how these models can and should be constructed, given the complexity of the filament wound composite structure. To achieve accurate results it is important to take the details of the manufacturing process into account. This can be achieved by filament winding simulation as shown in Figure 2 [9].

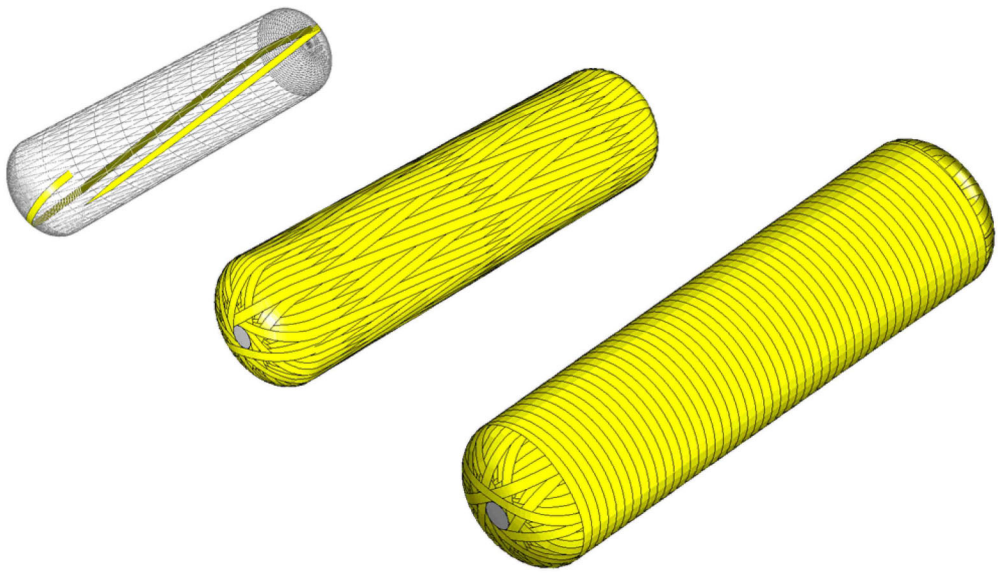

Figure 2: Filament Winding Simulation.

5 Filament Winding Simulation

The exact placement of the filament band on the winding surface is simulated for each wound layer. The final result is a detailed description of the entire composite laminate. A decisive requirement for an economic modeling of the composite structure is, that the detailed description of the laminate is transferred automatically into the finite element model. This can only be achieved by specialized software.

It is noteworthy that the helical layers show a complicated behavior in the end caps of the vessel. The winding angle changes continuously from the cylindrical part to the polar opening (Figure 3). Furthermore, the layer thickness increases due to the progressive overlap of the filament bands on the end caps. Thus, each helical layer is a complex entity in itself. The combination of multiple layers is even more intricate and no longer accessible to simple reasoning. This is reflected in the mechanical properties of the filament wound structure and is manifested in the deformation behavior of the pressure vessel and the stress distribution in the individual layers under internal pressure. The situation is made even more difficult by the dependence of the result on the shape of the dome contour.

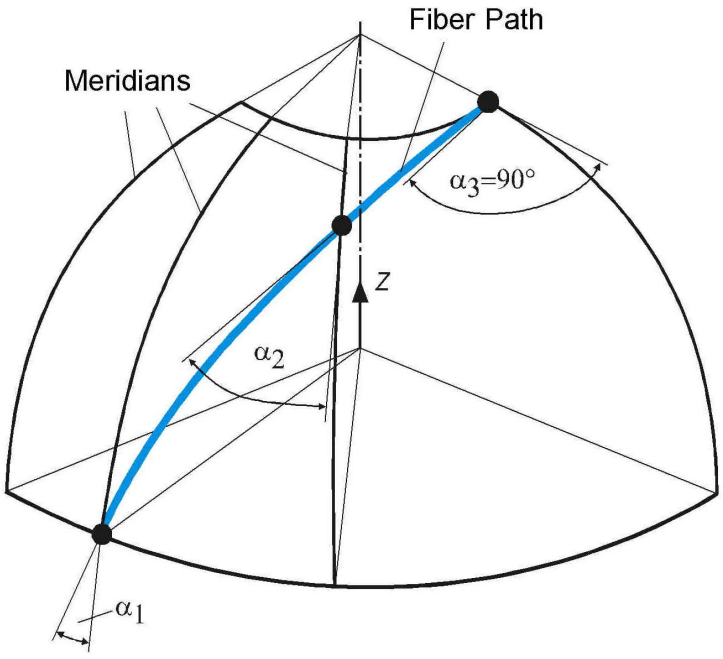

Figure 3: Filament winding path.

6 Iterative Analysis and Design

Under these circumstances neither optimal dome contour nor optimal winding angle combinations are obvious. The best strategy is to simulate the behavior of a given design, evaluate the result and feed back the understanding gained into the design of an improved pressure vessel. This process has to continue until an acceptable result is found. More ambitious optimization procedures (e.g. based on design of experiments) also require the generation and evaluation of large numbers of simulation models [12]. Again, this can only be achieved in an economic way by the support of specialized software. For instance, the evaluation of the stress or strain distribution in each individual layer of the composite laminate must be automatic and should be presented in an understandable way.

An effective way to do this is the creation of path evaluation diagrams of any quantity of interest along a meridian path of the structure (Figure 4).

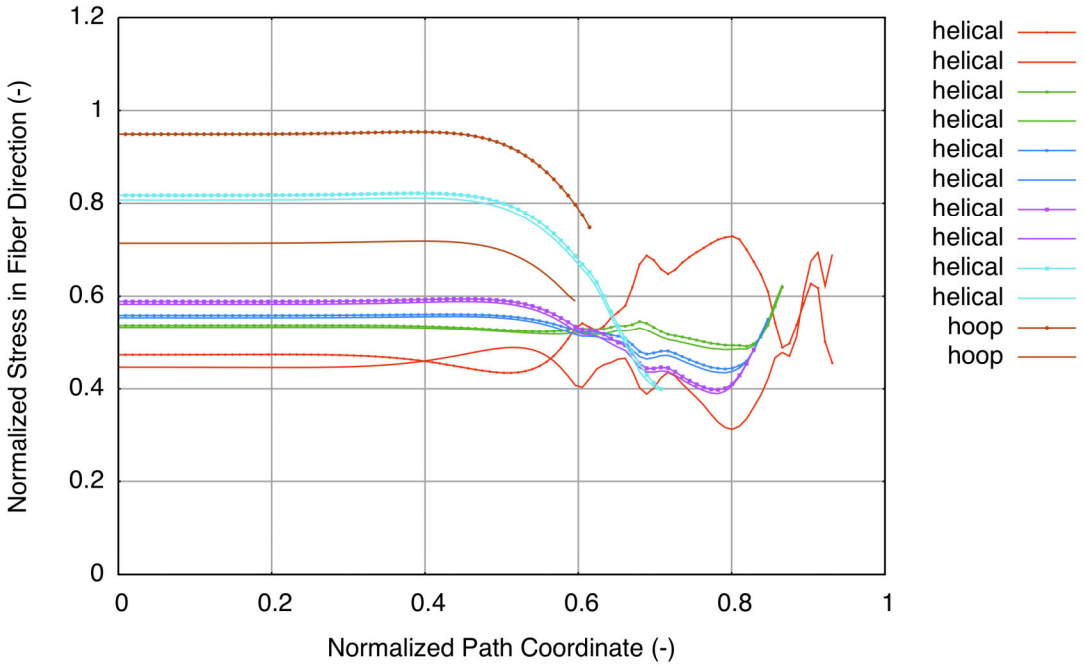

Figure 4: Sample path evaluation.

7 Analysis of Hybrid Vessels

The analysis of hybrid pressure vessels consisting of a composite overwrap on a load-carrying metal liner is more complicated due to the load sharing between the two structural components [2,10]. Fatigue of the metal liner is frequently the primary design issue. Therefore, analysis of the liner is as important as the analysis of the composite laminate. The behavior of the liner will depend strongly on the manufacturing process, namely any forming operation of the liner prior to filament winding as well as the so called autofrettage step. During autofrettage the over-wrapped liner will be pressurized beyond the yield point. This will result in compressive eigenstresses in the liner after pressure relief due to the plastic deformation of the liner. The net effects are a greater elastic stress range and a reduced maximum stress during operational load cycles as well as a negative mean stress – all beneficial factors with respect to fatigue.

Understanding and proper design of this process involves the simulation of multiple load steps as show in Figure 5. This simulation process is best set-up and evaluated automatically since multiple design iterations for liner and composite overwrap are inevitable.

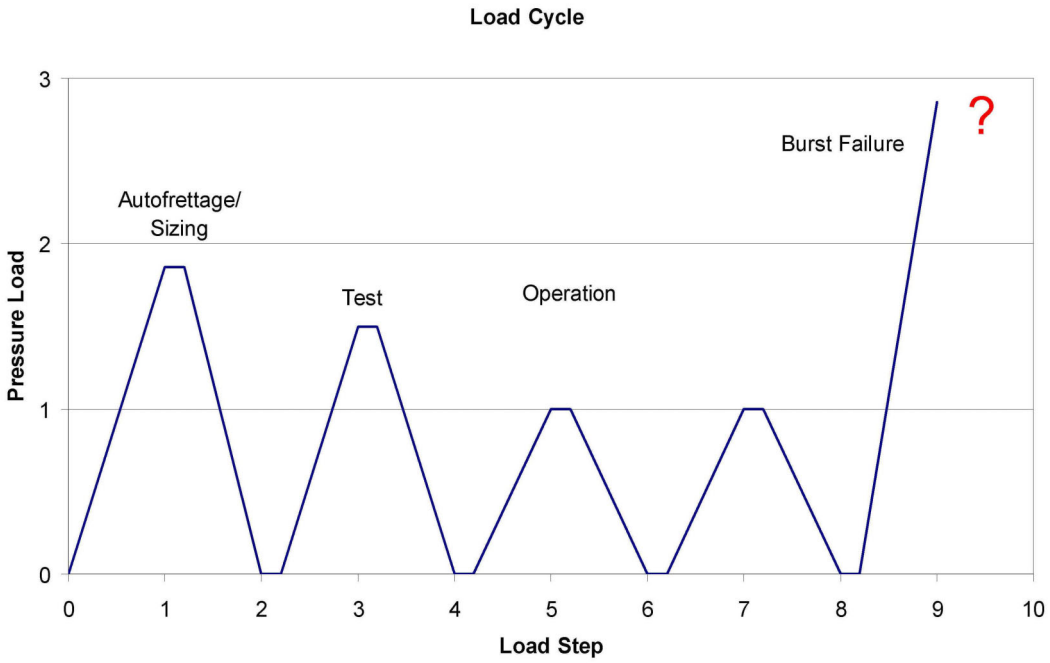

Figure 5: Simulated load steps.

8 Conclusions

As has been shown, analysis and design of composite pressure vessels is complicated and often time-consuming and expensive. On the other hand, the potential of detailed finite element analysis for the optimization of pressure vessels for the storage of hydrogen is undeniable. Therefore a great demand exists to make accurate modeling more timely and economic. ISATEC meats this demand by the development of the ISAWIND® software and process for rapid modeling and analysis of composite pressure vessels including hybrid vessels with metal liners. This process combines filament winding simulation and finite element analysis to an automatic end-to-end procedure for structural analysis from specification to result presentation. With ISAWIND® pressure vessel studies are conducted in a very efficient way. Vessels with different length and different diameters are easily compared concerning their gravimetric storage density, material and production effort. Alternatively a specific configuration is analyzed in detail and optimized by means of ISAWIND® in order to reach the best solution for the given specification in a very short time.

References

[1] European Integrated Hydrogen Project (EIHP): GRPE Informal Group: Hydrogen/Fuel Cell Vehicles, Draft ECE Compressed Gaseous Hydrogen Regulation, Revision 12b, www.eihp.org, 2003

[2] Anders, S.: Sensitivitätsanalyse des Eigenspannungszustandes eines Composite - Hybridhochdruckbehälters, BAM - Dissertationsreihe, Band 37, Berlin, 2008

[3] Betten, J., Multhoff, J.: Untersuchung des Versagensverhaltens von Höchstdruckbehältern aus Faserverbundwerkstoff, Abschlussbericht, DFG-Vorhaben

Be766/40-1 und Be 766/40-2, Lehr- und Forschungsgebiet Mathematische Modelle in der Werkstoffkunde, RWTH Aachen, 2003

[4] Herres, W.-U.: The Hydrogen Fuel Cell Vehicle – A Future Application For Composites, Proceedings of Filament Winding Congress, Brussels, 2005

[5] Krainz, G., Bartlok, G., Meinert, M., Novak, P.: Anwendungsorientierte Entwicklung von Wasserstoff-Speichersystemen für den automotiven Einsatz, Der 4. Deutsche Wasserstoff Congress 2008 – Tagungsband, Schriften des Forschungszentrums Jülich, Band 12, 2008

[6] Krieger, J.: Auslegung und Berechnung von Hochdruckbehältern aus Faserverbundwerkstoff, Dissertation, Lehr- und Forschungsgebiet Mathematische Modelle in der Werkstoffkunde, RWTH Aachen, 2003

[7] Krieger, J., Multhoff, J.B.: Auslegung von Composite-Hochdruckbehältern für H2-Speicherung bei 700 bar (im H2 700 NRW Projekt), Der 4. Deutsche Wasserstoff Congress 2008 – Tagungsband, Schriften des Forschungszentrums Jülich, Band 12, 2008

[8] Multhoff, J.B., Loures da Costa, L.E.V., Krieger, J., Betten, J.: Numerical Simulation of Damage and Failure of Composite Pressure Vessels, COBEM 2003, 17th International Congress of Mechanical Engineering, São Paulo, 2003

[9] Multhoff, J.B., Krieger, J.: Design of Composite Pressure Vessels Using Finite Element Analysis, Proceedings of Filament Winding Congress, Brussels, 2005

[10] Novak, P.: Ein Beitrag zur Strukturoptimierung dickwandiger Hybrid-Hochdruckspeicher, Fortschritt-Berichte, VDI Reihe 18, Nr. 306, VDI-Verlag, Düsseldorf, 2006

[11] Peters, S.T., Humphrey, W.D., Foral, R.F.: Filament Winding – Composite Structural Fabrication, SAMPE Publications, Covina, 1991

[12] Ribeiro, R.O., Loures da Costa, L.E.V., Multhoff J., Milioni, A.Z.: Composite Pressure Vessel Quality Evaluation using Design of Experiments and Simulation, ENEGEP 2002, XXII International Conference On Industrial Engineering and Operations Management, Curitiba, 2002

[13] Züttel, A.: Hydrogen storage methods, Review, Naturwissenschaften 91, Springer-Verlag, Heidelberg, pp. 157-172, 2004

A Model to Predict the Permeation of Type IV Hydrogen Tanks

Julien Bayle, **Dominique Perreux**, **David Chapelle**, **Frédéric Thiébaud**, MaHyTec
39100 Dole, France
Philippe Nardin, Université de Franche Comté, France

Abstract

In the frame of the certification process of the type IV hydrogen storage tanks MaHyTec aims to manufacture, this innovative SME is developing a numerical model dedicated to the study of permeation issues. Such an approach aims at avoiding complicated, time-consuming and expensive testing. Experimental results obtained under real conditions can moreover be significantly influenced by the scattering of material properties and liner dimensions. From simple testing on small-size flat membranes, the model allows to predict the gas diffusion flow through the whole structure by means of numerous parameters. On every step, theory can be compared with the results obtained from the samples.

This document presents a brief review of the mathematical theory describing gas diffusion and the different aspects of the study for better understanding the proposed approach.

1 Introduction

In a worldwide complex context of global warming, depletion of fossil fuel and increase of the general energy price, it is important to find new clean solutions. Hydrogen can be one of those future possibilities if we are able to produce, supply and storage it properly. Earth being full of this molecule, numerous solutions are available to extract it from water, gas or biological organisms… In different countries (Germany, Belgium, Netherlands, United States…), some installations or local production devices already exist to tank up vehicles. The actual real difficulty comes from its storage due to its low mass density. Among the three storage possibilities: solid (too heavy), liquid (too complicated and energy consuming to maintain -253°C), and gas, MaHytec believes in the high pressure tank of gaseous hydrogen. Four types of tanks exist, detailed on Fig.1, depending on utility and pressure wished.

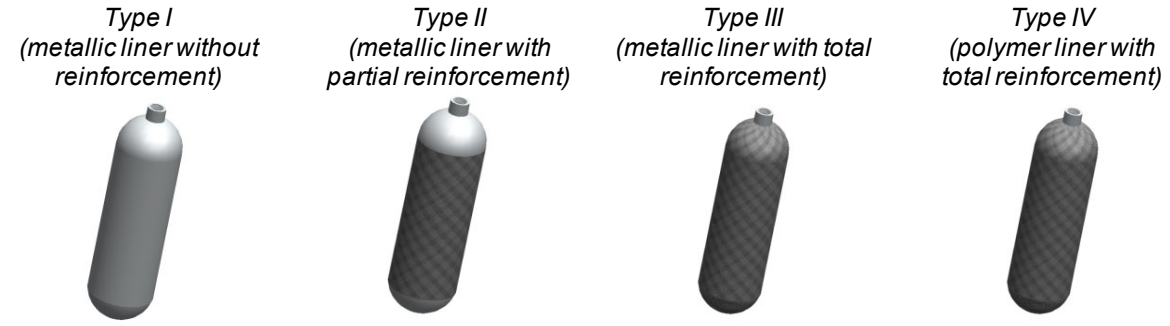

Figure1: Different types of gaseous hydrogen storage.

This study deals with the type IV hydrogen tank, which have the major drawback of a significant permeation. To be able to manufacture a good tank it is obligatory to respect legislation. In the perspective of being in compliance with the international standard ISO 11439:2000 defining the requirements for hydrogen tanks gastightness, it is of utmost importance to understand the gas transport phenomenon through polymers. Different mathematical theories have been proposed to represent the diffusion of a gas through a flat membrane but also through a cylinder or a sphere [1]. Inspired by Fourier's law on heat conduction, the Fick's first law is the most suitable theory for expressing the permeation of hydrogen :

$$J = -D\nabla C \quad (1)$$

J : hydrogen diffusion flow [cm^3(STP)/s.cm^3]

D : diffusion coefficient [cm^2/s]

∇C : concentration gradient [cm/s.cm^3]

The minus sign represents the direction of the flow, from the highest pressure side to the lowest pressure side. This equation can be combined with the mass conservation to obtain the Fick's second law (2, 3, 4). Depending on the shape of the material that is investigated, the law can be expressed as:

Flat membrane $$\frac{\partial C}{\partial t} = \frac{\partial}{\partial x}(D\frac{\partial C}{\partial x}) \quad (2)$$

Cylinder $$\frac{\partial C}{\partial t} = \frac{1}{r}\frac{\partial}{\partial r}(rD\frac{\partial C}{\partial r}) \quad (3)$$

Sphere $$\frac{\partial C}{\partial t} = D(\frac{\partial^2 C}{\partial r^2} + \frac{2}{r}\frac{\partial C}{\partial r}) \quad (4)$$

On the basis of these formulae, it is possible to develop a numerical model coupled with an experimental permeation system to predict the behavior of a type IV hydrogen tank.

2 Study

The permeation parameters of numerous materials can be readily found in the literature. However, the values of the diffusion, solubility and permeation coefficients are strongly influenced by the nature of the raw material, the production process or the conversion method, and the characteristics of a given polymer can vary from a specimen to another. The rigorous analysis of the permeation must rely on real parameters which must be determined experimentally rather than on unreliable theoretical values. On that purpose, a permeation vessel for the testing of flat membrane has been designed.

2.1 Experimental part

The system has been developed in view of simplicity and reliability (see Fig. 2). It makes it possible to test a polymer disc (a) under low or high pressure. The risk of bulging is overcome thanks to a reinforcement disk (c) made from a porous material. Hydrogen tightness between the two vessel blocks and the membrane is achieved by means of O-rings (b) to ensure that all the permeated gas is measured.

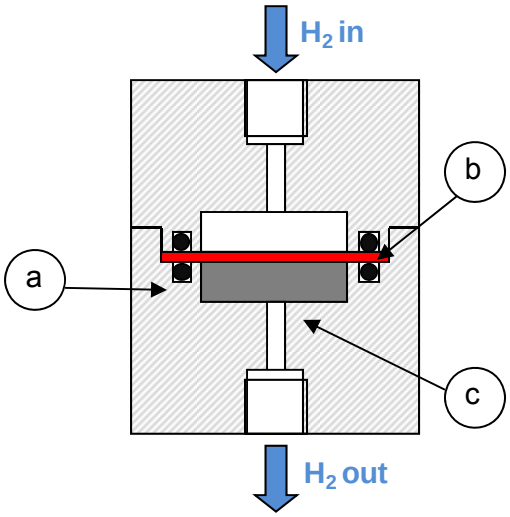

Figure 2: Schematic of the permeation vessel (refer to text for details).

The permeation testing is realized in a thermostatted environment to perfectly control the temperature, whose impact on diffusion kinetics is non-negligible. The low hydrogen flow is measured by a pressure sensor coupled with an acquisition device allowing us to obtain its evolution over time. With the help of equations obtained from the analytical analysis of a flat membrane, the permeation properties of the material can be assessed. This experimental qualification of the polymer should then contribute to estimate the permeation which may occur through a liner of type IV hydrogen storage tank.

2.2 Analytical analysis

Some publications [2-3] provide simplified methods for quantification of flat membranes permeation

$$Q(t) = eC_1\left(\frac{Dt}{e^2} - \frac{1}{6} - \frac{2}{\pi^2}\sum_{i=1}^{\infty}\frac{(-1)^i}{i^2}exp\left(-\frac{Di^2\pi^2t}{e^2}\right)\right) \quad (5)$$

$Q(t)$: amount of gas [cm^3 (STP)/cm^3]

e : thickness of the membrane [cm]

C_1 : gas concentration on the most pressurized side [cm^3(STP)/cm^3]

D : diffusion coefficient [cm²/s]

t : time [s]

Equation (5) gives a relevant approximation of gas permeation in a simple unidirectional case, where gas concentration C_1 is assumed to be constant and C_2, concentration on the

lowest pressure side, is assumed to be null. These hypotheses turn out to be satisfactory as long as the outlet pressure is relatively low.

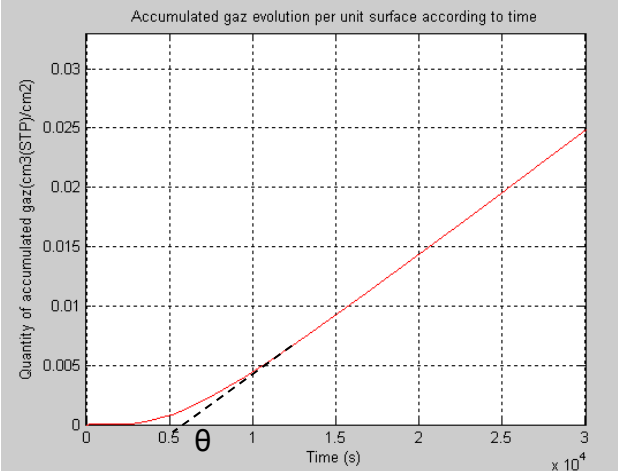

Figure 3: Typical permeation curve.

Fig. 3 shows the typical permeation curve obtained whether it be from experimental or theoretical investigations. It is then possible to determine material parameters like diffusion coefficient or gas concentration by using the evolution of Q over time. Thus, once the permeation has reached a steady state, the curve is a straight line which equation is:

$$Q(t) = \frac{DC_1}{e}\left(t - \frac{e^2}{6D}\right) \quad (6)$$

The intersection with the time axis of the submentioned line gives the "time lag" θ.

$$\theta = \left(\frac{e^2}{6D}\right) \quad (7)$$

The three main permeation parameters of a flat membrane made of any material can then be assessed.

- **Diffusion coefficient D**, obtained with equation (7) after having found θ experimentally.
- **Solubility coefficient S** [cm^3(STP)/cm^3.cmHg], obtained with Henry's law $C = S.P$, where P [cmHg] is the pressure and C the gas concentration from (6) on the same side.
- **Permeation coefficient Pr** [cm^3(STP).cm^2/cm^3.s.cmHg], obtained by multiplying D and S.

2.3 Numerical model for a type IV hydrogen storage tank

This model aims at predicting the diffusion behavior of hydrogen through a real liner of type IV tank as well as through a flat membrane. For the last, numerical and experimental results will be compared to check the model. The long-term objective is a full-numerical validation of the tanks permeation behavior. The model programming is based on the finite difference method with dimensionless quantities :

Flat membrane $$\frac{\partial \bar{C}_i}{\partial \bar{t}} = \frac{2}{h_i + h_{i-1}}\left(\frac{\bar{C}_{i+1} - \bar{C}_i}{h_i} - \frac{\bar{C}_i - \bar{C}_{i-1}}{h_{i-1}}\right) \quad (9)$$

Cylinder $$\frac{\partial \bar{C}_i}{\partial \bar{t}} = \frac{2}{h_i + h_{i-1}}\left(\frac{\bar{C}_{i+1} - \bar{C}_{i-1}}{2\bar{r}_i} + \frac{\bar{C}_{i+1} - \bar{C}_i}{h_i} - \frac{\bar{C}_i - \bar{C}_{i-1}}{h_{i-1}}\right) \quad (10)$$

Sphere $$\frac{\partial \bar{C}_i}{\partial \bar{t}} = \frac{2}{h_i + h_{i-1}}\left(\frac{\bar{C}_{i+1} - \bar{C}_{i-1}}{\bar{r}_i} + \frac{\bar{C}_{i+1} - \bar{C}_i}{h_i} - \frac{\bar{C}_i - \bar{C}_{i-1}}{h_{i-1}}\right) \quad (11)$$

Where $\bar{C}_i$ refer to the dimensionless concentration at point i, $\bar{r}_i$ is the dimensionless radius position of point , and h_i refer to the variable mesh size between point i and point $i+1$.

According to the analysis presented by Scheichl [4], a formulation which only considers a derivation in space is proposed. Then, using the commercial software matlab and dedicated functions (ode15s, quad) make it possible to have an assessment of the concentration through the thickness. Regarding the geometry of a type IV hydrogen tank, it can be assumed that its permeation behavior is obtained by combining the numerical results obtained separately for a cylinder and for a sphere. This hypothesis is only acceptable for ordinary totally closed hydrogen tanks (without filler cap).

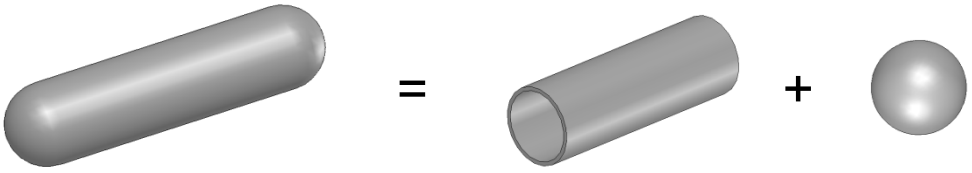

Figure 4: Geometrical decomposition of a type IV hydrogen tank.

The model is implemented in an easy-to-use program that allows to predict the permeation behavior of a structure depending on the shape, the material properties and the loading conditions. The results can be obtained numerically and graphically, under the form of a graph (Fig. 3) or cartography (Fig. 5). The latter represents the hydrogen concentration in regard of the time and wall thickness. On the figure here below, the blue color corresponds to the lowest concentration while the red color is used for the highest values.

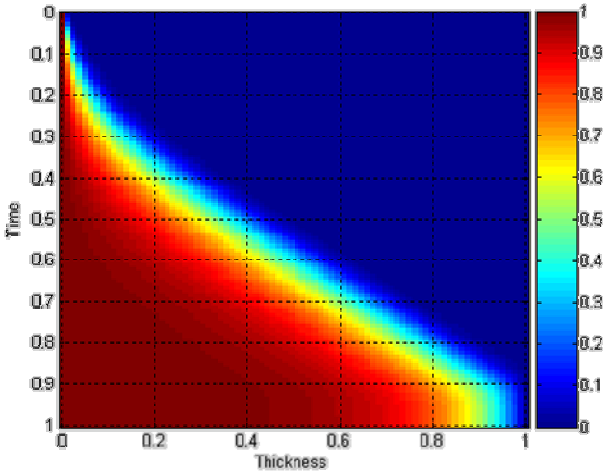

Figure 5: Evolution of concentration versus time and thickness.

3 Conclusion

Based on experimental investigations on flat membrane compared with both analytical modeling and numerical modeling, this study aims at predicting the permeation occurring in a type IV hydrogen storage tank which liner is made of polymer. Considering the first results that have been obtained up to now, the model turns out to be very promising. A good correlation was observed between theoretical, numerical and experimental approaches. Further developments will be carried out in order to improve the efficiency and accuracy of the program. The next step will consist in adding a mechanical aspect to take into consideration the free volume decrease under high pressure. It will be achieved by implementing the Cohen-Turnbull relationship [5] that will allow using non-constant diffusion coefficient.

References

[1] J. Crank, The Mathematics of Diffusion, 2nd ed., Clarendon Press, Oxford, 1975.

[2] B. Flaconnèche, J. Martin, M.-H. Klopffer, Transport properties of gases in polymers : experimental methods, Oil & Gas Science and Technology – Rev IFP, Vol 56 (2001), pp 245-259

[3] Vivekanand Saikumar, Ralph J. Jaccodine, Time lag and permeation in multilayer polymer coatings, IEEE transactions on components, Hybrids, and manufacturing technology, vol. 16, No. 5, (1993)

[4] R. Scheichl, M.-H. Klopffer, Z. Benjelloun-Dabaghi, B. Flaconnèche, Permeation of gases in polymers : parameter identification and nonlinear regression analysis, Journal of membrane Science 254 (2005) 275-293.

[5] A.J. Hill, S. Weinhold, G.M. Stack, M.R Tant, Effect of copolymer composition on free volume and gas permeability in poly(ethylene terephtalate)-Poly(1,4 cyclohexylenedimethylene terephtalate) copolyesters, European Polymer Journal, Vol. 32 (1996), No. 7, pp. 843-849

Optimisation of the IV Generation Tanks for Hydrogen Storage Applied in Vehicles. Modelling and Experiment

Jerzy Kaleta, Wojciech Błażejewski, Paweł Gąsior, Marek Rybaczuk, Wrocław University of Technology, Poland

1 Introduction

A prevalent technology is storing of hydrogen in a high pressure tanks/vessels (CH2) with increasing Nominal Working Pressure (NWP) to 70 MPa (vessel type IV). The outer layer of such vessel is made of high resistant carbon fibers and liner is made of high density plastics. A burst pressure (a safety ratio = 2.35), must be at least 164.5 MPa. Currently there is no vessel type IV on the market (omitting prototype vessels), which has sensible cost of production and fulfills all safety requirements at the same time. A high value of safety ratio cause that thickness of the composite layer of CH2 cylinders is at least 15 mm or even more. It brings a high price of complete storage system and exclude its mass applicability. The main efforts are presently focused on optimization of the production technology in order to mass and cost reduction. This requires application of new ideas of numerical modeling, experimental identification and sensoring. Good numerical model should allow: description of winding geometry, description of the stress and strain states in vessel for mezo- and macroscales, formulation of the problem of initiation of material damage, acceptance of quantity responsible for damage accumulation and formulation of fatigue hypothesis. The model should indicate location of sensors and their number what constitutes basis for experiment. The paper presents briefly selected methods of modelling and way of experimental verification of proposed models. Some results were obtained under StorHy project (6FP, Integrated Project), InGas project (7FP) and Polish research project No. POIG.01.01.02-00-016/08.

2 Geometry of Winding Composite Layers. Modelling

Analysis within construction of composite tank as well as applied structures of composite carrying layer in both cases CNG and CH2 bottles manufactured by leading firms in world allows to conclude that every manufacturer makes use of different arrangement of fibres. There are no differences in materials applied for a liner and braid, actually it is carbon fibres and aluminium or thermoplastic (IV generation) liner. However there are substantial discrepancies in composite carrying layer of tanks. Especially this concerns number of wound layers, angle of winding, layers sequence and finishing of outer layer, etc. This means that there is no widely accepted and documented methods of choice and determination of composite carrying layer. This problem is especially important in the case of designing of tanks, what is called fourth generation CH2. Our team has elaborated universal method of generation of interlace geometry and its application with the help of winders. It was proofed that only finite number of patterns is available. The Figure 1 below presents only four geometries around many possible. Experiment indicates that some structures allow reduction

of composite layer thickness thus reduction of mass and price without changes in safety requirements (level of strain, damage accumulation).

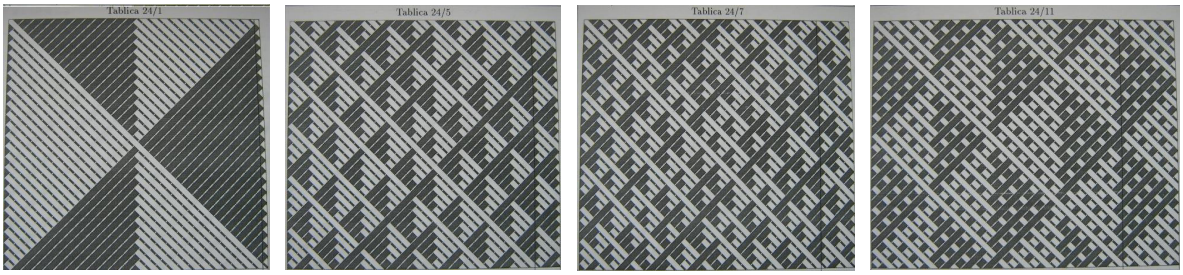

Figure 1: Diagrams of geometry of four chosen interlacing of wound fibres made with the help of winder.

Examinations of tanks with variety of interlace geometry, what is decisive but expensive (Figure 2a) were preceded by fatigue tests of tubes thus fragments of cylindrical tanks made with the help of hydraulic pulser MTS with application of elastometer as working medium (generating load). Two steel pistons situated at ends of tube compressed elastometer inside tube. The photo-elasticity coating method (PCM) was applied to determine strain field (Figure 2b) and temperature changes at the specimen surface were registered with IR camera (Figure 2c) in correlation with turn of winding. Examinations allowed to indicate optimal geometry of wind.

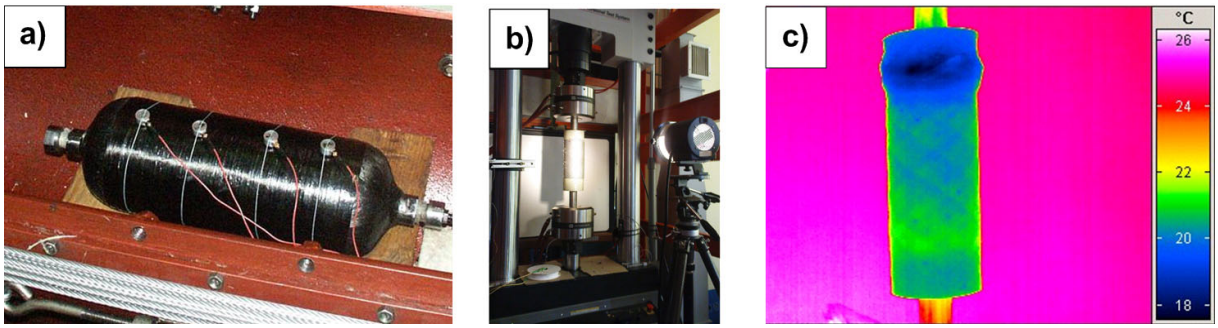

Figure 2: View of tank during pressure tests (a), stand for cyclic examinations of cylindrical tanks with MTS pulser and PCM (b) and distribution of temperature from thermovision camera (c).

In addition microscopic examinations were carried out, it was fund that there was substantial difference in numbers of voids i.e. air bubbles comprised between rowing and between fibres. Figure 3 presents view of metallographic specimens along generatrix of tank for two distinct structures (denoted as A and B). Difference in contained voids and resin may be correlated with suitable interlace structures.

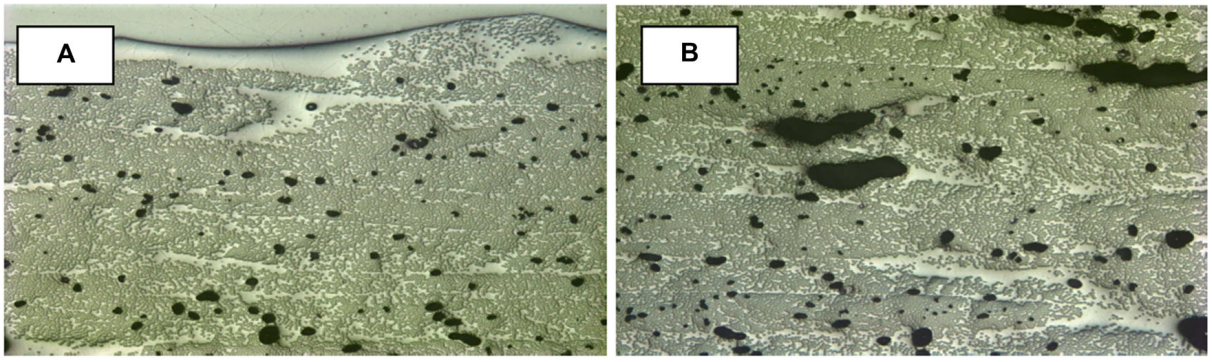

Figure 3: View of metallographic specimens (50X) along generatrix of tank for two different structures denoted as A and B. The substantial difference in voids and resin contents is clearly visible.

3 Modelling of Strain State and Damage Accumulation of Tank

Examination of running damage process and current damage level may be effectively performed as an effect of some **hybrid procedure**, i.e. it should consist of well verified numerical model (of the multi-scale type) of vessel together with local measurements making use of well located limited number of sensors.

Good numerical model (for every type of vessel) should allow:

- description of winding geometry (so called parquet problem, described above),
- the constitutive equation of composite (making use of some homogenization procedure for example)
- description of the stress and strain states in vessel (applying the model of continuum and FEM),
- formulation of the problem of initiation of material damage,
- acceptance of quantity responsible for damage accumulation (measure of damage) and formulation of fatigue hypothesis.

The model should indicate location of sensors and their number what constitute basis for experiment.

Dominating, till recent times, metal constructional materials and elaborated modelling methods are useless in the case of carbon/polymeric composites for high pressure vessels application. Here, the structure, orientation of fibres and interaction between fibres and epoxide matrix, have decisive meaning. Classical models do not provide reasonable safety of construction during computer aided designing. In turn, such modelling reduces costs of experimental works what entails reduction of construction costs. In practice effective methods of modelling becomes unavoidable.

Modelling of materials with complicated internal structure (corresponding to sufficiently short scales or equivalently to sufficient magnifications of observations) remains still an open problem. Modern constructional materials like fiber reinforced composites constitute a challenge. The basic problem is to find the correspondence between visible microscopic

structure and material properties, mainly mechanical ones, responsible for macro scales usually put forward in engineering applications.

The identification of material parameters based on experimental measurements has the key meaning. The experiment should allow:

- local measurements of strain at places indicated by the model (here, application of optical fibers sensors is preferred)
- measurement of quantity correlated with accumulation of damage of vessel (registration of AE for example),
- modelling and experiments for vessels (expensive ones) may be preceded by modelling and experiments for tube specimens.
- Especially useful In modelling of composite structures applied in tanks construction approaches are listed below [3,4,5,6]:
- Modelling making use of nonstandard models of continual media (using homoganisation),
- Modelling in terms of cellular automata,
- Modelling applying theory of dynamical systems.

Below only chosen aspects are briefly presented.

Modelling making use of nonstandard models of continual media. The main purpose of modelling of composite materials is establishing of constitutive equations describing entire large specimens due to known structure and material properties of separate phases forming composite as well as architecture of fibres (transition from micro through meso to large scales). The homogenisation method allows determination of material properties (for example Young module) and it consists in suitable averaging over chosen volume and over separate phases properties. At macro level, the structure of composite becomes invisible but one knows the stress-strain dependence which in fact corresponds to phase and fibres properties. It is possible to assume that fibre reinforced polymeric composites have periodic structure what enables establishing of the Representative Volume Element (RVE).

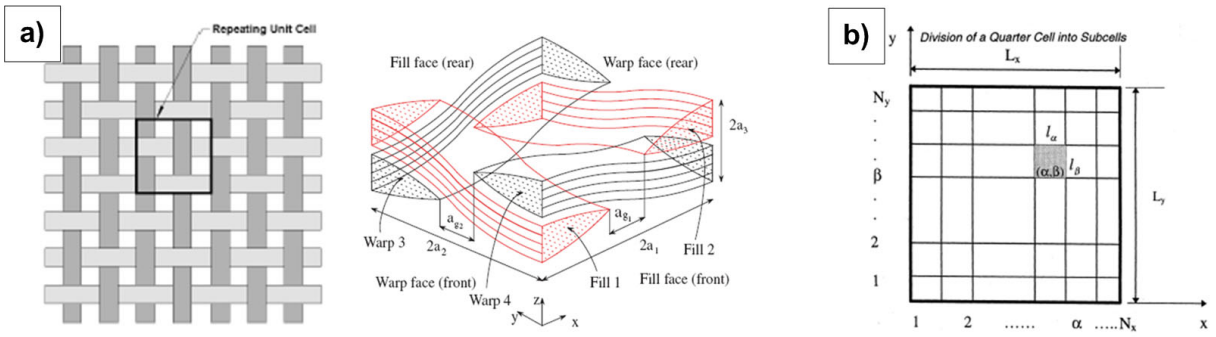

Figure 4: The structure and quarter of Representative Volume Element (a) and division of a quarter of unit cell into subcells in plane material properties homogenisation (b).

We predict the behaviour of composite making use the found RVE and the homogenisation procedure. According to distribution of fibres the RVE may be decomposed into subcells (Figure 4b) and the homogenisation procedure may run in few steps.

In turn application of fractal geometry methods allows modelling of acoustic emission (AE). Numerically simulated acoustic events may be compared with acoustic events registered during experimental examinations of specimens and pressure vessels.

4 Sensors, Measurements Methods

The problem of strain measurements and establishing of on board monitoring system [7,8,9,10], which may be applied during manufacturing phase and many years of its exploitation was presented in accompanying paper (Smart fibre optic methods for structural health monitoring of high pressure vessels for hydrogen storage. WHEC 2010; Vehicle and Infrastructure Safety/SI.1).

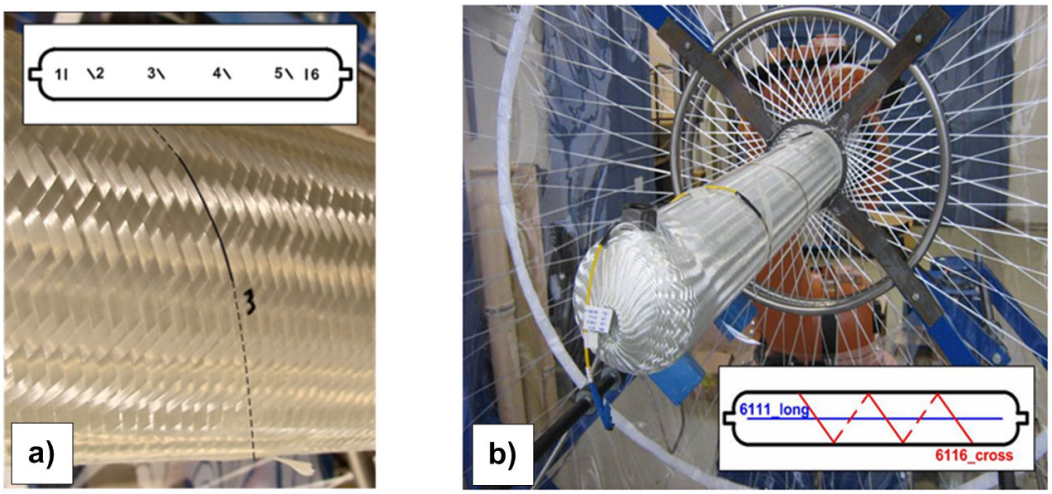

Figure 5: Scheme of FBG sensors arrangement (a) and SOFO® (b) and view of the braided structure with sensors installed on the penultimate braided layer [9].

Above, only ways of integration of optic fibres sensors FBG and SOFO® inside composite structure made up with braiding technique were presented (Figure 5). Digits 1,2,3,...,6 indicated positions of optical fiber sensors (FBG). System was tested for a pilot vessels made up from glass fibres.

Another effective measurement techniques were thermovision, photo-elastic method of surface layer, acoustic emission (for accumulation of damages). Resistance strain gauge method has limited importance.

5 Static and Fatigue Tests of Vessels

Norms assume that experimental examinations are decisive and cannot be replaced with modelling procedures. Therefore the special laboratory for high pressure tests was created at Institute of Materials Science and Applied Mechanics, Wroclaw University of Technology. Among others, it carries cyclic test within the range of pressures 2÷150 MPa (under room

temperatures and under extreme conditions , -45ºC, +80ºC and 90% humidity) as well as burst tests up to 200 MPa. There are also testing ground examinations (for example shoot down tests with penetrating bullet). Due to regulations the cyclic load test of tanks is carried out with the help of oil, up do damage or up to approaching 45000 tests in stages of 15000 cycles. Loads amount 20÷875 bars for Hydrogen with frequency not exceeding 10 cycles per minute (usually 2 cycles per minute).

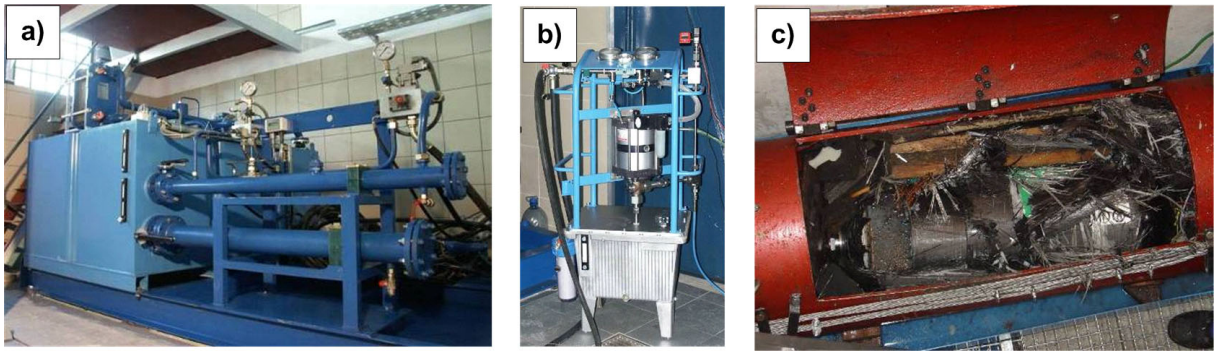

Figure 6: Hydraulic stand for cyclic examinations of vessels (a), stand for static tests of high pressure vessels (b) and vessel in safety chamber after burst test (c) [6].

In turn static tests, including burst tests, are carried out at stand depicted in Figure 6b. Maximal available pressure amounts 3000 bars. Before tests vessels are filled with water and degassed, next they become inserted in safety chamber.

6 Summary

1. Manufacturing of safety, light and relatively cheap composite tank of fourth generation for Hydrogen storage as fuel requires works on optimisation of wound geometry, modelling of effort state, damage accumulation and methods of modelling as well as application of sensors.
2. Methods of modelling allow substantially reduction of costs within constructions, technology and examination of CH2 tanks.
3. Experimental examinations still remain decisive especially within static and cyclic loads of bottles.

References

[1] Błażejewski W.: Influence of the winding fibers structures on mechanical strength of composite cylinder elements made up from epoxy-glass. W: 17th Danubia-Adria Symposium on Experimental Method in Solid Mechanics, Prague, October 11-14, 2000.

[2] Blazejewski W., Gasior P., Kaleta J.: Burst test of high pressure composite vessels for gasoues fuels storage. W: 25th Danubia-Adria Symposium on Advances in Experimental Mechanics, Ceske Budejovice, Cesky Krumlov, Czech Republic, September 24-27, 2008.

[3] Czapliński T., Maciejewski Ł., Przygoda A., Ziętek G. A model of textile reinforced composite; homogenisation and identification. 18th Conference on CMM. Zielona Góra, Poland, 2009, pp. 155-156.

[4] Aniszewska D., Rybaczuk M., Fractal characteristics of defects evolution in parallel fibre reinforced composite in quasi-static process of fracture, Theoretical and Applied Fracture Mechanics, 52, (2009), 91-95.

[5] Czopor J., Rybaczuk M., Fibers breaking process in composites models and numerical simulations applying cellular automata, Theoretical and Applied Fracture Mechanics, 52, (2009), 154-157.

[6] Aniszewska D., Rybaczuk M., Modelling defects growth in composites using fractals characteristics, Composites2009 2nd ECCOMAS, Thematic Conference on the Mechanical Response of Composites, 1-3 April 2009, Imperial College London, UK.

[7] Gasior P., Kaleta J., Sankowska A.: Optical fiber sensors in health monitoring of composite high pressure vessels for hydrogen, Proc. SPIE s. 66163G-1-66163G-10, cop. 2007.

[8] Blazejewski W., Gasior P., Kaleta J., Sankowska A..: Optical Fiber Sensors as NDT methods for strain state monitoring of high pressure composites vessels. Comparison of different types of OFS. 8th International Conference on Durability of Composite Systems, 16-18 July 2008, Porto, Portugal.

[9] Blazejewski W., Czulak A., Gasior P., Kaleta J., Mech R.: SMART composite high pressure vessels with integrated Optical Fiber Sensors. SPIE Smart Structures/NDE, San Diego, California, USA, 7 - 11 March 2010.

[10] Blazejewski W., Gasior P., Kaleta J., Sankowska A.: Optical fiber sensors integrated with composite material based constructions. Lightguides and Their Applications III, Proc. SPIE s. 66081L-1-66081L-10, cop. 2007.

An Innovative Technology for Hydrogen Storage in Portable and Mobile Systems

Dan Eliezer, C.En Ltd., Sonnhaldenstrasse 3, 8032, Zurich, Switzerland
Kai Holtappels, Martin Beckmann-Kluge, BAM Federal Institute for Materials Research and Testing, Division II.1 “Gases, Gas Plants”, Unter Den Eichen 87, 12205, Berlin, Germany

Central to the realization of the profound potential of the hydrogen economy is the resolution of obstacles related to hydrogen technologies- the primary obstacle being the development of an effective and applicable hydrogen storage method. Conventional storage methods are unable to reach necessary targets relating to: weight, volume, safety, cost, durability, as well as charging and permeation rates. This in turn limits the *applicability* of hydrogen and fuel-cell power technologies, curbing the development of the hydrogen economy.

The presentation will outline a novel method for the safe storage of highly pressurized hydrogen in arrays of thin sealed glass capillaries.

The C.En developed system ensures the **safe infusion, storage, and controlled release of hydrogen gas**, under storage pressures of over 1200 bar. These findings have been achieved in experiments conducted on individual and multiple (array) capillaries at the German Federal Institute for Materials Research and Testing (BAM), and demonstrate the unique properties of glass capillary arrays.

Testing at the BAM Federal Institute has lead to the determination of the pressure resistances of individual and multiple (array) capillaries. These were determined in relation to capillary glass materials (quartz, borosilicate, alumosilicate and soda-lime glasses), capillary dimensions, wall thickness, endurance capacities etc. These tests were conducted in order to ascertain the optimal parameters and materials for the utilization of the glass capillaries for a variety of applications. Results demonstrated that borosilicate capillaries were able to withstand pressures over 1000 bar. Endurance testing further established that borosilicate capillaries consistently performed higher than other glass materials through thousands of refill cycles, having the highest average value (1002 bar) and the highest burst pressure rates (1242 bar) (See Figure 1 adjacent). A central determinant of the pressure resistance of glass capillaries relate to defects in the glass structures, such as bubbles, grooves or crack flaws (shingles). These strongly increase stress peaks and therefore decrease pressure resistance. At the same rate, no ignitions were observed when capillaries where burst at different pressures.

The significant advantage of glass capillaries is that they are stronger than steel and are simultaneously of a lower density. In comparison to steel vessels, only a thin wall thickness is needed to achieve an equal pressure resistance. A polymer overwrap acts as a protective shell against mechanical damages and allows for a flexible design of the storage unit. Furthermore, a large number of capillary arrays can be stacked together in a solid tank made of lightweight materials (e.g. plastics). This means that less material is needed and a strong

and **lightweight** storage system is achieved. This is especially true as the apparatus of the system does not require additional bulky or heavy equipment, such as pressure reducers, to ensure its safe and efficient use (see details below).

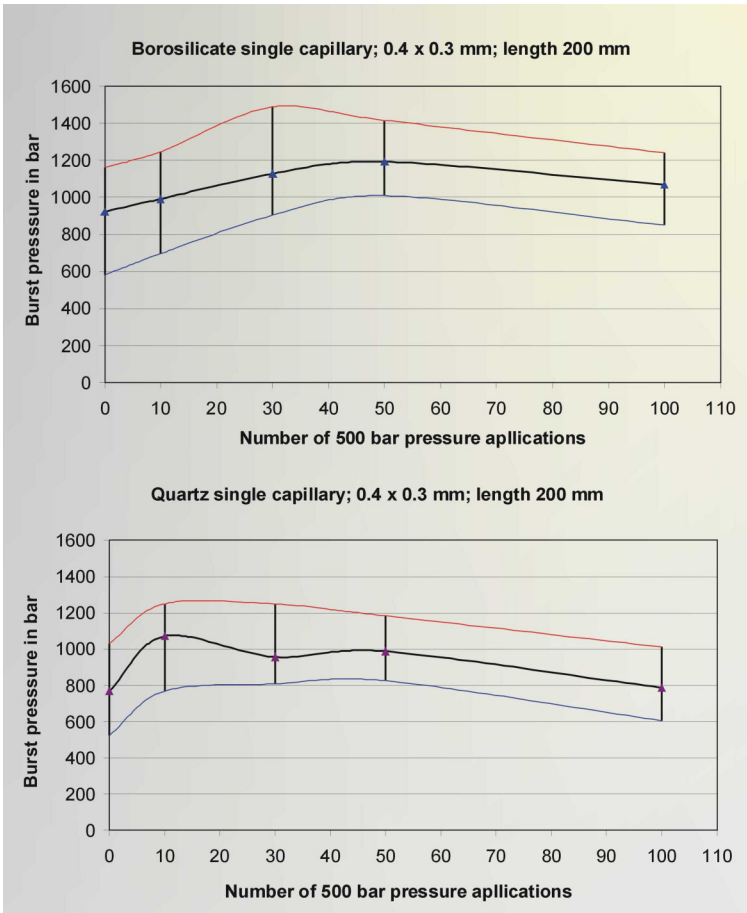

Figure 1: Burst pressure dependence on number of endurance tests.

The **safety** of hydrogen supply and storage is paramount. If a rupture occurs in a one-vessel hydrogen storage system the amount of hydrogen released would be very dangerous, likely creating an explosive atmosphere. The advantage of C.En's technology is in the bundling of many single capillaries. Acting as its own pressure resistant vessel, each capillary supports and strengthens the resistance of its adjacent capillaries. In the event that one "vessel" (capillary) is damaged the amount of hydrogen released would be too small to create an explosive atmosphere.

The major barriers to using hydrogen as a replacement for fossil fuels in cars and trucks have been the size and weight of the tank, as well as safety issues related to the infusion, transfer and release of the hydrogen. C.En Ltd. has developed an innovative technology based on capillary arrays that ensures the safe infusion, storage and controlled release of hydrogen gas. The hydrogen storage targets of the U.S. Department of Energy (DOE) are used as a standard to compare various on-board hydrogen storage technologies. In September 2009 the DOE lowered its 2010 gravimetric storage targets from 6% wt to 4.5

wt% and its 2015 gravimetric storage targets from 9 to 5.5% wt (% wt -net useful energy/ max system mass). Similarly the DOE's 2010 volumetric storage targets were lowered from 45 g/L to 28 g/L, and its 2015 targets were lowered from 81 g/L to 40 g/L (g/L - net useful energy/ max system volume). Storage targets were lowered due to the failure of DOE-sponsored hydrogen storage systems to approach original targets.

Storage tests conducted at a specially built state-of-the-art laboratory at the BAM Institute demonstrate that C.En's technology has a gravimetric storage capacity of **33 %wt** and a volumetric storage capacity of **45 g/L**, easily surpassing the U.S. Department of Energy (DOE) recently modified hydrogen storage goals for 2010 and 2015. Test results significantly exceed the published storage capacities of other storage systems, clearly demonstrating that the technology enables the storage of a significantly greater amount of hydrogen than other approaches

The presentation will delineate upon the various methods of: a) refilling capillaries with compressed hydrogen b) permeation through the walls of primarily sealed capillaries at elevated temperatures c) the sealing of capillaries. The theoretical analysis of the resistance of capillary arrays to hydrogen pressure, and the experimental matters of the charging and release of hydrogen will further be presented in detail

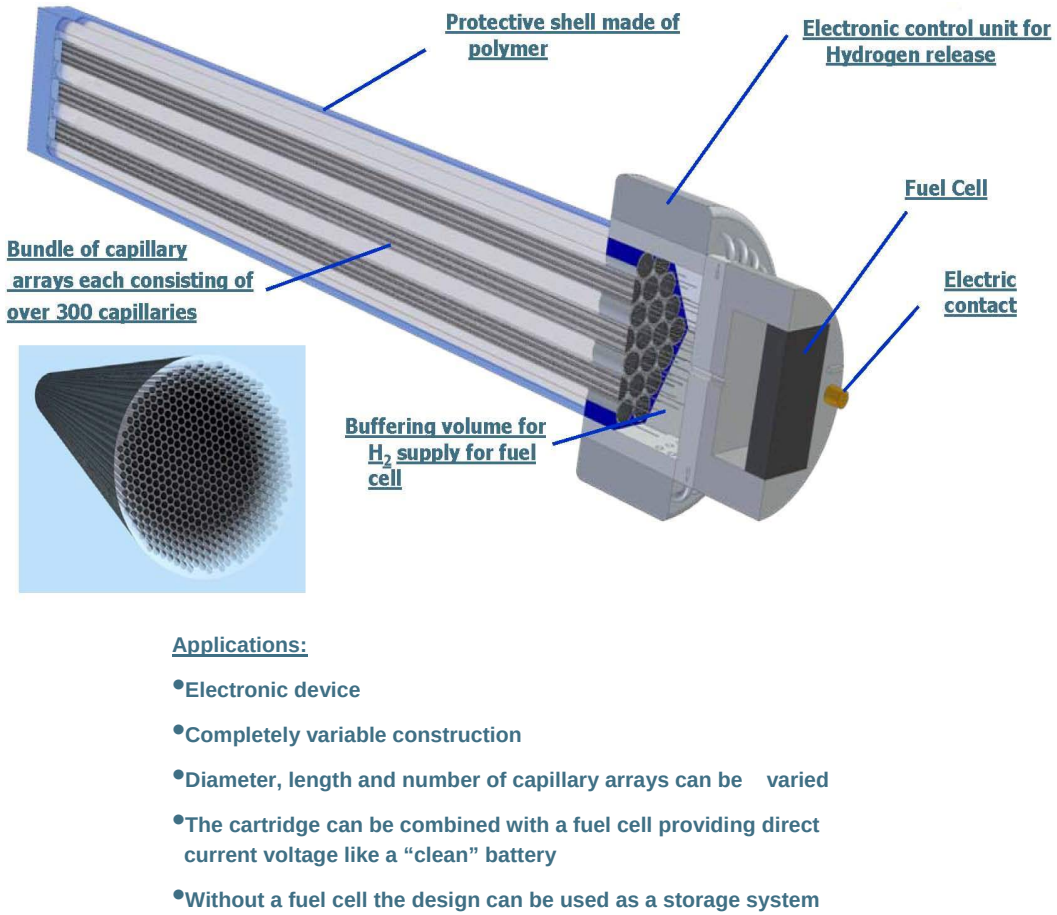

Figure 2: Hydrogen storage cartridge prototype.

The technology is founded upon established scientific principles, yet its employable structure is of a malleable nature. The structure of the storage system of arrays depends upon the specific requirements of the end-user applications, and therefore allows for the optimally designed storage system. The cartridge system prototype itself demonstrates the flexibility of the technology allowing for: the open scaling of arrays- in size, length and number; easy linkage to a variety of fuel cells and for the simple shaping of the device using a moldable polymer overwrap.

Testing of these advances prototypes at the BAM Institute have further clearly proven that the technology can be modified to suit the specific requirements of various end-user applications and can in turn enhance the applications by ensuring an efficient, light weight, safe and compact source of clean energy.

Experiments conducted at the BAM Institute have conclusively demonstrated the various uses of our system for a variety of applications, including those of the:

- **Transport industries** -automotive, aircraft/aerospace, ships, maritime vessels, submarines, trucks, rails
- **Electronic industries -**communications, defense industry, electric and power applications – mobiles, computers, laptops etc.)
- **Manufacturing Industries** fiber materials, containers)
- **Infrastructural projects** (large and bulk storage, stations).

The relationship between the properties of the storage system and potential end- user applications will be discussed in detail.

Large-Scale Hydrogen Underground Storage for Securing Future Energy Supplies

Fritz Crotogino, **Sabine Donadei**, KBB UT, Hanover, Germany
Ulrich Bünger, **Hubert Landinger**, LBST, Ottobrunn, Germany

1 Introduction

In recent years the role of hydrogen in future energy scenarios has moved somewhat into the background. Now its significance is being highlighted even more as it may play an important role during and after the transition from fossil fuels to renewable energy sources concerning two areas in particular.

1.1 Energy industry

The energy industry is facing the need to store extremely large quantities of energy for long-term to seasonal periods in order to adapt the fluctuating and non-dispatchable energy production from wind and solar resources to the actual demand, which is no longer feasible using conventional technologies. In today's fossil-based energy industry, seasonal fluctuations, strategic reserves, and compensation of shortages and shut-downs are largely balanced out by the storage of fossil fuels (e.g. Germany and France both have reserves covering around 2 months of demand). With a reach of only around 1 hour (Germany), today the storage of electrical energy plays a very subordinate role. The possibility to outsource the storage capacity to fossil fuels will decrease more and more in a future electricity-based energy industry, i.e. the long-term storage capacities for electrical energy will have to be much longer than 1 hour.

In recent years pumped hydro and compressed air energy storage (CAES) systems were almost exclusively seen as suitable methods for balancing out fluctuating wind and PV feed-in into the transmission grids. In contrast, the latest investigations - and particularly the comprehensive study published by VDE [1] have identified the limitations of these storage technologies, particularly with respect to total storage capacities. Hydrogen alone can facilitate the storage of large quantities of energy to balance out long periods of poor wind power supply and seasonal fluctuations. Hydrogen large scale storage will be the only means in the long term to provide electrical energy in quantities and at a quality level consumers are accustomed to, in parallel to the downscaling of major capacities from fossil power plants and nuclear power stations. Furthermore, the relevant large volumes which need to be stored can most likely only be accommodated underground in geological formations – primarily in man-made salt caverns.

1.2 Supplying fuel cell vehicles with hydrogen

The limited range and low storage capacity of battery electric vehicles as well as the limited availability of biofuels limiting its long term use to heavy duty transport such as trucks, rail and aircraft, require the use of hydrogen powered fuel cell vehicles for a wide range of vehicle segments. After a transition phase, hydrogen needs to be mainly produced from

renewable electricity such as wind and solar power [2]. Also for the transport sector it will be necessary to balance out seasonal fluctuations and to build up reserves to prepare for shortfalls, etc.

Most of today's infrastructure investigations on future hydrogen supply have either addressed the development of hydrogen demand or the build-up of hydrogen refuelling stations including onsite hydrogen storage capacities as well as onboard hydrogen storage. This paper contributes an assessment of the continuous supply of *green* hydrogen throughout the year which takes the utilisation of fluctuating and non dispatchable resources into account.

The first part of this paper looks at the future demand for hydrogen storage capacities for energy supply and for hydrogen as a vehicle fuel. The second part reviews the current status of hydrogen storage in salt caverns, engineering parameters, storage capacities and costs.

2 Demand for Energy Storage Capacity

2.1 Energy supply

The need for additional energy storage capacities at a grid scale has primarily been studied in the past with respect to providing balancing power, i.e. to level out deviations from wind energy forecasts. Pumped hydro and CAES power plants are as of now the most suitable systems for the electricity generation capacities in the order of a few Gigawatts and for periods of up to hours or a few days. Main reasons are their high efficiency level of 70%+ and specifically their moderate investment and operating costs.

In the long term, however, energy storage systems with considerably higher capacities will be needed. The required capacity will depend on the type of transition scenario (e.g. extended operating periods of nuclear power plants; substitution of coal based power generation to natural gas; nuclear phase-out or optimum or restricted grid extension).

In the *moderate*[1] *scenario,* the residual load, the difference between energy demand and energy generated by wind and solar power, can be largely provided from fossil and nuclear fuels for which no shortage is assumed even for the long-term. However, this would require a considerable extension of the existing electricity grid and a reliable long-term availability of additional very large quantities of natural gas imports should nuclear power be completely phased out. In this scenario, the expected demand for additional storage capacity is considered to be moderate. Assuming that an optimal extension of the electricity grid is not possible, the required storage capacities to compensate the *missing* grid extension may only be accomplished by providing large scale hydrogen storage capacities.

The *optimistic scenario* assumes to completely discard fossil and nuclear power plants and for this reason is the most extreme case. Balancing out seasonal fluctuations of wind power in particular - see Figure 2-1 - requires enormous storage capacities for electrical energy,. A comprehensive study by SIEMENS & ISET [3] has revealed the demand for storage capacity as shown in Table 2-1 under the assumption of an optimum Europe-wide extension of electricity grids. Furthermore, a storage capacity of 2% of the annual wind and solar energy production has been assumed in the study.

---

[1] Moderate with respect to the scaling down of fossil and nuclear power plant capacities.

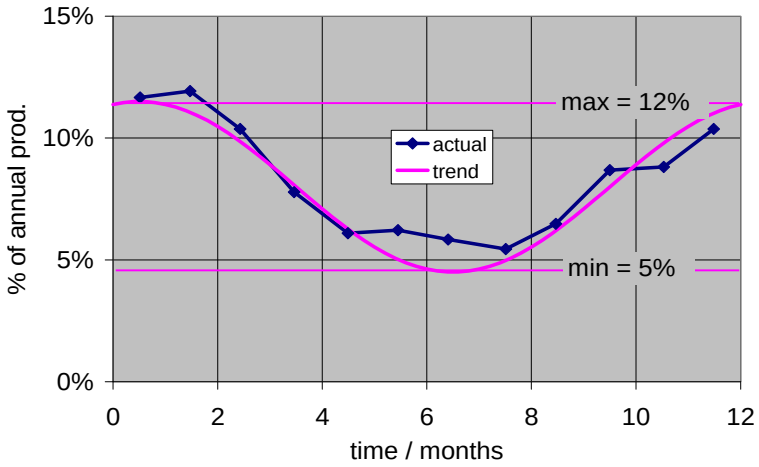

Figure 2-1: Seasonal wind power variations.

Table 2-1: European-wide storage requirements when power is only generated from wind and solar power[2] plants.

Hydrogen	167 TWh	0.41 km³
Pumped hydro	74 TWh	106 km³
Adiabatic CAES	80 TWh	29 km³

Achieving these enormous storage capacities using pumped hydro or CAES plants is completely unrealistic (106 km^3 of pumped storage volume corresponds to twice the volume of the Bodensee (Lake Constanz). Even the use of hydrogen storages goes very close to the feasibility limits.

The approach investigated in the *Kombikraftwerk* [4] project in which shortages of wind and solar power are primarily compensated by energy provided from biogas power plants is probably unfeasible because of the lack of adequate quantities of biogas.

2.2 Fuel supply for the transport sector

The study GermanHy [5] carried out on behalf of the German Federal Ministry of Transport, Building and Urban Development (BMVBS) in co-operation with the National Organisation Hydrogen and Fuel Cell Technology (NOW) has addressed the question “Where will the Hydrogen in Germany Come from by 2050?”, and forecasted a realistic hydrogen demand as a transport fuel. Whilst the future overall transport fuel consumption will strongly depend on the selected scenario (moderate, ambitious climate protection and resource shortages), the hydrogen demand by 2050 is predicted to be largely constant and independent of the scenarios and is estimated to around 470 PJ/a or on average 15 GW, which is approximately 20 % of the present grid load in Germany.

---

[2] The different figures for the energy storage requirements respect the different energy efficiencies of the various storage technologies. The different storage volume requirements also take the different storage densities into account.

Although fuel consumption is largely constant throughout the year, the availability of the main energy source wind is fluctuating both short term and seasonally, see Figure 2-1. In natural gas supply today the only solution for large scale energy storage is the use of underground geological formations for technical, economical and safety reasons. The storage of only 10 % of the annual hydrogen consumption forecast in GermanHy would result in the need to develop more than 50 salt caverns with a volume of about 500,000 m^3 each – corresponding to approximately one third of the number of underground gas caverns currently operated in Germany.

3 Storage Options

3.1 Comparison of large-scale storage options

3.1.1 Technical aspects

Given an average load in the German transmission grid of around 70 GW and a maximum output of all currently operated wind power plants of around 24 GW (62 GW expected in 2050), the storage of electrical energy at grid scale for minute reserve (tertiary control) and above is primarily only possible using pumped hydro schemes, CAES or hydrogen storage plants. Pumped hydro plants have the greatest degree of operational flexibility and comprise highest efficiencies of about 80%, yet providing relatively low volumetric storage densities. Furthermore, the potential to add new plants is limited. Future adiabatic CAES power plants are characterised by slightly lower operational flexibility and efficiency, but with higher yet still comparatively low volumetric storage densities. The potential to build new plants, however, is much higher because of the availability of suitable geological formations for underground storage caverns, in particular in regions with high wind power potential.

The storage options mentioned above are based on the *physical* storage of energy. In the case of hydrogen, storage is based on *chemical* principles, which is associated with much higher volumetric storage densities. The hitherto disadvantage is the much lower electricity-to-electricity conversion efficiency of less than 40% for converting electricity into hydrogen by electrolysis, storage and conversion back to electricity in a gas turbine. However, even despite these efficiency restrictions, hydrogen is the only storage option which enables the storage of much larger volumes of electrical energy. In addition, there is an even larger potential of suitable geological salt formations for hydrogen caverns compared to CAES caverns because hydrogen caverns can be installed at much greater depths. Figure 3-1 shows the preferential areas of application for the different storage options.

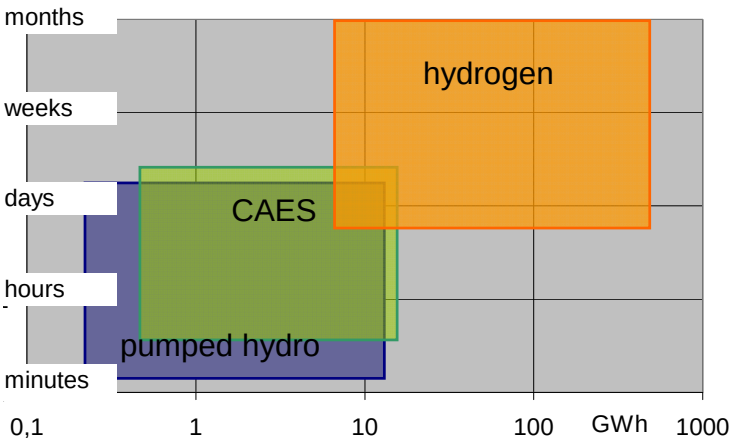

Figure 3-1: Preferential areas of large scale storage options.

3.1.2 Economic aspects

The VDE ETG study [1] has also quantified the storage costs for the three large-scale storage options: Figure 3-2 displays the results of the two scenarios *load levelling* to balance out short-term fluctuations and *long-term storage* to balance out larger amounts of energy over longer time periods. The parameters applied are power plant output and storage capacities. In the case of short-term storage, pumped hydro and CAES power plants are both associated with similar low costs as compared to hydrogen storage. This is primarily related to the high investment costs for the above ground facilities and the higher operating costs attributable to the lower overall efficiency in case of hydrogen. The situation reverses, however, when considering long-term storage: hydrogen becomes more attractive as a consequence of the dominant costs of long-term storage systems being associated with the number of storage caverns needed. In effect, hydrogen causes much lower storage costs because of its higher storage density reducing the required cavern volume by a factor of about 60.

In conclusion the benefits of hydrogen used as a storage medium for large energy volumes, needed to balance power over long periods, are not associated with technical aspects alone. Hydrogen underground storage also enables much lower costs for storing energy at large scale.

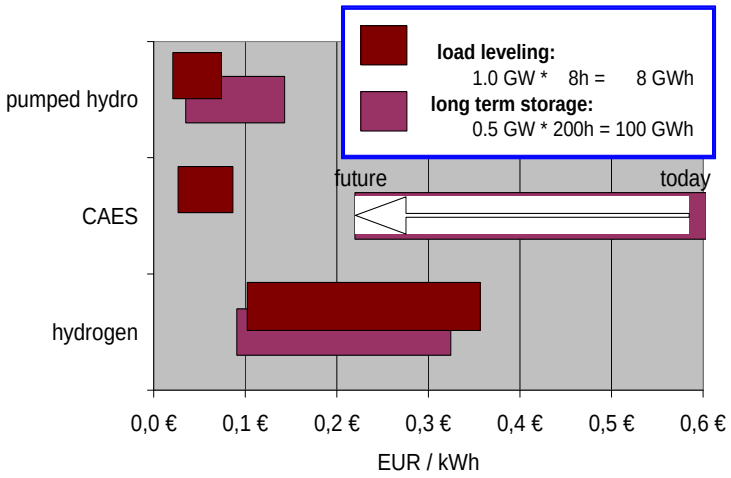

Figure 3-2: Costs (range) for storing one kWh electric power.

3.2 Options for underground storage of hydrogen

The safe and economic long-term storage of gases – primarily natural gas – in underground geological formations has been standard engineering practise for many decades. The most frequent technique is to use depleted gas fields and natural aquifer formations. Man made caverns in salt formations have gained increasing importance in recent years. Salt caverns are the best option for storing hydrogen because salt is inert with respect to hydrogen – as for natural gas – and is extremely gastight.

The disadvantages of natural reservoirs like depleted fields and particularly aquifer formations for hydrogen storage are possible reactions between hydrogen and micro-organisms, as well as between hydrogen and mineral constituents of the reservoir. Biological or mineralogical reactions of this kind can lead to the deterioration or depletion of the hydrogen storage, or that reaction products can plug the microporous pore spaces.

4 Hydrogen Storage in Salt Caverns

4.1 Technical parameters

Salt caverns have successfully been used for the storage of gases under high pressure for a long time, see Figure 4-1. The advantages of salt caverns are the extremely high tightness of the salt rock mass, low specific construction costs, and the small footprint required above ground. Typical parameters are 700,000m^3 geometrical volume and 20 MPa maximum operating pressure. In Germany about 170 caverns are currently used for the storage of natural gas for seasonal load balancing, shut-down reserve, reserve for extreme weather conditions, and as trading reserve. Interestingly, these major reasons for constructing and operating natural gas storage systems have hardly been discussed so far in the context of a future energy economy primarily based on renewable energy sources.

Despite its high level of fugacity, hydrogen has been successfully stored in salt caverns for decades. A plant with three relatively small single caverns is operated in the UK (Teesside).

Two much larger caverns are in operation in Texas, USA, and a third one is currently under construction. The minor differences to natural gas caverns primarily concern the selection of materials in the access well and the cavern head at the surface.

High pressure gas caverns function by compression and decompression between a minimum and a maximum pressure. The maximum pressure approximately corresponds to 80% of the initial formation pressure at the depth of the cavern roof, whilst the minimum pressure is around 30% of the maximum pressure. If the roof of the cavern is at around 1,000 m depth and the cavern has a geometrical volume of 700,000 m^3, the net storage capacity - also known as working gas - will be around 6,000 t. The gas volume remaining in the cavern once the minimum pressure has been reached and therefore not for use, also known as cushion gas, would be around 3,000 t hydrogen in this case.

The maximum acceptable rates for filling and emptying the caverns are governed by the maximum flow rates in the boreholes and the maximum pressure reduction rates in the caverns of 1 MPa/d. As a rule of thumb, maximum withdrawal rates correspond to approximately 10% of the storage capacity per day, with a maximum of 10 turnovers per year.

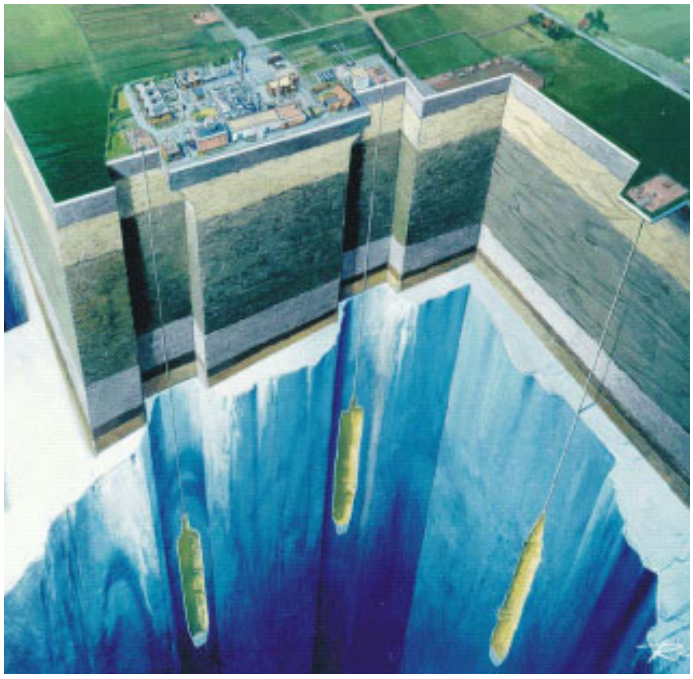

Figure 4-1: High pressure gas caverns in a salt dome.

4.2 Safety

Underground storage systems provide much higher safety levels than surface technologies do. The “thickness of the walls” in a given cavern is typically several 10 to 100 m, and the operating pressure is always below the encompassing formation pressure which is why a gas cavern can basically never explode. Salt rock is also extremely gas tight with theoretical leakage rates at some 0.01% p.a. The only connection between the cavern and the surface is the access borehole, see Figure 4-1. Several casing strings are cemented into this

borehole so that they are completely gas tight. Additionally, a production string is installed which can be replaced if required.

The worst case scenario which can affect the facility is a major damage to the cavern head. To prevent any blow-out, safety shut-off valves are installed in gas caverns about 50 m below the surface. They close automatically if any risk of a blow-out should occur.

4.3 Salt formations for constructing storage caverns in Europe

Figure 4-2 shows the – very uneven – distribution of salt formations across Europe, including existing and planned projects for storing fossil fuels. The individual structures can vary considerably with respect to their suitability for developing gas storage caverns. By far the most favourable geological conditions exist in the north-west of Germany and the north-east of the Netherlands. Extended regions in e.g. southern Germany or central France lack either salt formations completely or have unsuitable salt deposits. Another important prerequisite for the construction of caverns is the potential to dispose large quantities of saturated brine in an environment-friendly way produced during solution mining.

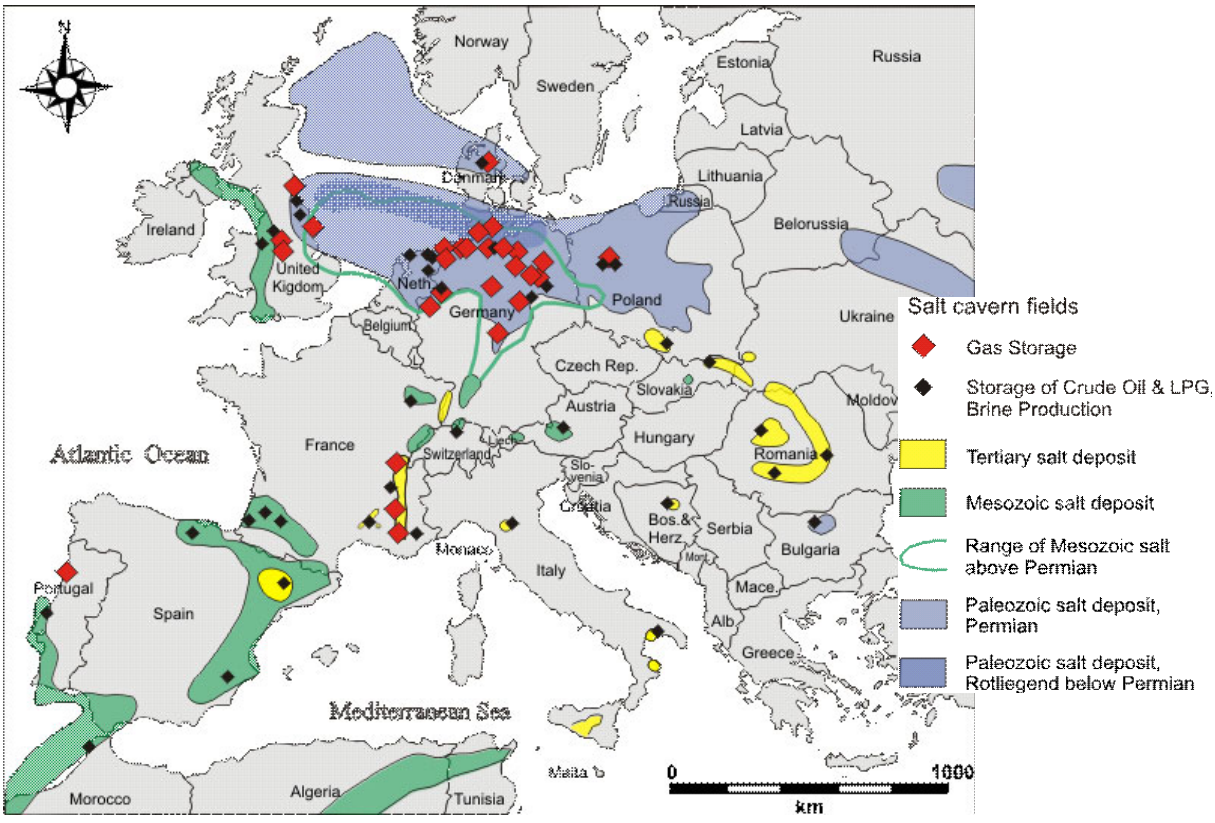

Figure 4-2: Salt structures and cavern storages in Europe.

5 Outlook

Now that hydrogen's potential role as a transport fuel and for energy storage has become obvious, it is time to improve our understanding of the technical and economic details for the whole pathway. A number of areas should be analysed more closely – specifically as this large-scale technology will need long development lead times.

Examples for further research & development are:

- The dimensioning and economics of surface gas handling equipment for drying, purification, compression or liquefaction
- The systems economy taking into account synergies from dual use (as a transport fuel and for re-electrification)
- The evaluation of regional energy storage potentials
- The future large-scale seasonal energy storage needs in Germany, Europe and the World
- The safety and associated certification issues for underground plants - and to a lesser extent - surface plants.

In preparing for real hydrogen storage applications, the relevant partners should be identified early, and the need for public support for these storage systems for renewable energy has to be addressed if considered important e.g. similar to the feed-in tariffs for renewable energy feed to the electricity grid.

References

[1] Energiespeicher in Stromversorgungssystemen mit hohem Anteil erneuerbarer Energieträger – Bedeutung, Stand der Technik, Handlungsbedarf; Energietechnische Gesellschaft im VDE (ETG), Frankfurt, Germany, 2009

[2] Schindler, J.; Wurster, R.; Blandow, V.; Zittel, W.; Where will the Energy for Hydrogen Production come from? Status and Alternatives; commissioned by the German Hydrogen and Fuel Cell Association; 2006; www.h2euro.org/wp-content/uploads/2009/01/eha_h2production_brochure_eng_0407.pdf

[3] Hoffmann, C.; Bremen, L., Storage and Transport Capacities in Europe for a full Renewable Power Supply System – Siemens-ISET Study. 14th Kassel Symposium Energy Systems Technology, 24-25 September 2009, Siemens Corporate Technology, Kassel, 2009

[4] www.kombikraftwerk.de

[5] www.germanhy.de/page/fileadmin/germanhy/media/090826_germanHy_Abschlussbericht.pdf

Underground Hydrogen Storage Problems in Russia

Kaplan S. Basniev, **Roman J. Omelchenko**, **Fatima A. Adzynova**, Gubkin Russian State University of Oil and Gas, Russia

1 Introduction

Utilization of organic fuel for covering the increasing demand for energy leads to global environmental pollution, greenhouse effect and lack of oxygen for the civilization. Therefore there is the necessity of reorientation from hydrocarbon to new universal energy resource. In this connection hydrogen is considered to be one of the most acceptable energy resources in the future. Hydrogen is a fuel for different purposes, it can be used as fuel and as chemical material. The convertion of transport, industry and household consumers to hydrogen doesn't request drastic changes in modern technology of fuel utilization. The important thing is that being burned hydrogen comes back to the atmosphere in the form of water. Increasing hydrogen consumption requires new kinds of hydrogen storage.

2 The Methods of Hydrogen Storage

At present the following methods of hydrogen storage are realized: gas bottles, gasholders (compressed gaseous hydrogen under the pressure of 40-100 MPa), stationary or transport cryogenic containers (liquid hydrogen under the pressure of 20 MPa), metal hydrides (metal absorption), underground storage. To evaluate the effectiveness of each particular method of hydrogen storage the functioning of the whole chain from production to consumption, including storing, transport and distribution, has to be analysed. Underground hydrogen storing will be necessary for regulation of seasonal, monthly and daily fluctuation of energy consumption and production when moving to the industrial use of hydrogen. The irregularity of gas consumption depends on the industry, way of life of the population and the climatic conditions of different regions of the country. The most effective ways of large-scale hydrogen storage is underground storage in depleted oil and gas fields, the subterranean aquifers, underground reservoirs in salt deposits, permafrost grounds. These methods should be located close to its heavy consumers. Due to less viscosity and density hydrogen has got greater mobility than natural gas does. Therefore hydrogen leaks through different seals or the storage cap are more probable.

3 Hydrogen Properties

It is reasonable to store a mixture of hydrogen and carbon dioxide. The dynamic viscosity coefficient of such mixture is higher than the dynamic viscosity coefficient of pure hydrogen and is close to methane (fig. 1). To get the mixture with necessary properties we can manage our composition by carbon dioxide inclusions.

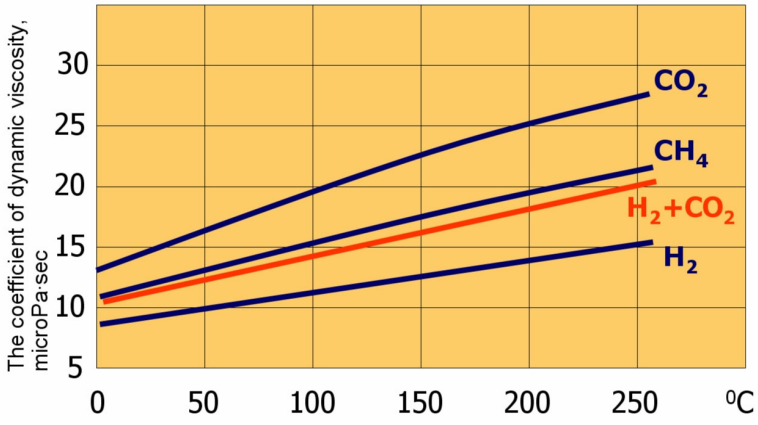

Figure 1: The dependence of viscosity from temperature at atmospheric pressure.

Practical impermeability, ability to stand at high pressures, opportunity of quick changing technology of injection and recovery while exploiting the underground storage, chemical inertness of rock salt to the stored products make storage of gaseous hydrogen in rock salt probably most effective for covering peak demands. The experience in exploitation of UGS in rock salts shows that the parametric variations during storage production are monotonous and sufficiently slow. The gas can be extracted from such storages very quickly. According to the estimations of the foreign authors, the underground hydrogen storage in such rocks costs more expensive than the cost of creation of underground hydrogen storage of the same capacity in depleted oil and gas fields, but on the other hand the operating costs when storing hydrogen in salt caverns are substantially lower.

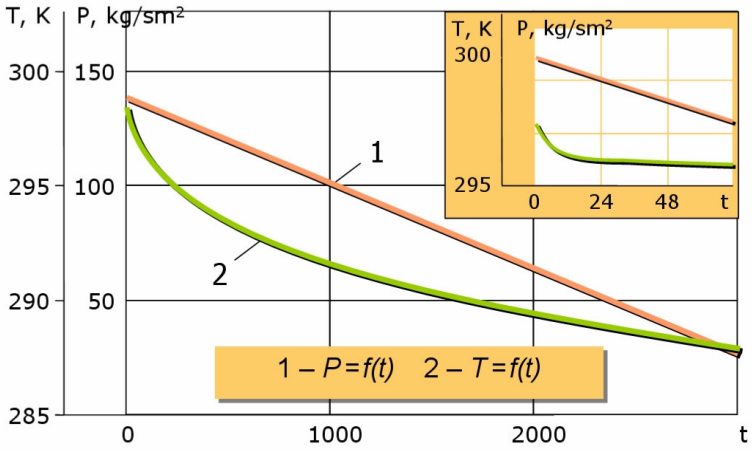

Figure 2: Hydrogen temperature and pressure variations during production from cavern.

Rock salt deposits of various shape and depth of occurrence are widely spread in Russia. According to the estimations of the specialists, the area of salt expansion reaches several tens and even hundreds of thousand square kilometers (for example, Podmoskovnoe - 50 th. km^2). Rock salt deposits can be found in Caspian Sea region, central part of Russia, on the territories of Tulskaya, Belgorodskaya and Irkutskaya regions, also at the Urals and

other parts of the country. Its storage in aquifers, natural caverns and spent mines requires very expensive preliminary researches and operations for improvement its impermeability. Due to less viscosity and density hydrogen has got greater mobility than natural gas does. Therefore hydrogen leaks through different seals or the storage cap.

4 Underground Hydrogen Storage at Yakshunovskoe Field

The geological model of Yakshunovskoe UGS is on fig.3. The red zone is gas-water contact (Fig.3). Green is for the observation wells, red is for developing well. Fig.4. shows the dependence between pressure and time for methane and hydrogen while injection and producing, calculated in Gubkin Russian State University of Oil and Gas. Geotechnological methods of cavern production through drill holes allowing to create steady caverns of given geometrical proportions and shape are developed in Russia (underground desalinization of salt cavern by water, underground explosions).

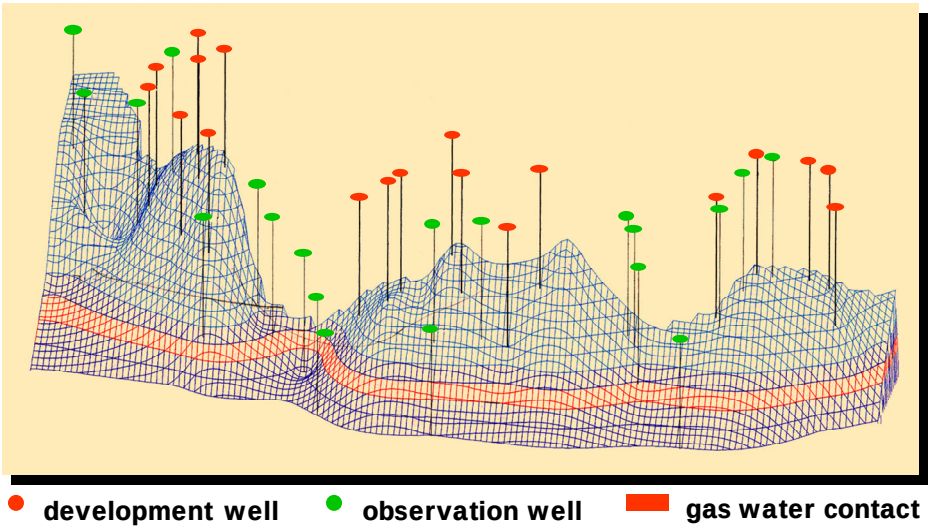

Figure 3: Jakshunovskoe UGS.

The underground desalinization technology is realized by four methods: desalinization in the bottom-up direction, desalinization in the top-down direction, combined method, cavern production without using nonsolvent. When designing the underground reservoirs in salt deposits it is very important to determine the permissible width of the cavern subject to production pressure, laying depth and its expected design shape.

5 Underground Hydrogen Storage in Salt Deposits

The permissible minimum laying depth of an underground storage $H_{\min}$ can be defined from

$$H_{\min} = \frac{p_{\max}}{\gamma_f g \rho_r} + C \qquad (1)$$

where $p_{\max}$ - maximum pressure at the shoe of the casing column, Pa; γ_f - reliability coefficient under the load, assumed equal to 0,85 in the case of lenticular salt deposits and impermeable overlying bed, and 0,75 – in other cases; ρ_r - averaged density of the rocks overlying the shoe of the casing column, kg/m^3; *C* –uncased hole length, m.

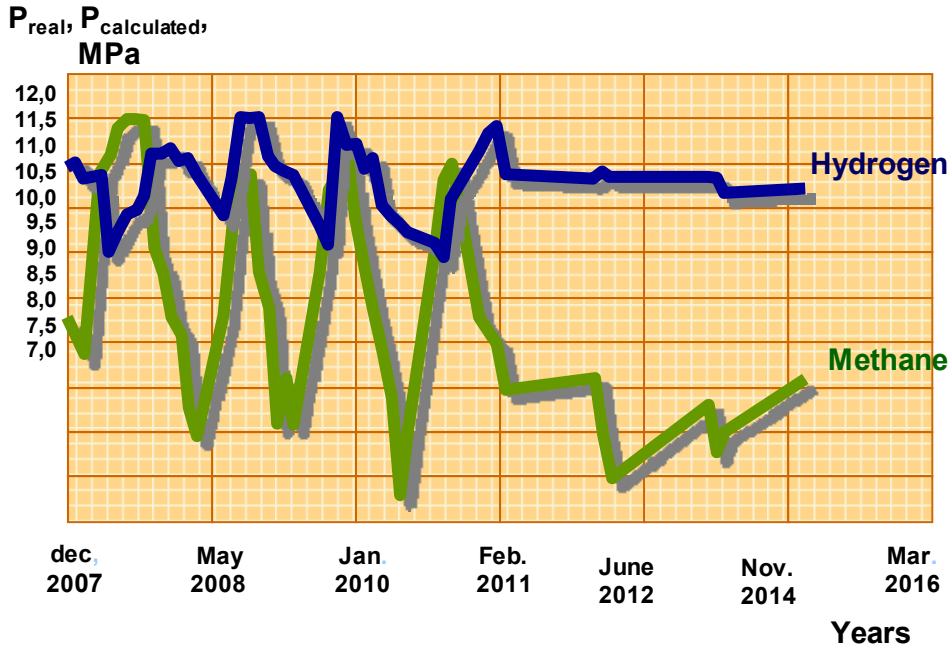

Figure 4: Recovery – injection of H_2 and CH_4 in Jakshunovskoe UGS.

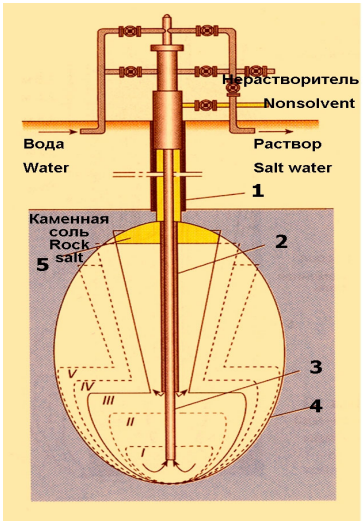

Figure 5: Combined method scheme: I-V – steps; 1 – casing column; 2 – production casing; 3 – central column; 4 – cavern production shape; 5 – nonsolvent.

$$\rho_r = \frac{\sum_{i=1}^{n} \rho_i m_i}{\sum_{i=1}^{n} m_i} \quad (2)$$

where ρ_i - formation density, kg/m^3; m_i - formation thickness, m. The permissible minimum rock salt thickness $M_{\min}$ is given by:

$$M_{\min} = H + m_1 + m_2 + C \quad (3)$$

where *H* – cavern height, m; m_1, m_2 - pillar thickness в at the cavern roof and at the cavern sole respectively, m. Minimum and maximum production pressures in the cavern in the case of the brine production scheme are defined by the height of a brine column subject to possible changes of the brine density and the hydraulic losses. The permissible maximum pressure $p_{\max}$ at the shoe of the casing column is defined from

$$p_{\max} = \rho_r g\left(H_k - C\right) \quad (4)$$

where H_k - interval from the ground surface to the cavern roof, m. The permissible minimum pressure $p_{\min}$ produced by the stored product at the cavern roof level is given by

$$p_{\min} = \rho_r g H_k - \frac{2}{\sqrt{3}} \frac{c+1}{c} \sigma_i^{\infty} \quad (5)$$

where *c* and σ_i^{∞} - parameters of the rock salt equation of state. The cavern width at the roof level *l* (m) can be derived from

$$l = \sqrt[3]{\frac{V_{adm}}{\alpha}\left(\frac{\sigma_i^{\infty}}{\rho_r g H - p_э}\right)^w} \quad (6)$$

where V_{adm} - permissible volume of the evanescent straining zone in the neighborhood of the cavern roof, m^3; $p_э$ - minimum production pressure at the cavern roof level, Pa; α, *w* – dimensionless parameters depending on height-to-width rate.

$$\tau \overline{w}_b = \sum R_i \quad (7)$$

where τ - total cavern production time, days; $\overline{w}_b$ - average linear velocity of salt dissolution by almost fresh water, m/day; $\sum R_i$ - a sum of radii of a cavern produced by fresh water, m.

$$\sum R_i = R_1 + R_2 + ... + R_n = nR_b + 0{,}5nhtg\alpha \quad (8)$$

where R_i – initial radius of each step where fresh water was used for the desalinization, m; n – number of desolution steps; h – height from the hydrocut roof (I step) to the cavern roof, m. A number of the desalinization steps in terms of the total cavern production time is represented by:

$$n = \frac{\tau\overline{\omega}_b}{R_b + 0{,}5htg\alpha} \quad (9)$$

Dissolution time is defined from the equation

$$\tau = z + 10^{-2} k_Q V \quad (10)$$

where z – constant coefficient equal to 45 days; V – underground storage design volume, m^3; k_Q - dimension factor depending on water injection capacity Q, days/m^3. The brine strength coming up to the surface when constructing the cavern is defined by

$$C = C_н - (C_н - C_0)\exp(-A) \quad (11)$$

where C – The brine strength coming up to the surface, kg/m^3; $C_н$ – limiting concentration of the saturated brine in the cavern, kg/m^3; C_0 – solvent strength, kg/m^3; A – dimensionless parameter depending on cavern production technology, size and shape of the cavern and rock salt properties. The brine extent radius in the reservoir bed around the bore-hole R (m) is given by

$$R = \sqrt{\frac{V}{\pi m_{эф} n}} \quad (12)$$

where V – injected brine volume, m^3; $m_{эф}$ - effective height of the aquifer, m; n – effective porosity. For the layer dissolution process nonsolvent layer thickness $h_н$ at the cavern roof remains constant for a single step and is assumed equal to 0,1-0,2 m. In our case the value of $q_н$ (m^3/h) is derived from

$$q_н = 2\pi r_к v_{рг} h_н \quad (13)$$

where $r_к$ - cavern radius at the place of nonsolvent-brine contact, m; $v_{рг}$ - horizontal dissolution velocity at the place of nonsolvent-brine contact, m/h.

6 Conclusions

Hydrogen can be used for different purposes. It is almost inexhaustible resource and the absence of harmful impact on the environment makes it possible to consider hydrogen as one of the most acceptable energy resources in the future. The most effective ways of hydrogen storage is its underground storage in depleted oil and gas fields, in the subterranean aquifers (by analogy with underground storing of methane and hydrocarbon liquids), underground reservoirs, salt deposits, permafrost grounds, etc. located close to its heavy consumers. Practical impermeability, ability to stand at high pressures, opportunity of quick changing technology of injection and recovery while exploiting the underground storage, chemical inertness of rock salt to the stored products make storage of gaseous hydrogen in salt rock probably most effective for covering peak demands.

References

[1] Russian R&D in Hydrogen Energy. Ministry of Education and Science of Russian Federation, Federal Agency for Science and Innovations, Moscow, 2007.

[2] Kazaryan V.A., Underground hydrocarbons storage in salt deposits, Moscow, Izhevsk: Institute of computer research, 2006. – 464 p.

[3] Bulatov G.G. Underground hydrogen storage: PhD thesis.-Moscow, 1979. –234 p.

[4] Kozlov S.I., Hydrogen energy industry. Current situation, problems and prospects. VNIIGAS, 520 p.

[5] “Science and Technics in Gas Industry”, Technical and Science Magazine, #3(35), 2008.

Experimental and Numerical Evaluation of Transient Temperature Distribution inside a Cylinder during Fast Filling for H_2 Applications

Emanuel Demaël, **Mathilde Weber**, **Philippe Renault**, Air Liquide R&D, Paris, France

1 Introduction

For practical use in near-term applications as transition and automotive markets, high pressure compressed gas storage of hydrogen remains a robust technology whose feasibility has been already demonstrated for working pressure up to 700 bar (European project Storhy for instance [1]). Safety issues are of critical importance in the context of hydrogen energy and must be clearly addressed. To guarantee the integrity of pressure vessels during successive refuelling processes in service, standards have been defined for vehicular applications which limit the gas temperature within the cylinder to 383 K and the gas pressure to 1.25 times the cylinder's design pressure.

Challenge consists in improving the efficiency of refuelling process while ensuring the safety of cylinders. In order to evaluate thermal and mechanics effects or damages on wall structure, a key issue is at first to give an accurate estimation of the temperature evolution at the surface of the interior cylinder wall and to highlight the hot spots where the temperature rises to a maximum associated with a the time of exposure.

To address this question, both experimental and numerical works may be found in the literature. To evaluate temperature distribution within the cylinder wall, a simple approach consists in coupling a single gas temperature evolution prediction and a one-dimensional conduction calculation within the wall (e.g. [2]). Such a method was also applied in Air Liquide R&D [3] and allowed to understand the influence of filling parameters such as initial conditions, targeted pressure and geometry of the cylinder as the ratio between the length and the diameter. Experimental studies using measurement devices placed inside the vessel have been also carried out, allowing evaluating the temperature in few points (e.g. [3], [4], [5]) or in a more extended region using a large matrix of sensors [6]. Two-dimensional CFD simulations with *Fluent* Software have also been also performed by the authors on a test corresponding to 350 bars for a filling duration inferior to one minute [7].

This paper proposes an accurate evaluation of transient temperature distribution within the gas during fast filling process with nitrogen gas. This experimental work has been coupled with numerical simulations on 2D and 3D geometries including the calculation of thermal conduction inside the walls.

In a first part, the experimental setup and devices are presented and main results are addressed. In a second part, the numerical settings of CFD calculations are described and first results are discussed in regard to measures.

2 Experiments

The instrumented cylinder is a 46L type 4 cylinder whose wall consists in a plastic liner (here polyethylene) and fully wrapped with a carbon-epoxy composite. The cylinder features are given Table 1.

Table 1: Cylinder characteristics (* with boss).

Working Pressure (bar)	Mass (kg)	Length* (m)	Diameter(m)	L/D ratio
200	18	1.47	0.235	6.2

To facilitate the instrumental device development, the gas used here is nitrogen and not hydrogen, which would have imposed heavier leak prevention and safety procedures, without being necessary to achieve the experiments objectives to understand the physics of fast filling. The experimental bench is composed of a nitrogen buffer at a pressure of 100 to 200 bars depending on test, a regulator, a calibrated throat, a long duct, a cylinder and a data acquisition system. The regulator decreases the pressure the buffer pressure to 100 bars. Two diameters have been considered (6 mm and 1 mm) leading to filling rates equal to 150 bar/min and 21 bars/min and corresponding to durations of around 30 s and 2 min 30s to reach a targeted pressure inside the cylinder of around 50 bars. The overall experimental bench is illustrated Fig 1 (left). The reproducibility of measures has been also investigated. Table 2 presents examples of experimental conditions for the two calibrated throat diameters.

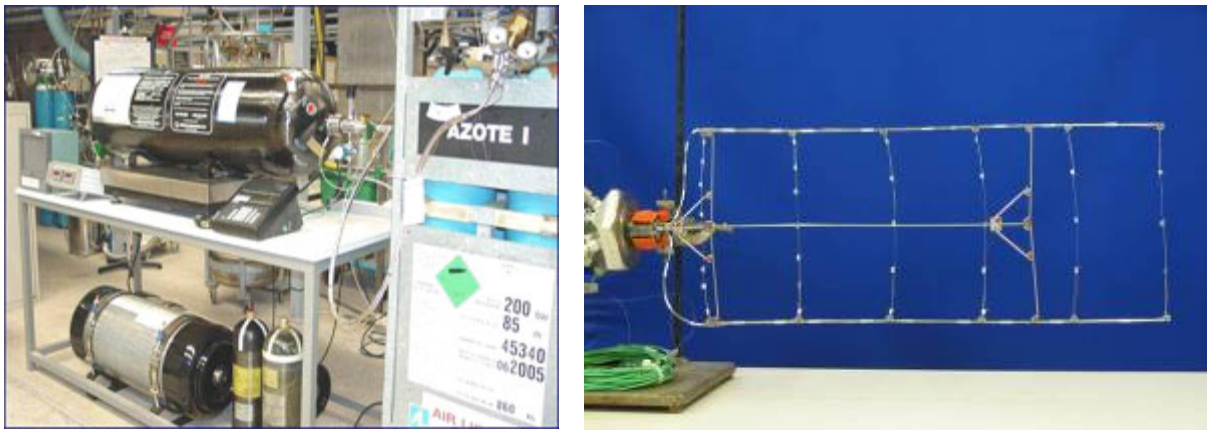

Figure 1: Experimental facilities in CRCD (left: experimental bench, right: second thermocouples matrix introduced at the bottom of the cylinder).

Table 2: Tests conditions.

Test	Throat diameter (mm)	P Buffer (barg)	P after expansion (barg)	P_i cylinder. (barg)	P_{final} (barg)	Charge duration (s)	Filling rate (bar/min)	T amb (°C)
#1	6.0	160	100	0.0	50	19.95	150	21.4
#2	1.1	185 - 190	100	0.0	50	141.40	21	22.3

Two experimental devices have been successively used to measure the temperature distribution in the vertical plane of the cylinder. These devices are composed of type K thermocouples with a diameter of 0.25 mm. The measure uncertainty is +/- 2.5 K and the time sampling during the filling is set to 50 ms. Note that on these tests, filing has been made horizontally. The large number of sensors (57) allows to accurately following the temperature evolution at any point of the interest zone. A view of the matrix #2 is given Figure 1 (right) and a schematic representation of sensors locations obtained with the two devices is given Figure 2.

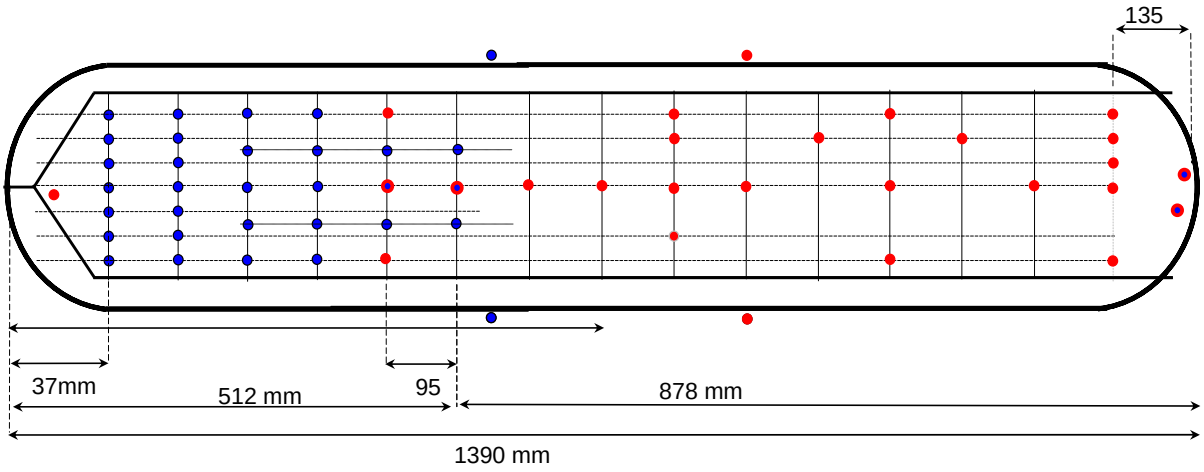

Figure 2: Matrix of sensors installed within the cylinder (in red: first device, in blue: second device, points in blue and red correspond to covering points). Note that gas entrance is placed here on the right.

2.1 Physics of fast filling

The gas entrance is depicted by a jet whose regime evolves during the filling time. Indeed, the instantaneous nozzle pressure ratio which drives the jet behaviour decreases during filling process as internal pressure increases. Therefore, an under-expanded regime is expected at the beginning and an over-expanded one at the end of the filling time. Hence, the jet characteristics (length, velocity and turbulence level) are directly correlated to the filling rate for which corresponds a given filling duration. Note that the jet confinement in the vessel leads to recirculation zones all around the jet. Moreover, depending on the jet and cylinder lengths, a flow zone characterized by very low Reynolds numbers may extend from the end of jet zone to the cylinder bottom. This zone may be seen as a stagnation zone where buoyancy effects may initiate free convection mechanism.

2.2 Experimental results and discussion

Figure 3 depicts the temperature evolution during filling for the sensors located along the jet direction. It shows clearly two distinct transient regimes. In a first zone going from the gas entrance to approximately a distance of x / L = 2/3 (corresponding to sensor #105), the temperature at any location increases continuously during time and reaches a maximum at the end of time filling. This observation is in accordance with measures from the literature

[3, 4, 5, 6] and calculations obtained with zero-dimensional models [2, 3] and also three-dimensional calculations [7].

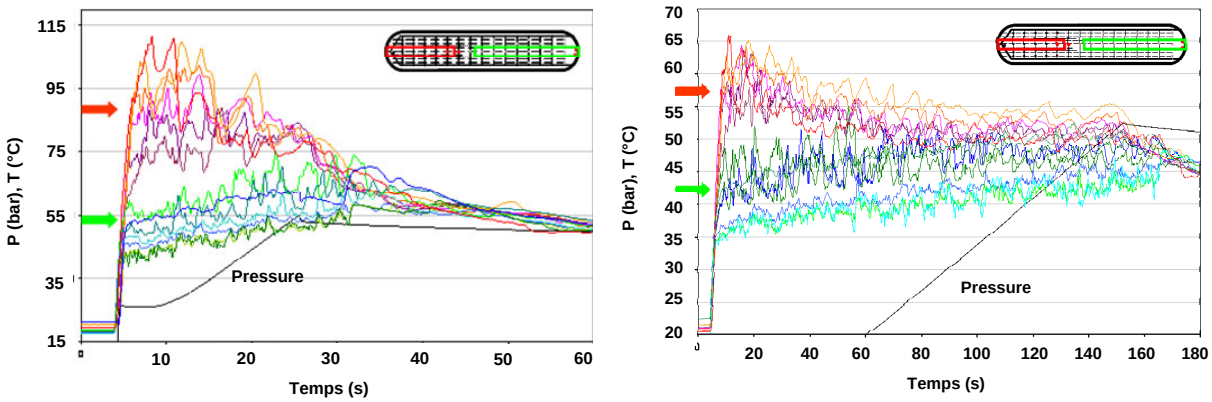

Figure 3: Temperature evolution along the cylinder centreline during fast filling (left: for a filling rate of 150 bar / min ; right: for a filling rate of 21 bar / min).

In a second zone located at the cylinder bottom, the maximum temperature at each position is observed very quickly (before 5 s for a filling rate of 150 bar/min and before 20 s for 21 bar/min) and one can observe a constant cooling thereafter to recover a quasi homogeneous temperature at the end of filling period.

Moreover, a longitudinal temperature gradient is also clearly highlighted. This gradient is not constant along the longitudinal distance: the smaller gradient is observed within the jet and the greater at a distance between the two zones previously mentioned (i.e. at a distance such as x / L is around 2/3).

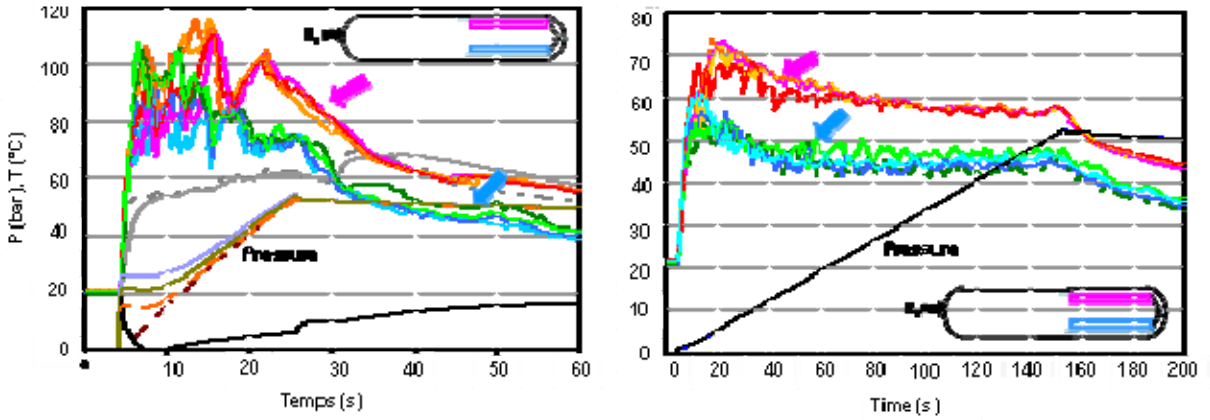

Figure 4: Temperature evolution at sensors located along the wall, in red on the left-figure (left: for a filling rate of 150 bar / min ; right: for a filling rate of 21 bar / min).

Figure 4 shows the temperature evolution on sensors located on two longitudinal lines at a same radial distance from the centreline but one at the top of the cylinder and the second below. All these sensors belong to the second region where higher temperatures are reached. Stratification in the transverse direction appears clearly with a constant difference of

15°C between the two levels for the lowest filling rate. This observation suggests that transient free convection mechanism appears in that region.

3 CFD Numerical Simulations

3.1 Numerical setup

CFD (Computational Fluid Dynamics) simulations have been carried out to reproduce the test #1 (150 bar / min). Both 2D axi-symmetric and 3D geometry for the half-cylinder have been handled (Figure 5). The mesh for the 2D geometry contains 20000 hexahedrons control volumes. This mesh is suitable to reproduce the expanded jet inside the cylinder and to predict the temperature evolution in the first part of the cylinder where buoyancy effects are negligible. The 3D mesh contains 1 million control volumes. The compressible pressure-based solver is used with a realizable k-ε turbulence closure model. For time discretization, implicit formulation is used with an optimized time-stepping strategy to reduce the computational time without impairing the solution's accuracy. The walls are taken into account and thermal conduction is resolved inside. Usual thermal exchange coefficients are defined for outside natural convection with air whereas coupled heat exchanges are handled by the solver inside the vessel. At inlet condition, a total pressure ramp is imposed according to experimental measures.

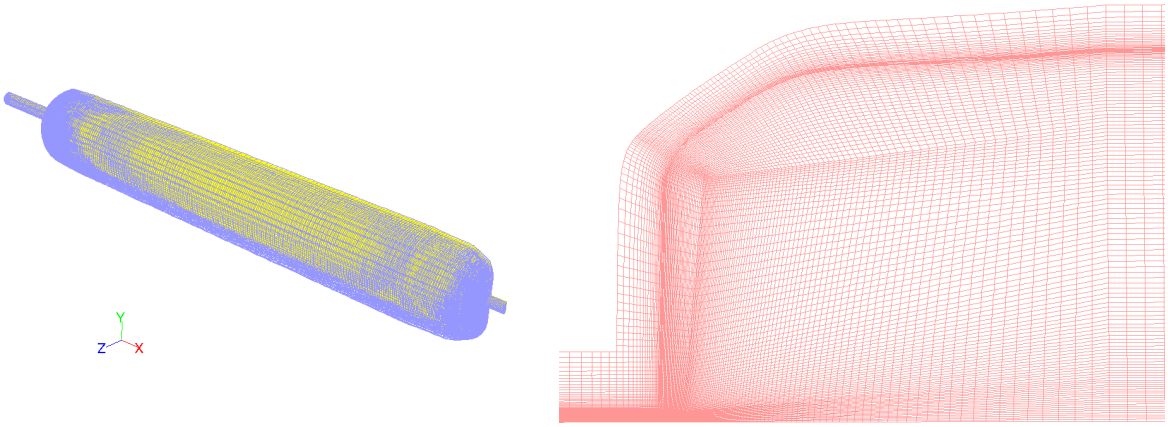

Figure 5: Mesh visualization for the 3D geometry (left) and zoom on near-field jet region (right) in a cut plane.

3.2 Main results

For 2D simulations, typical flow patterns are well reproduced with the development of an under-expanded jet extending to half the cylinder length surrounded by recirculation zones. The predicted temperatures inside the jet and more downstream are in relative good agreement with measures collected on matrix #1. An example is given Figure 6. However, comparisons made more downstream for the matrix #2 (note shown here) confirm that a simple 2D axi-symmetric approach is inappropriate to reproduce the thermal effects at the cylinder bottom. Indeed, neglecting free convection phenomena leads to a significant

overestimation of temperature rise in that region and including buoyancy effects in 3D simulations should improve the results in future work.

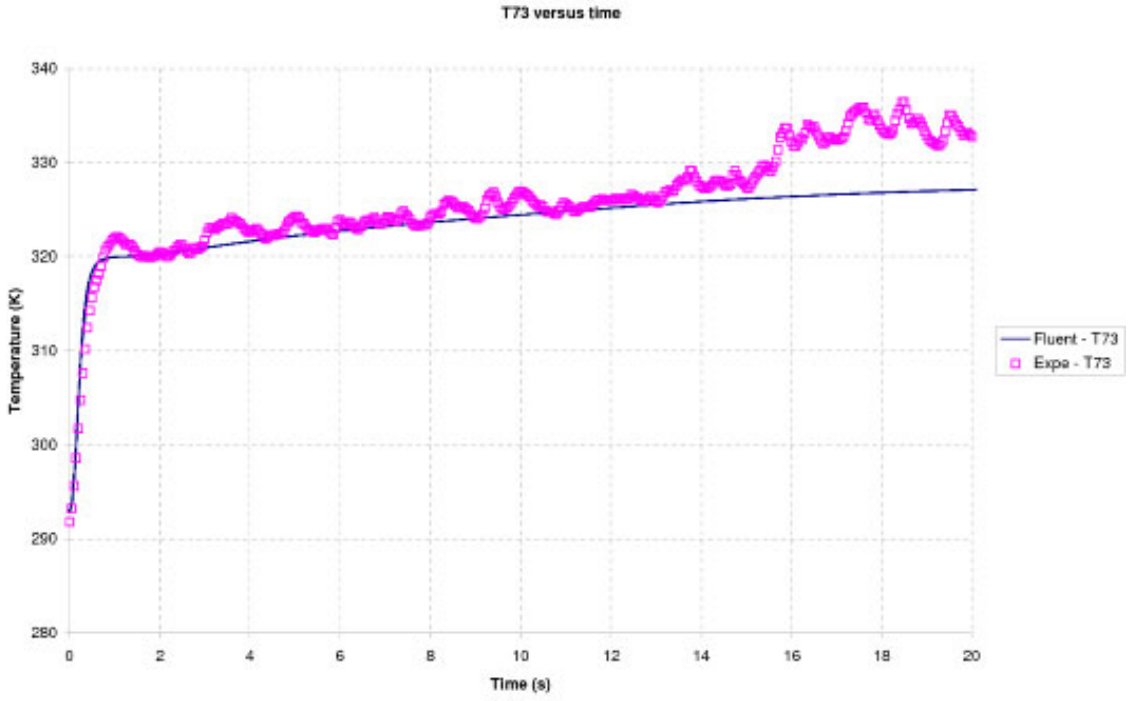

a)

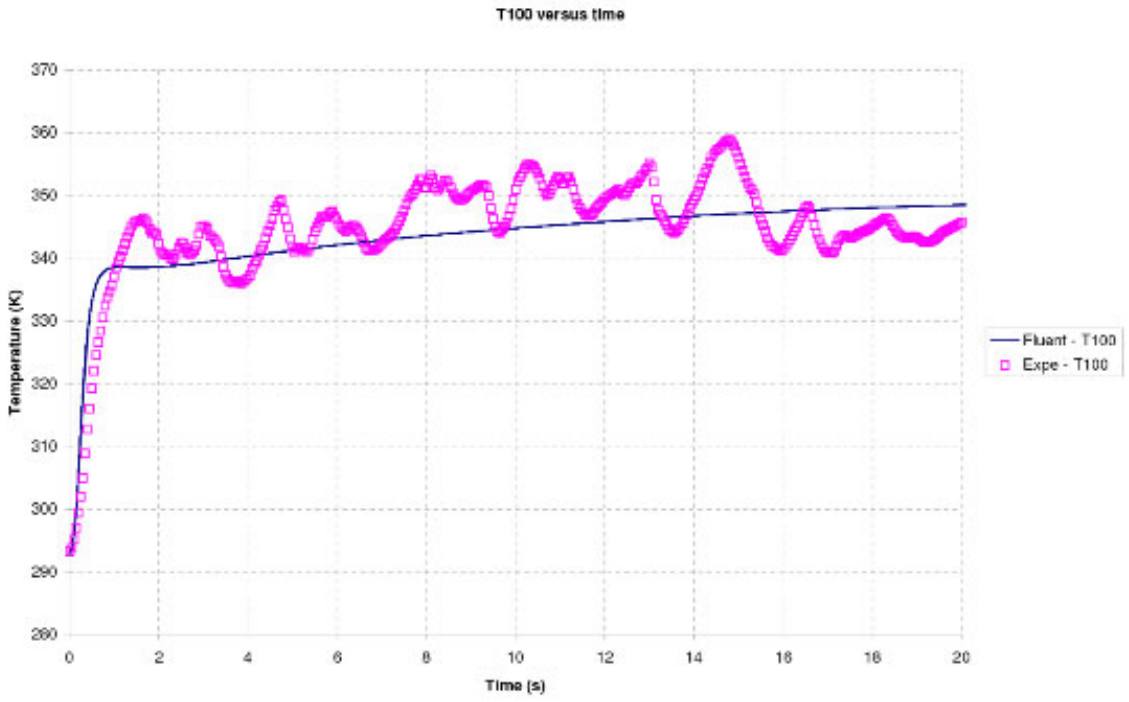

b)

Figure 6: Temperature evolution during filling up to 20 s at sensors #73 (a) and sensor #110 (b) for a filling rate of 150 bar/min.

4 Conclusions

This paper presents a large part of ongoing work at AIR LIQUIDE R&D on the understanding and evaluation of transient temperature distribution during filling process of high pressure gas cylinders and for two filling rates. The originality of the study consists in the geometric features of cylinder whose large scale ratio leads to the establishment of a secondary zone at the bottom of the cylinder in which free convection mechanism appears, even for very fast filling process. This zone is the place of a significant temperature rise up to about 100°C during a few seconds. The numerical study performed with Fluent CFD tool for a 2D axi-symmetric problem gives a relatively good agreement with measures for the prediction of transient temperature distribution in a first part of the cylinder where buoyancy effects remain negligible. Challenges ahead are to perform 3D simulations to understand natural convection establishment and better predict the temperature distribution at the bottom of the cylinder. Furthermore, and once the gas phase behaviour simulation would be considered validated against experimental work, it will be part of future work to extend the focus of the numerical study to the prediction of transient thermo-mechanical cycles in the cylinder structural shell.

References

[1] S. Colom, M. Weber and F. Barbier, 'Storhy: A European development of composite vessels for 70MPa Hydrogen storage', *World Hydrogen Energy Conference*, Brisbane (2008)

[2] M-T-I. Khan, M. Monde and T. Setoguchi, 'Hydrogen gas filling into an actual tank at high pressure and optimization of its thermal characteristics', *Journal of Thermal Science*, 18 (2009), 235-240.

[3] E. Werlen, P. Pisot, K. Barral and P. Renault, 'Thermal effects related to H2 fast filling in high pressure vessels depending on vessels types and filling procedures: modelling, trials and studies', *European Energy Conference*, September 2003.

[4] Y.L. Liu, Y.Z. Zhao, L. Zhao, X. Li, H.G. Chen, L.F. Zhang, H. Zhao, R.H. Sheng, T. Xie, D.H. Hu and J.Y Zheng: 'Experimental studies on temperature rise within a hydrogen cylinder during refuelling', *International Journal of Hydrogen Energy, to be published.*

[5] S.H. Lee, Y.G. Kim, S.C. Kim and K.B. Yoon, 'Temperature change of a type IV cylinder during hydrogen fueling process', Proceeding of *The 3rd International Conference on Hydrogen Safety,* Ajaccio (2009)

[6] C.J.B Dicken and W. Mérida, ''Measured effects of filling time and initial mass on the temperature distribution within a hydrogen cylinder during refuelling', *Journal of Power Sources,* 165 (2007), 324-336.

[7] C.J.B Dicken and W. Mérida 'Modeling the transient temperature distribution within a hydrogen cylinder during refuelling', *Numerical Heat Transfer Part A,* 53 (2008), 685-708.

Rapid Reaction Valve – New System for Flow Control

Jiri Vondricka, GSR Ventiltechnik, Im Meisenfeld 1, Vlotho, Germany
Dietmar Neuhaus, DLR, Linder Höhe, Cologne, Germany

1 Introduction

In the DLR (Deutsches Zentrum für Luft- und Raumfahrt – German Aerospace Centre) a fast reacting valve for gases and liquids has been developed with promising properties for aviation and space flight applications [1]. The valve company GSR is further developing new design options of the Rapid Reaction Valve (RRV®) for industrial applications.

2 Operating Principle

The special of the valve is its operating principle. The valve is constructed in a manner, that the plug of the valve, here a valve ball, is pressed into the valve seat only by a pressure difference between the valve input and the valve output. The valve is opened by rolling the valve ball from the valve seat. The closing process is caused by the streaming of gas or liquid through the valve, which carries forward the valve ball and move it back to the valve seat.

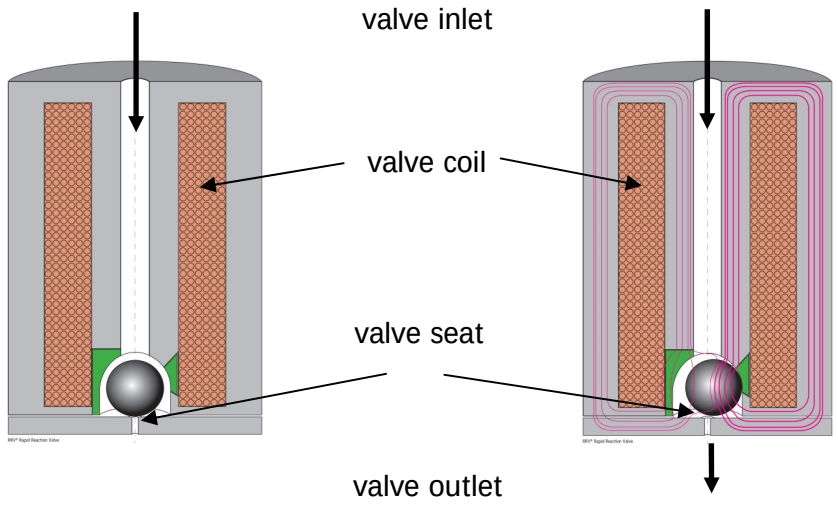

Figure 1: Schematic drawing of a RRV®. The shape of a magnetic field line is shown.

In Figure 1 the principle set up of a RRV® in a schematic drawing is shown. The valve ball is lying on the valve seat and is kept to the seats only by the pressure difference between the valve input and the valve output. (Figure 1a)

The valve is opened by rolling the valve ball from the valve seat due to the interaction with a magnetic field which, related to the axis of the valve, lateral effects the valve ball. Therefore

the valve ball must be magnetizable. (Figure 1b) In the RRV® the valve ball is the only moveable part. The rapid reacting magnetic valves can be designed to have one or several valve balls. In this paper valve with one valve ball is described.

Using the leverage effect, the valve ball is pulled from the valve seat very efficiently. The lever arm reaches from the middle of the valve ball to a contact point of the valve ball on the valve seat. By the lever action the valve ball can be moved from the valve seat by a small effort, in comparison with the effort necessary to lift up the ball upwards from the valve seat. The magnetic field acting lateral on the valve ball is caused by a coil surrounding the valve. The flux is guided in a magnetic circuit made of magnetizable materials which shows a gap made of a non magnetizable material on the same level as the middle of the valve ball. The non magnetizable material guides the magnetic flux through the magnetizable ball and creates force acting on the valve ball. To close the valve, the valve ball has to be reliably carried back to the valve seat by the streaming, which is achieved by limiting the free space where the valve ball can be moved, which keeps it close to its respective valve seat, in areas with high streaming velocities.

The streaming of gaseous or liquid media transports the valve ball back to the valve seat. With high viscose media friction forces are the dominant forces acting on the ball. In case of low viscose media high streaming velocities next to the ball, close by the valve seat, generate pressure differences which moves the ball. The liquid media can be cryogenic liquefied gases like liquid oxygen or liquid hydrogen.

3 Valve Design and Futures

The magnetic force acting on the valve ball is calculated from the magnetic force density:

$$\vec{f} = -\left(\vec{H}\right)^2 .grad\mu$$

$$\vec{H} \rightarrow \text{magnetic auxiliary field strength}$$

$$\mu \rightarrow \text{magnetic permeability}$$

Based on the formula of the magnetic force becomes clear, a small gap width between the valve ball and the inside wall is required to reach high magnetic auxiliary field strength $\vec{H}$ with a given current through the coil. The calculated distribution of the absolute value of the magnetic field strength in the magnetic circuit of the rapid reacting valve is shown in Figure 2.

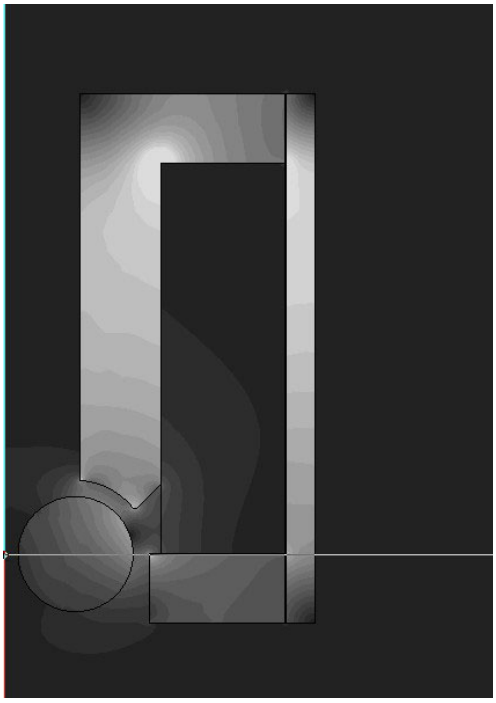

Figure 2: Model of the magnetic circuit of the RRV®. The qualitative distribution of the value of the magnetic field B was calculated and shown as grey levels. The lighter the grey level the stronger the magnetic field strength.

The pressure difference between the valve input and the valve output, the diameter of the valve seat and the diameter of the valve ball determines the force necessary to roll the valve ball from the valve seat. In Figure 3, related to the rapid reacting magnetic valve type 250 the minimum necessary electrical power input of the magnet coil, to open the valve, is shown as function of the pressure difference. A linear relation between the pressure difference and the power consumption is visible, in agreement with the mentioned formula of the magnetic force density. The value of the auxiliary magnetic field strength is proportional to the square root of the electrical power consumption of the magnet coil, and therefore the magnetic force density proportional to the electrical power consumption. The simple relation between the pressure difference and the minimum necessary electrical power to open the valve can be used to measure pressure differences with the rapid reacting magnetic valve.

With the assumption, that, related to Figure 1, the mentioned gap in the magnetic circuit of the valve is not changed, a doubling of the length of the magnetic coil halves the necessary electrical power consumption to open the valve. This is a result of the fact that a doubling of the length of the magnet coil halves the necessary current intensity through the magnet coil, the ohmic resistance doubles and due to the fact that the electrical power is proportional to the square of the current intensity the necessary electrical power halves.

This consideration is true if the magnetic permeability of the magnetizable material in the magnetic circuit is very high if compared with the non magnetizable material and the magnetic stray losses can be neglected. Therefore there is a connection between the minimum electrical power to open the valve and the dimension of the valve, which has to be

considered in the construction of rapid reacting magnetic valves for aviation and space flight applications.

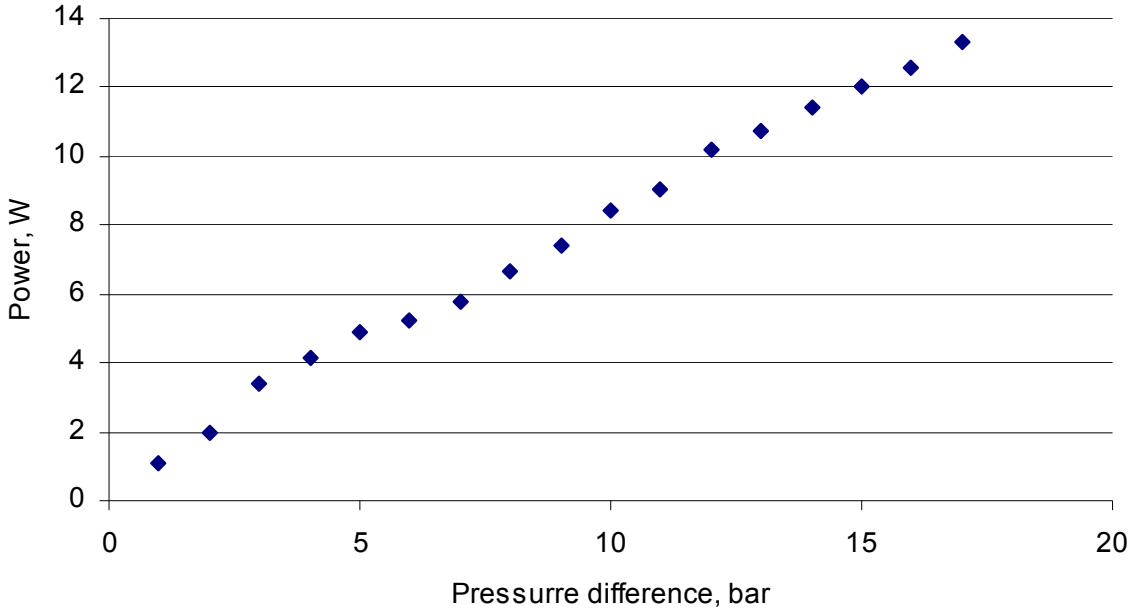

Figure 3: Relation of the minimum necessary electrical power to open the RRV® 250 as function of the pressure difference.

A compact and therefore also light magnetic valve has higher electrical power consumption.

With the rapid reacting magnetic valve gas pulses (nitrogen) were generated and measured with a hot wire anemometer, to investigate the switching properties of the valve. The wire of the hot wire anemometer was connected to a constant current source and the resistance changes of the wire, a consequence of temperature changes due to the streaming, measured. In Figure 4 a result of these measurements is shown. The magnet coil was driven by a rectangular voltage pulse marked with S: frequency 500 Hz, duty cycle 40%. Marked with H, the voltage drop over the hot wire as function of the time is shown. It becomes clear from Figure 4, that the rapid reacting magnetic valves does not opens simultaneously with the increase of the voltage S, a time delay of approximately 2.5 [ms] was observed.

The time delay is a consequence of the inductivity of the coil, which delays the current increase in the coil and therefore also the magnetic field generation, which can clearly be shortened by an as low as possible inductivity of the coil and an increased starting voltage. The valve closes immediately with the switch down of the voltage supply of the coil, here only a small time delay (<1 ms) can be observed. With the RRV® , gas pulses with frequency up to 1000 Hz were generated in the laboratory.

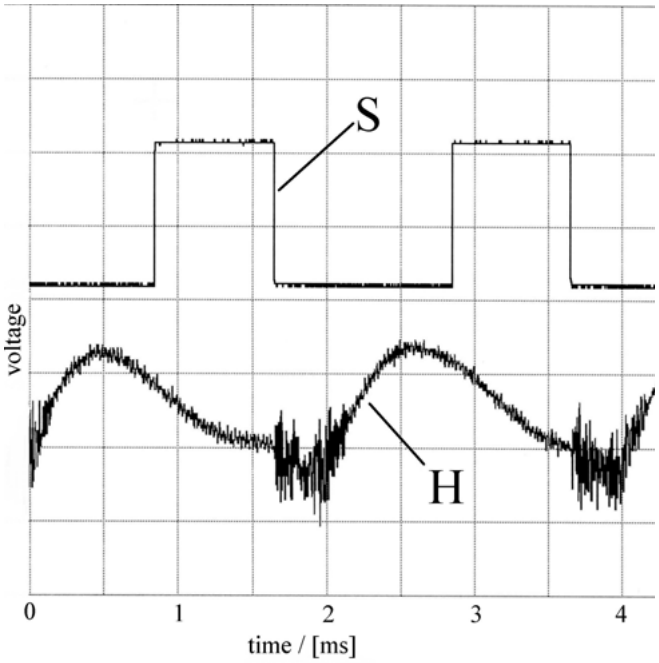

Figure 4: Switching properties of a RRV® The voltage on the magnet coil S and the voltage measured on the hot wire H is shown as function of the time. Switching frequency: 500 Hz, duty cycle: 40%.

4 Conclusion

Modern designs of gas turbines burning chambers [2] are driven, if possible, with a meagre fuel/ air mixture in the primary zone of the combustion to reduce the emission of pollutants; this applies for the aviation gas turbine as well as for the stationary gas turbine. The meagre and even more the meagre premixed burning in a combustion chamber are susceptible for burning vibrations. We can observe therefore, on the manufacturer side of gas turbines, a tremendous interest in devices and techniques to damp these vibrations. However the fast response of the RRV®, the “clean” internal design and a high life time makes the valve appropriate not only for the aerospace applications. Fast response and appropriate dosing is required in industrial and other research applications as well. For example the University of Bonn, Germany uses the valve for dosing and injection of pesticides [5,6] on the field sprayer, the research center in Jülich, Germany uses the valve for injection of fuels in the kerosene reformer for hydrogen production [3,4] and the company Materflex BZ is for almost two years successfully testing the valve for dosing of hydrogen in the fuel cell. Other applications where further tested in the pharmaceutical, food and engineering industry. Here the Rapid Reaction Valve developed by DLR and GSR can make a contribution.

References

[1] Neuhaus, D. (2000) Magnetisch betätigbares Ventil (Electromagnetic valve), European Patent: EP 1 052 441.

[2] L. Neuhaus L., Schulz J. , Neise W., Möser M. (2003) Active control of aerodynamic performance and noise of axial turbomachines. Proc. Instn. Mech. Engrs. Journal of Engineering for Power Vol 217 Part A:375-383.

[3] Pasel, J.; Meißner, J.; Porš, Z.; Samsun, R.C.; Tschauder, A.; Peters, R. (2007) Int. J. Hydrogen Energy 32, 4847. Germany.

[4] Peters, R., Eds. Ertl, G., Knözinger, H., Schüth, F., Weitkamp, J (2008) Fuel Processors in Handbook of Heterogeneous Catalysis. Wiley-VCH Verlag. Weinheim. Germany.

[5] Vondricka, J. and Schulze Lammers, P. (2009) Measurement of Mixture Homogeneity in Direct Injection Systems. Transactions of the ASABE, Vol. 52(1):61-66. USA.

[6] Vondricka, J. and Schulze Lammers, P. (2009) Real-time Controlled direct Injection System for Precision Farming. Precision Farming. Elsevier. United Kingdom.

Metal Hydrides

Etsuo Akiba

Abstract

The concept of hydrogen storage materials was proposed in late 1960's. Mg-based Mg_2Cu and Mg_2Ni are the first examples and $LaNi_5$ that works at room temperature was followed. In these early days, hydrogen storage materials are interstitial hydrides or hydrides of intermetallic compounds. Investigations on interstitial hydrides, a plenty of experimental results and empirical rules based on experiments have been reported. At the first part of this review, these achievements were briefly introduced because they are extremely suggestive for the research on non-interstitial hydrides as well as interstitial hydrides. In the later part, recent progress on interstitial hydrides and Mg based hydrides and their applications were briefly reviewed.

Design of a Metal Hydride

Lorenzo Castrillo, **Leire Romero**, **Marcos Rupérez**, **Luis Correas**, Aragon Hydrogen Foundation, Spain

1 Introduction

Metal hydrides hydrogen storage tanks are chemical reactions based systems that enable the storage of hydrogen. The equation (1) notes the heterogeneous characteristic of the process.

$$M(s)+H_2(g)\leftrightarrow MH_x(s) \quad (1)$$

The process is based on a chemical equilibrium influenced by the reaction materials and the container design factors. The factors that influence the reaction are thermodynamic, kinetic, containers design and materials.

2 Thermodynamics

The most important thermodynamic parameters are presented in van't Hoff equation(2) [1-4]

$$Ln P_{eq} = \frac{\Delta S_f^o}{R} - \frac{\left|\Delta H_f^o\right|}{RT} \quad (2)$$

Where P_{eq} is the pressure in the region of equilibrium between phases α - β, R is the ideal gas constant, ΔH_f^o is the standard variation of enthalpy of formation in the region of phase equilibrium and ΔS_f^o is the standard variation of entropy in the process of formation and temperature expressed as T.

The values of ΔH_f^o are employed to identify the amount of energy generated or consumed. Allowing the design of the heat management systems. The equations (3) and (4) calculates the heat generated or absorbed by the system, and the heat flow in unit time.

$$Q = m \cdot \Delta H \quad (3)$$

$$\dot{Q} = \dot{m} \cdot \Delta H \quad (4)$$

As seen on the equation(1), the process is reversible. Theoretically both processes behave similar, but in real cases both processes behave different way by effect of the hysteresis. This results in two van't Hoff plots, one for the absorption process and one for the desorption process, as shown in Figure 1.

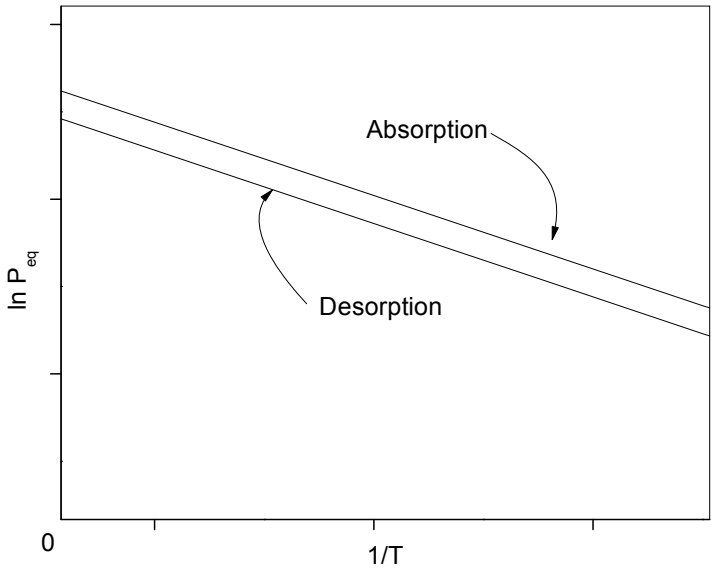

Figure 1: Van't Hoff plots for the reversible process.

Hysteresis affects temperature, pressure and composition values. Kinetics can be also affected by hysteresis, but its influence is lower in this case.

The most important thermodynamic variable to design a storage system is the enthalpy of the process, which is obtained from the slope of the equation (2). Considering an hysteresis process there are two solutions the first one is to select the highest value of enthalpy and the second one is to select one enthalpy value for charge and other one for discharge to calculate an optimal heat exchanger.

3 Kinetics

The hydrogen supply processes are influenced by the kinetic factors and dead volumes in the systems [5].

The dead volume resulting from porosity. So during the release and filling processes (transitory processes) the system may behave as pressurized storage systems.

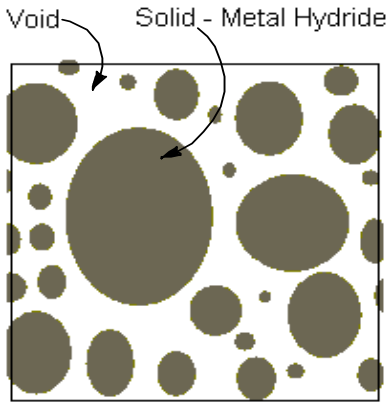

Figure 2: Porosity of the medium.

In Figure 2 there is a representation of the interior of the solid porous material. The porosity is at a value of ε = 0.5. It means that half of the container volume is dead volume.

Once steady state is reached, the hydrogen absorption rate is determined by the kinetics of the process. Thus the selection of the total dead volume of the system allow the design the initial flow capabilities of the system. Depending on the required initial flow, the amount of dead volume increase or decrease. Systems internal hydrogen combustion engines require high volumes in short periods of time so that dead space has to be greater.

This transitory flow present the stationary conditions of metal hydrides (before starting discharge). This is because the system was in equilibrium with the hydrogen storage alloy. This pressure is the maximum hydrogen supply pressure. The maximum pressure is just reached in case the metal hydride was in equilibrium before discharge. In case there isn't sufficient time to reach equilibrium, the system will behave dependent on kinetic process.

Although the kinetic processes affects during the entire operation of the system, in the transitory those processes are overlap with the effects of dead volumes previously mentioned. These effects, even getting significantly increase the initial values of discharge flows, do not influence the overall system behaviour.

For the determination of charge and discharge flows and rates a preliminary kinetic analysis has to be done. For this reason it's necessary to analyze the metal hydrides charging and discharging times.

The hydrides kinetic processes depend on several factors like pressure, temperature and the amount of hydrogen absorbed by the alloy (filling ratio α). The equation (5) shows the model of rate equation to obtain the adjusted formula [6-9].

$$r = \frac{d\alpha}{dt} = k \cdot f(P) \cdot h(\alpha) \tag{5}$$

Where k is:

$$k = A \cdot e^{\left(\frac{-E_a}{R \cdot T}\right)} \tag{6}$$

Therefore two functions have to be determined to obtain the optimal model, f (P) and h (α).

Once the model is determined, the hydrogen flows and the heat fluxes can be predicted through the equations (4) and (5).

4 Heat Exchange

Another factor that has high influence in the design of the tanks is the heat exchange process. As seen, the system temperature is an important variable for the kinetic (equation (6)) and for the thermodynamics of the process. Therefore it requires a thermal management of the system flows.

Thermodynamically, the charging and discharging of metal hydrides are exothermic and endothermic processes respectively. So that heat management is important for the deposits

optimal operation. This requires knowledge of the physical characteristics of the deposit to design an optimized canister.

As a first step to managing the heat exchange is necessary to determine the global heat transfer coefficients of the porous media. Thus the hydrogen storage medium presents different thermal characteristics for the gas phase than for the solid phase.

There are different ways to calculate the parameters of the bed. The effective thermal conductivity of the substrate can be calculated with the equation (7) [10].

$$K_{eff} = K_{H_2}\left(1-\sqrt{1-\Psi}\right)\cdot\frac{1}{\Psi-1+\frac{1}{K_{H_2}}}+\sqrt{1-\Psi}\cdot\left[\varphi\cdot K_p + K_{pgp}\cdot(1-\varphi)\right] \quad (7)$$

Where K_{H_2} is the thermal conductivity of hydrogen, Ψ is the porosity factor, φ contact materials factor, K_p is the thermal conductivity of the particles, K_{pgp} factor is the thermal conductivity of the particle gas particle interface.

Although there are less accuracy equations that allow obtaining values more quickly and simpler, one example of this equation is the equation (8). These equations do not take into account the contact factors and consider the porous medium as a homogeneous system of two components, the gas phase and solid phase [11].

$$\lambda_e = \varepsilon\lambda_g + (1-\varepsilon)\lambda_s \quad (8)$$

The systems have thermal conductivity values around 1W·m $^{-1}$·K^{-1}.For these reason it is necessary to increase the heat transfer capabilities, there is some know solutions for this problem. For example copper fins and metal sponges, increase the values of the bed thermal conductivity up to 2 - 9W·m^{-1}·K^{-1}.

The use of these systems improves the thermal conductivity of the system and thereby improves the performance of the reservoirs. But those thermal systems add to the canister dense material that does not store hydrogen, thus it decrease the energy density; volumetric and gravimetric.

After determining the global heat transfer from the bed, it is necessary to determine the heat transfer coefficients of the whole system. For this proposal it is necessary to know the geometry of the system to use the proper equations.

In the case of a cylindrical metal hydride tank the global coefficient of heat transfer is expressed by the equation (9) [12].

$$\frac{1}{h_{global}\cdot A} = \frac{1}{h_{medium}A_e} + \frac{\ln\left(\frac{D_e}{D_i}\right)}{2\pi L\lambda_c} + \frac{e_s}{\lambda_s A_i} \quad (9)$$

Where h_{global} is the global heat transfer coefficient of the system, A the contact surface area, h_{medium} the coefficient for the external medium (usually water or air), A_e outer area of the tube contacts, and D_e, D_i of the outer and inner diameters of the tubes respectively, L total length of the tube, λ_c heat transfer coefficient of tube material and e_s thickness of the storage layer . So the determination of the total value requires knowledge of all materials involved in heat exchanges.

To facilitate the exchange of heat is common to use heat exchange systems such as the ones shown in Figure 3, where the usual heat exchanger fluid is water.

Figure 3: Heat exchange systems. Left: external Shirt. Centre: internal coil. Right: external envelope for various segments.

5 Size

Size of the metal hydride storage is the first parameter to design a canister. It represents the amount of hydrogen stored, limiting dimension and capabilities to employ a heat exchanger. For example, a canister which takes up all the space of a device could useful, or a system which needs a 5lpm and the design only give 4lpm. It is necessary to fix a several parameters, how capacities, to start a design of a deposit.

6 Materials

Polymers, alloys, metals, gases and thermal fluids can be part of a canister. It is important to know all the compatibilities.

Currently, stainless steel, aluminium, hydrogen, several alloys and different polymers conforms typical hydrogen canister. However, in a novel system, with novel materials, it is necessary to check compatibilities.

Materials employed in containment structures need to be stable with other materials in contact. Containment structures are in contact with air and thermal fluid, like other systems.

But with these systems appears news materials in contact, such as hydrogen and the proper metal hydride. It needs to be analysed to avoid accidents. In a first term, working with hydrogen can appears permeation, embrittlement, or another reaction that promote hydrogen leak and a loss of security.

Materials, such as austenitic stainless steel, copper, gold, nickel and aluminium, present lower permeation than others, such as carbon steels. This a property related to crystal lattice,

systems with low permeation have face-centered cubic structure (FCC) because this structure is more resistant to embrittlement. It means that these materials can be used to contain hydrogen gas [13,14]. And the polymers can be a novel material possibility to construct metal hydride storage like high pressure canisters.

Another material in contact is the metal hydride or its metal or alloy. If there are two or more metals in contact it can appear redox reactions. It is important to study the redox potentials before putting in contact metal hydride and canister. This redox reaction can create a region which can be fracturated by action of hydrogen gas, which is a serious risk.

7 Conclusions

To design a container there are parameters which are important to take into account.

One of the first parameter is the dimension available or the hydrogen storage. These parameters allow to get a first idea of the system characteristics.

The selection of the proper metal hydride influence on several aspects like kinetics and thermodynamics. With enthalpy and a proper kinetic model, the hydrogen and heat flow can be calculated.

It is important to note that the system has a porosity which gives properties like heat transfer coefficient, and it gives special characteristics to the hydrogen flow. To calculate the global heat transfer coefficient it is important to know the porosity, the materials involved and the geometry to select a proper equation.

And a last term, the materials employed to design the container are important in terms of security and get an optimal design.

References

[1] B. Sakintuna, F.-D. M. (2007). Metal hydride materials for solid hydrogen storage: A review. *International Journal of Hydrogen energy , 32*, 1121-1140.

[2] Züttel, A. (2004). hydrogen storage methods. *Naturwissenschaften , 91*, 157–172.

[3] Latroche, M. (2004). Structural and thermodynamic properties of metallic hydrides used for energy storage. *Journal of physics and chemistry of solids , 65*, 517-522.

[4] Tarasov, B. P., Lototskii, M. V., & Yartys, V. A. (2007). Problem of hydrogen storage and prospective uses of hydrides for hydrogen accumulation. *Russian journal of general chemistry , 77* (4), 694-711.

[5] Melnichuk M, et al., Hydrogen discharge simulation and testing of a metal-hydride container,International Journal of Hydrogen Energy (2010), doi:10.1016/j.ijhydene.2009.12.127.

[6] Dhaou, H., Askri, F., Ben Salah, M., Jemni, A., Ben Nasrallah, S., & Lamloumi, L. (2006). Measurement and modelling of kinetics of hydrogen sorption by LaNi5 and two related pseudobinary compounds. *International journal of hydrogen energy* , 576-587.

[7] Sewry, J. D., & Brown, M. E. (2002). "Model-free" kinetic analysis? *Thermochimica Acta* (390), 217-225.

[8] Soriano, D., Mazo, A., Rubio, J., Rubio, F., & Oteo, J. L. (2006). Degradación térmica de nanocomposites TEOS/resol y gamma-APS/resol. *Bol.Soc.Esp.Ceram.V. , 45* (6), 379-388.

[9] Romero Ramirez, M. M. (2004). Expresiones analíticas de los modelos cinéticos para la reduccion a temperautra programada en la ecuacion generalizada de Kissinger. *Mineria y geologia* (3-4), 78-86.

[10] Walker, G. (2008). *Solid-state hydrogen storage - Materials and chemistry.* Woodhead publishing & CRC press.

[11] Yang, F., Meng, X., Deng, J., Wang, Y., & Zhang, Z. (2008). Identifying heat and mass transfer characteristics of metal hydride reactor during adsorption-Parameter analysis and numerical study. *International journal of hydrogen energy* , 1014-1022.

[12] Green, D. W., & Perry, R. H. (2007). *Perry's chemical engineers' handbook, 8th edition.* McGraw-Hill.

[13] Rusli, R. (2008). Role of hydrogen environment induced hydrogen embrittlement of Ti-8Al-1Mo-2V alloy. *Materials science and engineering A* , 494:143-146.

[14] Dantzer, P. (2002). Properties of intermetallic compounds suitable for hydrogen storage applications. *Materials science and engineering A , 329-331*, 313-320.

Optimization of Hydrogen Uptake and Release in Automotive-scale Metal Hydride Systems

Daniel E. Dedrick, **Michael Kanouff**, **Jay Keller**, Sandia National Laboratories, CA, USA
Tyler Voskuilen, Purdue University, IN, USA

Abstract
Metal hydride systems provide a technology pathway for high energy density hydrogen storage systems for a variety of transportation, APU, and man-portable power applications. Since metal hydride based systems include highly coupled heat transfer, mass transfer, and chemical kinetics, many opportunities exist for bottlenecks in the engineered system. For example, large variations in pressure and temperature can develop in the hydride material during refueling processes that can effectively starve parts of the system of hydrogen while other parts become over heated and cease to absorb hydrogen. In order to accurately resolve the local reaction environments present, the transport of gas through the bed must be understood. Towards this end, we have developed mass transport, heat transport, and chemical kinetics models that allow us to accurately predict hydrogen refueling and release processes for metal hydride based hydrogen storage systems. We have validated these models by comparing predicted results to experimental bulk hydrogen uptake/release rates and the associated thermal response of a 1.7kg sodium alanate system. Numerical experiments using these validated models resulted in a subset of design concepts that allow for optimized hydrogen uptake and release for transportation applications.

1 Metal Hydride Based Systems

Sodium aluminum tetra-hydride ($NaAlH_4$), a complex hydride historically used as a reducing agent in chemical synthesis, was found to release and accept hydrogen reversibly in a two-step phase change process in 1997. The discovery of destabilization by titanium doping made sodium alanates ($NaAlH_4$, Na_3AlH_6) promising materials for hydrogen storage systems 0], 0]. Sodium alanates reversibly absorb and release hydrogen in a two step recombination and decomposition reaction as shown here:

$$NaH + 1/3Al + 1/2H_2 \Leftrightarrow 1/3Na_3AlH_6 \quad \text{Eq. 1}$$

$$1/3Na_3AlH_6 + 2/3Al + H_2 \Leftrightarrow NaAlH_4. \quad \text{Eq. 2}$$

Although sodium alanates do not meet the US DOE goals 03] for vehicle hydrogen storage performance, these materials provide an opportunity to understand the highly coupled processes that present design challenges for implementation of complex metal hydrides into hydrogen storage systems.

Sodium alanates have been used for up-scaled engineered system development efforts 0], 0]. Most notably, the authors designed, optimized, and demonstrated an automotive-scale hydrogen storage system capable of meeting the drive-cycle requirements of the automobile

in collaboration with General Motors 0]. This program developed key technology to enable the use of metal hydride system for applications with high rates of refueling and aggressive fuel release requirements. The completed system is shown in Figure 1. For this study, a portion of the full-scale system was utilized – a 1.7 kg cylindrical bed measuring 5 cm in diameter and 95 cm long.

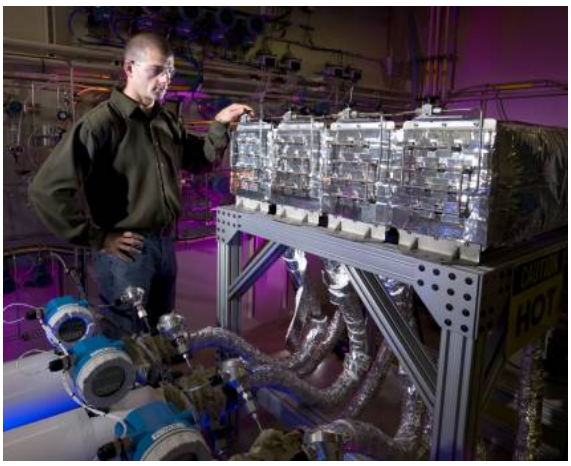

Figure 1: A full scale hydrogen storage system designed for automotive fuelling requirements.

2 Heat Transport, Mass Transport and Kinetics Relations

To facilitate the design and analysis of the up-scaled system, Sandia developed experimentally based models for heat transfer, mass transfer, and chemical kinetics 0]. These models were assembled using physically relevant mathematic expressions with empirically determined coefficients.

A chemical kinetics model was assembled from experimental measurement combined with a geometric representation of the packed particle bed. The model assumed that the equilibrium hydrogen pressures are functions only of temperature and independent of any solid species concentrations. This implies that the various alanate species do not form solid solutions, i.e., they are not intermingled at the molecular level. Reactions between species occur only at interfaces, and the rates of these surface reactions can depend only on gas or surface phase concentrations (and temperature). On the other hand, the volumetric reaction rates within an alanate bed depend on the amounts of the various solid species present, while maintaining thermodynamic consistency. The resulting expressions are outlined in the appendix of Dedrick et al 0].

Permeability was not explicitly measured during the design process of the automotive-scale hydrogen storage system. Upon testing of the full scale system, the authors identified that transport bottlenecks existed due to hydrogen flow limitations in the porous solid. The permeability properties of the compacts at various pressures and temperatures were subsequently quantified and an accurate model was produced that was appropriate for the range of flow regimes present within a hydrogen storage system for automotive applications. A variety of permeability models were investigated for the model development effort. The Young and Todd model was found to fit the requirements of the flow regimes within the

system and was used as a general permeability model. It should be noted that an Ergun expression with Knudsen number modifications would also adequately represent the flow regimes present within the system, but is less suited for modeling multidimensional flows. The Young and Todd model is as follows,

$$K = \frac{\phi}{\tau^2} d_p^2 \left[\frac{1}{32} + \frac{5}{12} Kn \right], \quad \text{Eq. 3}$$

where d_p is the pore diameter and τ is the tortuosity. Porosity is determined through sample mass and volume measurements and tortuosity is determined experimentally. While this model is limited to a characteristic pore diameter, a set of parameters were identified that were appropriate for all relevant flow regimes 0].

The effective thermal conductivity is another important property of the packed hydride material. A large conductivity is desired, which was obtained in the system under study here by using Expanded Natural Graphite (ENG) additives, bed densification, and excess aluminum as thermal conductivity enhancement strategies 0]. The resulting composite material demonstrated an order-of-magnitude improvement in heat transfer performance and was an enabling component to achieving the goals for rapid refueling. The mathematical expression for the enhanced thermal conductivity is represented by the following polynomial in the units of 10^{-2} W/cm-K:

$$k(\psi, E) = 11.7\psi^4 - 32.5\psi^3 + 33.2\psi^2 - 14.8\psi + 40E + 3.4 \quad \text{Eq. 4}$$

where ψ is the fractional hydrogen content (0-1, relative to 4.4 wt%) and E is the weight fraction of ENG flake.

The coupling of each of these models through the energy and momentum equations allows for the prediction of processes within arbitrary bed geometries and operating conditions.

3 Verification at the Application Scale

Verification of the coupled heat transfer, mass transfer, and chemical kinetics models was achieved through two methods; 1) a filling measurement that resulted in the temporally resolved quantity of hydrogen absorbed, and 2) the direct pressure drop measurement across the bed.

The figure below (Figure 2) shows the filling measurement for the hexahydride absorption process. The predicted absorption rate indicates that the bulk permeability is insufficient to resolve the total effective permeability through the bed, indicating a need for a channeling model. A channeling model consisting of 2% of the cross-sectional flow area was found to most closely represent the actual transport within the system observed in experiments [9].

As can be seen in Figure 2, application of the wall-channeling model to the filling measurements under predicts the absorption rate at first (at ~200 s) before over predicting the absorption at later times. The latter discrepancy appears to be due to an over prediction of the capacity of the hydride material, which points to a problem with our kinetics model, while the former discrepancy suggests that our model under predicts the permeability. We focus here on the model permeability issues. In contrast to Figure 2, the comparison shown

in Figure 3 suggests our model over predicts the permeability. Here, four hydride tube vessels were modified to allow hydrogen to flow into the tube on one end and out the other, where a fixed pressure drop was applied to each tube and the flow rate measured. The results show the model over predicts the hydrogen flow rate for a tube temperature of 30°C, although the agreement is better for a tube temperature of 71 °C.

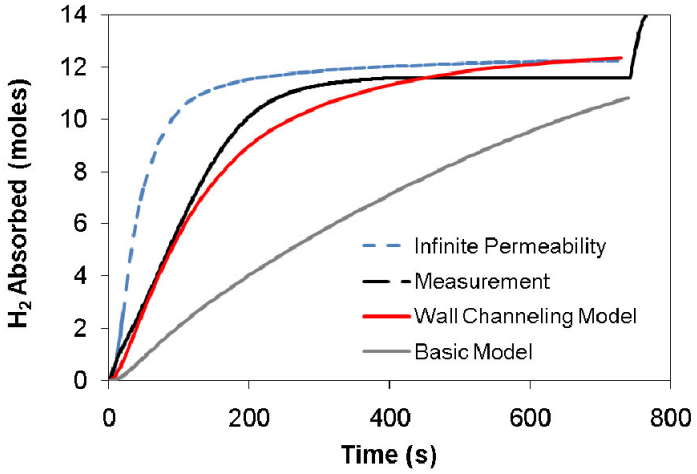

Figure 2: Verification measurements of the coupled models using the large-scale bed. Results indicate that the characteristic permeability of the bed is larger than the bulk permeability of the sodium alanate composite.

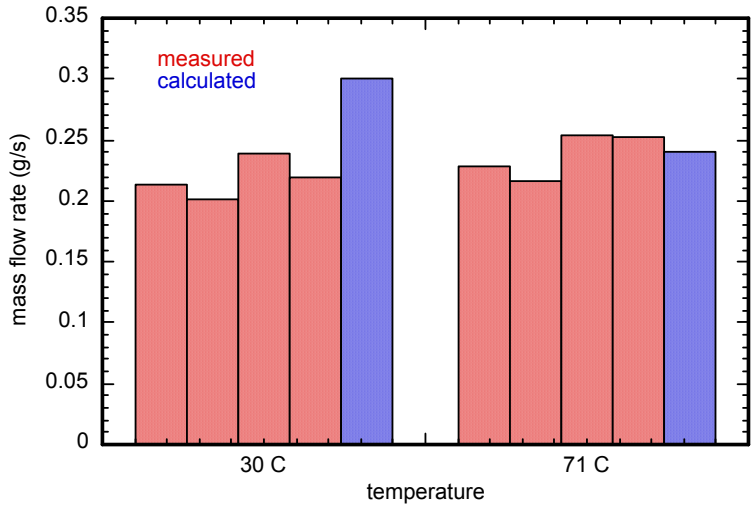

Figure 3: The comparison of measured and calculated mass flow rates for 4 individual tubes is inconsistent.

To investigate the origin of the apparent contradictions shown in Figure 2 and Figure 3 regarding the permeability used in our model, the bed was disassembled to quantify the channeling. Upon removal of the sodium alanate composite, a flow channel of ~0.127 mm was measured indicating that the material had pulled away from the wall and formed a small free flow channel. In addition, significant flow channels were observed to have formed along the near the vessel wall. These were present in the form of both discontinuous fissures and

continuous worm holes (see Figure 4). So, while a wall channel running the length of the tubes is confirmed, the channel we used in the model was too large and should be reduced in size, which would improve the agreement between model and experiment shown in Figure 3. Meanwhile, the fissures and worm holes observed after examining the hydride packed bed provide radial pathways into the material. By including these in the model it would improve the agreement shown in Figure 2 for the absorption rate, without contributing to an over prediction of the flow rate in the axial direction. The combination of these feature changes may likely explain the permeability discrepancy discussed above.

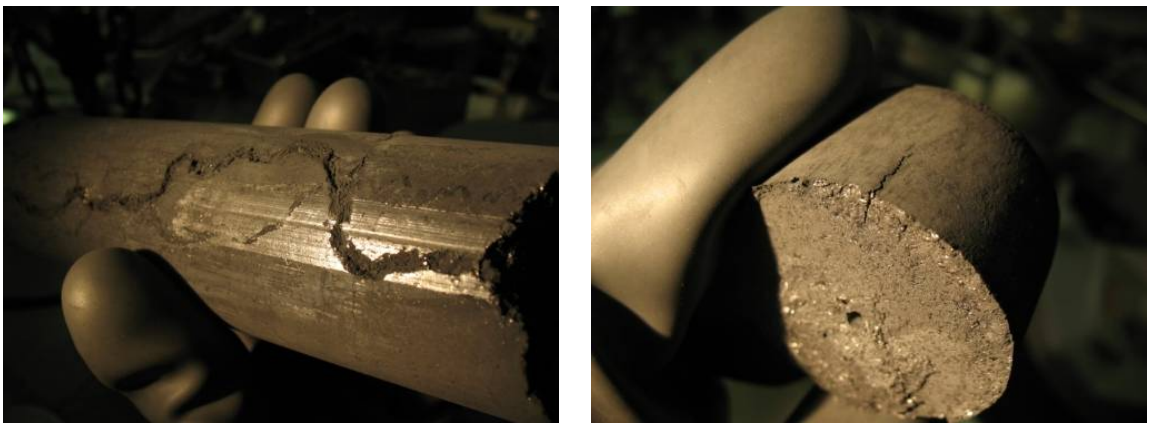

Figure 4: The presence of continuous "wormholes" were observed (left) in addition to discontinuous fissures (right).

4 Design and Optimization Concepts for Future Systems

The detailed understanding of transport within the context of the full scale system allows for the optimization of future designs. Using the models for transport, concepts were developed for the optimization of future systems.

Figure 5 shows two design concepts. The concept on the left represents a cross-section of the bed utilized for this analysis. A single frit exists at the entrance of the vessel. The figure on the right indicates a design concept for improving the permeability of the bed with an annular frit down the center of the bed along the axis.

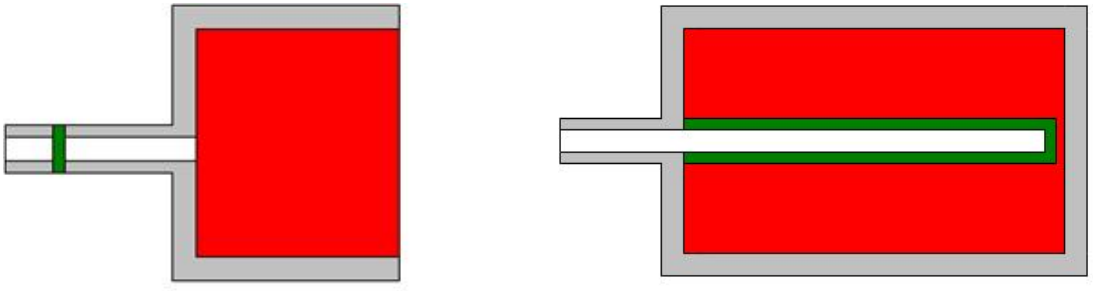

Figure 5: Two bed designs of arbitrary diameter considered for future development. The design on the left utilizes a single frit at the inlet while the design on the right integrates an annular frit along the axis of the bed.

Using the models for heat transfer, mass transfer, and chemical kinetics, the impact of this design feature can be compared on a performance basis to the baseline system. The plot below shows the relative fill speed as a function of vessel diameter. In this case, the Θ refers to the relative rate of hydrogen absorption (Fill Speed) that accounts for the coupled thermodynamics, kinetics, heat transfer, and mass transfer. Three cases are plotted; 1) the thermal-kinetic limit as realized by infinite permeability, 2) the baseline system permeability case, and 3) the axial frit case. For each of the cases, it can be seen that an optimal diameter exists near 3 cm. The fill speed reduction due to permeability is shown in green below the vertical axis and represents the margin for performance improvement with permeability enhancement. The axial frit case approaches the thermal kinetic limit and at larger diameters actually exceeds the performance of the thermal kinetic limit. This seemingly contradictory behavior is due to the added convection cooling effect that increases the effective thermal conductivity of the bed. This convection cooling effect can be exploited in future designs for further system optimization [8]. The above analysis can be performed on systems with more challenging characteristics, such as faster kinetics. These systems behave with the same overall trends; however, the optimal bed diameter is generally smaller.

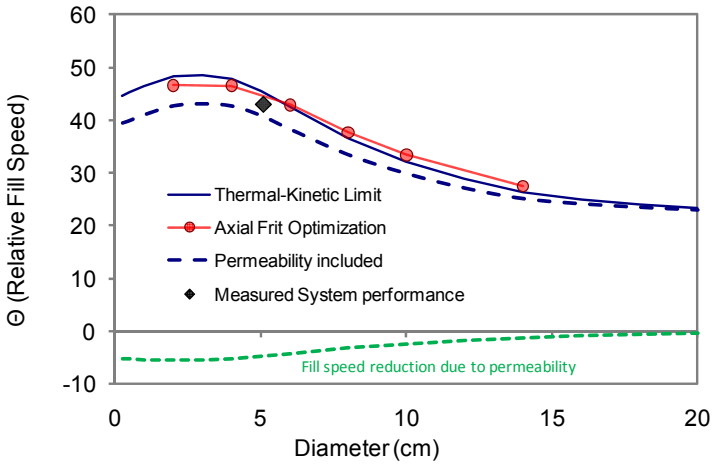

Figure 6: Characteristic fill speed as a function of bed diameter for the two different design concepts in comparison to the infinite permeability case.

5 Conclusions

A fully coupled model of heat transfer, mass transfer, and chemical kinetics has been assembled from experimental measurements for a sodium alanate-based metal hydride system. The coupled models were verified and validated at the relevant automotive scales. Although the coefficients of the individual models are specific to sodium alanates, the same principles can be applied to reactive porous systems in general. The authors utilized these models to quantify the specific transport mechanisms within the sodium alanate complex and subsequently proposed alternative designs that approach the thermo-kinetic limit of the sodium alanate based system.

Acknowledgments

This effort was completed under contract with the USDOE EERE Hydrogen Program. The full scale system was developed under contract with General Motors Research and Development. The authors are indebted to the mechanical design, electrical design and experimental expertise of Ken Stewart, George Sartor, Yon Perras, and Mark Zimmerman, Sandia is a multiprogram laboratory operated by Sandia Corporation, a Lockheed Martin Company, for the United States Department of Energy's National Nuclear Security Administration under Contract DE-AC04-94-AL85000.

References

[1] B. Bogdanovic, and M. Schwickardi, "Ti-doped alkali metal aluminium hydrides as potential novel reversible hydrogen storage materials". Journal of Alloys and Compounds, **253-254** (1997) 1

[2] Bogdanovic, B. et al. "Metal-doped sodium aluminium hydrides as potential new hydrogen storage materials" Journal of Alloys and Compounds **302** (2000), 36–58

[3] The Hydrogen, Fuel Cells & Infrastructure Technologies Program 2006 Multi-year Research Demonstration and Development Plan (MYRDDP)

[4] B. Mason, (2005, March 30). GM seeks help from Sandia Labs. The Valley Times, Vol.93, Num. 281

[5] T. A. Johnson, S. W. Jorgensen, and D. E. Dedrick, A Vehicle-Scale Sodium Alanate Hydrogen Storage Demonstration System, (in preparation for publication)

[6] D. Anton, "High Density Hydrogen Storage System Demonstration Using NaAlH4 Complex Compound Hydrides", 2004 DOE Hydrogen Program Annual Review, May 24-27, 2004 Philadelphia, PA

[7] D. Dedrick, M. Kanouff, R. Larson, T. Johnson, S. Jorgensen. "Heat and mass transport in metal hydride based hydrogen storage systems", HT2009-88231 Proceedings of HT2009 ASME Summer Heat Transfer Conference July 19-23, 2009, San Francisco, California

[8] D. Dedrick, "Chapter 4 - Solid-state hydrogen storage system design" SOLID-STATE HYDROGEN STORAGE: MATERIALS AND CHEMISTRY" Edited by G Walker, The University of Nottingham, UK, Woodhead Publishing Ltd, 2008. ISBN 1 84569 270 5, Sept 2008.

[9] T. Voskuilen, D. Dedrick, M. Kanouff, "System Level Permeability Modeling of Porous Hydrogen Storage Materials", Sandia Report, SAND2010-0254, Printed January 2010

Optimization of Heat Transfer in Metal Hydride Reactor

D.O. Dunikov, V.I. Borzenko, S.P. Malyshenko, Joint Institute for High Temperatures of Russian Academy of Sciences, Russia

Heat management is the design bottleneck in creation of efficient metal hydride systems. Inefficient heat transfer in metal hydride beds is connected with relatively low effective thermal conductivity (0.1-1 W/m K) and high reaction heat (25-70 kJ/mole H_2) of activated hydrogen storage materials, which are the fine powders with particle sizes down to 1-10 micrometers. As the result even for water cooled metal hydride reactors heat transfer coefficient from hydride bed to coolant is only about 100 - 120 W/m^{2}K (Borzenko, 2008; Kaplan, 2009) and determined mostly by poor heat transfer in the metal hydride bed.

The goal of current investigation is to find relationship between operational parameters of metal hydride accumulator (hydrogen capacity V_H, inlet/outlet pressure P_{in}, P_{out} and hydrogen flow rate g), reactor design (heat transfer area A) and properties of hydrogen storage material (PCT-diagram, heat of reaction ΔH, thermal conductivity k, heat transfer coefficient α).

Heat and mass transfer was experimentally investigated at sorption of pure hydrogen and desorption in metal hydride reactor filled with m_{MH} =4.69 kg of $Mm_{0.8}La_{0.2}Ni_{4.1}Fe_{0.8}Al_{0.1}$ alloy, ΔH_{in} = 13,1 MJ/kg H_2, ΔH_{out} = 13,5 MJ/kg H_2. The reactor consists of O-ring shaped capsules filled with MH bed, the capsules are assembled in cylindrical casing with water heat exchanger at outer wall (see Figure 1).

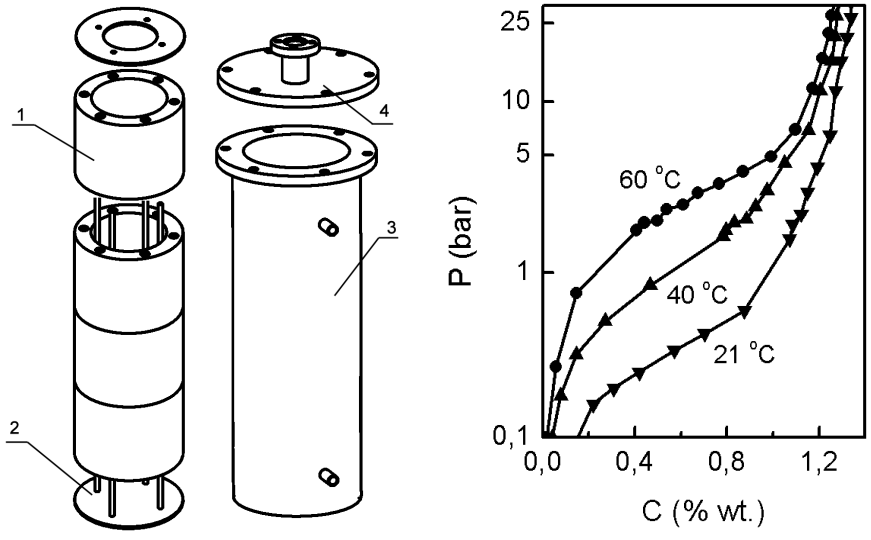

Figure 1: Reactor design (left) and desorption isotherms of alloy (right): 1 – capsule with storage material, 2 – hydride cartridge, 3 – casing with water heat exchanger, 4 – cover.

During charging and discharging of the reactor initial hydrogen flow at inlet and outlet was limited by flow regulator at different values between g_{max} = 24 (10% of maximal flow) and g_{max} = 240 st. l/min (100%) in order to measure parameters of heat and mass transfer for different operational regimes, hydrogen pressure in supply system was set to P_{in} = 9 bar for charging and discharged hydrogen was thrown into the atmosphere P_{out} = 1 bar. Hydrogen capacity of the reactor is found to be V_H = 690±5 st. l (1.33 %wt.) and charging time was t_H =18±1 min for g_{max} > 60 st. l/min.

It is found that the reactor for most of the regimes of charging and discharging cannot maintain the initial hydrogen flow rate g_{max}, and with increasing of g_{max} amount of hydrogen charged at initial flow rate decreasing significantly (Figure 2). Results for discharging are similar.

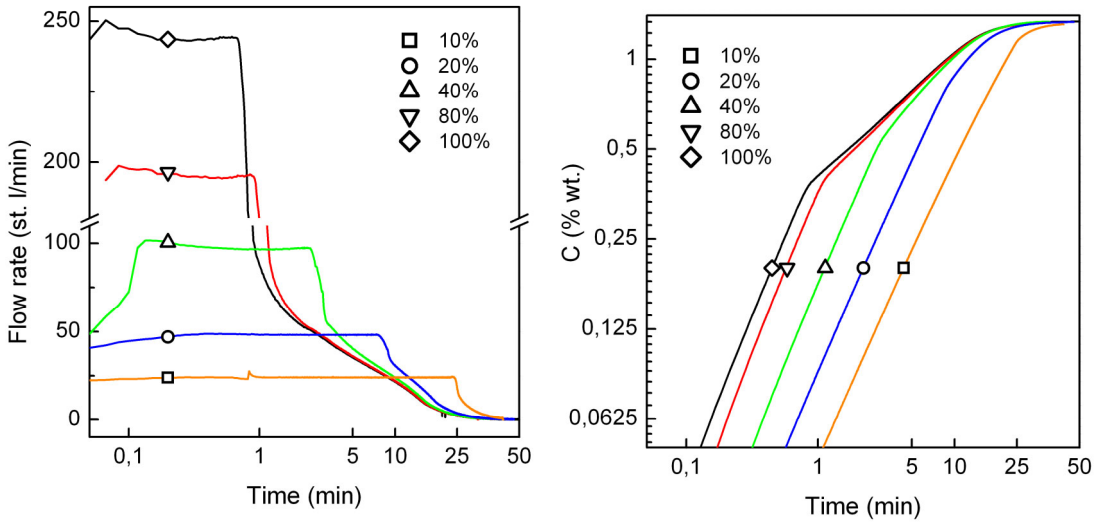

Figure 2: Hydrogen flow rate at inlet (left) and hydrogen content in MH bed (right) for different charging regimes.

We can divide the process of charging and discharging of MH reactor into three stages (Figure 3). Transition from the first to the second stage is connected with dramatic decrease of hydrogen flow rate at reactor inlet – and we can call this crisis of heat and mass transfer in MH reactor.

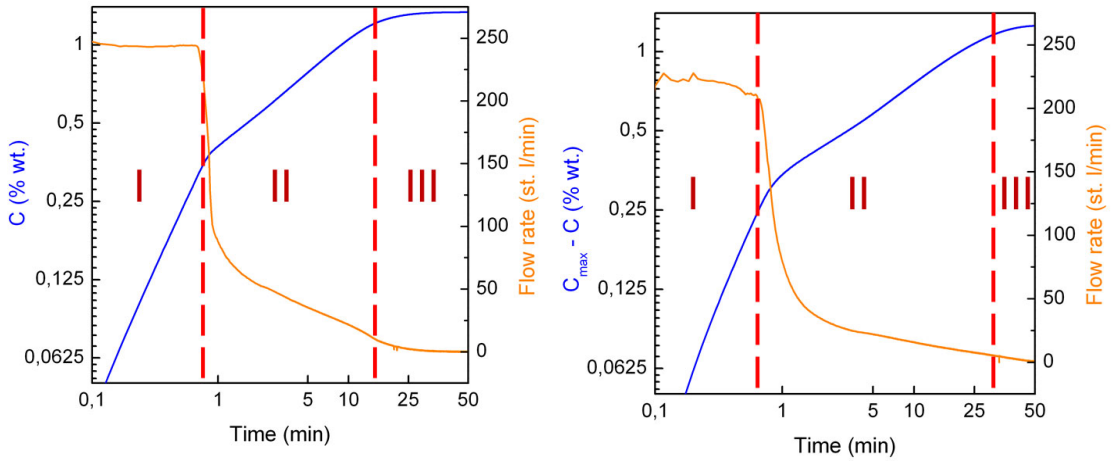

Figure 3: Hydrogen flow rate and hydrogen content in hydride bed for charging at 100% (left) and discharging at 90% (right) and three stages of the process.

These three stages can be explained from the analysis of temperature and pressure evolution inside the metal hydride bed during the process (Figure 4).

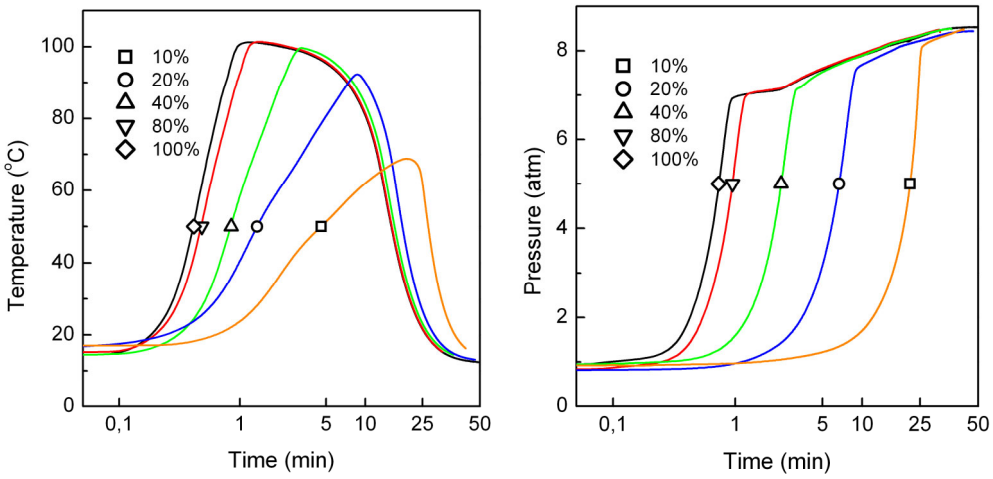

Figure 4: Temperature in the center of MH bed (left) and pressure in the reactor (right) for different charging regimes.

Stage I is characterized by rapid heating of the MH bed connected with pressure increasing. Transition I – II is connected with heat and mass transfer crisis: when maximum temperature is reached, hydrogen flow rate dramatically decreases. Stage II is characterized by steady temperature and pressure changing, hydrogen flow decreases, and at stage III pressure inside the reactor reaches inlet pressure and temperature goes down to coolant temperature. Discharging of the reactor shows similar picture: minimum temperature is reached at stage I, crisis, steady temperature and pressure changing at stage II and finishing at stage III. We can connect these stages with heat and mass transfer processes in the MH bed (see Figs. 5 and 6):

I stage – heating/cooling to reaction temperature. Hydrogen sorption in hydride bed is limited only by regulator at reactor inlet. Heat of reaction cannot be efficiently removed from the bed.

II stage – equilibrium sorption/desorption. Most of hydrogen (>50%) is charged at this stage, and it corresponds to plateau of *PCT*-diagram.

III stage – finishing. Reaction slows down and MH bed is cooled down or heated up to coolant temperature.

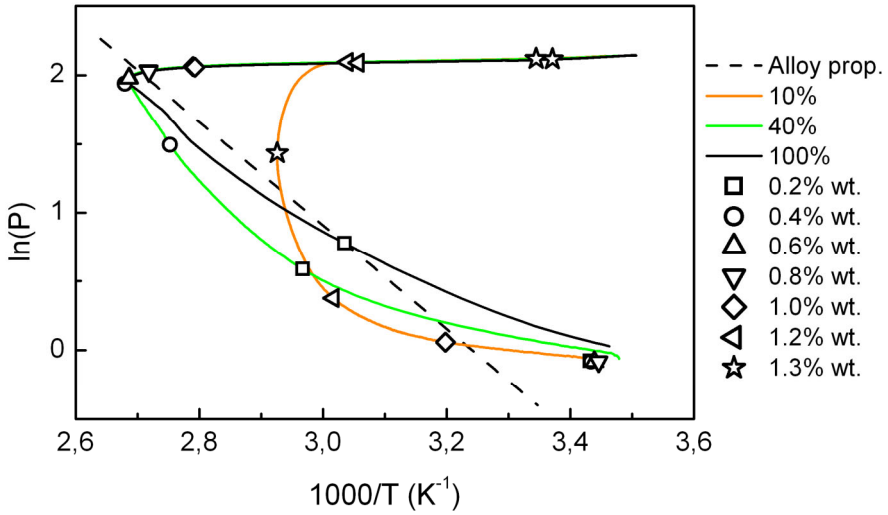

Figure 5: **Charging of the reactor (solid lines) in comparison with alloy properties (dashed line, corresponds to the middle of plateau of *PCT*-diagram), symbols on the solid lines show hydrogen content in the MH bed during the process.**

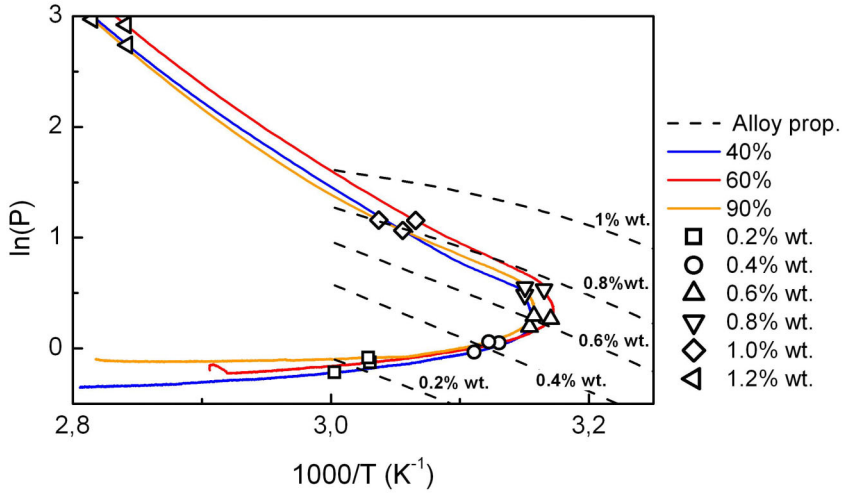

Figure 6: **Discharging of the reactor (solid lines) in comparison with alloy properties (dashed lines, corresponds to hydrogen content on the plateau of *PCT*-diagram), symbols on the solid lines show hydrogen content in the MH bed during the process.**

Two important things can be noticed after the analysis:

Unbalanced regimes with extreme reaction temperature – due to inefficient heat transfer for regimes with high hydrogen flow the hydrogen sorption and desorption reaction temperature is determined by inlet pressure not by coolant temperature, in this case the process is accompanied with crisis.

Heat-balanced regimes – in some regimes with low hydrogen flow rate the heat of reaction is efficiently removed from (moved to) the MH bed, these regimes are not accompanied with the crisis and constant hydrogen flow rate is preserved during the whole process (for example see regime 10% at Figure 5). These regimes are useful for practical applications.

Let determine a criteria for hydrogen flow rate at heat-balanced regime (Figure 7). Reaction heat is equal:

$$Q_{reaction} = m_{MH}\, g\, \Delta H,$$

Heat flow at heat exchanges is equal:

$$Q_{heat\ exchanger} = \alpha\, A\, (T_{MH\ bed} - T_\infty)$$

Heat-balanced regime necessary condition:

$$Q_{heat\ exchanger} > Q_{reaction}$$

Thus for sorption:

$$g_{balanced} < \alpha\, A\, (T_{eq}(P_{in}) - T_\infty)/\, m_{MH}\, \Delta H$$

And for desorption:

$$g_{balanced} < \alpha\, A\, (T_\infty - T_{eq}(P_{out}))/\, m_{MH}\, \Delta H$$

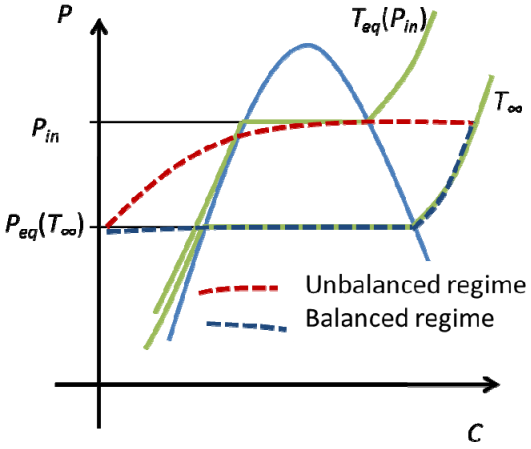

Figure 7: Scheme of heat-balanced and unbalanced regimes for charging of MH reactor.

Conclusions

Charging and discharging of MH reactor is the three stage processes:

I – Heating/cooling to reaction temperature $T_{eq}(P_{in})$ or $T_{eq}(P_{out})$

II – Equilibrium sorption/desorption at reaction temperature

III – Finishing (cooling/heating to T_∞)

I – II transition is connected with heat and mass transfer crisis due to insufficient cooling or heating of MH bed.

There exist heat-balanced regimes with sufficient heat transfer and constant flow rate at reactor inlet, which are useful for practical applications. Criteria for maximum flow rate in heat balanced regime:

for sorption: $g_{balanced} < \alpha A (T_{eq}(P_{in}) - T_{\infty})/ m_{MH} \Delta H$

for desorption: $g_{balanced} < \alpha A (T_{\infty} - T_{eq}(P_{out}))/ m_{MH} \Delta H$

Acknowledgments

Authors would like to thank Zhemerikin V.D. and Blinov D.V. for the aid in experimental work and Russian Ministry for Education and Science (state contracts 02.516.11.6150, 02.516.11.6016 и 02.516.11.6017) and Russian Foundation for Basic Research (grants 06-08-01614 and 07-08-12181) for financial support.

References

[1] Borzenko V., Dunikov D., Malyshenko S. Experimental investigations of heat and mass transfer in metal hydride hydrogen storage devices, Proc. of 17th World Hydrogen Energy Conference, Brisbane, Australia, 17-19 June 2008.

[2] Kaplan Y. Effect of design parameters on enhancement of hydrogen charging in metal hydride reactors, International Journal of Hydrogen Energy. - 2009. V. 34. p. 2288.

Open Sorption Cooling System Based on Metal Hydrides

M. Linder, **R. Mertz**, **E. Laurien**, IKE, University of Stuttgart, Germany

1 Introduction

Onboard hydrogen storage is one key issue for efficient hydrogen fuelled cars. Besides the chemical storing method in e.g. metal hydrides, two physical techniques, liquefaction and compression, are mainly used to increase the energy density of hydrogen storage tanks. Due to the low specific storage capacity of available metal hydrides, the physical storing techniques - especially the compression of hydrogen - seem currently more promising. However, the energy consumption due to the compression of hydrogen is around 15.5 % (800 bar) of its lower heating value and reduces the overall energy efficiency of the car [1].

Therefore, this work focuses on the utilization of the potential energy of the hydrogen storage tank that is available onboard. Based on conventional metal hydride sorption systems, an open sorption system is proposed that is able to utilize this energy to generate a cooling effect usable for e.g. air-conditioning.

2 Background and Working Principle of the Open Sorption System

In Figure 1 idealized van't Hoff diagrams of metal hydride based sorption cooling systems are shown. In both cases, the cooling effect is generated during the cooling half-cycle by the endothermic desorption of hydrogen of metal hydride A at the low pressure p_{Cool}. As the amount of hydrogen stored in metal hydride A is limited, it has to be recharged at the higher pressure level p_{Reg} during the subsequent regeneration half-cycle. The respective pressures (p_{Cool} and p_{Reg}) depend on the van'f Hoff characteristic of the applied metal hydride A and on the temperature boundary conditions.

The underlying principle of the closed sorption cooling system (left) is the coupling of an adapted second metal hydride (B) that operates as a thermally driven compressor between both pressure levels. Therefore, hydrogen is used as working fluid that is cycled between both metal hydrides but not consumed. Several closed metal hydride sorption systems have been realized within the last years with different metal hydrides as well as various metal hydride reaction bed designs. In order to reduce the half-cycle time of the respective system, different measures to increase the heat transfer within the powder bulk, like metal foams [2, 3] or metal hydride pellets [4, 5], have been intensively investigated. Very recently, a review article has been published that summarizes the practical state of the art of closed metal hydride sorption systems [6].

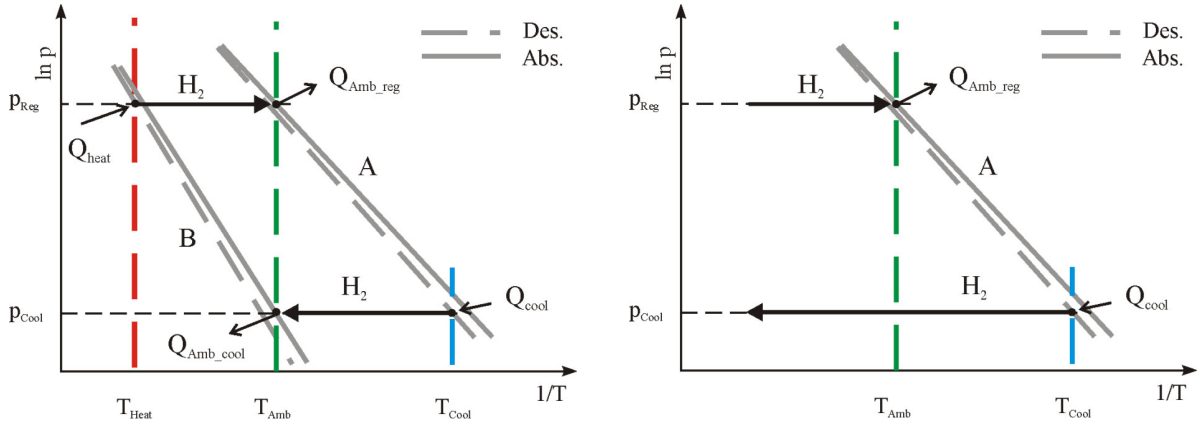

Figure 1: Van't Hoff diagrams of the closed (left) and the open (right) sorption cooling system.

Contrary to the closed metal hydride sorption system, the proposed new system operates with one single metal hydride (A). It is an open process which demands a hydrogen source at a high pressure level (p_{Reg}) and a hydrogen consumer at a low pressure level (p_{Cool}). If hydrogen is stored onboard in compressed state, both boundary conditions are available (hydrogen storage tank and fuel cell) and the open sorption system can be integrated and utilize the pressure difference. This system is schematically shown in Figure 2. In order to reach quasi-continuous cold output, it consists of two reactors that are connected to the fuel cell (FC) and to the hydrogen storage tank (PH_2). Two water cycles (pump, heat exchanger, two 3-way valves) are necessary to remove/supply the thermal energy of the reaction.

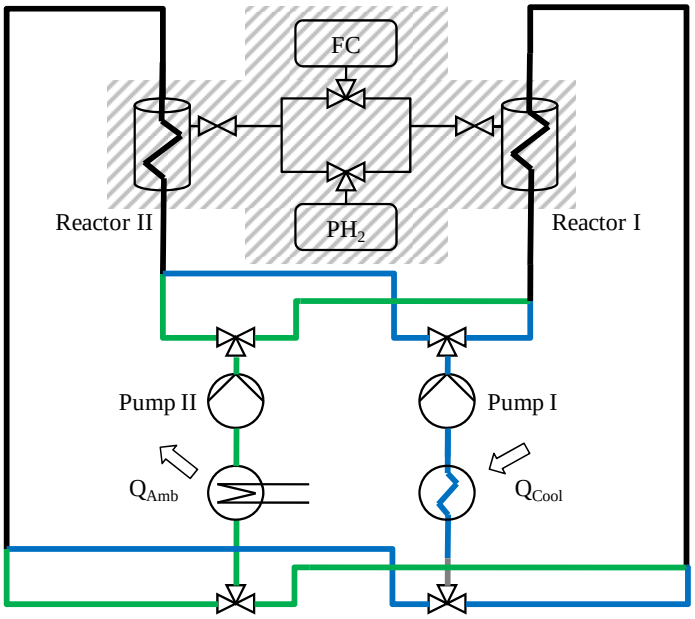

Figure 2: Schematic principle of the pressure-driven sorption system including all major secondary components.

The cooling effect is generated by the reactor that is connected to the hydrogen consumer (e.g. fuel cell) and desorbs hydrogen at the pressure p_{Cool}. The necessary heat of reaction (endothermic desorption) has to be supplied by the blue water cycle that operates at the cooling temperature (T_{Cool}). At the same time, the second reactor is regenerated with hydrogen (at p_{Reg}) from the storage tank and the generated heat of absorption is transferred to the ambient by means of the green water cycle.

Therefore, the metal hydride characteristic has to be adapted to the supply pressure of the hydrogen consumer and to the required cooling temperature. The necessary regeneration pressure for the sorption system is then defined by the ambient temperature.

3 Test Bench and Applied Metal Hydride Reaction Bed

The test bench used for experimental investigations of one reactor of the open sorption system is shown in Figure 3. It consists of a hydrogen part (thin lines) and a water cycle to supply/remove the thermal energy of the chemical reaction (thick lines). As the hydrogen part is separated by valve V7 into two areas, area 1 can be separately prepared for the respective experiment. In case of an absorption experiment, the hydrogen volumes are filled with hydrogen (p_{Reg}) and as soon as valve V7 is opened, the chemical reaction is monitored by several temperature (T1-T4) and pressure sensors (p1, p2). In order to keep the pressure change in the closed system reasonably small, hydrogen bottles with a total volume of around 52 l are used.

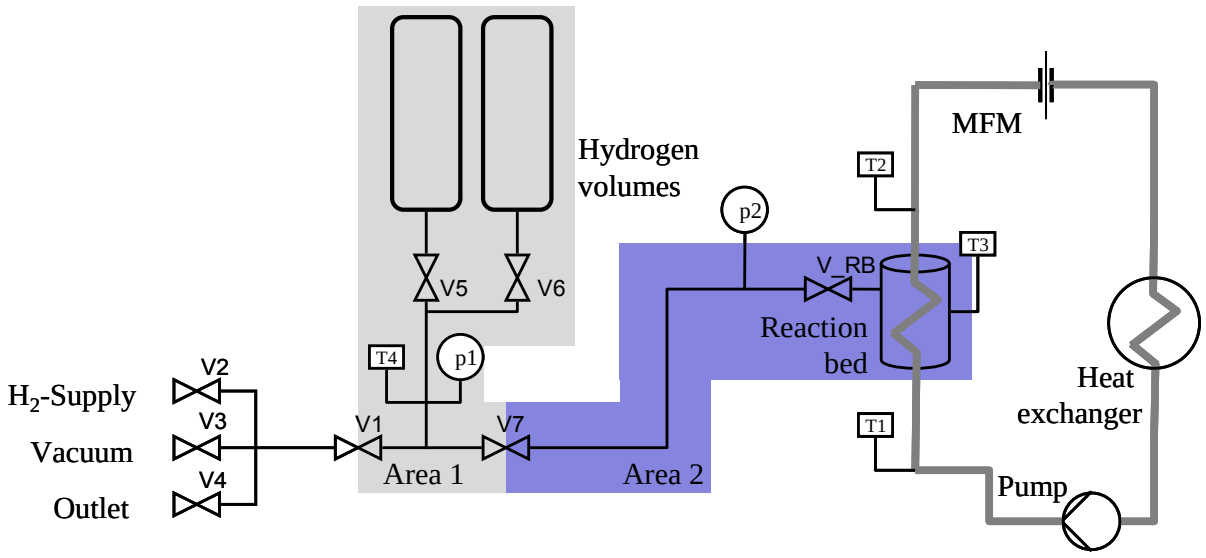

Figure 3: Schematic diagram of test bench.

In Figure 4 the applied reaction bed is shown. It consists of a capillary tube bundle heat exchanger (left) that is surrounded by a sintered metal filter tube (middle). The heat transfer fluid flows through the 372 capillary tubes (inner diameter of 1.4 mm) and the metal hydride powder is located in the outer part of the tube bundle. Hydrogen is distributed around the filter tube through an annular gap that is formed by the cladding tube of the reactor (right).

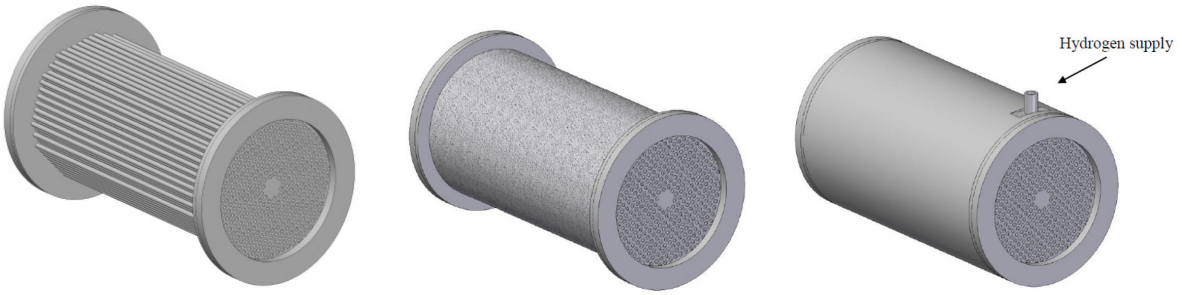

Figure 4: The capillary tube bundle reaction bed.

The total length of the assembled reaction bed is 135 mm. With an outer diameter of 76 mm the total volume of the reaction bed is around 0.6 l. Its weight without metal powder is around 1.7 kg. The volume within the sintered metal tube ($V_i \approx 0.23$ l) is sufficient to charge 800-1000 g of powder, depending on the density of the alloy.

4 Preliminary Experimental Results

Based on PCI measurements of different metal hydrides, $T_{0.99}Zr_{0.01}V_{0.43}Fe_{0.09}Cr_{0.05}Mn_{1.5}$ was chosen for first experimental investigations with one reactor of the open sorption system. The measurement results were obtained with the capillary tube bundle reaction bed and a metal hydride mass of 800 g. The measured cooling and regeneration half-cycles are shown in Figure 5 and Figure 6, respectively.

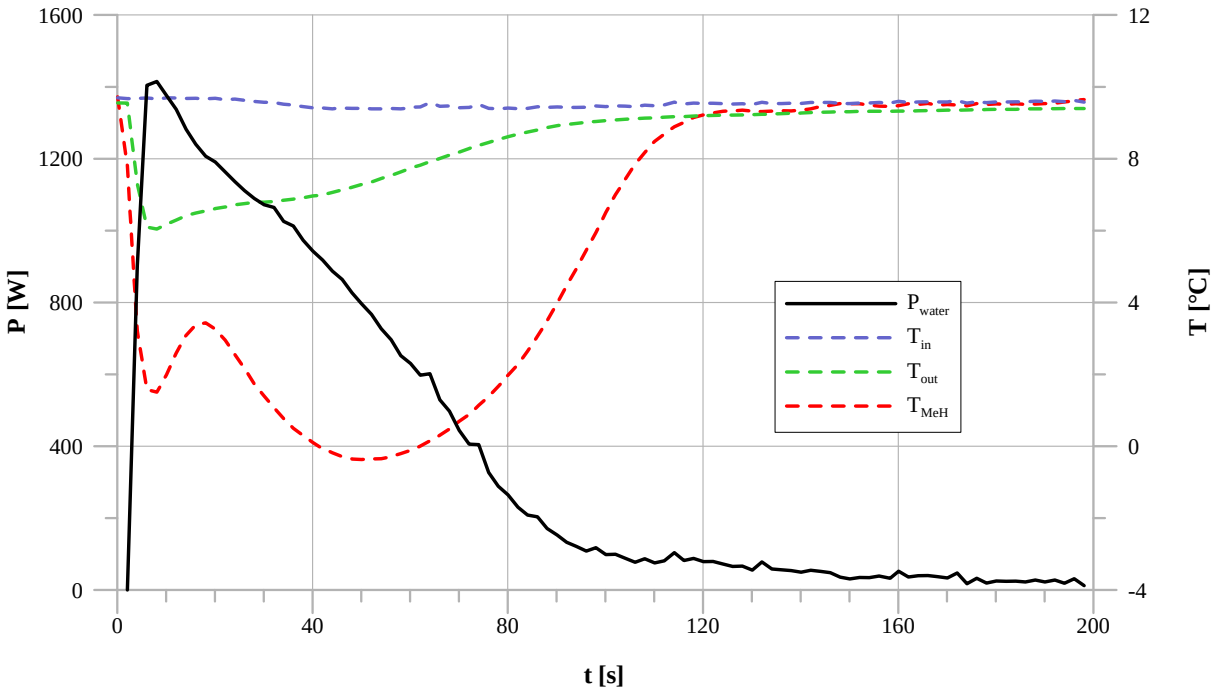

Figure 5: Measured cooling half-cycle for T_{in} = 10 °C with $p_{H2} \approx 5$ bar.

The thermal power P_{water} corresponding to the left y-axis is drawn as solid line and the respective temperatures (right y-axis) are drawn with dashed lines. The desorption pressure during the cooling half-cycle experiment (Figure 5) was set to 5 bar. With an inlet temperature of around 10 °C, a peak cooling power of around 1,400 W is achieved. The average cooling power is 800 W and the necessary half-cycle time is around 100 s.

The system pressure during the regeneration half-cycle (absorption, see Figure 6) was adjusted to 50 bar. For an inlet temperature of 35 °C, the time necessary to charge the metal hydride completely is comparable to the time of the desorption process (~ 100 s). Due to the very fast reaction at the beginning of the experiment, the maximum thermal power during regeneration is about 2,700 W.

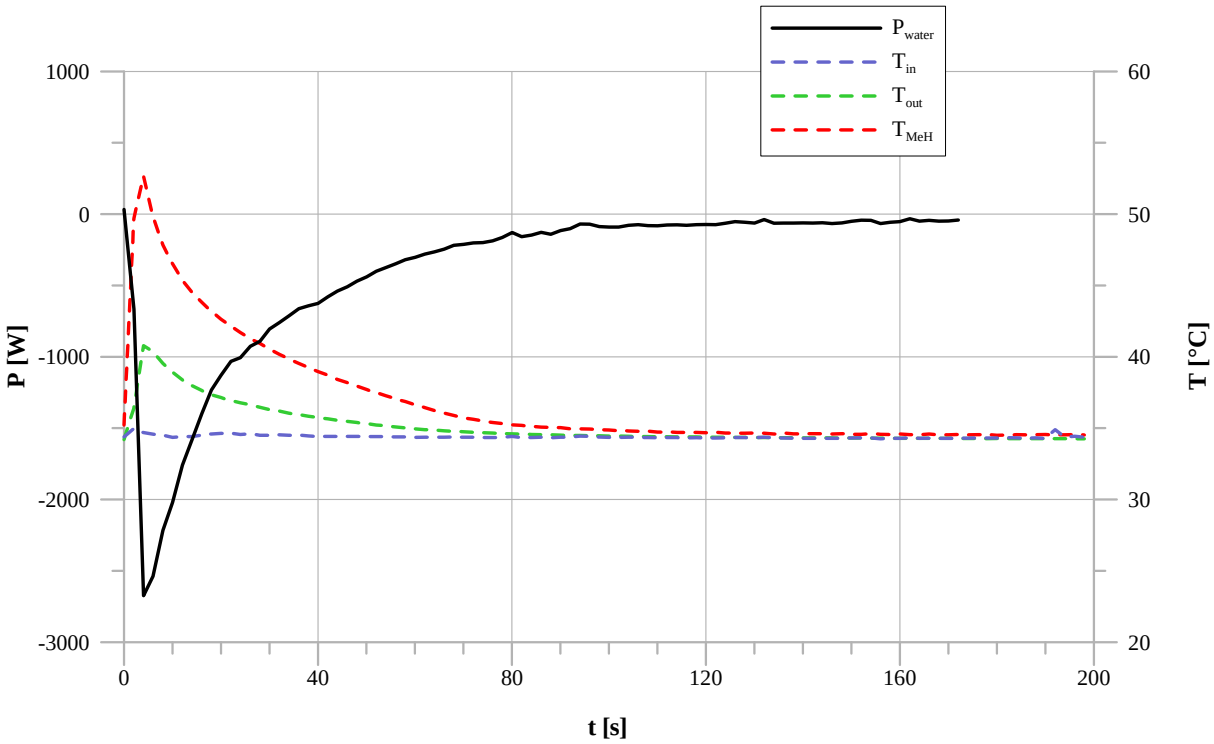

Figure 6: Measured regeneration half-cycle for T_{in} = 35 °C and p_{H2} ≈ 50 bar.

Both experiments show the possibility to operate an open sorption system between 5 bar and 50 bar hydrogen pressure. The achievable cooling temperature is below 10 °C and the regeneration at 35 °C (ambient temperature) is demonstrated in Figure 6. As the temperature and pressure boundary conditions of the cooling system depend on the implemented alloy, the system principle can be adapted to the hydrogen consuming unit, e.g. fuel cell by modifying the alloy composition.

Weight and volume constraints

Due to the simple system set-up consisting of only two reaction beds, the complete system can be very compact and lightweight. The weight of the reaction bed used for the described experiments is around 2.5 kg, including 800 g of metal hydride. A linear up-scaling to an average cooling power of 2 kW leads to a total weight of the hydrogen part of around 12.5 kg

(two reaction beds for continuous cold output). The volume of this part can be estimated to around 3 l (not including the hydrogen valve and connections).

Necessary hydrogen flow rate

Due to the coupling of the open sorption system to a hydrogen consuming unit (e.g. fuel cell), the cooling effect is only generated as long as hydrogen is consumed. Therefore, the generated cooling power of the open sorption system depends directly on the consumed hydrogen flow rate. This dependency is comparable to conventional air-conditioning systems that are mechanically coupled to the engine. Based on the desorption enthalpy of the applied metal hydride (22.6 kJ/mol) and neglecting the losses due to the heat capacity of the reactor (operation temperatures between T_{Amb} and T_{Cool}), the necessary hydrogen flow rate is around 0.09 mol/s if a cooling power of 2 kW is required. If more hydrogen is consumed by the fuel cell than desorbed by the metal hydride, a bypass solution could ensure the necessary hydrogen supply rate.

5 Conclusions and Outlook

In this work an open sorption system based on metal hydrides is described. According to preliminary experimental results with one reaction bed using 800 g of $T_{0.99}Zr_{0.01}V_{0.43}Fe_{0.09}Cr_{0.05}Mn_{1.5}$ the system is able to generate a cooling effect at a temperature below 10 °C with a desorption pressure of 5 bar and can be regenerated at 35 °C with an absorption pressure of 50 bar. However, more detailed experimental investigations are necessary and will be performed on the test bench of the complete system that is currently under construction at the Institute of Nuclear Energy and Energy Systems (IKE).

References

[1] J.O. Jensen, A.P. Vestbo, Q. Li and N.J. Bjerrum: The energy efficiency of onboard hydrogen storage, J. Alloys Comp. 446-447, 723-728 (2007)

[2] E. Willers, M. Wanner and M. Groll: A multi-hydride thermal wave device for simultaneous heating and cooling, J. Alloy Compd. 293-295, 915-918 (1999)

[3] H.-P. Klein and M. Groll: Development of a two-stage metal hydride system as topping cycle in cascading sorption systems for cold generation, Applied Thermal Engineering 22, 631-639 (2002)

[4] K.J. Kim K.T. Feldman Jr., G. Lloyd, A. Razani and K.L. Shanahan: Performance of high power metal hydride reactors, Int. J. Hydrogen Energy 23, 355-362 (1998)

[5] K.J. Kim, B .Montoya, A. Razani and K.-H. Lee: Metal hydride compacts of improved thermal conductivity, Int. J. Hydrogen Energy 26, 609-613 (2001)

[6] P. Muthukumar and M. Groll: Metal hydride based heating and cooling systems: A review, International Journal of Hydrogen Energy 35, 3817-3831, (2010)

Metal Hydride Hydrogen Storage Units for LT PEMFC Power Systems

Ø. Ulleberg, M. Lototskyy, B. Ntsendwana, Ye. Klochko, J. Ren, HySA Systems, SAIAMC, University of the Western Cape, South Africa

Uninterrupted power systems (UPS) for telecommunication installation (mobile phone transmitting towers, internet backbone computing facilities, etc) has been identified as a niche market for hydrogen based low temperature proton exchange fuel cells (LT PEMFCs). Typical power requirements for telecom backup systems range from 1 - 10 kW for single small-scale installations [1] to 5-100kW for larger multipurpose installations [2]. Field experience made by fuel cell companies in this market (e.g. Hydrogenics) show that the required time of continuous operation of such facilities typically varies from 1 to 24 hours, and that the total annual duration of the operation is typically less than 300 hours per year [1]. Other fuel cell companies (e.g., Ballard) have demonstrated PEMFC stack lifetime up to 11,000 hours [3]. Hence, there seems to be a good business case for hydrogen based LT PEMFCs for UPS telecoms.

A national competence centre on Hydrogen & Fuel Cell Technology Systems (HySA Systems) has newly been established at the South African Institute for Advanced Materials Chemistry (SAIAMC), University of the Western Cape (www.saiamc.org). HySA Systems is part of a large and long-term (15-year) research, development and innovation programme, sponsored by the Department of Science and Technology in South Africa. The main objective with HySA Systems is to perform technology validation and system integration in three key areas relevant to hydrogen and fuel cell technologies: (1) Combined Heat and Power, (2) Portable Power, and (3) Hydrogen-fuelled Vehicles.

The HySA portable power programme includes several R&D projects related to the UPS telecom market, including a project entitled “Metal Hydride H_2-Storage for LT PEMFC Power Systems” (Project KP2-S01). The main objective with the project is to develop and manufacture MH-based hydrogen storage units in South Africa, and supply these units to local and international portable and small-scale stand alone power system markets. The specific goals in the project are to: (1) Develop a series of MH-storage units suitable for 0.5-5 kW portable and stand-alone power H_2-based LT PEMFC and (2) Integrate MH-storage units into power systems based on LT PEMFCs with fast start-up and efficient control at variable loads. Preliminary results from this project, which started up in 2009, are presented in this paper.

Storing hydrogen in the solid-state hydride form holds a volumetric advantage over (compressed) gaseous and liquid hydrogen. Solid hydrogen storage systems also have features of low-pressure operation, compactness, safety, delivery pressure, and scalability (modular design) [4]. Commercial MH companies (e.g. Texaco Ovonic Hydrogen Systems LLC) have successfully manufactured MH hydrogen storage systems for portable power applications [5,6]. These MH-systems, consisting of several MH-units, were capable of storing 320 g (~3.5 Nm^3) of hydrogen in total, which is sufficient to run a 1 kW PEM fuel cell

for more than 240 minutes at full power. These pre-commercial MH-units showed no degradation after more than 500 charge/discharge cycles.

The work in this project focuses on the development and system integration of MH hydrogen storage units for PEMFC power systems to be operated below 120°C. Hence, the focus is on "low-temperature" AB_5- (A=rear earth; B=Ni, Co, Mn, Al), AB-alloys (A=Ti; B=Fe, Mn, V), or AB_2- (A=Ti, Zr; B=Mn, Cr, V) type of hydrogen storage materials, which are characterized by fast hydrogen absorption / desorption kinetics at moderate temperatures (10-100°C). In order to achieve fast start-up of the PEMFC and to minimize the power consumption during hydrogen supply (MH hydrogen discharge), the MH-unit must have a hydrogen equilibrium pressure (P_D) higher than the pressure of hydrogen to be supplied to the PEM fuel cell.

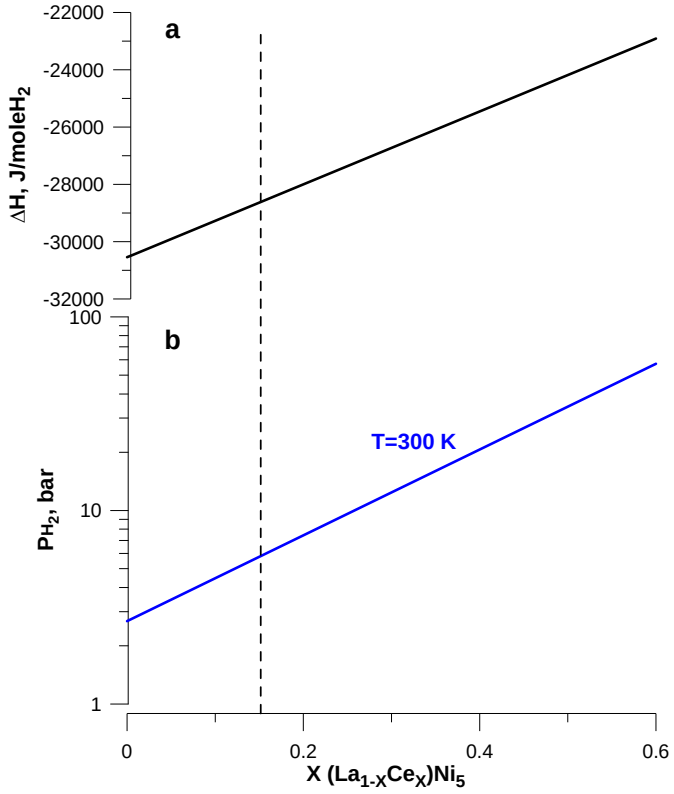

Figure 1: (a) Estimated enthalpies of hydride formation for cerium-substituted intermetallide $LaNi_5$ and (b) corresponding values of equilibrium hydrogen pressure at room temperature calculated assuming the entropy of the hydride formation equal to –110 J/(mole H_2·K).

An AB_5-type of material with a P_D = 5-10 bar (i.e. the required operating pressure for the hydrogen storage system) at room temperature was selected for the first phase of this project (other materials suitable for hydrogen storage pressures will be investigated in the next phase). AB_5-alloys are the most frequently used materials for MH-applications. Their main advantages are: low sensitivity to poisoning by impurities, easy activation, fast hydrogen absorption / desorption kinetics, and wide pressure range at near ambient temperatures [7]. Figure 1a shows our estimated values for formation enthalpies of the intermetallic hydrides $La_{1-x}Ce_xNi_5H_y$ based on available reference data [8], while Figure 1b show the corresponding

calculation of hydrogen equilibrium pressures assuming ΔS^0= -110 J/(mole H_2·K). From this it can be deducted that the composition $La_{0.85}Ce_{0.15}Ni_5$ can give an equilibrium pressure at room temperature of about 5 bar, which satisfies the pressure requirements of the given application.

Two batches of 100 kg with a $La_{1-x}Ce_xNi_5$ alloy specified for the project were manufactured by two independently Chinese industrial companies. Results from characterization (XRD, SEM, TEM, H sorption) of the MH-materials showed that both batches had almost identical properties. Hence, the MH-material can be produced on a larger industrially scale, and is suitable for high volume production of MH-units for portable and/or stand-alone power LT PEMFC applications.

Figure 2 shows the XRD-patterns (Cu-K_α) of the delivered alloy and the product of its hydrogenation (Hydrogenation was carried out in a Sieverts setup at a H_2 pressure of 50 bar and room temperature, followed by stabilization of hydride phase by the exposition of the hydrogenated material on air at the liquid nitrogen temperature). The starting alloy contained a single AB_5-phase (space group P_6/mmm, #191; a = 4.9919 Å, c = 3.9960 Å; V_0 = 86.236 Å^3; ρ_{calc} = 8.327 g/cm^3) (Figure 2a), while the product after hydrogenation was found to be a two-phase containing AB_5H_x hydride (70 vol.%) with increased unit cell volume (a = 5.3877 Å, c = 4.2617 Å; V = 107.133 Å^3; $\Delta V/V_0$=24.2%; ρ_{calc} = 6.703 g/cm^3), and α-solid solution $AB_5H_{\sim 0}$ (30 vol.%) (Figure 2b). The appearance of the α-phase is most probably caused by decomposition of the unstable β-hydride during carrying of the sample to the difractometer and XRD. Volumetric measurements of the pressure, composition, and temperature relationships (*PCT*) for the $La_{0.85}Ce_{0.15}Ni_5$ - hydrogen system were carried out at T = 0-80°C and P = 0.01-100 bar. Quite small hysteresis was observed (P_{ABS}/P_{DES}<1.2), so both absorption and desorption datasets were processed together. The experimental data was fitted using the model of phase equilibrium in metal – hydrogen systems [9]. Figure 3 and Table 1 summarize the results.

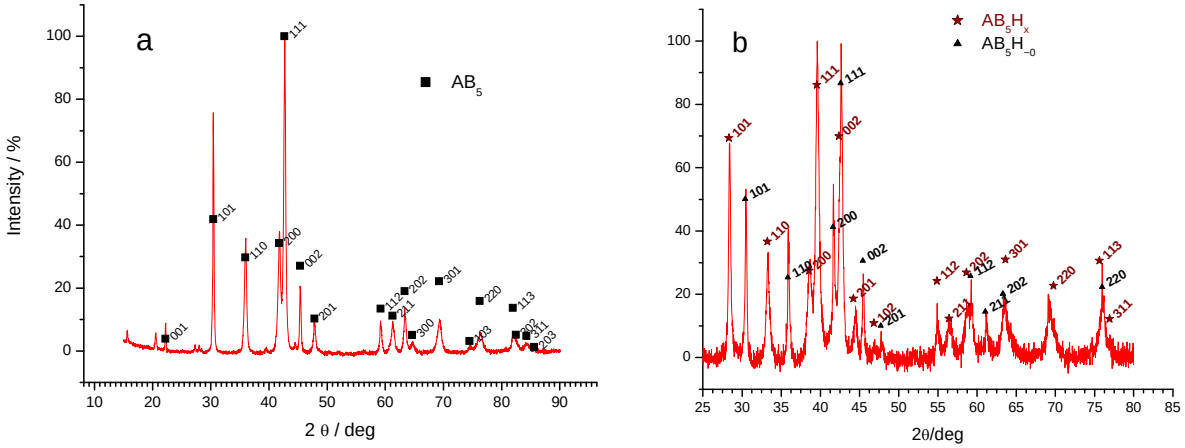

Figure 2: (a) Indexed XRD patterns of the as-delivered and (b) hydrogenated $La_{0.85}Ce_{0.15}Ni_5$ alloy.

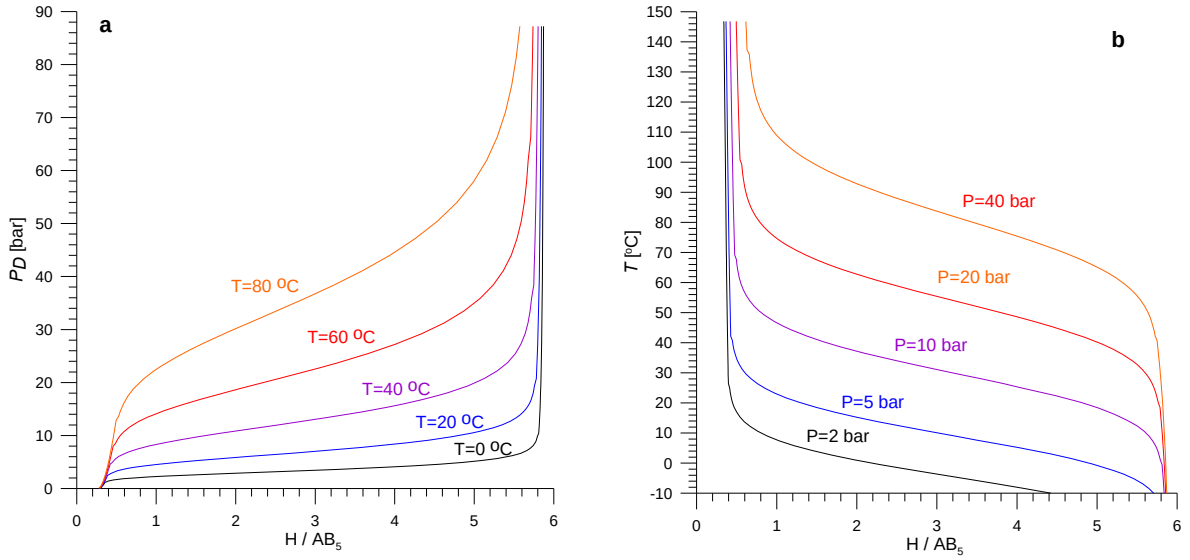

Figure 3: **(a) Calculated isotherms and (b) isobars of hydrogen sorption in $La_{0.85}Ce_{0.15}Ni_5$ alloy.**

Table 1: **Summary of calculated *PCT*-properties for the $La_{0.85}Ce_{0.15}Ni_5$ hydrogen storage alloy.**

Parameter	T = 20°C	T = 40°C	T = 60°C
Plateau midpoint (C_0), H/AB$_5$	3.060	3.041	3.015
ΔS^0, J/moleH$_2$/K (C=C_0)	-96.61		
ΔH^0, kJ/moleH$_2$ (C=C_0)	-23.548		
d(Ln P)/d(H/ AB$_5$)	0.171	0.175	0.181
P (C =C_0), bar	7.09	13.14	22.62
C (P =1 bar), H/AB$_5$	0.34	0.33	0.33
C (P =20 bar), H/AB$_5$	5.76	5.02	2.35

From the above it can be deducted that the equilibrium hydrogen pressure (P_D) for the selected alloy (Table 1) is greater than 1 bar at temperatures T > 0°C. In practice, this means that the MH-unit will be able to supply sufficiently high hydrogen pressure to the LT PEMFC stack, as long as the MH-unit operates at T > 0°C. In an air cooled/heated MH-unit these operating conditions can be achieved by providing ambient heat or hot exhaust air from the PEMFC-stack. In a water cooled/heat MH-unit more direct heat exchange with the PEMFC-stack can be achieved, but this requires a water cooled PEMFC-stack. The reversible hydrogen capacity of the material at T=30°C and P=1-10 bar is higher than 5 H/AB$_5$, or 130 L H_2 STP per 1 kg of the alloy.

The dynamic behavior of the hydrogen absorption /desorption in the selected AB$_5$-material was studied in a 150 cm^3 cylindrical reactor equipped with four thermocouples for the measurement of radial temperature distribution in the middle of MH bed (Figure 4a). The reactor was filled with 600 g of the $La_{0.85}Ce_{0.15}Ni_5$ H storage alloy. The alloy showed

reproducible H_2 absorption / desorption dynamics after completion of just one activation cycle: (1) initial evacuation, (2) 24-hours charging with H_2 at *P*=50 bar, (3) H_2 desorption at *P*=1 bar, and (4) final evacuation. All the operations were carried out at *T*=30°C. The evacuation was done using a rotary pump with a residual pressure of $5*10^{-2}$ bar. Both charge and discharge of the MH-reactor were carried out at constant pressures (1.5-5 bar for the desorption and 10-50 bar for the absorption); the unit was immersed in a thermostat (*T*=20-50°C). During the charge / discharge, hydrogen flow rate was logged, together with the temperatures in the centre of the MH-bed (T1), in between the centre and the wall of the reactor (T2), and on the inner (T3) and outer (T4) surfaces of the reactor wall.

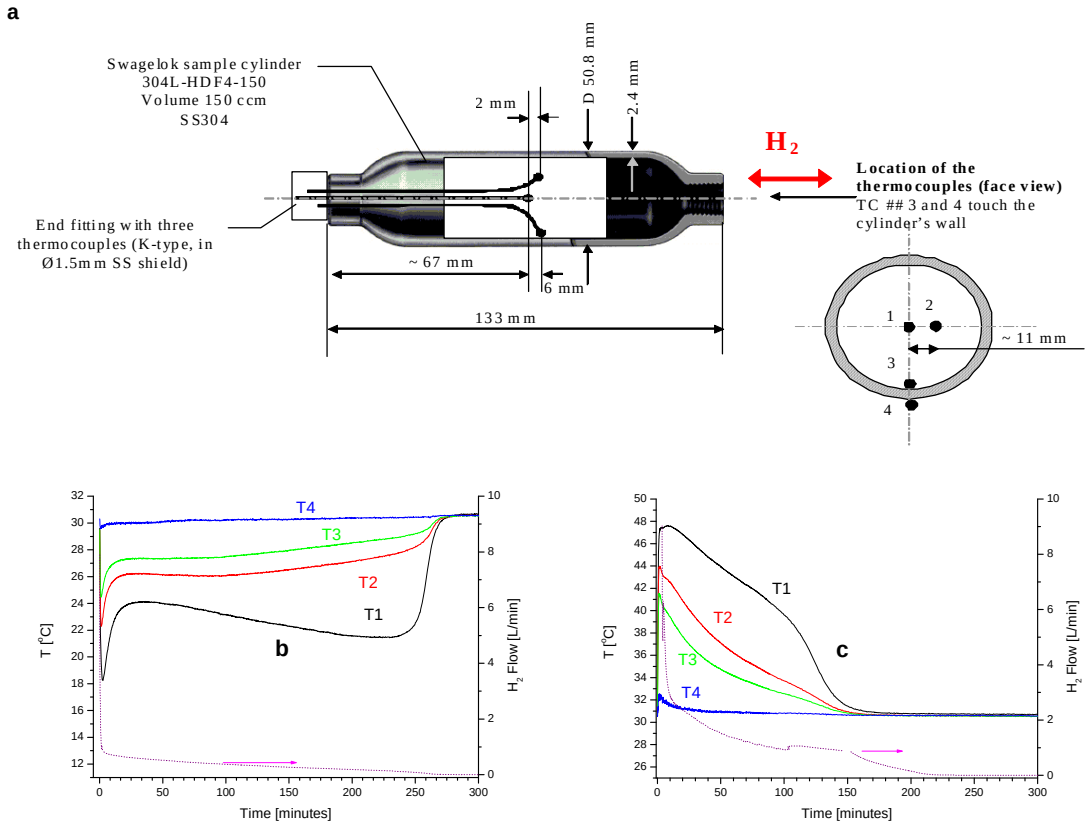

Figure 4: (a) Schematic of placement of thermocouples (1-4) in experimental MH-unit, (b) temperatures during desorption (*P*=2 bar, *T*= 30°C), and (c) temperatures during absorption (*P*=10 bar, *T*= 30°C).

Examples of the dynamic behavior of the MH-reactor are illustrated in Figure 4b (desorption, *P*=2 bar, *T*= 30°C) and Figure 4c (absorption, *P*=10 bar, *T*= 30°C). The heating/cooling of the MH-reactor during desorption (endothermic) and absorption (exothermic), which is limited by poor thermal conductivity in the MH-powder, significantly affects the hydrogen desorption/absorption flow rates. Initially, (first 2-3 minutes) the flow rates rapidly slow down from ~10 L H_2 (STP)/min to ~1 L/min during desorption, and 2.5 L/min during absorption. Over time the temperature approaches its initial value (thermostat setting), and the hydrogen flow rates slows down. The hydrogen desorption and absorption processes are fairly slow, ca. 5 and 2.5 hours respectively. The desorption is slower than the absorption due to a

smaller difference between the operating pressure and the equilibrium pressure (driving force for both absorption and desorption), slower reaction rates, and a more complicated thermal behavior in the MH bed (as observed in the temperature profile in the centre of the MH bed (T1) Figure 4b). This is likely to be caused by exothermic re-absorption of hydrogen in the cold central region, resulting in the temporary temperature increase. Similar effects have been observed in other studies [10], where it was concluded that temperature gradients induce composition gradients within the hydride bed, making the local temperatures, composition or reactions rates very different from the average values.

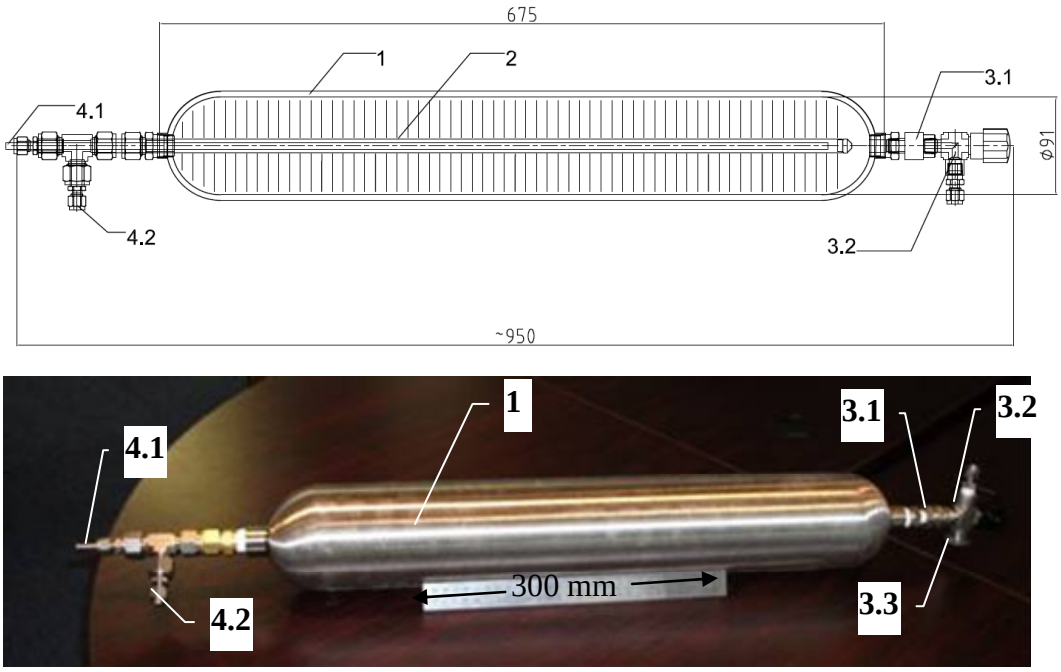

Figure 5: Schematic drawing (top) and photo (bottom) of the MH hydrogen storage unit, where
1 = stainless steel container; 2 = heat exchanger; 3 = H_2 manifold: 3.1 = filter, 3.2 = valve, 3.3 = overpressure protection (rupture disc); 4 = water manifold: 4.1 = inlet, 4.2 = outlet.

A prototype water-cooled MH hydrogen storage unit for a LT PEMFC application has been designed and developed (Figure 5) on the basis of the characterizations and heat and mass transfer analyses described above. The MH-unit (Figure 5) was assembled from standard components (Swagelok), except for the self-made heat exchanger (2) consisting of ½-inch OD copper tubing with copper fins (thickness 0.5 mm, pitch 10 mm). The supply of the heating/cooling water is provided via an internal ¼'-inch OD stainless steel tube connected to input pipeline (4.1) of the water manifold (4). Hydrogen charging of the MH-unit and hydrogen supply to the input pressure regulator of PEMFC-stack is provided via a hydrogen manifold (3) consisting of an in-line gas filter (3.1), shut-off valve (3.2), and a rupture disc with a burst pressure of 133 bar (3.3). The main part of the MH-unit is an one gallon (3.7 liter) Swagelok sample cylinder filled with 12 kg of $La_{0.85}Ce_{0.15}Ni_5$ H storage alloy. This gives a bulk density of the material of ca. 3.5 g/cm^3, or ca. 52% density of the material in the hydrogenated state, which is below the upper limit (61%) for safe packing of AB_5-type

hydrides in MH containers [11]. The MH-unit, with a total weight of 22 kg, has a hydrogen storage capacity of 1560 liters with H_2 (STP), which can provide more than 2 hours of full-load operation of a 1 kW LT PEMFC-stack. Additional hydrogen storage capacity can simply be achieved by integrating several units in a modular hydrogen storage system. Detailed thermal modeling studies on the MH-unit are currently being performed by a research group at Tswhane University of Technology, a HySA Systems partner. The results from these studies will be used to re-design new and more efficient MH-units.

Acknowledgements

This work is supported by the HySA Programme (project KP2-S01), Department of Science and Technology, South Africa and the South Africa Norway Research Cooperation Programme (project 180344), Research Council of Norway and and National Research Foundation of South Africa.

References

[1] Jonathan Dogterom, “Hydrogen and Fuel Cell Business Development in Canada. Case Study: Fuel Cell Telecom Installations”, HySA Systems Business Seminar, 2 November 2009, Cape Town.

[2] Teledyne Brown Engineering report, Fuel cell power systems for remote application, DOE/GO/10217-T1,1998.

[3] Felix N. Büchi, Minoru Inaba, Thomas J. Schmidt (Eds) Polymer Electrolyte Fuel Cell Durability, Springer 2009.

[4] Yartys V.A., Lototsky M.V., An overview of hydrogen storage methods, In: Hydrogen Materials Science and Chemistry of Carbon Nanomaterials, ed. by T. Nejat Veziroglu, SvetlanaYu. Zaginaichenko, Dmitry V. Schur, B. Baranowski, Anatoliy P. Shpak, and Valeriy V. Skorokhod, Kluwer Academic Publishers, 2004, pp. 75-104

[5] Young R.C., Advances of Solid Hydrogen Storage Systems, 14th Annual Conference of NHA, March 4-6, 2003, http://www.h2fc.com

[6] Chao B.S., Young R.C., Myasnikov V., Li Y., Huang B., Gingl F., Ferro P.D., Sobolev V., Ovshinsky S.R., Recent Advances in Solid Hydrogen Storage Systems, Mat. Res. Soc. Symp. Proc. Vol. 801, 2004, pp. BB1.4.1-BB1.4.12, http://www.mrs.org

[7] Sandrock G., A panoramic overview of hydrogen storage alloys from a gas reaction point of view, J. Alloys and Compounds 293–295 (1999) 877–888

[8] Kolachev B.A., Shanin R.E., Il’in A.A., Hydrogen Storage Alloys / Reference Book, Moscow, “Metallurgy” Publ., 1995 (in Russian)

[9] Lototsky M.V., Yartys V.A., Marinin V.S., Lototsky N.M., Modelling of phase equilibria in metal–hydrogen systems, J. Alloys and Compounds 356–357 (2003) 27–31

[10] Dantzer P., Metal-Hydride Technology: A Critical Review, In: Hydrogen in Metals III. Properties and Applications (Topics in Applied Physics Volume 73), Ed. by H. Wipf, Springer-Verlag, Berlin, Heidelberg, 1997, pp.279–340

[11] Nasako K., Ito Y., Hiro N., Osumi M., Stress on a reaction vessel by the swelling of a hydrogen absorbing alloy, J. Alloys Comp 264 (1998) 271–276

Pellets of MgH_2-based Composites as Practical Material for Solid State Hydrogen Storage

Giovanni Principi, **Ashish Khandelwal**, **Filippo Agresti**, **Giovanni Capurso**, **Amedeo Maddalena**, Materials Section, Dept. of Mechanical Engineering, University of Padova, Italy
Sergio Lo Russo, Dept. of Physics, University of Padova, Italy

1 Introduction

MgH_2 is one of the most studied materials among those able to store hydrogen in solid state, having many assets in its favour, like low cost, abundance, light weight and a theoretical storage capacity of 7.6 wt%. However, concerning the practical applications, it has the limitations of high thermodynamic stability and slow hydrogen absorption/desorption (a/d) kinetics. To come out of these practical shortcomings MgH_2 is used in nano-crystalline form obtained by high energy ball milling mixed with transition metal oxides, e.g. Nb_2O_5 [1,2], acting as catalysts to improve the hydrogen a/d kinetics with little reduction in the gravimetric capacity. During scaling up studies of MgH_2 based powders in a specially designed reactor it was observed that the hydrogen storage capacity, as well as the a/d kinetics, decreased with the ongoing cycles [3]. It was argued that this degradation was due to a close compaction of the powder particles inside the reaction chamber associated with local overheating, with the detrimental effect of strongly reducing the free flow of hydrogen through the storage material. The compaction of the powders was probably due to a pressure gradient that built up during the first stages of hydrogen absorption process given by the difficult gas transport through the Mg bed. These observations motivated us to study MgH_2 based powders moderately pressed in the form of pellets with the addition of some binding agent in order to retain stable mechanical consistency and structure with persistent free paths for hydrogen diffusion. The use of pellets instead of powder should improve the hydrogen transport inside the storage vessel avoiding pressure gradients and further compaction of the material. Moreover, in principle, each pellet should behave as an independent system reducing scaling up effects on the a/d kinetics.

In this work we have tested MgH_2 catalysed ball milled powders mixed with Al powder as a binder pressed with an electro-mechanical press, following an approach already preliminarily tested [4]. The crystalline structure, the hydrogen a/d properties and the mechanical strength of the samples have been analysed before and after hydrogen a/d cycling. The incorporation of aluminium is supposed also to enhance the thermal conductivity in the pellets.

2 Experimental

MgH_2 powder mixed with Nb_2O_5 (5 wt %) and graphite (1 wt%), as catalysts of the gas-solid reaction, was ball-milled in a SPEX 8000 shaker mill for 20 hours using steel balls with ball to powder ratio of 10:1 (samples denoted as cat-MgH_2). Two types of pellets were studied: one made up of as-milled cat-MgH_2 powder and in the other case 5 and 20 wt% of Al powder was

homogenously mixed by ball-milling for 5 min with cat-MgH_2 to act as a binding agent (samples denoted as cat-MgH_2-Al5 and cat-MgH_2-Al20, respectively). All pellets were obtained by pressing the powders in Ar atmosphere with a uniaxial pressure of 180 MPa by means of an Instron 1121 tester. Kinetic and thermodynamic tests were performed using a Sievert's type gas reaction controller. Annealing of samples containing Al powder was performed at 450 °C in the same Sievert's apparatus for 10 min under a rotary pump vacuum before starting the hydrogen a/d cycles. In order to test the compressive strength resistance of the pellets after different a/d cycles, compression tests were performed using the same Instron 1121 tester at the compressive strain rate of 1 mm/min. For all samples the hydrogen release processes were performed at the temperature of 320°C and H_2 pressure of 1.2 atm, while the soak processes were performed at the same temperature and H_2 pressure of 15 atm.

3 Results and Discussion

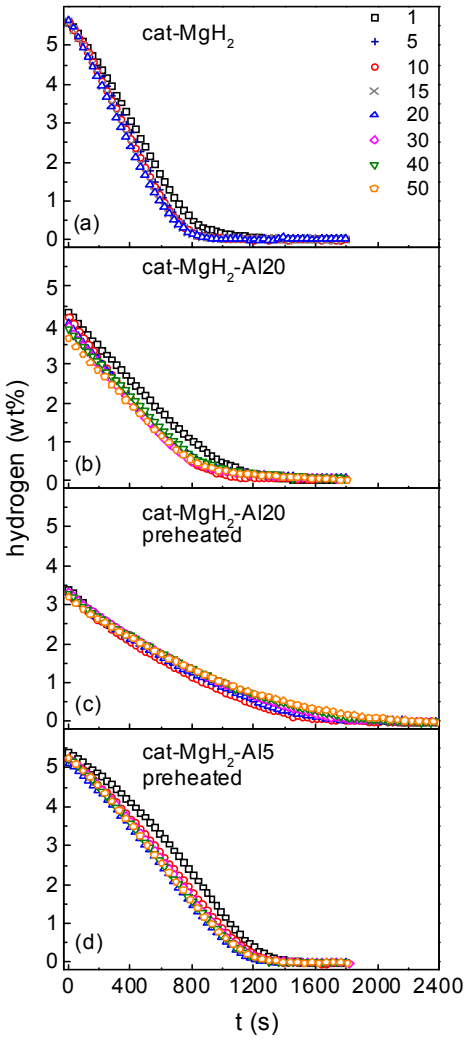

Figure 1: Desorption cycles of pellets cat-MgH_2 (a), cat-MgH_2-Al20 without preheating (b), cat-MgH_2-Al20 with preheating (c) and cat-MgH_2-Al5 with preheating (d).

Figure 1a) shows the release kinetics for the pellet of cat-MgH_2 and indicates that the maximum stored and released hydrogen in this case was 5.6 wt %, which remained stable for all the hydrogen a/d cycles. During cycling, the pellet lost gradually its mechanical consistency and after 20 cycles got completely powdered. This behaviour is in agreement with the observed continuous reduction of desorption time by cycling, considering that a not close compacted powder favours the hydrogen flow through the material. The breaking of the pellets is due to the stress induced during absorption with an increase of 32% of the volume for the host Mg forming MgH_2.

Figure 1b gives the desorption curves for pellet cat-MgH_2-Al20, where is shown that the hydrogen content goes from the initial 4.3 wt% to about 3.6 wt% after 50 cycles. This decrease can be explained in terms of Mg-Al phases formation during cycling, slowly reacting with hydrogen due to a higher plateau pressure with respect to pure Mg. The compactness of this pellet started degrading before 20 cycles and was completely lost before 50 cycles. Another similar pellet was then first heated in vacuum at 450 °C, for 10 minutes, in order to facilitate the formation of some intermetallic phases and/or solid solution and then submitted to 50 a/d cycles. As shown in figure 1c, the maximum hydrogen content of this pellet was about 3.3 wt% and the time for 90% desorption increased to 1320 s. The hydrogen content was now almost constant under cycling, in contrast to the pellet without pre-heating, and the degradation of mechanical compactness resulted less. However, the pellet started to degrade before about 50 cycles. Cat-MgH_2-Al5 pellets were cycled under similar conditions after pre-heating as in the previous case. Figure 1d shows that in this case almost all the absorbed hydrogen (5.3 wt%) was released in about 1500 s. The desorption behaviour became almost stable just after 10 cycles and the pellet remained mechanically consistent and hard even after 50 cycles.

The XRD measurements of cat-MgH_2-Al5 and cat-MgH_2-Al20 hydrogenated and dehydrogenated pellets after heat treatment and 50 hydrogen a/d cycles give the relative abundance of the phases, estimated by means of the Rietveld refinement, reported in Table 1. These results agree with the study of hydrogenation process of ball milled Mg-Al powders by Crivello et al. [5,6], which occurs in two completely reversible steps:

$$Al_{12}Mg_{17}+9H_2 \leftrightarrow 9MgH_2+4Al_3Mg_2 \quad (1)$$

$$4Al_3Mg_2+8H_2 \leftrightarrow 8MgH_2+12Al \quad (2)$$

Reaction (2) did not reach completion in our operating conditions, probably due to the higher relevant plateau pressure. The estimated amount of Al (4 wt%) in the cat-MgH_2-Al20 hydrogenated sample is larger than in the case of dehydrogenated sample. This is due to the fact that a certain amount of Al is in solid solution in the structure of Mg and during hydrogenation is expelled, according to the disproportionation reaction

$$Mg(Al_x) + H_2 \leftrightarrow MgH_2 + xAl \quad (3)$$

Table 1: Results of Rietveld refinement of the XRD patterns of the cycled pellets.

Sample	β-MgH_2 (wt %)	Mg (wt%)	MgO (wt %)	Al (wt %)	Al_3Mg_2 (wt %)	$Al_{12}Mg_{17}$ (wt %)
cat-MgH_2-Al20 450 °C (dehydrogenated)	<2	39	14	<3	-	43
cat-MgH_2-Al20 450 °C (hydrogenated)	51		17	4	15	13
cat-MgH_2-Al5 450 °C (dehydrogenated)	5	73	22	-	-	-
cat-MgH_2-Al5 450 °C (hydrogenated)	72	7	18	<3	-	-

According to the Mg-Al phase diagram, the small amount of Al is not sufficient for the precipitation of the eutectic phase and leads only to a solid solution of Al in Mg. The presence of Al in solid solution is also supported by the fact that the estimated amount of Al in the dehydrogenated sample is negligible.

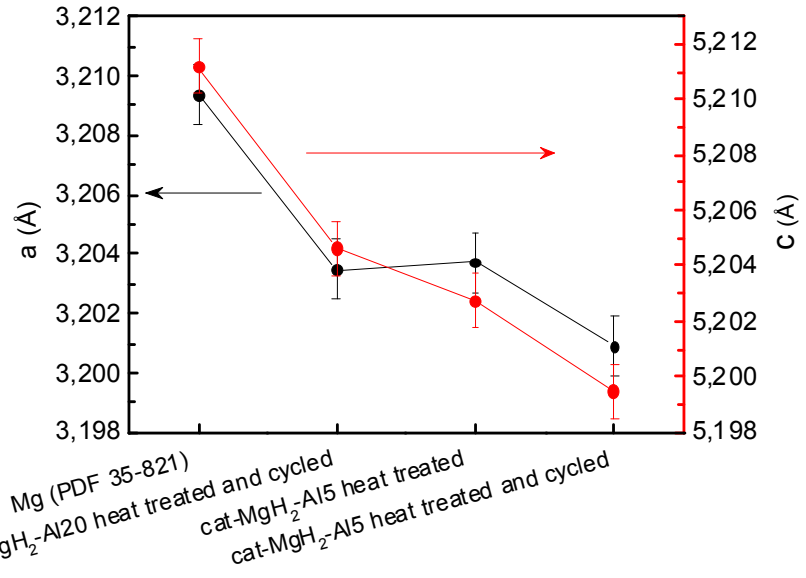

Figure 2: Lattice parameters of Mg estimated by Rietveld refinement for some of the studied dehydrogenated samples.

The lattice parameters of Mg obtained by the Rietveld refinement for some of the dehydrogenated samples are shown in Figure 2. These values are smaller compared to those of pure Mg and this is certainly due to the presence of Al in Mg(Al) solid solution, considering the smaller metallic radius of Al compared to that of Mg. The smallest lattice parameters are observed for the cat-MgH_2-Al5 sample after heat treatment and 50 a/d cycles, which shows that in this case Al prefers to enter in the Mg(Al) solid solution instead of forming Mg-Al intermetallic phases. On the contrary, in the case of the cat-MgH_2-Al20 sample the precipitation of the eutectic phase $Al_{12}Mg_{17}$ slows down the formation of Mg(Al) and the lattice parameters of Mg are larger.

Figure 3 shows the results of the mechanical tests for hydrogenated pellets without Al and with 5 wt% Al after 0 and 50 a/d cycles. It is evident the better behaviour of pellets containing Al, while, in absence of aluminium, a stress of 30.1 N/mm^2 and of 8.1 N/mm^2 was sufficient to break the pellet after 10 and 20 a/d cycles, respectively. As said before, it was not possible to recover the pellet after 50 a/d cycles. The better behaviour of samples containing Al can be attributed to the presence, according to reaction (3), of an Al matrix surrounding the MgH_2 particles. Anyway, also in this case the strength decreases, likely due to the progressive increase of porosity: 43.7 N/mm^2 and 13.9 N/mm^2 after 20 and 50 cycles, respectively.

Work is in progress to better understand, with a high resolution investigation, the micro-structural evolution of the pellets in the different stages of a/d cycling. Moreover, the preparation of a small vessel to study the hydrogen a/d behaviour of a metal hydride in form of pellets instead of powder, in order to overcome the shortcomings of the scaling up effects, is under way.

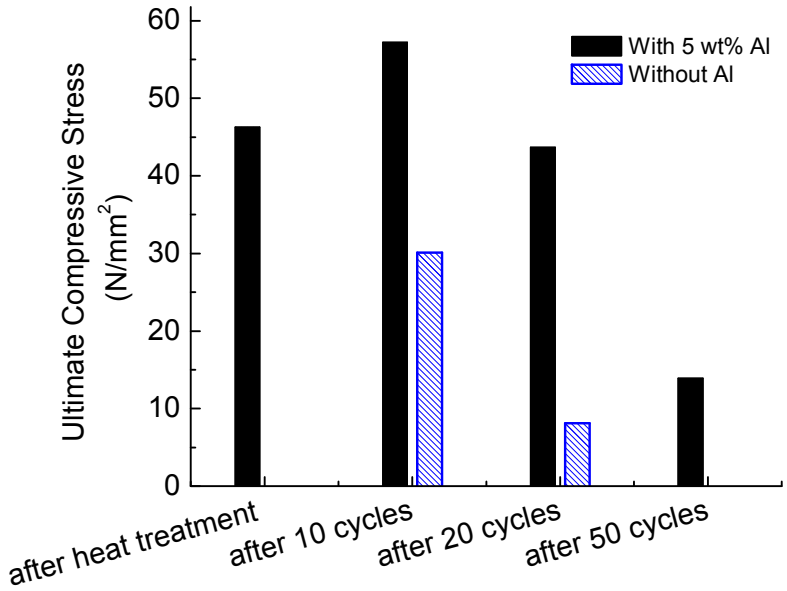

Figure 3: Results of the compression tests to estimate the mechanical strength of the pellets without and with 5 wt% Al.

References

[1] Barkhordarian G, Klassen T, Bormann R. Fast hydrogen sorption kinetics of nanocrystalline Mg using Nb_2O_5 as catalyst. Scr Mater 2003;49:213-7.

[2] De Piccoli C, Dal Toé S, Lo Russo S, Maddalena A, Palade P, Saber A, Sartori S, Principi G. Hydrogen storage in magnesium hydride doped with niobium pentaoxide and graphite. Chem Eng Trans 2004;4:343-7.

[3] Verga M, Armanasco F, Guardamagna C, Valli C, Bianchin A, Agresti F, Lo Russo S, Maddalena A, Principi G. Scaling up effects of Mg hydride in a temperature and pressure-controlled hydrogen storage device. Int J Hydrogen Energy 2009;34:4602-10.

[4] Glage A, Ceccato R, Lonardelli I, Girardi F, Agresti F, Principi G, Molinari A, Gialanella S, A powder metallurgy approach for the production of a MgH_2-Al composite material, J Alloys Compd 2009;478:273-280.

[5] Crivello JC, Nobuki T, Kato S, Abe M, and Kuji T. Hydrogen absorption properties of the γ-$Mg_{17}Al_{12}$ phase and its Al-richer domain. J Alloys Compd 2007;446:157-61.

[6] Crivello JC, Nobuki T, Kuji T. Improvement of Mg-Al alloys for hydrogen storage applications. Int J Hydrogen Energy 2009;34:1937-43.

Reversible Solid State Hydrogen Storage System Integrated with PEM Fuel Cell

V.I. Borzenko, **D.V. Blinov**, **D.O. Dunikov**, **S.P. Malyshenko**, Joint Institute for High Temperatures RAS, Russia

Abstract

The results of International IPHE Project "Reversible Solid State Hydrogen Storage and Purification System for FC Power Supply" are presented. The project focused on the thermal and integration aspects of metal hydride technology of hydrogen storage and purification. The experimental part of the project included various system –scale metal hydride devices for purification and storage tests. Basing on the results of mathematical modeling, the optimized from the heat and mass transfer point of view low temperature metal hydride (AB_5 type) devices for the purification system were created and tested within the fully automatic purification system with capacity of 3000 st.l/hour. The test results of the 100 kg alloy hydrogen storage device integration with PEM FC also presented. It was shown experimentally, that, taking into account overall energy balance of the integrated system, it is possible to increase the total efficiency of the PEM FC based power supply system with low temperature traditional metal hydride storage. The ways for metal hydride units thermal performance improvement and capacity increase for different cases of the technology application are also presented and discussed.

1 Introduction

The basic barriers of metal-hydride hydrogen storage and purification technology are the following [1,2]**:**

- low weight capacity of hydrogen absorbing materials;
- low effective thermal conductivity of hydrogen absorbing materials beds;
- negative impurity influence on sorption process;
- the lack of knowledge of system effects at the integration of solid-state hydrogen storage systems and fuel cells.

In spite of the above mentioned disadvantages of traditional low temperature metal hydrides (wt. capacity <2%), the stationary applications on their base can find their niche at the market for example in back-up power, hydrogen purification for turbo generator cooling systems, energy accumulation for power production using renewable energy and others [3]. The transition from laboratory scale amounts of hydrogen absorbing materials and experimental MeH devices to system scale demands concentration on design optimization from the point of view of better heat transfer and system integration.

2 Optimized Hydrogen Absorbing Materials

New, low temperature AB_5 type alloys were manufactured in cooperation with Moscow State University [3] both for hydrogen storage and purification subsystems with respect to the

requirements of MeH storage and purification system and the requirements of commercial 5 kW PEM FC for initial pressure and hydrogen purity.

3 Experimental Apparatus

Complex test facility for investigations of heat and mass transfer peculiarities at hydrogen sorption in MeH devices of reactor and system scales was created at H2Lab [3], JIHT RAS, which included hydrogen preliminary purification subsystem (de-oxygenizer and dryer), experimental MeH hydrogen fine purification subsystem (5 kg of AB_5 alloy reactors, Figure 1), hydrogen storage subsystem (81 kg of AB_5 alloy single reactor, Figure 2) and commercial GenCore 5T (PlugPower) PEM fuel cell.

Type 1.

Type 2.

Type 3.

Figure 1: AB_5 (5kg) alloy hydrogen storage and purification reactors: Type 1 – cartridge type, Type 2, 3 – tube and shell type.

Figure 2: Tube-and-shell type hydrogen storage device, combined air and liquid cooling/ heating, 81 kg of AB_5 alloy.

4 Calculation Model

Mathematical model, created in cooperation with Moscow Power Engineering Institute [4-6], includes a set of 3D Navier-Stokes unsteady equations of mass and energy conservation for solid and gas and momentum equation for gas.

The main assumptions taken for the calculations are the following:

- Gaseous phase is homogeneous mixture of *N* components, one of which is hydrogen;
- Solid phase includes impermeable structures (unit walls), permeable “passive” structures (internal tube with porous wall), permeable “active” structures (layers of intermetallic particles);
- The gaseous phase is ideal from the thermodynamic viewpoint;
- Specific isobaric heat capacity of gas mixture components is constant;
- The viscous dissipation and compression work are negligible.

Closing equations: interface interaction, absorption/desorption kinetics, effective permeability and coefficient of effective thermal conductivity

5 Results of Calculation and Modeling

The qualitative correspondence of the experimental and calculation results (Figure 3.) gave good background for the optimization of real geometry of MeH reactors. The proposed heat exchanger types ranged from separate cartridge (Type 1) to tube-and-shell (Type 2,3) with two side cooling and heating.

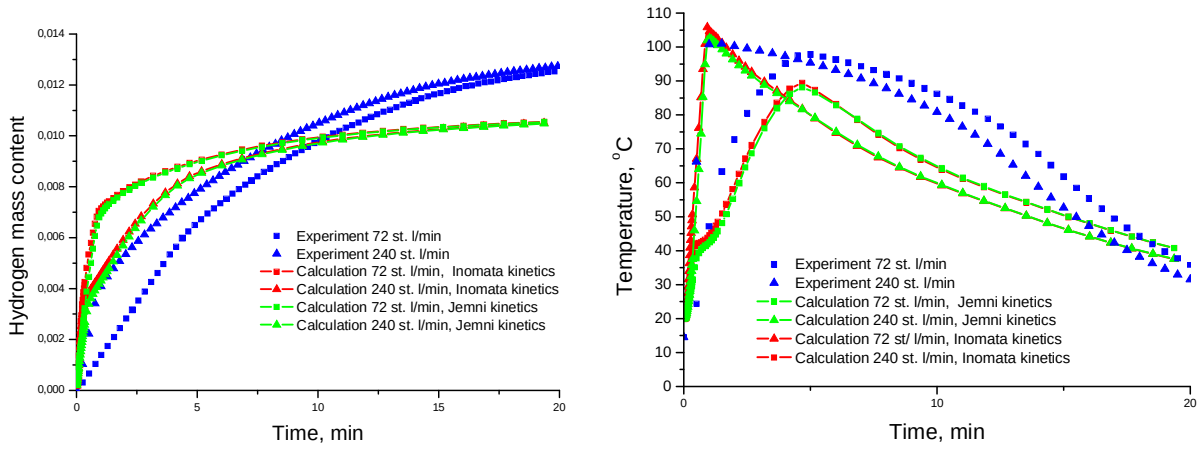

Figure 3: Hydrogen sorption in Type 1 reactor, verification of kinetics, constant hydrogen flow.

The problem of calculations and measurements correspondence can be solved by reliable PCT measurement and also by taking into account the scaling effect at transition from lab-scale to reactor-scale amounts of hydrogen absorbing materials.

6 Integration Results

Commercial GenCore 5B(T)48 Fuel Cell system was successfully supplied with hydrogen for nearly 4 hours with total hydrogen volume of up to 13 st. m^3 (Figure 4,5). The resources of low potential heat (FC coolant) cover the storage tank desorption needs, i.e thermal integration is possible.

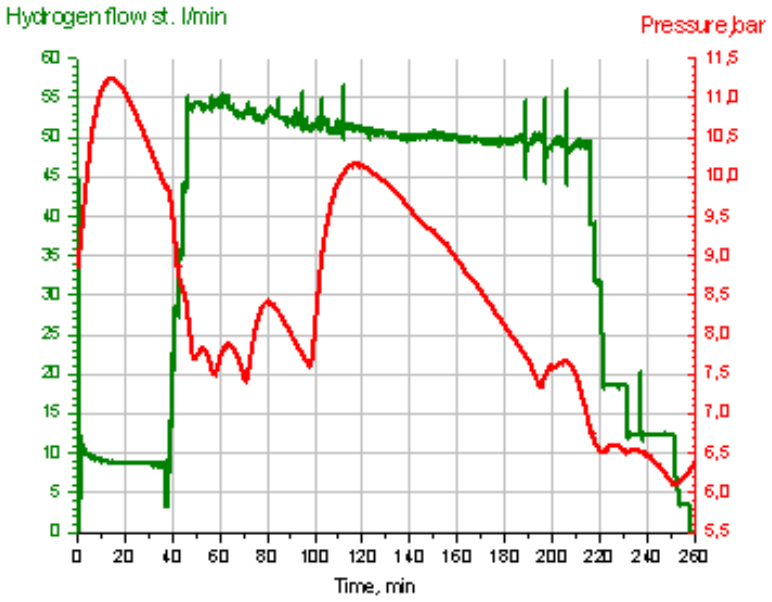

Figure 4: Operation of hydrogen storage device at FC supply.

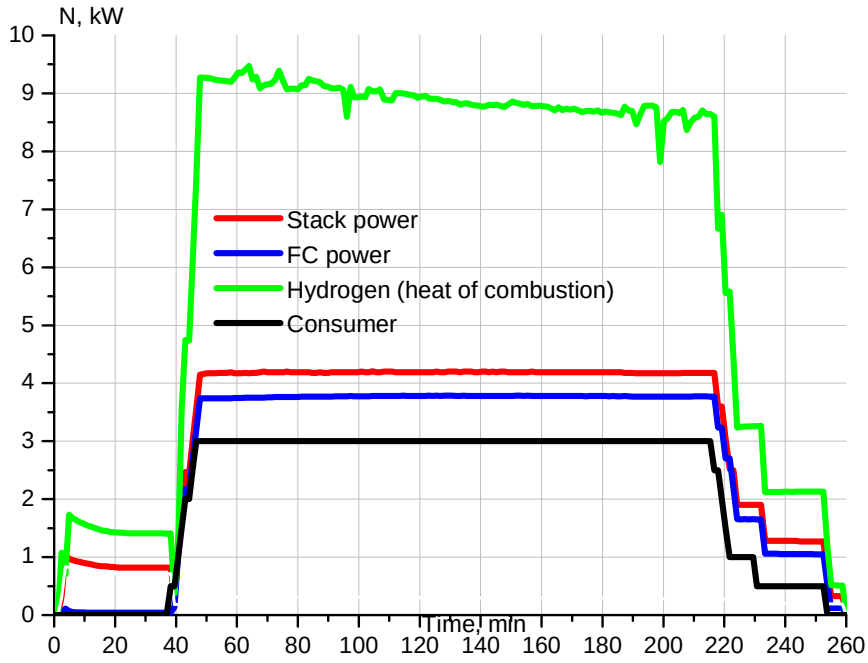

Figure 5: Energy parameters at operation of FC supplied by MeH hydrogen storage unit.

7 Purification

The approach to MeH fine purification is based on the useful feature of metal hydrides to selectively absorb hydrogen from the hydrogen containing gas. With this, the problem of metal hydride poisoning is very critical and must be solved according to the specific application. The investigations of purification in our experiments were carried out using inert gas admixtures and using low-cost technical hydrogen.

PSA-like mode for fine purification was proposed basing on the results of the experiments on MeH purification subsystem using reactors of Type 3. The essence of the operation mode is periodic admixture evacuation from the spare volume of MeH reactor which can be done in various ways, depending on the optimization target function (deeper purification or hydrogen saving): constant duration, constant final pressure and constant amount of gas. For the further development of the purification subsystem “constant lower pressure (atmospheric)” mode was selected (Figure 6.).

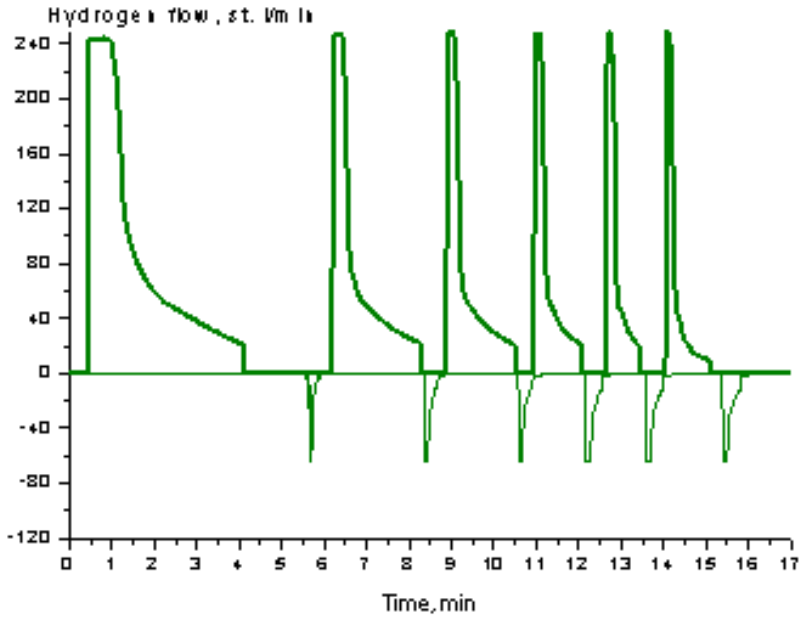

Figure 6: MeH reactor charging at PSA-like mode with admixture (3% inert gas) evacuation down to atmospheric pressure in the spare volume of the reactor.

The losses of hydrogen at this operation mode can reach 23% of the total flow, however other modes fail to provide the purity required by FC (99.95%).

8 Conclusions and Acknowledgements

The peculiarities of heat and mass transfer processes in fine-dispersed porous beds of solid hydrogen absorbing materials were studied both theoretically by modeling and experimentally in model reactor.

Reactor optimization on the base of developed 3D heat and mass transfer model was carried out and new types of reactors with enhanced thermal characteristics were created.

The feature of selective hydrogen sorption from hydrogen containing gas admixture was used for the creation of metal-hydride purification system for use in variable applications , PSA-like mode of purification was proposed and verified experimentally.

The ways for MeH storage and purification units integration with PEM FC were studied and the opportunity for overall efficiency of the fuel supply system was shown.

The possibility of system-scale utilization of traditional low temperature metal hydrides (AB_5) in power production units was experimentally proved.

The research was carried out as a part of the IPHE International Project “Reversible Solid State Hydrogen Storage and Purification System for FC Power Supply” (HSSS), endorsed in 2005 and was supported by Russian Federal Agency for Science and Innovations (State contracts #: 02.516.11.6150, 02.516.11.6016 and 02.516.11.6017) and Russian Foundation for Basic Research (Projects #: 06-08-01614-a, 07-08-12181-ofi)

References

[1] *Verbetsky V.A., Malyshenko S.P., Mitrokhin S.V., Solovey V.V*. Metal hydrides: Properties and practical applications // International Journal of Hydrogen Energy. 1998. V. 23. № 12. P. 1165.

[2] *Tarasov B.P., Lototskii M.V., Yartys V.A.* Problem of hydrogen storage and prospective uses of hydrides for hydrogen accumulation. Russian Journal of General Chemistry. 2007. T. 77. № 4. C. 694-711.

[3] Malyshenko S.P., Borzenko V.I., Dunikov D.O. et. al. Modeling of Thermophysical Processes in Me-H Cleaning Systems, Hydrogen Energy Progress XIII. Proc. of the 13th World Hydrogen Energy Conference, Beijing, China, June 12-15, 2000. V.2. P. 1323-1327

[4] *Artemov V.I., Lazarev D.O., Yan’kov G.G., Borzenko V.I., Dunikov D.O., Malyshenko S.P.* The effect of non-absorbable gas impurities on heat and mass transfer in metal-hydride devices for storage and purification of hydrogen. High Temperature. 2004. T. 42. № 6. C. 987-995.

[5] *Artemov V.I., Yankov G.G., Karpov V.E.* and Makarov M.V. Numerical Simulation of Processes of Heat-and-Mass transfer in Items of Heat and Power Equipment //Thermal Engineering. 2000. ‹ 7. V. 47. P. 632.

[6] *Borovskikh O.V., Lazarev D.O., Yan’Kov G.G., Artemov V.I.* Finning efficiency of a metal-hydride reactor’s active volume. Thermal Engineering. 2009. T. 56. № 3. C. 235 - 238.

Reactivity Improvement of Magnesium with Hydrogen by Carbon Nano-Material Mixing

Kenji Aikawa, Course of Metallurgical Engineering, Tokai University, Japan
Hideki Niimuma, **Haru-Hisa Uchida**, Department of Human development, Tokai University, Japan
Yoshitake Nishi, Department of Materials Science, Tokai University, Japan

Abstract

Proposing magnesium as a hydrogen storage material, we demonstrate quite interesting results of carbon nano-materials mixed into magnesium by mechanical milling in this study. Higher hydrogen reactivity can be obtained by multi wall carbon nano-tube (MWCNT) mixing which may enlarge the diffusion path in the sample powder particles. As a result, Mg with 0, 10, 20, 40 and 60 mass% of MWCNT exhibits drastically modified hydrogen absorption and desorption kinetics with more than 5 mass% H (including weight of catalyst) at 573-673K within 10min. under 6MPa of H_2.

1 Introduction

Hydrogen is expected in many application fields, especially in H_2 storage technique for fuel cell vehicle, where the available hydrogen density is an important factor. If the technological standard is considered, the hydrogen density of 5 ~ 7 mass% is required for the fuel cell vehicle [1]. Liquid hydrogen, which is one of the way of H_2 storage, realizes about 5 mass% of hydrogen density including the mass of container. However, the liquid hydrogen needs a lot of energy in cooling and yields unavoidable gas boil-off. On the other hand, H_2 storage materials exhibit higher hydrogen density even at room temperature. The volume density is, in most cases, higher than liquid hydrogen. However, a typical hydrogen storage material of $LaNi_5$ exhibits lower hydrogen density of only 1.4 mass%, which cannot be used for the vehicles.

Alkali-earth element of magnesium has been expected as a hydrogen storage material with a large hydrogen capacity. However, low hydrogen reactivity even at higher temperature is a significant problem for the practical utilization. Recently, for improving the sorption characteristics, we have reported the reaction kinetics of chemical hydrides with higher hydrogen density by mixing rare-earth oxide [2]. We have concluded that catalytic effect seems to be attributed to the hydrogen diffusion path generated in the hydride phase layer by rare-earth oxide.

In this study, carbon nano-material mixed into Mg has been demonstrated where the hydrogen sorption reactions and the density of hydrogen are drastically improved.

2 Experimental

2.1 Sample preparation

The mixture of MgH_2 (98%) and MWCNT(φ20~50nm) was mechanically milled in a rotary mill (IRIE SHOKAI Co., Ltd)(see Figure 1). MgH_2 and MWCNT were obtained from Wako Pure Chemicals. The mixing ratios of CNT / Mg were 1, 10, 20, 40 and 60 mass% in weight ratio, respectively. In this study sample preparation was carried out in a glove box under argon atmosphere. The condition of ball milling process is shown in Table 1.

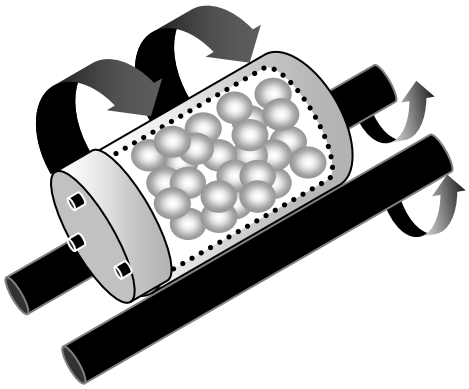

Figure 1: Rotaly ball-milling.

Table 1: Ball milling condition.

Rotating rate	180 rpm
Milling samples	Mg, MWCNT
Total weigth of the sample	1.5 g
Millimg period	25 hr
Milling atmosphere	Ar (99.999%)
Ball diameter and number	0.95mm×35
Volume ratio of vial vs. balls	1.7 : 1
Outside / Inside vial diameter	70.59 / 39.75 mm
Capacity of vial	70.33cm^3
Materials of vial / ball	18Cr-12Ni-2.5Mo-Low C. / 18Cr-8Ni

2.2 Sample analyses

The micro structure observation was carried out using SEM (Hitachi, S-3200N) and FE-SEM (Hitachi, S-4200) for the sample after ball milling. In addition samples were also observed by STEM (Hitachi HF-2200, 200kV) EDX (NORAN) and FIB (Hitachi) after the thinning preparation.

2.3 Measurement of hydrogen reactivity

Hydrogenation was carried out using high pressure Sievert's type apparatus. Sample in reaction tube was heated up to 673K . Dehydrogenation was carried out at 673K for several hours and cooled down to 573K under the high vacuum. After that, high purity hydrogen (7N) of 6MPa was then supplied at 573K. Afterwards hydrogenation was carried out at 573K. The process was repeated and initial reaction rate and hydrogen amount absorbed confirmed to be stabilized.

3 Results and Discussions

3.1 STEM image after ball milling

STEM image of MgH_2+ 40mass% MWCNT mixture after the ball milling of 25 hours is shown in Figure 2-(a). Fibrous form of WMCNT can be recognized. TEM image of MgH_2 + 40mass% MWCNT is shown in Figure 2-(b). Pillar form at the lower left is WMCNT. The difference of contrast indicate hole structures of MWCNT. From the figures we can understand that MWCNT is not broken even after long time of ball milling.

TEM cross section image and elementary distribution measured by EDX for the sample of Mg+ CNT 40mass% are shown Figure 3. Fiber forms of MWCNT can be confirmed also in the sample particle of Mg. Distribution of carbon indicates observed by EDX analysis, MWCNT exists also in the granulose Mg particle. These results show the possibility that MWCNT supply Mg particle diffusion passes for hydrogen inside.

3.2 Hydrogen Reactivity

Hydrogenation curves of MgH_2 and MgH_2 + MWCNT under 1MPa H_2 at 573K are shown in Figure 4. Addition of MWCNT exhibits an extremely accelerated reaction rate of hydrogen absorption. The sample absorbs H of 4wt% (excluding catalyst) within 10min.

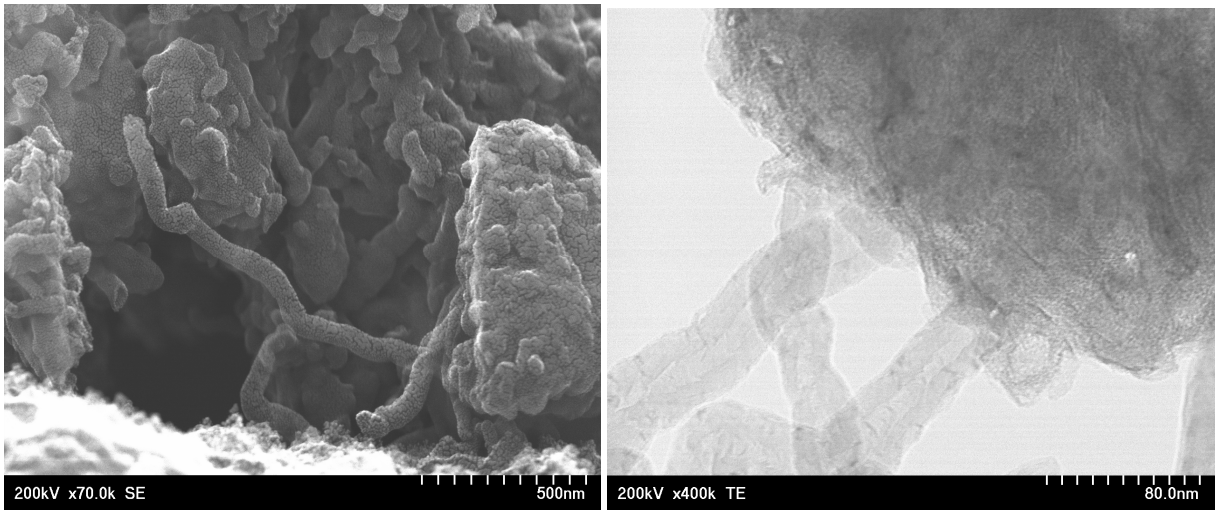

Figure 2: (a) STEM, (b) TEM images of After the ball milling of 25 hour of MgH_2+ CNT 40mass%.

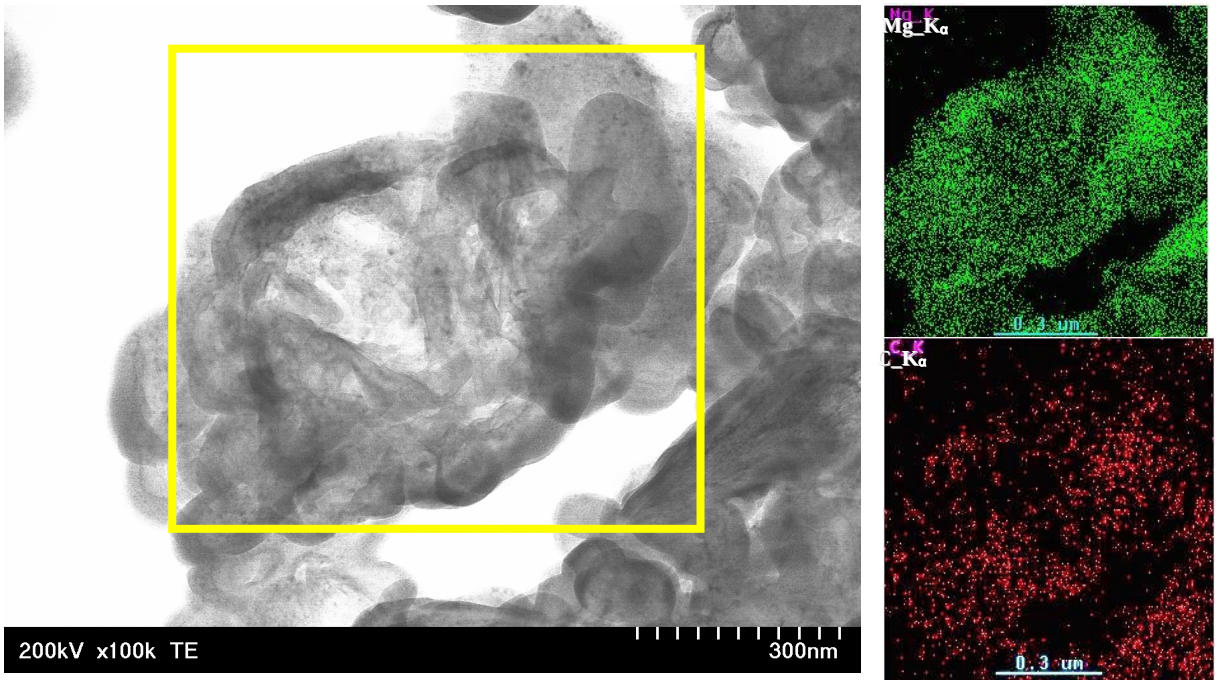

Figure 3: TEM and EDX images of Cross section observation of Mg+ CNT 40mass%.

In general, hydrogen absorption of Mg is controlled by diffusion of H atom through hydride layer in surface region. The precise reaction mechanism is not well known; however, catalysis of MWCNT distributed in the particle of Mg accelerates the diffusion of H atoms into the particle. Pressure dependence of the initial rate indicates a tendency of a change from diffusion to dissociation controlled reactions by the addition of MWCNT. The mechanisms of the reaction should be investigated further more.

Amount of MWCNT is also an interesting factor. Initial reaction rate and hydrogen absorption (including catalyst) at 10800 sec with different amount of MWCNT are shown in Figure 5. Initial reaction rate depends on the amount of MWCNT. From the Figure 5, increasing amount of MWCNT accelerates the initial sorption rate while decreasing the hydrogen density absorbed if the mass of MWCNT is included. In this study, therefore, 1~10mass% seems to be the best ratio of the mixture for both initial reaction rate and hydrogen absorption density.

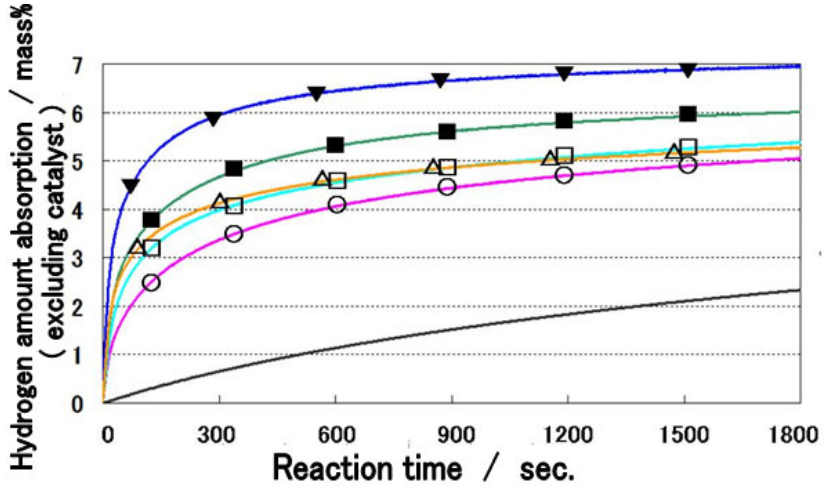

Figure 4: Hydrogen absorption of Mg and Mg + MWCNT with different amount of MWCNT.

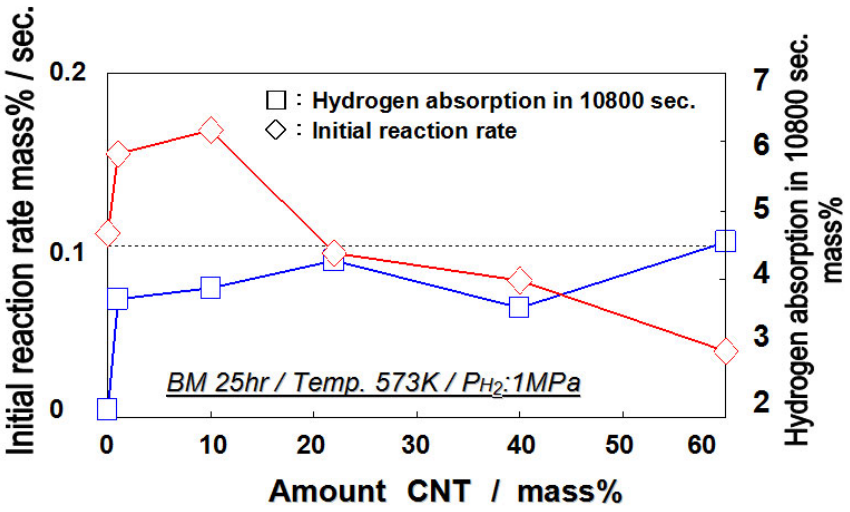

Figure 5: Initial reaction rate and hydrogen absorption density (excluding MWCNT) after 10800 sec for the sample with different amount of MWCNT.

4 Conclusion

A fuel cell vehicle needs to carry hydrogen of 7kg in the near future. In case of utilizing $LaNi_5$ (1.4wt% H), metal of 500kg is necessary. On the other hand, in case of Mg (6.0wt% H), only 120kg is enough for carrying the same amount of hydrogen, where the weight can be reduced to 25% if Mg is available.

Mg + MWCNT mixture by ball milling shows a more suitable reactivity for the practical hydrogen sorption reaction. Rate controlling step of hydrogenation of pure Mg is in generally considered as diffusion of H atom in magnesium hydride layer on the surface because of the ion bonding with matrix. In this study, mixing of MWCNT is demonstrated for realizing an increased reaction rate, where the MWCNT may give the paths of fast ab- and desorption. Additionally, amount CNT is a dominant factor for the sorption rate. By increasing amount

MWCNT, initial reaction rate also increases, while if the hydrogen density is considered, 1~10 mass% is the appropriate amount of the mixing.

References

[1] NEDO: Development for Safe Utilization and Infrastructure of Hydrogen, 2008

[2] Atsushi Uemura et al: J. Mat. Sci. Vol.72, No.3, p.224-228, 2008

Improvement of the Electrochemical Hydrogen Storage Performance of Mg-Based Alloys by the Various Partial Replacement Elements

Mustafa Anik, **Gizem Özdemir**, Eskisehir Osmangazi University, Metallurgical and Materials Eng. 26480, Eskisehir, Turkey

1 Introduction

Mechanically alloyed Mg-based hydrogen storage alloys attract great attention as the negative electrodes for the nickel–metal hydride (Ni/MH) rechargeable batteries which have considerable potential for the utilization in cordless tools and electric vehicles [1-8]. The large scale practical applications, however, can only be possible if these alloys could be developed with the superior rate capabilities.

Modification of the alloy composition by the partial replacement of Mg is a common practice to improve the electrode performance of the Mg-based alloys [9]. In this work, as the continuation of our attempts to develop a high performance Mg-based negative electrode alloy by the composition modifications [9-13], MgNi, $Mg_{0.9}Zr_{0.1}Ni$, $Mg_{0.9}Ti_{0.1}Ni$ and $Mg_{0.9}Al_{0.1}Ni$ alloys were synthesized by mechanical alloying and the effects Zr, Ti and Al replacement elements on the electrochemical hydrogen storage characteristics of MgNi alloy were observed .

2 Materials and Methods

Elemental Mg, Ni, Ti, Zr and Al powders were mixed in various compositions and charged into the stainless steel vials under the high purity Ar atmosphere. The diameter of the stainless steel balls was 5 mm and the ball to powder weight ratio was selected as 20:1. The mechanical alloying was performed with a planetary ball mill and the milling speed was 500 rpm. The ball milling duration was selected as 25 h. The mechanical alloying was carried out by milling for 30 min in the forward direction then cooling for 15 min and then milling for 30 min in the reverse direction.

The phase structure of the alloy powders was examined by the X–ray diffractometer (Bruker axs D8) using Cu Kα radiation. The powder morphologies were observed by ZEISS SUPRATM 50 VP Scanning Electron Microscope (SEM). The size of the powders was measured by Model ALV CGS-3 compact goniometry system (dynamic light scattering).

Working electrodes were prepared by mixing 0.2 g alloy powder with 0.6 g nickel powder and then cold pressing into pellets of 10 mm in diameter, under a pressure of 10 ton cm^{-2}. $NiOOH/Ni(OH)_2$ counter electrode and a Hg/HgO reference electrode were used to set up a three-electrode cell in 6 M KOH solution. Tests were performed with PARSTAT Model 2273 potentiostat/galvanostat unit. The charge current density was 100 mA g^{-1} and the charging

was carried out down to the severe gassing potential. The discharge current density was 25 mA g^{-1} and the discharge cut-off potential was -0.6 $V_{Hg/HgO}$.

3 Experimental Results and Discussion

3.1 The structural and morphological characteristics

The overlaid XRD patterns of MgNi, $Mg_{0.9}Zr_{0.1}Ni$, $Mg_{0.9}Ti_{0.1}Ni$ and $Mg_{0.9}Al_{0.1}Ni$ alloys are shown in Figure 1. All the alloys give almost the same pattern with a broad peak around 41.5° which can be assigned to amorphous structure (or to the mixture of amorphous/nano-crytalline structure). The peaks for any particular structure and for any element in each alloy could not be observable in Figure 1.

The typical powder morphology of 25 h milled alloys is illustrated in the scanning electron micrograph in Figure 2a. The fragmentation of the coarse, cold-welded particles into the fine powders in these figures shows the typical morphology of the powders synthesized by the ball milling. The size distribution of the disintegrated particles of 25 h milled alloys is provided in Figure 2b. The average radius of the particles looks approximately 0.9 micron in Figure 2b.

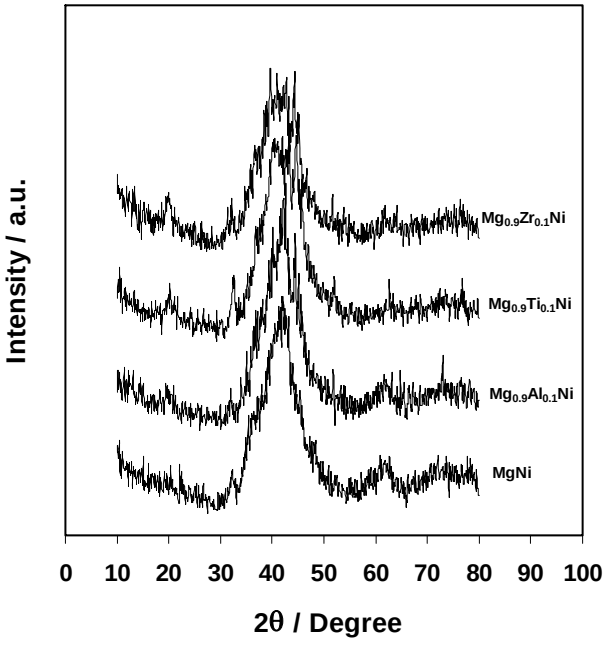

Figure 1: Overlaid XRD patterns of the alloys synthesized by 25 h milling.

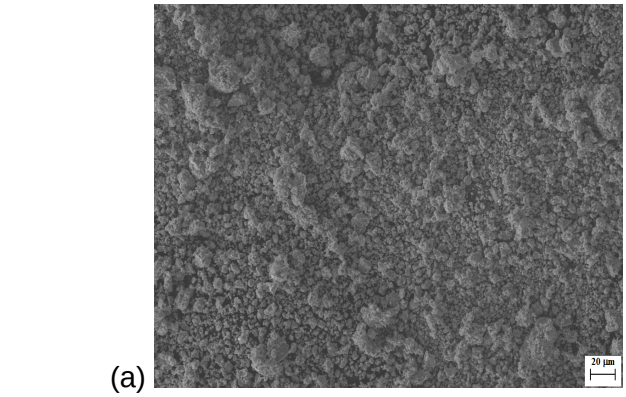

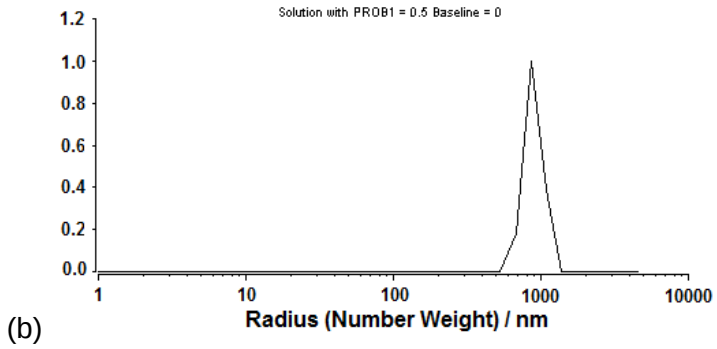

Figure 2: (a) Typical powder morphology and (b) powder size distribution of the alloys.

3.2 The cycle stability of the alloys

The variations in the discharge capacities of 25 h milled MgNi, $Mg_{0.9}Zr_{0.1}Ni$, $Mg_{0.9}Ti_{0.1}Ni$ and $Mg_{0.9}Al_{0.1}Ni$ alloys depending on the charge/discharge cycle numbers are depicted in Figure 3. The cyclic stabilities of the alloys are also evaluated by observing the capacity retaining rates, which are defined as $C_n/C_{max.}$ x 100% ($C_{max.}$ is the initial discharge capacity and C_n is the discharge capacity at n^{th} charge/discharge cycle), as in Figure 4.

The initial discharge capacities of MgNi, $Mg_{0.9}Zr_{0.1}Ni$, $Mg_{0.9}Ti_{0.1}Ni$ and $Mg_{0.9}Al_{0.1}Ni$ alloys were 495, 507, 491 and 403 mA h g^{-1}, respectively. Zirconium increases the initial discharge capacity slightly in Figure 3. In fact, the big-size Zr atoms (Mg = 1.72 A°, Ni = 1.62 A°, Zr = 2.16 A°) can create extra sites for the hydrogen storage in the alloy crystal structure and thus the alloy capacity increases. The cyclic performance of the alloy in the presence of Zr, however, did not show considerable improvement in Figure 4 ($Mg_{0.9}Zr_{0.1}Ni$ alloy keeps 52% of its initial capacity at 10^{th} charge-discharge cycle). The alloy cyclic performance increases significantly in the presence of Ti replacement element. While MgNi keeps 48% of its initial capacity, $Mg_{0.9}Ti_{0.1}Ni$ alloy keeps at least 70% of its initial discharge capacity at 10^{th} charge-discharge cycle in Figure 4. It is believed that Ti segregates to the surface and makes the alloy surface more penetrable by atomic hydrogen during the alloy cycling [14]. Although $Mg_{0.9}Al_{0.1}Ni$ alloy has low initial discharge capacity, the capacity retention rate of this alloy is acceptable. The capacity retention rate of Al-including alloy was 60% at 10^{th} charge-discharge cycle in Figure 4. This positive contribution of Al replacement element is generally attributed to the selective dissolution of the disseminated Al_2O_3 throughout the barrier

$Mg(OH)_2$ surface layer [9,10]. The selective dissolution makes the barrier hydroxide layer porous and more permeable for hydrogen, and thus the alloy cyclic stability gets better.

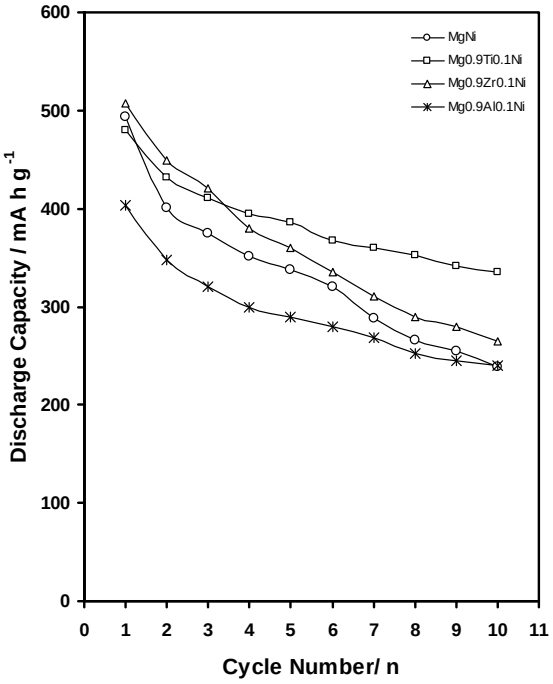

Figure 3: Discharge capacities as a function of cycle number.

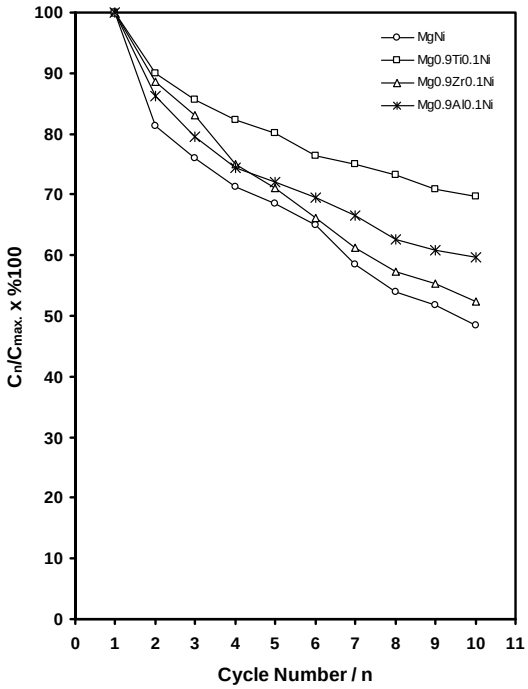

Figure 4: Cyclic stability as a function of cycle number.

References

[1] P. Selvam, B. Viswanathan, C.S. Swamy, V. Srinivasan, Int. J. Hydrogen Energy 11 (1986) 169-192.

[2] N. Cui, B. Luan, H.K. Liu, H.J. Zhao, S.X. Dou, J. Power Sources 55 (1995) 263-267.

[3] L. Zaluski, A. Zaluska, J.O. Ström-Olsen, J. Alloys Comp. 217 (1995) 245-249.

[4] S. Orimo, H. Fujii, Intermetallics 6 (1998) 185-192.

[5] N. Cui, P. He, J.L. Luo, Acta Mater. 47 (1999) 3737-3743.

[6] M. Dornheim, S. Doppiu, G. Barkhordarian, U. Boesenberg, T. Klassen, O. Gutfleisch, R. Bormann, Scripta Mater. 56 (2007) 841-846.

[7] M. Jurczyk, L. Smardz, I. Okonska, E. Jankowska, M. Nowak, K. Smardz, Int. J. Hydrogen Energy, 33 (2008) 374-380.

[8] X. Zhao, L. Ma, Int. J. Hydrogen Energy 34 (2009) 4788-4796.

[9] M. Anik, J. Alloys Comp. 486 (2009) 109-114.

[10] M. Anik, H. Gasan, S. Topcu, I. Akay, N. Aydinbeyli, Int. J. Hydrogen Energy, 34 (2009) 2692-2700.

[11] M. Anik, I. Akay, S. Topcu, Int. J. Hydrogen Energy 34 (2009) 5449-5457.

[12] M. Anik, I. Akay, G. Ozdemir, B. Baksan, Int. J. Hydrogen Energy 34 (2009) 9765-9772.

[13] M. Anik, J. Alloys Comp. 491 (2010) 565-570.

[14] J.J. Jiang, M. Gasik, J. Power Sources 89 (2000) 117-124.

Development of Intermetallic Compounds for Hydrogen Supply System Integrated with PEM Fuel Cell

D.O. Dunikov, I.A. Romanov, Joint Institute for High Temperatures of Russian Academy of Sciences, Russia
S.V. Mitrokhin, Moscow State University, Russia

Fuel cell power units require high quality hydrogen [1] and problem of their hydrogen supply with the use of intermetallic compounds, which selectively absorb hydrogen from gas mixture and can desorb it at needful parameters, thus excluding hydrogen purification and compression and utilizing waste heat from the fuel cell increasing overall energy efficiency of the power unit.

On the other hand not all the admixtures are safe for intermetallic compounds during hydrogen sorption. The admixtures can be divided into five groups according their influence on sorption capacity and durability of intermetallic compounds [2, 3], Table 1 summarize results for T = 20–100°C and P = 0.001–50 bar. Thus metal hydride hydrogen supply system can purify hydrogen from admixtures of groups 1-3 and requires preliminary purification from oxygen, water and CO (burner and dryer), and sulfur compounds.

Table 1: Influence of admixtures on hydrogen sorption properties of intermetallic compounds.

Group	Admixture	Type of interaction with surface of particles	Number of cycles, N*
1	Ar, He, N_2, CH_4, C_2H_6,…	«Inert»	>1000
2	CO_2, (NH_3),…	Chemisorption without poisoning	~1000
3	C_2H_4, C_2H_2, (C_3H_6),…	Catalytic hydrogenation	~1000
4	O_2, H_2O,…	Chemical reaction	~100
5	CO, SO_2, H_2S, (CH_3SH),...	«Poisoning»	1–2

The following design scheme of metal hydride system can be proposed:

1. Purification system (preliminary purification and metal hydride purification units) – fast operating, compact, easily replaceable high durable intermetallic compound;
2. Metal hydride hydrogen storage unit – thermally coupled with fuel cell, intermetallic compound with high hydrogen capacity.

JIHT RAS experimental setup consist of source of hydrogen, solid-state purification and storage system and 5 kW PEM fuel cell. Water at temperatures from 293 up to 353 K (25 and 80 °C respectively) is used to control absorption and desorption process. Main advantages of

* Number of hydriding/dehydriding cycles for which hydrogen capacity of storage material decreasing in 2 times for concentration of admixture 0.1% vol.

this scheme are possibility of using of impure hydrogen, simplicity, reliability and safety (Figure 1).

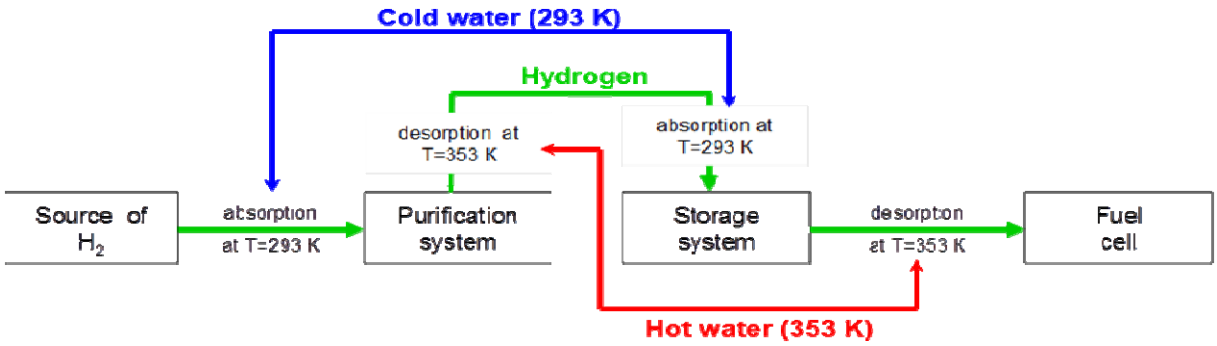

Figure 1: Principle design of 5 kW PEM fuel cell based power unit with solid state purification and storage system.

Two types for hydrogen storage materials are used: purification alloy and storage alloy. Requirements for the purification alloy are: (i) hydrogen absorption pressure must be lower than 1 bar at 293 K to minimize hydrogen losses during purification process; (ii) hydrogen desorption pressure must be as high as possible at 353 K for efficient charging of hydrogen storage unit; (iii) alloy must have good cycle ability. Requirements for the storage alloy are: (i) low absorption pressure at 293 K to make charging easier; (ii) desorption pressure along the whole plateau at 353 K must higher than 6 bar to meet fuel cell power unit requirements for hydrogen supply; (iii) alloy must have good cycle ability.

Alloys compositions was chosen with the use of semi empirical mathematical model, which represents thermodynamic parameters of unknown alloy at hydrogen desorption as a sum of the parameters of the well-investigated alloys with different coefficients [4]. Experimental samples was prepared and investigated by Siverts method and two alloys was chosen [5] for purification and storage units (Table 2).

Table 2: Properties of alloys.

Alloy composition	P_{eq}, bar		Hydrogen storage capacity, % wt.		ΔH_{des}, kJ/mole H_2
	298 K	353 K	298 K	353 K	
Storage alloy $La_{0.5}Nd_{0.5}Al_{0.1}Fe_{0.4}Co_{0.2}Ni_{4.3}$	1.1	11.6	1.1	1	35.3
Purification alloy $LaFe_{0.1}Mn_{0.3}Ni_{4.8}$	0.66	7.6	1.3	1.2	40.4

Purification alloy $LaFe_{0.1}Mn_{0.3}Ni_{4.8}$. was tested on admixture resistance and durability. To model the operation of purification unit a sample of alloy was placed into the autoclave and cycled with impure (nitrogen, oxygen, water) hydrogen at 7 bar and 353 K. Hydrogen storage

capacity was measured after each cycle by Siverts method. It is found that absorption of technical hydrogen leads to decreasing of hydrogen capacity down to 20-30% during 25 cycles (Figure 2, left). After 30 absorption/desorption cycles autoclave was set under vacuum conditions and alloy sample was cycled with high purity hydrogen from metal hydride accumulator at 7 bar and 353 K. Hydrogen storage capacity is measured after each cycle (Figure 2, right). There was performed 3 consecutive series of experiments. It is found that making of 7-10 absorption/desorption cycles with high purity hydrogen allows to regenerate hydrogen capacity up to 95% from the initial value.

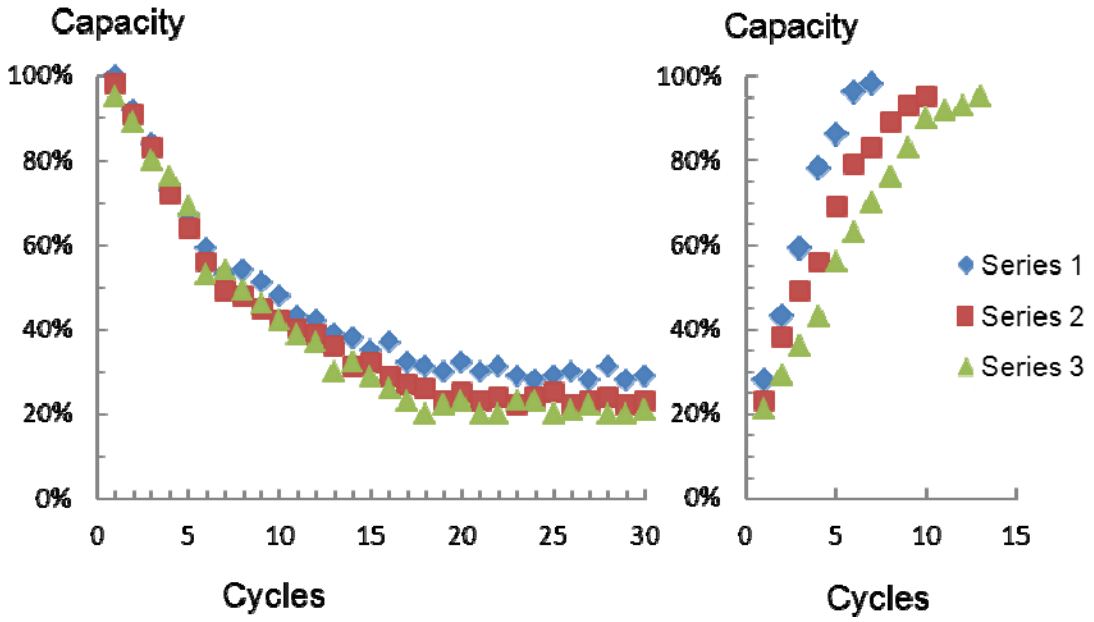

Figure 2: Degradation in impure hydrogen (left) and regeneration in pure hydrogen (right) of 4 g sample of $LaFe_{0.1}Mn_{0.3}Ni_{4.8}$ in three consecutive series of experiments.

It is obvious that multiple regeneration cycles are inconvenient for practical applications, losses of hydrogen and energy will be too high. In this connections experiments with single regeneration cycle were made. An experimental reactor was filled with 489 g of purification alloy $LaFe_{0.1}Mn_{0.3}Ni_{4.8}$. The reactor is a cylindrical vessel with thick steel walls, placed inside liquid bath of thermostat. Between sorption/desorption cycles alloy was poisoned with air from atmosphere. Parameters of experiments are presented in Table 3. Results (Fig. 3) show that dynamics of hydrogen sorption is influenced by air poisoning of alloy but not as great as experiments on smaller sample predict. Also even one cycle of regeneration with pure hydrogen improves the situation.

Table 3: Parameters of experiments on air poisoning of $LaFe_{0.1}Mn_{0.3}Ni_{4.8}$ alloy.

#	Regime	Gas	Thermostat	#	Regime	Gas	Thermostat
1	Sorption	H_2, 7 bar	10°C	4	Sorption	H_2, 7 bar	40°C
	Desorption	to 1 bar	90°C		Desorption	to 1 bar	90°C
	Poisoning	Air for 3 h	90°C		Poisoning	Air for 1 h	40°C
2	Sorption	H_2, 7 bar	10°C	5	Sorption	H_2, 7 bar	40°C
	Desorption	to 1 bar	90°C		Desorption	to 1 bar	90°C
3	Sorption	H_2, 7 bar	10°C	6	Sorption	H_2, 7 bar	40°C
	Desorption	to 1 bar	90°C		Desorption	to 1 bar	90°C

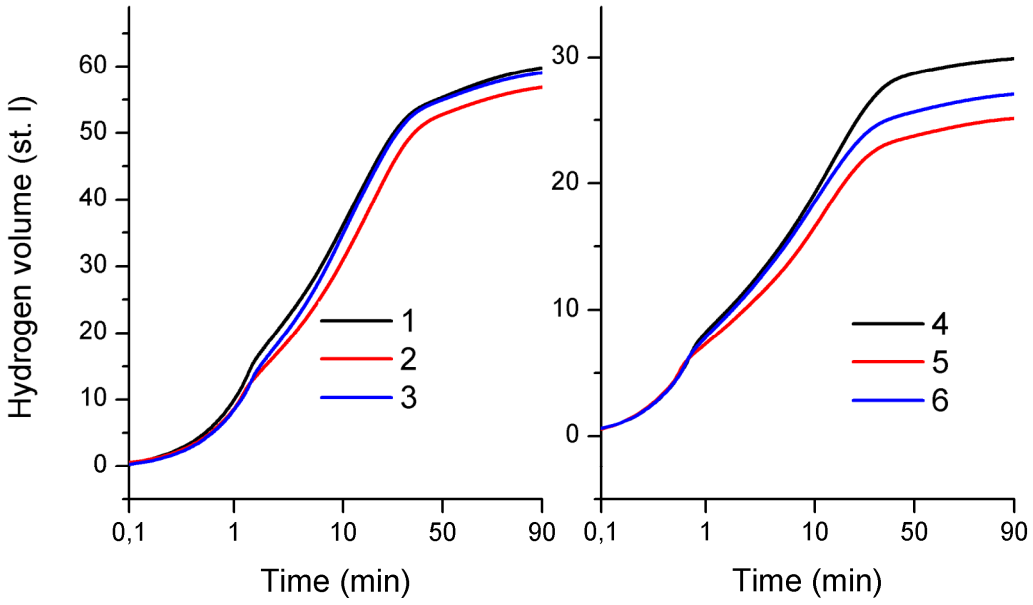

Figure 3: Charged hydrogen for different cycles during experiments on alloy poisoning/regeneration (parameters see in Table 3).

Conclusions

Due to selective absorption of hydrogen intermetallic compounds are good for hydrogen storage and purification in hydrogen supply systems for PEM fuel cells. On the other hand properties of hydrogen storage materials are influenced by impurities in hydrogen and several types of impurities (water, oxygen, sulfur, etc.) can greatly reduce their sorption capacity and durability. It is proposed to use preliminary purification to avoid poisoning of hydrogen storage materials.

For experimental 5 kW PEM fuel cell it is proposed to use the following design of hydrogen supply system:

1. Purification system – fast operating, compact, easily replaceable high durable intermetallic compound. Consists of preliminary purification unit (catalytic burner and dryer) and metal hydride purification unit (LaFe0.1Mn0.3Ni4.8 alloy is chosen);
2. Metal hydride hydrogen storage unit – thermally coupled with fuel cell, intermetallic compound with high hydrogen capacity (for further experiments La0.5Nd0.5Al0.1Fe0.4Co0.2Ni4.3 alloy is chosen).

Experiments on $LaFe_{0.1}Mn_{0.3}Ni_{4.8}$ shows that impurity can greatly reduce quality of the storage material, but it can be regenerated with pure hydrogen. Experiments on reactor scale sample show that even one recharging with pure hydrogen can improve hydrogen sorption rate after air poisoning of alloy.

Acknowledgments

Authors would like to thank Tarasov B.P. for consultation, Borzenko V.I and Zhemerikin V.D. for the aid in experimental work and Russian Ministry for Education and Science (state contracts 02.516.11.6150, 02.516.11.6016 и 02.516.11.6017) and Russian Foundation for Basic Research (grants 06-08-01614 and 07-08-12181) for financial support.

References

[1] Besancon B., et al., Hydrogen quality from decarbonized fossil fuels to fuel cells, International Journal of Hydrogen Energy. 2009. V. 34. № 5. P. 2350

[2] Tarasov B.P., Shilkin S.P., Interaction of LaNi5 and CeCo3 intermetallic compounds with hydrogen in the presence of Ar, CH4 and CO2, Russian Journal of Inorganic Chemistry. 1994. V. 39(1), PP. 16-19.

[3] Tarasov B.P., Shilkin S.P., Effect of O2, CO and SO2 on hydrogen sorption properties of LaNi5 and CeCo3 intermetallic compounds, Russian Journal of Inorganic Chemistry. 1995. V. 40(5), PP. 713-718.

[4] Smirnova T.N., Mitrokhin S.V., Verbetsky V.N., Hydrogen Interaction with alloys of Ti(Zr)-Mn-V Systems, in Hydrogen Materials Science and Chemistry of Metal Hydrides. NATO Science SeriesII: Mathematics, Physics and Chemistry, vol.82, 2002, 107-112.

[5] Mitrokhin S., Romanov I., Development of intermetallic compounds for hydrogen supply of PEM fuel cell, Proc. of 17th World Hydrogen Energy Conference, 15-19 June 2008, Brisbane, Australia.

The Effect of the Self-Heating Rate on Hydrogen Generation in Quasi-Adiabatic Systems "Aluminum Nanopowder – Water"

A. A. Gromov[*], **A. G. Kabardin**, Tomsk Polytechnic University, Lenin Prospekt, 30, Tomsk, 634050, Russia
A. B. Vorozhtsov, Institute for Problems of Chemical & Energetic Technologies, SB RAS, Biysk, 659322, Russia

1 Introduction

Studies of the interaction of aluminum nanopowder (ANP, a_s = 100 nm) with water are conducted to determine the physicochemical properties of ANPs themselves, prepare ecologically friendly reactive monofuels (whose condensed combustion products are aluminum oxides and hydroxides) [1,2] and high-porosity oxide hydroxide structures (metalloceramic and filtering materials etc.), and design mobile hydrogen sources on the basis of ANP hydroreaction systems for combustion or catalytic oxidation. Chemical reagents that decompose with the release of hydrogen are of the greatest interest as mobile hydrogen generators. The largest amount of hydrogen is contained in alkali metal hydrides and borohydrides (LiH, NaH, LiBH, and NaBH). Hydrides are, however, hydrophilic, and borohydrides are toxic. Alkali metals are reactive, expensive, and require storage under organic liquids. They vigorously react with water in the combustion mode (with the ignition of hydrogen released). Conversely, group IV–VII metals are unreactive toward water. The Al and Mg metals are of interest for creating mobile "hydrolysis" sources of hydrogen. Their properties are stable, and hydrolysis products are not toxic. The problem with using compact Al and Mg in reactions with water is their low activity (passivation of metal surfaces with insoluble compounds during hydrolysis). It was found in preliminary experiments that the hydrolysis of aluminum plates or magnesium and aluminum–magnesium alloy powders can be performed in solutions in alkalis at pH 11–12. Ideally, a hydrogen-generating system should consist of only two substances, a reducing agent (metal) and oxidizer (water), and hydrogen release should begin at room temperature. The "water–Al" system is capable of producing 1.2 liters of H_2 per 1 g of aluminum under normal conditions. Studies directed to the optimization of the characteristics of systems "water–Al" concentrate on the problem of increasing the reactivity of aluminum powder. For instance, coarse-grained aluminum powders (aluminum spherical disperse ASD-1 and ASD-4, aluminum powder, and aluminum pigment powder) passivated with paraffin completely react with 5 % aqueous NaOH during several months and are of no interest for designing mobile hydrogen sources. ANPs passivated, for instance, with Al_2O_3 are fully hydrolyzed in 5 % aqueous NaOH in 1–2 min [3]. If a solution does not contain alkali, solution temperature increasing from 20 to 80°C results in an explosive reaction between ANP and water [4]. The hydrolysis of ANP yields insoluble

[*] Corresponding author, email: a_a_gromov@yahoo.com

aluminum oxides and hydroxides, but their high dispersity does not interfere with the supply of new liquid oxidizer portions to the fresh surface of aluminum. In this work, we studied the influence of heating temperature, medium pH, admixtures of metal cations, and the type of passivating coating on ANP on the kinetics of self-heating in reactions between aluminum nanopowders and water. The objects of study (ANP) were nanopowders prepared by the electrical explosion of wires [5]; these powders are produced on an industrial scale, their properties are stable, and the content of metal in them does not change during 5–6 years [6].

2 Experimental Part and Discussion

Aluminum nanopowders

The ANPs were prepared by electrical explosion in gaseous argon with 10 vol. % hydrogen at an excess pressure of 0.15 MPa. The diameter and length of aluminum wires were 0.3 and 75 mm, respectively. After the preparation of ANP, it was passivated by slow oxidation with air (particles were coated with aluminum oxide) and various reagents, including nickel, boron, fluorine, and aluminum stearate and oleate (Table 1).

H_2O–ANP suspensions

Aqueous suspensions were prepared from ANP and warm (~50°C) distilled water, and various reagents and additives were introduced into them. A suspension was continuously stirred and heated in a thermostat to 64–66°C , and stirring was then continued without heating. Temperatures were measured from the beginning of suspension heating (~50°C) to its cooling after reaction termination (~25°C). The reaction products were dried in air at room temperature and analyzed.

An analysis of the phase and chemical composition and morphology of the reagents and products

The phase composition of reaction products was determined on a Rigaku D-MAX/B diffractometer. The content of aluminum metal in ANP and reaction products was determined volumetrically, from the volume of hydrogen released in the reaction of samples with a 10% solution of NaOH. The microstructure of initial ANPs and hydrolysis products was studied using a JEOL 6500F scanning electron microscope. The specific surface area of initial powders and hydrolysis products was measured by the Brunauer–Emmett–Teller (BET) method on an ASAP 2020 instrument.

Table 1: Characteristics of ANP and, for comparison, industrial PAP-2 powder (scaly particles, GOST (state standard) 5494-95)

No.	Powder (coating)	s_{sp}, m^2/g	a_s, nm	c_{Al}, wt %
	PAP-2 (paraffin)	5.4	397	94
1	ANP (Al_2O_3)	18.6	115	78
2	ANP (B)	12.0	179	84
3	ANP (Ni)	40.7	237	53
4	ANP (F)	11.6	284	81
5	ANP (stearate)	12.1	177	79
6	ANP (oleate)	14.3	150	45

Note: s_{sp} is the specific surface area; a_s is the mean-surface diameter of particles, for spherical Al particles, $a_s = (6/2.7)s_{sp}$; and c_{Al} is the content of aluminum metal in ANP.

The characteristics of passivated ANPs

A decrease in the specific surface area of samples 4, 5, and 6 (Table 1) passivated in fluorinated dodecanol and stearic and oleic acids, respectively, compared with samples 1–3 passivated by the "dry" method is related to a substantial amount of residual solvents on particles (Table 1). This is substantiated by a decrease in the content of aluminum in samples 4–6 and 3. The decrease is maximum for aluminum nanopowder passivated by stearic acid (up to 45 wt %). Coating with organic reagents substantially decreases specific metal contents in powders. With a boron coating, the decrease is less substantial. For ANP coated with nickel, metal content is low, but the specific surface area is high.

ANPs in the reaction with water

According to the stoichiometry, the complete oxidation of 27 g (1 mol) of Al requires 54 g (3 mol) of H_2O (1).

$$Al + 3H_2O \rightarrow Al(OH)_3 + (3/2)H_2\uparrow + 459\ kJ. \quad (1)$$

Because of heat release in the reaction, the temperature of the mixture increases. When an "open" reaction system is heated to 100°C, the oxidation of Al requires an additional amount of water because of its intense vaporization.

The influence of heating on the kinetics of heat release in the H_2O–ANP system

In spite of the high chemical activity of ANP, the oxidation of aluminum with water must be initiated, because aluminum nanoparticles are always coated with a passivating oxide film. The oxidation of ANP with water was intensified by heating suspensions. The temperature of heating (64–66°C) was adjusted experimentally (Figure 1). At this temperature, spontaneous suspension self-heating began because of heat release in the chemical reaction. When

suspensions were heated to lower temperatures, the rate of oxidation was comparatively low, and the reaction occurred without self-heating. Heating above 66°C caused a rapid acceleration of self-heating without an induction period, which complicated recording thermograms of the hydrolysis of ANP. When an H_2O–ANP suspension heated to 64–66°C was continuously stirred (Figure 1, I) in the absence of external sources of heating (Figure 1, II), the thermal process was characterized by induction period τ followed by an increase in temperature to its maximum value *T* max (Figure 1). After this, the colour of the suspension changed from black (the colour of ANP) into light gray (the colour of suspensions after oxidation).

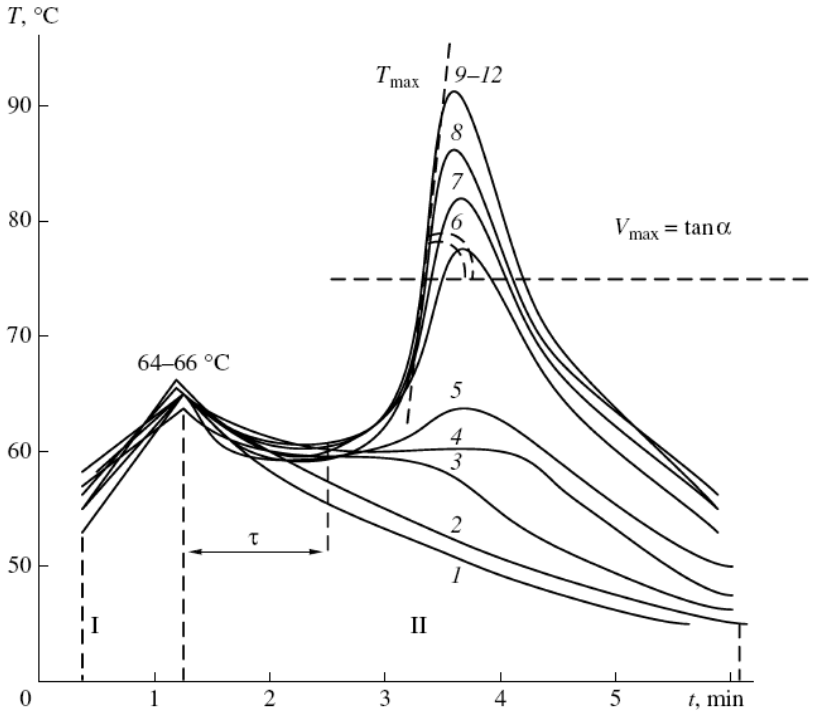

Figure 1: Kinetic curves of temperature variations during the interaction of ANP with liquid water; I, simultaneous suspension heating and stirring; II, suspension stirring only; τ is the induction period, min; v_{max} is the highest temperature growth rate, K/s; T_{max} is the highest suspension (water) temperature; 1,2, …, 12 are suspension numbers with different ANP contents (Table 2)

The maximum suspension self-heating temperature when ANP interacted with water depended on the content of ANP. At an H_2O : ANP ratio of from 84 to 126, the process occurred at a low rate and without suspension self-heating (Table 2, samples 1–3). At higher ANP contents (H_2O : ANP = 56–72), no self-heating was recorded (Figure 1, Table 2, samples 4, 5), but aluminum was oxidized. This follows from hydrogen release and the presence of aluminum hydroxides in the dried product according to the X-ray data. Suspensions with still higher ANP contents (H_2O : ANP = 8–25) were characterized by self-heating with intense heat release (Figure 1, Table 2, samples 9–11) and the formation of aluminum hydroxide and oxyhydroxide in substantial amounts, whereas the content of

unreacted aluminum in hydrolysis products was low (Figure 2). An increase in the content of ANP to H_2O : ANP ratios of 7 and lower resulted in suspension self-heating to 100°C during aluminum oxidation. Under water deficiency conditions, powder sintering in open systems was possible, and the weight ratio H_2O : ANP = 2 calculated from the chemical reaction equation was insufficient for complete aluminum oxidation. At an H_2O : ANP ratio of 6, the oxidation of aluminum and suspension self-heating were accompanied by intense water vaporization and ANP sintering.

Table 2: Parameters of the interaction of ANP with water (v_{max} is the highest temperature growth rate, T_{max} is the highest suspension temperature, and c'_{Al} is the content of aluminum metal in hydrolysis products).

Sample	H_2O : Al (±0.5%)	v_{max}, K/s	T_{max}, °C	c'_{Al}, wt % (±0.5)
1	126	–	–	76.1
2	101	–	–	75.2
3	84	–	–	76.2
4	72	0.00	60	3.1
5	56	0.18	62	2.3
6	50	0.42	78	1.8
7	42	0.53	83	1.7
8	33	0.68	87	1.4
9	25	0.83	92	1.4
10	16	0.83	92	1.4
11	13	0.84	92	1.4
12	8	0.85	92	1.4

Note: Data on sample 2 (Table 1, 78 wt % Al in ANP) are given. For samples 1–3, no formation of H_2 bubbles was noticeable. For samples 5 and 6, the formation of H_2 bubbles was observed. With samples 6–12, hydrogen was released vigorously. The reaction with sample 13 was accompanied by water vaporization.

3 Conclusion

To summarize, we experimentally found the range H_2O: ANP weight ratios (8–25) at which the reaction occurred under optimum conditions (Figure 1, Table 2, samples 9–12) with the most complete conversion of ANP in its oxidation with liquid water (the residual content of aluminum in hydrolysis products was 1.4 wt %). We showed experimentally that the oxidation of aluminum nanopowder with liquid water in a suspension preliminarily heated to 64–66°C

was characterized by an induction period (0.8 – 6.0 min) and self-heating to 92°C with heat and molecular hydrogen release.

Acknowledgement

The work has been supported by CRDF project RUX0-016-TO-06 and Russian President Grant MD-237.2009.8.

References

[1] Zhen-Yan Deng, Joseph M. F. Ferreiraw, Yoshio Sakka. Hydrogen-Generation Materials for Portable Applications // J. Am. Ceram. Soc., 91 [12], 3825–3834 (2008).

[2] I.E. Smith. Hydrogen generation by means of the aluminum-water reaction // J. Hydronaut., 6 [2], 106–109 (1972).

[3] Alexander A. Gromov, Yulia I. Strokova, Ulrich Teipel. Stabilization of Metal Nanoparticles – A Chemical Approach // Chem. Eng. Technol., 32 [7], 1049–1060 (2009).

[4] A.A. Gromov, A.G. Kabardin, A.B. Vorozhtsov. Hydrogen Generation in Systems "Aluminum Nanopowder – Water" // Proceedings of 40th International Annual Conference of ICT "Energetic Materials (Characterisation, Modelling and validation)" (June 23 - June 26, 2009), Karlsruhe Federal Republic of Germany, V 26, 6 p.

[5] Gromov A., Ilyin A., Ulrich Forter-Barth, Ulrich Teipel Characterization of Aluminum Powders: II. Aluminum Nanopowders Passivated by Non-Inert Coatings // Propellants, Explosives, Pyrotechnics. 5, pp.401-409 (2007).

[6] A. Gromov, A. Vorozhtsov, Yu. Strokova, U. Teipel. Experimental Study of Metal Nanopowders Effect on HMX, AP and AN Decomposition // Propellants, Explosives, Pyrotechnics, 34 [6], p 506-512 (2009).

ERDA: Technique for Hydrogen Content and Depth Profile in Thin Film Metal Hydride

I P Jain, **Ankur Jain**, **Pragya Jain**, Centre for Non Conventional Energy Resources, University of Rajasthan, Jaipur-302004, India

Abstract

The use of thin films for hydrogen storage has become very important as the main process of absorption and desorption of hydrogen takes place on the surface of the material. The incorporation of hydrogen into thin film form is relatively new field of research and provides an opportunity to examine a number of unusual properties, which are not visible in the bulk hydrides. Considerable amount of work has been done in our laboratory to investigate hydrogen absorption mechanism in FeTi, LaNi, and $MmNi_{4.5}Al_{0.5}$ thin film metal hydrides.

Over the past few decades thin films are analyzed using ion beam analysis techniques where an energetic incident ion provides depth information on the basis of the energy lost by it and the creation of possible secondary particles in the sample. Rutherford Back Scattering (RBS) technique is based on the principle of elastic scattering of α particles of about a few MeV energy. One of the main drawbacks of RBS is its poor sensitivity for light elements present in a heavier matrix. Hence hydrogen cannot be detected using RBS as backscattering of ions from hydrogen is not possible.

The limitations of RBS are overcome by another technique, Elastic Recoil Detection Analysis (ERDA), in which the yield and energy of particle ejected out of thin film sample under swift heavy ion beam irradiation is detected giving the quantitative information concerning the depth distribution of light elements in a sample. In the present work ERDA technique is being presented with its principle, design, working and application for hydrogen content and depth profile in thin film hydride.

1 Importance of ERDA

- This has become the predominant ion beam technique for quantitative analysis of light elements in thin films.
- The technique is especially for Depth Profiling of light elements overcoming the limitations of RBS, over a wide range of elements from hydrogen to rare earth elements using particle identifying techniques.
- The sensitivity for light elements is enhanced by detecting the recoiled particles instead of the scattered primaries.
- It helps in background free detection of the light elements as different recoiled particles can be identified by their mass or atomic numbers and can be separately counted and measured their energy.
- This is a primary technique for studying content of hydrogen in thin films.
- It has large recoil cross sections with heavy ions and hence good sensitivity and the cross section remains about the same over a wide mass range of atoms.

2 ERDA Technique

In elastic detection (ERD) one determines the yield and energy of particles ejected out of the surface region of samples under MeV ion bombardment, which is an ion beam analysis technique for quantitative analysis of light elements in solids. The sample which has to be analyzed is irradiated with ion beam energy (e.g. O, He, Li, Ag, Au) of several MeV. Light elements (e.g. H, D) from the sample are scattered in forward directions and can be detected with a solid state detector. ERDA makes use of the fact that the information about the target is carried by the target nuclei themselves and not by the backscattered primaries as in RBS which enables us to identify the particles under investigation. Detection in ERDA especially occurs in forward geometry, and therefore, both scattered and recoiled particles will move in the direction of detector.

ERDA was first demonstrated by Ecuyer et al. [1] in 1978 and by Doyle and Peercy [2] in 1979. It is the most frequently used method for hydrogen depth profiling and content measurement in thin films and surfaces [3-5], hydrogen in chemical vapour deposited diamond films [6-7], diamond like carbon films [8-9], plasma deposited amorphous silicon nitride films [10] and in hydrogenated Pb/semiconductor devices [11].

3 Principles of ERDA

In an elastic collision of the incident particle of mass m_p (in atomic mass units) and energy E_p, with the atom of mass m_r (in atomic mass units) present in the sample, the atom in the sample which is at rest, recoils in forward direction after the collision. The energy E_r of the recoiling atom can be derived from the basic principle of conservation of energy and momentum which for atom with mass m_r at an angle ϕ with respect to the beam direction is given by

$$E_r = kE_p, \tag{1}$$

where k is kinematic factor given by

$$k = 4m_p m_r \cos 2\phi / (m_p + m_r)^2 \tag{2}$$

The projectile mass, its energy and recoil angle remains fixed under a given experimental condition, therefore atoms of different masses in the sample come out with different recoil energies as governed by eq. (1). If $m_p > m_r$, projectiles can only be scattered in a limited angular range with a maximum angle ϕ defined by

$$\phi = \arcsin (m_r/m_p)$$

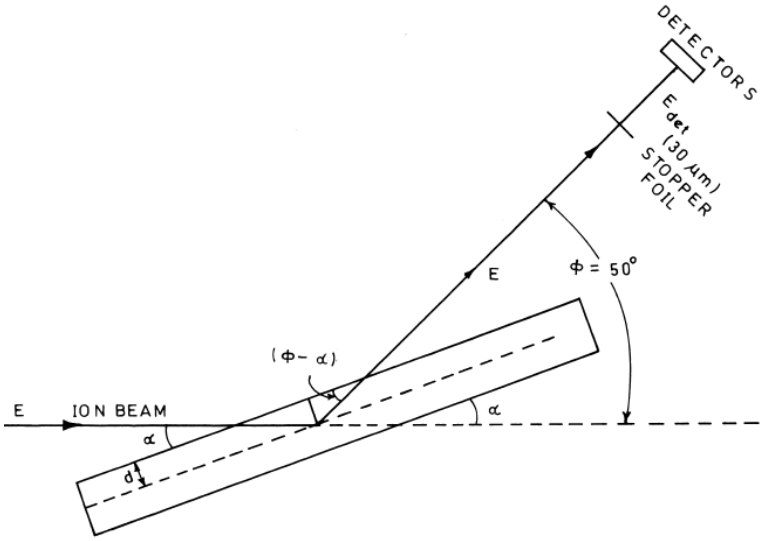

Figure 1: Schematic experimental set up of ERDA indicating path of ion beam and recoil through the sample.

This fact can be used to avoid scattered projectiles by placing the detector for the recoils beyond this angle. Normally the heavier scattered projectiles or recoils of the sample are stopped in a stopper foil of appropriate thickness in front of the detector. Light element recoils are not stopped in the stopper foil due to smaller energy loss during traversal. Figure 1 shows the schematic of an ERDA set up and explains the principle of ERDA.

4 Quantification

The concentration of sample atoms *N*r (in atoms/cm^2) can be determined by the following relation

$$Y_H = N_P N_H \left(\frac{d\sigma}{d\Omega}\right)_R \frac{\Omega}{\sin \alpha} \tag{3}$$

Where hydrogen concentration, N_H is atm/cm^2, N_p is the number of incident ions; Ω is the solid angle subtended by the detector, α is the tilt angle of the sample with respect to ion beam direction and $(d\sigma/d\Omega)_R$ is the Rutherford recoil cross section for H in laboratory frame. The Y_H defined in Eq. (1) is the area under H recoil peak is given by,

$$\left(\frac{d\sigma}{d\Omega}\right)_R = \left[\frac{Z_p Z_t e^2}{2E}\right]\left[1 + \frac{m_p}{m_t}\right]^2 \frac{1}{\cos^3 \phi} \tag{4}$$

Where m_p m_t Z_p and Z_t are the atomic masses and atomic number of the projectile and the target sample respectively, *e* is the electronic charge, E is the incident ion energy and *ϕ* is the recoil angle. It was observed that H concentration decreases during ion irradiation. The H

loss was monitored as a function of dose and was taken into account to evaluate the H concentration in thin films.

5 Depth Profiling

The energy of recoils as detected by the detector depends on kinematics as per eq. (1), energy loss of the incoming ion in the sample up to a certain depth *d*, energy loss of the recoil in the sample from depth *d* where it originates, and energy loss of the recoil atom in the stopper foil.

If the recoil originates from the surface, the energy of the recoil atom is determined only by the kinematics according to eq. (1). This is the maximum energy of recoil of particular mass originating from the sample's surface. The energy of a recoil ion generated at depth *d* is given by

$$E_d = k[E_p - (d/\sin\alpha)(dE/dx)_{in}], \quad (5)$$

where $(dE/dx)_{in}$ is the energy loss of incoming ion in the sample material.

The energy of recoil E_{ds}, originating at depth *d*, coming out at the surface is

$$E_{ds} = E_d - \{d/\sin(\phi-\alpha)\}(dE/dx)_{out}, \quad (6)$$

where $(dE/dx)_{out}$ is the energy loss of recoil in the sample. The recoil energy as detected by the detector is given by

$$E_{det} = E_{ds} - \Delta E_{foil}(E_{ds}), \quad (7)$$

where ΔE_{foil} is the energy loss of recoil in the foil, which is dependent on energy. The recoil energy is converted to depth scale using the eqs. (5) to (7) given above.

6 Mass Identification

Recoil energy provides the information about the mass of the elements in the sample as per eq. (1) at fixed ϕ. The identification of the elements from the recoil energy is possible as long as the recoil energy difference of the elements is larger than the energy resolution of the set up. Higher mass recoils have higher energy as per eq. (1), if $m_p > m_r$ and appear as separate groups.

7 Sensitivity

Sensitivity is defined as the minimum quantity of an element, which can be detected for a moderate charge of incident ions (say 10 μC). It is dependent on the recoil cross section and the detector solid angle. The latter is kept normally in such a way that the opening of detector has an acceptance angle, which is comparable or smaller than the kinematic broadening. Typically, the minimum detection limit is about 0.1 atomic per cent.

8 Depth Resolution

Depth resolution depends on the energy resolution d*E*, which is governed by various factors such as, incident ion beam energy spread, straggling in the stopper foil and the detector system, inhomogeneities in the stopper foil and the entrance window of the detector, detection system resolution, which is composed of the electronics noise and the detector resolution, kinematic broadening and angular and lateral spread due to multiple scattering, which adds to the kinematic broadening. Incident beam resolution is typically 50 keV. Detection system resolution is typically 1% and is therefore about 200 keV for 20 MeV heavy ion recoils. One has to choose the experimental parameters in such a way that the recoil energy spread due to various factors is minimized.

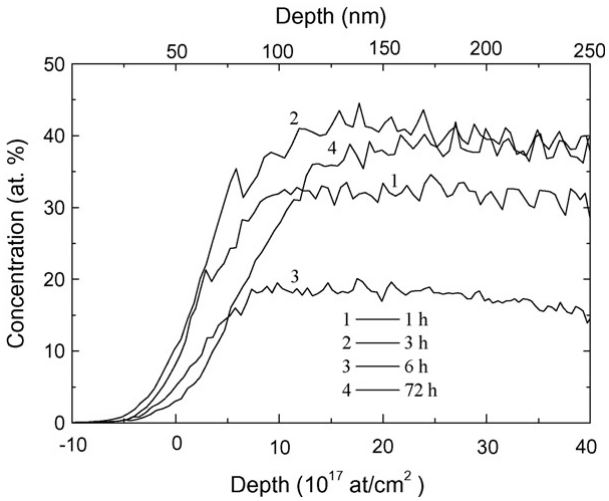

Figure 2: Hydrogen distribution profiles in MgNi films at 250 8C [13].

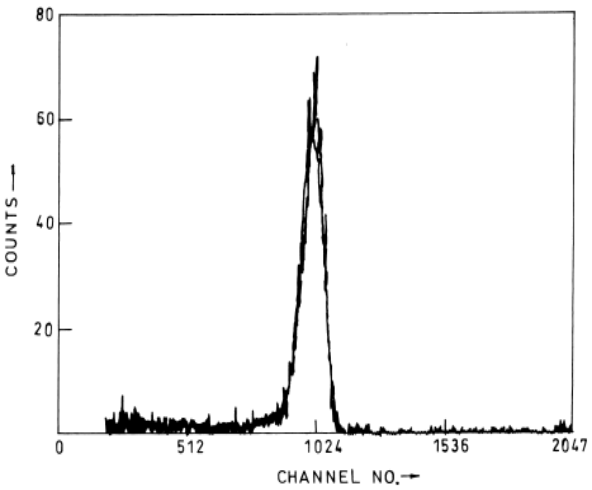

Figure 3: Hydrogen content in hydrogen loaded FeTi thin films [15].

9 Hydrogen Depth Profiling

The hydrogen content has a great influence on the chemical, physical and electrical properties of many materials. Therefore, it is necessary to monitor the H-concentration by depth profiling. Wielunski et al [12] has compared the hydrogen depth resolution in multilayered metal structure (Al/Cu/Ag/Au) by ERDA and NRA techniques. Pranevicius et al. [13] investigated the Hydrogen distribution profiles in Mg-Ni films (Figure 2). Wirth et al. [14] studied the changes in surface barrier layer of Mg-Ni films by hydrogen profile. Hydrogen concentration in unloaded and hydrogen loaded FeTi thin films were measured by Jain et al [15] by ERDA with 160MeV Ag ^{107} ions and found that hydrogenation of the films increased the H-content by a factor of 5-10 atm% (Figure 3).

10 Conclusions

ERDA technique is important as it provides the yield and energy of particle ejected out of thin film sample under swift heavy ion beam irradiation giving the quantitative information concerning the depth distribution of light elements in a sample with 1nm resolution. ERDA is already a very useful technique having good sensitivity and high resolution, but it needs to be

further improved. It has the excellent capability for fast quantitative concentration depth profiling of elements and capable of giving the total abundances of light elements in surface layers. It is an important technique which helps in our understanding of hydrogen content and its depth profile in a thin film samples, which is very important for the hydrogen storage in various materials for ultimately solving world's energy problem. In our laboratory lot of work is being done and is under progress using ERDA to understand the actual hydrogen absorption mechanism in alloys and compounds.

References

[1] L'Ecuyer, J., Brassard, C., Cardinal, C. and Terreault, B., Nucl. Instr & Methods in Physics Research B, 1978, B149, pp 271.

[2] Doyle B. L. and Peercey P. S., Appl. Phys. Lett., 1979, 34, pp 812.

[3] Weilunski LS, Beneson RE, Lanford WA. Nucl Instr & Meth 1983;218:120.

[4] Turos A, Meyer O. Nucl Intsr and Meth B 1984;4:92.

[5] Baglin JEE, Kellock AJ, Deline VR, Crockett MA, Shih AH. Nucl Intsr and Meth B 1992;64:469.

[6] Sharda T, Mistra DS, Avasthi DK. Vacuum, 1996;47:1264.

[7] Yagi H, Tanida K, Hatta A, Ito T, Hiraki A. Nucl Instr & Meth B 1996;118:318-21.

[8] Avasthi DK, Kabiraj D, Jaipal, Metha GK, Barshilia HC, Sah HC, Somna, Metha BR, Vankar VD. Vacuum 1995;46:633.

[9] Konishi Y, Konishi L, Sakuchi N, Hasyashi S, Hirakimoto A, Suzuki J. Nucl Instr and Meth B 1996;118:312

[10] Avasthi DK, Acharya MG, Tarey RD, Malhotra LK, Mehta GK. Vacuum 1995;46:265.

[11] Srivastava PC, Singh UP, Pandey SP, Avasthi DK., Vacuum 1996; 47(12):1427.

[12] L. S. Wielunski, D. Grambole, U. Kreissing, Nucl Instr & Meth 2002, 190: 1-4,693.

[13] L. Pranevicius, E. Wirth, D. Milcius, M. Lelis, L.L. Pranevicius, A. Bacianskas, Applied Surface Science 255 (2009) 5971–5974

[14] E. Wirth, F. Munnik, L.L. Pranevicius, D. Milcius, J. of Alloys & Compounds, 2009, 475, 917-922.

[15] I. P. Jain, Babita Devi, P. Sharma, A. Williamson, Y. K. Vijay, D. K. Avasthi, A. Tripathi, Int. J. of Hydrogen Energy, 2000, 25,pp 517-521.

Development of V-rich V-Ti-Cr and V-Ti-Cr-Al Alloys with High Hydrogen Desorption Pressure for High Pressure MH Tank

Takahiro Kuriiwa, **Atsunori Kamegawa**, **Masuo Okada**, Department of Materials Science, Graduate School of Engineering, Tohoku University, Japan
Takahiro Maruyama, Department of Materials Science, Faculty of Engineering, Tohoku University, Japan (Now at Department of Materials Science, Graduate School of Engineering, Tohoku University, Japan)

1 Introduction

Recently, high-pressure metal hydride (MH) tanks attract many attentions for on-board usage due to its high volumetric hydrogen storage density and easiness of heat management[(1)]. In order to enhance its merits, especially improving of cold-starting capability, increment of hydrogen desorption pressure of MH at ambient temperature is strongly required[(2)]. Besides, from viewpoint of materials as on-board fuel storage media, durability or cyclic properties are quite important issue. V-Ti-Cr alloys with BCC crystal structure are known to its relatively high volumetric hydrogen capacity[(3)], in addition, alloys with high V content possess good cyclic properties. Therefore V-Ti-Cr alloys are regarded as one of the most promised candidates for on-board hydrogen storage media. In this ternary system, reducing of Ti and increasing of Cr content in alloys lead to increment of hydrogen desorption pressure of alloys. But excess substitution of Ti by Cr causes declination of hydrogen capacity of alloys[(4)](this compositional restriction is called as “limitation line”). Therefore, to overcome this limitation, introduction of adequate substitutional element(s) into this system is one of the effective techniques to increase hydrogen desorption pressure. In addition, recently, it was revealed that in V-Ti-Cr system, not only Ti/Cr ratio but also V content is important factor to make alloys high hydrogen desorption pressure with high hydrogen capacity[(5)]. Al and Mo are known to its effectiveness of increasing of hydrogen desorption pressure of V-based alloys. In our previous study, introducing of Al or Mo into alloys reduces the minimum optimum content of Ti in alloys with high hydrogen capacity. But degree of increment of hydrogen desorption pressure of Al substitution is higher than that of Mo substitution.

In this study, effects of Ti/Cr on 75at%V and substitutional element of Al in 75at%V-Ti-Cr-Al alloys were investigated with prospect of increment of hydrogen desorption pressure for improvement of cold starting capability of high-pressure MH tanks.

2 Experimental Procedures

Purity of starting materials was as follows. V : 99.95%(N200, provided by TAIYOKOKO co.,LTD), Ti:99.99% ,Cr:99.995%, Al:99.999%, respectively. The samples of approximately 13.5g were weight out and then arc-melted four times in order to improve its homogeneity. In this study, composition of the samples is described by atomic%. Crystal structure and lattice parameter were measured by X-ray diffraction with Cu-Kα radiation. Pressure composition

isotherms (PCT curves) were measured by Sieverts-type apparatus (Suzuki-shoukan). First, sample was crushed into particles, weighted out about 1g and placed into pressure vessel for PCT measurement. Then the vessel was connected to PCT apparatus and flushed with hydrogen for three times. Each time, before commencing of PCT measurement, sample was evacuated with rotary pump for 2hrs at measuring temperature, and beginning point (or zero-point) of PCT curves were adjusted. Effective hydrogen capacity is defined as difference between amount of hydrogen stored at 9MPa in absorption step and remained in the sample at 0.1MPa in desorption step.

3 Results

3.1 Hydrogen storage properties of 75at%V-Ti-Cr alloys

Figure 1 shows PCT curves of 75at%V-xat%Ti-Cr as-cast samples (x=3 to 5) measured at 273K. The 75at%V-5at%Ti-Cr sample showed flat plateau region and relatively large hydrogen storage capacity. But 75at%V-4at%Ti-Cr sample showed declination of hydrogen storage capacity and 75at%V-3at%Ti-Cr sample showed quite small or almost no hydrogen storage capacity. This declination of hydrogen storage capacity with inclination of Cr content is regarded as Cr content is exceeding limitation line of corresponding V content and causing of reduction of hydrogen storage property[3]. In this study, all the samples were confirmed as BCC single phase.

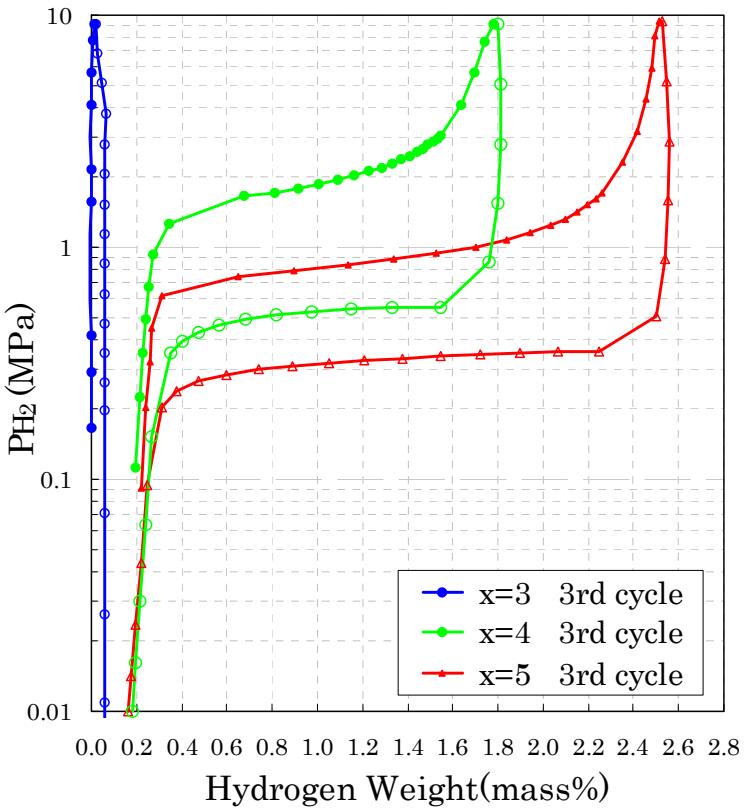

Figure 1: PCT curves of 75at%V-xat%Ti_Cr as-cast samples (x=3 to 5) measured at 273 K.

Figure 2 shows PCT curves of 75at%V-5at%Ti-Cr as-cast sample measured at 243K to 313K. At 273K, effective hydrogen capacity was about 2.3mass% (at 10th cycle). Hydrogen desorption pressure was 0.35MPa at 273K and 0.107MPa at 253K, respectively. From 243K through 313K, amount of hydrogen uptake maintained almost the same value.

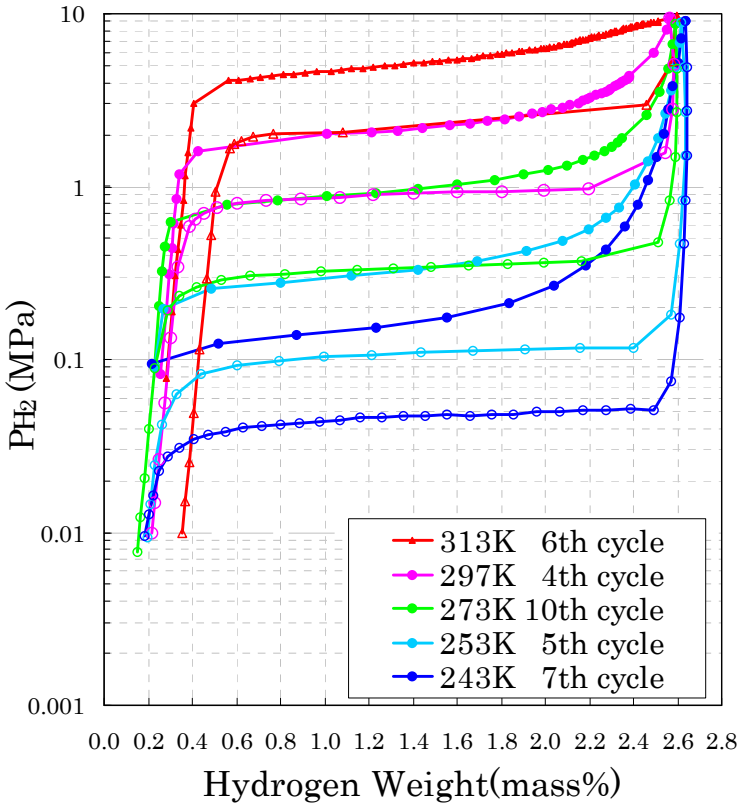

Figure 2: PCT curves of 75at%V-5at%Ti-Cr as-cast sample measured at 243 K to 313 K.

Figure 3 shows relationship of hydrogen desorption pressure and Ti content of 75at%V-Ti-Cr samples at 273K along with those of 60at%V-Ti-Cr and 80at%V-Ti-Cr. Open diamond marks in Fig.3 refer to samples with poor hydrogen storage capacity. This deterioration of hydrogen storage capacity for alloys with low Ti content might be attributed that Cr content of the sample might have exceeded “limitation line” as mentioned above. From the results of Fig.3, in V-Ti-Cr alloys, further increment of hydrogen desorption pressure without declination of hydrogen storage capacity is quite difficult without introducing of substitutional element(s).

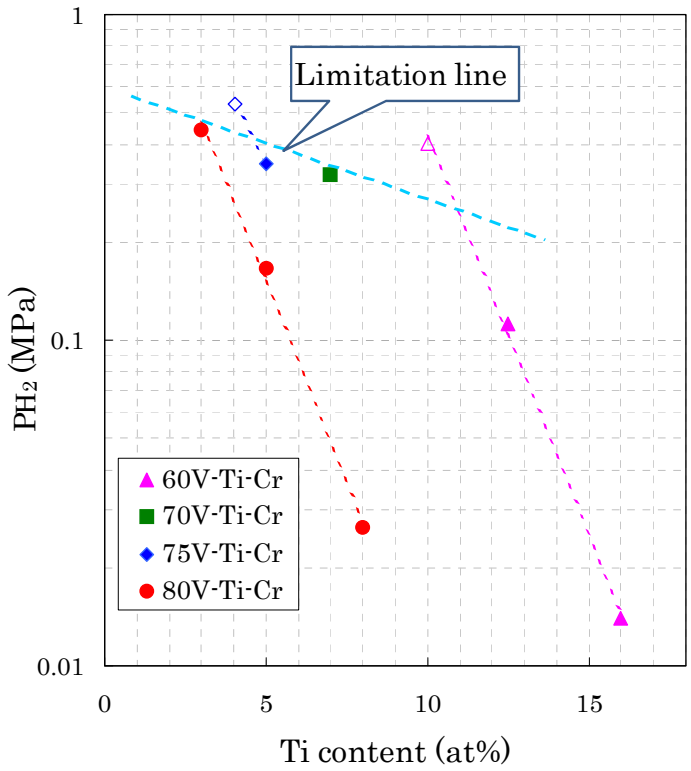

Figure 3: Relationship of hydrogen desorption pressure and Ti content of 75at%V-Ti-Cr samples at 273 K along with those of 60at%V-Ti-Cr and 80at%V-Ti-Cr. (Open marks refer to sample with poor capacity)

3.2 Hydrogen storage properties of 75at%V-Ti-Cr-Al alloys

Figure 4 shows PCT curves of 75at%V-xat%Ti-Cr-1Al% samples (x=3 to 5) measured at 273K. Compared to 75at%V-4at%Ti-Cr sample, hydrogen storage properties of 75at%V-4at%Ti-Cr-1at%Al, such as hydrogen storage capacity and hydrogen desorption pressure, were improved significantly. But declination of hydrogen storage capacity is observed in this sample, so, in the case of 75at%V-Ti-Cr-1at%Al samples, limitation line lies between 75at%V-4at%Ti-Cr-1at%Al and 75at%V-5at%Ti-Cr-1at%Al samples. 75at%V-3at%Ti-Cr-1at%Al showed further declination of hydrogen storage capacity along with increment of hydrogen desorption pressure. This deterioration of hydrogen storage capacity might be attributed to exceeding of “limitation line”.

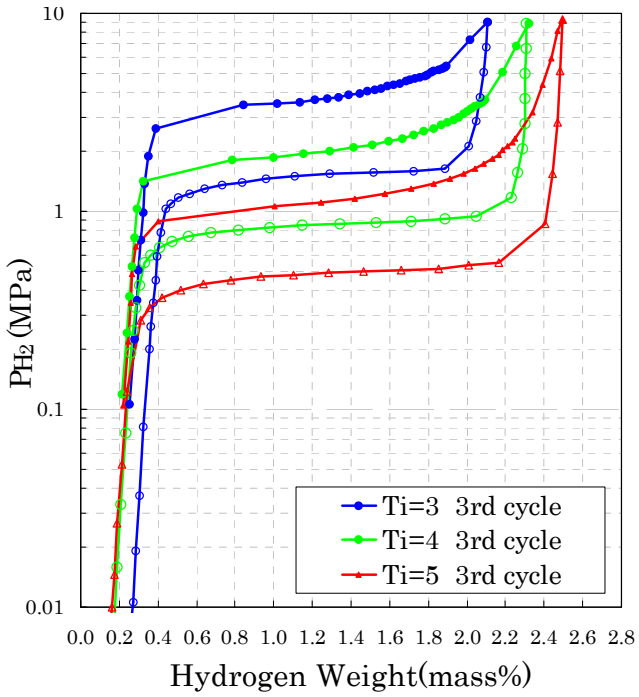

Figure 4: PCT curves of 75at%V-xat%Ti-Cr-1Al% samples (x=3 to 5) measured at 273 K.

Figure 5 shows PCT curves of 75at%V-xat%Ti-Cr-2at%Al samples (x=3 to 5) measured at 273K. 75at%V-4at%Ti-Cr-2at%Al sample shows high hydrogen capacity and improvement of hydrogen desorption pressure. In this 75at%V-Ti-Cr-2at%Al series, limitation line is raised between 75at%V-3at%Ti-Cr-2at%Al and 75at%V-4at%Ti-Cr-2at%Al samples.

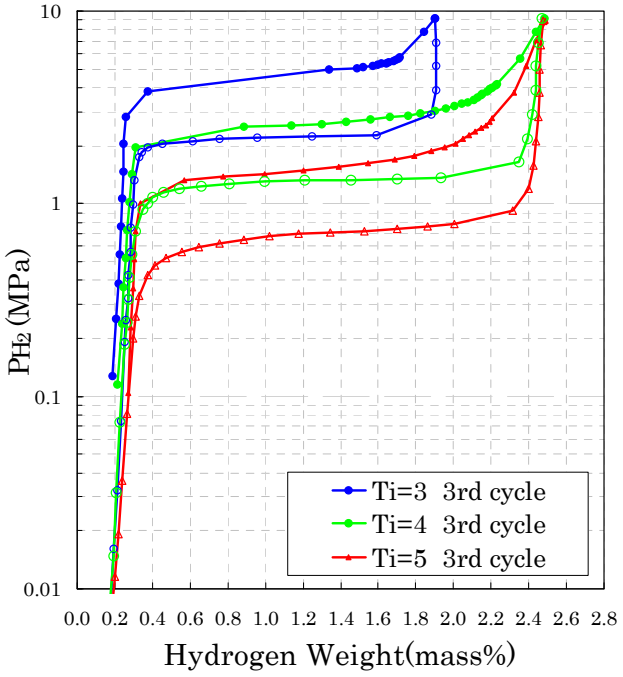

Figure 5: PCT curves of 75at%V-xat%Ti-Cr-2at%Al samples (x=3 to 5) measured at 273 K.

Figure 6 shows PCT curves of 75at%V-xat%Ti-Cr-3at%Al samples (x=3 to 5) measured at 273K. It is quite unique and clearly confirmed that 75at%V-3at%Ti-Cr-3at%Al sample shows high hydrogen capacity and improvement of hydrogen desorption pressure. In this 75at%V-Ti-Cr-3at%Al series, limitation line is raised above 75at%V-3at%Ti-Cr-3at%Al sample.

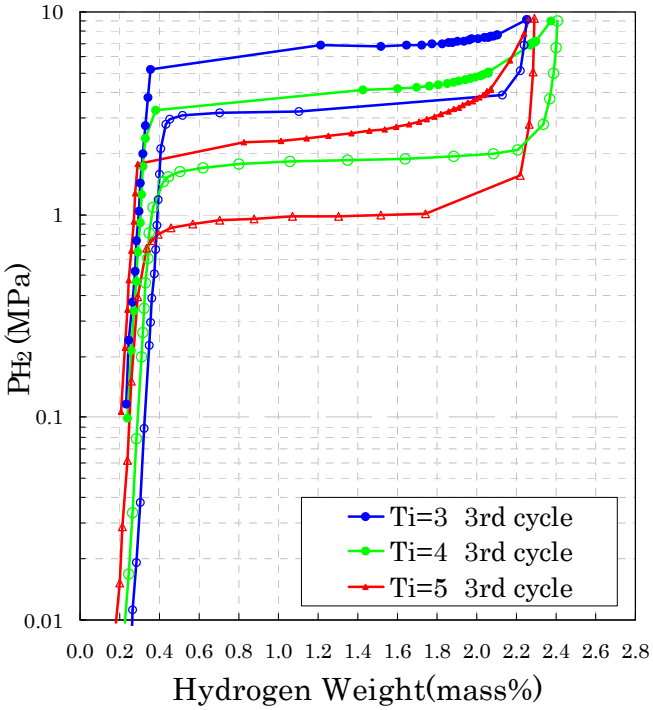

Figure 6: PCT curves of 75at%V-xat%Ti-Cr-3at%Al samples (x=3 to 5) measured at 273 K.

4 Discussion

Figure 7 shows relationship of hydrogen desorption pressure at 273K and Ti content for 75at%V-Ti-Cr, 75at%V-Ti-Cr-1at%Al, 75at%V-Ti-Cr-2at%Al and 75at%V-Ti-Cr-3at%Al samples of this study (open marks in Fig.7 refer to samples with poor hydrogen storage capacity). In 75at%V-5at%Ti-Cr-yat%Al samples (y=0 to 3at%), raising of hydrogen desorption pressure with increment of Al content is observed and thus, introduction of Al of adequate amount is effective method for improvement of hydrogen desorption pressure in this system. Without Al substitution, minimum adequate Ti amount for 75at%V-Ti-Cr is around 5at%. But with introducing and increasing of amount of Al substitution, minimum optimum content of Ti reduced. In the case of sample with 3at%Al substitution, minimum optimum Ti content reduced to around 3at%. From these results mentioned above, introducing of adequate amount of Al substitution are effective for not only raising hydrogen desorption pressure by Al substitution effect itself but also for enhancing limitation, in resulting in enabling alloys with more less Ti composition. With this latter effect, further improvement of hydrogen desorption pressure of V-Ti-Cr-Al alloys could be possible.

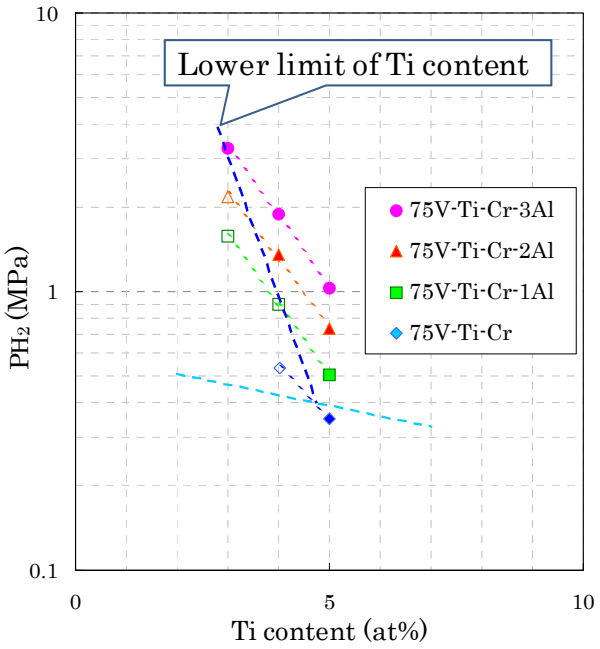

Figure 7: Relationship of hydrogen desorption pressure and Ti content for 75at%V-Ti-Cr, 75at%V-Ti-Cr-1at%Al, 75at%V-Ti-Cr-2at%Al and 75at%V-Ti-Cr-3at%Al samples for 273 K. (Open marks refer to sample with poor capacity)

As summary, figure 8 shows PCT curves of 75at%V-Ti-Cr-Al alloys of various Al content measured at 243K. 75at%V-xat%Ti-Cr-3at%Al (x=3, 4) and 75at%V-4at%Ti-Cr-2at%Al alloys show desorption pressure higher than 0.23Mpa at 243K with large hydrogen capacity.

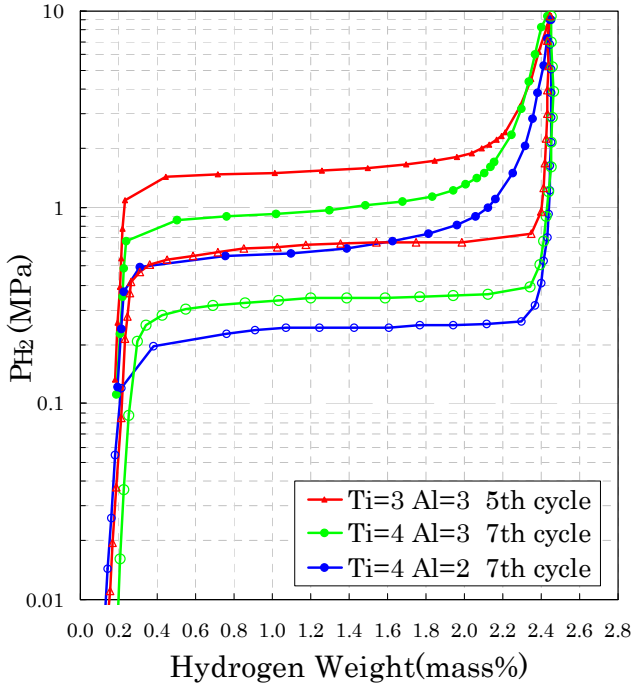

Figure 8: PCT curves of 75at%V-Ti-Cr-Al alloys of various Al content measured at 243 K.

5 Conclusion

In this study, effects of Ti/Cr on 75at%V and substitutional element of Al in 75at%V-Ti-Cr-Al alloys were investigated with prospect of increment of hydrogen desorption pressure for improvement of cold starting capability of high-pressure MH tanks.

The 75at%V-5at%Ti-Cr sample showed flat plateau region and relatively large hydrogen storage capacity. But 75at%V-4at%Ti-Cr sample showed declination of hydrogen storage capacity. So, limitation line is located between 4at%Ti and 5at%Ti in 75at%V-Ti-Cr series.

In 75at%V-5at%Ti-Cr-yat%Al samples (y=0 to 3at%), raising of hydrogen desorption pressure with increment of Al content is observed and thus, introduction of Al of adequate amount is effective method for raising hydrogen desorption pressure in this system. Without Al substitution, minimum adequate Cr amount for 75at%V-Ti-Cr is around 5at%. But with introducing and increasing of amount of Al substitution, minimum allowed Cr content reduced and in the case of sample with 3at%Al substitution, minimum optimum Ti content reduced less than 3at%. From these results mentioned above, introducing of adequate amount of Al substitution are effective for not only raising hydrogen desorption pressure but for also enhancing limitation and enabling alloys with more less Ti composition. With this latter effect, further increment of hydrogen desorption pressure of V-Ti-Cr-Al alloys could be possible. As V-Ti-Cr-Al system, introducing of adequate amount of Al is quite effective tactics to make alloys high hydrogen desorption pressure that would be effective for improvement of cold starting capability of high-pressure MH tank for on-board usage.

Acknowledgement

This work was partially supported by KAKENHI 22760528. (Grants-in-Aid for Scientific Research 22760528)

References

[1] N.Takeichi et.al. Int J Hydrogen Energy 28 (2003) 1121

[2] D.Mori et.al. Int J Hydrogen Energy 34 (2009) 4569

[3] E. Akiba et.al. Intermetallics 6 (1998) 461–70

[4] T.Tamura et.al. J. Alloys Comp. 356–357 (2003) 505

[5] T. Kuriiwa et.al. Collected Abstracts of Autumn Annual Meeting of the Japan Inst. Metals (2010) 372

Hydrogen Storage in Melt-spun Nanocrystalline Mg-Ni-Y Alloys

Lars Röntzsch[*]**, Thomas Schmidt**, Fraunhofer IFAM-Dresden, Germany
Siarhei Kalinichenka, TU Dresden, Germany
Bernd Kieback, TU Dresden; Fraunhofer IFAM-Dresden, Germany

1 Introduction

Magnesium-rich alloys are attractive materials for the reversible solid-state storage of hydrogen due to high gravimetric hydrogen storage densities that can reach up to more than five weight percent [1]. Further, Mg alloys are suitable for commercial use because of their cycle stability, their high abundance and the moderate cost of Mg as lightweight base material. However, the very slow hydrogen sorption kinetics of common bulk material requires strong improvement in view of practical applications. In the past decade, much attention has been devoted to the research and development of Mg alloys for hydrogen storage. It is now well established that, in order to improve the hydrogen sorption kinetics, magnesium alloys ought to possess a sub-micrometer crystal structure and should contain highly disperse catalyst particles [2]. For this purpose, Mg alloys can be ground by high-energy ball-milling techniques to reduce the average grain size and to disperse such catalyst particles [3-8]. Alternatively, nanocrystalline Mg alloys can be produced by rapid solidification processes such as melt-spinning [9-17]. With this high-yield rapid cooling technique an amorphous or super-fine microstructure solidifies in the form of ribbons which are a few tens of micrometers thin.

In this contribution, nanocrystalline magnesium-rich Mg-Ni-Y alloys were produced by melt-spinning and were studied in view of their crystal structure, crystallization behaviour and their cyclic hydrogenation/dehydrogenation properties that render them attractive materials for the reversible storage of hydrogen. The alloy composition was chosen for several reasons: From the literature it is known that the addition of Ni to Mg significantly improves the hydriding/dehydriding kinetics and decreases the working temperature compared to that of pure Mg [18-20]. Further, Y is widely known as glass-forming element in Mg alloys [21]. Moreover, ultrafine yttrium hydride particles improve the hydrogen sorption kinetics of Mg [22]. Finally, ultra-fine crystal phases like yttrium hydrides might stabilize the nanostructure of the alloys by preventing further crystal coarsening during thermal processing.

2 Experimental

Mg-Ni-Y master alloys with two different chemical compositions ($Mg_{90}Ni_5Y_5$ and $Mg_{80}Ni_{10}Y_{10}$) were produced by induction-melting of a mixture of pure Mg metal, Ni powder and a Ni-Y alloy under Ar atmosphere. During melt-spinning of these alloys, continuous ribbons (35 µm in thickness, 10 mm in width) were obtained from a single roller melt-spinning device (surface

[*] Corresponding author, email: lars.roentzsch@ifam-dd.fraunhofer.de

velocity of 40 m/s). The melt-spinning experiments were carried out under Ar atmosphere. The melt-spun ribbons were thermally activated during three cycles at 350°C and hydrogen partial pressures between 2 and 30 bar for 11 h. This activation procedure is widely found in the literature (cf. Refs. [11, 12, 19]). The crystal structure characterization of the samples has been performed by X-ray diffraction analysis (XRD). The microstructure characterization of the specimens has been carried out using a scanning electron microscope (SEM) and a transmission electron microscope (TEM). The hydrogenation/dehydrogenation properties (reaction kinetics) and cycle stability of the melt-spun Mg-Ni-Y ribbons were studied using a magnetic suspension balance.

3 Results and Discussion

XRD patterns of the as-spun $Mg_{90}Ni_5Y_5$ and $Mg_{80}Ni_{10}Y_{10}$ ribbons are shown in Figure 1. It can be seen that the as-quenched $Mg_{80}Ni_{10}Y_{10}$ ribbon shows a typical amorphous structure. $Mg_{90}Ni_5Y_5$ ribbons consist of Mg-crystals embedded in an amorphous Mg-Ni-Y phase (002)-peak at 40° (2Θ). According to TEM, the Mg-Ni-Y alloys produced here consisted in the as-spun state indeed of mixtures of nanocrystalline grains that are embedded in an amorphous matrix (cf. Figure 2).

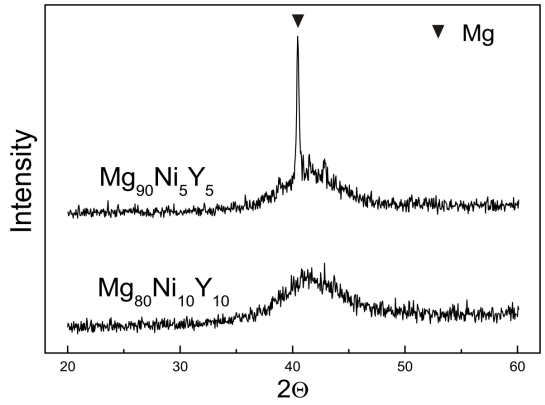

Figure 1: X-ray diffraction patterns for $Mg_{90}Ni_5Y_5$ and $Mg_{80}Ni_{10}Y_{10}$ in the as-spun state.

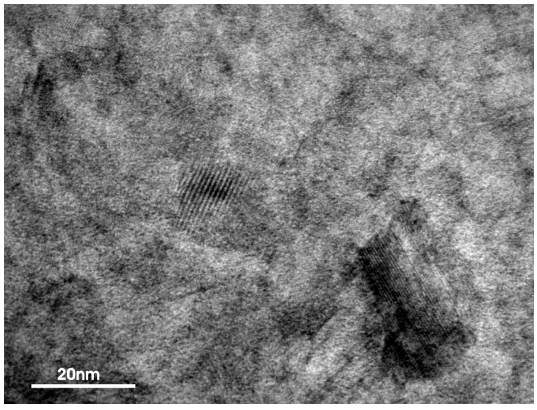

Figure 2: High resolution TEM micrograph of as-spun $Mg_{90}Ni_5Y_5$.

The average crystal size was about 20 nm in the case of $Mg_{90}Ni_5Y_5$ (cf. Figure 2) and about 5 nm in the case of $Mg_{80}Ni_{10}Y_{10}$ (TEM results not shown). The crystallization temperatures of the as-spun Mg-Ni-Y ribbons were determined by DSC which displayed two and three exothermic peaks for $Mg_{90}Ni_5Y_5$ and $Mg_{80}Ni_{10}Y_{10}$, respectively [13]. The characterization of the hydrogenation and dehydrogenation properties of activated Mg-Ni-Y alloys was carried out at different temperatures between 280°C and 180°C. Figure 3 shows the hydrogen content vs. time (reaction kinetics) of the activated $Mg_{80}Ni_{10}Y_{10}$ alloy for the absorption of hydrogen at 20 bar H_2 and the desorption of hydrogen at vacuum. Obviously, the velocity of hydrogenation is nearly equal (approx. 1 wt.%-H per minute) in the first minutes of hydrogenation during which about 5 wt.%-H can be achieved. After 4 hours of hydrogenation a saturation of 5.3 wt.%-H was observed [13]. In the case of dehydrogenation (cf. Figure 3),

there is a clear dependence on the sample temperature in the temperature range investigated. At 280°C and 250°C a 90% desorption is obtained after 5 minutes, at 200°C after 15 min and in the case of 180°C after about 60 minutes. This result of dehydrogenation kinetics is still good enough for automotive application where full desorption needs to be reached after 4 to 5 hours under continuous operation conditions. Thus, it can be expected that $Mg_{80}Ni_{10}Y_{10}$ can be desorbed even at lower temperatures of about 150°C to 160°C which is the operation temperature range of most high-temperature PEM fuel cells [23], thus, waste heat from the fuel cell could be directly used the dehydrogenate the hydride in the tank.

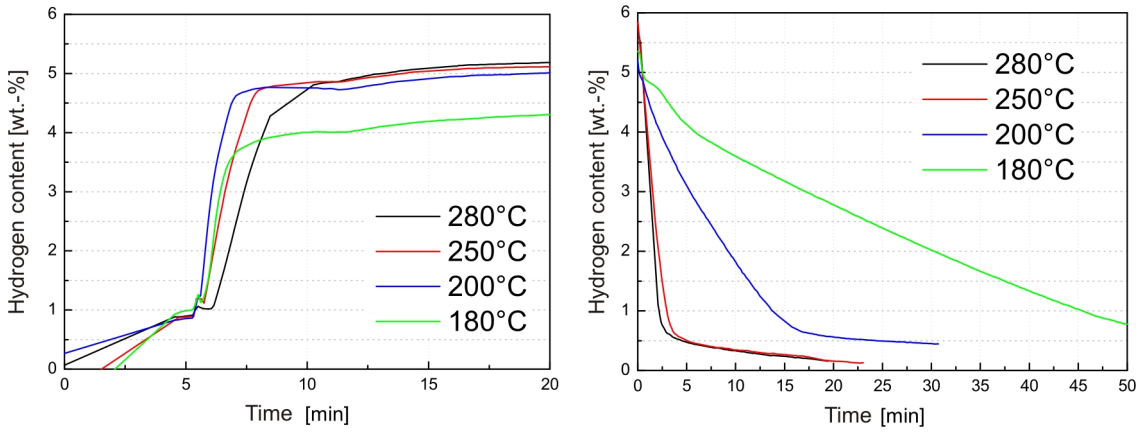

Figure 3: Hydrogenation (left, 20 bar) and dehydrogenation (right, vacuum) kinetics of melt-spun $Mg_{80}Ni_{10}Y_{10}$. measured in a magnetic suspension balance.

From the reaction kinetics point of view, Y is known to form very stable hydrides which act like Mg-Ni hydride phases as catalysts for the hydrogenation of magnesium [22, 24]. Moreover, finely dispersed Y hydride phases might be beneficial regarding the conservation of a sub-micrometer structure of the alloy.

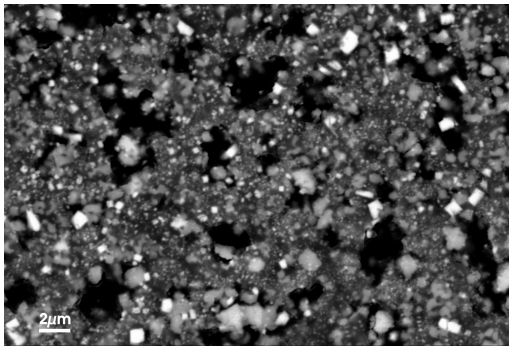

Figure 4: Scanning electron micrograph (BS imaging mode) of a hydrogenated $Mg_{80}Ni_{10}Y_{10}$ ribbon after 10.5 hydrogenation/ dehydrogenation cycles.

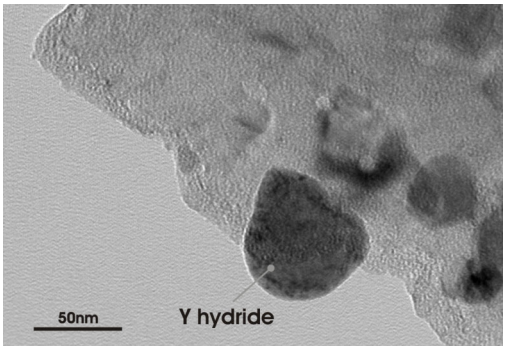

Figure 5: High resolution TEM micrograph of hydrogenated $Mg_{80}Ni_{10}Y_{10}$ after 10.5 hydrogenation/ dehydrogenation cycles.

In this regard, in Figure 4 a SEM micrograph of a hydrogenated $Mg_{80}Ni_{10}Y_{10}$ ribbon after 10.5 hydrogenation/dehydrogenation cycles is shown. Evidently, the material preserves mainly a

sub-micrometer crystal structure which in return might be the case for a fast reaction kinetics during hydrogenation/dehydrogenation.

The cyclically hydrogenated Mg-Ni-Y ribbons were very brittle and could be powderized easily. As shown in Figure 4, the microstructure of ribbons in the hydrogenated state consisted mainly of coarse Mg_2NiH_4 grains with 1 to 2 µm in size and of nanocrystalline yttrium hydride particles embedded in a MgH_2 matrix whose average crystal size is in the range of 100 nm (cf. Figure 5). In the literature, there are only a few investigations on the hydrogenation kinetics of magnesium-rich Mg-Ni-Y alloys. For example, Spassov *et al*. [9, 10] reported results of hydrogen storage properties of the various nanocrystalline and amorphous Mg-Ni-Y alloys ($Mg_{87}Ni_{12}Y_1$, $Mg_{63}Ni_{30}Y_7$, $Mg_{76}Ni_{19}Y_5$, $Mg_{78}Ni_{18}Y_4$, $Mg_{83}Ni_{9.5}Y_{7.5}$) produced by rapid solidification. They found that these Mg-Ni-Y alloys show rather slow rate of hydrogen absorption (0.15 to 0.3 wt.%-H per minute) and a maximum gravimetric hydrogen capacity of about 3.2 wt.%-H. In Ref. [23] the hydrogen sorption properties of Mg-20 wt.% Ni-Y composites prepared by reactive mechanical alloying were studied after the total milling time of 40 h. This composite does not need activation for hydrogen storage process and it can absorb 5.59 wt.%-H at pressures of 30 bar H_2 at 200°C in 10 min and desorb 4.67 wt.%-H at 250°C in 30 min at a hydrogen pressure of 0.2 bar. Compared to these values, the Mg-Ni-Y alloys investigated in this study exhibit even higher hydrogen storage capacities and/or faster hydrogenation/dehydrogenation kinetics. Nonetheless, there is still a need for decreasing the temperatures of hydrogen desorption down to the range of 120°C to 150°C which could be achieved by catalytically more active elements, for example. In conclusion, it could be shown that the melt-spinning technique is very effective in producing nanocrystalline magnesium-rich and catalytically activated alloys, in particular Mg-Ni-Y, which are suitable for the reversible solid-state storage of hydrogen.

Acknowledgement

The authors would like to acknowledge financial support of the Boysen-Stiftung and the Fraunhofer Attract program. Furthermore, we thank Chr. Mickel (IFW Dresden) for TEM analyses and to R. Leuschner, V. Pacheco and M. Ruhnow for practical support.

References

[1] L. Schlapbach, A. Züttel, Nature 2001, 414, 353 - 358.

[2] M. Fichtner, Adv. Eng. Mater. 2005, 7, 443 - 455.

[3] O. Gutfleisch, S. Dal Toè, M. Herrich, A. Handstein, A. Pratt, J. Alloys Compds. 2005, 404–406, 413 - 416.

[4] G. Liang, J. Huot, S. Boily, A. van Neste, R. Schulz, J. Alloys Compds. 1999, 292, 247 - 252.

[5] J. Bystrzycki, T. Czujko, R. A. Varin, J. Alloys Compds. 2005, 404–406, 507 - 510.

[6] F. C. Gennari, M. R. Esquivel, J. Alloys Compds. 2008, 459, 425 - 432.

[7] C. X. Shang, M. Bououdina, Y. Song, Z. X. Guo, Int. J. Hydrogen Energy 2004, 29, 73 - 80.

[8] J. L. Bobet, E. Akiba, B. Darriet, Int. J. Hydrogen Energy 2001, 26, 493 - 501.

[9] T. Spassov, U. Köster, J Alloys Compd 1998, 279, 279 - 286.

[10] T. Spassov, U. Lyubenova, U. Köster, M. D. Barò, Mater. Sci. Eng. A 2004, 375–377, 794 - 799.

[11] K. Tanaka, Y. Kanda, M. Furuhashi, K. Saito, K. Kuroda, H. Saka, J. Alloys Compds. 1999, 293–295, 521 - 525.

[12] M. Y. Song, S. Kwon, J. S. Bae and S. H. Hong, Int. J. Hydrogen Energy 2008, 33, 1711 - 1718.

[13] S. Kalinichenka, L. Röntzsch, B. Kieback, Int. J. Hydrogen Energy 2009, 34, 7749 - 7755.

[14] S. Kalinichenka, L. Röntzsch, C. Baehtz, B. Kieback, J. Alloys Compds. 2010, available online: doi:10.1016/j.jallcom.2010.02.128.

[15] Y. Wu, J. K. Solberg, V. A. Yartys, J. Alloys Compds. 2008, 446–447, 178 - 182.

[16] K. Tanaka, T. Miwa, K. Sasaki, K. Kuroda, J. Alloys Compds. 2009, 478, 308 - 316.

[17] C. Suryanarayana, ed., Non-equilibrium Processing of Materials, Pergamon, Oxford, 1999.

[18] J. J. Reilly, R. H. Wiswall, J. Inorg. Chem. 1968, 7, 2254 - 2256.

[19] G. Friedlmeier, M. Arakawa, T. Hirai, E. Akiba, J. Alloys Compds. 1999, 292, 107 - 117.

[20] C. D. Yim, B. S. You, Y. S. Na, J. S. Bae, Catalysis Today 2007, 120, 276 - 280.

[21] S. G. Kim, A. Inoue, T. Masumoto, Mater. Trans. JIM 1990, 31, 929 - 934.

[22] S. Orimo, H. Fujii, M. Tabata, J. Alloys Compds. 1994, 210, 37 - 43.

[23] J. O. Jensen, Q. Li, R. He, C. Pan, N. J. Bjerrum, J. Alloys Compds. 2005, 404, 653 - 656.

[24] Z. Li, X. Liu, L. Jiang, S. Wang, Int. J. Hydrogen Energy 2007, 32, 1869 - 1874.

Effect of O_2 Preadsorption on the Rate of H_2 Absorption on the Surface of Rare Earths (La, Ce, Pr, Nd, Gd, Tb, Dy and Y) at 298K

H. Uchida, Department of Energy Science and Engineering, School of Engineering, Tokai University, Japan
M. Enomoto, S. Murakami, Course of Applied Science, Graduate School of Engineering, Tokai University, Japan

Abstract
Rare earths (RE) thin film with a clean surface was prepared under an ultra high vacuum condition. The reactivities of H_2 and O_2, with the La, Ce, Pr, Nd, Gd, Tb, Dy and Y surface were quantitatively measured by a volumetric method at pressures ranging from 10^{-8} to 10^{-2} Pa at 298 K. At the initial stage, a clean surface of RE exhibited the highest reactivity in the reaction probability r=1 for H_2, and O_2 respectively. As the amount of O_2 preadsorption layers was increased, r_{H2} was decreased. The oxidized Ce surface exhibits the highest H_2 reactivity among other rare earths with oxide layers.

1 Introduction

Rare earths (RE) are widely used as constitutional elements of various functional materials, devices and catalyses. However, RE have high reactivities with H_2 , O_2 and H_2O gases even at room temperature. Especially, the formation of stable surface oxides/hydroxides is one of the serious problems in the production and the use of RE containing materials. Some RE oxides like Ce oxide are used as catalysis where the Ce oxides remain still metallic even with a high coverage of surface oxide.

We have investigated the reactivities of H_2, O_2 or H_2O with the clean surface of RE using ultra high vacuum technique [1, 2]. Based on our experience, we aimed to compare some RE in the effect of preoxidation on successive hydrogen reactivity. In this study, we measured systematically the effect of O_2 preadsorption layers on the H_2 reactivity of RE (La, Ce, Pr, Nd, Gd, Tb, Dy and Y). under ultra high vacuum condition. And the H_2 reactivity on the RE surface covered with oxide layers is compared at 298 K for various RE elements.

2 Experimental Procedure

The reaction probability r, defined by the ratio of the rate of reacted gas molecules to the rate of impinging by the gases on the surface, was volumetrically determined by means of Wagener method [3]. The Each block sample of a RE metal (La, Ce, Pr, Nd, Gd, Tb, Dy, Y) was carefully degassed in ultra high vacuum by increasing its temperature stepwise until 1300K where the total pressure of the system achieved less than 1×10^{-7} Pa. H_2 gas with a grade of 99.99999% or O_2 gas with a purity 99.99% were supplied through a hot Pd or a hot Ag diffusion cell. The reaction probability was calculated as a function of the amount of

coverage in a monolayer (ML) scale. More detailed information concerning the applied method is described elsewhere [3, 4].

3 Results and Discussion

3.1 RE metals–H_2 systems

As shown in Figs. 1(a) and (b), at the initial stage, the highest reaction probability, r=1, was observed for H_2 molecule. As shown in Figure 1(a), r_{H2}=1 holds at the initial stage of the H_2 absorption by these metals. At this initial stage, the H solid solution phase may be formed for each system. In the reaction with H_2 at N_{H2} > 1, the decrease in r_{H2} seems to be ascribed to the segregation of the dihydride phase from saturated hydrogen solid solution, and then to slower diffusion rate of H atoms inside the surface dihydride, and also to the retarded dissociation rate of H_2 molecules on the dihydride. Since the H_2 dissociation pressures of the dihydride of La, Ce, Pr, Nd, Gd, Tb, Dy and Y are lying at very low levels such 10^{-22} to 10^{-30} Pa at 298 K [2, 6], the dihydride phase of these metals can easily be formed at H_2 gas pressures higher than 10^{-8}–10^{-6} Pa in this experimental condition.

As shown Figure 1 (b), with increasing H concentration, r_{H2} gradually decreased until N_{H2}=300×10^{15} molecules cm^{-2} where two phases of H solid solutions and dihydride may coexist in the film samples.

The H_2 reaction probability r_{H2} with Ce is lying lower by an order of magnitude than those of the other metals. This may be caused because the H_2 equilibrium pressure for the Ce–H system is the highest among the systems [2, 6].

3.2 RE metals–O_2 systems

Figure 2 shows the change in the O_2 reactivity r_{O2} with La, Ce, Pr, Nd, Gd, Tb, Dy, and Y at 298 K as a function of the amount of adsorbed O_2 molecules N_{O2}. At the initial stage, all samples exhibited r_{O2}=1. Particularly, Ce exhibited a longer plateau at r_{O2}=1, meaning the highest O_2 reactivity compared with the other rare earths examined in this study.

3.3 Effect of O_2 preadsoption

Figure 3 shows the effect of the O_2 preadsorption layer on the H_2 reactivity for La, Ce, Pr, Nd, Gd, Tb, Dy, and Y. Each film surface was precovered with O_2 in the ranges of the precoverages from 28 MLO_2 to 230 MLO_2.

Generally, surface oxide layers strongly hinder the dissociation of H_2 molecules, and subsequent H absorption [6]. However, a Ce surface with the highest amount of the O_2 preadsorption layers, 230 ML, exhibits the highest r_{H2} among these metal samples with O_2 preadsorption layers. This suggests that Ce oxides remain metallic, and can dissociate H_2 molecules by exchanging electrons between the surface and the molecules

As shown in Figure 4, the influence of the Ce oxide deteriorates than the clean surface, however, the reactivity of hydrogen exhibits much higher in comparison with the other rare earths with lower amounts of oxide surfacelayers. This is a unique phenomenon to be found in only for Ce, and it is thought that a Ce oxide leaves a metallic property from this result.

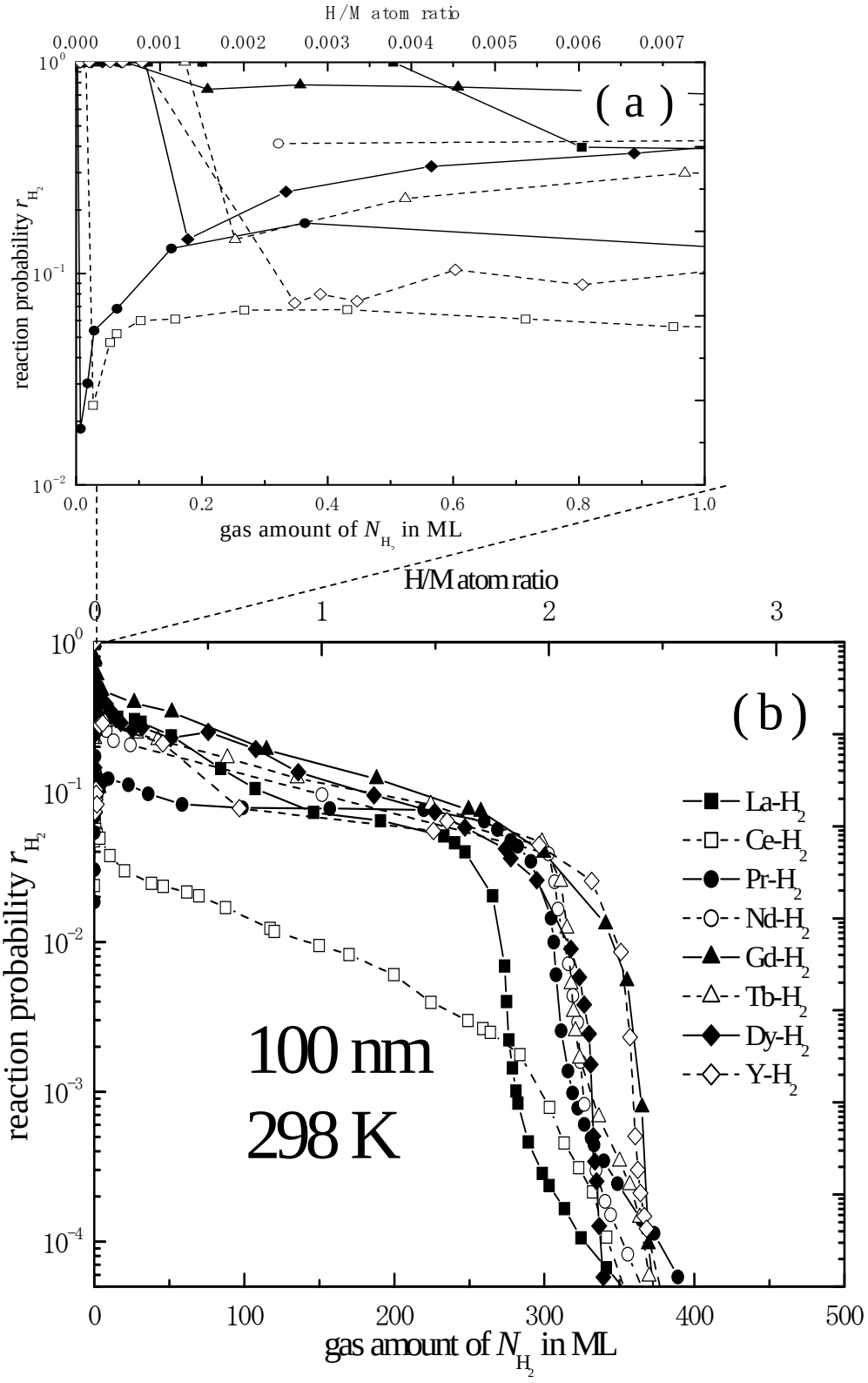

Figure 1: **Change in the reaction probabilities r_{H2} on the La, Ce, Pr, Nd, Gd, Tb, Dy and Y surface as a function of the reacted amount of N_{H2} of H_2 molecules. (a) N_{H2} < 1ML (b) N_{H2} <500ML.**

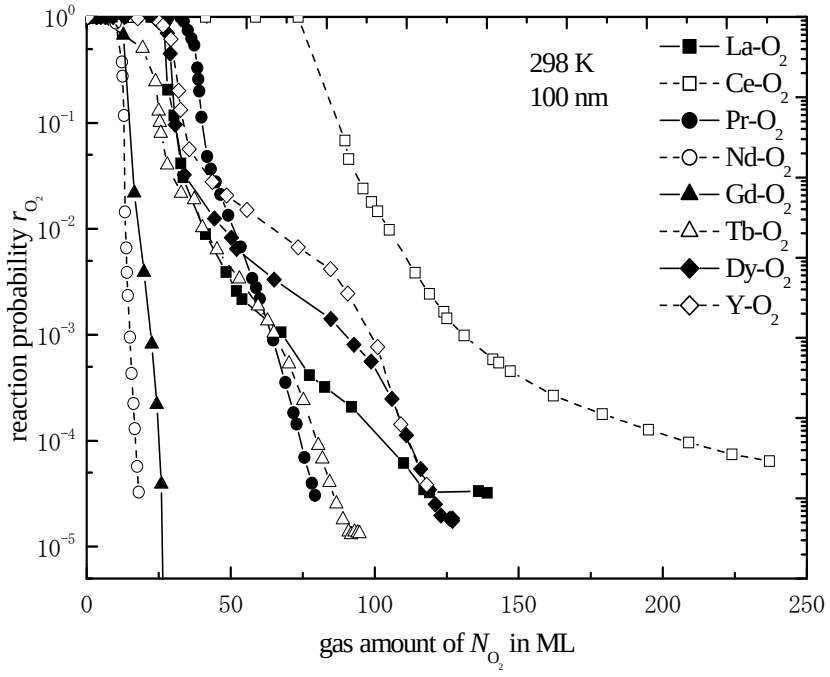

Figure 2: Change in the reaction probabilities r_{O2} on the La, Ce, Pr, Nd, Gd, Tb, Dy and Y surface as a function of the reacted amount of N_{O2} of O_2 molecules.

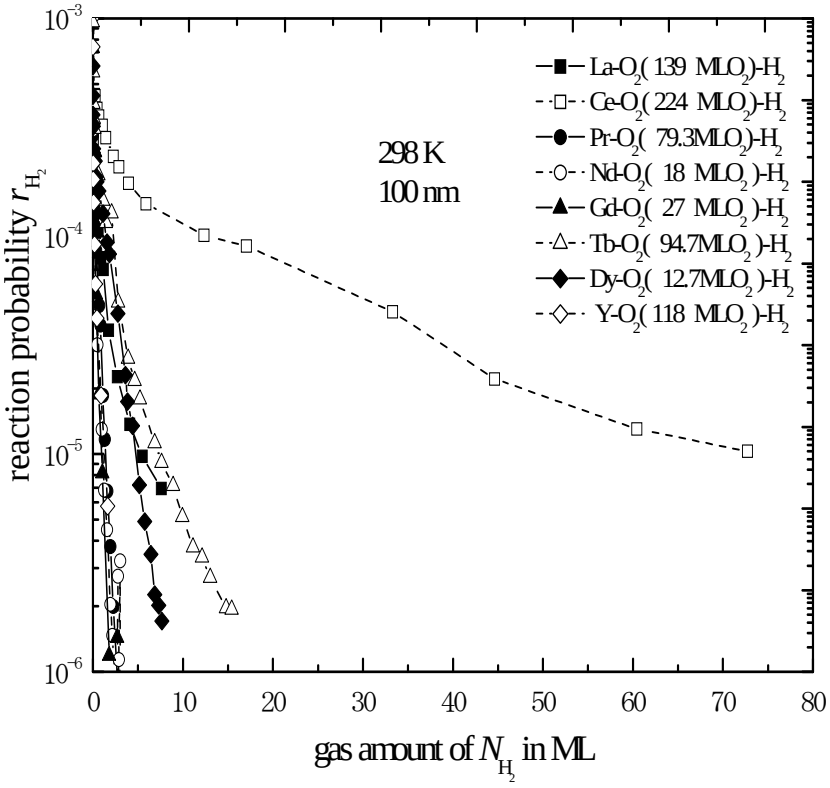

Figure 3: Effect of O_2 preadsorptions on the H_2 reaction probability r_{H2} on the La, Ce, Pr, Nd, Gd, Tb, Dy and Y surface as a function of the reacted amount of N_{H2} of H_2 molecules.

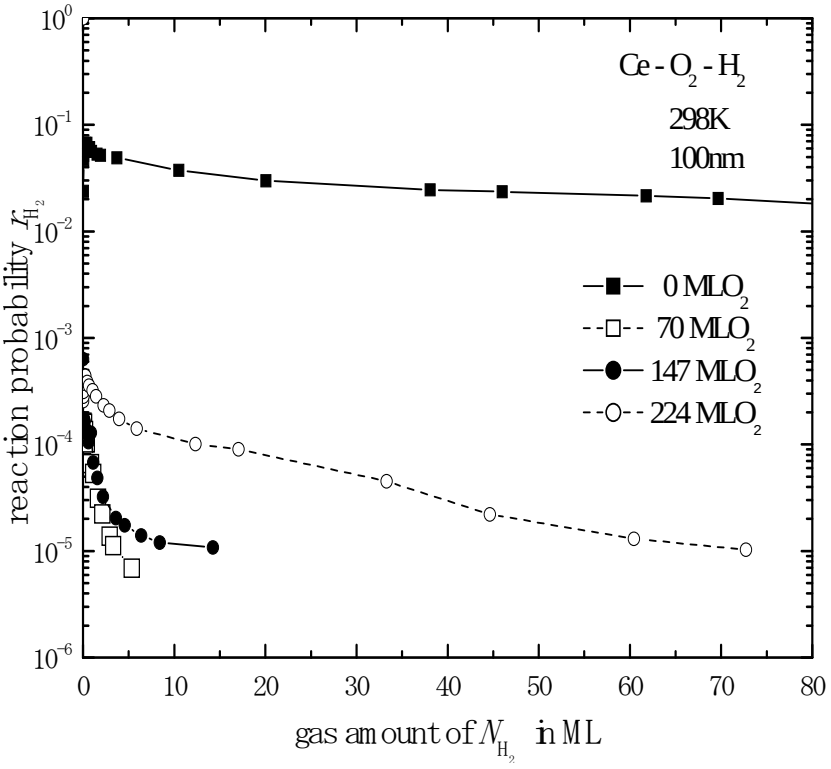

Figure 4: Effect of O_2 preadsorptions on the H_2 reaction probability r_{H2} on the Ce surface as a function of the reacted amount of N_{H2} of H_2 molecules.

4 Conclusion

At the initial stage, the highest reaction probability, r=1, was observed for the reactivity of H_2 and O_2 molecule on RE (La, Ce, Pr, Nd, Gd, Tb, Dy and Y) surface at 298 K. This means that all molecules can dissociate by fast dissociation of covalent H_2 and O_2 molecules on a clean RE surface. The oxidized Ce surface exhibits the highest H_2 reactivity among the other oxidized rare earths examined, indicating the strong metallic features of the CeO_x in comparison with the oxides of La, Pr, Nd, Gd, Tb,Dy and Y.

References

[1] M.Hadano, N.Urushihara, T.Inoue, H.Uchida, J. Alloys Compd. 293-295 (1999) 403-406.

[2] H.Uchida, S.Kato, J. Alloys Compd. 408-412 (2006) 319-322.

[3] S. Wagner, Br. J. Appl. Phy. 1 (1950) 225-231.

[4] H. Uchida, E. Fromm, J. Less Common Met. 172-174, (1991) 832-840.

[5] K. Toguchi, M. Tada and Y.C. Hunag. *J. Less-Common Met.* 88 (1982), 469-478.

[6] H. Uchida, *Int. J. Hydrogen Energy* 24 (1999) 861-869.

Combinational Effect of Charged Particle Irradiation and Alkaline Pretreatment on Hydriding Property of a Mm-Ni Based Alloy

Hirohisa Uchida, Department of Energy Science and Engineering, School of Engineering, Tokai University, Japan
Masahiko Kishimoto, Course of Applied Science, Graduate School of Engineering, Tokai University, Japan
Hiroshi Abe, Radiation Effects Group, Quantum Beam Science Directorate, Japan Atomic Energy Agency, Japan

Abstract

This study deals with surface modifications of a misch metal-nickel (Mm-Ni) based hydrogen storage alloy. This alloy is widely used as negative electrode of nickel-metal hydride (Ni-MH) battery. The surface modification was conducted by electron irradiation. The initial hydriding rate of the alloy was measured. Results are compared among those at different irradiation conditions, and also for additional surface alkaline pretreatment using a KOH solution [1,2]. The electron irradiation on the alloy surface was found effective to increase the initial hydrogen absorption rate.

1 Introduction

Recently, global environmental issues such as greenhouse effect, climate change and air pollution are serious matters to be solved. The use of clean hydrogen energy technologies is one of the most prominent solutions to reduce CO_2 emission presumably causing greenhouse effect.

The application of hydrogen storage alloys may contribute to energy saving and the reduction of CO_2 emission as is proven by hybrid vehicles which are drive both an electric motor and a combustion engine. Most of these hybrid vehicles use Ni-MH rechargeable battery. In 1988, Tokai University proved that a Ni-MH rechargeable battery can be use more than 1000 charge and discharge cycles. Since that time, we have been involved in improving kinetic of electrode performance by surface modifications.

The alkaline pretreatment of the alloy surface using LiOH, NaOH or KOH was found to accelerates the rate of the initial activation [1,2]. Alkaline atoms in the surface oxides lower the work function of electron of the surface, and this facilitates the rate of dissociation of H_2 or H_2O molecules, resulting in the acceleration of hydrogen absorption. In addition, the surface modification of materials, ion/electron irradiation was found to be a quite useful method [3,4]. Then, ion/electron irradiation onto the surface of a metal effectively induces defects such as vacancies, dislocations and micro-cracks in the surface region of the materials.

In this study, we adopted electron as charged particles, and applied electron irradiation to surface modifications of the electrode of the Ni-MH battery. And the effect of electron

irradiation on the initial rate of hydriding of Mm-Ni based alloys was investigated in electrochemical process.

2 Experimental Process

2.1 Mm-Ni based alloy sample

In this study, a negative electrode material of NI\MH battery a Mm-Ni based hydrogen storage alloy, $MmNi_{3.48}Co_{0.73}Mn_{0.45}Al_{0.34}$ (Mm = $La_{0.35}Ce_{0.65}$), was prepared by arc melting. The alloy was then crushed to produce powder samples by cyclic hydriding and dehydriding treatments. The produced powder samples had an average grain size of about 38 μm. The powder was then mixed with Cu powder at a rate of alloy/Cu=1 : 3 in weight, and the pressed under a pressure of 7 t/cm^2 to prepare a pellet sample as cathode for the measurement of hydriding rate in electrochemical process.

2.2 Surface modifications

Surface modifications were made by electron irradiation and/or alkaline treatment. Electron irradiation onto the surface of a sample was made in an acceleration energy of 2 MeV, and a dose range from 5 x 10^{16} cm^{-2} to 1 x 10^{17} cm^{-2} in the atmospheric air, low vacuum (~10^{-2} Torr) or in a He gas atmosphere respectively, using a 2 MV Cockcrfoft-Walton electron accelerator in Japan Atomic Energy Agency.

Alkaline treatment was made by heating a sample at 398 K for 30 min in a 6M KOH solution. This treatment put K ions in the surface oxide layers of the alloy [3,4].

2.3 Measurement of the initial hydriding rate

The initial hydriding rate was measured in electrochemical process where a pellet sample was used as a cathode, and $Ni(OH)_2$ as an anode. An Hg/HgO electrode was used as a reference electrode in an open cell. The rate of hydriding of the sample was measured in a 6 M-KOH using the open cell at a constant voltage –0.93 V and at 298 K.

3 Results and Discussion

3.1 Effect of electron irradiation

Figure 1 shows hydriding curves for samples with and without electron irradiation before electrochemical process. Samples with electron irradiations in the air exhibit much higher hydriding rates than a sample without irradiation.

As known, electron irradiation induces vacancy type defects in the surface region of the alloy [3]. These defects may act as hydrogen trapping sites, and increase hydrogen concentration in the surface region. This may enhance the initial hydriding rate, which was similarly observed for other metals pretreated by various charged ions [4].

3.2 Effect of alkaline pretreatment

Figure 2 shows hydriding curves for samples with and without electron irradiation. After the electron irradiations in air, samples were treated in an alkaline solution of 6 M KOH. Samples with electron irradiations show higher reaction rates that a sample without irradiation. The

reaction rates for samples with both the irradiation and the alkaline treatment are much higher than those of samples only with electron irradiations (Figure 1). After the irradiation, samples were exposed to air before the measurement of electrochemical hydriding rate. In this step, surface oxidation of samples surely took place. Therefore, the additional alkaline treatment was effective to enhance the rate, because the alkaline treatment induces the K atoms in the surface oxides, and reduces the work function of electron of the surface to facilitate the dissociation of H_2O and the subsequent hydriding rate [1,2], .

3.3 Effect of electron irradiation conditions

Figure 3 shows hydriding curves for samples irradiated under different conditions. A sample irradiated in the air exhibits a higher hydriding rate than the other samples irradiated in low vacuum or in a He atmosphere. According to surface analyses using ESCA, samples treated under different conditions showed the presence of complicated oxides of alloy components. Since Mm consists mainly of La and Ce, the contribution of conductive rare earth oxides like CeOx or LaOx to the fast kinetics [5-10] should be taken into account to explain the different kinetic behaviors measured in this work. In this study, we report limited information for surface of samples examined.

ESCA analyses revealed that the sample irradiated in a He atmosphere was found to have rather reactive surface conditions with thinner surface oxide layers than the sample irradiated in low vacuum. All samples were exposed to air before electrochemical hydriding process. As well known, even at room temperature, surface oxidation proceeds more profound for a metal with a clean surface than for a metal covered with thin oxide layers [11]. Therefore, the sample with reactive surface was heavily oxidized during the air exposure. And this resulted in a subsequent low H_2O dissociation and hydriding rates. The sample treated in low vacuum was covered by stable oxide layers after the irradiation, and this seems to have inhibited the subsequent H_2O dissociation and hydriding.

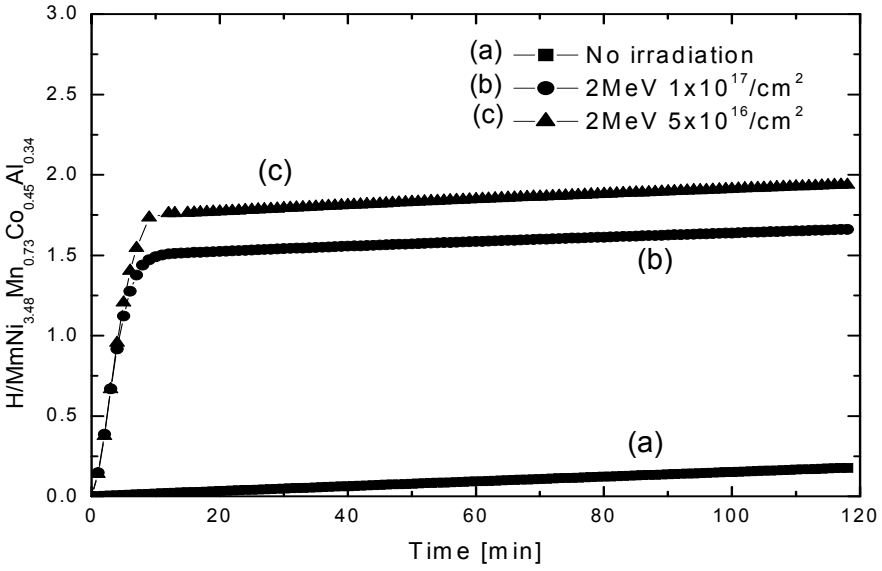

Figure 1: Hydriding curves for samples with and without electron irradiation.

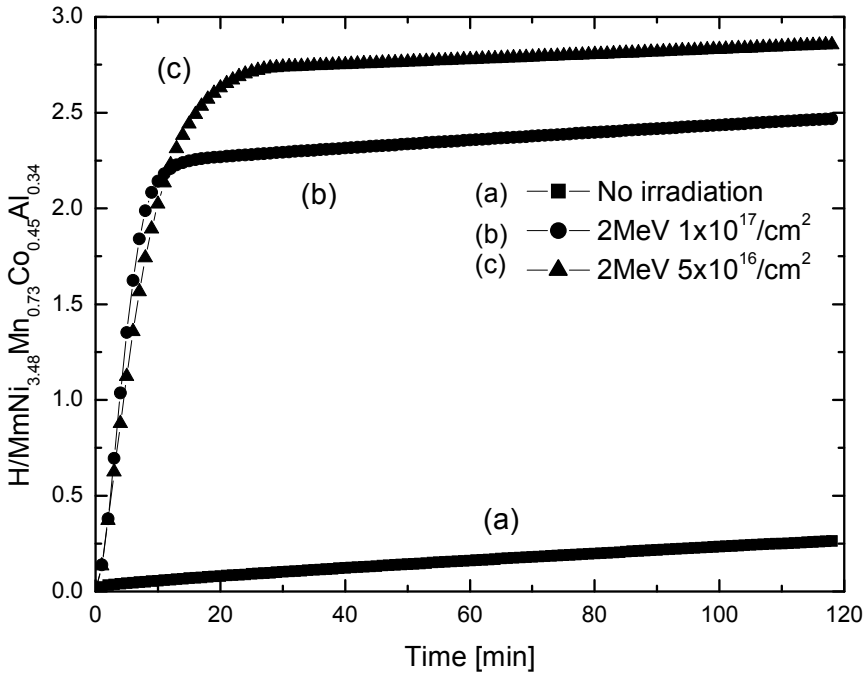

Figure 2: Hydriding curves (a) for a sample without electron irradiation and with alkaline treatment, and (b) and (c) for samples with electron irradiations and alkaline treatment.

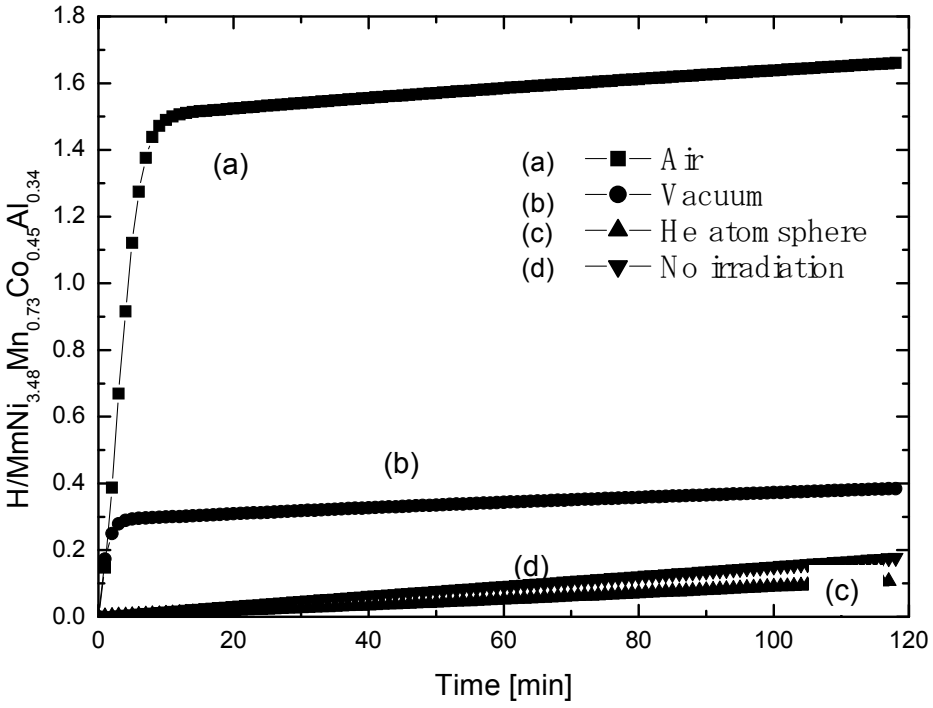

Figure 3: Hydriding curves for samples (a) with electron irradiation in the atmospheric air, (b) with electron irradiation in low vacuum, (c) with electron irradiation in a He atmosphere, and (d) without irradiation.

4 Conclusion

Electron irradiation onto the surface of a Mm based hydrogen storage alloy was found very effective. Additional alkaline treatment was found also to contribute to the enhancement of the hydriding rate. These effects should be interpreted in terme of the induced vacancy defects by electron irradiation, and surface oxidation of the alloy surface. Because the irradiated surface and subsequent oxidation seem to form complicated surface conditions, further investigation with surface analyses is needed.

References

[1] H.Uchida et al., J Alloys Comp., 330(2002)622.
[2] H.Uchida et al., J Alloys Comp., 293(1999)751.
[3] H.Abe et al., Mater. Sci. Forum, 363(2001)156.
[4] H.Abe et al., Nucl. Inst. Meth. B, 206(2003)224.
[5] H. H. Uchida et al., J. Alloys Comp. 231(1995)679.
[6] H. Uchida et al., J. Less Common Met. 172-174(1991)1018.
[7] H. Uchida et al., J. Less Common Met. 172-174(1991)983.

[8] S. Seta et al., J. Alloys Comp. 231(1995)448.
[9] H. Uchida et al., Z. Phys. Chem. 181(1993)417.
[10] H. Uchida et al., Z. Phys. Chem. 181(1993)429.
[11] E.Fromm, Chap.5 “Low Temperature Oxidation” p.78 in “Kinetics of Metal-Gas Interactions at Low Temperatures”, Springer, 1998, ISSN 0931-5195.

HT-PEM Fuel Cell System with Integrated Complex Hydride Storage Tank

R. Urbanczyk, **D. Bathen**, Institut für Energie- und Umwelttechnik e.V., Germany
M. Felderhoff, Max-Planck-Institut für Kohlenforschung, Germany
J. Burfeind, Zentrum für Brennstoffzellentechnik GmbH, Germany

1 Introduction

The growing gap between demands for economic growth and better standard of life on one hand and care for global climate and decreasing energy resources on the other hand require sustainable solutions in the near future. One answer to these problems might be the increased use of renewable energies and “clean” energy carriers like hydrogen wherever possible. Among other things, hydrogen storage is one of the major challenges encumbering hydrogen economy. There are three common techniques of hydrogen storage:

- Pressurized hydrogen
- Liquefied hydrogen
- Hydrogen reversibly chemisorbed or physisorbed (metal hydrides, MOF, carbon materials)

However, the energy required to store hydrogen in each storage method is quite different. For instance, the necessary cooling energy for liquefied hydrogen amounts to 30 % of the stored chemical energy of hydrogen in relation to its lower heating value. An energy input of 12 % for pressurizing hydrogen up to 200 bar [1] and 9 % for storing it at 100 bar in a metal hydride (e.g. $NaAlH_4$) will be required.

A fuel cell system described here was developed and tested with a hydrogen storage tank based on the metal hydride sodium alanate which was thermally coupled to a high temperature fuel cell (HT-PEM). The fuel cell was fed by hydrogen desorbed from the storage tank while the fuel cell provided the reactor with the necessary heat for desorbing hydrogen. The project was carried out by following institutions: Zentrum für BrennstoffzellenTechnik (ZBT) in Duisburg, Max-Planck-Institut für Kohlenforschung in Mülheim (Ruhr) and Institut für Energie und Umwelttechnik (IUTA) in Duisburg. ZBT has developed the HT-PEM fuel cell stack (Figure 1), MPI produced the metal hydride sodium alanate material and IUTA constructed and tested the hydrogen storage tank.

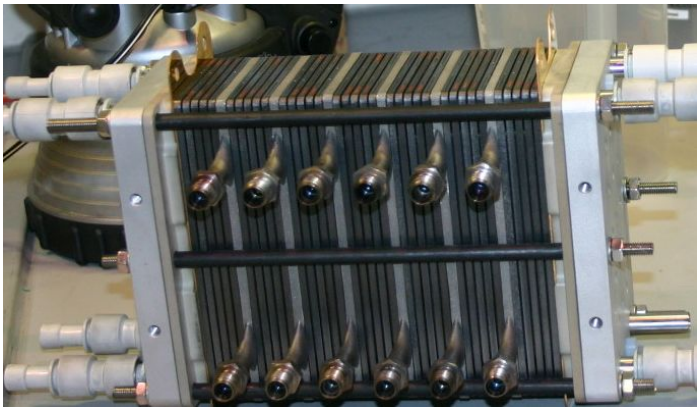

Figure 1: Liquid cooled HT-PEM-Stack with 28 cells by ZBT.

2 Experimental

For gaining experience in constructing and operating hydrogen storage tanks based on sodium alanate the reactor was developed in three steps. The first tank had an inner volume of 245 ml and 67 g of hydride material charged inside. The material was doped with 4 mol-% of $TiCl_3$ and the hydrogen capacity reached 3.35 wt.-% (theoretical reversible storage capacity is about 5.5 wt.-% [2]). The hydrogen mass adsorbed in the hydride was 2.2 g. The heating of the tank was performed by thermal oil flowing in two 1/8 " u-bends welded at the lid. Contrary to the first prototype, the second tank was designed with two flanges. This facilitated the charging of the reactor with the metal hydride and made the changing of the heating systems inside the tank for test purposes more flexible. The first version of the second prototype included a spring-plate system connected to the lid in order to compensate for the volume change of metal hydride during the operation [3]. The heat transfer in this tank was realized by thermal oil flow in annulus. The fluid was led in helically wound rectangular channels inside for heat transfer improvement. The 2nd reactor was charged with 241 g of sodium alanate at 4 mol-% of $TiCl_3$, which resulted in 8 g of hydrogen evolved in the first cycle. This relates to 3,35 wt.-% of hydrogen content in the material. The tank was operated both in stand alone mode and coupled with the HT-PEM as well. In the stand alone operation the absorbing and desorbing characteristics were investigated. In each case the system was heated up and at the end of the test cooled down by a thermostat. The hydrogen flow was adjusted by a mass flow controller. The cumulated hydrogen mass was then calculated by the measurement software. The absorbed hydrogen mass was estimated either volumetrically or with mass flow meter. The mass flow of the cooling medium was measured by a coriolis mass flow meter. The sketch of the test rig is shown in Figure 2.

It was necessary to heat up the system at the beginning of the test. The oil flew first through the heat exchanger system in the tank and then in the channels of the fuel cell. After both components reached appropriate temperature levels, the pump of the thermostat was switched off and the oil flow was driven by the second pump (in Figure 2 between tank and fuel cell).

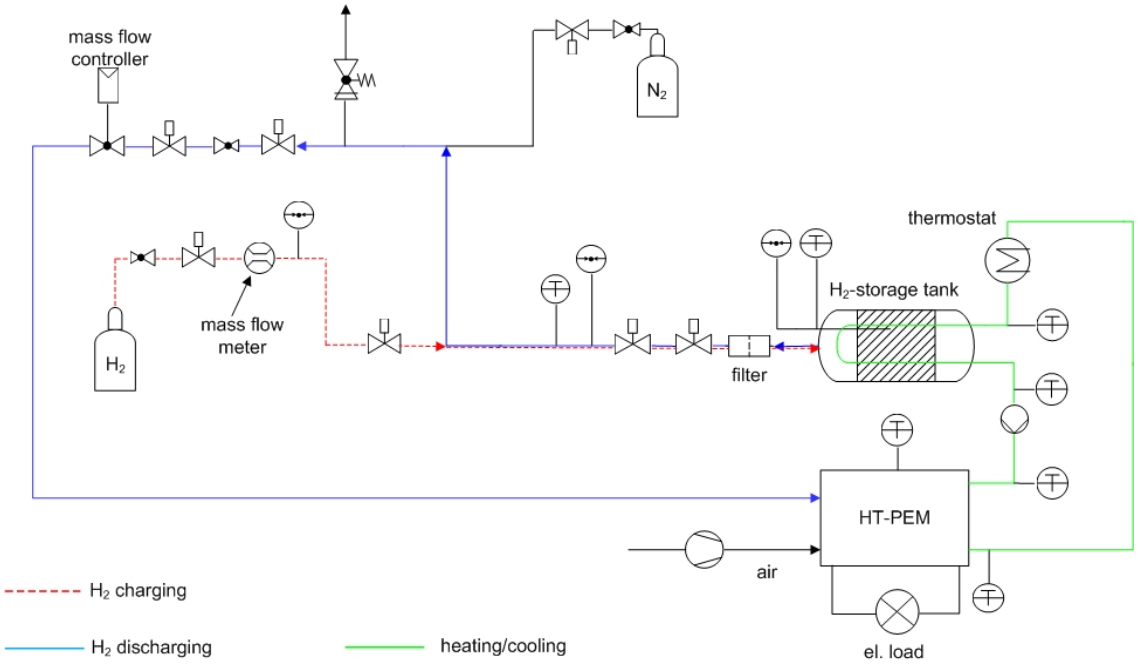

Figure 2: Sketch of the test rig.

The experiments carried out with the above mentioned two reactors led into construction and subsequent tests with the scaled up version of the tank depicted in Figure 3. The vessel contained 2676 g of sodium alanate doped with 4 mol-% of $TiCl_3$. The inner volume of the tank amounted to 5.1 l and 7 thermocouples were installed for temperature measurements. The heat transfer was realized by a system of a double coiled helical winding inside the tank and additionally in the annulus. In the last one the oil flow was led by a rectangular coil with 8 turns. The inner and outer coil inside of the reactor was made of 15 turns of 6 mm outer diameter pipe. The pressure vessel was machined from austenitic steel X 6 CrNiMoTi 17-12 2.

In this project ZBT developed a HT-PEM fuel cell stack with 28 cells with an output power of 260 W_{el}. The operating temperature range of the stack was 120-190°C. The heat transfer in the fuel cell was realized by oil flow inside of 6 cooling plates.

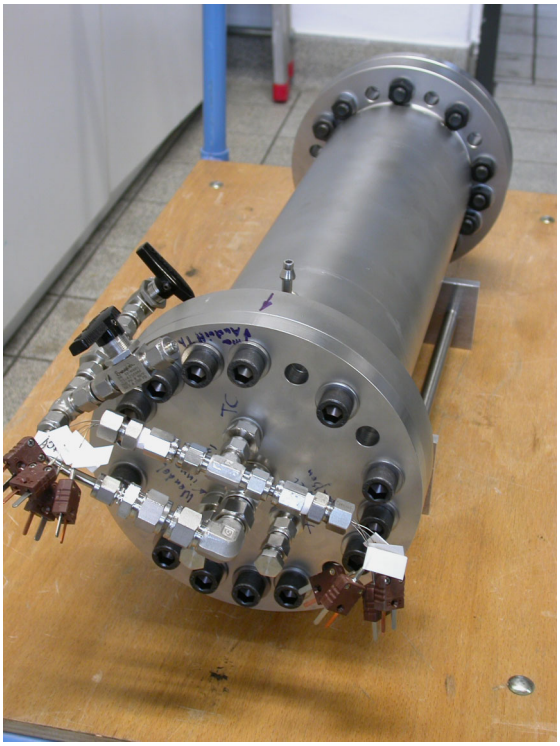

Figure 3: Final version of the hydrogen storage tank.

3 Results

Figure 4 depicts the load profile, hydrogen flow and cumulated electrical energy provided by the fuel cell during one of the experiments. The system was heated up until the fuel cell temperature exceeded 120°C in minute 90 of the experiment time. Subsequently, load cycling was performed on the fuel cell beginning with 206 W, afterwards increased to 235 W and to 240 W, then changed to 190 W, returned to 240 W, lowered to 165 W and finally increased up to 212 W. The hydrogen and the air flow supplied to the fuel cell were adjusted accordingly at the air ratio of 2 before changing the load. Sometimes the load dropped suddenly as can be seen in the figure. This resulted from decreased cell voltage in some cells of the stack. Probably the achieved temperature of the stack was not sufficient for these electrical loads. However after a short time the single cell voltages stabilized and the fuel cell stack began to operate well during the entire testing period. The cumulated electrical energy at the end of the experiment was 660 Wh while the liberated hydrogen mass reached 60 g corresponding to 2.24% of the inserted mass of sodium alanate.

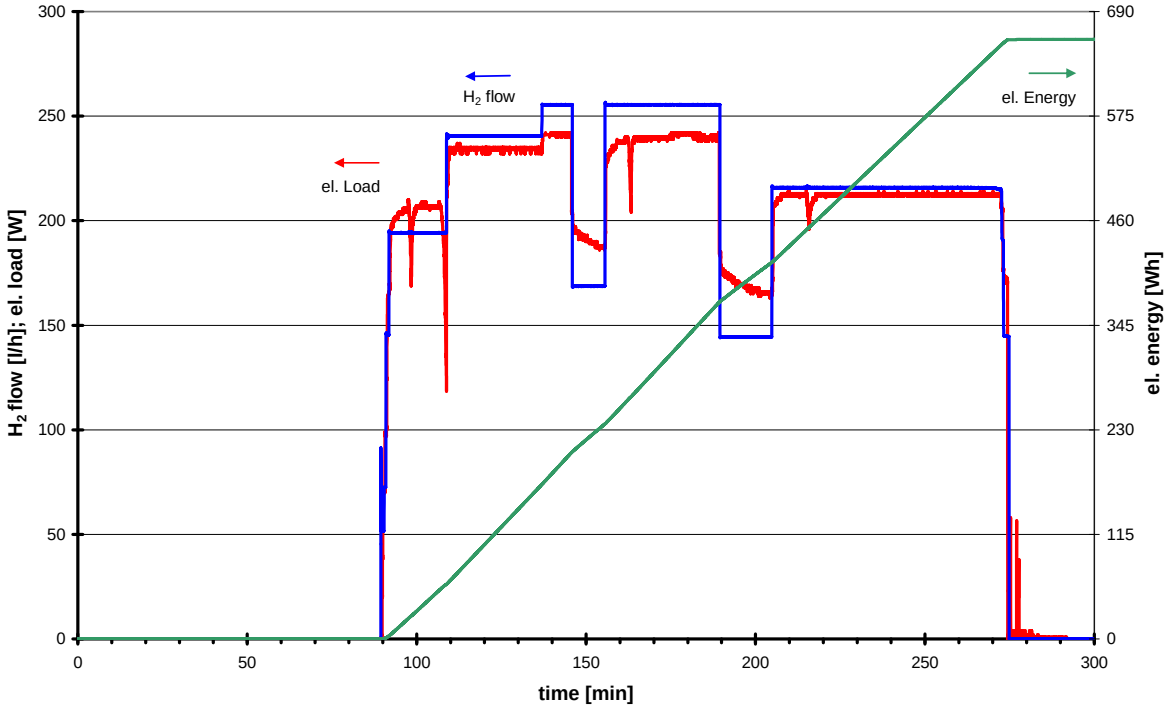

Figure 4: Load profile, hydrogen flow and cumulated el. energy.

The development of temperature of the cooling medium and the fuel cell stack is illustrated in Figure 5. Furthermore, the temperature of the oil at the tank inlet\outlet and at fuel cell inlet\outlet and also the temperature of the fuel cell stack are depicted in Figure 5. There is a huge temperature difference between the oil inlet and outlet in the reactor at the beginning of the test because of the mass of the vessel and additional metal hydride that had to be heated up. The maximum of the heat flow in the warm up phase was 1530 W in the tank and 470 W in the fuel cell at approx. 31 kg/h mass flow of the oil. After the thermostat was switched off (90^{th} minute) the oil temperature in tank inlet was decreased sharply because of a sudden loss of auxiliary heat supply.

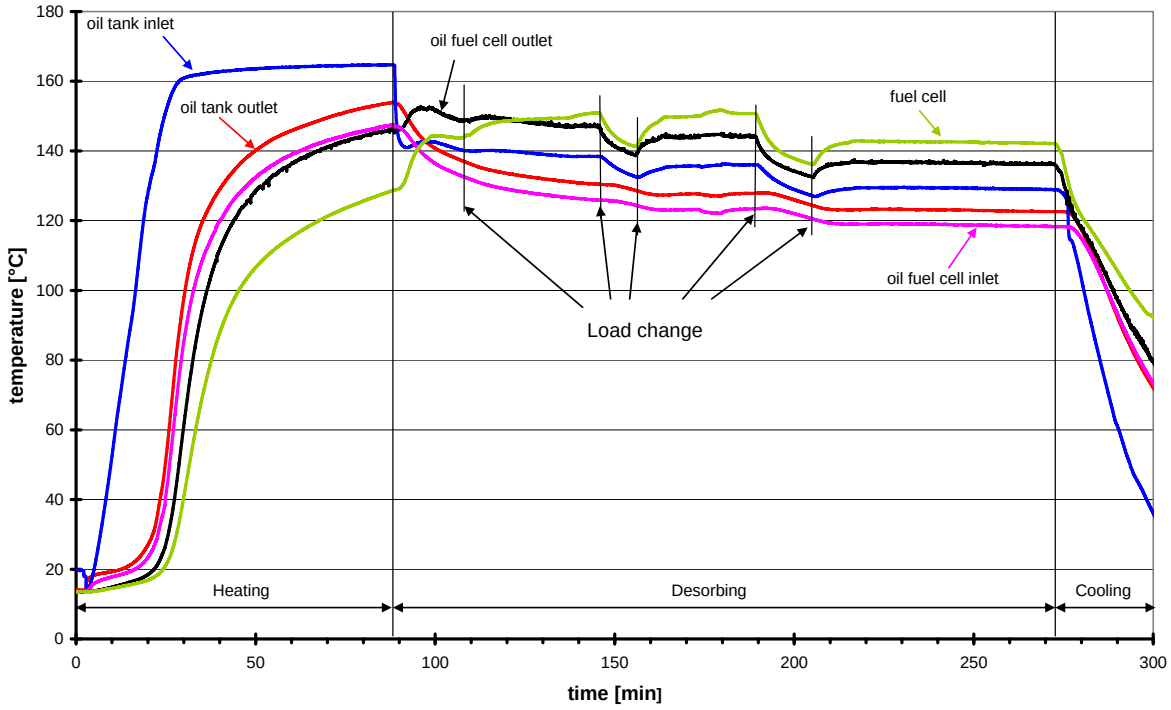

Figure 5: Oil and fuel cell temperature.

From this moment this temperature was lower than the oil temperature in fuel cell outlet, which can be explained by heat losses between both components. A similar trend can be observed between oil temperature in tank outlet and fuel cell inlet. Each time the load was increased, both the temperature of the oil in fuel cell outlet and of the stack increased but the stack temperature rose at bigger ratio and also at the moment, when the oil temperature rise already had stopped. In the stack the generated heat during the operation was therefore transferred both to the cooling fluid and to the housing of the fuel cell. However the temperature in the tank inlet was influenced too, but at lower ratio, because of the heat losses. The pressure in the tank at the beginning of H_2 release reached 77 bar and the temperatures of the sodium alanate were in the range of 136-156°C.

4 Conclusions

A high temperature fuel cell was operated together with a hydrogen storage tank based on complex metal hydride sodium alanate. Both components were thermally coupled so the heat generated by the fuel cell was transferred to the sodium alanate in the hydrogen storage tank for desorbing hydrogen which was then supplied to the fuel cell. The system was operated at different current loads applied to the fuel cell. The temperatures in the thermal circuit followed the loads and although the oil temperature in the tank inlet was approximately 8 K lower than the oil temperature in the fuel cell outlet due to heat losses, 2,24% of hydrogen content of the metal hydride could be liberated during 3 h (in comparison to 3% in the very first cycle). The generated electrical energy was 660 Wh. In comparison to theoretical hydrogen content in sodium alanate of 5,5% the evolved hydrogen amount is lower but the

experiment began at relatively low stack and reactor temperatures (128°C and approx. 150°C respectively) and probably during the second reaction step which is more temperature sensitive not the whole amount of hydrogen could be desorbed at the available reaction rate. On the other hand the warm up procedure should not be exceeded because the auxiliary heat source does not really exist in real life technical system and the heat needed for the desorption of hydrogen should only be provided by the fuel cell. In future systems the heat losses in the thermal circuit have to be radically reduced. For example in the last part of the test the heat flow consumed by the tank was 125 W. At the same time the heat dissipated between the fuel cell and the tank was 144 W and between tank and fuel cell on the other side the heat loss was 82 W. Because of the poor thermal conductivity of the sodium alanate (0,6-0,7 W/m*K) [4] the heat transfer is relatively low. It can be improved by increasing the flow of the thermal fluid on the one hand and by increasing the heat transfer area on the other hand [5]. But it should be kept in mind that the heat transfer resistance is primarily offered by the sodium alanate particles.

References

[1] R. v. Helmolt, *Fuel Cells* 2004, 4, 264

[2] F. Schüth, B. Bogdanovic, M. Felderhoff, *Chem. Commun.* 2004, 2249-2258, 20

[3] G. Sandrock, K. Gross, G. Thomas, C. Jensen, D. Meeker, S. Takara, *J. Alloys and Compounds* 2002, 330-332, 696

[4] D. E. Dedrick, M.P. Kanouff, B.C. Replogle, K.J. Gross, *J. Alloys and Compounds*, 2005, 389, 299

[5] M. Groll, *Heat Recovery Systems & CHP*, 1993, 13, 341

Complex Hydrides

Andreas Borgschulte, Robin Gremaud, Oliver Friedrichs, Philippe Mauron,
Arndt Remhof, and Andreas Züttel

Abstract

The complex hydrides, particularly borohydrides, are currently under discussion as potential solid hydrogen storage materials. Their gravimetric hydrogen density exceeds that of transition metal hydrides by one order of magnitude. The electronic structure of complex hydrides such as $LiBH_4$ differs significantly from that of metallic hydrides, in which the hydrogen atoms occupy the interstitial sites of the metal host lattice. This has severe consequences for their physical and chemical properties such as the crystalline and electronic structure of the compound and ultimately their applicability as hydrogen storage materials. In a broader sense, certain organic hydrides have properties similar to those of complex hydrides and therefore are possibly suitable as hydrogen storage materials. In this chapter, we give an overview on the various materials and hydrogen storage solution based on them.

Liquid Organic Hydrogen Carriers (LOHC): An auspicious alternative to conventional hydrogen storage technologies

J. von Wild, T. Friedrich, BMW Group Research and Technology, Germany
A. Cooper, B. Toseland, G. Muraro, Air Products & Chemicals
Ward TeGrotenhuis, Yong Wang, Paul Humble, Ayman Karim, Pacific Northwest National Laboratory, USA

1 Introduction

Due to the limited availability of fossil fuels – the finite nature and instability of fossil fuel supply and limited production rate – mankind is facing increasing pressure to establish a sustainable alternative energy economy. At least since the so-called “oil crises” in the 1970’s, the automotive industry has started to strive towards a possible substitution of an oil-based energy carrier. As the optimum long-term solution, hydrogen has been identified as an energy carrier, produced on the basis of renewable energy sources (water, sun, wind, biomass) and distributed and stored within adapted infrastructure with new or modified facilities for car refueling.

The realistic implementation of this vision, among others, has been pursued at BMW for more than 30 years in the framework of the “CleanEnergy” program [1]. The results that have been obtained are promising, showing the feasibility of that vision in principle. For instance, the BMW hydrogen record car H2R [2-4] has proven the performance of a hydrogen car powered by an internal combustion engine. The fleet of BMW Hydrogen 7 serial cars [5-7] persuasively demonstrated the suitability and durability for daily use. Another conclusion in the course of these 30 years: the costs to install a new and nationwide infrastructure of fueling stations for hydrogen distribution will be the biggest hurdle for a substantial implementation of the hydrogen economy in the automotive vehicle sector. This is due to the currently established methods of hydrogen storage in the form of cryogenic liquid or pressurized hydrogen. In this respect, it is worth thinking about alternative methods of hydrogen storage [8], which require less energy and cost efforts for distribution and vehicle storage.

2 Discussion

Looking at alternative ways of hydrogen storage for mobile applications, both the systems at fueling stations and onboard the vehicle must be considered concurrently. Thereby, the biggest technical challenge remains onboard the vehicle, as fuel systems in mobile systems have to be compact and lightweight to maintain the best driving dynamics and transportation performance. Additionally, a number of safety relevant criteria have to be fulfilled. Vehicle refueling has to be simple, fast and – last, but not least – affordable. Fulfilling of all these parameters is not an easy task considering the physical and chemical properties of hydrogen. Hydrogen is the element with the lowest specific volumetric density (ca. 84 g / m^3). Confining a lot of hydrogen in a small space is rather challenging. On the other hand, hydrogen possesses a very high gravimetric energy density of 120 kJ / g (lower heating value), which is three times higher than that of gasoline. For a mileage of 500 km, a medium-sized sedan needs 5 kg of hydrogen stored onboard the vehicle. The volumetric and gravimetric goal for a

suitable hydrogen storage system should remain under realistic considerations below 125 l und 100 kg, translating into a volumetric density of 40 g H_2 per liter system volume and a gravimetric storage density of 50 g H_2 per kg system mass (= 5 mass%).

A postulated power demand of such a car (with 100 kW nominal power) requires the supply of ca. 150 g / min. or 9 kg / hr. hydrogen, to be fulfilled by the storage system. Technologically, the most common (automotive) storage of hydrogen is in a physical way as cryogenic liquid and compressed gas. Cryogenic liquid hydrogen offers in combination with lightweight tanks built of aluminum or carbon fiber composite structures currently the greatest potential with respect to gravimetric and volumetric storage densities. The biggest disadvantage is the unavoidable loss of hydrogen due to evaporation of liquid hydrogen during longer stand-still periods. Compressed H_2 tanks require, at acceptable volumetric storage densities, very high storage pressure up to currently 700 bar. Increasing pressure compels more demanding requirements to the structural design of the (always cylindrical) tank. Promising are so-called cryo-compressed tank systems, where hydrogen is stored simultaneously under high pressures and cryogenic temperatures. BMW has developed such a cryo-compressed hydrogen storage concept, which is now undergoing a system and component validation to prove compliance with automotive requirements before it can be demonstrated in a BMW test vehicle [9]. All physical storage systems require a new fuelling station infrastructure, a topic which is currently elaborated in the German *H_2-Mobility* initiative.

Besides the above-mentioned physical storage, a variety of alternative storage methods exist. Alternative storage means the sorption of hydrogen, either chemically or physically, to an additional chemical element. Hydrogen is released from that chemical bonding through heating (thermolysis) or via a direct chemical reaction with additional reagents. Figure 1 shows a choice of the various existing storage technologies.

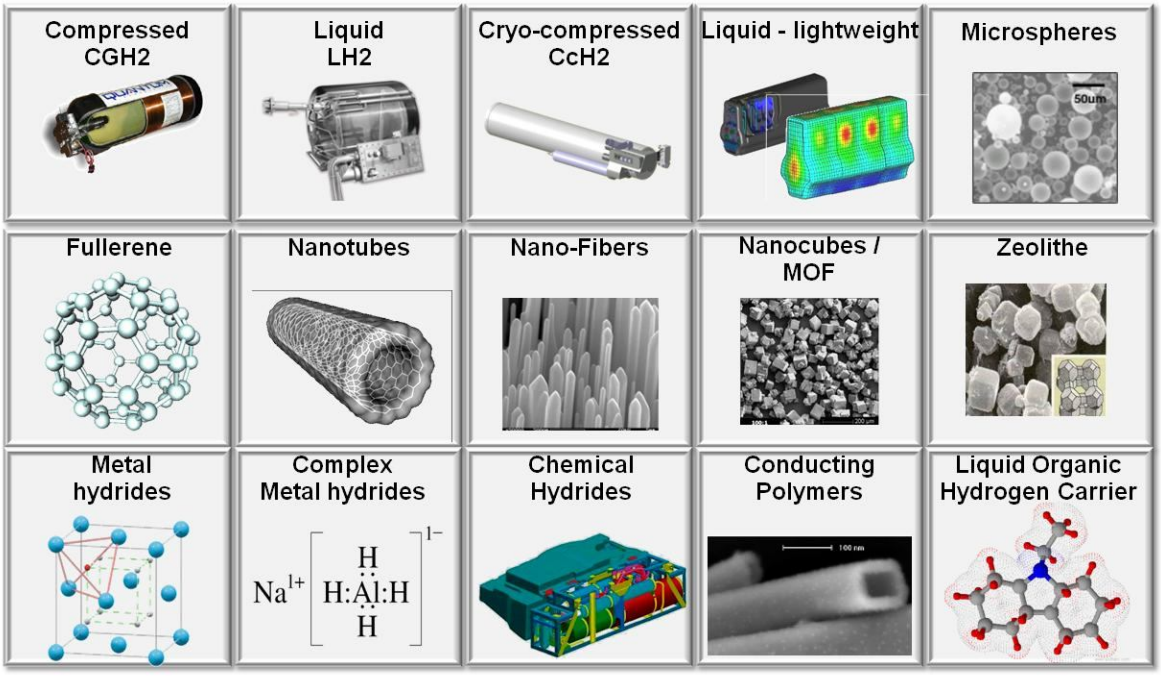

Figure 1: Overview of different hydrogen storage alternatives.

The different hydrogen storage technologies vary in the nature and strength of the hydrogen binding, measured as binding enthalpy ΔH. By using the free energy, ΔG, and the Van't Hoff equation, operation pressure and temperature and thermodynamic stability of the chemical reaction are interrelated.

This leads to the following consequences for the previously mentioned vehicle: Let's take into account an alternative storage material with a binding enthalpy of ΔH = 40 kJ / mol H_2 (e.g. Sodium Alanate). For the loading or unloading of 5 kg hydrogen, an effective thermal energy of ca. 100 MJ is involved. If the tank should be loaded with hydrogen in 3 minutes (as convenient for gasoline tanks), a thermal load of ca. 0.6 MW (!) has to be cooled through a heat exchanger during the exothermic reaction. By contrast, the unloading during full load driving conditions with the dehydrogenation rate of 9 kg H_2 / hr. requires a maximum heat load of only 50 kW. This example shows that especially the loading of alternative hydrogen storage materials with hydrogen is not an easy matter. On the one hand, the required stability of the hydrogen storage materials requires a relatively high binding enthalpy. On the other hand, a higher enthalpy demands a higher cooling power during hydrogen loading, especially if fast fueling is necessary. Against this background, the question is whether it would be a better solution to fuel fully loaded H_2 storage materials directly to the car than the onboard hydrogenation of the storage materials with the inevitable high thermal loads. Needless to say, this fueling method benefits from alternative storage materials in liquid form.

The class of so-called Liquid Organic Hydrogen Carriers (LOHC), where the carrier material is built of organic molecules, seems to be predestinated for a usage onboard of vehicles, because most of them are liquid under ambient conditions in the temperature regime of automotive applications and can be easily rehydrogenated with hydrogen. Therefore, LOHC-tank systems do not need to be insulated or pressurized and could be manufactured as free form tanks in conventional gasoline architecture. Dehydrogenation requires a reactor device, where the hydrogen-rich molecule „LQ∗H_{2x}" is separated under heat supply and in contact with a catalyst to yield a hydrogen-poor carrier material „LQ" and hydrogen:

$$LQ^*H_{2x} + \text{Heat} \rightarrow LQ + x\ H_2.$$

The separation of the functionalities „storage" and „dehydrogenation" also allows the heating of just the required amount of liquid to the reaction temperature, than warming-up the full tank system as in solid storage materials. The dehydrogenated carrier material can be stored in a two-chamber tank system and can be transported back to a centralized facility for rehydrogenation. Ideal hydrogen binding enthalpies for LOHC are between 40 and 70 kJ / mol H_2. Rehydrogenation is possible under moderate H_2 pressures (ca. 70 bar) and temperatures (ca. 150 °C) under heat dissipation.

The basic idea of hydrogen storage in organic liquids is not new [10-13]. With the obtained gravimetric and volumetric material storage density (with up to 7.2 % and 70 g H_2 / l), these LOHC have always been in the field of vision of the research engineers. However, a major issue for an automotive usage was the high temperatures necessary for the dehydrogenation of the material. Recently, new research activities at Air Products now have lead to novel LOHC materials with a significant reduction of the required operation temperature to approx. 200 °C [14]. For a further elucidation of that visionary idea, BMW Group Research and Technology has joined forces with Air Products, United Technologies Research Center (UTRC)

and Pacific Northwest National Lab (PNNL) inside the U.S. DOE-funded project “Reversible Liquid Carriers for an Integrated Production, Storage & Delivery of Hydrogen“. As mentioned, a primary need to realize the use of LOHC in practical applications is an efficient reactor system for the separation of hydrogen from the carrier. Therefore, the project focus is the setup of a reactor prototype with a hydrogen production rate of 1g H_2 / min. to demonstrate the technical feasibility. The necessary energy input, as heat, requires good heat transfer properties within the reactor. An additional challenge is the clean separation of the large amount of gaseous hydrogen generated from the LOHC (>600:1 ratio of hydrogen gas volume to liquid carrier volume at ambient temperature and 1 bar pressure).

The initial research on dehydrogenation reactors were concentrated on two types of continuous flow reactors, packed beds with pelleted catalysts and monolith structured packings. Our test compound, perhydro-N-ethylcarbazole, was dehydrogenated over a variety of pelleted catalysts, (e.g. Pd on alumina) in a packed bed. In all cases, the dehydrogenation proceeded normally, and reactor behavior was typical of a trickle bed reactor. The hydrogen purity was >99.9% even though only a simple tangential flow separator was used to isolate the gaseous product. We anticipated that packed beds would suffer from inefficiencies due to the high hydrogen gas flow rate and catalyst size. An understanding of the flow limitations was obtained by feeding hydrogen to the inlet of the reactor to simulate high gas flow rates which would be found in a full-scale reactor. The addition of hydrogen caused a “drying out” of the catalyst surface. The dry catalyst surface is not effective for reaction, and the flow of product hydrogen decreased. We anticipated a second limitation on reaction rate because of the slow diffusion of large molecules like N-ethylcarbazole through catalyst pores (i.e. intraparticle diffusion). The effectiveness factor, defined as the ratio of measured reaction rate for the catalyst particle to the rate for the catalyst with no diffusion effects, captures this effect. Our developed model for the kinetics of the reaction on micron size particles was used to predict the reaction rate with no diffusion effects. For the packed bed reactor, an effectiveness factor of about 0.08 was estimated, i.e. the rate of reaction for the pellet is only 8% of that for very small particles.

One way to reduce the diffusion effect and to increase the efficiency of the catalyst is to decrease the diameter of the particle. This was done by using a monolith, coated in its interior surfaces with a thin layer of catalyst as a continuous-flow reactor. Corrugated, 0.05 mm iron-chromium alloy foils were coated with a tightly-adhering alumina washcoat. The coated foils were then assembled to form a 400 cpsi (cells per square inch) honeycomb monolith. The desired catalytic metal was then introduced as a washcoat onto the monolith surface. Metal usage was now excellent, with effective factors > 0.5 as compared to 0.08 for the pellets. Initial studies showed that reaction rates using monoliths are diminished by high gas flow rate. Two-phase flow proceeds through four regimes as gas flow rate increases: bubbly, Taylor flow (slug flow), annular flow and gas-continuous with liquid mist. These flow effects are complicated and further data was needed to develop rational scale-up guidelines. Our flow studies showed temperature fluctuations in the flow upstream of the monolith, indicating an unstable fluid flow field. Analysis of causes of this unstable flow led to the surprising finding that there was a small amount flow out of the entrance of the monolith against the overall pressure gradient. Recent literature references show that several types of oscillations are possible when bubbles grow during flow in microchannels, and for high rates of bubble generation, alternating flow patterns both upstream and downstream, are predicted [15;16]. This alternating flow field complicates reactor design, since it affects the residence time of

the fluid in the reactor. We conclude that while microchannel reactors such as monoliths can give high conversion and selectivity, feed distribution will be important for the final design.

Since the structure of the flow field strongly affects reactor performance, an investigation of the fluid mechanics of single- and two-phase flow in a microreactor using Computational Fluid Dynamics (CFD) was undertaken. The simulation showed that using a triangular shape of the individual channels in the monolith causes areas of low flow at the vertices of the triangle, which potentially allows for gas buildup at the wall (Figure 2).

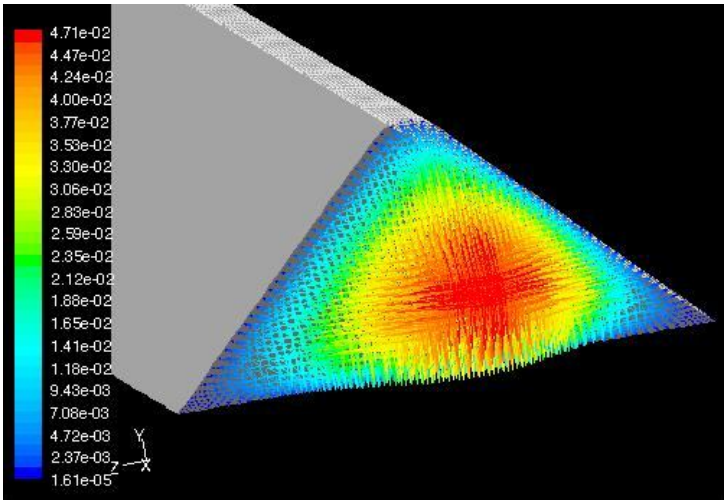

Figure 2: Computational Fluid Dynamics (CFD) simulation of velocity vectors of LOHC flow in triangular channels of a monolith reactor.

Additional work found that circular tubes have only thin layers of low flow and would be less susceptible to such buildup. The combination of high gas flow rate relative to liquid flow rate and the generation of gas at the wall results in a flow pattern in which the gas flow is along the inside of the tube wall instead of the centerline of the tube, as would be expected for the usual case of mixed gas-liquid flow entering the tube. This flow pattern seems to promote early transition to spray flow. The spray flow regime means that the concentration of liquid on the reactor walls is low. This would reduce reactor efficiency, since the liquid must be in contact with the catalyst for reaction to occur. Thus, the study shows that generation of gas at the walls of the reactor leads to novel design issues. Tube shape, catalyst distribution and gas flow pattern must all be part of the final reactor design consideration.

Microchannel reactors were considered to have design characteristics that are suitable for dehydrogenation of LOH. A microchannel reactor concept was pursued with the intent of segregating the liquid carrier from the H_2 being produced. The concept, which is illustrated in Figure 3, deploys the catalyst in a thin porous substrate that is wetting for liquid carrier and placed in a microchannel. A vapor plenum adjacent to the wick allows the H_2 to separate from the liquid as it is generated, preventing the catalyst from drying out. Proper balancing of the liquid and vapor pressures keeps the liquid in the wick by capillarity and causes the liquid to flow through the wick. This reactor concept addresses the issues of catalyst drying out and other effects of 2-phase channel flow. Experiments with the microwick reactor concept showed significantly reduced performance as indicated in Figure 3 for the wick only configuration. The test apparatus was configured to cool the vapor stream leaving the reactor caus-

ing condensation of carbazole vapors in that stream. As the liquid flow rate was decreased, more and more of the unreacted carrier was volatilized and bypassing the catalyst. To compensate, Pt/Al_2O_3 coated aluminum foam was added to the vapor channel of the wick reactor resulting in significantly improved performance, as indicated by the wick+foam data in Figure 4. However, reactor performance did not surpass performance of a packed bed of 210-420 micron particles.

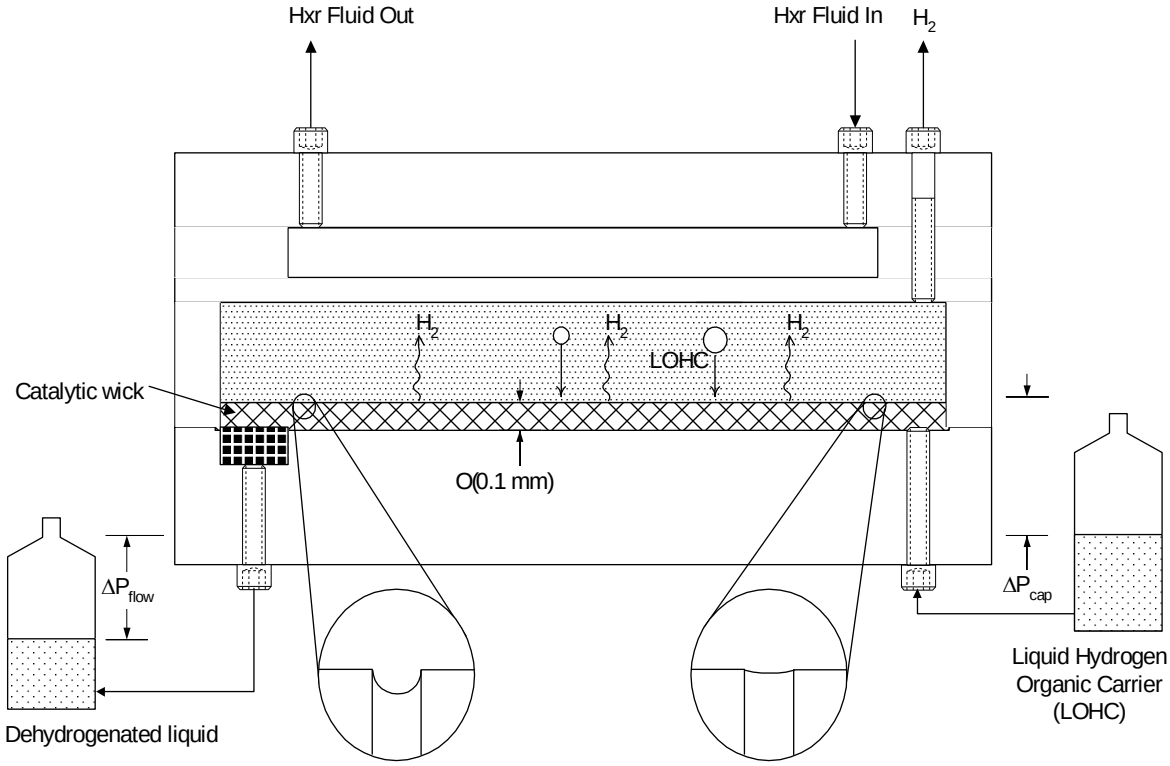

Figure 3: Microwick reactor concept for dehydrogenating a Liquid Organic Hydrogen Carrier.

The results in Figure 3 imply that phase segregation and maintaining wetted catalyst is not dictating performance in a packed bed reactor. An analysis of diffusion limitations in the packed-bed revealed that the reaction kinetics are an order of magnitude faster than the H_2 diffusion rate within the pores of the carbazole-filled catalyst particles. In addition, the kinetic rate is of the same order of magnitude as the H_2 diffusion rate through the liquid boundary layer surrounding the particles. The analysis also explains that much lower conversions from the wick reactor concept were caused by lower liquid velocities through the wicks that increased boundary layer thickness. The mass transfer analysis was further confirmed through experiments with smaller catalyst particles. Working with particles an order of magnitude smaller than the packed-bed particles has successfully improved catalyst productivity from 0.02 g H_2/g Pt/min at 90% conversion for the packed bed to 1.5 g H_2/g Pt/min, which is 75% of the original target.

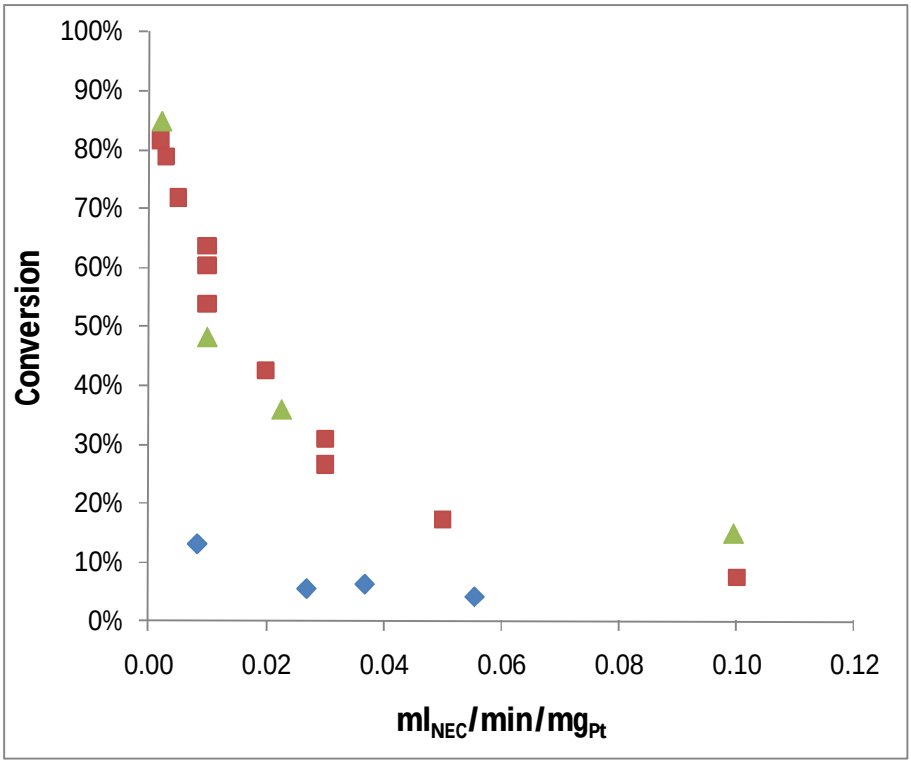

Figure 4: Conversion of n-ethyl carbazole as a function of liquid flow rate normalized by catalyst loading for a packed bed of 210-420 micron particles (■), a microwick reactor (♦), and a microwick reactor with a catalyst-loaded foam insert in the vapor space (▲).

The team is now working to realize this level of performance in a proof-of-concept reactor producing 0.1 g/min of H_2. This will be followed by a gas-heated prototype reactor capable of supplying a 1 kWe scale PEM fuel cell. If successful, the engineered catalyst volume will be less than 40 ml.

At BMW, the existing test bench to operate liquid carrier materials during dehydrogenation in microstructured reactors has been changed. Additionally, a new facility has been constructed for analysis during rehydrogenation. Regarding onboard car application, first simulation results have shown that BMW hydrogen combustion engines can offer the necessary heat quantities at temperature levels necessary for the dehydrogenation of LOHCs. Therefore, an application of LOHC-storage system in a hydrogen combustion engine propelled vehicle is in principle possible.

Usage of Liquid Organic Hydrides shows a relatively simply way for the entire distribution, storage and usage of hydrogen in vehicles. The handling procedure would be, as depicted in Figure 5 largely comparable to today's usage of gasoline or diesel fuels.

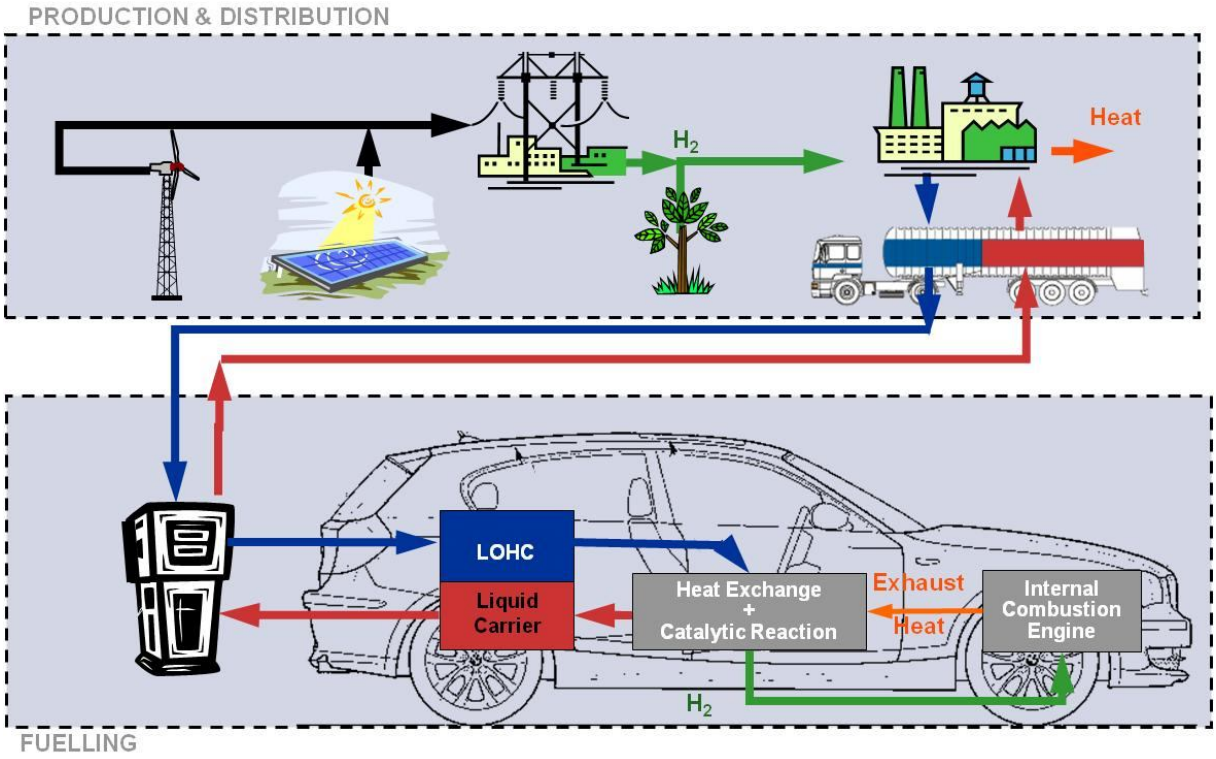

Figure 5: Vision of Liquid Organic Hydrogen Carriers in a Hydrogen based alternative energy economics.

3 Conclusion

Liquid Organic Hydrogen Carriers (LOHC) are liquid pumpable, easily rechargeable and have, at acceptable gravimetric storage densities, similar volumetric storage densities than cryogenic liquid hydrogen.

The off-board recycled fuel can be stored and transported at ambient conditions and does not need an entirely new filling station infrastructure.

Inside the above mentioned DOE-funded project, we are striving to make that vision reality.

The Authors would like to thank the Department of Energy for financial support through contract #DE-FC36-05GO15015.

References

[1] Freymann, R., Pehr, K, Strobl, W. : Twenty-five Years of Continuous Hydrogen Research at BMW. JSAE Paper Number 20025305. Proceedings of the JSAE Annual Congress, Yokohama, Japan (2002).

[2] Strobl, W. : BMW H2R. NHA Annual Hydrogen Conference, Washington, D.C., USA (2005).

[3] Fickel, HC, Heller, K, Kresse, T, von Wild, J.: Ist der Wasserstoffverbrennungsmotor schon auf der Überholspur? 6. Dresdner Motorenkolloquium (2005).

[4] Freymann, R., Strobl, W, Kübler, J. : Wasserstofftechnologie im Automobilbau: nachhaltig, sauber, leistungsfähig. Erste Österreichische Wasserstoff-Konferenz, Graz (2005).

[5] The BMW Hydrogen 7. Available at: http://www.bmw.com/com/en/insights/technology/efficient_dynamics/phase_2/clean_energy/bmw_hydrogen_7.html;. Accessed 01.09.2008.

[6] Danner, S., Fürst, S. : BMW Hydrogen 7 series - a safe way to a clean future. FISITA, Yokohama, Japan (2007).

[7] Fürst, S, Gräter, A, Pehr, K.: Hydrogen 7: The First Premium Saloon with a Bivalent Internal Combustion Engine. JSAE Paper Number 20075338. JSAE Proceedings 28, 5-8 (2007).

[8] von Wild, J., Freymann, R, Zenner, M. : Potentiale von alternativen Wasserstoff-Speicherungstechnologien. VDI-Berichte: Innovative Fahrzeugantriebe 2008, Dresden/Germany , 2030, 273-298 (2008).

[9] Aceves, SM, Espinosa-Loza, F, Ledesma-Orozco, E, Ross, TO, Weisberg, AH, Brunner, TC, Kircher, O.: High-density automotive hydrogen storage with cryogenic capable pressure vessels. Int J Hydrogen Energy 35, 1219-1226 (2010).

[10] Scherer, GWH, Newson, E.: Analysis of the seasonal energy storage of hydrogen in liquid organic hydrides. International Journal of Hydrogen Energy 23, 19-25 (1998).

[11] Taube, M, Rippin, D, Knecht, W, Hakimifard, D, Milisavljevic, B, Gruenenfelder, N.: A prototype truck powered by hydrogen from organic liquid hydrides. International Journal of Hydrogen Energy 10, 595-599 (1985).

[12] Hodoshima, S, Arai, H, Takaiwa, S, Saito, Y.: Catalytic decalin dehydrogenation/naphthalene hydrogenation pair as a hydrogen source for fuel-cell vehicle. International Journal of Hydrogen Energy 28, 1255-1262 (2003).

[13] Kariya, N, Fukuoka, A, Ichikawa, M.: Efficient evolution of hydrogen from liquid cycloalkanes over Pt-containing catalysts supported on active carbons under "wet-dry multiphase conditions". Applied Catalysis A: General 233, 91-102 (2002).

[14] Pez, G, Scott, A, Cooper, A, Cheng, H, Bagzis, L, Appleby, J, inventor: HYDROGEN STORAGE REVERSIBLE HYDROGENATED OF PI-CONJUGATED SUBSTRATES. patent WO 2005/000457 A2. 06.01.2005 (2005).

[15] Xu, J, Feng, Y, Cen, J.: Transient flow patterns and bubble slug lengths in parallel microchannels with oxygen gas bubbles produced by catalytic chemical reactions. Int J Heat Mass Transfer 50, 857-871 (2007).

[16] Wang, G, Cheng, P, Wu, H.: Unstable and stable flow boiling in parallel microchannels and in a single microchannel. Int J Heat Mass Transfer 50, 4297-4310 (2007).

Ammonia Borane and Sodium Borohydride: Boron Hydrides as Hydrogen Storage Materials Intended to Specific and Different Applications

Umit B. Demirci, Julien Hannauer, R. Chamoun, Philippe Miele, Université Lyon 1, CNRS, UMR 5615, Laboratoire des Multimatériaux et Interfaces, France

1 Introduction

Hydrogen storage is still today one of the most significant issues hindering the development of a 'hydrogen energy economy'. It is a significant challenge and to take up it several solutions, based on either physisorption of H_2 or chemisorption of H, have been considered up to now [1]:

- Physical storage: i.e. compressed H_2, liquid H_2, (cryo-)adsorption in adsorbents such as zeolites;
- Chemical storage: i.e. hydrolytic hydrides (e.g. sodium borohydride $NaBH_4$ (SB)), metal hydrides (e.g. MgH_2), complex hydrides (e.g. sodium alanate $NaAlH_4$), amine-borane adducts (e.g. ammonia borane NH_3BH_3 (AB)), amides/imides, hydrocarbons, glass microspheres, ice hydrates.

From all of these possibilities, hydrolytic hydrides and amine-borane adducts are noticeable by their high hydrogen densities[1]. For example, the 2000s have seen the emergence of, first, SB and, then, of AB, which are constituted of 10.8 and 19.5 wt% of hydrogen respectively [2].

As noticed by Eberle et al. [1], "storage of hydrogen is a substantial challenge, especially for applications in vehicles" and the automotive industry is the eagerest in expecting an efficient storage solution. Accordingly the U.S. Department of Energy (US DOE) has set quite severe application targets [3]. For example, one of the most known targets, which is also one of the most used to discuss the potential of a storage solution, is the gravimetric hydrogen storage capacity [2]. Even though the GHSC targets have been recently revised downwards, meeting them is a significant challenge. For example, the US DOE recommended a no-go for SB for automotive applications in 2007 because of too low eHDs and therefore too low GHSCs [4]. Nevertheless $NaBH_4$ still has a potential for portable [5] and niche fuel cell applications [6]. While recommending the no-go for SB, the US DOE strongly suggested intensifying the efforts devoted to AB while valorizing the know-how on SB.

For both SB and AB, one of the main challenges is to release efficiently the maximum of the stored hydrogen. To succeed in that, several dehydrogenation routes (Figure 1) have been considered so far: the SB hydrolysis [7] and methanolysis [8]; and the AB hydrolysis [9],

[1] In accordance with the definitions set by the US DOE, the term "gravimetric hydrogen storage capacity" (denoted GHSC) will only be used for a complete storage system (including the tank, storage media, safety system, valves, regulators, piping, and so on). The term "theoretical hydrogen density" (denoted HD) will define the gravimetric content of hydrogen in the storage media (e.g. SB or AB). The term "effective hydrogen density" (denoted eHD) will refer to the content of hydrogen really released from the storage media.

methanolysis [10] and thermolysis [11]. Note that thermolysis of SB needs too high temperatures, even in the presence of a catalyst, to be considered suitable for applications (i.e. T > 400 °C) [3]. With respect to the solvolysis reactions (with liquid water and methanol), the HDs of the systems $NaBH_4$-$2H_2O$, $NaBH_4$-$4CH_3OH$, NH_3BH_3-$2H_2O$ and NH_3BH_3-$4CH_3OH$ are 10.8, 4.8, 9.0 and 3.8 wt%, respectively (Figure 1). However these theoretical values (taking into account only the stoichiometric amount of solvolytic agent) are difficulty achieved because of some problems: e.g. excess of the solvolytic agent that is used also as solvent, formation of thermodynamically stable borate hydrates, limited solubility of the hydrogen storage materials as well as that of the borates, weight of the by-products, and volume expansion (borates/SB or borates/AB, %). Today the yield of the H_2 release is not an issue anymore as very reactive catalysts have showed to convert 100 % of SB or AB with variable hydrogen generation rates (HGRs). The issue with the catalytic materials is rather durability [8].

Hydrolysis @ <85°C	
$NaBH_4 + 2\ H_2O \rightarrow NaBH_2 + 4\ H_2$	10.8 wt%
$NH_3BH_3 + 2\ H_2O \rightarrow NH_4BO_2 + 3\ H_2$	9.0 wt%
Methanolysis @ <85°C	
$NaBH_4 + 4\ CH_3OH \rightarrow NaB(OCH_3)_4 + 4\ H_2$	4.8 wt%
$NH_3BH_3 + 4\ CH_3OH \rightarrow NH_4B(OCH_3)_4 + 3\ H_2$	3.8 wt%

Thermolysis @ 120-500°C	
$NaBH_4$ *not considered*	
$n\ NH_3BH_3 \rightarrow [NH_2BH_2]_n + H_2$	6.5 wt%
$[NH_2BH_2]_n \rightarrow [NHBH]_n + H_2$	6.5 wt%
$[NHBH]_n \rightarrow [NB]_n + H_2$	6.5 wt%
$n\ NH_3BH_3 \rightarrow [NB]_n + 3\ H_2$	19.5 wt%

Figure 1: Ideal solvolysis of SB and AB and thermolysis of AB.

We are currently much involved in the solvolysis of SB and AB and we are working especially on the development of reactive, durable metal-based (mainly Co) catalysts as well as on optimizing the eHDs of the systems specified above. Hereafter are reported our main results concerning both topics. In a last section entitled 'outlook and conclusion', the AB thermolysis is briefly considered as it appears to be the most promising route for the automotive applications despite storage irreversibility.

2 Short Survey About the Metal Catalysts in the Solvolysis of SB and AB

With respect to the hydrolysis of SB, a great number of studies have been published since the late 1990s and the Amendola et al.'s pioneer work [12]. Most of them are about catalytic materials. Liquid or solid acids [13, 14], metal salts in solution [14] or loaded into solid SB [15], metals [16], metal borides [17], metal alloys [18] and supported metals (mainly Ru or Co) [19, 20, 21, 22] have been considered. Highly reactive catalysts that are mainly based on Co have often been reported and, frankly speaking, preparing such catalysts is not an issue anymore. We have investigated acids such as acetic acid [15] and metal-based catalysts such as cobalt [16] and aluminum [23] salts, cobalt fluorides and borides [24], and Ru or Co supported catalysts [20, 25], and the main conclusion of our works is that variable hydrogen generation rates with total conversions of almost 100 % can be easily obtained with various types of catalysts. This is illustrated by the data listed in Figure 2. Note that the conclusion given above holds also to the SB methanolysis.

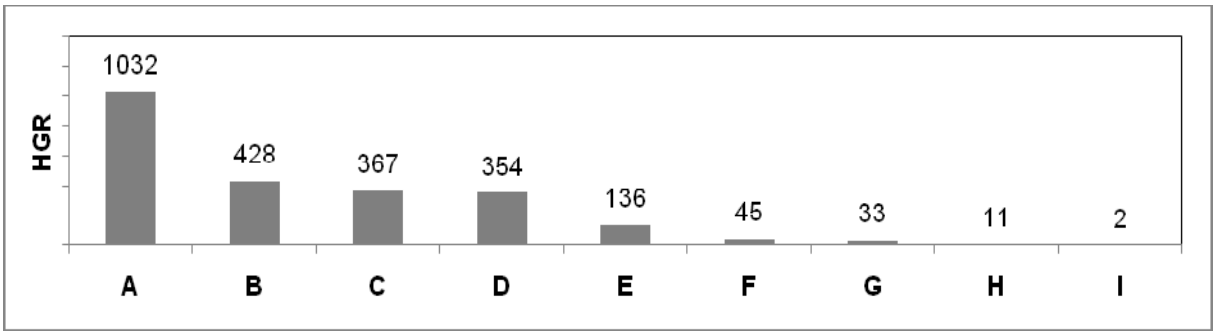

Figure 2: Hydrogen generation rates (L min^{-1} g^{-1}(metal)) for some metal-based heterogeneous catalysts at ambient conditions: A: $RuCl_3$-$AlCl_3$ [24]; B: 10 wt% Ru-LiCoO2 [21]; C: 15 wt% Pt-$LiCoO_2$ [22]; D: $AlCl_3$ [21]; E: 10 wt% Co-C [24]; F: $CoCl_2$-Al_2O_3 [26]; G: Co [25]; H: 1 wt% Ru-ZrO_2-SO_4^{2-} [20]; I: $CoCl_2$ [16].

Regarding the AB hydrolysis, the first published studies date back the middle of the 2000s. Xu's group may be considered as the leader group in this area [26]. Similarly to SB, most of the works focused on the reactivity of the developed metal-based (heterogeneous [10] and homogeneous [27]) catalysts. For example, the following hydrogen generation rates have been reported to occur at ambient conditions: e.g. 10 mL min^{-1} for Pt-Ru/C at 20 °C [28], 12 mL min^{-1} for 1 wt% Rh/TiO_2 at 40 °C [29], 25 mL min^{-1} for Rh^0 nanoclusters at 35 °C [28], 67 mL min^{-1} for Co-Mo-Fe/Ni foam at 25 °C [30], 100 mL min^{-1} for Pd^0 nanoclusters at 25 °C [31] and 140 mL min^{-1} for Ru^0 [32]. Recently we have reported a hydrogen generation rate of 21 mL min^{-1} for $CoCl_2$ [33]. Hydrogen generation rates > 600 mL min^{-1} for Ru-based catalysts have even been achieved at 40 °C. However that may be, similarly to SB it is not so problematic to synthesize reactive catalytic material for hydrolyzing AB.

In fact, the main problem with the metal catalysts used in the hydrolysis of both SB and AB is their limited durability. Agglomeration of particles, surface oxidation and component dissolution in alkaline SB solutions are common reasons for catalysis deterioration of a catalyst [8]. Synthesizing stable catalysts is one of our concerns. For example, in a previous study it was considered fluorination of Co nanoparticles in order to prevent them from oxidation or boronation [25]. In this case, the catalyst was in powder form and this is another problem. Handling of powder catalyst is not easy and above all it is not convenient for start-and-stop applications, that's why we are also working on shaped catalysts, which are evidently much more practical. Our criteria of success are as follows: shaped catalysts as reactive as powder catalysts; and durable shaped catalysts that will permit start-and-stops without reactivity degradation, which is important since in practical uses support failure of the catalyst support and catalyst erosion are reasons to the catalyst deterioration due to mechanical constraints of the generated hydrogen bubbles and flushing of the SB or AB solution [8]. Accordingly, we are working on developing 2D shaped catalysts consisting of Co^0 or supported Co catalysts deposited over Ni foam by electrodeposition or electroless deposition, over polymeric films by electrodeposition, and over Cu/stainless steel plates by electrophoretic deposition (Figure 3). Our preliminary results show that for optimized shaped catalysts high reactivity, even higher than that of equivalent catalysts in powder form, and relative durability can be achieved.

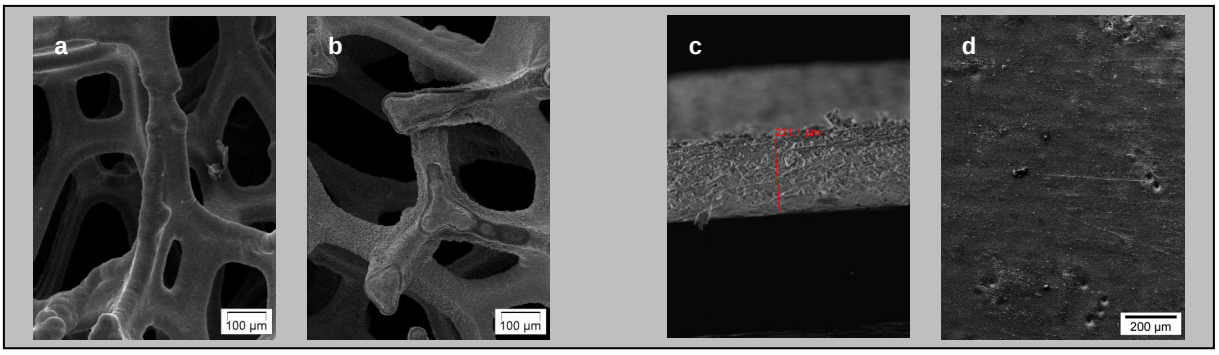

Figure 3: SEM images of (a) Ni foam, (b) Co-Ni foam, (c) and (d) Co-Al_2O_3-Cu thickness and surface.

3 Effective hydrogen Densities

Recently, we concluded that "none of both boron hydrides is mature enough to envisaging applications, especially automotive applications, both suffering from low, but not-optimised, effective hydrogen storage capacities" [3]. It was for example showed that to date the highest effective GHSCs are 4.5 and 2.5 wt% for the systems $NaBH_4$-H_2O and NH_3BH_3-H_2O, respectively. The question that is then asked is: may SB and AB be envisaged for automotive applications when their hydrolysis is considered? For the former hydride, the answer was given by the US DOE when a no-go was recommended [5]. With respect to the latter compound, the answer is quite evident. Given that the HD of NH_3BH_3-$2H_2O$ is only of 9.0 wt%, the highest GHSC that could be obtained is 4.5 wt%[2], that is, far from the targets for automotive applications by 2015 [4]. However portable applications can still be considered even if there is no target clearly set [3].

In the hydrolysis of SB, several issues make reaching the HDs given in Figure 1 difficult. Actually the hydrolysis takes place in an excess of water owing to two reasons. The 1st reason is that the thermodynamically stable form of the borate by-products is the hydrated one, namely $NaBO_2.xH_2O$:

$$NaBH_4 + (2+x)\ H_2O \rightarrow NaBO_2.xH_2O + 4\ H_2$$

For example, Marrero et al. [34] particularly showed that $NaBO_2.2H_2O$ predominates over $NaBO_2.4H_2O$ at ambient conditions. Accordingly the HDs of SB-(2+2)H_2O and SB-(2+4)H_2O are only of 7.3 and 5.5 wt%, respectively. It is noteworthy that this can also be applied to the AB hydrolysis even though as far as we know no study about its by-products has been reported yet:

$$NH_3BH_3 + (2+x)\ H_2O \rightarrow NH_4BO_2.xH_2O + 3\ H_2$$

[2] Assuming that the AB weight is 50 % of the weight of the complete storage system.

The HDs of AB-(2+2)H_2O and AB-(2+4)H_2O will then be of 5.8 and 4.3 wt%. To get round such a problem, it has been suggested to methanolyze SB or AB as $B(OCH_3)_4^-$ is not hydrated in ambient conditions. This has been confirmed through our works as we showed, by XRD and IR, the formation of only $NaB(OCH_3)_4$ through the hydrolysis of SB [35]:

$$NaBH_4 + (4+x)\ CH_3OH \rightarrow NaB(OCH_3)_4 + 4\ H_2 + x\ CH_3OH$$

The 2nd reason of using an excess of solvolysis agent is that both SB and AB as well as the respective by-products have a limited solubility. For example, the solubility of SB, AB and $NaBO_2$ in water are 55, 28 and 34 g per 100 g(H_2O). Actually the limited solubility is problematic to the catalytic material since any by-product precipitation may be detrimental to its reactivity. These last years, the utilization of SB or AB in a solid state [34, 37, 36] has discarded such an issue as for portable applications it is more and more often considered a single use of the catalyst, the catalyst likely deactivation being then unimportant.

The HDs given in Figure 1 are theoretical and the eHDs can be at best equal to the HDs[3]. Accordingly we carried out a series of experiments in order to determine the eHDs that can be achieved in our experimental conditions and in the presence of a Co catalyst. Typically we followed the solvolysis of SB or AB by injecting various amounts of water in accordance with the hydrolysis equations given above and with *x* varying from 0 to 8. The SB/AB total conversion (TC, %) was determined and the eHDs were calculated as (TC×HD)÷100. Figure 4 shows the results we obtained, which can be summarized as follows:

- SB-(2+*x*)H_2O: the highest eHD, i.e. 7.3 wt%, is obtained for *x* = 2, the TC being 100 %;
- SB-(4+*x*)CH_3OH: the highest eHD, i.e. 3.4 wt%, is obtained for both *x* = 0, the TC being 74 %, and *x* = 2, the TC being 100 % [37];
- AB-(2+*x*)H_2O: the highest eHD, i.e. 7.8 wt%, is obtained for *x* = 0, the TC being 96 % [34];

In every case the catalyst weight was taken into account for the eHD calculations. It is noteworthy that the by-products precipitated for the small *x* values (i.e. *x* = 0-4). To summarize, eHDs of 7-8 wt% can be achieved with SB or AB, suggesting therefore GHSCs up to 4 wt% [35].

When SB is envisaged to be stored as a solid, there is another problem that reduces the eHDs. The problem is the volume expansion since the borates volume is larger than the volume of solid SB [37]. For example, a volume expansion of 173 and 197% has been reported elsewhere [38, 39]. We studied the volume expansion for SB and AB. As $NaBO_2.2H_2O$ is the predominating borate, the volume expansion at 20 °C and in the presence of a Co-catalyst (10 wt% of $NaBH_4$+Co) was determined for *x* = 2. It was found to be 156 %, which is consistent with the values reported above (while considering the Co presence). With respect to AB, no volume expansion was noticed. Surprisingly, for *x* = 2, it

[3] It can be considered to use steam from a fuel cell in order to hydrolyze SB or AB. By this way, the respective HDs are 21.1 and 19.5 wt% (the 2 water molecules are not taken into account in the calculation of the HD). However, such an approach is not considered here as in our opinion this is only feasible for the automotive applications.

was found a volume regression of 50 %. Hence, with SB the tank must be 64%-filled (the amount of stored hydrogen will then be 64%-lower) whereas with AB the tank can be 100%-filled.

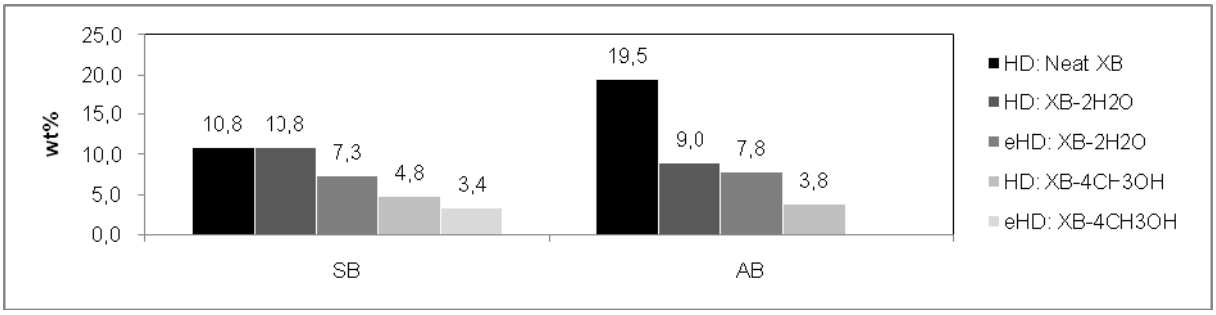

Figure 4: HDs and eHDs of neat XB (with X = S or A), XB-2H_2O and XB-4CH_3OH systems (the determination of the eHD of AB-4CH_3OH has been discarded because of a low HD, i.e. 3.8 wt%).

4 Outlook and Conclusion

None of the routes discussed heretofore can be envisaged for automotive applications but this is not the case for the thermolysis of AB. The thermolysis of AB is a simple reaction to implement for releasing stored hydrogen but in the meantime it is the most difficult to chemically achieve [3]. The 1st equiv. H_2 is generated at temperatures up to 120 °C (Figures 1 and 5). It can also be released at 85 °C after 17 h [40]. The 2nd equiv. H_2 is released at < 200 °C (Figure 5) and the 3rd one at temperatures up to 500 °C [12]. Such releasing rate is unacceptable for applications and to improve it several solutions (dispersion of AB in ionic liquid [43] or solvent [41], its incorporation into a nanoporous scaffold [42], catalysis [44,43]) have been considered. The objective is simply to decrease the dehydrogenation temperatures of the 2 equiv. H_2 (corresponding to an eHD of 13.0 wt%) towards 85 °C (Figure 5), which is the target set by the US DOE [4]. According to Stephens et al. [44], a rapid rate and acceptable extent of dehydrogenation have not been achieved yet, even despite a catalyst. Be that as it may, the AB thermolysis is the route having the highest potential for on-board hydrogen storage for automotive applications.

Neither SB nor AB are mature enough to envisaging technological applications. Both suffer from various issues [3]: catalyst inefficiency in terms of durability in the cases of the SB and AB hydrolysis; low, but not-optimised, eHDs in all cases; and too low hydrogen generation rates for the AB thermolysis. There are many other issues [5, 47, 45, 46]. One of the most significant ones, which has not been discussed yet, is related to the storage irreversibility, that is, the inefficiency in spent fuel recycling (off-board process). Other examples are the purity of generated H_2 (i.e. presence of gaseous by-products such as B_2H_6 [12] in the gas stream from the AB thermolysis or NH_3 released during the AB hydrolysis), the borates crystallisation in the case of the hydrolysis, the thermal management, especially in the case of SB hydrolysis, and so on.

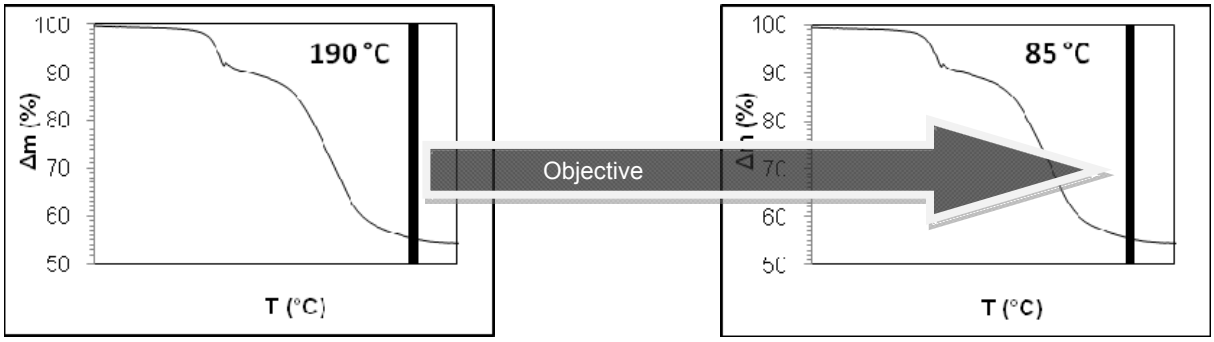

Figure 5: Thermolysis of AB: the objective is to release 2 equiv. H_2 at temperatures up to 85 °C.

SB is not really competing with AB and each may be intended to specific applications [3]. The SB hydrolysis has a higher potential for portable applications owing to its eHDs, commercial availability, and cost while the AB thermolysis has the highest potential for automotive applications owing to high eHDs and a real potential of improvement [47].

References

[1] U. Eberle, M. Felderhoff, F. Schüth. Angew. Chem. Int. Ed 48 (2009) 2; and references therein.

[2] U.B. Demirci, P. Miele. Energy Environ. Sci. 2 (2009) 627; and references therein.

[3] U.S. Department of Energy, Office of Energy Efficiency and Renewable Energy and The FreedomCAR and Fuel Partnership, Targets for onboard hydrogen storage systems for light-duty vehicles, September 2009, available at http://www.eere.energy.gov.

[4] U.S. Department of Energy Hydrogen Program. Independent review. Go/no-go recommendation for sodium borohydride for on-board vehicular hydrogen storage. NREL/MP-150-42220, can be found under www.hydrogen.energy.gov/. November 2007.

[5] U.B. Demirci, O. Akdim, P. Miele. Int. J. Hydrogen Energy 34 (2009) 2638; and references therein.

[6] G. Principi, F. Agresti, A. Maddalena, S.L. Russo. Energy 34 (2009) 2087.

[7] B.H. Liu, Z.P. Li. J. Power Sources 187 (2008) 527; and references therein.

[8] R.E. Davis, J.A. Gottbrath. J. Am. Chem. Soc. 84 (1962) 895.

[9] Q. Xu, M. Chandra. J. Power Sources 163 (2006) 364.

[10] P.V. Ramachandran, P.D. Gagare. Inorg. Chem. 46 (2007) 7810.

[11] V. Sit, R.A. Geanangel, W.W. Wendlandt. Thermochim. Acta. 113 (1987) 379.

[12] S.C. Amendola, S.L. Sharp-Goldman, M. Saleem Janjua, et al. Int. J. Hydrogen Energy 25 (2000) 969.

[13] H.I. Schlesinger, H.C. Brown, A.E. Finholt, et al. J. Am. Chem. Soc. 75 (1953) 215.

[14] O. Akdim, U.B. Demirci, P. Miele. Int. J. Hydrogen Energy 34 (2009) 7231.

[15] O. Akdim, U.B. Demirci, D. Muller, P. Miele. Int. J. Hydrogen Energy 34 (2009) 2631.

[16] C.M. Kaufman, B. Sen. J. Chem. Soc. Dalton Trans. (1985) 307.
[17] C. Wu, F. Wu, Y. Bai, et al. Mater. Lett. 59 (2005) 1748.
[18] J.C. Ingersoll, N. Mani, J.C. Thenmozhiyal, A. Muthaiah. J. Power Sources 173 (2007) 450.
[19] U.B. Demirci, F. Garin. J. Mol. Catal. A 279 (2008) 57.
[20] P. Krishnan, T.H. Yang, W.Y. Lee, C.S. Kim. J. Power Sources 143 (2005) 17.
[21] R.S. Liu, H.C. Lai, N.C. Bagkar, et al. J. Phys. Chem. B 112 (2008) 4870.
[22] D. Xu, P. Dai, X. Liu, et al. J. Power Sources 182 (2008) 616.
[23] U.B. Demirci, O. Akdim, P. Miele. J. Power Sources 192 (2009) 310.
[24] O. Akdim, U.B. Demirci, A. Brioude, P. Miele. Int. J. Hydrogen Energy 34 (2009) 5417.
[25] O. Akdim, U.B. Demirci, P. Miele. Int. J. Hydrogen Energy 34 (2009) 4780.
[26] T. Umegaki, J.M. Yan, X.B. Zhang, et al. Int. J. Hydrogen Energy 34 (2009) 2303; and references therein.
[27] F. Durap, M. Zahmakiran, S. Özkar. Appl. Catal. A 369 (2009) 53.
[28] C.F. Yao, L. Zhuang, Y.L. Cao, et al. Int. J. Hydrogen Energy 33 (2008) 2462.
[29] V.I. Simagina, P.A. Storozhenko, O.V. Netskina, et al. Catal. Today 138 (2008) 253.
[30] H.B. Dai, L.L. Gao, Y. Liang, X.D. Kang, P. Wang. J. Power Sources 195 (2010) 307.
[31] H. Erdogan, Ö. Metin, S. Özkar. Phys. Chem. Chem. Phys. 11 (2009) 10519.
[32] Ö. Metin, Ş. Şahin, S. Özkar. Int. J. Hydrogen Energy 34 (2009) 6304.
[33] U.B. Demirci, P. Miele. Hydrolysis of ammonia borane. J. Power Sources (2010) doi:10.1016/j.jpowsour.2010.01.002.
[34] E.Y. Marrero-Alfonso, J.R. Gray, T.A. Davis, M.A. Matthews. Int. J. Hydrogen Energy 32 (2007) 4117.
[35] J. Hannauer, U.B. Demirci, C. Geantet, et al. (2010) to be submitted.
[36] O. Akdim, U.B. Demirci, P. Miele. Int. J. hydrogen Energy 34 (2009) 9444.
[37] L. Zhu, D. Kim, H. Kim, et al. J. Power Sources 185 (2008) 1334.
[38] J.E. Stearns, M.A. Matthews, D.L. Reger, J.E. Collins. Int. J. Hydrogen Energy 23 (1998) 469.
[39] P.P. Prosini, P. Gislon. J. Power Sources 161 (2006) 290.
[40] M.E. Bluhm, M.G. Bradley, R. Butterick III, U. Kusari, L.G. Sneddon. J. Am. Chem. Soc. 128 (2006) 7748.
[41] M.C. Denney, V. Pons, T.J. Hebden, D.M. Heinekey, K.I. Goldberg. J. Am. Chem. Soc. 128 (2006) 12048.
[42] A. Gutowska, L. Li, Y. Shin, C.M. Wang, et al., Angew. Chem. Int. Ed. 44 (2005) 3578.
[43] F.Y. Cheng, H. Ma, Y.M. Li, J. Chen, Inorg. Chem. 46 (2007) 788.
[44] F.H. Stephens, V. Pons, R.T. Baker, Dalton Trans. (2007) 2613.
[45] B. Peng, J. Chen, Energy Environ. Sci. 1 (2008) 479.
[46] J.H. Wee, K.Y. Lee, S.H. Kim. Fuel Process. Technol. 87 (2006) 811.
[47] T.B. Marder. Angew. Chem. Int. Ed. 46 (2007) 8116.

Tailoring Thermodynamics of Hydrogen Storage Materials

Wiebke Lohstroh, Karlsruhe Institute of Technology, Germany
Francesco Dolci, Institute for Energy, DG Joint Research Centre, European Commission, The Netherlands
Maximilian Fichtner, Institute of Nanotechnology, Karlsruhe Institute of Technology, Germany

Hydrogen has the potential to serve as clean and versatile energy carrier, but efficient, reliable and safe storage systems have to be developed for a future hydrogen economy. Besides pressurized gas or liquid hydrogen tanks, solid state storage systems are a viable alternative. However, the materials investigated so far for solid state storage still show too low capacity at sufficiently low working temperatures to meet the targets set by the automotive industry. This is not necessarily due to the amount of stored hydrogen but thermodynamic and kinetic reasons restraining the application. Two alternative pathways to adjust thermodynamic properties are currently discussed: (i) restriction of particle sizes of the active material or (ii) the use of a reaction system introducing a second partner to alter the final products and thus the reaction enthalpy [1, 2].

Among the materials with the largest amount of hydrogen stored are complex hydrides such as aluminohydrides (e.g $NaAlH_4$) or borohydrides (e.g. $Mg(BH_4)_2$, $LiBH_4$) or amides ($Mg(NH_2)_2$ + x LiH composites). They have in common that hydrogen is released in a solid state reaction and the desorbed state is comprised of two or (more) segregated solid phases. Upon rehydrogenation the opposite reaction has to take place and the reaction kinetics is mainly determined by mass transfer. That is the reason why initial investigations on free standing small particles of $NaAlH_4$ suffered from insufficient reversibility. One possibility to circumvent this problem is the encapsulation of a complex hydride in a mesoporous host [3, 4, 5, 6].

1 $NaAlH_4$ and Mesoporous Host Materials

Among the most studied materials for solid state hydrogen storage is $NaAlH_4$. Using a transition metal based additive e.g. $TiCl_3$, or $ScCl_3$ reversible hydrogen uptake can be achieved at moderate temperature and pressure conditions (temperatures and pressures below 150°C and 100 bar H_2, respectively). Hydrogen is released in a two step reaction [7]:

$$3\ NaAlH_4 \ <\!\!-\!\!> Na_3AlH_6 + 2\ Al + 3\ H_2$$
$$Na_3AlH_6 <\!\!-\!\!> 3\ NaH + Al + 3/2\ H_2$$

and in total 5.6 wt% H_2 are liberated. Under the condition outlined above, NaH can not be decomposed (T_{des} > 400°C) nor does uncatalysed $NaAlH_4$ show any significant H_2 desorption.

In order to elucidate the hydrogen sorption properties of nanoscaled particles of $NaAlH_4$ composites of $NaAlH_4$ and different carbon host material have been studied.

$NaAlH_4$ (Albemarle, purity 96%) was used as received, while the carbon materials were heated in Ar/H_2 gas stream prior to any use to remove water and other volatile impurities. Various composites were prepared either by melt infiltration ($T_m(_{NaAlH4})$ = 181°C) under H_2 pressure or by ball milling in Ar atmosphere. The pore widths distributions of the host materials (except graphite) show the majority of pores to be in the range of 1-4 nm. The samples were chosen as to compare different hosts (i.e. surface area, ash content and transition metal impurities of the carbon) and preparation methods (melt infiltration, ball milling), a summary is given in table 1.

Table 1

Carbon (surface area / free pore volume)		**$NaAlH_4$ content [wt%] Preparation method**	**Remarks**
ACF 25 (transition metal and ash free carbon fibre made form organic precursors)	1815 m^2/g 0.66 cm^3/g	ACF #1 (M):48 wt% ACF #2 (M): 31.6 wt% Melt infiltrated (185°C, 160 bar H_2)	#1:(crystallographic) $NaAlH_4$ volume equals free pore volume
Activated carbon AC Alfa Aesar Transition metal impurities	1170 m^2/g 0.48 cm^3/g	AC (M): 50 wt% Melt infiltrated (185°C, 150 bar H_2), AC (BM): 50 wt% Ball milled 10 min (600rpm)	Excess $NaAlH_4$ compared to free pore volume
PFA 600 preparation according to Ref. [8] Transition metal and ash free carbon	774 m^2/g 0.33 cm^3 /g	PFA (BM): 50 wt% Ball milled 10 min (600rpm, Si_3N_4 vial and balls)	Excess $NaAlH_4$ compared to free pore volume
Graphite	-	GR (BM): 50 wt% Ball milled 10 min	

Figure 1 shows the first and second desorption for the various samples measured in a Sieverts' type apparatus (T = 150 °C, reabsorption took place at 125 °C and 100 bar H_2). The amount of released hydrogen has been normalized to the weight of the active material $NaAlH_4$ to facilitate comparison of the data. All composites show reversible H_2 uptake, independent from the preparation method with the exception of non-porous graphite. The ball milled samples AC (BM) and PFA (BM) release almost 5 wt.% H_2 in the initial desorption while the melt infiltrated samples show considerably lower values. Presumably, some hydrogen is already released during melt infiltration. This is in agreement with the XRD data which show some Al and Na_3AlH_6 alongside $NaAlH_4$ after preparation. In the second desorption (after rehydrogenation) less hydrogen is released. However, there is no clear trend for the reversible capacity in dependence on the carbon host.

It is well known that carbon based additives enhance kinetic performance of the hydrogen sorption of $NaAlH_4$ [9]. In order to investigate the influence on the thermodynamic properties, pressure-composition isotherms were measured for the various composites (except

graphite). In the former case, the smaller particle size increases the surface contribution to the free energy in both the hydrogen rich and poor phase and thus changes of the reaction enthalpy are expected [10]. However, the relevant particle sizes are quite small e.g. for Mg /MgH_2 significant changes are predicted to occur at particle sizes below 1.3 nm [11]. The results for $NaAlH_4$ – carbon composites are summarized in Figure 2. The measurements were done during absorption at 140 °C and the pressure was increased stepwise following by some rest time (typically 20 000s) to allow the sample to reach equilibrium.

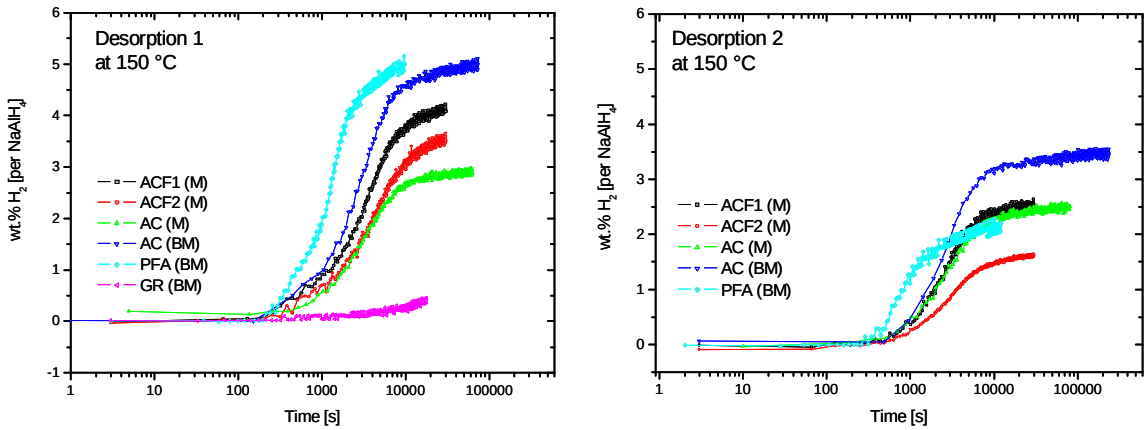

Figure 1: Desorption 1 and 2 of various $NaAlH_4$-carbon composites at 150 °C. Composites of $NaAlH_4$ and mesoporous carbon show reversible H_2 uptake while composites with graphite show hardly any hydrogen release.

The obtained PCI curves are significantly changed compared to the data obtained for $NaAlH_4$ (doped with 4 mol % $CeCl_3$, shown in the inset). Besides the lower H_2 capacity, most prominently, the two plateaus (originating from the two reaction steps) get smaller while simultaneously a sloping region develops extending to low pressures and low hydrogen concentrations. This feature is most prominent for sample ACF 1 (M) where the original plateaus have completely vanished. A similar PCI is observed for sample ACF 2 (M) (not shown)[12]. For these two samples, the $NaAlH_4$ content is chosen in such a way that the volume of the active material equals or is smaller than the available free pore volume. In all other samples a surplus of $NaAlH_4$ was contained in the samples. These results suggest that the small remains of the original plateau stem from $NaAlH_4$ outside the pores. This is catalysed although not very efficiently by the carbon, and as a result, “bulk” like plateaus are observed in the PCI measurements. In contrast, $NaAlH_4$ that is in close contact with the mesoporous host (i.e. inside the pores) exhibits altered thermodynamic properties.

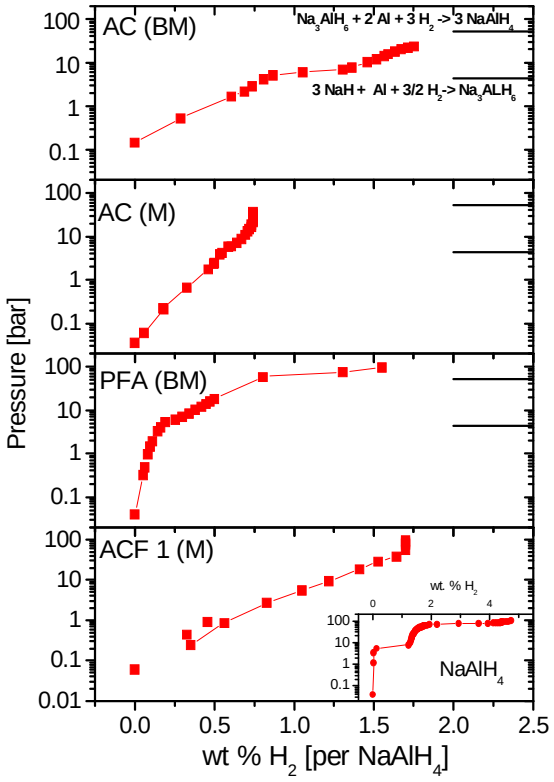

Figure 2: Pressure composition isotherms of various $NaALH_4$ –carbon composites at 140 °C. The inset shows the PCI obtained for $NaALH_4$ catalysed with 4 mol% $CeCl_3$, moreover the expected plateau pressures for reaction step 1 and 2 are indicated (Data from Ref [7]).

2 Reaction Based Systems: $Mg(NH_2)_2$ + x LiH

Another potential route changing thermodynamics is by use of so called reactive hydride composite mixtures. For these compounds thermodynamic parameters of a single component are changed by the presence of a second one. In 2000, Chen et al. [13] presented a Lithium amide based reaction system that reversibly takes up hydrogen according to the following reactions:

$$LiNH_2 + 2\ LiH <-> Li_2NH + LiH + H_2$$
$$Li_2NH + LiH <-> Li_3N + H_2$$

and in total 10.4 wt% H_2 are liberated at temperatures up to 320°C. The single compounds emit either ammonia ($LiNH_2$) or need higher temperatures for decomposition (T_{LiH}>600°C). Substituting $LiNH_2$ with the analogue magnesium compound lowers the operating temperature to ~ 200°C and the overall reaction can be described as [14, 15]

$$Mg(NH_2)_2 + 2\ LiH <-> Li_2Mg(NH)_2 + 2\ H_2 \qquad 5.6\ wt.\%\ H_2$$

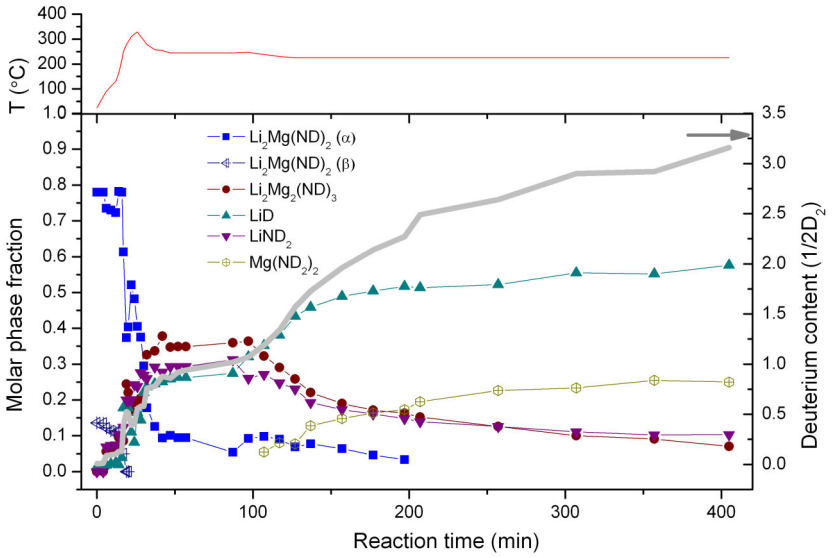

Figure 3: Phase evolution of $Li_2Mg(NH)_2$ during hydrogen uptake. The initial H_2 pressure was 60 bar, and it was increased to 70 bar at $t_{reaction}$ = 100 min.

Moreover, $Mg(NH_2)_2$ + x LiH compounds with x = 3/8, and 4 have been proposed for storage purposes with hydrogen capacities of 6.9 wt% and 9.1 wt% H_2, respectively. The reactions were proposed [16,17] as follows:

$Mg(NH_2)_2 + 8/3\ LiH <-> 1/3\ Mg_3N_2 + 4/3\ Li_2NH + 8/3\ H_2$ 6.9 wt% H_2

$Mg(NH_2)_2 + 4\ LiH <-> 1/3\ Mg_3N_2 + 4/3\ Li_3N + 4H_2$ 9.1 wt% H_2

To get deeper insight into the mechanism of hydrogen release the different $Mg(NH_2)_2$ + x LiH were studied using in-situ neutron diffraction. Experiments were carried out at the SPODI instrument, FRM II (Munich) and the D20 beamline, ILL (Grenoble). Prior to the neutron scattering experiments the samples have been cycled in a Sieverts type apparatus using D_2 gas to exchange hydrogen with deuterium and the scattering experiments have been done during absorption.

Starting from $Li_2Mg(NH)_2$ (1:2 system) a new intermediate phase was identified during the initial stages (p= 60 bar, T = 245°C) of hydrogen uptake [18]. Moreover, $LiNH_2$ as well as LiH occur in the scattering patterns, while $Mg(NH_2)_2$ only is formed as the pressure is raised to 70 bar H_2 (and T lowered to 225°C). The composition of the intermediate phase is proposed to be $Li_2Mg_2(NH)_3$ and its structure is related to $Li_2Mg(NH)_2$ and $LiNH_2$: the underlying crystal structure can be referred to as anti-fluoride type with cations/vacancies residing on tetrahedral sites and nitrogen occupying fcc lattice sites. The phase evolution during hydrogen uptake was evaluated using Rietveld analysis and the results are shown in Figure 3.

Thus, the hydrogen uptake reaction is proposed to be:

$2\ Li_2Mg(NH)_2 + H_2 <-> Li_2Mg_2(NH)_3 + LiNH_2 + LiH$ 1.5 wt% H_2

$Li_2Mg_2(NH)_3 + LiNH_2 + LiH + H_2 <-> 2\ Mg(NH_2)_2 + 4\ LiH$ 4.4 wt% H_2

The hydrogen uptake in composites with higher LiH content (x = 3/8 and 4) has also been measured using in-situ neutron scattering technique (starting from the desorbed state). The results show that the same phases $Li_2Mg_2(NH)_3$, $LiNH_2$ and LiH appear initially when the hydrogen pressure is increased stepwise while $Mg(NH_2)_2$ is formed only at pressures above 40 bar (T = 200 °C). A quantitative analysis using Rietveld refinement yields a ratio of $Li_2Mg_2(NH)_3$: $LiNH_2$ of 1:1 at the intermediate hydrogenation step. For x = 8/3 and 4, the LiH content is naturally higher, however there are no indications that under the given conditions (T = 200°C) the additional LiH takes part in the reaction. Consequently, for all three $Mg(NH_2)_2$: x LiH compositions (x = 2, 8/3, and 4) the same hydrogen uptake reaction occurs (for T < 250 °C) albeit the gravimetric hydrogen density decreases with increasing LiH content. The additional hydrogen in these systems is only accessible at higher temperatures.

3 Conclusions

The above presented examples demonstrate the possibility of tailoring thermodynamic properties of hydrogen storage materials. $NaAlH_4$ in close contact with a mesoporous host shows drastically altered pressure-composition isotherms compared to “bulk” material whereby the porous nature of the material and its high surface area seems to be essential.

Amide based materials are one example how hydrogen release can be obtained in a reaction based system. The occurrence of the intermediate phase at intermediate H_2 pressures is representative for the potential and the difficulties of this approach: Suitable material combinations and their reaction pathway are hard to predict but new promising systems potentially remain to be discovered.

References

[1] J.J. Vajo, F. Mertens, C.C. Ahn, R.C. Bowman Jr., and B. Fultz, J. Phys. Chem. B 108, (2004) 13977–13983.

[2] J.J. Vajo, S.L. Skeith, F. Mertens, J. Phys. Chem. B 109, (2005) 3719-3722.

[3] F. Schüth, A. Taguchi, S. Kounosu, J.P. Saitama, and B. Bogdanovic, German Patent DE 10332438 A1 2004.

[4] R.D. Stephens, A.F. Gross, S.L.Van Atta, J.J. Vajo, and F. Pinkerton, Nanotechology 20, (2009) 204018.

[5] C.P. Balde, B.P.C. Hereijgers, J. H. Bitter, and K.P. de Jong, J. Am. Chem. Soc. 130, (2008) 6761–6765.

[6] Ph. Adelhelm, K.P. de Jong, and P.E. de Jongh, Chem. Comm. (2009) 6261-6236.

[7] B. Bogdanovic, R. Brand, A. Marjanovic, M. Schwickardi, and J. Tölle, J. Alloys Compd. 302, (2000) 36-58.

[8] Ch. L. Burket, R. Rajagopalan, A.P. Marencic, Kr. Dronvajjala and H. C. Foloey, Carbon
44 (2006) 2957.

[9] C. Cento, P. Gislon, M. Bilgili, A. Masci, Q. Zheng, P.P. Prosini, J. Alloys Compnd. 2007, 437,
360–366.

[10] V. Bérubé, G. Radke, M. Dresselhaus, and G. Chen, Inter. J. Energy Res. 31, (2007) 637-663.

[11] R. W. P. Wagemans, J.H. van Lenthe, P.E. de Jongh, A.J. van Dillen, and K.P. de Jong,
J. Am. Chem. Soc. 127, (2005) 16675–16680.

[12] W. Lohstroh, A. Roth, H. Hahn. and M. Fichtner, Chem. Phys. Chem. (2010), DOI: 10.1002/cphc.200900767

[13] P. Chen, Z.T. Xiong, J.Z. Luo, J. Y. Lin, and K.L Tan, Nature 420, (2002) 302.

[14] Z. Xiong, G. Wu, J. Hu and P. Chen, Advanced Materials, 16 (2004) 1522.

[15] W. Luo, Journal of Alloys and Compounds, 381 (2004) 284.

[16] H.Y. Leng, T. Ichikawa, S. Hino, N. Hanada, S. Isobe and H. Fujii, Journal of Power Sources,
156 (2006) 166.

[17] Y. Nakamori, G. Kitahara, K. Miwa, S. Towata and S. Orimo, Applied Physics A: Materials Science and Processing, 80 (2005) 1.

[18] E. Weidner, F. Dolci, J. J. Hu, W. Lohstroh, T. Hansen, D. J. Bull, and M. Fichtner, J. Phys. Chem. C 113, (2009) 15772.

Advantages of Organic Chemical Hydrides for Long-term Storage and Over-sea Transportation of Hydrogen

Atsushi Shono, **Susumu Kawaguchi**, **Noriaki Matsushima**, **Kiyoshi Aramaki**, **Jun Kuwano**, **Katsuto Otake**, Department of Industrial Chemistry, Faculty of Engineering, Tokyo University of Science 12-1, Funagawara-machi, Shinjuku-ku, Tokyo, Japan, 162-0862
Yasukazu Saito, New Energy Lab. Co., 1-3, Kagurazaka, Shinjuku-ku, Tokyo, Japan, 162-8601

Summary

Wind-power hydrogen is convertible into methylcyclohexane via catalytic hydrogenation of toluene and becomes storable for long term as well as transportable over sea. Catalytic dehydrogenation of methylcyclohexane would contribute to CO_2 reduction at energy-demand sites in industries, e.g., electric power, steel making, automobile, town-gas, etc.. Key technology in the present system lies on dehydrogenation catalysis, which involves endothermic hydrogen evolution.

It was elucidated for the first time that heating temperatures could be lowered down to 300-C and below, where adsorbed species were removed under vigorous boiling conditions, making it possible to accelerate the regeneration of active sites. A flow-type catalytic reactor, driven by low-quality heats, was discussed from the viewpoint of exergy analysis in contrast to liquefied hydrogen.

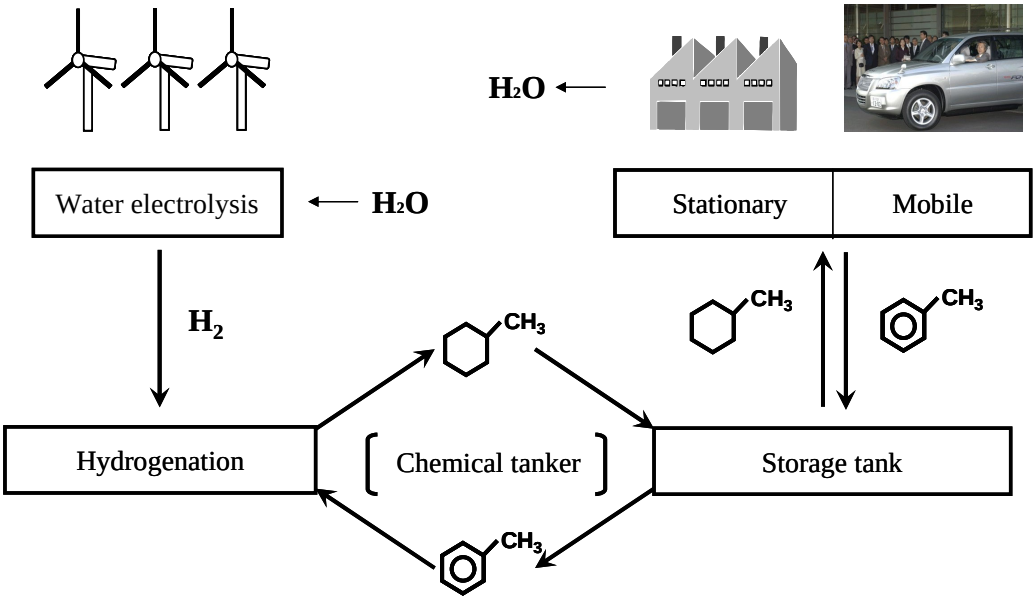

Figure 1: Storage and Transportation System for Hydrogen by Organic Chemical Hydride.

1 Introduction

The most important for hydrogen storage is to be safe in addition to be easy-to-handle. Organic chemical hydrides are hydrocarbons with moderate boiling points and volatilities (Table 1), the ranges of which belong to gasoline. A catalytic reaction couple of toluene hydrogenation and methylcyclohexane dehydrogenation makes it possible to store hydrogen at the levels of 6.16% in weight and 1.33 times larger than liquefied hydrogen in volume [1]. Among secondary energies, electricity is superior to others in many aspects, but is disadvantageous to transport over the sea in contrast to chemicals. A series of renewable-energy technologies, consisting of wind power, water electrolysis and hydrogenation catalysis, is particularly attractive, because organic chemical hydrides are storable for long term and can connect foreign industrial countries with emblessed wind-firm areas at any place in the world.

Hydrogen regeneration from organic chemical hydrides has a serious task, however, where the endothermic reaction heat is required at the energy-demand sites. By this reason, a certain kind of waste heats ought to be utilized at the temperatures as low as possible. Hydrogen storage with organic chemical hydrides will therefore be discussed with special emphasis of dehydrogenation catalysis in the present work.

2 How to Make and Carry Hydrogen at a Large Scale

Renewable energy is concentrated and stored as wind power on earth in the polar regions. From the North Pole, strong wind blows through the Behring Sea to the North Pacific, which brings the Aleutian Islands tremendous wind resource at annual average of ca. 10 m/s. Since a large-scaled windfirm as 50 GW is capable to be built there, wind hydrogen is now planned to convert it into organic chemical hydrides. Production of hydrogen from the windmill at Aleutians will amount to 3.8 million tons per year. Dutch Harber, a famous unfrozen fishery port in Alaska, had long been connected with Los Angeles and Yokohama, both being apart from ca. 5000 km. This area is assumed to be the center for the factories of water electrolysis and catalytic hydrogenation of toluene to yield methylcyclohexane.

$$\text{methylcyclohexane (MCH)} \rightleftharpoons \text{toluene (TOL)} + 3\,H_2 \qquad \Delta_r H\text{: } 67.5 \text{ kJ mol-}H_2^{-1}$$

Table 1: Molecular properties of organic chemical hydrides.

	bp/℃	mp/℃	vapor press. (25℃)/kPa	hydrogen content/wt%
MCH	101.1	-126.6	6.1	6.16
TOL	110.6	-95.0	2.9	

3 How to Regenerate Hydrogen from Organic Chemical Hydrides

Methylcyclohexane, imported to an industrial country and kept at the port storage tank, is transferred by lorry or pipe to hydrogen-demand sites, where the reaction heat of 67.5 kJ mol-H_2^{-1} is provided with waste heats from both economical and safety reasons. In this context, developments in low-temperature catalysis for dehydrogenation are strongly required.

An appropriate wettedness, defined as the amount ratio of liquid MCH to carbon-supported catalyst, was found to take the essential role for dehydrogenation under boiling conditions. As shown in batch-type performances (Fig. 2) [2], subtle differences in wettedness were decisive in hydrogen evolution rates as well as 2 h-conversions. Equilibrium attainments were observed in flow-type reactors at the catalyst-layer temperatures in the range of 200~300-C (Fig. 3) [3]. The temperature gradient inside the catalyst layer and bubble evolution from the catalyst surface would couple vector-wise thermodynamically, by which the reverse path or toluene hydrogenation was prohibited irrespective of temperatures [4]. Preparation of nano-catalysts is essentially important [5].

In order to carry hydrogen with organic chemical hydride, a moderate thermal exergy is required for endothermic dehydrogenation, while the reverse process of toluene hydrogenation proceeds by removing the exothermic reaction heat. Total exergy loss for hydrogen storage is dramatically decreased, if compared to the extensive loss of mechanical exergy for hydrogen liquefaction.

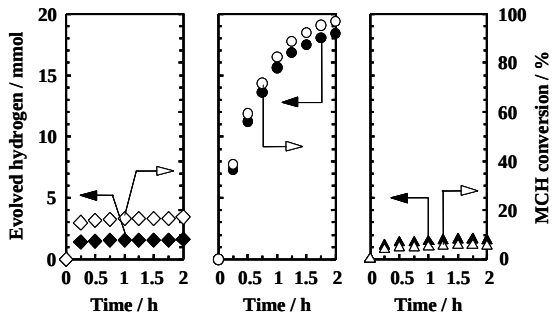

Pt-Ir / C (5 wt-metal%, Pt / Ir = 4, 0.30 g), Heated at 210℃
MCH charged / ml (◆, ◇ : 0.4, ●, ○ : 0.8 , ▲, △ : 1.2)

Figure 2: Time courses of hydrogen evolution from methylcyclohexane in a batch-type catalytic reactor under boiling and refluxing conditions.

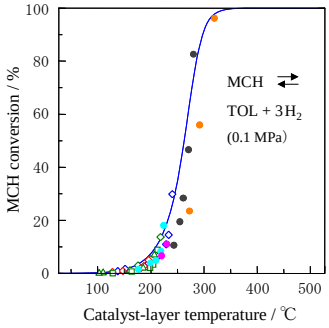

Pt / AC Cloth (3 ~ 5 cm ϕ & 10×20 cm^2, 5 wt%),
Fed at 0.3 ~ 3.5 ml-MCH min^{-1} without refluxing

Figure 3: Observed conversion from MCH in a flow-type catalytic reactor under boiling conditions.

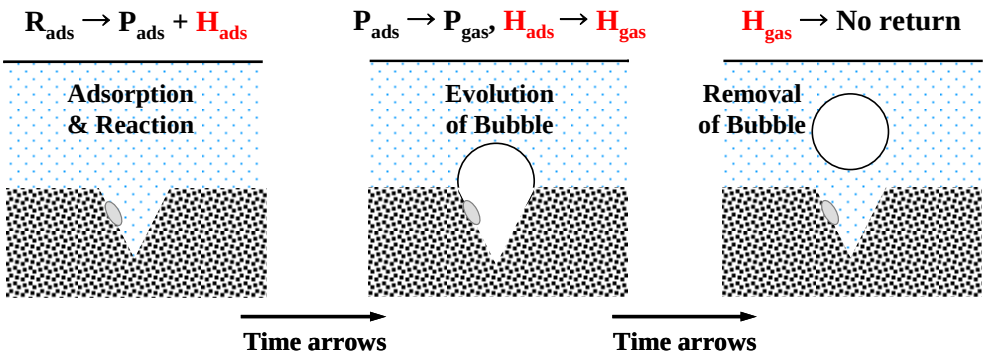

Figure 4: Contrariety from micro-reversibility principle in bubble evolution during dehydrogenation catalysis.

4 How to Utilize Hydrogen of Organic Chemical Hydride

Japan is surrounded and isolated by the sea from all kinds of energy resources. For example, American or Eurasian countries could choose pipe-line transportation of natural gas, whereas Japan had to start with LNG from the beginning. Either oil or coal had long been imported from abroad.

The present project of hydrogen storage and transportation as organic chemical hydride seems to open a new era on the following grounds.

1. Hydrogen is originated from the renewable energy of North-Polar wind.
2. Annual speed average (> 10 m/s) generates electricity (50 GW) at the Aleutian Islands.
3. Electrolysis hydrogen (3.8 million ton-H_2/y) is carried as organics in oil tankers.
4. Industrial waste heats (< 300-C) are available for endothermic hydrogen regeneration.

Renewable hydrogen, brought into Japan extensively, would contribute to CO_2 reduction (15 million ton-CO_2/y in calorie equivalent to H_2) through various industrial and domestic fields.

- Electric power: Hydrogen fuel to Molten Carbonate and Solid Oxide Fuel Cells.
- Steel making: Coke reduction in blast furnace processes by direct injection and ore prereduction.
- Town gas: Combustion-heat adjustment by hydrogen addition within the range of legal regulation.
- Domestic cogeneration: H_2 supply at Polymer Electrolyte Fuel Cell with use of its waste heats.
- Automobile: H_2 station for Fuel Cell Vehicles and on-board use for Internal Combustion Engines.

5 Conclusions

Both prolonged storage and distant transportation are superior properties of hydrogen to electricity as secondary energies. Organic chemical hydride has not only peculiar advantages to be safe and easy-to-handle, but also to be responsible to utilize waste heats for industrial and domestic consumers at the moments of hydrogen regeneration. Developments of large-scaled renewable energies will open a new paradigm of hydrogen economy.

References

[1] S. Hodoshima, H. Arai, Y. Saito, Inter. J. Hydrogen Energy, 28, 197 (2003).

[2] Y. Saito, K. Aramaki, S. Hodoshima, M. Saito, J. Kuwano, K. Otake, Chem. Eng. Sci., 63, 4935 (2008).

[3] S. Hodoshima, A. Shono, J. Kuwano, Y. Saito, Energy Fuels, 22, 2559 (2008).

[4] S. Hodoshima, Y. Saito, Hydrogen fuel: Production, Transport and Storage (Ed. R. B. Gupta), CRC Press (2008), 437-474.

[5] K. Aramaki, S. Kawaguchi, M. Saito, J. Kuwano, Y. Saito, Key Eng. Mat., 388, 65 (2009).

Unstable Complex Hydrides as New Hydrogen Storage Materials

Michael Felderhoff, Claudia Weidenthaler, André Pommerin, Ferdi Schüth
Max-Planck-Institut für Kohlenforschung, Germany

1 Introduction

After several years of research in the field of solid state hydrogen storage no optimized material was developed which can be used for hydrogen storage in mobile applications [1]. One of the most discovered material over the last decade is the complex sodium aluminum hydride, $NaAlH_4$, which can store 5.6 wt.% H_2 and releases hydrogen over two decomposition steps. An important disadvantage, which limits the practical use of complex metal hydrides, is the high amounts of energy which must be dissipate during the refilling process in a short time of less than 5 min. Therefore high efficient heat exchangers are necessary, which decreases the overall storage capacity of the whole tank system.

One possible solution to overcome low storage capacities of tank systems is the combination of different types of hydrogen storage processes. The combination of conventional metal hydrides (storage capacity roughly 2 wt.% H_2) and a high pressure tank (350 bar) was developed in the last years [2]. Such systems show increased storage capacities for hydrogen in mobile applications. But the limiting factor of the storage capacity is the low hydrogen amount of the metal hydride. With new types of unstable metal hydrides the storable hydrogen amount in a metal hydride/high pressure tank can be significantly increased.

2 Transition Metal Complex Aluminium Hydrides

Figure 1 shows the theoretical hydrogen content of several transition metal complex aluminium hydrides, reaching more than 9 wt.% H_2 for $Ti(AlH_4)_4$. Most of these materials are unknown and were not prepared or characterized. Only several of these compounds were synthesized in the past in ether solutions according to the following metathesis reaction at low temperature of -110 °C (Equation 1) [3]. These materials are unstable under conditions of 1 bar pressure and at a temperature of 298 °C.

$$TiCl_4 + 4\,LiAlH_4 \xrightarrow[Et_2O]{-110°C} Ti(AlH_4)_4 + 4\,LiCl \qquad \text{Eq. 1}$$

They decompose during heating up to room temperature releasing hydrogen and different metallic decomposition products. The decomposition products and the decomposition mechanism are not fully discovered yet.

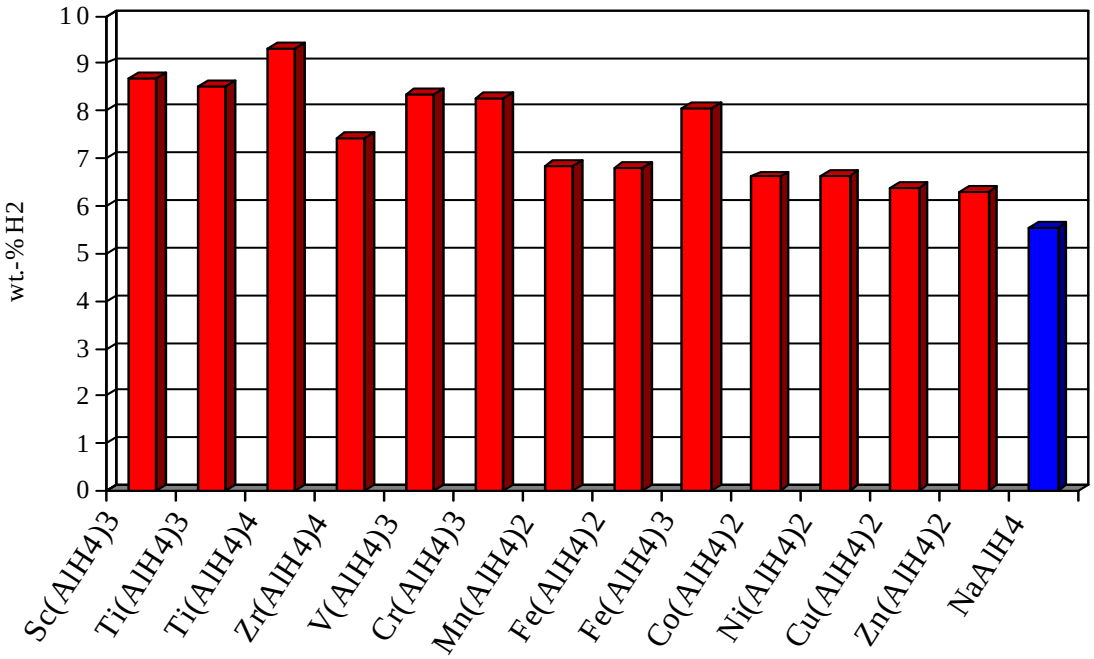

Figure 1: Theoretical hydrogen content of several transition metal complex aluminium hydrides.

With the combination of an unstable metal hydride and a high pressure tank the storage capacity of a tank system can significantly increased. Such a combination releases hydrogen in three steps (Figure 2):

1. pressure reducing step from 350 bar to 200 bar reaching the (assumed) equilibrium pressure of the unstable complex aluminium metal hydride
2. hydrogen release from the decomposition of the unstable complex aluminium hydride (equilibrium pressure)
3. pressure reducing step from 200 bar to 0 bar

The combination of an unstable metal hydride (complex hydride) system / high pressure tank shows several advantages over conventional storage systems:

- high gravimetric and volumetric storage capacity
- reduced heat release during the refilling step
- no cold start problem

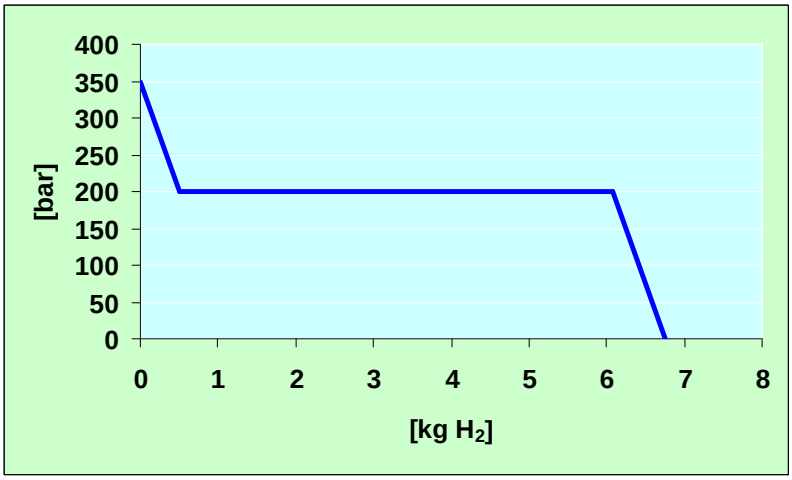

Figure 2: Hydrogen releasing process of a hydrogen storage tank consisting of the combination of an unstable complex hydride and a high pressure tank.

3 Synthesis and Characterization of New Rare Earth Complex Hydrides

Recently it was shown that complex hydrides can be prepared in pure form and without any decomposition products starting from a simple alkaline metal hydride and aluminium hydride through cryo milling according to Equation 2 [4].

$$MeH + AlH_3 \ (Me = Li, Na, K) \xrightarrow[b.m.]{-196°C} MeAlH_4 \qquad \text{Eq. 2}$$

Starting from these experiments unstable metal hydrides should be synthesized from transition metal hydrides and aluminium hydride at -196°C with the ball millling method. These experimenst are currently under evaluation.

According to the metathesis reaction shown in Eq. 1 new types of rare-earth complex aluminium hydrides (Figure 3) were prepared and characterized [5]. These materials can serve as model substances to learn more about the stability, preparation methods and handling of unstable transition metal hydrides with high hydrogen storage capacity.

Rare-earth chlorides ($LaCl_3$, $CeCl_3$, $PrCl_3$, $NdCl_3$) react with 3 moles of $NaAlH_4$ in a ball milling experiment at room temperature prodcucing unstable rare-earth aluminium hydrides $RE(AlH_4)_3$ in a first reaction step. These materials decompose during the synthesis and produce stable $REAlH_6$ compounds. The decomposition reactions of $REAlH_6$ are endothermic with about 30 kJ mol^{-1} H_2, as revealed by DSC analysis. This suggests that these compounds are reversible at lower temperatures and/or higher pressure, and thus, these compounds may constitute a new class of intermediate temperature hydrides.

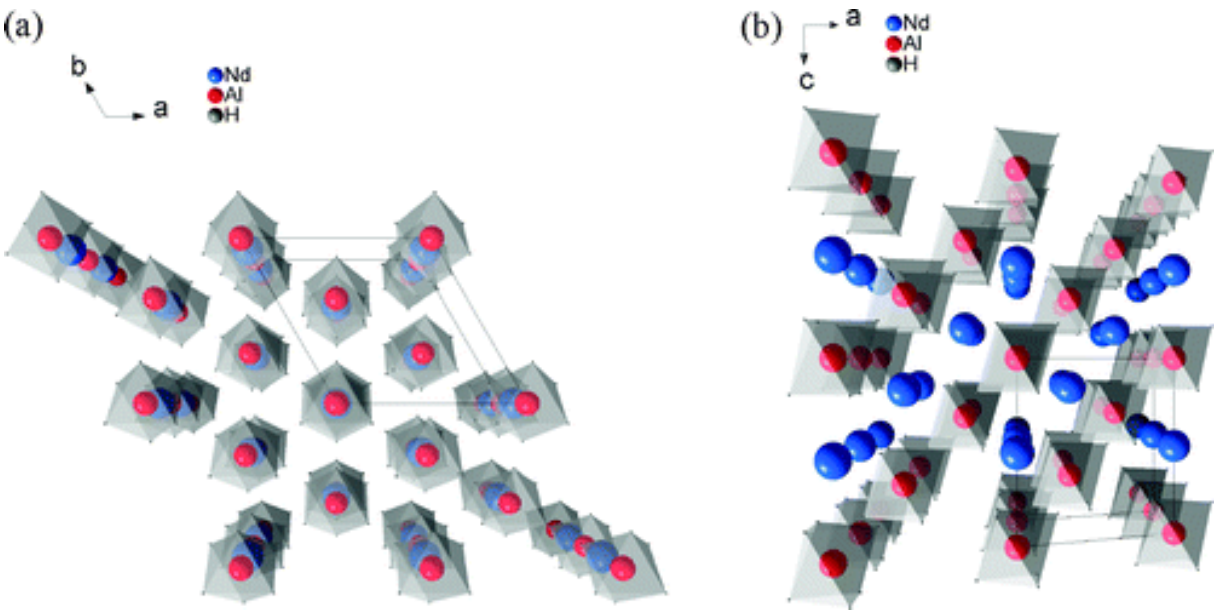

Figure 3: Crystal structure of $NdAlH_6$, from Ref. [4].

References

[1] U. Eberle et al., Angew. Chem. Int. Ed. 48 (2009) 6608.

[2] D. Mori et al. J. Japan Inst. Metals 69 (2005) 308.

[3] E. Wiberg, R. Uson, Z. Naturforschg. 6b (1951) 392.

[4] M. Felderhoff et al. Scr. Mater. 62 (2010) 576.

[5] C. Weidenthaler, et al. J. Am. Chem. Soc. 131 (2009) 16735.

In-situ Study of Hydriding Kinetics in Pd-based Thin Film Systems

Renaud Delmelle, Joris Proost[*], Division of Materials and Process engineering, Université catholique de Louvain Place Sainte-Barbe 2, B-1348 Louvain-la-Neuve, Belgium

Abstract

The hydriding kinetics of Pd thin films has been investigated in detail. The key experimental technique used in this work consists of a high resolution curvature measurement setup, which continuously monitors the reflections of multiple laser beams coming off a cantilevered sample. After mounting the sample inside a vacuum chamber, a H-containing gas mixture is introduced to instantaneously generate a given hydrogen partial pressure (p_{H2}) inside the chamber. The resulting interaction of H with the Pd layer then leads to a volume expansion of the thin film system. This induces in turn changes in the sample curvature as a result of internal stresses developing in the Pd film during a hydriding cycle. Based on such curvature date obtained in-situ at different p_{H2}, a two-step model for the kinetics of Pd-hydride formation has been proposed and expressions for the hydrogen adsorption and absorption velocities have been derived. The rate-limiting steps have been identified by studying the p_{H2}-dependence of these velocities. Furthermore, from our in-situ experimental data, relevant kinetic parameters have been calculated. The effect of dry air exposure of the Pd films on the hydriding kinetics has been considered as well.

1 Introduction

Among the major obstacles to the technological reconversion of mobility and transport applications towards green and sustainable hydrogen technologies are a number of issues related to H-storage [1, 2]. Solid-state hydrogen storage is the most promising solution since its potential in terms of hydrogen volume and weight density is higher than that of conventional tanks [3 - 5]. The storage issues related to the wide family of solid-state hydrides can be classified as thermodynamic and kinetic issues [6]. On-board storage applications require restrictive operation temperature and pressure ranges. The reversibility of hydriding is another critical parameter. This requirement implies low driving forces for both hydriding and dehydriding reactions, thus usually poor kinetics.

In this context, the hydrogen-palladium system is a good model system in view of the design of effective hydrogen storage materials. Indeed, the Pd hydriding mechanism is fast, spontaneous and reversible at room temperature. It has been the most extensively studied hydrogen-metal system for more than a century [7]. Nevertheless, the Pd hydriding mechanism is still an issue of debate, especially regarding its kinetic details [8, 9].

[*] Corresponding author, email: joris.proost@uclouvain.be

In this respect, this work focuses on a more detailed understanding of the hydriding kinetics of the Pd-based model system. The kinetic model presented here takes into account the mechanisms of adsorption and absorption of hydrogen into the Pd lattice. This extended abstract will first focus on the main ideas from which the kinetic model has been built. It will then elaborate an identification of the rate-limiting steps of the Pd hydriding mechanism and the calculation of relevant kinetic parameters (bulk and surface coverage) from in-situ hydriding curves obtained at different p_{H2}. Finally, the effect of long-term dry air exposure of the samples on the hydriding kinetics is discussed as well.

2 In-situ Measurement Principle

The experimental setup considered for our in-situ approach, as well as the sample characterization, are already described in detail in another publication [10]. The samples used here were cut approximately 3x0.5 cm^2 in size from two oxidized, 425 µm thick Si wafers. These were coated by e-gun evaporation with a pure Pd thin film on top of a 5 nm thick Ti adhesion layer. The Pd thin film thicknesses and the initial stresses in those films after deposition have been characterized for two different batches and are listed in Table 1. The error is on the order of 1% for the thickness measurements and 0.1% for the initial stress measurements. The table also mentions the approximate time spent by the samples in the desiccator between their deposition process and their cycling with hydrogen.

Table 1: Sample characterization of the palladium films.

	Sample 1	Sample 2
Pd thickness [nm]	128	112
Initial stress level [MPa]	435	409
Dry air exposure time [months]	12	2

The cantilevers obtained this way are embedded in a vacuum chamber, with a base pressure on the order of 10^{-6} mbar. A ultra-pure Ar/H_2 gas mixture is then instantaneously introduced into the chamber in order to impose a desired p_{H2}. The sample curvature is measured in-situ with a high resolution curvature measurement setup, including a laser beam source mechanically fixed onto the chamber. A CCD camera mounted onto the chamber continuously detects the position of 5 laser beams reflected off the cantilevered sample, allowing to monitor the sample curvature $\Delta\kappa$ in real time. The internal compressive stresses developing in the Pd film during hydriding are a result of the prohibited volume change during Pd-H interaction in the thin film geometry. They can be deduced from the measured changes in the sample curvature thanks to Stoney's equation [11].

3 Results and Discussion

The four major steps involved in Pd hydriding are H_2 molecular adsorption, dissociative chemisorption, atomic hydrogen diffusion and finally hydride formation. The present kinetic model considers two main steps, as inspired from Wagner's seminal work [7]. The first step, called here "adsorption", involves H_2 molecular adsorption and dissociative chemisorption. Diffusion and hydriding constitute the second step, called here "absorption". In fact, the

absorption step does not take explicitly into account the hydrogen diffusion mechanism. Indeed, it can easily be shown that bulk diffusion can be considered to be non-rate limiting in our thin film geometry [10]. The adsorption and absorption reactions and their equilibrium constants are presented in Eqs. (1) - (4):

$$H_2 + 2s \Leftrightarrow 2H - s \tag{1}$$

$$K_{ad} = \frac{k_{ad}^{'}}{k_{ad}^{''}} = \frac{\theta_{eq}^2}{(1-\theta_{eq})^2}\frac{1}{p_{H_2}} = \frac{1}{K_S^2} \tag{2}$$

$$H - s + i \Leftrightarrow H - i + s \tag{3}$$

$$K_{ab} = \frac{k_{ab}^{'}}{k_{ab}^{''}} = \frac{1-\theta_{eq}}{\theta_{eq}} \cdot \frac{n_{eq}}{1-n_{eq}} \tag{4}$$

Here, *s* is a surface adsorption site and *i* is a bulk absorption site. θ_{eq} and n_{eq} are the equilibrium surface coverage and bulk H/Pd atomic ratio, and K_s is the well-known Sievert's constant describing the ideal solution behavior [7].

Starting from those expressions, a kinetic model has been built according to two main hypotheses. Firstly, it is assumed that θ reaches values close to θ_{eq} much before n reaches its equilibrium value. This reasoning leads to the following expressions for the adsorption and absorption velocities:

$$\frac{d\theta}{dt} = \overbrace{\left[k_{ad}^{'}(1-\theta)^2\right]}^{S_{ad}} \cdot p_{H_2} \overbrace{-k_{ad}^{''}\theta^2}^{I_{ad}} \tag{5}$$

$$\frac{dn}{dt} = \overbrace{\left[\frac{k_{ab}^{'}}{K_S}\left[1 + n\left(\frac{1-K_{ab}}{K_{ab}}\right)\right]\right]}^{S_{ab}} \cdot \sqrt{p_{H_2}} \overbrace{-k_{ab}^{''}n}^{I_{ab}} \tag{6}$$

Secondly, every parameter in Eqs. (5) and (6) is assumed to be independent of p_{H2} (and hence, so are the slopes S_{ad} - S_{ab} and the intercepts I_{ad} - I_{ab}). This second statement is inspired from experimental observations [10]. As seen in Figure 2, two linear kinetic regimes are observed during hydrogen loading of our samples. The latter are separated by a brutal, instantaneous transition. As shown in Figure 1, these constant slopes further exhibit a linear relationship with respect to $\sqrt{p_{H2}}$ in the first regime, and vary linearly with p_{H2} in the second regime.

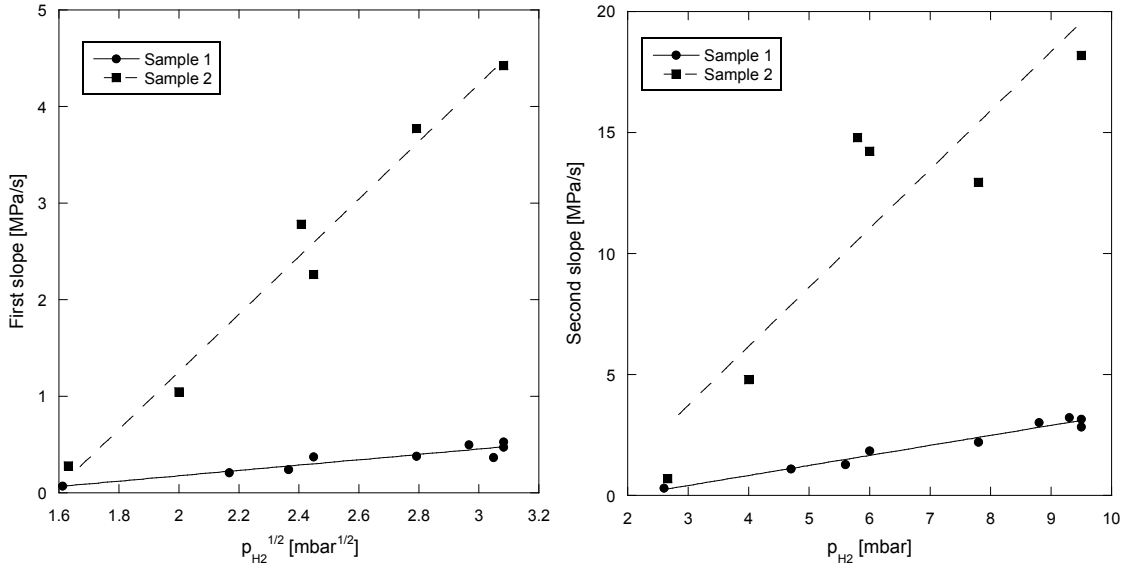

Figure 1: First and second slopes as functions of $\sqrt{p_{H2}}$ and p_{H2}, respectively.

Moreover, the effect of dry air exposure time clearly appears in Figure 1. The more important is this time interval, the slower is the hydriding kinetics. This effect is attributed to a long-term chemical reaction between the Pd surface and oxygen in air, which is believed to affect the initial palladium surface coverage [7].

All the experiments presented here have been carried out in the α phase region of the Pd-H phase diagram (p_{H2} < 10 mbar [10]). In this phase, the equilibrium compressive stress levels are located between 300 and 500 MPa, thus leading to exclusively elastic deformation if one takes into account the initial tensile stresses in the Pd films (cfr. Figure 2). Consequently, the measured stresses are directly proportional to the hydrogen concentration in the fcc palladium lattice [12]. If t_{tr} is the transition time between the linear kinetic regimes, one can then write:

$$t_{tr} \propto \frac{1}{S_{ad} p_{H_2} - S_{ab} \sqrt{p_{H_2}} + (I_{ad} - I_{ab})} \tag{7}$$

Taking the calculated slopes and intercepts from sample 2 as an example, observations from Figures 1 and 3 confirm that the first kinetic regime is limited by absorption and the second one by adsorption. Indeed, if one assumes the contrary statement, the resulting reasoning would lead to the opposite function in Eq. (7) and therefore to the prediction of negative transition times, which is physically impossible.

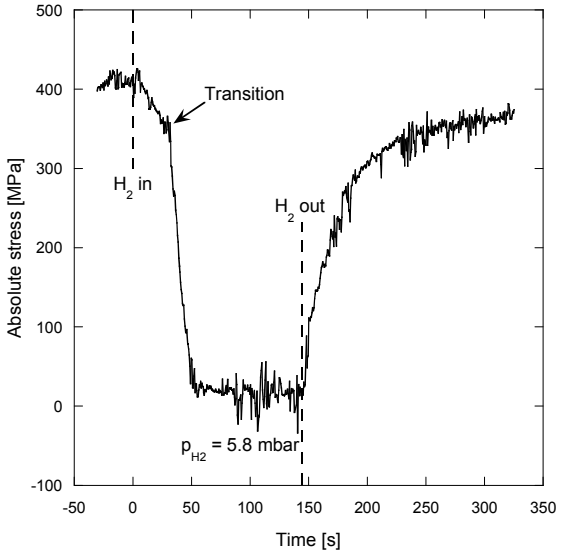

Figure 2: Typical hydriding cycle (sample 2).

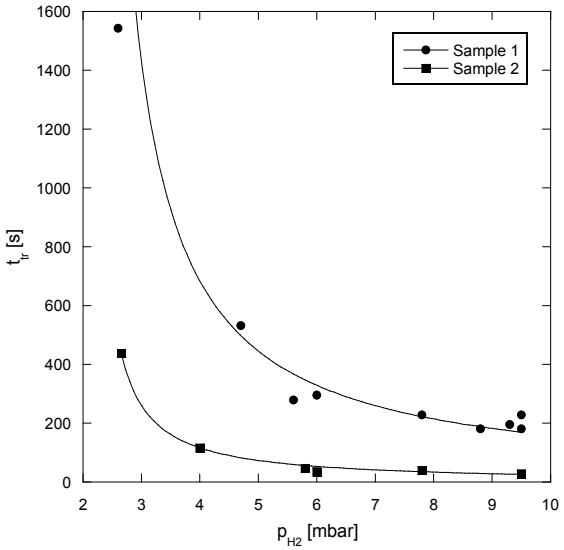

Figure 3: Transition times as functions of p_{H2} fitted with Eq. (7).

Moreover, if one takes the value of K_s already calculated in [10] and assumes that $K_{ab} = 1$ (so $n_{eq} = \theta_{eq}$), the resulting calculation from Eqs. (5) and (6) gives $\theta = 3.4.10^{-3}$ in the second kinetic regime and $n = 3.5.10^{-3}$ in the first kinetic regime. Those values make sense because they are indicative for bulk H-concentrations corresponding to the α phase region of the palladium hydride [7].

4 Conclusion

The quantitative analysis of in-situ recorded hydriding cycles according to our kinetic model enabled to identify the rate-limiting steps of Pd hydriding and to calculate surface coverage and bulk H/Pd atomic ratios in the α phase of the Pd hydride. The first linear kinetic regime is limited by absorption and the second one is limited by adsorption. The samples presented here have been compared in terms of dry air exposure time. The results show a strong influence of this parameter on the hydriding kinetics. The slowing down of the kinetics is attributed to a partial occupation of the palladium surface by oxygen. Further characterization is necessary in order to identify the chemical nature of the surface.

Acknowledgements

R. Delmelle acknowledges support from the Belgian National Science Foundation through a FRIA doctoral fellowship.

References

[1] L. Schlapbach, *MRS Bulletin* 27 (2002) 675-676.

[2] P. Chen and M. Zhu, *Materials Today* 11 (2008) 36-43.

[3] R. S. Irani, *MRS Bulletin* 27 (2002) 680-682.

[4] J. Wolf, *MRS Bulletin* 27 (2002) 684-687.

[5] R. C. Bowman Jr. and B. Fultz, MRS Bulletin 27 (2002) 688-693.

[6] W. Osborn et al., *JOM* 61 (2009) 45-51.

[7] E. Wicke and H. Brodowsky. In: G. Alefeld and J. Voelkl eds. *Hydrogen in metals vol. 2*, pp. 73-155, Berlin, Germany, 1978. Springer.

[8] M. Johansson et al., *Surface Science* 604 (2010) 728-729.

[9] R. J. Matelon et al., *Thin Solid Films* 516 (2008) 7797-7801.

[10] R. Delmelle, G. Bamba and Joris Proost, *Int. J. Hydrogen Energy* (2009), doi:10.1016/j.ijhydene.2009.11.087.

[11] J. Proost and F. Spaepen, *J. Appl. Phys.* 91 (2002) 204-216

[12] A. Pundt *et al.*, *Acta Mat.* 52 (2004) 1579-1587.

Catalytic Ammonia Decomposition in Molten Salt and Ionic Liquid Media

D. W. Assenbaum, **J. Beil**, **D. Schmitt**, **N. Taccardi**, **P. Wasserscheid**, Lehrstuhl für chemische Reaktionstechnik, Universität Erlangen-Nürnberg, Germany

1 Introduction

The increasing daily consumption of energy per person in the industrialised countries like Europe or the U.S. along with the upcoming developing countries like China or India has triggered a deep reflection about the way to generate and store energy. The actual society way of life, indeed, is pushing the consumption of electrical energy higher and higher. Thus, to store and to provide the energy necessary to at least preserve the actual life standards is going to be one of the biggest challenges the mankind is going to face in the nearly future.

Hydrogen has emerged as viable medium as energy carrier as its high energy density. Thanks to well known fuel cell technologies or combustion applications and due to the easy availability of co-reactant oxygen, its usage in energy production is almost universally possible. However, the main problem for energy supplying systems based on hydrogen is its storage. In fact, a devices like a common gas bottle reaches a storing capacity of 1,5 wt.-% for hydrogen (calculation made considering a 50 l steel tank weighting ca.95 kg charged at 200 bar hydrogen). On the other hand, storing hydrogen in liquid form will not solve the problem, requiring a huge amount of energy for the liquefaction, high pressure resisting tanks those will have, in addition, the known problem of loss over time by effusion, without considering the risk of handling hydrogen at high pressures. Other systems provide hydrogen through physically bound metal hydrides, which show good results for releasing velocity but have only limited storing capacities [1]. Therefore, alternative hydrogen storing systems with high capacities, low releasing temperatures and high purity of the released gas are needed. These systems use compounds with mostly chemically bound hydrogen like ammonia-borane [2,3]. The problem here is hidden in the difficult production and recycling process of these compounds. To overcome the various difficulties in this field a chemically storing system should be easy to produce and recycle. With its 17,6 wt.-% of hydrogen, ammonia is an interesting possibility. As a matter of fact, it is widely produced in big amounts and easy to liquefy at the relatively low pressure of 8 bar, leading to a capacity of 120 kgH_2/m^3 [4]. The decomposition of ammonia occurs at temperature around 400 °C releasing hydrogen and nitrogen, which was taken from the air during production, as only side product [5,6]. This product gas mixture can in principle directly be used in a hydrogen fuel cell or combustion system.

Ionic Liquids and Molten Salt media are well known as electrolytes in batteries or heat transfer media in various applications [7]. Moreover, especially for Ionic Liquids, great interest has been devoted to these materials as solvents or co solvents in catalytic reactions [8]. Ionic Liquids are pure salts of melting points below 100°C [9]. Besides their low volatility and high thermal stability, compared to common organic solvents, Ionic Liquids dissolve

hydrogen and nitrogen in negligible amount whereas they show high solubilisation capability for ammonia [10]. Another property of these solvents is the stabilization effect on catalysts in chemical reactions. Our contribution deals with the idea to generate a catalytic reaction system consisting of a catalyst stabilized in Ionic Liquid or Molten Salt as solvent, being able to decompose ammonia to hydrogen and nitrogen. The underlying idea is that due to the high solubility of ammonia in such a media and the very low solubility of hydrogen and nitrogen, the ammonia decomposition equilibrium might be shifted towards the latter, so allowing the decrease of the reaction temperature but reaching same conversions.

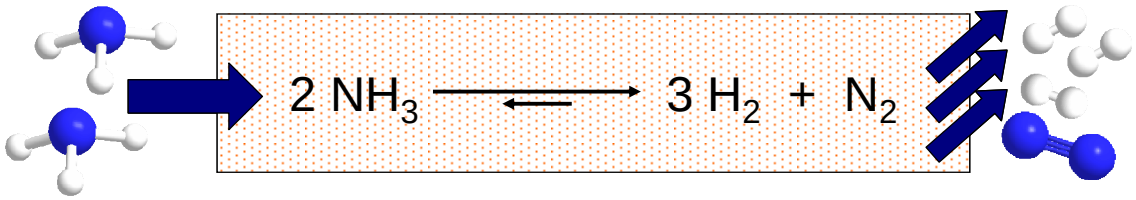

2 Results and Discussion

At first, Ionic Liquids were investigated as solvent media. Therefore, the thermal stable Ionic Liquid [EMIM][NTf_2] (1,2-Dimethyl-3-ethylimidazolium Bis(trifluorosulfonyl)imide) with its favourable solubility performance was chosen. As catalyst, Ruthenium supported on MgO was suspended into the system. The results obtained in experiments at different temperature are shown in Figure 1.

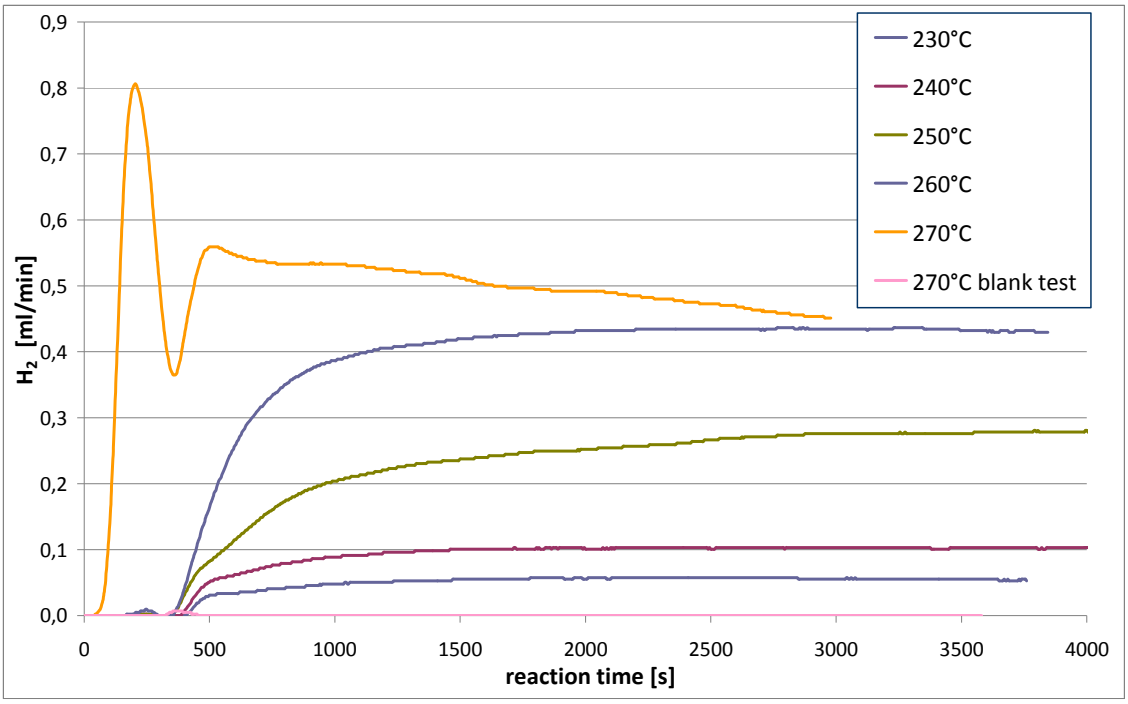

Figure 1: Hydrogen evolution during decomposition of ammonia at different temperatures in [EMIM][NTf_2] with Ru on MgO.

During the reaction, the conversion reaches a stable level, with the highest stable conversion got at 260 °C. In these conditions, the Ionic Liquid and the dispersed catalyst showed to be unaffected after the reaction was stopped. Conversely, at 270 °C, the ionic liquid decomposed as indicated by the decreasing profile of conversion *vs.* time, as well as by the tarry substance which form from the ionic liquid in the reactor. It could be concluded that the thermal limit for the actually known Ionic Liquids had been reached. As solvent with higher stability is necessary, molten Salts mixtures were examined for their possible application. To reach better catalyst dispersion, eutectic mixtures with low melting point were chosen. An eutectic salt mixture of K/Li/Cs Acetate was found a suitable candidate [11]. As catalyst in this reaction setup, $RuCl_3$ was used. The results of this experiment at different temperatures are shown in Figure 2.

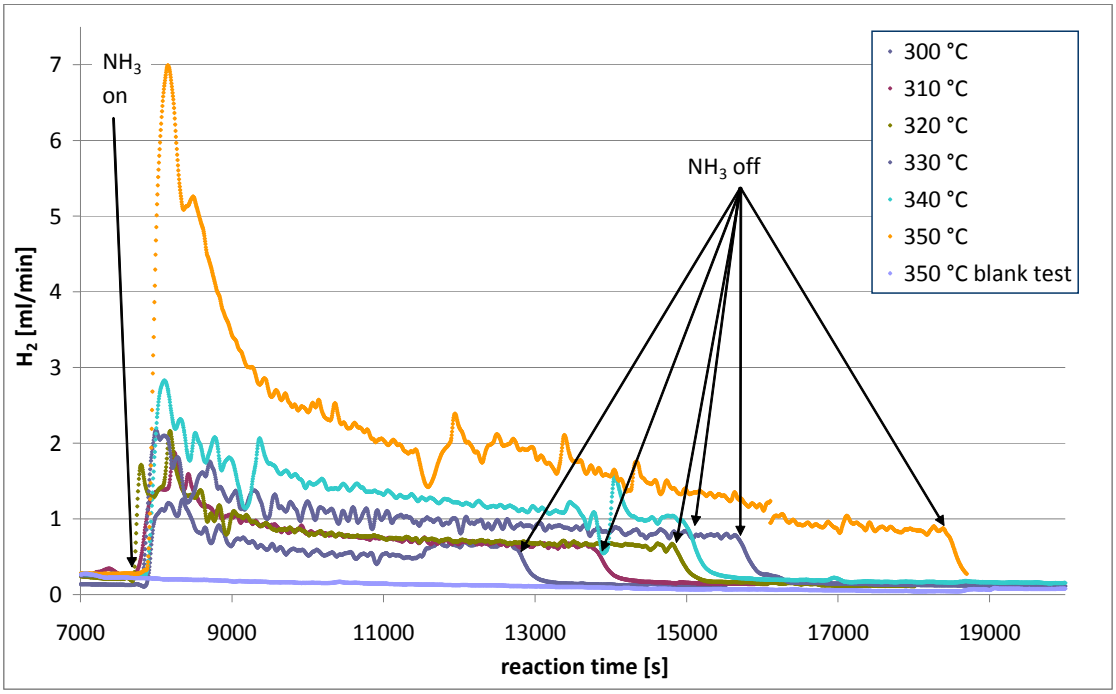

Figure 2: Evolution during decomposition of ammonia at different temperatures K/Li/Cs Acetate with Ru Cl_3.

As expected, the decomposition rate of ammonia is higher at increased temperatures. However, the conversion is decreasing over the time indicating a catalyst deactivation. This reasonably occurred due to agglomeration. In fact, it is reasonable to assume that the Ru salt formed Ru nano-particles in the reaction conditions, which are the active species. These particles agglomerated during the reaction leading to less active metal centres. Highest conversions were achieved at 350 °C with a hydrogen production rate of about 7 ml/min which corresponded to a yield of 23 % of the ammonia feed introduced into the system.

3 Conclusion

In summary, the feasibility of the decomposition of ammonia to hydrogen and nitrogen in a reaction system comprising Ionic Liquids or Molten Salts as solvent media has been proven.

The hydrogen output rates of about 0,5 ml/min at stable level in the Ionic Liquid system is relatively low. However, the maximal reachable reaction rate in this experiment was limited by the thermal stability of the solvent media. Thus, the use of higher thermally stable Eutectic Molten Salt mixtures like K/Li/Cs Acetate allowed overcoming this problem. This second reaction system shows higher conversion and the highest hydrogen production rate of 7 ml/min, 14times bigger than in the former series of experiments. Moreover, although the rapid deactivation of the catalyst, a stable hydrogen production rate of 1 ml/min, more than double as in the experiment with the Ionic Liquid solvent, was obtained.

The results obtained are quite promising and this work gives insights into new approaches for known reactions leading to innovative ways of hydrogen supply and with this an improving support for energy. The catalyst deactivation and the improvement of overall conversion are currently under investigation.

References

[1] Miura, Shinichi; Fujisawa, Akitoshi; Nenryo Denchi ,2009, 9(2), 108-112

[2] D.W. Assenbaum, D. Gerhard, P.S. Schulz, P. Wasserscheid, Chemie Ingenieur Technik 2009, 81(8), 1048.

[3] Gerhard, Dirk; Wasserscheid, Peter; Assenbaum; Schulz, Peter; Eur. Pat. Appl. 2009, 7pp

[4] Rasmus Zink Sorenden, Asbjorn Klerke, Jacob Birke Reves, Jens Kehlet Norskov, Claus Hviid Christiansen; GSC-3 Symposium, Delft, 2007, 164

[5] F.R. Garcia-Garcia, Yi Hua Ma, I. Rodriguez-Ramos, A. Gierrero-Ruiz, Cat. Comm. 9, 2008, 482-486

[6] S.F. Yin, B.Q. Xu, X.P. Thou, C.T. Au, Appl. Cat. A General 277, 2004, 1-9

[7] Michel Armand, Frank Endres, Douglas R. MacFarlane, Hiroyuki Ohno and Bruno Scrosati, Nature Materials, 2009, 8 621–629

[8] P. Wasserscheid, P. S. Schulz in P. Wasserscheid, T. Welton (eds.) „Ionic Liquids in Synthesis“, Wiley-VCH, 2nd edition, 2007, pp. XX-YY.

[9] P. Wasserscheid, W. Keim, Angew. Chem., Int. Ed. 2000, 3776-XXX

[10] Yokozeki, A.; Shiflett, Mark B Industrial & Engineering Chemistry Research 2007, 46(5), 1605-1610.

[11] S. Allulli, Laboratorio di Chimica delle Radiasioni e Chimica Nucleare del C.N.E.N Rome, Italy, Received May 2, 1968

Improved Hydrogen Generation from Formic Acid

Albert Boddien, Björn Loges, Henrik Junge, James R. Noyes, Felix Gärtner, Matthias Beller, Leibniz-Institut für Katalyse e.V. an der Universität Rostock (LIKAT), Germany

An adequate and sustainable supply of energy is one of the essential challenges for our future. Due to ever-increasing energy demands further improved technologies for the production, distribution, storage and conversion of energy are stringently necessary. In this respect a hydrogen economy would allow both for the increasing energy demand as well as the reduction of greenhouse gases. In this respect, a key issue is the current lack of safe and practical methods for onboard storage of hydrogen. Recently we and the groups of G. Laurenczy and S. Fukuzumi demonstrated independently that formic acid can be used as efficient storage material for hydrogen [1].

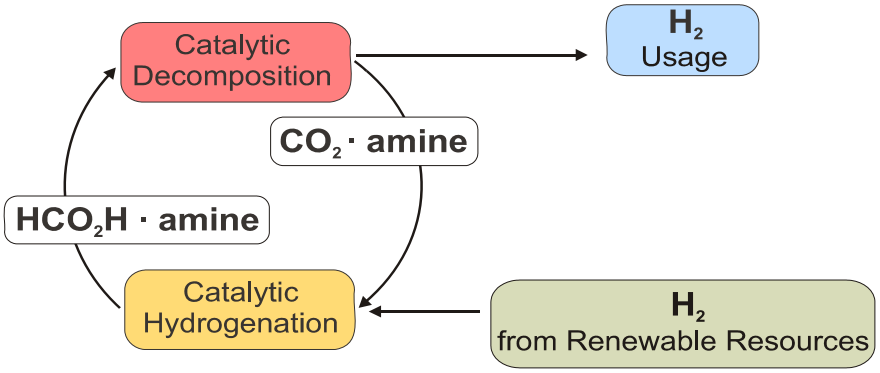

Figure 1

Applying *in situ* prepared ruthenium phosphine catalyst systems we could show the continuous generation of hydrogen at mild conditions (RT) from formic acid amine adducts [2]. More recently we investigated the influence of organic bases and of inorganic salt additives on the productivity and activity of the Ru-catalyzed hydrogen generation from formic acid [3]. While weaker bases decelerate the process, stronger bases like HexNMe2, DBN or MTBD gave excellent activities (Figure 2).

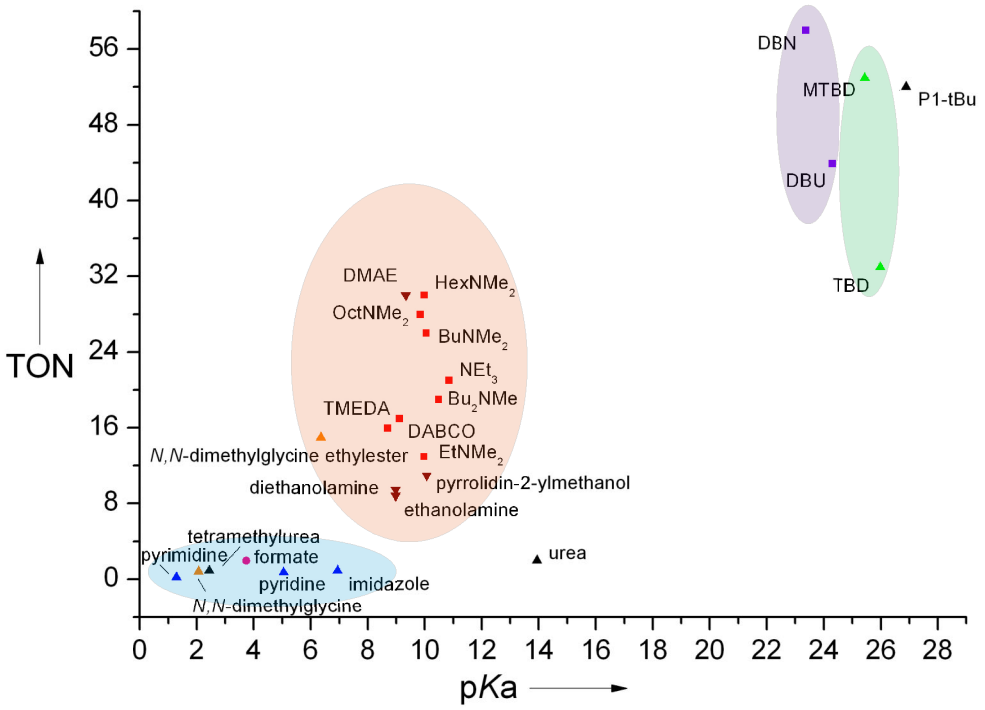

Figure 2

Moreover the presence of halide ions has also a significant influence. While the catalyst activity increase by >450% with a [RuCl2(*p*-cymene)]2 pre-catalyst by addition of 10 eq. of KI, a decrease of the catalyst activity is observed by addition of KBr to a phosphine containing catalyst system. Noteworthy, applying a catalyst system containing [RuCl2(benzene)]2 and dppe with triethylamine (3:4; amine to HCO2H) or *N,N*-dimethyl-*n*-hexylamine (4:5) a fast hydrogen generation is possible with full conversion within 2 hours.[4] Applying 20 mL of 5HCO2H/4HexNMe2 as substrate a TON of 5716 within 3 hours at 40 °C was reached, which constituted the highest activity for our approach to hydrogen generation so far. After gas evolution had ceased, the catalyst was reactivated ten times by addition of formic acid. In the first run, a prolonged induction period was observed. The activity did not decrease significantly within the next 10 runs, and an overall TON > 60000 was achieved (Figure 3a).

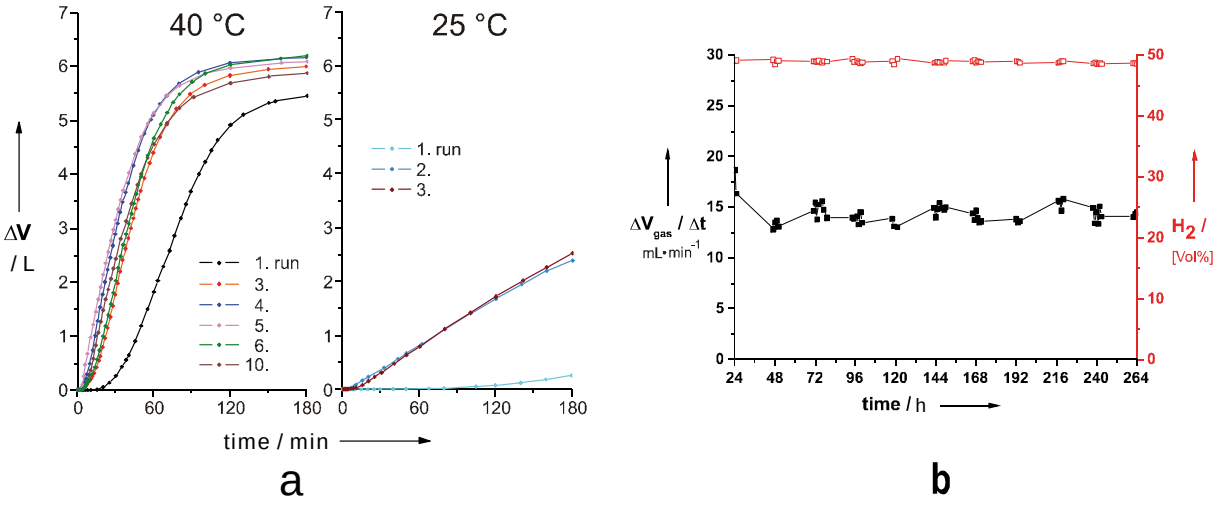

Figure 3

Based on these results, a continuous reactor was set up with 9.55 µmol [RuCl2(benzene)]2 / 6 dppe 17.5 mL HexNMe2. The system worked for more than 11 days using commercial 99% formic acid from BASF SE as received. Gas output and hydrogen concentration were virtually constant during this time, and no signs of catalyst deactivation were observed (Figure 3b). Overall, 260000 turnovers were achieved, corresponding to TOF > 900 h-1. This concept was proven to work in a small prototype model car driven by a hydrogen/air fuel cell, which has been coupled to an onboard hydrogen generation system using formic acid and a similar catalyst.

Furthermore, we could reveal the first light-driven iron-based catalytic system for hydrogen generation from formic acid, where hydrogen generation is possible under visible light irradiation and ambient temperature.[5] Applying a catalyst formed *in situ* from inexpensive Fe3(CO)12, 2,2':6'2''-terpyridine and triphenylphosphine hydrogen generation is possible under visible light irradiation and ambient temperature. Applying 1,10-phenanthroline as *N*-ligand significant catalyst turnover numbers (>100) are observed, which is the highest activity known to date for non-precious metal catalyzed hydrogen generation from formic acid. NMR, IR studies, and DFT calculations of iron complexes, which are formed under reaction conditions, confirm that PPh3 plays an active role in the catalyst cycle and that *N*-ligands enhance the stability of the system (Figure 4).

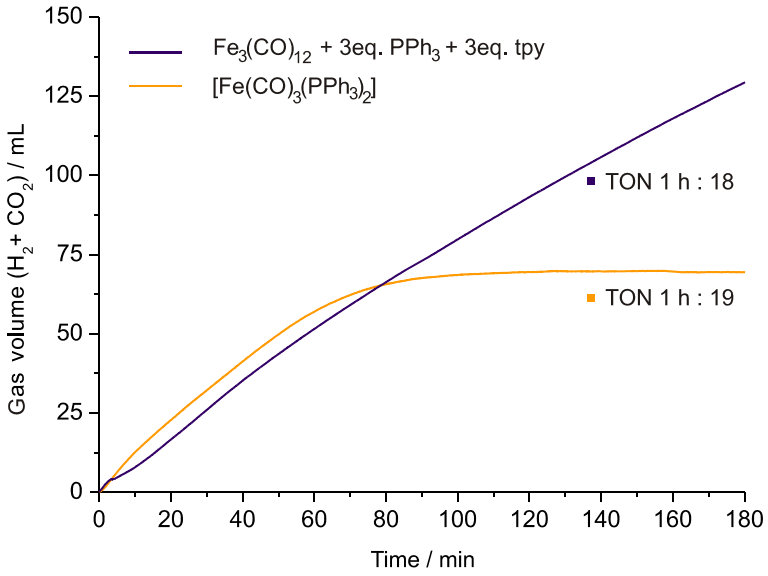

Figure 4

It is shown that the reaction mechanism includes iron hydride species which are generated exclusively under irradiation with visible light.

The present work demonstrates that hydrogen can be produced on demand even at room temperature without the need of high temperature reforming processes. In conclusion, we have shown that depending on the ruthenium pre-catalysts amines and halide additives have a significant influence on the catalyst activity. Moreover, under optimized conditions >330 ml hydrogen/h is generated from 5 mL formic acid/amine mixture, which allows for electrical applications. Beside we could show for the first time that also Fe-catalysts are capable of generating hydrogen from formic acid.

References

[1] C. Fellay, P. J. Dyson, G. Laurenczy, *Angew. Chem. Int. Ed.* **2008**, *47*, 3966–3968; Fukuzumi, S.; Kobayashi, T.; Suenobu, T. *ChemSusChem.* **2008**, *1*, 827-834; B. Loges, A. Boddien, H. Junge, M.Beller, *Angew. Chem. Int. Ed.* **2008**, *120*, 4026-4029.

[2] A. Boddien, B. Loges, H. Junge, M. Beller, *ChemSusChem.* **2008,** *1*, 751-758.

[3] H. Junge A. Boddien, Francesca Capitta, B. Loges, James R. Noyes, Serafino Gladiali,, M. Beller, *Tetrahedron Letters.* **2009**, 1603-1606

[4] A. Boddien, B. Loges, H. Junge, F. Gärtner, J.R. Noyes, M. Beller, *Adv. Synth. Catal.* **2009**, *351*, 2517.

[5] A. Boddien, B. Loges, F. Gärtner, C. Torborg, K. Fumino, H. Junge, R. Ludwig, M. Beller, *J. Am. Chem. Soc.* **2010**, DOI: ja-2010-00925n.

Hydrogen-Deuterium Exchange experiments to probe the decomposition reaction of Complex hydrides.

Andreas Borgschulte, Robin Gremaud, Arndt Remhof, Andreas Züttel, Empa Switzerland

Hydrogen storage in complex metal hydrides offers a safe alternative for transportation and storage of hydrogen. Among those storage materials, $LiBH_4$ is a promising candidate, as it can store up to 18.4 mass\% hydrogen. Storage capacity, thermodynamic stability and sorption rate are the most important properties of hydrogen storage materials and are intensively studied, but in particular the slow sorption kinetics of complex hydrides is controversial [1]. Diffusion of hydrogen is one of the main mechanisms in hydrogen sorption. Insight into the specific diffusion processes could help to improve sorption kinetics. While the diffusion of H in metals is relatively well understood, only rudimentary knowledge exists for the dynamics of hydrogen in complex hydrides. The reason for this originates from the different electronic structures of the hydrides. Hydrogen in most transition metals occupies interstitials [2]. The covalent contribution to the hydrogen-metal bond is small and thus hydrogen can easily jump from interstitial to interstitial. Accordingly, the diffusion of hydrogen in transition metals is fast with small activation energies [3]. Hydrogen in complex hydrides, on the contrary, is covalently bound and arranged in subunits ('complexes'). It is not known, whether hydrogen can be removed from such a subunit without degradation of the whole compound, i.e. diffusion of hydrogen would then require the movement of the whole subunit and/or degradation of it. Indeed, first quasi-inelastic neutron scattering measurements indicated a very slow diffusion of hydrogen in $NaAlH_4$ [4]. Nuclear magnetic resonance measurements failed in determining the hopping rate of hydrogen, as most relaxation processes are associated with the molecular reorientation of the complex anion. An alternative method to shed light onto the specific diffusion process is to label the diffusing atoms. This is experimentally realized by hydrogen-deuterium exchange either by exposing deuterium to hydrides or by solid-solid exchange.

The first method allows the investigation of the decomposition of $NaAlH_4$ [5] and $LiBH_4$ [6] by thermogravimetry, mass spectrometry and Raman spectroscopy. By these experiments we are able to obtain specific information on the surface processes, diffusing species and formation of intermediates.

The second method is realized by the investigation of hydride/deuteride diffusion multiples (see Figure 1). We demonstrate the use of spatially resolved Raman spectroscopy to derive the tracer diffusion parameters and mechanism of hydrogen containing species in complex hydrides, exemplarily on $LiBH_4$ [7]. The measurements confirm recent NMR and Raman experiments and thereby clarify the mechanism of hydrogen diffusion in $LiBH_4$. Hydrogen is directly exchanged between BH_4 units at an extremely low rate and then transported through the ionic crystal by intact BH_4 units at diffusion rates similar to rates in isoelectronic ionic compounds. This results in an effectively fast diffusion of hydrogen. We compare the

diffusion of various species in $LiBH_4$ to similar materials and discuss possible diffusion mechanisms (Figure 2).

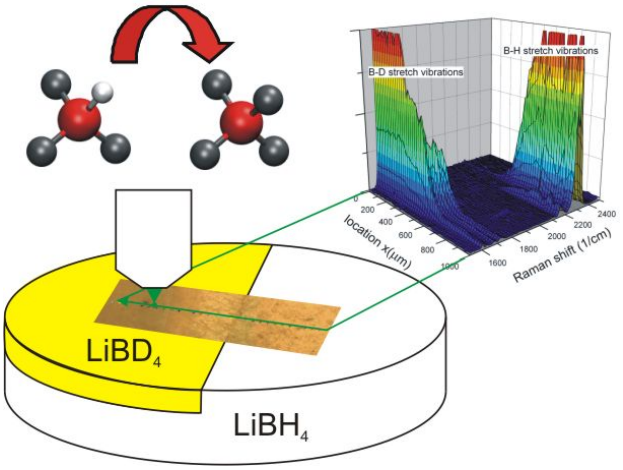

Figure 1: Raman spectroscopy on hydride/deuteride diffusion multiples.

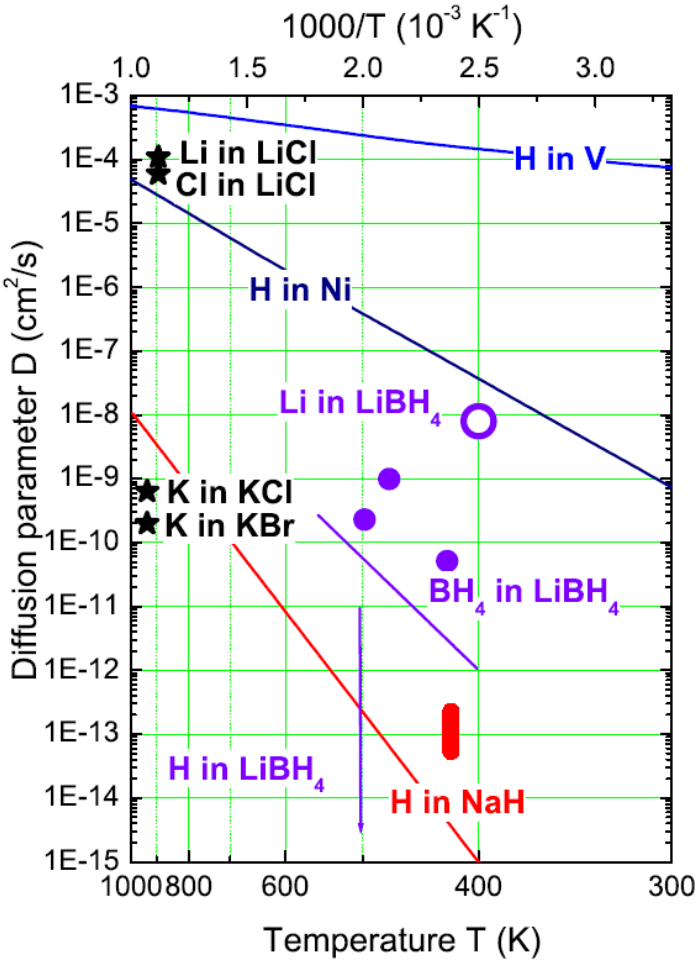

Figure 2: Diffusion of hydrogen in various metal hydrides.

The measurement of ion motilities is a generally important subject in research on complex hydrides [8]. The here presented method is not restricted to hydrogen, but can be applied to all possible ions in the compound. By interdiffusion of different hydrides, samples with locally different compositions are obtained. Spatially resolved Raman spectroscopy allows the determination of possibly formed new phases in one single sample, and with further characterization the corresponding pseudo-binary phase diagram is obtained. Thus the method is suitable as a novel high-throughput method (hydrogenography [9]) using spatially resolved Raman spectroscopy. As an example of technologically high relevance, we apply the method on $LiBH_4$ – LiI and $LiBH_4$ – $LiNH_2$, being superionic Li-ion conductors [8].

References

[1] A. Züttel and S.I. Orimo, in *Hydrogen as a Future Energy Carrier*, edited by A. Züttel, A. Borgschulte, and L. Schlapbach, Wiley-VCH, Weinheim, 2008.

[2] Y. Fukai, *The metal-Hydrogen System, Basic Bulk Properties*, pp. 207, Springer Series in Materials Science 21, Springer Berlin, 1993.

[3] H. Smithson et al., Phys. Rev. B 66, 144107 (2002).

[4] Q. Shi, et al. J. All. Compds. (2007), 446,469-473.

[5] A. Borgschulte, et al., Phys. Chem. Chem. Phys., 2008, 10, 4045 – 4055.

[6] A. Borgschulte et al. J. Phys. Chem. A 112, 4749–4753 (2008).

[7] A. Borgschulte, et al. Phys. Chem. Chem. Phys. in press (2010), DOI:10.1039/C000229A

[8] M. Matsuo,et al. J. Am. Chem. Soc., 2009, 131 (45), pp 16389–16391.

[9] R. Gremaud, et al. , Adv. Mater. 19, 2813–2817 (2007).

Making Hydrogen Work – Sustainable, Emission-free-Energy Carrier for Local Power Generation on Demand

Gregor Fornol, Jaap Korevaar, Gerard Lugtigheid, Tjitte Nauta, H2Fuel, Systems bv, The Netherlands

1 Introduction

We have a unique inexhaustible and environmentally friendly energy carrier which can be produced worldwide and which can easily be stored, transported and refueled (H2FUEL). This H2FUEL enables the on-demand and emission-free production of electric energy and/or heat both at static and mobile locations. To that effect we have developed a unique compact and scalable generator (H2FUEL energy system). The released energy can in principle be used for any application and the spent H2FUEL can be completely recycled.

Our H2FUEL energy concept may play a crucial role in the future of our energy supply, not just for providing vehicles, vessels and airplanes with emission-free energy but also as an emission-free energy concept for households, companies and institutions. Furthermore, the mobile application of our H2FUEL energy concept amply meets the targets which have been formulated by the US Department of Energy (DOE) en her European counterpart StorHy.

Just to give you an impression: if we compare the lithium-ion battery pack in a Tesla Roadster to an equal volume H2FUEL energy system, then our system is 45% lighter and provides 5 times more electrical energy, resulting in a 5 times longer driving range.

Table 1

Volume equivalent	Li-ion	H2FUEL	Delta
• Volume	180 L	180 L	n/a
• Weight	450 kg	250 kg	- 45%
• System energy	53 kWh	260 kWh	+ 500%
• System mass per kWh output	8.5 kg/kWh	1.0 kg/kWh	- 90%
• System volume per kWh output	3.4 L/kWh	0.7 L/kWh	- 80%
• Range (EPA highway)	322+ km	1610+ km	+ 500%

In case of an equal mass H2FUEL system, our system indeed is 1,5 times larger yet provides 12,5 times more energy. Obviously, the driving range in that case is 12,5 times longer. An H2FUEL powered electric car has the benefit that the ratio of useable space to driving range can be drastically revised.

Table 2

Weight equivalent	Li-ion	H2FUEL	Delta
• Volume	180 L	280 L	+155%
• Weight	450 kg	450 kg	n/a
• System energy	53 kWh	663 kWh	+1250%
• System mass per kWh output	8.5 kg/kWh	0.7 kg/kWh	- 92%
• System volume per kWh output	3.4 L/kWh	0.4 L/kWh	- 88%
• Range (EPA highway)	322+ km	4025+ km	+1250%

Several prominent strategic parties have an interest to further develop and apply the H2FUEL energy concept in cooperation with us. Since this requires a substantial financial injection, not just from the strategic parties but also from us, we are approaching different organizations

The strategic partners we are deeply engaged with in setting up the joint development projects include amongst others the research organization TNO (Defense and Safety, Industry and Technology), the German national research centre for aeronautics and space (DLR), an important airplane manufacturer and a German industrial supplier for emergency electrical power for aviation and other industrial applications.

2 Background

Electrically powered vehicles, vessels and airplanes play a prominent role in the growing global need for emission-free mobility. Major challenge is to bring electrical energy on board. At first sight the battery seems to be a suitable solution. However, batteries are harmful to the environment and furthermore the recoverable raw material reserves are insufficient. These reserves will de depleted quicker than oil wells and thus we exchange dependence from one sources to the other. Batteries make electrically powered vehicles expensive to buy and maintain, and the massive application of batteries provides enormous logistic problems, for which the power grid is not designed. The relatively low energy density furthermore limits the driving range and the required charging time does not match the current driving experience.

It is very clear that the solution lies in an inexhaustible and environmentally friendly energy carrier which can easily be stored, transported and refueled, and from which electrical energy can be generated on board while driving and on demand, such that the driver of a conventional fossil fuel vehicle becomes motivated to change over to an electric vehicle.

For a long time the clean energy carrier hydrogen appeared to be the most promising solution. Electrical energy can be generated instantaneously from pure hydrogen and ambient air using a fuel cell. Application of pure hydrogen appears not to be economically viable, particularly due to the precautions required to safely and efficiently store, transport

and refuel pure hydrogen. In addition, the present day industry does not succeed in increasing the energy density, as a result of which the targets formulated by the US Department of Energy (DOE) and her European counterpart StorHy cannot be met by a long run.

Initially our project objective was to develop a renewable energy carrier as an alternative for pure hydrogen, and a plug & play energy system able to release energy from this carrier on board a vehicle and emission-free. Our desire was to develop a mobile energy concept that meets the targets formulated by the US Department of Energy (DOE) and her European counterpart StorHy, such that electric driving better matches the present day driving experience. In the mean time we realize that our H2FUEL energy concept has a much broader applicability.

3 A Unique and Promising Energy Concept: H2FUEL

The H2FUEL energy concept can play a crucial role in the future of our energy supply, not just for providing emission-free energy to vehicles, vessels and airplanes but also as emission-free energy concept for households, companies and institutions.

An H2FUEL energy system instantaneously releases pure hydrogen from H2FUEL, subsequently the released hydrogen reacts with oxygen in stacked fuel cells to form water, while an electric current is created in an efficient way. If desired, the same energy system may for certain applications be limited to an instantaneous, emission-free hydrogen production on demand.

H2FUEL is better to handle and therefore its application is more economically viable than compressed pure hydrogen. H2FUEL is a liquid by itself and can be stored under slightly adapted conditions, without serious degradation of storage materials. The risk profile of H2FUEL is more or less equal to that of gasoline and in addition, pure hydrogen is not released prior to any demand. Furthermore, the energy density of H2FUEL per liter energy system is larger than that of compressed pure hydrogen. All this results in an energy carrier having a large driving range and a short refueling time at a large number of potential refueling locations, and an energy system having a long life expectancy.

The instantaneous release of pure hydrogen from H2FUEL causes no harmful emissions. Furthermore, combustion of pure hydrogen in an internal combustion engine or the use thereof in a fuel cell to produce an electrical current does not result in harmful emissions. In both cases the released hydrogen reacts with oxygen to produce energy, while the only exhaust gases released comprise water vapor.

H2FUEL has enormous potential as a renewable, emission-free energy carrier. The major component of this energy carrier, viz. a modified type of chemically bound hydrogen, can be produced from virtually all primary energy sources including renewable sources such as solar energy, wind energy, hydropower, biomass and geothermal energy. As energy carrier H2FUEL will never be depleted.

4 Status

Obviously, we have applied for patents both for the energy system and the energy carrier. The basic design of the H2FUEL energy system has been positively assessed by several renowned scientific institutes and the manufacture thereof is considered to be feasible. Furthermore the H2FUEL proposed by us (including its application in the H2FUEL energy system) has been positively assessed.

Although H2FUEL is not commercially available, the basic processes for its manufacture are known. Research organization TNO (Defense and Safety) claims that for performing prototype tests, TNO can produce H2FUEL according to our specifications. The particular expertise of TNO is producing and applying the major component of H2FUEL: a modified type of chemically bound hydrogen. Currently the basis thereof is used in ammunition, as rocket fuel and as emergency ignition fuel for military aircrafts.

The moment our strategic partner(s) and us have made a fist H2FUEL energy system and an amount of H2FUEL, we can prove not just in theory but also in practice that the energy capacity of the H2FUEL concept, both in terms of system volume and system mass, by far outclasses other innovative and environmentally friendly energy concepts allowing the on demand generation of electrical energy and/or heat on location. In fact, this enables us to prove in practice that the ultimate targets formulated by the US Department of Energy (DOE) and her European counterpart StorHy for hydrogen based energy systems (to be used in vehicles), are actually achievable with our H2FUEL concept; and we herewith close a time gap of more than a decade.

TNO Industry and Technology, business unit Automotive, has made us an offer to provide and electrical vehicle with the H2FUEL energy concept, with support from the Dutch Government. In addition, TNO Defense and Safety has offered to produce H2FUEL for prototypes and to develop a scalable and economically viable manufacturing model for the longer term, also with support from the Dutch Government. A contribution from us is required. This contribution obviously increases as the development risks decrease.

The NESSHY Hydrogen Sorption Properties Database

N. Frischauf, **C. Filiou**, **P. Moretto**, Institute for Energy, Joint Research Centre of the EC

1 Introduction

The final aim of NESSHY project is to identify the most promising solid storage solutions for such applications. To assess the potential of the various materials as hydrogen stores and to identify the most promising storage systems, it is important to have access to materials respective hydrogen sorption performance data and related information, and also to means for their comparison and evaluation. This is the need that the NESSHY hydrogen sorption properties database (NESSHY-DB) came to fulfil. It was built by the JRC-IE, as a tool to manage, store and exchange data and information from researchers between the different NESSHY laboratories.

Moreover, NESSHY-DB meets also a requirement of DG RTD, to have a permanent repository of the experimental results acquired by NESSHY, which could guarantee their availability beyond the time frame of the project.

1.1 State-of-the-art

To our knowledge there is only one other database dedicated to hydrogen solid-state storage publicly available on the internet. In 1995, G. Sandrock at the Sandia National Laboratory started a “On-line Hydride Database”, in the frame of the Task 12 of the Hydrogen Implementation Agreement of the International Energy Agency (IEA-HIA) [1].The database was created as a literature reference service for the scientists in Task 12 and has grown up to almost 2000 hydride alloys and 1200 references. The Sandia database has not been updated in the last years, and its structure is optimised for classic metal hydrides only [2,3].

The NESSHY-DB is not in competition with the Sandia one. Objectives and structure differ considerably. This will appear clear in the detail in the following chapters. To mention here just some of these differences, NESSHY-DB can accommodate primary experimental data such as pcT, TPD and kinetics curves, and to respect intellectual property rights (IPR) issues, it offer scientists different access levels.

2 Description of the NESSHY-DB

2.1 Overview

The NESSHY-DB was built for the archiving, exchange and comparison of experimental results and material properties data generated in the NESSHY laboratories. The main driver was to ensure that all scientific and research data are available within the NESSHY Consortium .Therefore all data are organised centrally for maximising their usability, efficient management, exploration and ultimately conservation for the future. In addition, the tool had to facilitate the data exchange without compromising the confidentiality of the information. These requirements dictated the actual structure and functionalities of the database.

The NESSHY-DB is based on the JRC portal ODIN (On-line Data Information Network, https://odin.jrc.ec.europa.eu), which provides web-enabled access to a number of engineering and materials databases. These applications share fast cabling, firewall, secure connection, redundancy to guarantee high availability, central data and user management, common hard- and software infrastructure in order to facilitate maintenance and further development (see Figure 1). Further details on the JRC databases hardware and software system and structure can be found in general in references [4 and 5], while [6] describes the content of HIAD, the Hydrogen Incidents and Accidents Database developed in the frame of Network of Excellence HySafe.

The NESSHY-DB has been designed with an appropriate interface for data content, entry, retrieval and reporting. The database contains public and restricted data and has the necessary access control implemented via a central registration and login procedure. It offers also the possibility for data evaluation employing special graphical development environments. It is dedicated to experimental hydrogen sorption and thermo-physical properties data obtained on mainly new materials generated by the NESSHY participating laboratories. It also includes already published hydrogen storage material data and results from inter-laboratory comparison exercises run within the project for the data harmonisation and the development of testing protocols. The NESSHY-DB is currently restricted to partners only. It serves for data organisation, comparison, reporting and ultimately for the material down-selection, which feeds in the engineering task of the programme of work of NESSHY.

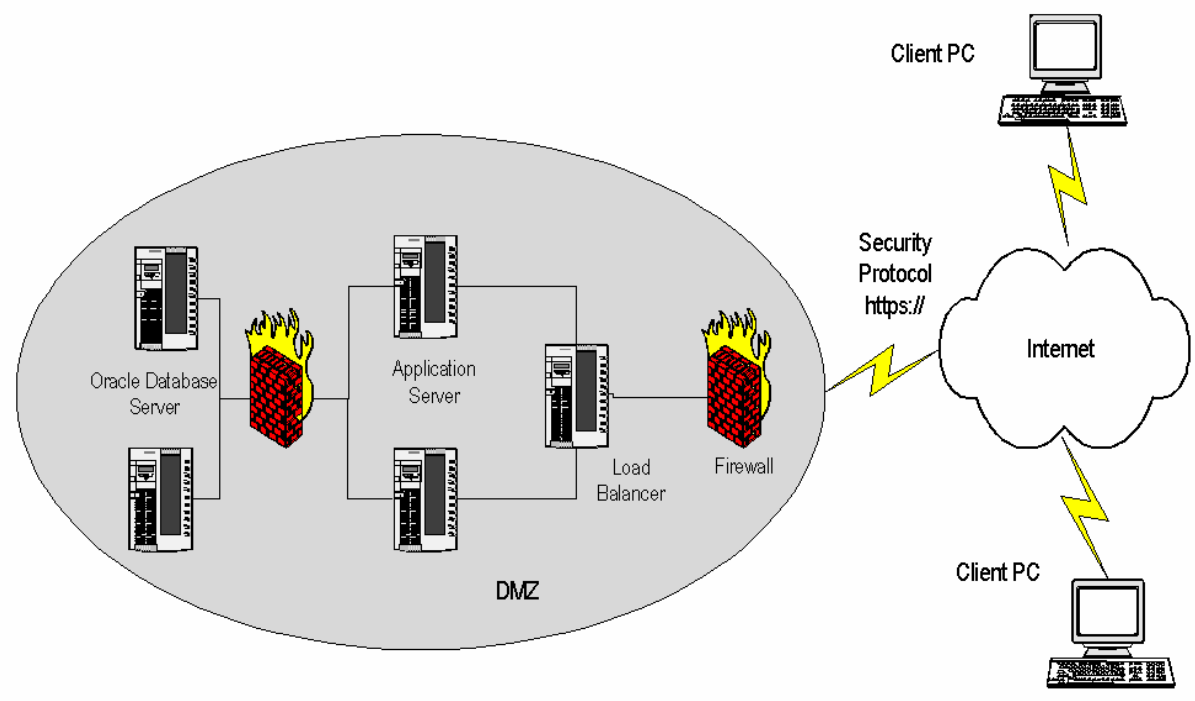

Figure 1: Structure of the web-enabled JRC ODIN portal.

2.2 Database structure

The NESSHY-DB has basically three modules. The first two modules focus on experimental data produced in the various NESSHY laboratories. They comprise an experimental data retrieval module and a data upload module with a web-enabled interface for the direct remote upload of data. The third module serves as repository for the physical and engineering data as well as a structured collection of engineering data necessary for the design and construction of the solid-state storage tanks.

2.3 Access rights and handling of data

The database is built in such a way to ensure that different levels of access rights are possible and implemented to separate the confidential/restricted data from public data. The data owner decides which parties can access and enter data. There is also an option for the so-called 'power users' allowing them to manage their own sources. A method for “de-classifying” parts of data, as opposed to the whole source, to change from confidential to restricted or public has also been introduced. By default, all authorised users belong to the “NESSHY_Public Group”. These members have “read rights” (can retrieve but neither write new data nor edit existing data) to all data sources that are identified as “read-accessible”. If a data source is identified as “restricted” then no one apart from the data owner (or specific users following data owner’s authorisation and an action by the administrator) can see its content. A “source” is visible to a user only if the user has read rights for this source. There is also a possibility for restricted write access rights, enabling the users retrieval and modification of data. For a group of users (for instance work package leaders within NESSHY) specific access rights/characteristics can be created. Every user can also belong to certain (sub)group(s) with extra privileges and access rights to restricted sources of data, which can be set as required and authorised by data owners. Access permissions apply to the whole (sub)group allowing for easier management.

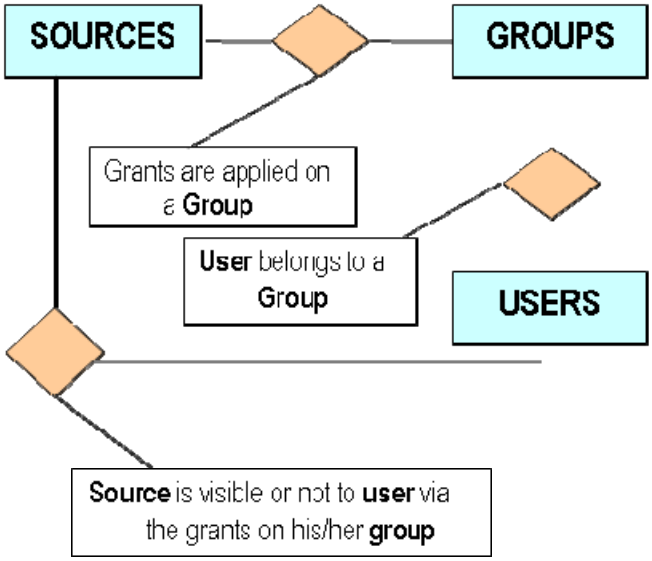

Figure 2: Entity/relation diagram for NESSHY user authorisation.

Every organisation gets by default two data source folders/source identifiers for entering data – one where data which will be viewed by all authorised NESSHY users are placed and another source folder for confidential/restricted data. More Source folders can be created as required and following approval of organisation/company main contact person in NESSHY and their request to the DB administrator. Users belonging to one organisation are linked to the respective sources through confirmation by their organisation's main contact person in NESSHY. One or more users per organisation may also be assigned as data validators to control the quality of the data entered.

2.4 Intellectual property rights

Scientific data sharing and access to collectively generated data sets constitute important knowledge and their dissemination and management are essential for scientific progress but can also be quite sensitive and subject to Intellectual Property Rights. As stated earlier, for the time being the NESSHY-DB is restricted within the NESSHY Consortium. The platform, under which the database runs, its structure and operation, are JRC property. The general rules described under Article 9 on Intellectual Property Rights of the NESSHY Consortium Agreement hold for the access to, use and exploitation of the NESSHY DB. Ownership of and access to the data, information and knowledge entered in the NESSHY DB lie with the Contractor (Laboratory) that has generated the data. Any use or exploitation of these data must be directly requested from the respective Laboratory. In the near future, and pending the Consortium members' agreement, the NESSHY-DB will be released for use by the European research community.

2.5 Functioning of the NESSHY-DB

The NESSHY-DB database consists of a web enabled interface and three modules for remotely uploading, retrieving & managing data. The entry module allows uploading hydrogen sorption materials data, which can be retrieved via the retrieval module. The third module is dedicated to Physical & Engineering Parameters. The DB has an 'import/export' data feature and an elaborated 'advanced selection' option for retrieval, and good graphical data presentation. Introductory manuals dedicated to each module have been uploaded, along with online help screen shots with detailed instructions for every step.

3 Summary and Follow-up

The Novel Efficient Solid Storage for Hydrogen Database (NESSHY-DB) is a web-enabled tool designed and running under the JRC ODIN platform and it is currently at the disposal of the NESSHY Consortium. It was developed for storing hydrogen sorption test data generated on new materials, as well as literature available data and the results of inter-laboratory comparison exercises. A part from exchanging and conserving data and knowledge, it is a flexible and robust tool for managing and fully exploring experimentally derived information for assessing the performance of materials as potential hydrogen stores.

At the moment, the database is populated only with results from JRC and from the three NESSHY Round Robin Exercises. It has been made publicly available and is waiting for input from partners.

Acknowledgement

This work was conducted under the auspices of NESSHY European project. Funding by the European Commission DG Research (contract SES6-2006-518271/NESSHY) is gratefully acknowledged.

References

[1] G. Sandrock and G. Thomas, The IEA/DOE/SNL On-Line Hydride Databases, Project 7 of the Task 12 of the IEA/HIA, in “IEA Agreement on the Production and Utilization of Hydrogen Annual Report 2000, Edited by Carolyn C. Elam, National Renewable Energy Laboratory, Golden, CO USA, NREL/TP-510-31287

[2] http://hydpark.ca.sandia.gov/ieaframe.html

[3] G. Sandrock, G. Thomas, The IEA/DOE/SNL on-line hydride databases, Appl. Phys. A 72, 153–155 (2001)

[4] H.H. Over, W. Dietz, The web-enabled database of JRC-EC, a useful tool for managing European Gen IV materials data, Journal of Nuclear Materials 376 (2008) 346–352

[5] H. H. Over, E. Wolfart, The Web-enabled ODIN Portal -Useful Databases for the European Nuclear Society, International Conference Nuclear Energy for New Europe 2005, Bled, Slovenia, September 5-8, 2005

[6] C. Kirchsteiger, A.L. Vetere Arellano, E. Funnemark, Towards establishing an International Hydrogen Incidents and Accidents Database (HIAD), Journal of Loss Prevention in the Process Industries 20 (2007) 98–107

Formic Acid – Convenient Liquid Hydrogen Storage for Mobile Applications

Henrik Junge, Björn Loges, Albert Boddien, Matthias Beller, Leibniz-Institut für Katalyse e.V. an der Universität Rostock, Germany

1 Introduction

In the last decade hydrogen has become an increasingly attractive source for energy generation. Advancements in hydrogen technology such as the generation of hydrogen, its storage and its conversion to electrical energy are the prerequisite for the application of hydrogen as power source. Recently, the use of carbon dioxide as storage material for hydrogen and the controlled decomposition of formic acid to hydrogen have received considerable attention for energy storage [1].

In 2008, we have demonstrated that hydrogen can be generated from formic acid under mild conditions [2]. Commercially available Ru-catalysts are suitable for this reaction in the presence of amines. However, an improvement of the catalytic activity is possible applying in situ catalysts based on ruthenium and various phosphine ligands [3].

2 Results and Discussion

Unprecedented high rates at ambient temperature were obtained with a catalytic system which contains $[RuCl_2(benzene)]_2$ and the bidentate ligand dppe (1,2-bis(diphenylphosphino)ethane). This ruthenium/phosphine catalyst is able to generate hydrogen with high rates and high stability at room temperature. In order to allow for practical electric applications, >1 L H_2 per hour of hydrogen should be produced continuously for several hours. By application of $[RuCl_2(benzene)]_2$/dppe hydrogen evolution is achieved with up to 2.9 Liters per hour (Figure 1).

Besides the activity another important practical feature is the reuse of the catalyst system. Notably, our ruthenium phosphine complex showed no significant decrease of activity even after 10 restarts of the reaction by addition of formic acid during a period of two months! Hence, a total turnover number (TON) of approximately 60000 at 40 °C in 30 hours reaction time was obtained.

Applying the *in situ* ruthenium catalyst, usually the first run showed an induction period followed by a linear increase of gas evolution. The induction period is more pronounced for lower temperatures. The subsequent runs proceeded with an induction period of less than one minute (Figure 1).

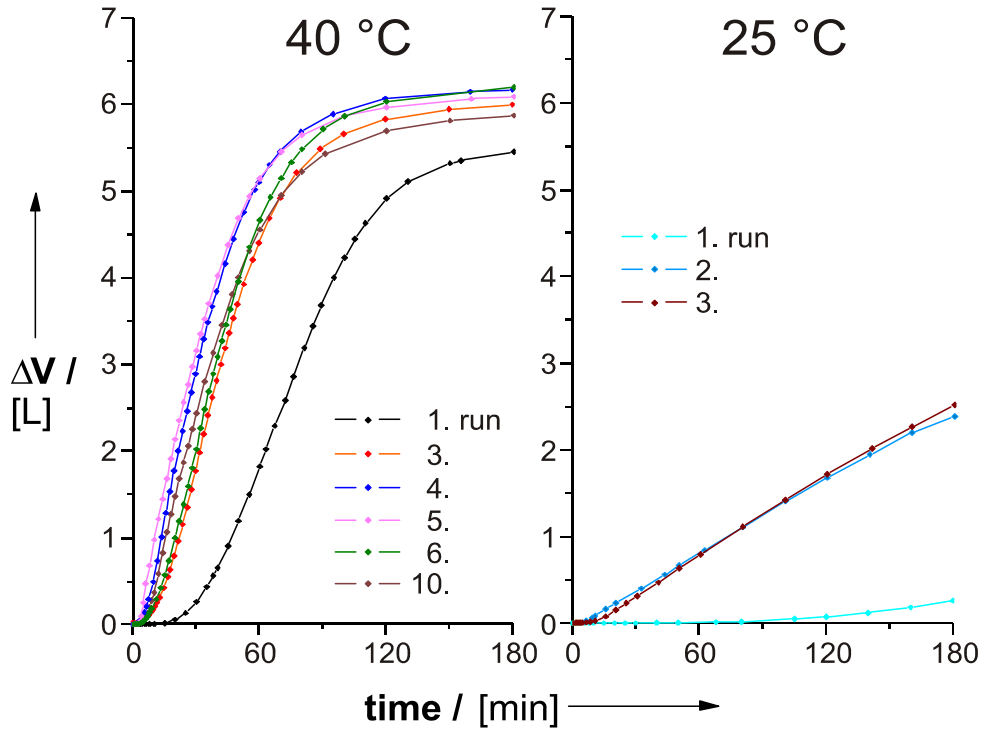

Figure 1: Recycling experiments; 4.75 mL HCO_2H added to a solution of 9.55 µmol $[RuCl_2(benzene)]_2$ /3 equiv dppe in 17.5 mL $HexNMe_2$.

To investigate the long time stability of our system, we constructed a device for continuous hydrogen generation (Figure 2). In a typical experiment 0.74 mL formic acid per hour were added to the reaction vessel containing 9.55 µmol $[RuCl_2(benzene)]_2$ / 3 eq. dppe in 17.5 mL *N,N*-Dimethylhexylamine ($HexNMe_2$). The gas mixture was quantified constantly with a gas flow meter "EL-FLOW" (Bronkhorst) and the hydrogen content was measured with a hydrogen sensor supported by GC analysis of the collected gas every 24 h.

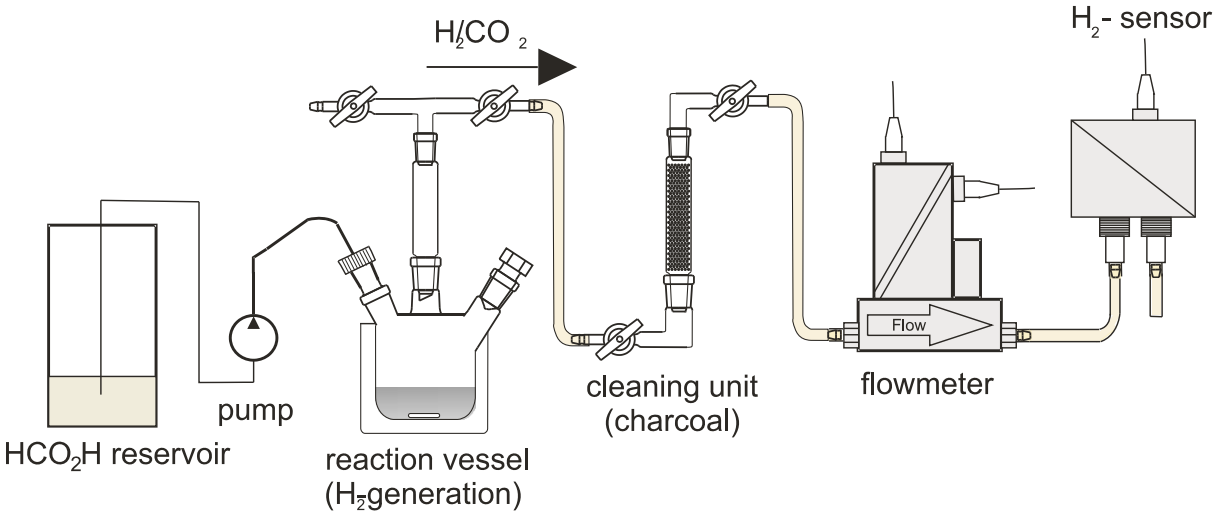

Figure 2: Device for continuous hydrogen generation from formic acid.

As shown in Figure 3 no decrease of catalyst activity was observed over a period of 264 h resulting in an outstanding TON of 260000! To the best of our knowledge, this is the highest value ever reported for selective formic acid decomposition. With respect to feedstock commercially available formic acid (99% grade, BASF) was used as received. Notably, also formic acid with 2% water content can be used without any loss of activity, underlining the robustness of the catalytic system. Applying the continuous conditions, the hydrogen outflow was approximately 0.45 L H_2/h [4].

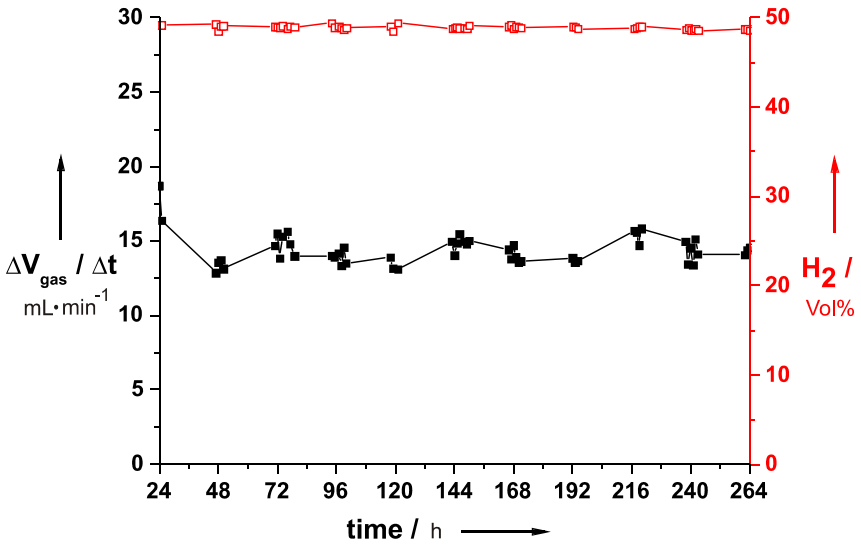

Figure 3: Continuous hydrogen production at room temperature.

The produced hydrogen (1:1 mixture with CO_2) meets already the qualitative and quantitative requirements for an application in small electric devices. It contains < 10 ppm CO and can be directly used in fuel cells. For demonstration we successfully implemented our hydrogen generation unit in a commercial available PEMFC toy car (Figure 4).

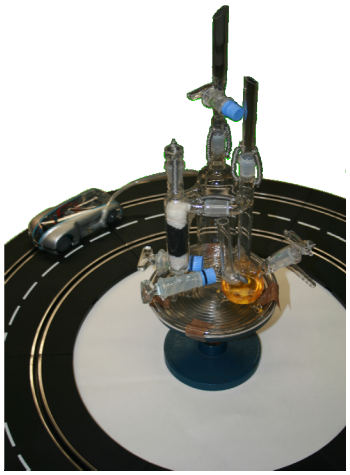

Figure 4: HCO_2H based H_2 supply for a commercial PEMFC toy car.

It is noteworthy to mention that the hydrogen generation can be accelerated by light and in fact can be triggered by switching on and off the light source (Figure 5).

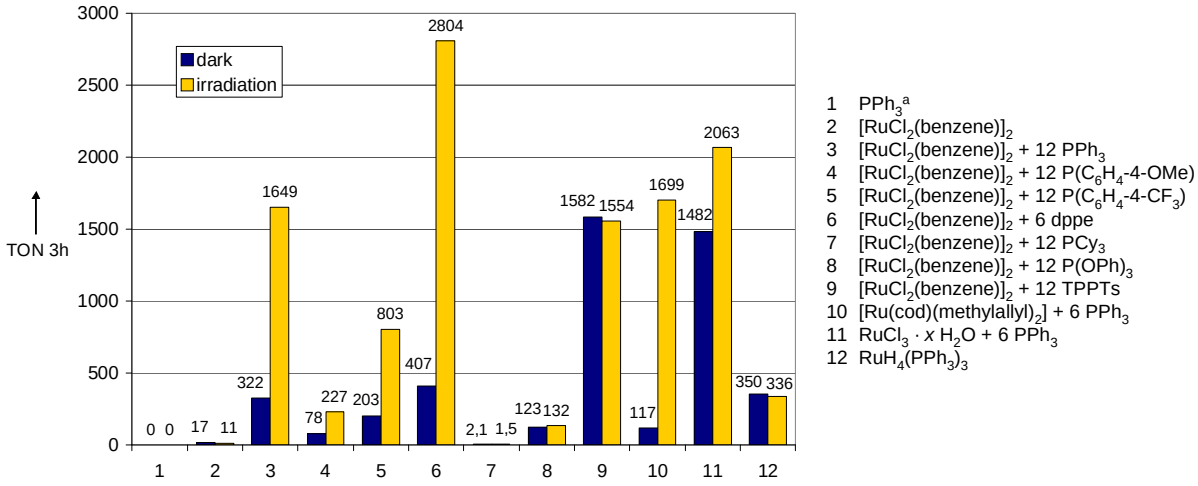

Figure 5: Influence of light on the performance of Ru-catalysts. (5.0 mL 5 HCO_2H • 2 NEt_3, 19.1 µmol [Ru], 3h at 40 °C, Xe-Arc lamp/hot mirror; P : Ru = 6. [a] no hydrogen detected by GC.

This is the first example of the light-accelerated hydrogen generation reaction from formic acid with a catalyst system based on a ruthenium precursor and arylphosphines. In comparison to the non photo-assisted system, a more than one order of magnitude increase of gas evolution is achieved in the light-accelerated reaction. Thus the productivity of our best catalyst system $[RuCl_2(benzene)]_2$/dppe could be further increased [5]. Hence, the catalyst activity is almost double the activity of the best non-light activated system.

A careful analysis of our results reveals that irradiation has at least two effects: first the generation of the active species is promoted and second the deactivation of the catalyst is prevented.

Notably, this offers the opportunity to control hydrogen generation with light. After an initial formation of a stable photo-active catalyst, gas evolution could be almost stopped by switching off the light source, and restarted after turning it on again. Thus in addition, we could demonstrate for the first time that hydrogen evolution can be triggered by switching on and off the light source! (Figure 6)

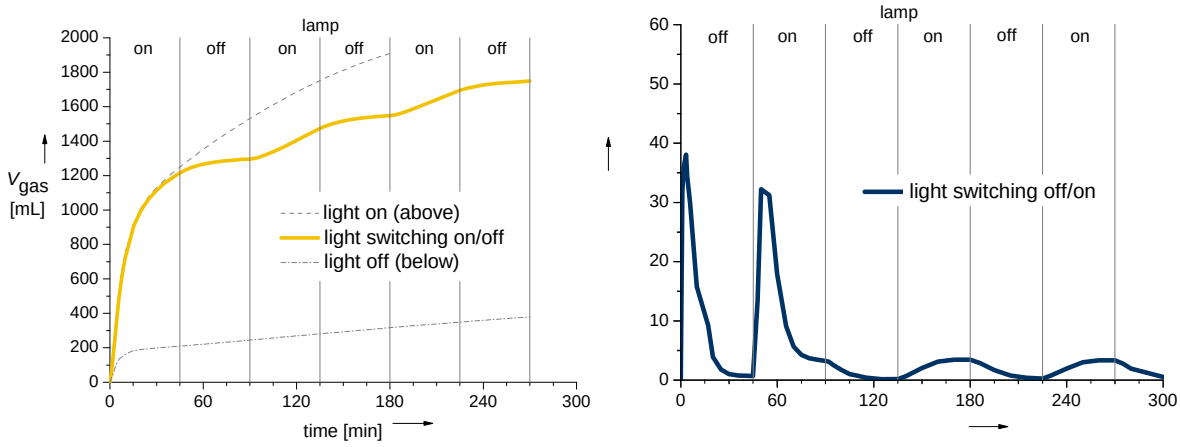

Figure 6: Light-triggered gas evolution from 5 mL 5 HCO_2H • 2 NEt_3 with $[RuCl_2(benzene)]_2$ / 12 PPh_3 (320 ppm Ru).

Left: After an initial formation of a stable photo-active catalyst, gas evolution can be almost stopped switching off the light source, and restarted after turning it on again.

Right: (Differential plot) Irradiation with light after 45 min further activates the catalyst in the first cycle of irradiation. In the following irradiation cycles, hydrogen generation is started and stopped by turning the light on or off.

In the light assisted reaction ruthenium can be substituted by the non noble metal iron. Recently the first light-driven iron-based catalytic system for hydrogen generation from formic acid could be developed. The catalyst is formed in situ from inexpensive $Fe_3(CO)_{12}$, 2,2':6'2''-terpyridine and triphenylphosphine.

3 Conclusion

Active and stable catalysts for the generation of hydrogen from formic acid at ambient conditions could be developed, which allow for an application of formic acid as hydrogen source especially in portable electric devices. Here the combination of hydrogen generation from formic acid and a PEMFC could be a suitable alternative for direct methanol fuel cells.

References

[1] a) S. Enthaler, *ChemSusChem* **2008**, *1*, 801-804; b) F. Joó, *ChemSusChem* **2008**, *1*, 805-808.

[2] a) B. Loges, A. Boddien, H. Junge, M. Beller, *Angew. Chem.* **2008**, *120*, 4026-4029; *Angew. Chem. Int. Ed.* **2008**, *47*, 3962-3965.

[3] a) A. Boddien, B. Loges, H. Junge, M. Beller, *ChemSusChem* **2008**, *1*, 751-758; b) H. Junge, A. Boddien, F. Capitta, B. Loges, J. R. Noyes, S. Gladiali, M. Beller, *Tetrahedron Lett.* **2009**, *50*, 1603-1606.

[4] A. Boddien, B. Loges, H. Junge, F. Gärtner, J.R. Noyes, M. Beller, *Adv. Synth. Catal.*, **2009**, 351, 2517-2520.

[5] B. Loges, A. Boddien, H. Junge, J. R. Noyes, W. Baumann, M. Beller, *Chem. Commun.* **2009**, 4185-4187.

Graphitic Nanofibres as Catalyst for Improving the Dehydrogenation Behavior of Complex Aluminium Hydrides

M. Sterlin Leo Hudson, Himanshu Raghubanshi, D. Pukazhselvan, O.N. Srivastava*, Hydrogen Energy Center, Department of Physics, Banaras Hindu University, Varnasi, India

Abstract

In the present work, we explored the catalytic effect of graphitic nanofibres (GNF) particularly of two different morphology, namely planar graphitic nanofibre (PGNF) and helical graphitic nanofibre (HGNF) for enhancement of hydrogen desorption from complex aluminium hydrides such as $LiAlH_4$ and $LiMg(AlH_4)_3$. We found that the catalytic activity of fibres depends mainly on its morphology. Hence helical morphology fibres possess superior catalytic activity than planar graphitic nanofibres. The desorption temperature for 8 mol% HGNF admixed $LiAlH_4$ gets lowered from 159°C to 128°C with significantly faster kinetics. In 8 mol% HGNF admixed $LiMg(AlH_4)_3$ sample, the desorption temperature gets lowered from 105°C to ~70°C. The activation energy calculated for the first step decomposition of $LiAlH_4$ admixed with 8 mol% HGNF is ~68 $kJmol^{-1}$, whereas that for pristine $LiAlH_4$ it is 107 kJ/mol. The activation energy calculated for as synthesized $LiMg(AlH_4)_3$ is ~66 kJ/mol. Since the first step decomposition of $LiMg(AlH_4)_3$ occurs during GNF admixing, the activation energy for initial step decomposition of GNF admixed $LiMg(AlH_4)_3$ could not be estimated.

1 Introduction

The growing interest on finding effective catalyst for improving the dehydrogenation/re-hydrogenation behavior of complex metal hydrides after the pioneering work of Bogdanovic et al [1] on the reversibility of $NaAlH_4$ triggers research on various catalysts including transition and rare earth metal based catalysts. Aluminium hydrides, $LiAlH_4$ and $LiMg(AlH_4)_3$ possess quite high gravimetric hydrogen capacity of 10.6 and 9.7 wt.%H_2, respectively. The fast desorption of hydrogen from these compounds becomes feasible with the use of a suitable catalysts. There is an ongoing search for finding an effective catalyst for improving the dehydrogenation/re-hydrogenation behavior of complex hydrides [2]. Recent studies by Berseth et al [3] reveal that carbon nano-variants are found to possess catalytic effect on complex hydrides. Among the carbon nanovariants, graphitic nanofibres are very promising due to their large number of localized σ bond electrons around the edges of parallel graphitic sheets, which provides more catalytically active sites [4, 5]. Advantageous features of carbon nanofibre are that it is light weight, not prone to oxidation nor gets substituted in the alanate lattice. In the light of above, we explored the use of graphitic nanofibres of two different morphology namely planar graphitic nanofibre (PGNF) and helical graphitic nanofibre

* Corresponding author: Email: hepons@yahoo.com

(HGNF) for possible improvement in dehydrogenation characteristics of $LiMg(AlH_4)_3$ and $LiAlH_4$. The catalytic activity of GNFs has been proven for binary hydride, MgH_2 [6]. The optimum concentration of GNFs on $LiAlH_4/LiMg(AlH_4)_3$ for the present study has been found to be 8 mol%. Our present investigation reveals that HGNFs possess superior catalytic activity than PGNFs.

The motivation behind our present investigation is to show the catalytic activity of HGNF on $LiMg(AlH_4)_3$ and $LiAlH_4$ for reducing the decomposition temperature and increasing the dehydrogenation kinetics, and hence we deduce the activation energy for initial decomposition reaction, which is comparable to that obtained by using known transition metal based catalysts (e.g. $TiCl_3$, VCl_3 etc.). We found that admixing HGNF greatly improves the desorption kinetics and decreases the decomposition temperature of both $LiMg(AlH_4)_3$ and $LiAlH_4$.

2 Experimental Method

As received $LiAlH_4$ (Aldrich, 95%) and $MgCl_2$ (Alfa Aesar, 99%) have been used without further purification. $LiAlH_4$ and $MgCl_2$ in the molar ratio 3:1 was ball-milled together with two steel balls of 12.5 mm each and one ball with 4 mm in a chrome-nickel stainless steel milling vial under argon atmosphere in a locally fabricated attritor ball-miller with ball-to-powder mass ratio 10:1. The expected reaction $3LiAlH_4 + MgCl_2 \rightarrow LiMg(AlH_4)_3 + 2LiCl$ has been found to get completed in one hour of ball-milling. All operations on the samples were done under dry argon atmosphere in a glove box to prevent reaction with moisture and oxygen in the air. The graphitic nanofibres are being synthesized in our laboratory through dissociation of hydrocarbon (acetylene/ethylene) over Ni/Fe nanoparticles catalyst in an open furnace at 650°C under flowing He and H_2 gas both with an optimized flow rate of 1500 sccm. In keeping with the known results [7, 8], we have found that morphology of GNF is dependent on the shape of the Ni/Fe nanoparticles. Whereas for faceted Ni/Fe nanoparticles helical GNF get formed and for non-faceted Ni/Fe nanoparticles, planar GNF are found to grow. Thermal decompositions of GNF admixed $LiAlH_4$ and $LiMg(AlH_4)_3$ samples were monitored using computerized pressure composition isotherm (P-C-I) measurement system supplied by Advanced Materials Corporation.

Structural characterization of the samples was carried out through XRD, Philips PW-1710 and X'Pert PRO (PANalytical) X-ray diffractometer equipped with graphite monochromator employing CuK_α radiation (λ= 1.5402Å). Exposure of the sample to atmosphere has been avoided by covering the XRD holder by fine layer of Parafilm (Pechiney plastic packing). The microstructural characterization has been done through Transmission electron Microscope (Technai, 200 kV).

3 Results and Discussions

3.1 Lithium-magnesium alanate

$LiMg(AlH_4)_3$ has been synthesized mechano-chemically through the following reaction

$$3Li(AlH_4)_3 + MgCl_2 \rightarrow LiMg(AlH_4)_3 + 2LiCl \quad (1)$$

by using a locally fabricated attritor ball-miller. The above reaction gets completed in ~1 hour of ball-milling, which gets confirmed from the X-ray diffractogram, a representative XRD profile is shown in Figure 1(a). Since peaks corresponding only to the reaction product were present in the XRD profile, it becomes evident that complete conversion of the above said chemical reaction (eq. (1)) has taken place. Figure 1(b) shows the XRD of purified (through acid treatment) helical GNF used as catalyst for our present study.

Following the known results [9], the thermal decomposition behavior of $LiMg(AlH_4)_3$ can be described as follows,

$$LiMg(AlH_4)_3 \rightarrow LiMgAlH_6 + 2Al + 3H_2 \quad (\sim 100^\circ C) \quad (2)$$

$$LiMgAlH_6 \rightarrow LiH + MgH_2 + Al + 3/2H_2 \quad (\sim 150^\circ C) \quad (3)$$

$$2MgH_2 + 3Al \rightarrow Al_3Mg_2 + 2H_2 \quad (\sim 340^\circ C) \quad (4)$$

The temperature programmed desorption (TPD) curve was monitored from room temperature to 240°C at the heating rate of 1°C/min. It has been observed from the TPD profile that the peak decomposition temperature of Eq. (2) is 105.5°C and that of Eq. (3) is 149.6°C. For 8 mol% HGNF admixed $LiMg(AlH_4)_3$, Eq. (2) occurs at the time of catalyst admixing. However, for the heating rate of 1°C/min, the peak desorption temperature for 8 mol% HGNF admixed $LiMg(AlH_4)_3$ corresponds to Eq. (3) has been lowered from 149.6°C to 127.9°C**.** A representative TPD curve is shown in Figures 2(a) and 2(b).

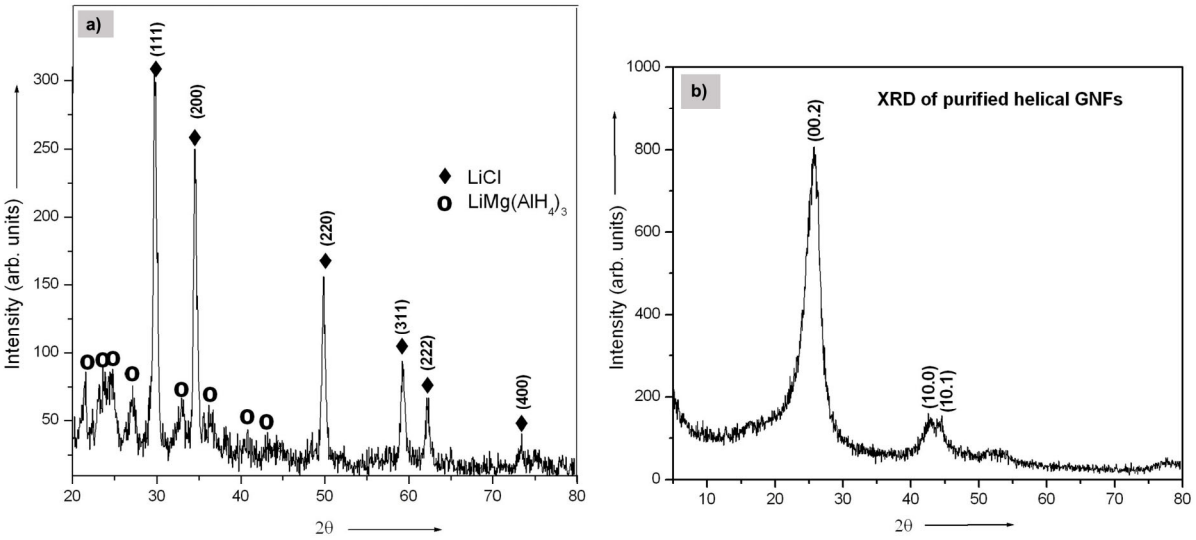

Figure 1: X-ray diffractorgram of a) as synthesized $LiMg(AlH_4)_3$ + 2LiCl mixture and b) purified GNFs used as catalyst.

The LiCl in the reaction product acts as a dead weight and it does not take part in the above mentioned reactions. Purification of LiCl from $LiMg(AlH_4)_3$ + 2LiCl mixture is a tedious and time consuming process which may also leads to the decomposition of $LiMg(AlH_4)_3$. Therefore purification may not be of help for practical applications [10]. In order to calculate

the rate constant of reaction and hence to calculate the activation energy, a comparative study without considering the dead weight of LiCl has been made. A representative TPD curve of $LiMg(AlH_4)_3$ without considering the weight of LiCl is shown in Figure 2 (a), curve (B). We have found that the TPD curve corresponding to 8 mol% HGNF admixed $LiMg(AlH_4)_3$ sample (Figure 2(a), curve (D)) shows an enhanced desorption kinetics than that of PGNF admixed $LiMg(AlH_4)_3$ (Figure 2(a), curve (C)) but with a loss in hydrogen capacity of ~4 wt.%. This suggests that the $LiMg(AlH_4)_3$ phase decomposes and liberates hydrogen during HGNF admixing through ball-milling.

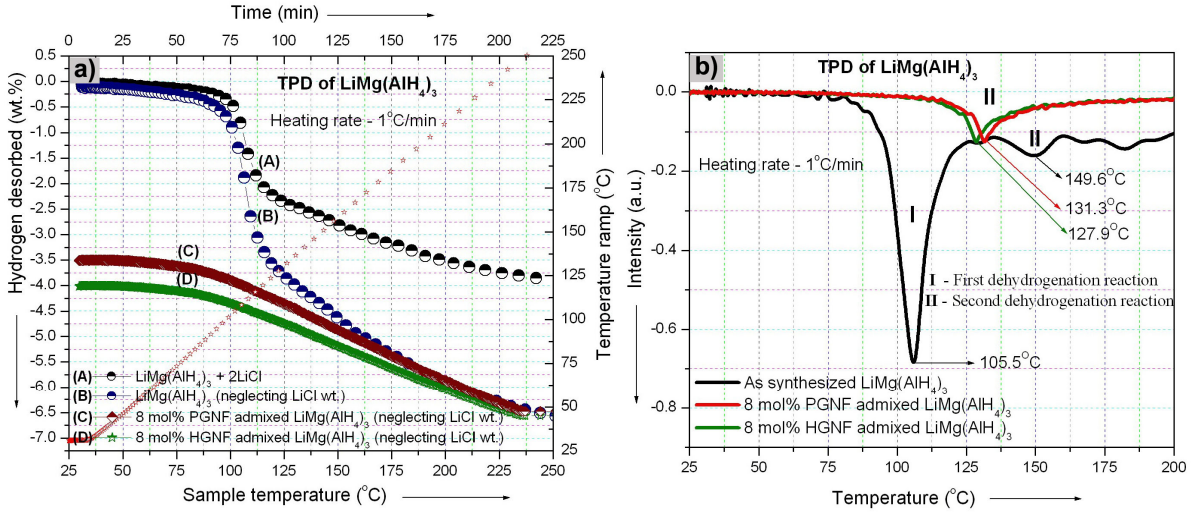

Figure 2: Temperature Programmed Desorption (TPD) a) with respect to hydrogen desorbed (doted curve represents the temperature ramp profile) and b) with respect to peak desorption temperature.

Table 1: Difference between HGNF and PGNF used as catalyst.

Types of GNFs	Catalyst used for synthesis	Surface area (m^2/g)	Average diameter (nm)
Helical GNF (HGNF)	Faceted Ni nanoparticle	125	150
Planar GNF (PGNF)	Spherical Ni nanoparticle	109	200

Representative TEM micrographs of HGNF and PGNF are shown in Figures 3(a) and 3(b).

In order to find the catalytic effect of HGNF in decreasing the activation energy of $LiMg(AlH_4)_3$, we proceed to evaluate this energy from the Arrhenius plot, as described by Janot et al. [11].

The activation energy of desorption process is estimated by plotting the maximum reaction rate (k) as a function of the temperature (T). The reaction rates are obtained from the slopes of the tangents at the inflection points of desorption kinetic curves.

The maximum reaction rates (k) of Eq. (2) at different temperature were calculated from desorption kinetic curves as shown in Figure 4(a). Since the inclusion of LiCl mass in the

kinetic measurement of $LiMg(AlH_4)_3$ affects the rate constant value, we have not considered the weight of LiCl for desorption kinetic measurements.

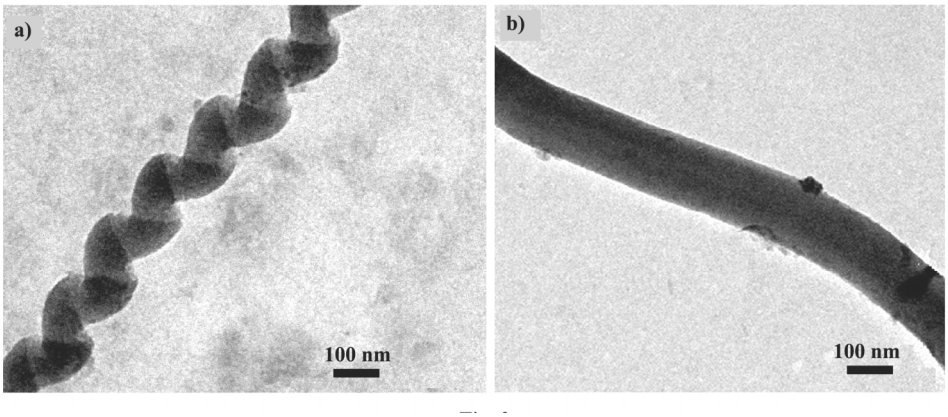

Figure 3: TEM micrograph of GNF a) helical morphology GNF (HGNF) and b) planar morphology GNF (PGNF) (difference between HGNFs and PGNFs are given in table 1).

Quantitative estimation of kinetic barrier was then carried out by the determination of the activation energy (*Ea*) from the well known Arrhenius equation of the form

$$\ln(k) = -Ea/RT + \ln(A) \quad (5)$$

By plotting ln *k* versus *1/T*, *Ea* can be extracted from the linear slope. Figure 4(b) shows the Arrhenius plot for the first-step dehydrogenation of $LiMg(AlH_4)_3$. A good linearity between ln *k* and 1/*T* is obtained with R^2 = 0.99. The activation energy (*Ea*) as calculated corresponds to ~66 kJ/mol.

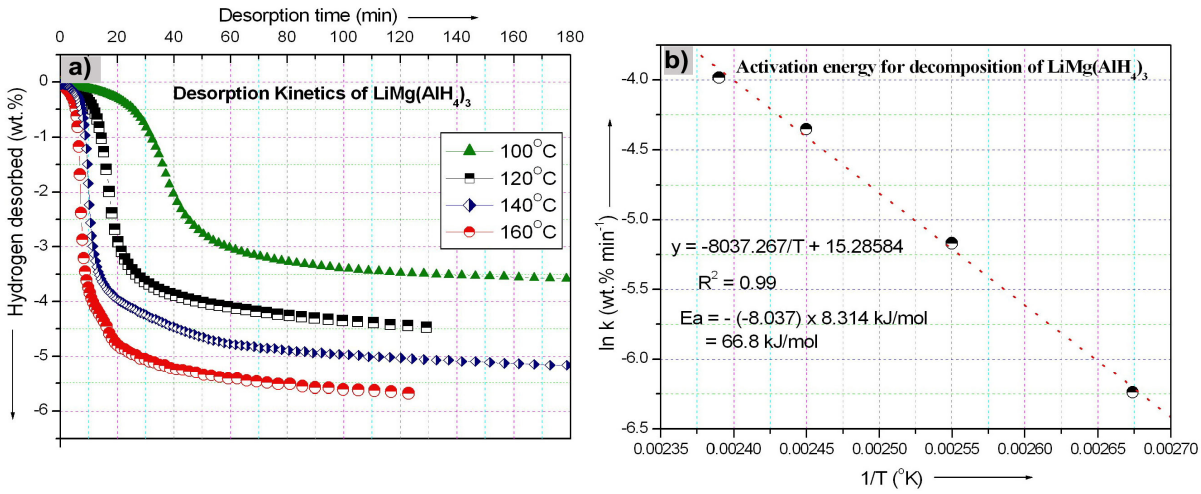

Figure 4: a). desorption kinetic curve of $LiMg(AlH_4)_3$ at different temperatures b) plot of ln *k* vs 1/T for $LiMg(AlH_4)_3$.

3.2 Lithium alanate

In general, $LiAlH_4$ has three-stage decomposition, as represented by the following equations:

$$3LiAlH_4 \rightarrow Li_3AlH_6 + 2Al + 3H_2 \quad (\sim 150°C) \quad (6)$$

$$Li_3AlH_6 \rightarrow 3LiH + Al + 3/2H_2 \quad (\sim 180°C) \quad (7)$$

$$3LiH + 3Al \rightarrow 3LiAl + 3/2H_2 \quad (>400°C) \quad (8)$$

Eq. (6) approximately releases 5.3 wt.% hydrogen and eq. (7) and eq. (8) both release approximately 2.6 wt.% H_2 each. However, eq. (8) is generally not considered usable because it involves very high temperature for decomposition [12].

The catalyst admixing was carried out through ball-milling for 15 min, using the same ballmiller as mentioned above. The optimum molar concentration of GNFs for $LiAlH_4$ has been found to be 8 mol%. Lower concentration of GNF does not produce enhancement in kinetics similar to that from 8 mol% and increasing the molar concentration of GNFs further leads to the decrease in hydrogen storage capacity. For comparison, the dehydrogenation behavior of one hour ball-milled $LiAlH_4$ is also compared with 8 mol% HGNF admixed $LiAlH_4$ sample. Figures 5(a) and 5(b) show representative TPD profile of $LiAlH_4$ sample. There is a loss of ~2 wt.% H_2 in the 8 mol% GNFs admixed $LiAlH_4$ sample, this was estimated by comparing the TPD profile of the ball-milled and pristine $LiAlH_4$.

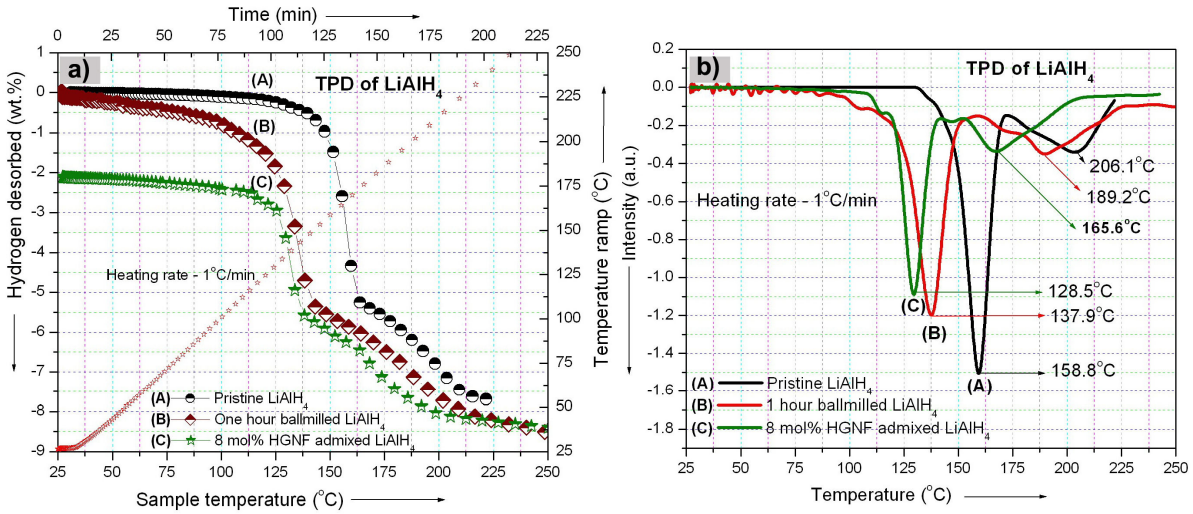

Figure 5: Temperature programmed desorption (TPD) of $LiAlH_4$ a) with respect to hydrogen desorbed (doted curve represents the temperature ramp profile) and b) with respect to peak desorption temperature.

A noticeable feature shown in Figure 5(b) is that for the heating rate of 1ºC/min, the peak desorption temperature for 8 mol% HGNF admixed $LiAlH_4$ sample corresponds to Eq. (6) has been lowered from 158.8°C to 128.5°C and as that for reaction corresponding to Eq. (7) has been lowered from 206.1°C to 165.5°C. It may be mentioned that the effect of increase in the interface area which will result due to ball-milling, will not be able to explain the significant decrease in desorption temperature. Apparently it is the catalytic effect of GNF which leads

to decrease of desorption temperature. The exact role of GNF in improving the dehydrogenation behavior of complex hydride is exactly not known. Based on the known results on the catalytic effect of carbon nanostructures in complex hydrides, it is believed that higher the curvature of catalyst, higher is the catalytic activity. The carbon nanostructures as for example fullerenes have higher curvature than CNTs or graphenes. Hence fullerene has higher catalytic activity [3]. In contrast to PGNF, HGNF has curved surface. Therefore it will have higher catalytic activity than PGNF.

When admixing 8 mol% HGNF with $LiAlH_4$, desorption kinetics of $LiAlH_4$ gets significantly improved. The effect of HGNFs on $LiAlH_4$ is estimated from the activation energy value (*Ea*) calculated for pristine $LiAlH_4$ and 8 mol% HGNF admixed with $LiAlH_4$. In order to find the activation energy of pristine $LiAlH_4$ using Arrhenius relation, the desorption kinetics of pristine $LiAlH_4$ at different temperatures was evaluated. A representative desorption kinetics plot of pristine $LiAlH_4$ at different temperatures and its ln *k* vs *1/T* plot is shown in Figures 6(a) and 6(b), respectively. A good linearity between ln *k* and 1/*T* is obtained with R^2 = 0.99. The activation energy calculated for pristine $LiAlH_4$ is 107 kJ/mol. This value is comparable to the recently reported value of 102 kJ/mol by Blanchard et al.[13].

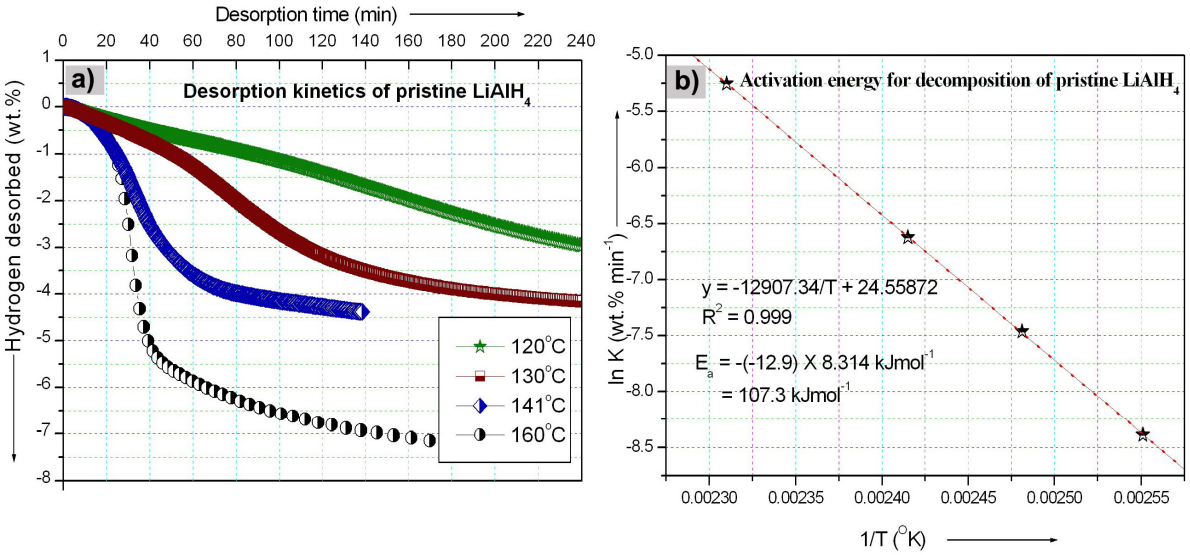

Figure 6: a) dehydrogenation kinetics of pristine $LiAlH_4$ at different temperatures b) plot of ln *k* vs 1/T for calculation of activation energy for reaction correspond to Eq. (5).

The activation energy (*Ea*) calculated for 8 mol% HGNF admixed $LiAlH_4$ is ~68 kJ/mol. This is slightly higher (~16 kJ/mol) than the reported activation energy value (42.6 kJ/mol) of $LiAlH_4$ with transition metal based catalysts (Chen et al, ref [14]). However, there exist some controversial results regarding the activation energy for $LiAlH_4$. For 2 mol% TiC_3.1/3($AlCl_3$) catalyzed $LiAlH_4$, the activation energy calculated by Blanchard et al. [13] is 90 kJ/mol, which is much higher than the estimate value of 42.6 kJ/mol, reported by Chen et al [14]. The dehydrogenation kinetics of 8 mol% HGNF admixed $LiAlH_4$ at different temperatures and its ln *k* vs *1/T* plot is shown in Figures 7(a) and 7(b), respectively.

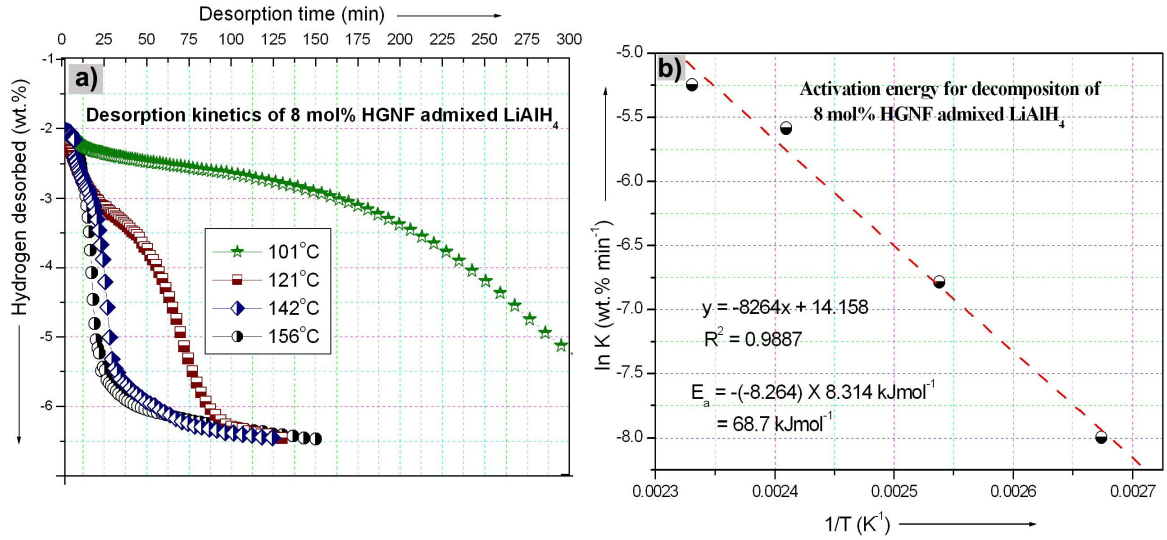

Figure 7: a) dehydrogenation kinetics of 8 mol% HGNF admixed $LiAlH_4$ at various temperatures b) plot of ln *k* vs 1/T for 8 mol% HGNF admixed $LiAlH_4$.

Thus the admixing of 8 mol% HGNF helps to decrease the activation energy for the decomposition of $LiAlH_4$ by 36% (for pristine $LiAlH_4$ calculated *Ea* is 107 kJ/mol, and for 8 mol% HGNF admixed $LiAlH_4$, it is ~68 kJ/mol.

4 Conclusions

The catalytic effect of graphitic nanofibres on $LiMg(AlH_4)_3$ and $LiAlH_4$ has been studied. The dehydrogenation behavior of the samples was studied through TPD and desorption kinetic measurements. We have found that helical morphology of GNF improves the dehydrogenation behavior of both $LiMg(AlH_4)_3$ and $LiAlH_4$. The lowering of desorption temperature for HGNF admixed $LiMg(AlH_4)_3$ as compared to its pristine phase is from 105°C to ~70°C. Whereas the lowering of desorption temperature of HGNF admixed $LiAlH_4$ as compared to pristine $LiAlH_4$ phase is from 159°C to 128°C. However, the decomposition rate of $LiMg(AlH_4)_3$ in the presence of HGNF is higher than that for $LiAlH_4$. The activation energy calculated for the first step decomposition of HGNF admixed $LiAlH_4$ is ~68 $kJmol^{-1}$, whereas that for pristine $LiAlH_4$, it is ~107 kJ/mol. The activation energy calculated for as synthesized $LiMg(AlH_4)_3$ is ~66 kJ/mol. Since the first step decomposition of $LiMg(AlH_4)_3$ occurs during GNF admixing, the activation energy for initial decomposition of GNF admixed $LiMg(AlH_4)_3$ could not be estimated.

Acknowledgement

The authors would like to thank Prof. T.N. Veziroglu, Prof. C.N.R. Rao, Prof. S.K. Joshi, Prof. S.P. Thyagarajan and Prof. D.P. Singh (VC:BHU) for their encouragement and support. Financial support from the Ministry of New and Renewable Energy, the University Grants Commission, DST: Nano Science Technology Unit (BHU) and the Council of Scientific and Industrial Research are thankfully acknowledged.

References

[1] Bogdanovic B, Schwickardi M. Ti-doped alkali metal aluminium hydrides as potential novel reversible hydrogen storage materials. J. Alloys Compd. 1997;253-254:1-9.

[2] Srinivasan S, Escobar D, Goswami Y, Stefanakos E. Effects of catalysts doping on the thermal decomposition behavior of $Zn(BH_4)_2$. Int. J Hydrogen Energy. 2008;33:2268 - 72.

[3] Berseth PA, Harter AG, Zidan R, Blomqvist A, Araujo CM, Scheicher RH, Ahuja R, Jena P. Carbon Nanomaterials as Catalysts for Hydrogen Uptake and Release in $NaAlH_4$. Nano Lett. 2009;9:1501-05.

[4] Serp P, Corrias M, Kalck P. Carbon nanotubes and nanofibers in catalysis. Applied Catalysis A: General. 2003;253:337-58.

[5] Kumar LH, Viswanathan B, Murthy SS. Dehydriding behaviour of $LiAlH_4$-the catalytic role of carbon nanofibres. Int. J Hydrogen Energy. 2008;33:366-73.

[6] Lillo-Rodenas MA, Guo ZX, Aguey-Zinsou KF, Cazorla-Amoros D, Linares-Solano A. Effects of different carbon materials on MgH_2 decomposition. Carbon 2008;46:126-37.

[7] Park C, Baker RTK. Catalytic Behavior of Graphite Nanofiber Supported Nickel Particles. 2. The Influence of the Nanofiber Structure. J. Phys. Chem. B 1998;102:5168-77.

[8] Blank VD, Alshevskiy YL, Zaitsev AI, Kazennov NV, Perezhogin IA, Kulnitskiy BA. Structure and phase composition of a catalyst for carbon nanofiber formation. Scripta Mat. 2006;55:1035-38.

[9] Tang X, Opalka SM, Laube BL, Wu FJ, Strickler JR, Anton DL. Hydrogen storage properties of Na–Li–Mg–Al–H complex hydrides. J. Alloys Compd. 2007;446-447:228-31.

[10] Hudson MSL, Pukazhselvan D, Sheeja GI, Srivastava ON. Studies on synthesis and dehydrogenation behavior of magnesium alanate and magnesium–sodium alanate mixture. Int. J Hydrogen Energy. 2007;32:4933-38.

[11] Janot R, Eymery JB, Tarascon JM. Investigation of the processes for reversible hydrogen storage in the Li–Mg–N–H system. Journal of Power Sources. 2007;164:496-502.

[12] Vittetoe AW, Niemann MU, Srinivasan SS, McGrath K, Kumar A, Goswami DY, Stefanakos EK, Thomas S. Destabilization of $LiAlH_4$ by nanocrystalline MgH_2. Int. J Hydrogen Energy. 2009;34:2333-39.

[13] Blanchard D, Brinks HW, Hauback BC, Norby P, Muller J. Isothermal decomposition of $LiAlD_4$ with and without additives. J. Alloys Compd. 2005;404-406:743-47.

[14] Chen J, Kuriyama N, Xu Q, Takeshita HT, Sakai T. Reversible Hydrogen Storage via Titanium-Catalyzed $LiAlH_4$ and Li_3AlH_6. J. Phys. Chem. B. 2001;105:11214-20.

Hydrolysis of Sodium Borohydride for Hydrogen Generation

V. Minkina, **S. Shabunya**, **V. Kalinin**, Heat & Mass Transfer Institute of NAS of Belarus
H. Yoshida, Kyoto University, Japan

1 Introduction

Hydrogen production in reaction of alkali metal borohydride with water is actively studied to develop hydrogen generators for fuel cells. Sodium borohydride $NaBH_4$ is the most promising one from the point of view of mass content of hydrogen storage and safety (non-flammable and solution is non-toxic). The aqueous solutions of $NaBH_4$ may be used for high purity hydrogen generation (99.99%). The reaction of hydrolysis

$$NaBH_4 + 2\,H_2O = 4\,H_2 + NaBO_2 - 212\ kJ/mole$$

is accompanied by heat release calculated by components enthalpies [1]:

H_{NaBH_4} = -191.84 kJ/mole, H_{NaBO_2} = -975.71, $H_{H_2O(liquid)}$ = -285.83 kJ/mole.

To develop hydrogen generator using $NaBH_4$ hydrolysis some decisions have to be accepted to determine basic features of the design.

2 Type and Working Volume of Reactor (single-pass or circulating)

The choice of either single-pass or circulation type reactor is one of the principal ones. Prima facie, single-pass system is more simple, $NaBH_4$ solution is supplied to reactor, and the yields are H_2 and a solution of sodium metaborate $NaBO_2$. Controlling solution flow rate, the production capacity of generator can be changed. In the car we are used to the fact that an increase in the fuel supply immediately leads to an increase in engine power. The catalytic hydrolysis of $NaBH_4$ is rather a quick process, but its rate is much less than the combustion one. This means that either the gradual change of generator efficiency must be accepted, or the receiver of sufficient volume must be set after the reactor in hydrogen line to match the rapid changes in the productivity desired by user with a slower response of reactor. The more the hydrogen mass in the receiver is, the weaker the limitations on reactor performance are. Inclusion of receiver into the working scheme is the first argument in favor of the circulation scheme.

Maximum capacity of the generator W_{max} (in moles of hydrogen) determines the ratio between water flow Q_{max} (in liters) and molality concentration $\mathcal{M}_{NaBH4}$ of working solution:

$$4Q_{max}\mathcal{M}_{NaBH_4} = W_{max}\,.$$

At maximum generator productivity the contact time of solution with catalyst will be the smallest and expressed in terms of volume V_{cat} of the catalytic unit of the reactor:

$$\tau_{min} = V_{cat}/Q_{max} = 4V_{cat}\mathcal{M}_{NaBH_4}/W_{max}\,.$$

This expression is equally applicable to single-pass reactor and circulating scheme; there is difference in flow through catalytic unit. In the first case fresh working solution is at inlet, and $NaBO_2$ solution has to be at outlet for single pass. The front part of catalytic unit is working with a concentrated solution, the output - with the lean one. In circulating scheme solution repeatedly passes through the catalytic unit, the velocity of solution flow and mass transfer processes are more intensive and the entire catalyst is working under approximately the same conditions. In light of these considerations the following benefits circulation schemes can be expected: thermal regime of catalyst is more uniform, it gets easier to control the ultimate hydrolysis rate, as a result, the less efficient catalyst can be used and / or the size of catalytic unit can be decreased. Circulating regime presumes cyclic repetition of three stages: filling the reactor with fresh working solution, the circulation of solution through catalytic unit and draining of $NaBO_2$ solution after the completion of hydrolysis.
Let's estimate the volume of catalytic unit required for the generator with H_2 production W_{max} = 180 mole/hr ≈ 4 Nm^3/hr and working solution with $\mathcal{M}_{NaBH4}$= 5 mole/l. Then Q_{max} = 0.15 l/min, i.e. required volume of catalytic unit has to be equal to 0.15 liters to ensure contact time of solution with catalyst about one minute. Time required for complete solution hydrolysis depends on catalyst activity, the total surface of catalytic centers, the working temperature and the efficiency of mass transfer processes.

3 Thermal Regime of Reactor and Catalyst Efficiency

Quite a lot of publications [2-7] are devoted to the study of the fine powder catalysts efficiency. Such catalysts are designed for disposable fuel cells, while they are not applicable to hydrogen generators. Discussed catalytic unit can be implemented as a filling of pellets, or a certain frame (a set of grids, highly porous ceramics) whose surface is covered with a catalyst. When filtering the solution through such structure the hydrolysis processes are controlled by the heterogeneous mechanism on the catalyst surface, and homogeneous one in working solution. Comparing catalyst efficiency it is considered that the more efficient catalyst provides higher hydrolysis rate at the same temperature and identical area of catalytic surface. At low hydrolysis rates (low temperature) the properties of catalytic material become important. At high temperatures the mass-exchange processes play the main role; they are controlled by the structure of porous medium and filtration velocity. Intensive hydrogen release and evaporation (boiling) of water further complicate the running processes. One should take into consideration that at high temperatures the homogeneous hydrolysis is also highly accelerated. It might be possible that when the processes of mass

transfer running in catalytic unit are rationally organized, the simple catalysts could be used instead of highly efficient ones. We have tested three kinds of granular catalysts, which are traditionally used in the processes of partial oxidation of hydrocarbons. The characteristics of these catalysts are collected in table 1 below.

Table 1: The characteristics of the used catalysts.

Catalyst	Content	Carrier	Form	Dimensions
Pd	1%	Al_2O_3	cylinder	∅ 3.2 mm, h=3.7 mm
Pt	0.5%	Al_2O_3	cylinder	∅ 3.2 mm, h=3.6 mm
Rh	0.1%	Al_2O_3	ball	∅ 5 mm

The comparison of these catalysts shown in Figure 1 was conducted at room temperature. It has merely technical sense, because at the same bulk amount of grains the catalyst content, shape and mean size of the grains are not identical. The process of hydrolysis is highly accelerated by temperature rise, while intensive evaporation of water affects limiting values of working temperature. According to [8] the actual range of operating temperatures will be 120-140°C. Though we could not conduct these experiments at this temperature range, the experimental results for the "slowest" catalyst (Rh) of three ones obtained at three temperatures, presented in Figure 2, can be used for qualitative assessment of hydrolysis acceleration rate. Based on these data the value of resident time equal to 1 minute accepted above would be sufficient to complete hydrolysis, when operating temperature is about 120°C. There is no sense in using the operating temperature higher than the required one, because it increases the amount of water vapor in outlet gas flow. In any case, the design of generator should contain cooling device for vapor condensation and water recycling. Uncontrolled water loss will result in increase of metaborate concentration and risk of its deposition on catalyst and tubes. Another problem caused by temperature increase might be generation of toxic gas diborane, whose formation is probable in conditions of high temperature hydrolysis at significant scarcity of water.

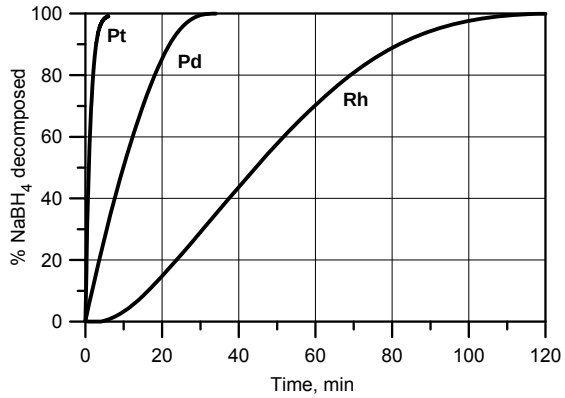

Figure 1: The rate of catalytic hydrolysis of $NaBH_4$ solution at 25°C.

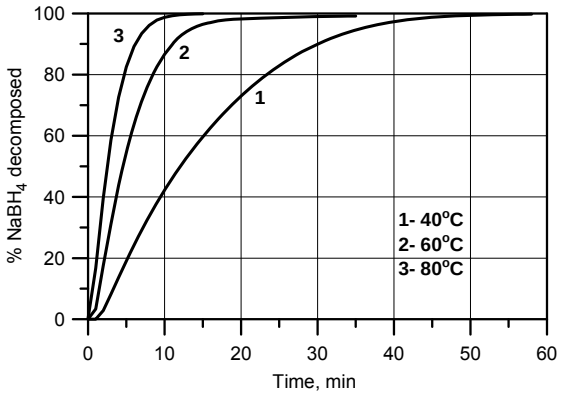

Figure 2: Effect of temperature on the rate of catalytic hydrolysis of $NaBH_4$ solution.

4 Concentration of Working Solution

The concentration of working solution should not be below the certain minimum $\mathcal{M}_{NaBH4,min}$, which maintains the working temperature T_{work}. This value can be estimated by condition of thermal balance:

$$\mathcal{M}^{min}_{NaBH_4} H_{Hyd} = (1+\varepsilon) c_{H_2O} (T_{work} - T_{in})$$

where H_{Hyd} is the heat of hydrolysis per one mole of $NaBH_4$, $c_{H2O} \approx 4.2$ kJ/kg – specific heat of water, T_{in} is the temperature of solution at reactor inlet and ε is parameter determining the portion of thermal losses. If $\varepsilon = 0.5$ and $T_{work} - T_{in} = 100$, $\mathcal{M}_{NaBH4,min} \approx 3$ mole/l. The upper molality concentration limit $\mathcal{M}_{NaBH4,max}$ is determined by solubility of generated $NaBO_2$. In order to avoid the deposition of solid metaborate from solution in catalytic unit and in tubes connecting the reactor and collection vessel, outlet concentration of $NaBO_2$ has to be lower than the solubility limit at temperature T_{out}. For example, if $T_{out} = 80$ °C the limiting value is $\mathcal{M}_{NaBH4,max\_80} \approx 12.3$ mole/l [9], and calculated value

$$\mathcal{M}^{max}_{NaBH_4} \text{ is } \frac{55.5\mathcal{M}^{max\_80}_{NaBO_2}}{55.5 + 2\mathcal{M}^{max\_80}_{NaBO_2}} \approx 8.5 \text{ mole/l.}$$

Within the range $\mathcal{M}_{NaBH4,min} - \mathcal{M}_{NaBH4,max}$ there is freedom of choice to meet additional optimality conditions, for example, minimum amount of water used, or absence of $NaBO_2$ condensation at a given temperature, etc.

5 Start-up and Shut-down of Generator

The problem of generator start-up can be solved by incorporating heater in the path of solution supply to catalytic unit. This solution is applicable to both types of reactors; it looks quite simple and, what is the most important, controllable. In this case the estimated value of start-up is about few minutes. In case of very effective catalyst the problem of cold start could be solved by catalyst self-heating. At usage of single-pass scheme the task is somewhat simpler than in circulating case, when preheating of catalyst and all elements is required to ensure the circulation of solution. Moreover the implementation of self-heating regime requires the usage of the most effective catalyst and working solution with concentration close to the maximum value. Nevertheless, even in such case at low temperatures (say about 0°C) start-up may fail. In circulating scheme the process of self-heating is additionally hampered by necessity to heat the catalyst and all elements ensuring the circulation of solution. Currently, the forced preheating at process start-up looks more preferable, but usage of efficient catalysts can significantly decreases the threshold of start temperature. At generator shut-down it is necessary to complete the solution hydrolysis in catalytic unit and to release (or even wash) it from $NaBO_2$ solution. In the circulation scheme, such operations are the parts of the natural cycle, for single-pass reactor it is an additional element of design.

6 Preparation and Storage of Working Solution

The problem of working solution preparation has two ways: preparation in advance and storage until usage, or dosing preparation just before hydrolysis. In first case the ready made “fuel” is loaded into the generator, while in “fuel tank” hydrolysis process runs without catalyst. This feature caused the problem of stabilization and storage of borohydride solutions, which is complicated with temperature growing. The increase of solution pH by adding alkali inhibits the hydrolysis. Experimental results of stabilization obtained at 25 и 40 °C are illustrated in Figure 3.

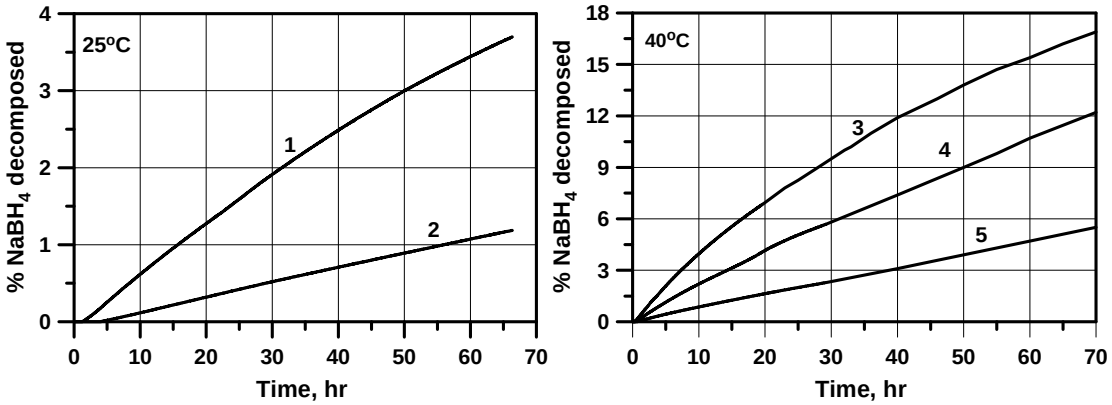

Figure 3: Effect of NaOH on hydrolysis rate for molar composition of solution $NaBH_4$/ H_2O = 1/9. C_{NaOH} = 1 wt. % (1), 2 wt. % (2), 3 wt. % (3), 4 wt. % (4), 5 wt. % (5).

Too high concentration of NaOH is required (> 3 wt. %) to maintain low rates of hydrolysis at temperature above 40 °C.

Excluding the usage of preliminary prepared working solutions can solve stability problem, but requires additional unit to prepare small portions of solution with generator running. Dosing hygroscopic powder $NaBH_4$ raises some technical difficulties, but they do not seem insurmountable. Immediate preparation of the solution just before hydrolysis is easier combined with circulating scheme of generator, where the dissolution of $NaBH_4$ may complete in circulation loop, where the temperature is high.

References

[1] NIST Chemical WebBook, http://webbook.nist.gov/chemistry

[2] Amendola S.C., Sharp-Goldman S.L., Janjua M.S. et al. An ultrasafe hydrogen generator: aqueous, alkaline borohydride solutions and Ru catalyst, J. of J. Power Sources, 2000, Vol. 85, Pp. 186-189.

[3] Rangel C.M., B. Bonnetot, Minkina V. et al. Production of hydrogen by borohydrides: in search of low cost non-noble efficient catalysts, Proceedings, WHTC, 4-9 November 2007, Montecatini Terme, Italy.

[4] Suda S., Sun Y.-M., Liu B.-H. et al. Catalytic generation of hydrogen by applying fluarinated-metal hydrides as catalysts, Appl. Phys., 2001, A 72, Pp. 209-212.

[5] Kojima Y., Hydrogen Storage and Generation Using Sodium Borohydride, R&D Review of Toyota CRDL, 2005, Vol. 40, No 2, Pp. 31-35.

[6] Ye W., Zhang H.M., Xu D.Y. et al. Cobalt boride catalysts for hydrogen generation from alkaline NaBH4 solution, J. Power Sources, 2007, Vol. 164, No 2, Pp. 544-548.

[7] Garron A., Bennici S. and Auroux A., In situ generated catalysts for $NaBH_4$ hydrolysis studied by liquid-phase calorimetry: Influence of the nature of the metal, Applied Catalysis A: General, 2010, Vol. 378, Issue 1, Pp.90-95

[8] Kojima Y., Suzuki K.-I., Fukumoto K. et al. Development of 10 kW-scale hydrogen generator using chemical hydride, J. of J. Power Sources, 2004, Vol. 125, Pp. 22-26.

[9] Adams R.M., Siedel A.R., in Boron, Metallo-boron compounds and Boranes, R.M. Adams Ed, Interscience Publisher, New-York, 1964, Pp.380-90.

Round Robin Hydrogen Sorption Performance Characterisation of Carbon Adsorbants, Complex and Metal Hydrides

P. Moretto, **C. Zlotea**, **E. Weidner**, Institute for Energy, Joint Research Centre of the European Commission

1 Introduction

In the frame of the European funded project NESSHY (Novel Efficient Solid State Storage for Hydrogen), three inter-laboratory comparative measurement campaigns have been undertaken for assessing the hydrogen physi- and chemi-sorption behaviour of storage materials. These Round Robin Testing (RRT) exercises aimed, in the absence of specific measuring standards, to guarantee that the performance parameters of novel hydrogen storage materials as measured in different laboratories are comparable and to identify possible weaknesses in the measurement steps. The overarching objective is to contribute with this work to the data harmonisation and the development of testing protocols for accurately and independently assessing the performance, safety and life cycle stability of hydrogen solid-state materials. This could ultimately serve future codes drafting and standardisation needs in the field.

Very few examples of RRT exercises in the hydrogen sorption field have been reported in the literature. Some RRT's have involved too few partners and had a limited scope, for example the interlaboratory comparison reported by C. Ahn et al. at the 2005 Annual Merit Review Proceedings of the DoE [1]. To our knowledge the RRT exercise has never been published. Some RRT exercises have been organised in Japan to validate the Japanese sorption standards issued by the Japanese Standard Association [2]. Also the results of these RRT's have not been published. A record of this can be found however in an article specifically on the accuracy of gas phase sorption measurements by Wang and Suda [3]. The RRT exercises focussed on classic metal hydrides such as $LaNi_5$ and the compared experiments used mild experimental conditions in term of temperatures and pressures.

The RRT exercises reported here have been organised in a formal way (see next section) and the material choices has taken into account the recent developments in the hydrogen solid-state storage field. We have not been able to identify any previous RRT specifically dedicated to the assessment of hydrogen sorption performances of the three materials chosen for this study, what brings to conclude that these RRT exercises are the first ever formally organised in the world.

2 The NESSHY Round Robin Test Exercises: Materials, Protocol and Organisation

One round robin testing exercise focused on adsorption capacity measurements on a carbon based material. The other two testing campaigns were dedicated to thermodynamic and kinetic properties measurements on alanate- and magnesium-based absorbents. A

significant number of laboratories, beyond the NESSHY European partners, participated in these exercises, including key, reputable international experimental facilities.

Table 1 gives an overview of the RRT's exercises, with materials, participants and experimental campaigns.

Table 1: Overview of the three Round Robin Tests.

Material	**Microporous carbon molecular sieve TAKEDA 4A**	**$NaAlH_4$ with 4% $CeCl_3$ additive**	**MgH_2 with 5% transition metals additives**
Participants	China: GRINM, France: Institut Néel, CNRS (2 laboratories) Germany: IFW Dresden, MPI für Metallforschung. Greece: Demokritos. Eur. Commission: JRC-IE Spain: University of Alicante (2 laboratories). UK: Johnson Matthey, University of Birmingham, University of Nottingham, University of Salford. USA: SwRI	China: GRINM. Germany: KIT-INR, IFW Dresden, GKSS European Commission: JRC-IE Norway: IFE. Swiss: EMPA. UK: Johnson Matthey. USA: SwRI.	China: GRINM, France: CNRS(3 laboratories) Germany: IFW Dresden, GKSS. Japan: AIST Eur. Commission: JRC-IE. Norway: IFE. Swiss: EMPA. Turkey: METU. UK: Johnson Matthey, University of Salford. USA: University of Nevada, JPL.
Experimental campaign	pcT isotherm absorption and desorption curves at 77 K (-193ºC) and room temperature ~ 288 K (15-20ºC).	pcT isotherm absorption and desorption curves at 298 K (125ºC) and 313 K (140ºC) temperatures.	pcT isotherm absorption and desorption curves at 553 K (280ºC) and 593 K (320ºC) temperatures.
		Absorption isotherm kinetic curves at 298 K (125ºC) and 323 K (150ºC).	Ab- and de-sorption isotherm kinetic curves at 523 (250ºC) and 573 (300ºC).
	Isostherical heat of absorption (optional)	Enthalpy of formation of $NaAlH_4$ and Na_3AlH_6	Enthalpy of formation of MgH_2

For each of the three RRT exercises a specific protocol has been prepared by a group of experts, defining the experiments to be performed, the material preparation required (outgassing, activation, etc.) and the data to be reported. The RRT materials have been carefully characterised to avoid sample-to-sample differences, to minimise handling and transport deterioration, and stability during hydrogenation. When the number of reporting participants was allowing it, the data has been analysed according to the ASTM standard setting a methodology for interlaboratory study evaluation [4]. The original length of 9 months for the performance of each RRTexercise had to be extended to more than one year, to accommodate delays of some participants.

3 Results and Preliminary Conclusions

It is not possible to give a complete report of all the achieved results. In the following only some selected results for each of the three RRT's are given, focussing on thermodynamic properties. The kinetics aspects will be published later.

3.1 RRT on physi-sorption (microporous carbon molecular sieve)

The results of this RRT exercise has been published in [5]. We limit here to present its final conclusions. From the detailed analysis of the experimental parameters of each participants, different types of error could be identified: 1) procedural errors such as gas leakage, measurement conditions not allowing for thermodynamic equilibrium and choice of the real equation of gases, 2) operator errors, such as low purity of hydrogen gas and incorrect measured or assumed dry mass, 3) calibration errors such as buoyancy evaluation for gravimetry, reactor and incorrect sample volume determination for volumetry, 4) poor equipment design which causes low accuracy of measurements.

Based on this, the following measurement recommendations can be proposed:

- Methodology: the choice of instrument should be a function of type, amount and geometry of the sample.
- Calibration of the volumes and determination of the gas leakage rate in order to assess the accuracy of the measurement (for example in term of uncertainty based on a value of moles of hydrogen).
- Outgassing of the sample under controlled conditions. Sometime an ultra high vacuum system is required for very small pores.
- Thorough characterisation of the sample before starting experiments.
- Controlling of the experiment in terms of equilibration time, temperature stability and gas state equation.
- Checking the repeatability of isotherms by performing more than one acquisition and always acquiring ad- and de-sorption curves.
- Analysis of the data by critical assessment of the type of isotherm, reason for hysteresis (if present) and nature of adsorption.

3.2 RRT on chemi-sorption: $NaAlH_4 + CeCl_3$

Only 9 laboratories have participated to this exercise, and very few have performed all the experiments mentioned in the measuring protocol. Therefore, it is not possible to perform a statistical analysis according to [4]. As an example of results, Figure 1 shows the absorption curves at 125°C. The pcT measurement results can be summarised as follows: the $NaAlH_4$ absorption plateau has been found between 5.0 and 6.0 MPa at 125ºC and between 6.0 and 7.5 MPa at 140ºC. For $NaAl_3H_6$ the plateau ranges between 2.5 and 4.0 MPa at 125ºC and between 4.5 and 6.0 MPa at 140ºC. The full H_2 capacity is evaluated by participants from 3.0 to 4.5 wt% (125°C).

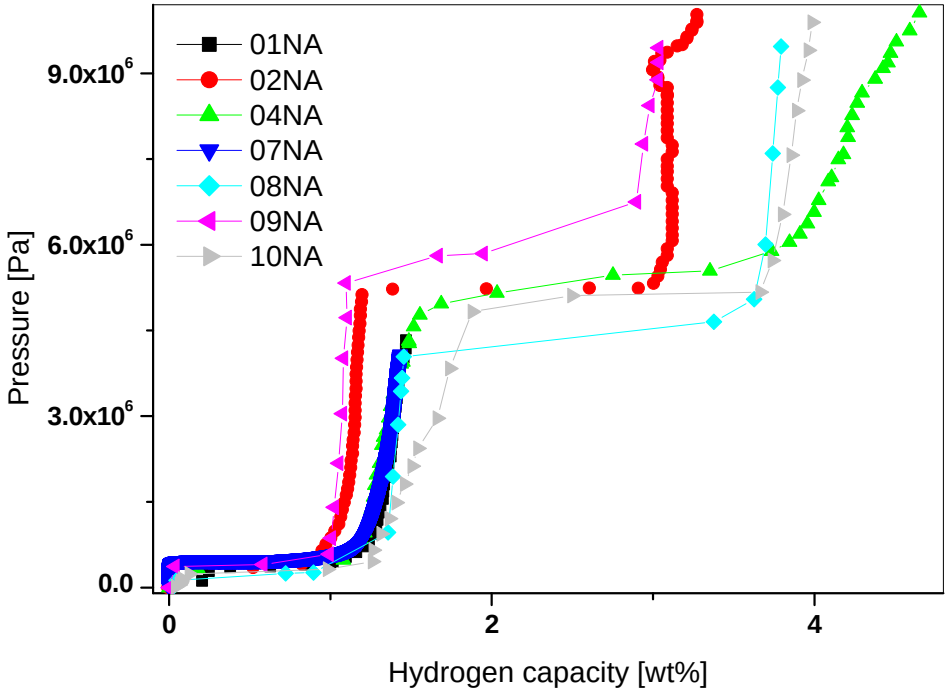

Figure 1: Absorption curves at 125°C for $NaAlH_4$ with $CeCl_3$ addictives.

The discrepancy remarked among the pcT curves of the individual participants could be cause by (a combination of) various causes such as material deterioration during distribution and/or handling, dishomogeneity of the as-produced material, not attainment of the full equilibrium during pcT acquisition, leakage. Since the material has been carefully prepared and sampled and characterised before shipping and the experiments performed, the most plausible, although not demonstrated, cause for the discrepancies is the different handling of the samples at the laboratory of each participant. In other words, partial oxidation of the material could have occurred in laboratories which show reduced capacity and higher plateau pressure.

3.3 RRT on chemi-sorption: MgH_2 + transition metals

Up to 15 laboratories have participated to this RRT exercise. The statistical analysis has not yet been completed because some participants reported very late in 2010. Figure 2 shows the absorption curves at 320°C. The MgH_2 absorption plateau has been found between 0.26 and 0.41 MPa at 320ºC. The full H_2 capacity measured at 1 MPa extend between 5.5 and 6.4 wt% and between 5.4 and 6.6 wt% respectively at 280°C and 320°C. The enthalpy of formation has been evaluated by participants in a range from -60.4 to -80.0 kJ/moleH_2 for absorption and between 60.7 and -80.3 kJ/moleH_2 in desorption.

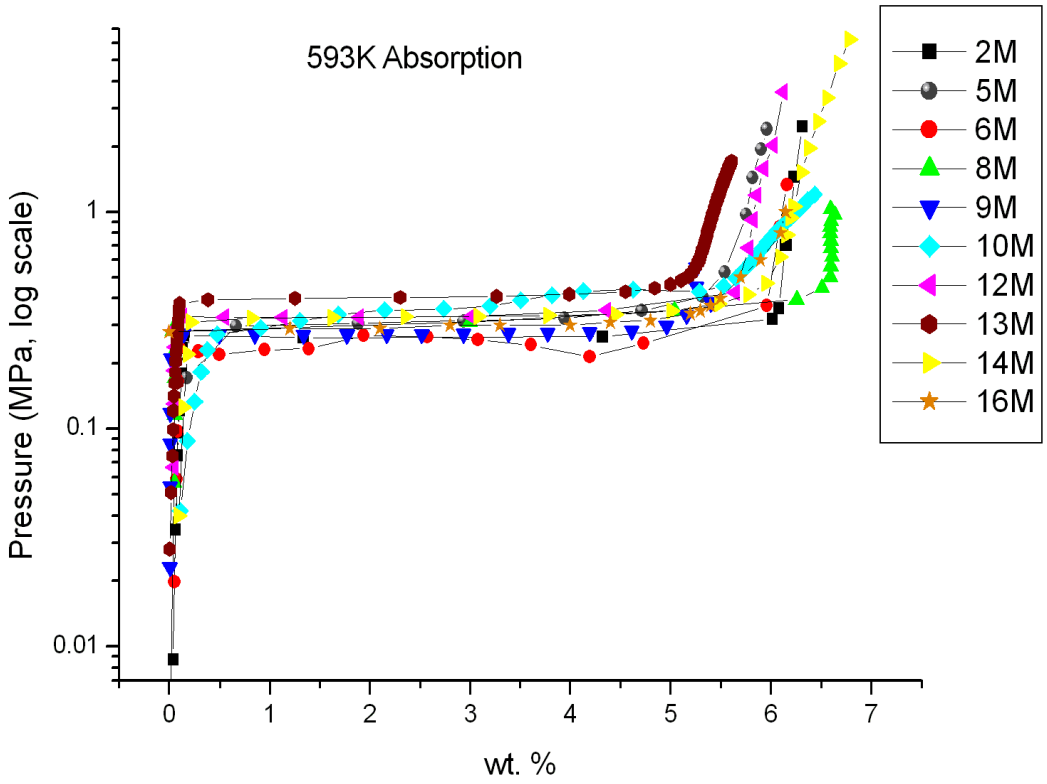

Figure 2: pcT curve of MgH2 at 593 K as measured by all participants.

The highest data dispersion occurs at higher pressure, and from the shape of many pcT curves, which do not appear vertical in the b-phase, it could be concluded that small leaks at high pressure (> 0.5 MPa) is the most frequently occurring cause of errors.

Acknowledgement

This work was conducted under the auspices of NESSHY European project. Funding by the European Commission DG Research (contract SES6-2006-518271/NESSHY) is gratefully acknowledged.

References

[1] Channing Ahn et al., Enhanced Hydrogen Dipole Physisorpion, 2005 Annual Merit Review Proceedings of the US Department of Energy, http://www.hydrogen.energy.gov/pdfs/review05/stp_34_ahn.pdf

[2] Japanese Industrial Standards JIS H 7201, 7202 and 7203:2007

[3] X.–L Wang., S., Suda, Journal of Alloys and Compounds, 231 (1995) 660-665

[4] Standard Practice for Conducting an Interlaboratory study to determine the Precision of a Test Method, ASTM International, E691-99, 1999.

[5] C. Zlotea et al., International Journal of Hydrogen Energy, 34 (2009) 3044-3057

Design of a Hydrogen Gas Generator Using Aqueous Sodium Borohydride Solution for Portable Fuel Cell Applications

Asli Yurdakul, Serdar Erkan, Saim Ozkar, Inci Eroglu, Middle East Technical University (METU), Turkey

1 Introduction

Due to increasing demand for power in portable electronic devices fuel cells attained considerable attention on replacement of lithium batteries. The last two century heavily depends on fossil fuels. Due to drawbacks of fossil fuels, researches have been concentrated on alternative energy sources. Hydrogen can be considered as ideal fuel for fuel cell. Since hydrogen can be stored, transported, and converted easily to other energy forms, there has been intense scientific, industrial, and governmental interest in the development of hydrogen based energy production technology [1,2]. Also it is considered as clean fuel but it has still a problem, storage that is crucial for the supply of hydrogen for portable fuel cells.

Hydrogen has been stored in tanks in compressed or liquefied form, in hydrogen-storing alloys, and on activated carbon or nanoscale materials such as carbon nanotubes but, none of these methods are suitable for portable applications due to the low volumetric and gravimetric efficiency of hydrogen storage as well as the associated safety issues. Instead of such hydrogen storage methods, liquid fuels (methanol, ethanol, gasoline, etc.) and chemical hydrides ($NaBH_4$, KBH_4, LiH, NaH, etc.) could be employed as hydrogen sources for portable PEMFC [2]. Among them, hydrogen generation from the hydrolysis reaction of an alkaline sodium borohydride solution ($NaBH_4$) has widely investigated due to its theoretically high hydrogen storage capacity (10.8 wt %). Also, because of the high purity of produced hydrogen, it can be used as hydrogen supplier for proton exchange membrane (PEM) fuel cells [3].

Hydrogen is produced from $NaBH_4$ according to the following irreversible, heterogeneous and highly exothermic, with the heat of reaction of 210kJ/mol:

$$NaBH_4(aq) + 2H_2O \xrightarrow[\text{catalyst}]{} 4H_2 + NaBO_2(aq) \qquad (1)$$

Catalytic generation of hydrogen from $NaBH_4$ solutions has several advantages listed below [4]:

- NaBH4 solutions are non-flammable and not toxic.
- NaBH4 solutions are stable in air for months.
- H2 generation only occurs in the presence of selected catalysts.

But this reaction can occur to some extent even without a catalyst if the solution pH < 9. However, to increase the shelf life of $NaBH_4$ solutions and to suppress the self hydrolysis of it, $NaBH_4$ solutions are typically maintained as a strongly alkaline solution by adding NaOH. According to the reactor type and amount of reactants, NaOH can be added in various amounts but generally in the range of 5-15 wt% of reactants. It must be noted that the excess amount of NaOH decreases the hydrogen yield. Mostly NaOH in the amount of 3-5% of reactant is thought to be sufficient to control hydrogen release. [4]

- The only other product in the gas stream is water vapour.

The presence of water vapour is beneficial for use in PEM fuel cells where the water vapour can be used to humidify the PEM membrane. The H_2 gas generated is sufficiently pure and it can be used directly in PEM fuel cells without further cleanup.

As a reactant, water is important since approximately 95% of the reactant mass is occupied by it. Furthermore fuel cell applications needs low weight hydrogen devices so, water content must be decreased as possible. [4]

- Reaction products are environmentally safe.

Since reaction (1) is totally inorganic and does not contain sulphur, it produces virtually no fuel cell poisons such as sulphur compounds, CO, soot, or aromatics.

- H_2 generation rates are easily controlled.

The heat generated by reaction Eq. (1), 75 kJ/mole H_2 formed, is considerably less than the typical > 125 kJ/mole H2, produced by reacting other chemical hydrides with water. This promises a safer, more controllable reaction.

Moreover, to generate H_2, $NaBH_4$ solution is allowed to contact catalyst either by dipping catalyst into a $NaBH_4$ solution or injecting $NaBH_4$ solution on catalyst. This ensures fast response to H_2 demand, i.e., H_2 is generated only when $NaBH_4$ solution contacts with catalyst. When H_2 is no longer needed, $NaBH_4$ solution is removed from catalyst and H_2 production ceases.

- Volumetric and gravimetric H_2 storage efficiencies are high.
- The reaction products can be recycled.
- H_2 can be generated even at 0°C.

Also hydrogen could be generated at temperatures below 0°C if water-methanol or water-ethylene glycol mixtures were used. [5]

2 Experimental

In this work, we construct a batch system for hydrogen production where hydrogen generating reactor is approximately 30mL three neck tube reactor that is stayed in a water bath. From one neck, alkaline $NaBH_4$ solution is introduced, from the other neck the reaction temperature is measured and recorded online. The generated gas that exits from reactor comes to the water displacement column that is filled with water. The scale is placed under the column for determining the change in the water amount and the scale is also connected to the computer for online recording the data. From that displacement of water the generated amount of hydrogen is determined. Figure 1 shows the experimental setup.

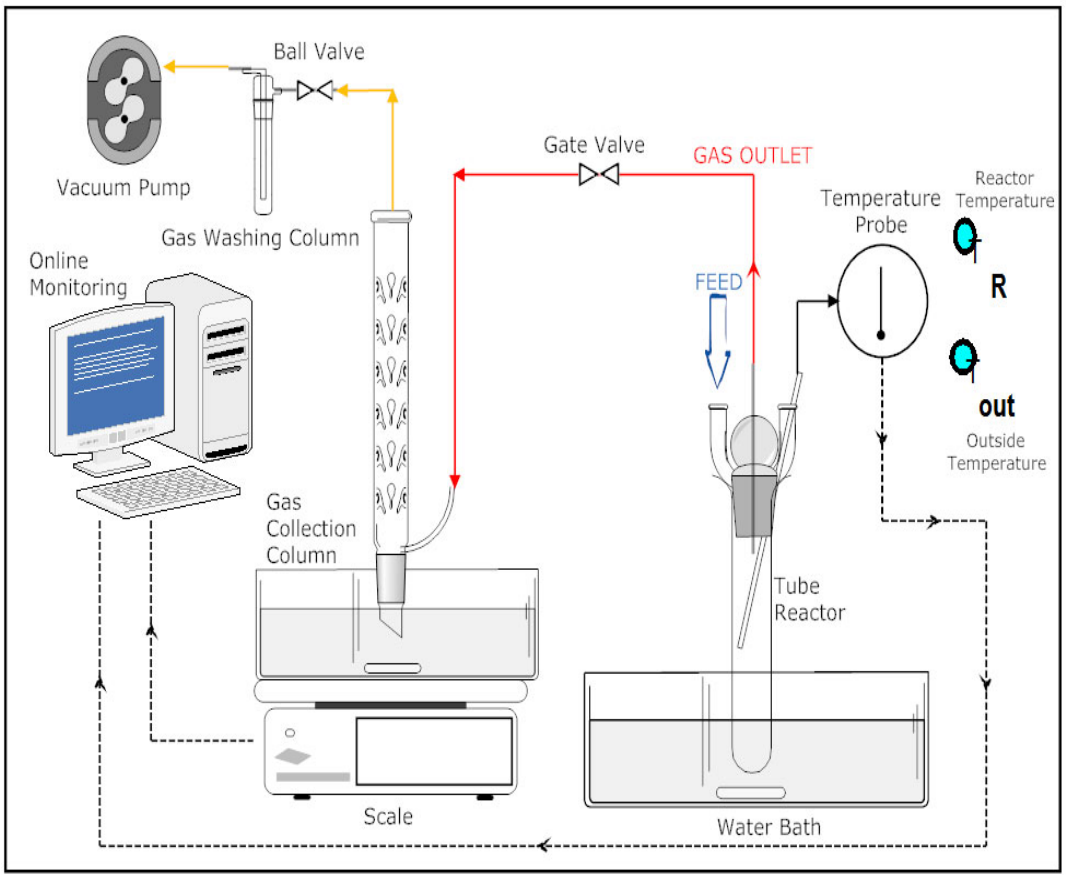

Figure 1: Experimental setup for hydrolysis of sodium borohydride.

In experiments first, water displacement column is filled with water by the help of vacuum pump. In order to prevent the water leakage to the pump, there is a gas washing column for collecting coming water. Then the solutions are prepared. Since $NaBH_4$ spontaneously reacts with water, while the spontaneous hydrolysis can be depressed in alkaline solutions, we prepared solutions on sodium hydroxide (NaOH) medium. The commercial catalyst that is 20% HP Pt on Vulcan XC-72 (ETEK®) is used in powder form to initiate the reaction. The desired amount of catalyst is weighted and placed into the reactor. Some amount of deionized water (1-2mL) is added on the catalyst to wet and introduce a homogenous medium. Then necessary amount of NaOH is weighted and dissolved in 14mL of deionized water. When alkaline medium is established the $NaBH_4$ is added to finish the solution preparation. During the set of experiments amount of water used is fixed. For the high temperature experiments this prepared solution is heated until it reaches to the reaction temperature before adding to the reactor. After that the solution is introduced to the reactor. When it comes to contact with catalyst the hydrogen is started to be generated. The generated gas comes to the water displacement column from the bottom. After it enters the column the water level reduces and this pressurizes the scale under it. The change in the scale is measured at every 0.2s. Also the temperature of the reaction and the ambient temperature are recorded at every 0.2s.

3 Results

There are mainly four parameters that are affecting the hydrogen generation such that $NaBH_4$ concentration, catalyst amount, NaOH concentration and temperature. To investigate the order of magnitude of their effects the controlled experiments were carried out. The effect of $NaBO_2$ is not considered in this work.

To analyze the effect of $NaBH_4$ concentration on H_2 generation rate three sets of experiment were prepared. In these sets, the only parameter that was changing is $NaBH_4$, others were kept as constant. These three experiments were carried out at constant temperature of 20°C. The pressure of system was 0.94atm. It was found that as $NaBH_4$ concentration increases the amount of hydrogen increases. The initial hydrogen generation rates are nearly the same for all these three experiments but, through the completion of reaction the rates were changing. This shows that the reaction rate is dependent of concentration of sodium borohydride solution catalyzed with Pt/C.

As mentioned before, the solutions of $NaBH_4$ were prepared in NaOH in order to prevent self hydrolysis of sodium borohydride. To investigate the effect of NaOH concentration again three sets of experiments were conducted that had 1ww% NaOH, 5ww%NaOH and 10%NaOH. It was found that the amount of hydrogen produced is same within 3 cases as expected since the $NaBH_4$ amount did not changed. Also, as NaOH concentration increases the H_2 generation rate decreases accordingly. So we conclude that for high production rates we have to optimize the amount of NaOH that also stabilize the solution.

When catalyst amount and temperature was considered as expected it is seen that the hydrogen production rate increases with increase of catalyst and temperature whereas the maximum amount of hydrogen produced does not changes.

To determine the kinetic model of hydrolysis reaction on commercial Pt/C catalyst, method of excess is used. After the experiments we concluded that the reaction rate depends on concentration of $NaBH_4$ and NaOH, catalyst amount and temperature. By using power law we propose a model:

$$r_{H_2} = f(T, C_{NaOH}, C_{NaBH_4}, C_{cat})$$

$$r_{H_2} = k e^{-E_a/RT} C_{NaBH_4}^{\alpha} C_{NaOH}^{\beta}$$

After calculations the rate model proposed is of the form that:

$$r_{H_2}' = 5.2 \times 10^{-3} \times \frac{C_{NaBH_4}^{0.235}}{C_{NaOH}^{0.405}} \qquad \text{for } 20^0\text{C and } 0.048\text{gPt/C with } R^2 = 0.994$$

For the temperature analysis Arrhenius plot is drawn shown in Figure 2.

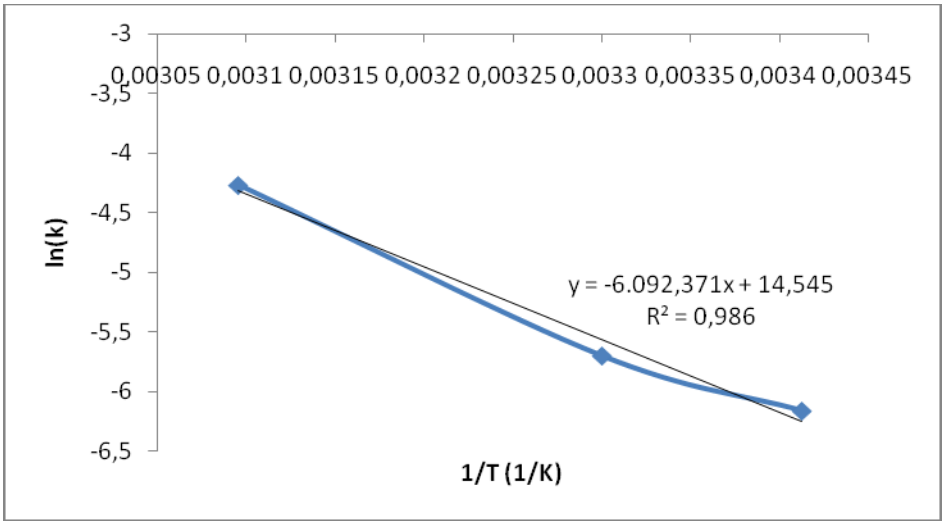

Figure 2: Arrhenius plot.

From Figure 2, the pre-exponential factor and activation energy are found as

$2\times10^{6}\,\frac{mol}{L.\min}$ and 50.65 kJ/mol respectively.

So the rate expression takes the form:

$$r_{H_2}' = 2\times10^{6}\times e^{-\frac{50.65}{RT}}\times\frac{C_{NaBH_4}^{0.235}}{C_{NaOH}^{0.405}} \qquad \text{for 0.048g Pt/C with } R^2 = 0.986$$

The catalyst effect must be introduced to the model in the activation energy but this is not investigated through this work.

4 Conclusions

Hydrogen generation from the hydrolysis of stabilized sodium borohydride solution offers a convenient, practical and effective way for portable fuel cell applications. Using $NaBH_4$ solutions reduces inherent safety concerns associated with long-term gaseous H_2 storage. H_2 production occurs on demand and reaction products are not toxic. Even the presence of water vapour is beneficial for use in PEM fuel cells where the water vapour can be used to humidify the PEM membrane. The H_2 gas generated is sufficiently pure and it can be used directly in PEM fuel cells without further cleanup.

In the present work, hydrogen generation system for portable applications has been studied and developed. The 20% Pt/C catalyst was utilized in the form of powder to initiate the hydrolysis reaction. The four parameters that are affecting the H_2 generation rate such as amount of catalyst, $NaBH_4$concentration, NaOH concentration and temperature has been widely investigated. It was seen that under Pt catalyst reaction behaves nearly zero order with respect to the $NaBH_4$. Also, the increase in NaOH concentration which is used to prevent self hydrolysis of $NaBH_4$ results decrease in the rate. The catalyst amount and

temperature significantly affect the H_2 generation rate in a positive manner as expected. At the end of controlled experiments the rate equation for hydrolysis reaction has been derived. Moreover, at ambient conditions the generation rate was estimated as 2.14L/min.g Pt catalyst for 0.23M $NaBH_4$-0.27M NaOH solution.

This indicates that our generator system is suitable for portable applications of PEM fuel cells.

References

[1] Erce Şengül, “Preparation and performance of membrane electrode assemblies with Nafion and alternative polymer electrolyte membranes” MS thesis, Chemical Engineering Department, METU, Ankara, September, 2007

[2] Kim et al. “Hydrogen generation system using sodium borohydride for operation of a 400W-scale polymer electrolyte fuel cell stack” Journal of Power Sources 170 (2007) 412-418

[3] Hung, A., Tsai, S., Hsu, Y., Ku, J., Chen, Y., Yu, C. “Kinetics of sodium borohydride hydrolysis reaction for hydrogen generation” International Journal of Hydrogen Energy 33 (2008) 6205–6215

[4] Çakanyıldırım, Ç., Gürü, M. “Hydrogen cycle with sodium borohydride” International Journal of Hydrogen Energy 33 (2008) 4634–4639

[5] Schlesinger, H.I., Brown, H.C., Finholt, A.E., Gilbreath, J.R., Hockstra, H.R., Hyde, E.K. “Sodium borohydride, its hydrolysis and its use as a reducing agent and in the generation of hydrogen” J Am Chem Soc 75 (1953) 215–219.

Adsorption Technologies

Barbara Schmitz and Michael Hirscher

Abstract

One promising possibility to store hydrogen is cryosorption of hydrogen molecules on nanoporous materials possessing large internal surfaces. The physisorption process is fast and fully reversible and, therefore, short refuelling times can be realized. This chapter introduces the basics of hydrogen adsorption and various classes of nanoporous adsorbents including the most advanced materials. The influence of the specific surface area, the pore size and the chemical composition on the hydrogen storage properties are discussed. Finally, the relevant parameters for technical applications and the requirements to possible storage materials are highlighted.

Analysis of Hydrogen Storage in Porous Adsorption Materials

Ulrich Bünger, **Erling Naess**, Norwegian University of Science and Technology, Norway
Maurice Schlichtenmayer, **Michael Hirscher**, Max Planck Institute for Metals Research, Germany
Irena Senkovska, **Stefan Kaskel**, Institute for Inorganic Chemistry, Universität Dresden, Germany

1 Introduction

In 2008 the research project “Advanced MOFs for Hydrogen Storage in Cryo-adsorption Tanks” was launched under the European collaboration program HyCo. It comprises three research partners, two from Germany (TU Dresden/Institute for Inorganic Chemistry, Max-Planck-Institute for Metal Research) and one from Norway (University of Science and Technology/Institute for Energy and Process Engineering).

The focus of the project is to carry the development of advanced hydrogen storage systems by adsorption in metal organic frameworks (MOF, coordination polymers) one step further by fundamental and applied research at three levels:

Synthesis of new promising adsorption type and highly porous MOF materials, characterization of their physical hydrogen adsorption and desorption characteristics and comparison with other known materials and prediction and measurement of the thermal behavior of hydrogen storage in 'real' cryogenic adsorption storage tanks.

Currently, first advanced and new adsorption type materials of coordination polymer type have been synthezised and characterized for their adsorption characteristics as well as thermally.

2 State-of-the art

Efficient hydrogen storage onboard fuel cell vehicles is one of the pre-requisites of a successful commercialization of this type of vehicles. To avoid complex storage system structures to contain hydrogen either under high (35 MPa) and highest (70 MPa) pressures or as a liquid (at -253 °C) and to reduce storage system weight and specifically volume the ambition is to obtain hydrogen system storage capacities in excess of 6 wt% (2010) and 9 wt% (2015) and 1.5 kWh/L (2010) and 2.7 kWh/L (2015), which is the 2003 storage commercialization goal of the U.S. Department of Energy.

Next to hydrogen absorption type tanks, typically based on chemisorption of hydrogen within a host material (some form of metal hydride) hydrogen adsorption comprises the attachment of one or more layers of gas molecules on solid material surfaces. Therefore, gas adsorption type materials are typically characterized by high and ultra-high specific surfaces of several thousand cm^2/g and high porosities.

Highly porous active carbon has early been identified as a candidate material for hydrogen adsorption. Also, it was found that the lower the temperature of adsorption, the higher the hydrogen adsorption rate. On one hand hydrogen adsorption typically requires cryogenic operating temperature, on the other hand increasing the gas pressure additional hydrogen can be stored in the void fraction, such that the total storage capacity of an adsorption type tank comprises the storage of compressed gas which is solely governed by the gas pressure and excess storage by adsorption which is characterized by the characteristics of the adsorbant as well as temperature and pressure.

3 MOF Synthesis

In the late 90s, a new class of materials, so called porous coordination polymers or metal-organic frameworks (MOFs), has been identified as efficient adsorbents, capable of even higher gravimetric storage densities than activated carbon in cryogenic operation, 77K being a practical temperature level. MOFs are formed by coordinative bonds of multidentate ligands to metal atoms or metal clusters resulting in 2D or 3D structure with pores or channels that are occupied by guest molecules (typically solvent used during synthesis) which can be removed by activation. For energy storage applications at 200 bar, larger pores (2-3 nm) are essential to achieve a shift of the excess adsorption maximum towards higher pressure resulting in high capacities.

Our task is the synthesis and characterization of new porous coordination polymers. Characterisation implies the determination of the structure by single crystal X-ray analysis or powder X-ray diffraction (PXRD) *via* Rietveld refinement as well as the specific surface area and pore volume by physisorption measurements of nitrogen at 77K up to 1 bar. Hydrogen adsorption measurements up to 1 bar and higher pressures were done testing the new MOF material for the desired application.

Within our research we synthesized several new MOFs namely DUT-4 (DUT = Dresden University of Technology; Al(OH)(2,6-ndc), 2,6-ndc = 2,6-naphthalenedicarboxylate) [5], DUT-5 (Al(OH)(bpdc), bpdc = 4,4'-biphenyldicarboxylate) [5], DUT-6 (Zn_4O(2,6-ndc)$(btb)_{4/3}$, btb = 1,3,5-benzenetribenzoate) [3], DUT-8(Cu) (Cu_2(2,6-ndc)$_2$(dabco), dabco = 1,4-diazabicyclo[2.2.2]octane) and DUT-8(Co) (Co_2(2,6-ndc)$_2$(dabco)) by solvothermal reaction in DMF (*N,N*-dimethylformamide) or DEF (*N,N*-diethylformamide). All samples were characterized by PXRD to ensure the phase purity and by nitrogen physisorption at 77K to determine the porosity. The resulting MOFs show different network topologies and pore dimensions. The aluminum containing coordination polymers offer rectangular channels 8.5 Å x 8.5 Å for DUT-4 and 11 Å x 11 Å for DUT-5. By using the longer ligand bpdc instead of 2,6-ndc slightly larger channels are observed. DUT-4 and -5 are stable in air and exhibit a permanent porosity. The framework of DUT-8(Cu,Co) consists of binuclear paddle wheel M_2-units (M = Cu, Co) bridged by 2,6-ndc anions to form a 2D square-grid layer with a mesh size of 9.6 Å x 9.6 Å in *c* direction. The framework of DUT-8(Cu) is rigid, in comparison the cobalt containing MOF shows flexibility during physisorption of different gases. In DUT-6 wide open dodecahedral mesoporous cages of 2.5-3 nm in diameter are formed by twelve Zn_4O^{6+} nodes, six 2,6-ndc linkers, and eight btb linkers. The six bridging carboxylate groups form an octahedral secondary building unit (SBU) with four btb linkers in a square arrangement, while

two additional 2,6-ndc linkers occupy the residual octahedral sites and further crosslink the network. The compound has a rigid framework and exhibits high permanent porosity, which has been confirmed by gas and liquid phase adsorption, and by the adsorption of large molecules. The storage capacity of porous system mainly depends on the specific surface area and pore volume of the material. DUT-4,-5 and DUT-8 (Cu, Co) can be classified as microporous materials. Due to the large pores DUT-6 is attributed to the mesoporous materials. By nitrogen physisorption (77K, 1 bar) the total pore volume (V_{pore}) and specific surface area (SSA, $p/p_0 = 0.3$) for all materials have been determined (DUT-4: V_{pore} = 0.68 cm^3g^{-1}, SSA = 1308 m^2g^{-1}; DUT 5: V_{pore} = 0.81 cm^3g^{-1}, SSA = 1613 m^2g^{-1}; DUT-6: V_{pore} = 2.02 cm^3g^{-1}, SSA ~ 4000 m^2g^{-1}; DUT-8(Co): V_{pore} = 0.58 cm^3g^{-1}, SSA = 1100 m^2g^{-1}; DUT-8(Cu): V_{pore} = 1.0 cm^3g^{-1}, SSA = 1920 m^2g^{-1}). The values of DUT-6 are among the highest values reported for MOFs today. The hydrogen storage capacities at high pressures were evaluated *via* volumetric measurements. The hydrogen adsorption isotherm for DUT-4 revealed an excess hydrogen storage capacity of 247 cm^3g^{-1} at 30 bar corresponding to 2.1 wt.%, DUT-5 of 381 cm^3g^{-1} at 40 bar corresponding to 3.3 wt.%, DUT-8(Co) of 333 cm^3g^{-1} at 35 bar corresponding to 2.9 wt.%, DUT-8(Cu) of 496 cm^3g^{-1} at 30 bar corresponding to 4.3 wt.% and DUT-6 of 666 cm^3g^{-1} at 50 bar corresponding to 5.6 wt.% which is one of the highest values reported so far for hydrogen adsorption on MOFs. So far DUT-6 is the most promising new MOF material for hydrogen storage at high pressures within this project.

4 MOF Characterization

The aim of MOF synthesis in the context of hydrogen storage is to develop new MOFs with high hydrogen capacities that allow storage with as little effort as possible. For finding an optimal storage material for a real tank it is therefore important to know how much hydrogen is adsorbed under different surrounding conditions (mainly pressure and temperature). Therefore for all promising materials the hydrogen uptake is measured at controlled temperatures between 77K and room temperature and pressures between 0 bar and 25 bar. These measurements are carried out using a Sieverts-type adsorption instrument (PCT Pro 2000 with microdoser from HyEnergy), that needs only small amounts of sample (about 200 mg), which is very practical due to the high effort for synthesizing large amounts of newly developed materials. From the isotherms also the heat of adsorption is calculated for all materials using the Van ‘t Hoff equation. This is also an important parameter for hydrogen storage, the higher the heat of adsorption, the stronger the hydrogen is attached to the adsorbent and less pressure or cooling is necessary to get the same relative hydrogen uptake.

As an example some isotherms of the absolute adsorption of a MOF and an activated carbon are shown in figure 1. Both materials have similar uptakes at 25 bar at all temperatures, however, at smaller pressures the activated carbon has a significantly higher uptake especially at low temperatures, thus indicating a higher heat of adsorption than the MOF.

In the choice of an adsorption material for a real tank also some more technical points have to be considered. One of them is not only to store as much hydrogen as possible but also to be able to release it again. Fuel cells need a certain supply pressure and, if there is no extra compressor, this is a lower limit for the tank pressure. For example assuming this supply

pressure as 2 bar, in the activated carbon AX21_33 there would remain about 3 wt% adsorbed at 77 K (see figure 1). In this case only 2.5 wt% of the adsorbed hydrogen at maximum pressure can be used. Under the same conditions the MOF DUT 6 would release 5 wt% of hydrogen. It turns out, that in these terms a high heat of adsorption can be disadvantageous because it leads to a high remaining hydrogen content at low pressures. However this can again be compensated when it is possible to raise the temperature of the system, since at low pressures and high temperatures the hydrogen uptake of all adsorbents is negligible. So for the choice of an adsorbent for a real tank, the exact knowledge of the operating conditions, especially pressure and temperature range, is necessary.

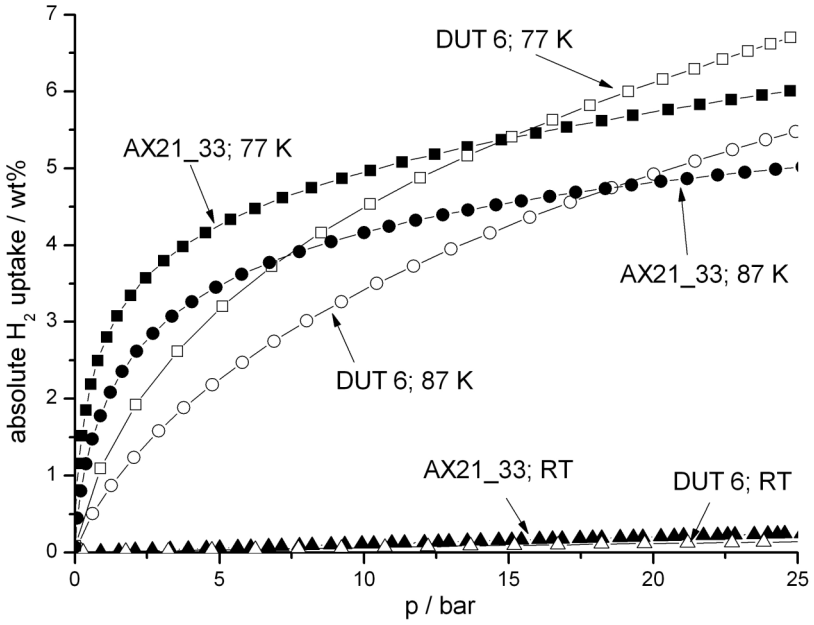

Figure 1: Hydrogen adsorption isotherms of the metal organic framework DUT 6, synthesized by the group of Stefan Kaskel at TU Dresden (open symbols) and of the activated carbon AX21_33, also known as Maxsorb III (closed symbols). The isotherms have been taken at three different temperatures, 77 K (squares), 87 K (circles) and room temperature (triangles).

In addition to the adsorbed layer, porous materials always also contain hydrogen gas inside their pores [4]. The sum of both is called total uptake, which is even higher than the absolute uptake given in figure 1.

In comparison with other porous materials, MOFs are very promising adsorbents for hydrogen storage. The best materials show a total hydrogen uptake of more than 10 wt% on materials basis.

5 Prediction and Measurement of Real Adsorption Tank Systems

In real tank systems using adsorption type hydrogen storage not only the static hydrogen uptake is relevant in operation i.e. onboard vehicles. Furthermore, the dynamic operational characteristics when drawing hydrogen from the tank, but specifically when rapidly filling the

tank require specific material characteristic. One such characteristic is how much hydrogen can be net-released from the tank given the possible temperature and pressure swing, the other is the need to rapidly remove heat from the tank during filling and adding heat when emptying to overcome the heat of adsorption. It can be shown that in a real vehicle tank the thermal power rapidly transferred from or to the tank across a cryogenic insulation can be in the order of 0.5 MW_{th} which poses the need to add efficient heat transfer devices.

The goal of this part of the work is to analyse and develop models to predict the kinetic heat and mass transfer in a real tank simulation tool to understand the charging and discharging process of hydrogen into/from selected MOF materials from the samples provided/synthesized by University Dresden and characterized by Max-Planck-Institute as well as different geometries and heat exchanger designs.

The following three tasks have been defined in the Norwegian part of the project:

- **Measurement and development of models for predicting the basic material quantities:** Of particular interest are the thermophysical and flow related properties (e.g effective thermal conductivity, specific heat capacity, density, porosity and permeability, as well as the kinetic properties),
- **Development of a simulation tool for hydrogen storage tanks, predicting the transient heat and mass transfer coupled with the material kinetic properties:** The outcome of this will form the basis of defining and developing internal heat exchanger surfaces and cooling systems enabling e.g. fast filling of storage tanks.
- **Experimental validation:** Selected materials will be tested experimentally in a relatively large (ca 9 l) cryo-storage tank, where flow, pressure and temperature distribution is mapped. Internal heat exchanger surface geometries can be fitted inside to optimize the tank behavior. Experimental data will be used to validate the simulation tools.

For the measurement of effective thermal conductivity a new rig for static measurements will be developed. The other measurements will be carried out with existing experimental setups available at NTNU.

An existing experimental rig, which was earlier used to analyse hydrogen ad- and desorption with isothermal tank boundaries [1], will be re-built to measure hydrogen ad- and desorption under near adiabatic operating conditions, i.e. with insulated tank walls. Hence, hydrogen will be filled into the pre-cooled test tank under cryogenic conditions and the dynamics and quantities of heat removed from the tank (emptying = desorption) and added to the tank (filling = adsorption) will be measured to study the system dynamics and hydrogen uptake of / removal from the tank.

A specific innovation of the project is to analyse the effect of heat exchangers integrated into the adsorption material. To efficiently add or replace heat to or from the adsorbant (= heat of ad- / desorption) these heat exchangers will have to fulfill several requirements simultaneously:

- Use up as little volume and add as little weight to the tank as possible,
- Offer highest possible systems dynamics for high ad- and desorption rates and

- Low cost material and design heat exchanger design with simple geometry for low cost tank assembly.

The heat & mass transfer simulation tool will be based on an existing simulation tool which has been used to predict thermal behaviour of MOF materials using a well measured active carbon as reference material [2].

In order to predict systems behaviour of the newly synthesized adsorbants a first rough tank layout was used to compare the gravimetric and volumetric storage densities of the bulk material and the tank system at various maximum gas operating pressures. It was assumed that the 2 m long and 30 cm wide tank will in future fuel cell vehicles be longitudinally be located between the seats. The tank is double shelled with a total wall thickness including liner, inner and outer wall and insulation of 2.5 cm, powdrous vacuum super insulation, instrumentation (ca. 30 kg), no heat exchanger, a gross tank weight about 105 kg and a total maximum hydrogen content of 1.5 – 3.6.

The gravimetric storage density is depicted in figure 2 for the pressure range 2 – 20 bar. It can be seen that for lower pressures the copper based MOF synthesized by TU Dresden (DUT8) is superior in gravimetric hydrogen uptake, both in the material and in the system whereas for higher pressures the well known MOF 177 and DUT6 take over and result in a gravimetric uptakes of about 7 wt% and 6.5 wt% at 20 bar. Only the material based hydrogen uptake reaches the required U.S. DoE storage goal of 6 wt%. For the (non-optimised) system gravimetric storage densities do not surpass 1.8 wt%. Systems storage density suffers specifically from tank ballast such as instrumentation. It can be envisioned that this can be reduced in the future.

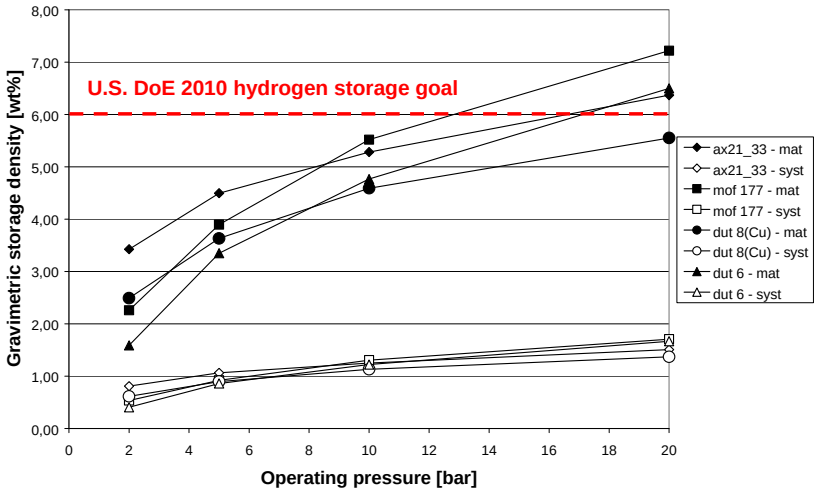

Figure 2: Gravimetric storage density of various MOF and activated carbon adsorbants at 77 K and 2 - 20 bar. Full symbols are capacities on materials basis and open symbols refer to system values.

Figure 3 presents extrapolated data for volumetric storage densities of the same material for the assumption that hydrogen storage by adsorption is asymptotically reaching its maximum

at about 20 bar and only compressed hydrogen in the voids adds to the increase of storage capacity of the tank with rising pressure.

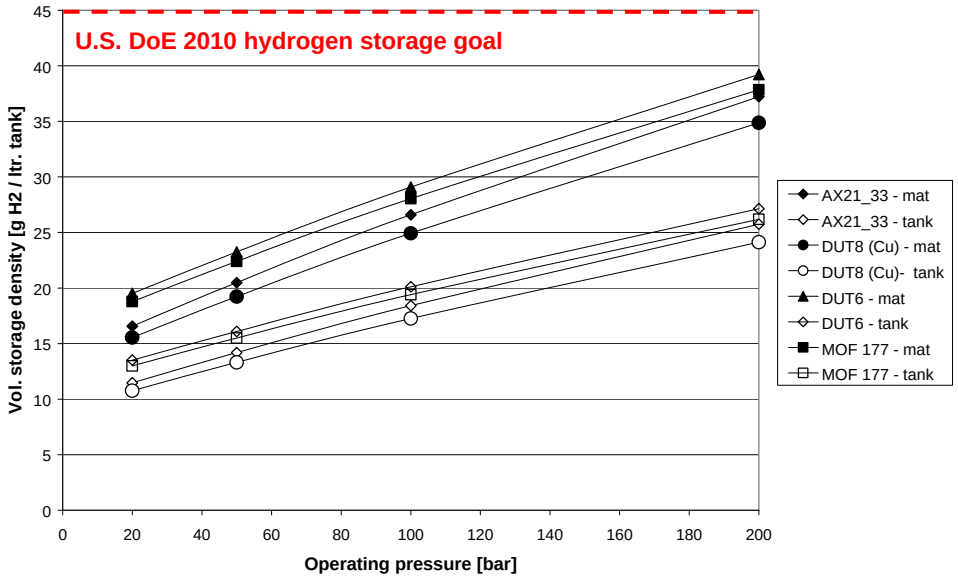

Figure 3: Total volumetric storage densities of various MOF and activated carbon adsorbants at 77 K and 20 – 200 bar. Full symbols are capacities on materials basis and open symbols refer to system values.

Figure 3 shows that the volumetric bulk material storage density of the newly synthesized MOF by TU Dresden (DUT6) is slightly higher than for MOF 177 and activated carbon for the full pressure range.

Today, none of the materials can fulfill the DoE 2010 hydrogen storage goals, by volume not even the bulk material at highest pressures. Further work will therefore study the tank systems behaviour in more detail, specifically also taking the amount of hydrogen into account which can not be taken out of the tank due to the steep gradients of the adsorption isotherms versus pressure. By regulating pressure and temperature by specific instrumentations such as efficient heat exchangers, we expect some potential for optimization.

References

[1] Aleksic, P.; Næss, E., Bünger, U.: An experimental investigation of thermal effects during discharging operations in a hydrogen cryo-adsorption storage system. 7th Int. Conf. Heat Transfer, Fluid Dynamics and Thermodynamics, 19.21 July 2010, Antalya, Turkey.

[2] Jensen S., Næss E., Bünger U., Sønju O.: A numerical study of the heat and mass transfer in an adsorption type hydrogen storage tank. HEFAT 2007, 5th Int. Conf. on Heat Transfer, Fluid Mechanics and Thermodynamics, Sun City, South Africa.

[3] Klein, N.; Senkovska, I.; Gedrich, K.; Stoeck, U.; Henschel, A.; Mueller, U.; Kaskel, S.: Angew. Chem. Int. Ed., **48,** 9954-9957 (2009).

[4] Schmitz B., Hirscher M.: Adsorption Technologies, in Hydrogen Energy, ed. Stolten D., Wiley-VCH 2010.

[5] Senkovska, I.; Hoffmann, F.; Froeba, M.; Getzschmann, J.; Boehlmann, W.; Kaskel, S.: Microporous Mesoporous Mater., **122** 93–98 (2009).

Mixed H_2-CH_4 Hydrates as Materials for Hydrogen Storage

Rodion Belosludov, **Hiroshi Mizuseki**, **Yoshiyuki Kawazoe**, Tohoku University, Sendai, Japan
Oleg Subbotin, **Vladimir Belosludov**, Nikolaev Institute of Inorganic Chemistry, Novosibirsk, Russia

1 Introduction

The present environmental factors and limited energy resources in future have led to a profound evolution of technical progress in the generation, storage and supply of energy. Although fossil and nuclear sources will remain the most important energy provider for nearest future, the technological solutions that involve alternative possibilities of energy supply and storage are in urgent need of development. To meet the request storage conditions, researches need to identify new materials and address a host of associated performance and system issues, such as operating pressure and temperature, the durability of the storage material, the reversibility of hydrogen uptake and release, the hydrogen delivery pressure, overall safety, toxicity, system-efficiency and cost [1].

The clathrate hydrate is material, which has a potential application as hydrogen storage. This is a special class of inclusion compounds consisting of water (red and white) and small guest (grey) molecules (see Figure 1), which form a variety of hydrogen-bonded structures.

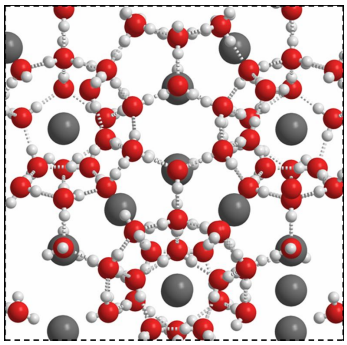

Figure 1: Crystal structure CS-II clathrate hydrate.

These compounds are formed when water molecules arrange themselves in a cage-like structure around guest molecules. As example, the methane in gas hydrates represents one of the largest sources of hydrocarbons on Earth. Interest in hydrogen clathrate hydrates as potential hydrogen storage materials has risen recently after a report that the clathrate hydrate of cubic structure II (CS-II) can store around 5.0 weight% of hydrogen at 220MPa and 234 K [2]. However, the extreme pressure required to stabilize this material makes it impractical. A significant reduction in the hydrate formation pressure, nearly 2 orders of magnitude, was found in the tetrahydrofuran (THF) – hydrogen – water system [3, 4]. In this case the THF molecules can be included only in the large cages of host lattice that

significantly reduces amount of hydrogen and hence makes such storage impractical. Moreover, it is already established that THF can be classified as an “irritant” compound with a low toxicity category and thus can be used only in modest amounts.

Thus first, it will be interesting to consider the possible formation of hydrogen hydrates stabilized by other guest molecules which, for example, may also fill small cavities and see, whether hydrates formed from mixtures of these guests and H_2 can be used as a basis for hydrogen storage material. Second, there are several types of gas hydrate structures with different cage shapes, and some of these hydrate structures can hypothetically store more hydrogen than the hydrate of structure CS-II. Therefore, for practical application of gas clathrates as hydrogen storage materials, it is important to know the region of stability of these compounds as well as the hydrogen concentration at various pressures and temperatures.

In this work, we calculate the thermodynamic properties and the degree of filling of the large and small cavities for mixed propane+hydrogen and methane+hydrogen hydrates in various range of pressures and temperatures. For these binary hydrates, we also analyze the possibility to realize the “composition tuning mechanism” proposed earlier for THF+H_2 hydrate [4].

2 Computational Details

In order to accurately estimate the thermodynamic properties of hydrogen hydrates, we developed a method based on the solid solution theory of van der Waals and Platteeuw (vdW-P) with some modifications that include multiple occupancies, host relaxation, and the description of the quantum nature of hydrogen behavior in the cavities. The following development of the model is based only on one of the assumptions of vdW–P theory: the contribution of guest molecules to the free energy is independent of mode of occupation of the cavities at a designated number of guest molecules. This assumption allows us to separate the entropy part of free energy:

$$F = F_1\left(V,T,y_{11}^1,\ldots,y_{nm}^k\right)+ \\ + kT\sum_{t=1}^{m} N_t\left[\left(1-\sum_{l=1}^{n}\sum_{i=1}^{k} y_{lt}^i\right)\ln\left(1-\sum_{l=1}^{n}\sum_{i=1}^{k} y_{lt}^i\right)+\sum_{l=1}^{n}\sum_{i=1}^{k} y_{lt}^i \ln\frac{y_{lt}^i}{i!}\right] \quad (1)$$

For a given arrangement $\{y^1{}_{11},\ldots,y^k{}_{mn}\}$ of the guest molecules in the cavities the free energy $F_1(V,T,\ y^1{}_{11},\ldots,y^k{}_{mn})$ of the crystal can be calculated within the framework of a lattice dynamics approach in the quasiharmonic approximation as

$$F_1\left(V,T,y^1{}_{11},\ldots,y^k{}_{nm}\right)=U+F_{vib}, \quad (2)$$

where U is the potential energy, F_{vib} is the vibrational contribution:

$$F_{vib} = \frac{1}{2}\sum_{j\bar{q}} \hbar\omega_j(\bar{q}) + k_B T \sum_{j\bar{q}} \ln\left(1 - \exp(-\hbar\omega_j(\bar{q})k_B T)\right), \quad (3)$$

where $\omega_j(\mathbf{q})$ is the *j*-th frequency of crystal vibration and **q** is the wave vector.

If the free energy *F* is known then the equation of state and the Gibbs free energy Φ(P, T, {y}) expressed in terms of chemical potentials of host and guest molecules can be found and the corresponding equations are presented elsewhere [5, 6].

3 Results and Discussions

The validity of the proposed approach was checked for pure CS-II hydrogen hydrates [6]. The calculated curve of the phase transformation between hexagonal ice and hydrogen hydrate agrees well with the available experiments. The hydrogen content continues to increase due to multiple filling of the large cages. At low temperature the mass percentage of hydrogen in the CS-II hydrogen hydrate can reach amount up to 3.8 wt % for pressures of 160-180 bar. This value corresponds to configuration of four hydrogen molecules in the large cavities and one molecule in the small cages of the CS-II hydrate structure. At higher pressure the hydrogen storage capacity can increase up to 4 wt% (see Figure 2) indicating the changes from one to twofold filling for a limited number of small cavities. Increasing the temperature up to 260 K significantly reduces the amount of stored hydrogen. The maximum amount of hydrogen stored at this temperature and high pressures is about 3.5 wt % [6].

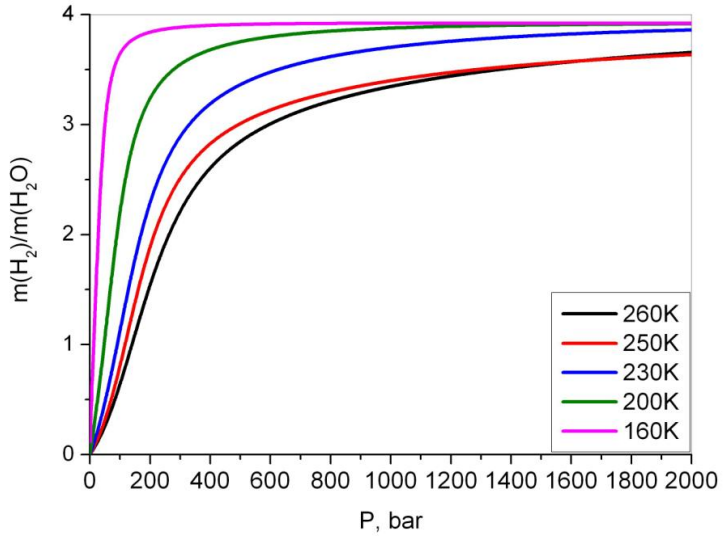

Figure 2: The amount of stored hydrogen in the pure CS-II hydrogen hydrate.

The phase diagrams of propane+hydrogen hydrate with structure II have been constructed and they are in agreement with available experimental data. The formation pressure can be significantly reduced in the presence of propane as a second guest in the binary hydrogen hydrate. At a low propane concentration of 0.1 % in the gas phase, the binary hydrate becomes stable at a pressure around 380 bar which is about four times lower than that

needed to form the pure hydrogen clathrate in the same temperature region [6]. By analogy with THF, propane brings the hydrate formation conditions closer to ambient conditions and it is undoubtedly favorable for a hydrogen storage material. The filling of the large cages by hydrogen molecules increases consecutively from one to four hydrogen molecules with increasing pressure. In contrast to hydrogen, the propane filling decreases with increasing pressure and in the high pressure region the propane molecules are gradually expelled by hydrogen molecules. The tuning of large cage occupancy can be attributed to the "composition tuning mechanism" proposed by Lee *et al.* [4]. The mass percentage of hydrogen in the mixed CS-II propane+hydrogen hydrate can amount up to 3.5 wt% at T=260 K and lower concentrations of propane in the gas phase and a pressure of 1000 bar. This value is comparable with the hydrogen content (3.5 wt %) estimated for pure hydrogen hydrate at the same temperature as shown in Figure 3.

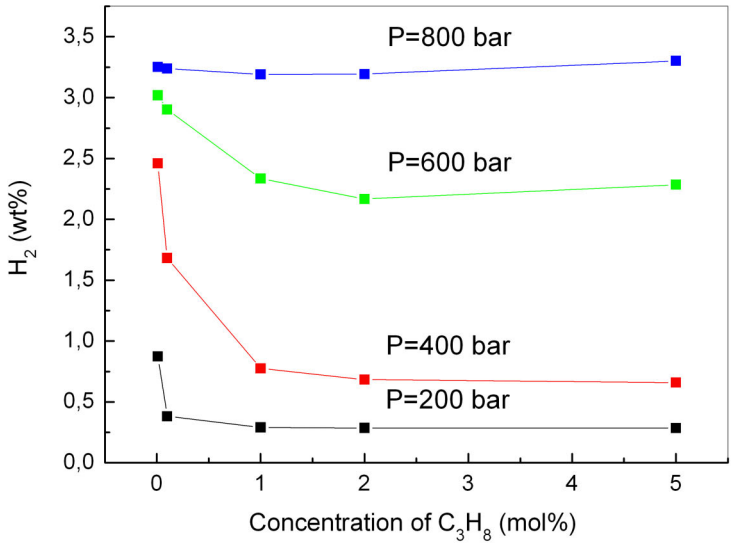

Figure 3: The amount of stored hydrogen in the mixed propane+hydrogen CS-II hydrate.

It has been also estimated that the pure hydrogen hydrate of CS-I structure can store more hydrogen but this structure is thermodynamically unstable as comparable with CS-II structure and hexagonal ice. Therefore, the mixed methane+hydrogen hydrates of CS-I and CS-II structures have been investigated with different methane and H_2 concentrations. The formation pressures of the binary H_2+CH_4 CS-I and CS-II hydrates depend on methane concentration in the gas phase and with increasing methane concentration in the gas phase was found to be lower in comparison with the pressure of pure hydrogen hydrate formation. At low methane concentration (less than 1 %), the mixed methane+hydrogen CS-II hydrate is more thermodynamically stable than CS-I hydrate with same composition of guest molecules. The "composition tuning mechanism" has been also observed for the methane+hydrogen CS-II hydrate as in the case of propane+hydrogen one. The introduction of methane as a second guest component in the binary hydrogen CS-II hydrate does not only

reduce the formation pressure but also reproduces the hydrogen storage ability of the pure clathrate hydrate. The calculations showed that the stabilization of CS-I hydrate can be also realized for H_2-methane-H_2O systems with relative large concentration of methane in the gas phase. However, in this case, the amount of storage hydrogen in CS-I structure reduced during increasing pressure. In contrast to CS-II structure, the methane filling of large cages increase with increasing pressure and in the high pressure region the hydrogen molecules are gradually expelled by methane molecules. By variation of methane concentration in gas phase, the mass percentage of hydrogen in mixed methane+hydrogen CS-I hydrate can reach amount 2 wt % at 250 K and 800 bar. However, the storage hydrogen amount depends on the methane concentration in the gas phase as well as thermodynamic conditions of hydrate formation. Therefore, it is important to determine the optimal balance between storage capacity and formation conditions for the practical feasibility of the binary hydrate as a hydrogen storage candidate. There are significant difficulties in experimental investigation and treatment of phase diagrams of multi-component clathrate hydrates that could result in a loss of important information related to the guest content in storage media. We believe that the proposed approach could support experimentalists in the practical realization of hydrogen storage material based on clathrate hydrate.

Acknowledgement

The authors would like to express their sincere thanks to the staff of the Center for Computational Materials Science of the Institute for Materials Research, Tohoku University for their continuous support of the SR11000-K2/51 supercomputing facilities. This work has been supported by New Energy and Industrial Technology Development Organization (NEDO) under “Advanced Fundamental Research Project on Hydrogen Storage Materials”.

Reference

[1] L. Schlapbach and A. Züttel. Nature **414** (2004) 353-358.

[2] W.L. Mao *et al.* Science **297** (2002) 2247-2249.

[3] L. J. Florusse *et al.* Science **306**, (2004) 469-471.

[4] H. Lee *et al.* Nature **434**, (2005) 743-746.

[5] V. R. Belosludov et al. Mater. Trans. 48 (2007) 704-710.

[6] R. V. Belosludov et al. J. Chem. Phys. 131 (2009) 244510.

Effects of Palladium Modification on Hydrogen Sorption by Boron Nitride with High Specific Surface Area

Nobuyuki Nishimiya, **Kozue Iimura**, **Takeshi Toyama**, **Yoshiyuki Kojima**, Nihon University, Japan

1 Introduction

Since Dillon et al [1] reported plausibly high hydrogen capacity of single walled carbon nanotubes at room temperature; numerous researches have been made in order to develop highly efficient hydrogen storage media with high specific surface areas [2]. The maximum hydrogen capacity of single walled carbon nanotubes prepared by the authors was 0.86 mass% at room temperature under 0.1 MPa of hydrogen [3]. Those nanotubes contained Y and Ni, since the starting material was graphite compounded with those metals, which would act as catalysts to form tubular structures. Modification of high surface area materials with metals would be promising for construction of novel hydrogen storage composites, since some cooperative effect was found, for example, in a system comprising activated graphite and Zr [4]. BN can be prepared in a turbostratic layered form with high specific surface area [5], and there are more degrees of freedom to modify the structure as compared with carbonaceous compounds. In the present work, BN and Pd-modified BN samples with high specific surface areas were thus prepared by varied methods and their hydrogen storage capacities were evaluated.

2 Experimental

Preparation of BN was carried out by heating melamine borate, which was synthesized by mixing melamine and boric acid in hot water, first at up to 720 K in air for 110 min and secondly at 1170 K under nitrogen for 60 min. Modification of BN was carried out by three different methods. Non-electrolytic deposition (A) was performed using an aqueous solution of $Pd(NH_3)_4Cl_2$, EDTA and ammonia reduced by hydrazine. Modified BN was filtered, rinsed and dried overnight at 340 K. Immersion (B) was performed by sonicating BN in a methanol solution of palladium acetate. After filtration, rinsing and overnight drying at 340 K, the sample was heat treated at 520 K. Premixing followed by BN formation (C) was performed by sonicating melamine borate in an acetone solution of palladium acetate, filtration, rinsing, overnight drying at 340 K and heating at 1170 K under nitrogen.

The samples were characterized by SEM, XRD, FTIR and nitrogen adsorption measurements at 77 K. Hydrogen storage capacities were volumetrically evaluated at 297 K and 77 K.

3 Results and Discussion

Specific surface area of BN increased with that of starting melamine borate as shown in Figure 1. Since specific surface area of melamine borate was controllable by adjusting concentrations of melamine and boric acid, specific surface area of the calcined product, BN,

was also controllable in a range of 200-900 m^2 g^{-1}. The shape of BN observed by SEM was similar to that of melamine borate. The high specific surface area of BN would not be due to finely divided nature, but due to some porous structure of the sample.

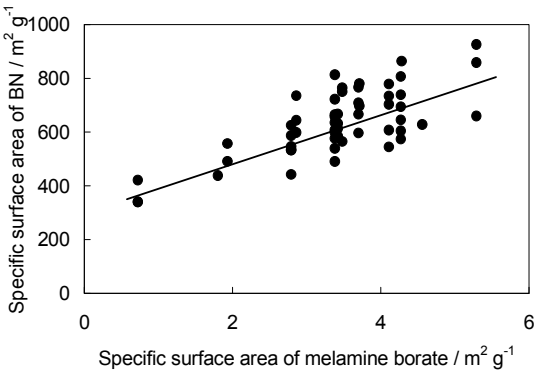

Figure 1: Variation of specific surface area of BN with that of melamine borate.

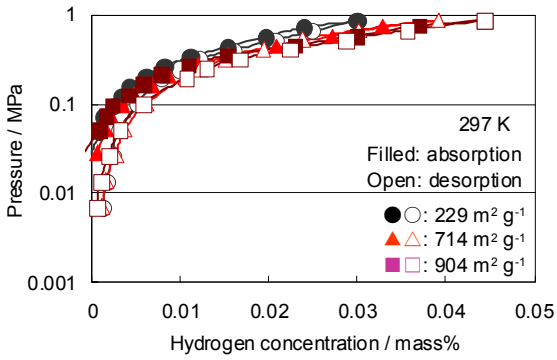

Figure 2: Hydrogen sorption isotherms at 297 K for BN with varied specific surface areas.

Hydrogen absorption-desorption isotherms in Figure 2 shows that the hydrogen storage capacity at room temperature was limited. Sorption was almost reversible and the amount of sorbed hydrogen rapidly increased under higher pressures. Sorption would proceed through physisorption. The hydrogen capacity increased with specific surface area as expected. Hydrogen sorption at 77 K was substantial as shown in Figure 3, and the amount of sorbed hydrogen again increased with specific surface area. Since the enhancement of sorption by cooling from room temperature to 77 K was about 50 times, the main scheme of sorption at 77 K would not be simple phisisorption, but would be pore filling.

When modification of BN with Pd was carried out by the method (A) or (B) after the preparation of BN, the turbostratic structure of BN was completely or partly destroyed as illustrated in Figure 4, and specific surface areas of the Pd-modified samples were diminished from 514 m^2 g^{-1} to 0.5 m^2 g^{-1} for the method (A) and to 9 m^2 g^{-1} for the method (B). In the case of the method (B), reflections from Pd were clearly observed in Figure 4. The intended dispersion of Pd was one Pd atom per nm^2 of the surface of BN, and the amounts of employed Pd compounds were weighed and added in accordance with that intension. Lowering of specific surface area of BN would cause excessive presence of Pd on the surface, and nucleation and growth of Pd particles would proceed to give the XRD pattern. On the other hand, the method (C), calcination of melamine borate preliminarily compounded with the palladium species, gave modified BN with large specific surface area as high as 800 m^2 g^{-1}, and the specific surface area value was adjusted by changing the nature of the starting melamine borate. The turbostratic layered structure of BN was clearly observed in the Pd-modified samples as shown in Figure 4.

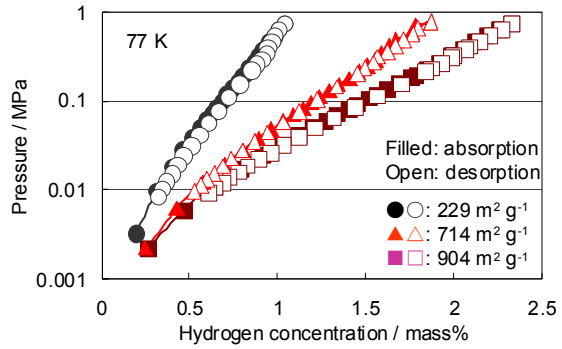

Figure 3: **Hydrogen sorption isotherms at 77 K for BN with varied specific surface areas.**

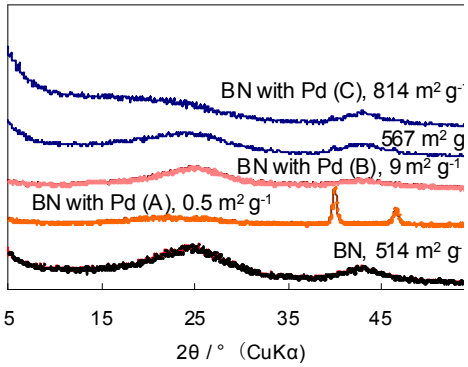

Figure 4: **XRD patterns from BN and Pd-modified samples through different methods.**

The method (C) gave porous structures to the modified samples, as was the case for BN itself, in addition to the layered structure. The presence of both micropores and mesopores was confirmed by the nitrogen adsorption isotherms in Figure 5 for the modified sample with specific surface area of 814 m^2 g^{-1}. Its feature was similar to a typical neat BN with close specific surface area of 714 m^2 g^{-1} as illustrated in Figure 5. While the difference of micropore volume between BN and the modified BN was reasonable considering the difference of specific surface area, the difference of mesopore volume between them was not. In other words, reduction of mesopore volume was observed for the modified BN through the presence of Pd.

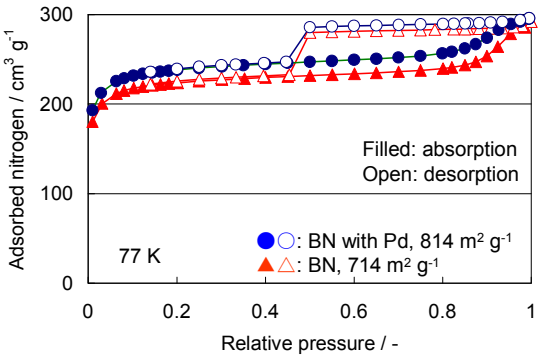

Figure 5: **Nitrogen adsorption isotherms at 77 K for BN and a typical Pd-modified sample.**

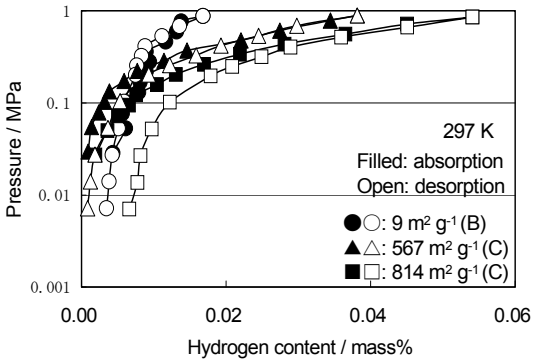

Figure 6: **Hydrogen sorption isotherms at 297 K for Pd-modified BN samples with varied specific surface areas.**

The modified BN with low specific surface area in Figure 6 sorbed less hydrogen than any BN in Figure 2. Collapse of the layered structure would be one of the causes of the reduction of the hydrogen capacity. The modified BN samples with high specific surface areas sorbed reasonable amounts of hydrogen as illustrated by the Isotherms in Figure 6. After the modification with Pd, some hydrogen irreversibly sorbed by the samples, although that was

not significant for the modified BN with specific surface area of 567 m^2 g^{-1}. Figure 7 comparatively shows actual isotherms for the modified BN with specific surface area of 814 m^2 g^{-1} and calculated isotherms based upon a linear combination of isotherms for Pd and BN with a little bit larger specific surface area of 904 m^2 g^{-1}. Hydrogen capacity of the modified sample exceeded the sum of that of neat BN and that of Pd, and a cooperative effect was observed at room temperature. That would be due to hydrogen dissociation sites provided by palladium and hydrogen accepting sites provided by BN. The irreversible nature again illustrated in Figure 7 for the modified BN suggested that those sites were chemisorption sites.

The cooperative effect would be found only for those modified samples with higher specific surface areas as suggested by Figure 8. The Pd modification would create the chemisorption sites on the victim of specific surface area nevertheless using the method (C).

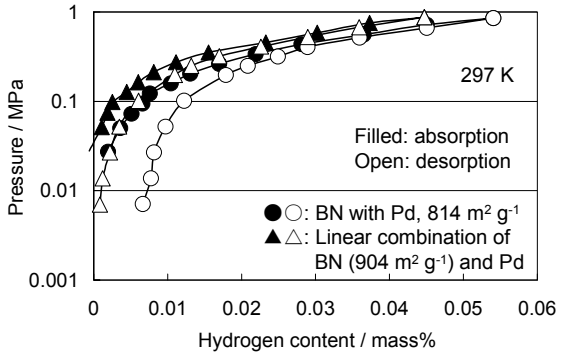

Figure 7: Comparative hydrogen sorption isotherms at 297 K for Pd-modified BN and a hypothetical mixture. The former is observed, and the latter is calculated on an assumption of simple mixing.

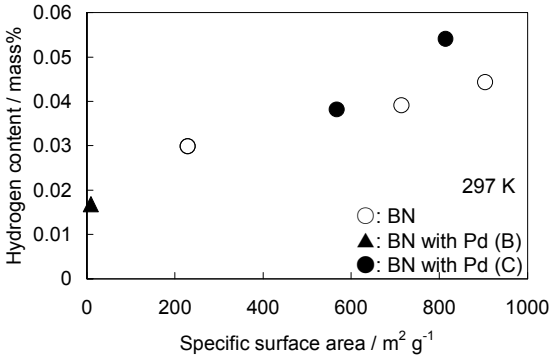

Figure 8: Variation of hydrogen sorption capacity at 297 K under 0.9 MPa with specific surface area for BN and Pd-modified samples.

The cooperative effect was not found at 77 K as shown in Figure 9. Isotherms for a modified sample with higher specific surface area almost coincided with those for BN with lower specific surface area. It is likely that pore filling of molecular hydrogen dominated at 77 K and that the presence of Pd would interfere with the filling flow of hydrogen. The reduction of the mesopore volume on the modification shown in Figure 5 supports that speculation. That is further depicted in Figure 10.

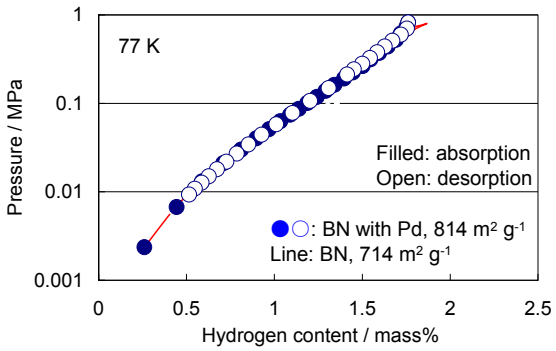

Figure 9: Comparative hydrogen sorption isotherms at 77 K for BN and a typical Pd-modified sample.

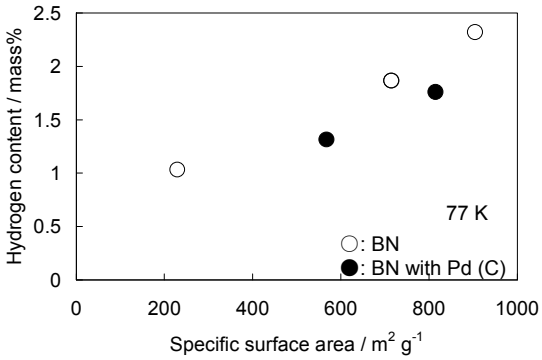

Figure 10: Variation of hydrogen sorption capacity at 77 K under 0.9 MPa with specific surface area for BN and Pd-modified samples.

4 Conclusion

BN modified with Pd had higher hydrogen capacity than the sum of hydrogen capacity of BN and that of Pd at room temperature, but such was not the case at 77K. Substantial hydrogen sorption of BN at 77 K would be due to micropores and mesopores, and that was not enhanced by the novel modification with Pd with high specific surface area retained. Specific surface area of BN increased with that of melamine borate, and hydrogen capacity increased with specific surface area of BN. That would be a guiding principle for constructing a new type of hydrogen storage material applicable at room temperature.

References

[1] Dillon A. C., K. M. Jones, T. A. Bekkedahl, C. H. Kiang, D. S. Bethune and M. J. Heben, “Storage of Hydrogen in Single-Walled Carbon Nanotubes,” Nature 386 (1997) 377-379.

[2] Panella B., M. Hirscher and S. Roth, “Hydrogen Adsorption in Different Carbon Nanostructures,” Carbon 43 (2005) 2209-2214.

[3] Nishimiya N., K. Ishigaki, H. Takikawa, M. Ikeda, Y. Hibi, T. Sakakibara, A. Matsumoto and K. Tsutsumi, “Hydrogen Sorption by Single-Walled Carbon Nanotubes Prepared by a Torch Arc Method,” J. Alloys and Comp. 339 (2002) 275-282.

[4] Mulana F., N. Nishimiya, H. Saito, A. Matsumoto and K. Tsutsumi, “Preparation and Characterization of Carbonaceous Material-Based Hydrogen Absorbing Composites,” J. Alloys and Comp. 372 (2004) 243-250.

[5] Hagio T., K. Kobayashi and T. Sato, “Formation of Hexagonal BN by Thermal Decomposition of Malamine Diborate,” J. Ceramic Soc. Japan 102 (1994) 1051-1054.

Influence of Metal Doping of a MOF-74 Framework on Hydrogen Adsorption

J.A. Botas, **G. Calleja**, **M.G. Orcajo**, Department of Chemical and Energy Technology, ESCET, Rey Juan Carlos University, Madrid, Spain
M. Sánchez-Sánchez, Instituto de Catálisis y Petroleoquímica, CSIC, C/ Marie Curie 2, 28049 Madrid, Spain

Abstract

Microporous Metal-Organic Framework (MOF) adsorbents are considered an interesting option for hydrogen storage. Due to their porous nature and unusually high surface areas, these materials show an exceptional H_2 uptake. Unfortunately, their interaction with H_2 molecules is weak, so cryogenic temperatures are required to reach competitive H_2 storage capacities. In this sense, the presence of coordinatively unsaturated and exposed metal centers in some MOF frameworks could increase the affinity for H_2 through stronger metal-H_2 interactions. In this preliminary work, the effect of doping a Zn^{2+}-MOF-74 framework with Co^{2+}, Cu^{2+} and Mg^{2+} on its adsorption properties for H_2 has been studied. Characterization studies suggest that the samples prepared have actually the MOF-74 structure, in which the different tested heteroatom ions have been successfully incorporated. The differences in H_2 adsorption at 77 K and 87 K between the MOF-74 samples doped with the mentioned divalent metal ions were discussed as a function of their free pore volume and amount of metal incorporation.

1 Introduction

Hydrogen is considered as the energy vector more promising because of its high efficiency and negligible environmental impact [1]. However, the difficulties associated to its producing, safely storing, and transporting in large quantities has limited its utility to date [2]. Hydrogen adsorption onto Metal-Organic Framework (MOF) materials is presented nowadays as a promising alternative among all technologies for hydrogen storage. It is now widely recognized that the interactions of hydrogen with porous host materials must be substantially increased in order to make MOFs efficient materials for H_2 storage.. In this sense, H_2-MOFs binding energies in the range 15-25 kJ/mol are clearly necessary [3], existing different approaches to face this challenge. Among them, the control of metal ion nature in open metal binding sites of certain metal-organic frameworks is probably one of the most promising. Crystallization of MOF materials with a given metal ion as well as metal doping of MOFs seem to be good alternatives to produce additional electrostatic forces contributing to increase the H_2 adsorption strength [4].

Kubas [5] described that the interaction metal-H_2 takes place through the *d* orbitals of a transition metal (M) with antibonding orbitals of the hydrogen molecule. The complexes M–H_2 can reversibly bind H_2, with a binding energy in the range 20–160 kJ/mol, which partially overlaps with the appropriate heat of adsorption range for high H_2 uptake at room

temperature [3, 6]. Kubas binding strategy has been recently followed to enhance H_2 binding with metal (transition metal) sites in MOFs [7a].

Theoretical [6] and experimental [7] studies with MOFs containing open metal sites of different elements (Zn, Mn, Co, Ni, Fe, Mg, V, Sc, etc.) have shown that it is possible to get high binding energies with H_2 up to 46.5 (theoretical studies) and 13.7 kJ/mol (experimental studies). Among these MOF materials, MOF-74 is an interesting material due to its relatively high affinity to hydrogen molecules, its thermal stability and its potential composition range [7c,d]. This material has been fully substituted with divalent metals ions such as Mg^{2+}, Ni^{2+}, Fe^{2+} and Co^{2+},but to the best of our knowledge, no partial substitution has been reported so far [8]. Apart from its application in gas adsorption uses, the doping of this material can have important implication in other fields like catalysis and semiconductor materials

In this work, partial isomorphic substitution of Zn-based MOF-74 clusters by Co^{2+}, Cu^{2+} and Mg^{2+} cations during the solvothermal synthesis, as well as its effect over their H_2 affinities and adsorption capacities, are studied and discussed.

2 Experimental Section

2.1 Synthesis

MOF-74 ($Zn_2(C_8H_2O_6)(DMF)_2(H_2O)_2$) was prepared basically following the procedure published elsewhere [10], in which 2,5-dihydroxybenzene-1,4-dicarboxylic acid and zinc nitrate tetrahydrated are dissolved in N,N-dimethylformamide. Once the reactants are dissolved, deionized water is added to form a mixture of molar composition 1 H_2DHBDC : 2,9 Zn : 523 DMF : 107 H_2O. This mixture is heated up to 100 ºC for 20 h to yield yellow needle crystals. After decanting and rinsing with DMF, the solid product was immersed in methanol for 6 days, during which the activation solvent was decanted and freshly refilled three times. The solvent was removed under vacuum at 150 °C, yielding the porous material. Metal-doped MOF-74 materials, denoted as Co10-MOF-74, Cu10-MOF-74 and Mg10-MOF-74, were synthesized following the same procedure but substituting 10 molar % of Zn by Co, Cu or Mg, respectively, using nitrate salts as metal sources.

2.2 Characterization techniques

Powder X-Ray Diffraction (PXRD) patterns were obtained in a Philips XPERT PRO using CuKα (λ = 1,542 Å) radiation. In order to avoid the effects of preferred crystal orientation, crystals were grounded. Mica sample was used as an internal standard to calculate the displacement error of the instrument. Thermogravimetric analyses (TGA) were carried out in a 100 ml/min flowing air atmosphere at a heating rate of 5 ºC/min up to 1000 ºC, using a TA Instruments SDT 2860 apparatus. Metal contents of the materials were measured by ICP (Inductively Coupled Plasma) atomic emission spectroscopy on a Varian Vista AX CD system. N_2 adsorption isotherms were measured on an AutoSorb equipment (Quantachrome Instruments). Previously, 0.02-0.04 g of the sample was in-situ evacuated under high vacuum for 18 h at 150 ºC. The micropore surface area values were calculated by the Brunauer-Emmett-Teller (BET) and Langmuir methods. Hydrogen adsorption isotherms were obtained in a Hiden Analytical Intelligent Gravimetric Analyser equipped with an ultra high vacuum system. The buoyancy effects were corrected as a function of temperature taking

into account the void volume of the cell determined with He at 77 K, and assuming that the amount of He adsorbed is negligible.

3 Results and Discussions

Powder X-ray diffraction (XRD) patterns of as-prepared non-doped and Metal-doped samples show that MOF-74 is the unique crystalline phase present in all samples [10], except for Cu10-MOF-74, where some reflections of an unidentified phase were detected (Figure 1).

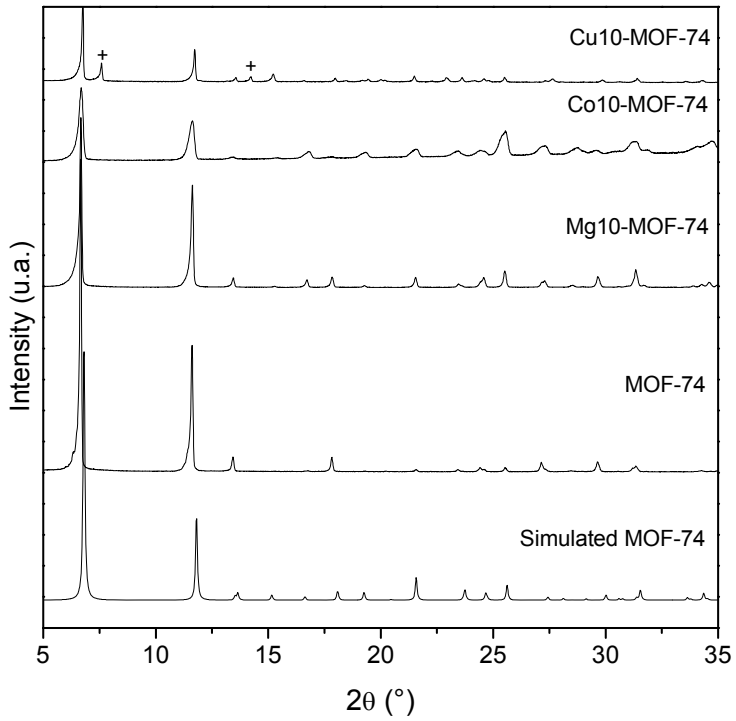

Figure 1: Experimental powder XRD patterns of MOF-74 materials. (+: Unidentified phase).

All powder XRD patterns were indexed on the basis of a face-centered hexagonal unit cell with resulting values summarized in Table 1, which are in good agreement with their ionic radii (Zn^{2+} > Cu^{2+} > Mg^{2+} > Co^{2+}). The differences in the unit cell parameters obtained qualitatively support the metal incorporation into the MOF-74 framework.

Table 1: Unit Cell Parameters of MOF-74 materials.

Sample	Co content (wt. %)	Parameter *a* = *b*	Parameter *c*
MOF-74	0	26.188	6.771
Co10-MOF-74	14	26.098	6.841
Cu10-MOF-74	17	26.144	6.781
Mg10-MOF-74	5	26.106	6.790

Thermogravimetric analysis (TGA/DTG) curves of as-synthesized MOF-74, Co10MOF-74, Cu10MOF-74 and Mg10MOF-74 samples are shown in Figure 2. The first weight loss produced around 115 ºC can be attributed to the solvent (DMF/H_2O) removal from the cavities. The next main weight loss in the range 300 - 375 °C, (precise temperatures are explicitly indicated in Figure 2), corresponds to the organic ligand decomposition and thus provides an indication of the thermal stability of MOF-74 framework in air atmosphere. The thermal stability is different for each MOF-74 sample, which indirectly confirms the incorporation of the doping metal into the framework.

The porosity of these materials was measured by nitrogen adsorption-desorption at 77 K. All of them exhibit permanent microporosity, as evidenced by the reversible type I N_2 adsorption isotherms, according to IUPAC, which correspond to microporous materials [11]. Textural properties estimated from N_2 isotherms of all MOF-74 samples, summarized in Table 2, are very similar, which is not surprising when the metal ions are incorporated in MOF-74 instead of forming extra-framework species. As an exception, Co10-MOF-74 exhibits slightly better textural properties than the rest, probably because the activation treatment was somehow more effective.

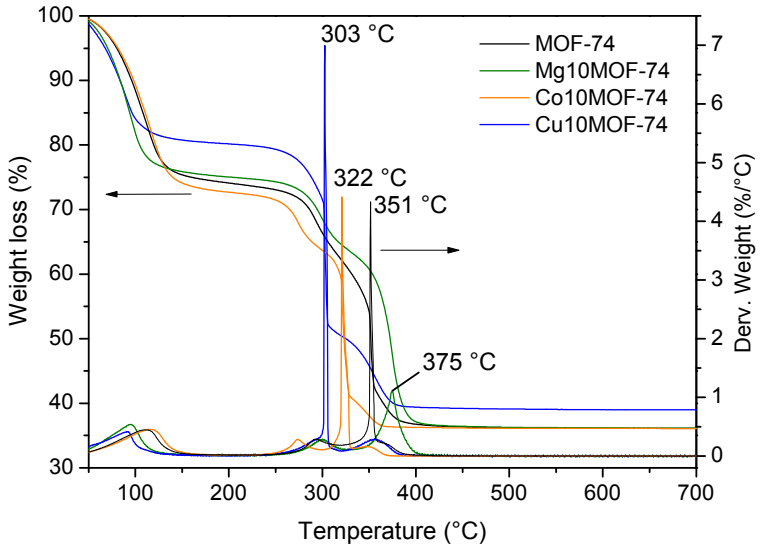

Figure 2: TGA/DTG in air atmosphere curves of MOF-74 samples.

Table 2: Textural properties and H_2 adsorption capacity of activated MOF-74 samples.

Sample	S_{BET} ± 40 (m^2/g)	S_{Lang} ± 50 (m^2/g)	Vm_{NL-DFT} ± 0.04 (cm^3/g)	H_2 adsorbed (wt. %) 77 K	Q_{st} H_2[a] kJ/mol
MOF-74	850	960	0.34	2.16	7.9
Co10-MOF-74	1111	1270	0.49	3.08	9.3
Cu10-MOF-74	822	935	0.41	1.62	9.6
Mg10-MOF-74	900	1024	0.44	3.01	8.2

[a] Q_{st} was measured for 0.3 wt. % of H_2 coverage.

Gravimetric hydrogen adsorption capacities for doped and non-doped MOF-74 materials were measured at 77 K and up to 10 bar (Table 2 and Figure 3). All doped samples adsorb significantly higher amount of hydrogen than the non-doped MOF-74 under the same conditions of temperature and pressure, except for Cu10-MOF-74 material, which is the only doped MOF-74 with hydrogen uptake lower than the Zn-based MOF-74. This low H_2 uptake value could be related to the presence of the unidentified phase observed by powder XRD, whose proportion increases along the adsorption process, as it was made clear by an XRD study after this treatment. The magnitude of interaction between hydrogen molecules and MOF framework was checked by measuring the isosteric heat of hydrogen adsorption, Q_{st} (Table 2), estimated from the hydrogen adsorption isotherms at 77 and 87 K. It is noteworthy that despite of the lower porosity of Cu10-MOF-74 compared to the other samples, the Q_{st} value of this material appears to be the highest. Therefore, the low H_2 uptake is a question of phase purity rather than simple gas affinity. The hydrogen uptakes of the materials was in the decreasing order Co10-MOF-74 > Mg10-MOF-74 > Zn10-MOF-74 > Cu10-MOF-74, whereas for Q_{st} was Cu > Co > Mg > Zn, a result which agree with the results published for CPO-27 (isostructural to MOF-74) prepared with Co, Mg and Zn [8a].

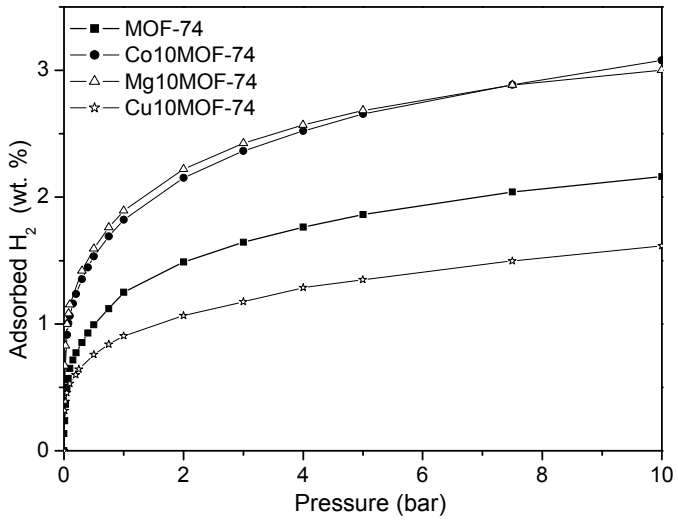

Figure 3: Hydrogen adsorption of MOF-74 materials at 77 K and up to 10 bar.

4 Conclusions

Partial doping of the open-metal-sites of a MOF-74 framework was carried out. Evidence for metal substitution of Zn sites by other divalent metals in the MOF-74 framework was provided by PXRD (unit cell parameters), TGA and N_2 adsorption at 77 K. MOF-74 materials doped with Co and Mg showed a significant enhance in H_2 uptake at 77 K and 10 bar, compared to the non-doped material. Nevertheless, Cu10-MOF-74 was not purely crystallized, so its H_2 uptake is much lower. Additionally, doped MOF-74 homologues exhibited higher affinity to H_2 molecules than Zn-based MOF-74, particularly for the sample doped with copper, a result that suggests the challenge of preparing all-Cu or pure Cu-doped MOF-74 materials. The important differences in hydrogen affinity and uptake, as well as the difference in thermal stability, support the assumption that metal ions are actually incorporated into the MOF-74 framework. This study opens the possibility of doping different MOFs materials, and particularly those which have exposed centers, thorough a non-post-synthesis strategy, for improving their adsorption properties as well as for catalysis applications.

Acknowledgment.

The authors wish to thank ‘‘Comunidad de Madrid’’ and Spanish Ministry of Science and Innovation for their financial support to the SOLGEMAC Project through the Programme of Activities between Research Groups (S2009/ENE-1617) and CICYT (Project CTQ2009-11934), respectively.

References

[1] D. Britt, H. Furukawa, B. Wang, T. Grant Glover and O.M. Yaghi, *PNAS*, 2009, **106**, 20637.

[2] S.R. Caskey and A.J. Matzger, *Material Matters*, 2010, **4**, 111.

[3] J.L.C. Rowsell and O.M. Yaghi, *Angew. Chem. Int. Ed*., 2005, **44**, 4670.

[4] L.J. Murray, M. Dinca and J.R. Long, *Chem. Soc. Rev*., 2009, **38**, 1294.

[5] G.J. Kubas, *Chem. Rev*., 2007, **107**, 4152.

[6] Q. Yang and C. Zhong, *J. Phys. Chem. B*, 2006, **110**, 655; M. Dinca, A. Dailly, Y. Liu, C.M. Brown, D.A. Neumann and J.R. Long, *J. Am. Chem. Soc*., 2006, **128**, 16876; M. Kosa, M. Krack, A.K. Cheetham and M. Parrinello, *J. Phys. Chem. C*, 2008, **112**, 16171.

[7] M. Dinca and J. Long, *J. Am. Chem. Soc*., 2007, **129**, 11172; B.L. Chen, N.W. Ockwig, A.R. Millward, D.S. Contreras and O.M. Yaghi, *Angew. Chem. Int. Ed*., 2005, **44**, 4745; P.M. Forster, J. Eckert, J.-S. Chang, S.-E. Park, G. Férey and A.K. Cheetham, *J. Am. Chem. Soc*., 2003, **125**, 1309; L. Kong, G. Roman-Perez, J. Soler and D. Langreth, *Phys. Rev. Lett*., 2009, **103**, 96103.

[8] W. Zhou, H. Wu and T. Yildirim, *J. Am. Chem. Soc*., 2008, **130**, 15268; P.D.C. Dietzel, Y. Morita, R. Blom and H. Fjellv, *Angew. Chem*., 2005, **117**, 6512; P.D.C. Dietzel, Y. Morita, R. Blom and H. Fjellv, *Angew. Chem. Int. Ed*., 2005, **44**, 6354; P.D.C. Dietzel, B. Panella, M. Hirscher, R. Blom and H. Fjellv, *Chem. Commun*., 2006, 959; P.D.C. Dietzel, R.E. Johnsen, R. Blom, and H. Fjellv, *Chem. Eur. J*., 2008, **14**, 2389; S.

Bhattacharjee, J-S. Choi, S-T. Yang, S. Choi, J. Kim and W-S. Ahn, *J. Nanosc. Nanotechnol*., 2010, **10**, 135.

[9] E. Klontzas, A. Mavrandonakis, E. Tylianakis and G. E. Froudakis, *Nano Lett*., 2008, **8**, 1572; S.S. Han and W.A. Goddard III, *J. Am. Chem. Soc*., 2007, **129**, 8422; Y.J. Choi, J.W. Lee, J.H. Choi and J.K. Kang, *Appl. Phys. Lett*., 2008, **92**, 173102; S.S. Han, J.L. Mendoza-Cortés and W.A. Goddard III, *Chem. Soc. Rev*., 2009, **38**, 1460.

[10] J.L.C. Rowsell and O.M. Yaghi, *J. Am. Chem. Soc.,* 2006, **128**, 1304.

[11] K.S.W. Sing, D.H. Everett, R.A.W. Haul, L. Moscou, R.A. Pierotti, J. Rouquerol and R. Siemieniewska, *Pure Appl. Chem*., 1985, **57**, 603.

Magnesium-based Nanocomposites Synthesized by High-energy Ball Milling for Hydrogen Storage

H. Imamura, **S. Nakatomi**, **K. Tanaka**, **Y. Hashimoto**, **Y. Sakata**, Yamaguchi University, Tokiwadai, Japan

Abstract

Nanocrystalline MgH_2 obtained by ball milling with cyclohexane or benzene showed excellent properties for hydrogen storage. 1 at% Al-added nanocrystalline magnesium samples obtained by milling of MgH_2 with solutions of $Al(C_2H_5)_3$ in benzene showed the reversible hydrogen absorption/desorption cycles even at 0.1 MPa of hydrogen. Moreover, the hydrogen storage properties of magnesium hydride were markedly improved upon nanocomposite formation by ball milling of MgH_2 with Sn or SiC. For MgH_2/Sn and MgH_2/SiC nanocomposites, the dissociation temperature at 0.1 MPa of hydrogen was raised, compared to that for MgH_2.

1 Introduction

Magnesium and magnesium-containing systems (alloys and composites) are potential materials for hydrogen storage due to the high hydrogen storage capacity, the low cost and weight. However, their slow sorption kinetics and high thermodynamic stability of the hydride is a serious barrier to practical applications. Interest has recently centered on the topic of modifying the hydrogen storage properties of magnesium hydride.

In the present work the hydrogen storage properties of the nanocrystalline magnesium hydride obtained by ball milling of MgH_2 with cyclohexane or benzene are studied by X-ray diffraction (XRD), differential scanning calorimeter (DSC), thermal desorption spectrometry (TDS), thermogravimetry (TG) and pressure-composition isotherm (PCT) [1,2]. For nanocrystalline MgH_2 thus obtained, interesting features of the hydrogen desorption behavior are presented. For MgH_2/Sn [2,3] and MgH_2/SiC [4] nanocomposites we elucidate the hydrogen storage properties of magnesium hydride which are markedly improved upon ball milling of MgH_2 with Sn and SiC, respectively.

2 Experimental Procedure

MgH_2 (98 %), SiC and Sn (99.9 %) powders were purchased from Wako Pure Chemical Ind., Ltd. and Rare Metallic Co., Ltd., respectively. Cyclohexane and benzene used were reagent grade (>99.5%).

The preparation of nanocrystalline MgH_2 [1,2] and Mg-based nanocomposites (MgH_2/Sn [2,3] and MgH_2/SiC [4]) was carried out using a planetary-type ball mill (Kurimoto Ltd.; High G, BX 254), being capable of operating at a 863-rpm maximum speed. In a typical preparation of nanocrystalline MgH_2, MgH_2 (3.0 g) and cyclohexane (2.0 cm^3) were placed in a grinding bowl (coated with zirconia; cylindrical shape with volume of 160 cm^3) flushed thoroughly with dry nitrogen. The mixtures were subjected to ball milling with balls (zirconia; diameter 3 mm;

112 g) for 3 h. All operations concerning the magnesium samples were carried out without exposure to air.

The magnesium samples thus obtained were examined by XRD (Rigaku X-ray diffractometer, RINT 2200), DSC (TA Instruments Q10), TDS, TG (TA Instruments, TGA 2850 Thermogravimetric Analyzer) and PCT measurements (Suzuki Shokan Co. Ltd., PCT-1SDWIN).

3 Results and Discussion

3.1 Nanocrystalline MgH_2

In the hydrogen storage properties of nanocrystalline MgH_2 obtained by ball milling techniques, ball milling of MgH_2 with cyclohexane or benzene resulted in improvement of the absorption and desorption properties [1,2]. Interestingly, the desorption temperatures of the nanocrystalline MgH_2 were strongly dependent upon the rehydrogenation temperatures; the sample rehydrogenated at 290 K showed a lower desorption temperature by about 90 K than that rehydrogenated at 453 K [2]. Such a desorption behavior is associated with lattice defects such as dislocation and vacancy introduced during rehydrogenation.

Moreover, as shown in Figure.1, the reversible hydrogen absorption by 1 at% Al-added nanocrystalline MgH_2, obtained by milling of MgH_2 with solutions of $Al(C_2H_5)_3$ in benzene, was observed with a maximal capacity of 7.3 wt% even at a 0.1 MPa H_2 atmosphere [1].

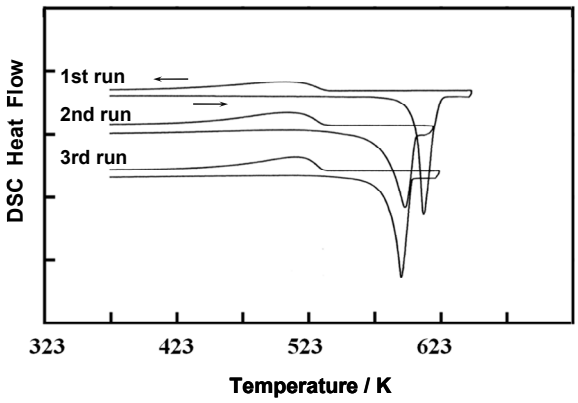

Figure 1: DSC traces of 1 at% Al-added MgH2 obtained by ball milling of MgH2 with solutions of Al(C2H5)3 in benzene for 3 h.

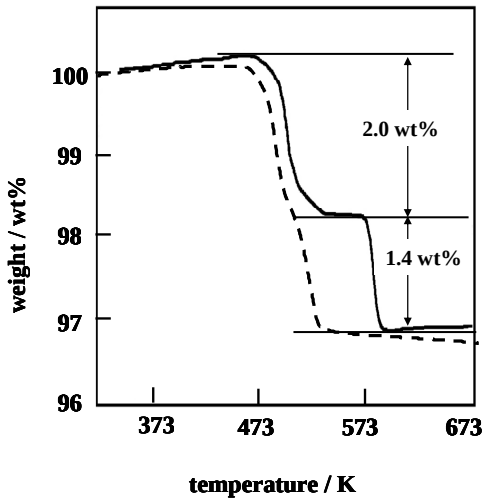

Figure 2: TG of MgH2/Sn measured in a flow of hydrogen (solid line) or helium (dotted line) at 0.1 MPa.

3.2 MgH_2/Sn and MgH_2/SiC nanocomposites

Upon ball milling of the nanocrystalline MgH_2 with Sn [2,3] or SiC [4], the properties of MgH_2 were further improved for hydrogen storage. TDS, TG, DSC and PCT measurements indicated the formation of MgH_2/Sn or MgH_2/SiC nanocomposites as a result of ball milling of MgH_2 with Sn or SiC, respectively, instead of a mere physical mixture.

As shown by TG measurements, the nanocomposite obtained when MgH_2 was ball-milled with 17 at% Sn contained two types of hydrogen species; the one was hydrogen (2.0 wt%) produced newly as a result of MgH_2/Sn nanocomposite formation and the other hydrogen (1.4 wt%) derived from MgH_2 remaining in MgH_2/Sn [3]. The properties of the MgH_2/Sn nanocomposite were further discussed in comparison with those of the physical mixture of MgH_2 and Sn [2].

Moreover, the hydrogen storage properties of MgH_2 were markedly modified upon ball milling with SiC [4]. The desorption temperatures of MgH_2/SiC tended to drop with increasing the composition of SiC (10-75 mol%) in the nanocomposites. The hydrogen desorption of MgH_2 as a starting material was observed around 705 K in TDS, while MgH_2 milled with 10 mol% SiC showed the desorption around 480 K. The hydrogen in MgH_2/SiC (75 mol%) was more destabilized, leading to lowering of the desorption temperature to about 437 K. XRD showed that in the nanocomposites with different compositions of SiC the magnesium constituent was highly dispersed in both the hydrogenation state and the dehydrogenation state. The hydrogen storage properties, especially desorption temperatures and thermodynamic parameters, were significantly improved as a result of nanocomposite formation by milling MgH_2 with 75 mol% SiC.

For MgH_2/SiC (75 mol%) obtained under different milling conditions, ball milling at 863 rpm for 0.5 h was fit to form the nanocomposites as shown in DSC traces (Figure. 3). In DSC measured under a 0.1 MPa hydrogen atmosphere, the two endothermic peaks assigned to dehydriding of MgH_2/SiC nanocomposites and MgH_2 remaining in MgH_2/SiC were observed around 520-570 K and 590-610 K, respectively. Taking into account the fact that the dissociation temperatures for the Mg-H system at 0.1 MPa hydrogen were about 560 K [5], the dehydriding temperature observed from 520 K was too low for MgH_2, indicating the formation of MgH_2/SiC nanocomposites. Ball milling at 650 rpm for 0.5 h was inadequate for the formation of nanocomposites; dehydriding of MgH_2 was exclusively observed around 590 K. In ball milling at 863 rpm for 0.5 h, the DSC peak corresponding to dehydriding of MgH_2 decreased, whereas that for the nanocomposites increased conversely.

PCT measurements of MgH_2/SiC (75 mol%) were carried out to evaluate further the properties of the hydrogen in the nanocomposites [4]. The sample was first subjected to the desorption isotherm measurements at 573 K with lowering hydrogen pressures from 10 MPa to 0.001 MPa, followed by pressurizing hydrogen to 10 MPa to measure the absorption isotherms. Finally the desorption isotherms were measured with the same procedures again. As shown in Figure. 4, the PCT traces obtained in the first desorption process were obviously different from that of MgH_2; the equilibrium pressures at 573 K were much higher than those predicted for MgH_2. This is consistent with the DSC results (Figure. 3) described previously. Thus MgH_2 was destabilized upon ball milling with SiC.

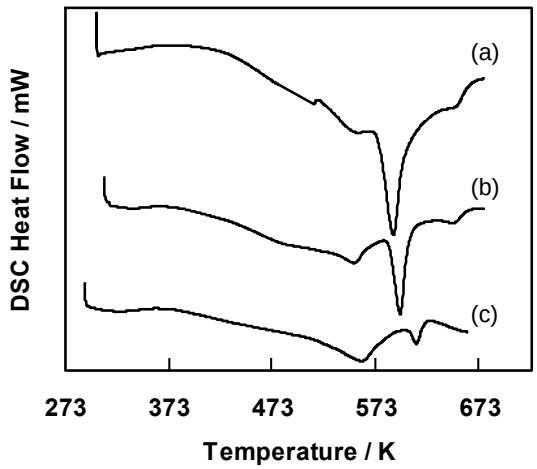

Figure 3: DSC traces at 0.1 MPa of hydrogen for MaH2/SiC (75 mol%) prepared under different milling conditions: (a) 650 rpm, 0.5 h; (b) 863 rpm, 0.25 h; and (c) 863 rpm, 0.5 h.

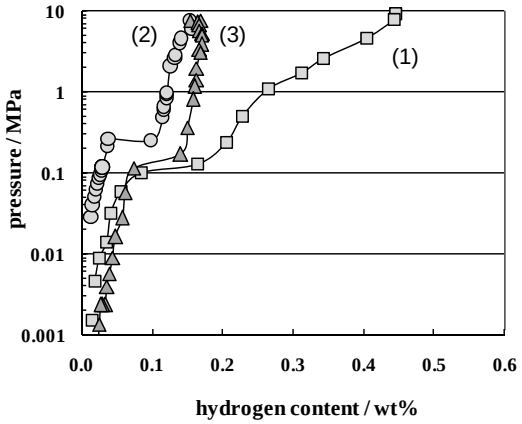

Figure 4: Pressure-composition isotherms at 573 K for MgH2/SiC (75 mol%). Desorption/adsorption cycles, (1) → (2) → (3).

However, the equilibrium pressures obtained for the following absorption (2) and desorption (3) processes at 573 K were very close to those of MgH_2. This indicates that the nanocomposites irreversibly broke down partly into magnesium and SiC at temperatures above 573 K. The absorption (2)/desorption (3) isotherms observed in Figure. 4 is probably attributed to the magnesium component generated after a breakdown at elevated temperatures.

For MgH_2/SiC nanocomposites, the reversibility of hydrogen absorption/desorption was certainly observed at lower temperatures.

References

[1] H. Imamura, K. Masanari, M. Kusuhara, H. Katsumoto, T. Sumi and Y. Sakata, J. Alloys Comp. 386 (2005) 211.

[2] H. Imamura, K. Tanaka, I. Kitazawa, T. Sumi, Y. Sakata, N. Nakayama and S. Ooshima, J. Alloys Comp. 484 (2009) 939.

[3] H. Imamura, K. Yoshihara, M. Yoo, I. Kitazawa, Y. Sakata and S. Ooshima, Int. J. Hydrogen Energy, 32 (2007) 4191.

[4] H. Imamura, S. Nakatomi, Y. Hashimoto, I. Kitazawa, Y. Sakata, H. Mae and M. Fujimoto, J. Alloys Comp. 488 (2009) 265.

[5] J. F. Stampfer Jr., C. E. Holley Jr., J. F. Suttle, J. Am. Chem. Soc. 82 (1960) 3504.

Hydrogen Storage by Functionalised Poly(ether ether ketone)

R. Pedicini, **G. Giacoppo**, **A. Carbone**, **E. Passalacqua**, CNR-ITAE, Institute for Advanced Energy Technologies, Messina, Italy

Abstract

In this work a functionalised polymer was studied as potential material for hydrogen storage in solid state. A Poly(ether ether ketone) (PEEK) matrix was modified by a manganese oxide *in situ* formation. Here we report the functionalisation process and the preliminary results on hydrogen storage capability of the synthesised polymer.

The polymer was characterized by Scanning Electron Microscopy, X-ray diffraction, Transmission Electron Microscopy and Gravimetric Hydrogen Adsorption measurements. In the functionalised PEEK, morphological changes occur as a function of oxide precursor concentration and reaction time. Promising results by gravimetric measurements were obtained with a hydrogen sorption of 0.24%wt/wt at 50 °C and 60 bar, moreover, reversibility hydrogen adsorption and desorption in a wide range of both temperature and pressure was confirmed.

1 Introduction

The development of hydrogen as a reliable energy vector is strongly connected to the cost, performance and level of safety of the storage system components. The actually investigated hydrogen storage methods are based on high-pressure gas tank, cryogenic tank for liquid hydrogen, adsorbed hydrogen on materials with a large specific surface area, absorbed hydrogen on interstitial sites in a host metal (at ordinary temperature and pressure), chemical storage in complex hydrides and oxidation of reactive metals with water (e.g. Li, Na, Mg, Al, Zn) [1-4]. In the last years, nevertheless the research progresses, no one of these methods meets the DOE targets for a real application. Several materials for physical and chemical hydrogen storage have been proposed, but few research works were devoted to polymer based materials, that are generally low cost and weight, easy to be managed and manufactured. A new approach based on polymers able to store hydrogen has been proposed by Cho et al.[5], by using a HCl-treated polyaniline and polypirrole, even if other authors [6] have tried to reproduce this results without success. In fact, a functionalised polymer containing a nanometric metal oxide was developed as a hydrogen storage material. A commercial Poly-ether-ether-ketone (PEEK) was selected as a matrix for its chemical-physical characteristics. A manganese oxide was linked onto the polymeric matrix as a metal compound able to promote the hydrogen storage. The manganese oxide was chosen as a hydrogen storage material for both its crystalline structure [7] and its easy production in the in-situ reaction. The preliminary results show that this approach can be useful for the hydrogen storage

2 Experimental

2.1 Materials Preparation

A commercial PEEK (Victrex 450PF) was functionalised via an electrophilic aromatic substitution with chlorosulfonic acid (Aldrich) at 30 °C under stirring for 24 h. Successively, the obtained chlorosulfonated polymer (SPEEKCl) was precipitated in cold water and completely dried in an oven at 70 and 120 °C. A $KMnO_4$ solution was added to chlorosulfonated polymer, under stirring for 2.5 h at room temperature, then the temperature was increased at 50 °C maintaining it for different reaction times (tab.1). During the reaction time, the yellow starting polymer has changed its colour until to dark brown, meaning that the formation of manganese oxide occurred. Then, the material was filtered and washed several times until to a neutral pH and the redox reaction that produces manganese oxide was followed through the identification of Cl^- ions (Chlorine test) by using a $AgNO_3$ 1N solution. Three different powders were prepared changing the permanganate concentration and reaction time, as reported in Table1.

Table 1

Sample	[$KMnO_4$]	$T_{reaction}$	$time_{reaction}$
SPMnO2A	0.02M	50 °C	1h
SPMnO2B	0.02M	50 °C	3h
SPMnO2E	0.1M	50 °C	1h

2.2 Material characterisation

The SPEEKCl sulphonation degree (DS) was determined from the experimental and theoretical S/C ratio, through elemental analysis (CHNS-O Analyzer Thermo Flash mod. EA 1112), where the theoretical S/C was calculated assuming the complete sulphonation of the polymer [8]. The qualitative difference among the obtained powders were evidenced with an optical microscope (Nikon SMZ 1500). The acidity of the functionalised polymers was checked by measuring the slurry pH. The amount of the produced oxide was calculated weighting the residual mass at 1000 °C, temperature above the decomposition temperature of the polymer [9]. A field emission Scanning Electron Microscope equipped with EDAX microprobe (Philips mod. XL30 S FEG) was used to investigate the morphology and to reveal the presence of the elements on the polymeric powders. The X-ray powder diffraction (XRD) analyses were performed by using a Philips X-ray automated diffractometre (model PW3710) with Cu Kα radiation source. The 2θ Bragg angles were scanned between 5 ° and 100 °.

The morphology of the prepared powders was observed by using a Philips CM12 transmission electron microscope (TEM), with a LaB_6 filament at an accelerating voltage of 120kV. Samples were prepared by placing few drops of a sonicated alcoholic dispersion on the surface of a copper grid. Hydrogen storage capability on SPMnO2A was measured by Magnetic Suspension Balance (Rubotherm), consisting of a measuring cell with a sample holder magnetically coupled with an external balance. The percentage variation is calculated respect to the initial sample weight for each pressure step. At the beginning, the sample was

treated at about 100 °C for 24h in the same measurement chamber. The measurements were carried out by varying the pressure and temperature in a range of 1-60 bar and 32-110 °C, respectively.

3 Results and Discussion

The PEEK polymer was functionalized with chlorosulphonic acid to obtain an highly chlorosulphonated precursor able to participate to the redox reaction producing manganese oxide and acting as a polymer support [10]. From CHNS-O analyses, a S/C ratio experimental value of 0.141 was found for the sulfonated polymer, that corresponds to the theoretical value (0.140) for a sulfonation degree of 100%, so we deduced that the complete functionalisation reaction is occurred. In Fig.1 are reported the photos of the precursor and the prepared samples, it is evident that a low $KMnO_4$ concentration and reaction time produce a brown spongy powder (b), while more strong reaction parameters allow to produce a dark grey and compact powders.

(a) (b) (c) (d)

Figure 1: Photos of the samples a) SPEEKCl, b) SPMnO2A, c) SPMnO2B, d) SPMnO2E.

The precursor and the obtained powders were dispersed in water monitoring the pH. The highly chloro-sulfonated precursor decreases the water pH from 5.5 to 3.8, meaning that the functionalisation reaction produces a partial chlorosulfonation associated to a sulfonation (SO_3H) responsible of the acidic groups presence. A different behaviour is found depending on the synthesized material, in fact, a less acidic pH was found for SPMnO2A (pH=4.5), which underwent a mild reaction conditions. In a strong reaction environment (prolonged time or more concentrated reactant) the pH values increase to approach the neutral pH (5.1 for SPMnO2B and 6.0 for SPMnO2E). To determine the amount of produced oxides an aliquot of samples was calcined obtaining a dry residue of 15%, 20% and 38% for SPMnO2A, SPMnO2B and SPMnO2E respectively, attributable to the oxides presence. In Fig. 2, SEM images, at a magnification of 5000X are reported. The precursor (Fig. 2-a) presents agglomerates in a filamentous form, the successive introduction of the manganese oxide in mild condition reaction (Fig. 2-b) does not produce a significant morphological modification but a more compact morphology is obtained when more strong reaction conditions are used (Fig. 2-c and d).

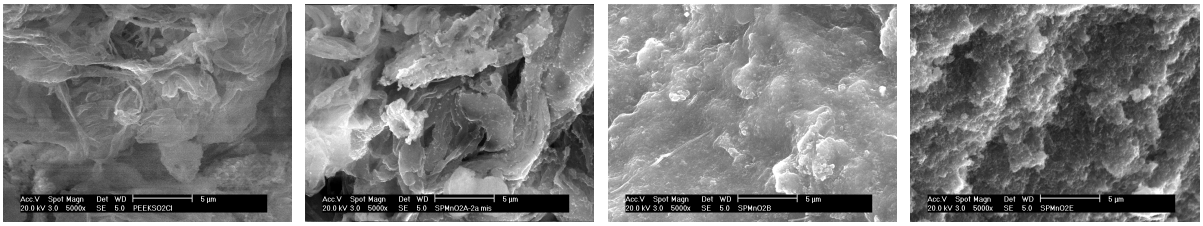

(a) (b) (c) (d)

Figure 2: SEM images of the samples a) SPEEKCl, b) SPMnO2A, c) SPMnO2B, d) SPMnO2E.

The EDX mapping performed during SEM measurements has revealed the contemporary presence of the manganese, potassium and chlorine elements indicating that the redox reaction between the precursor and the permanganate is probable incomplete, even if the amount of potassium and chlorine decreases by using more strong reaction conditions. To evaluate the presence of oxide supported on to the polymeric matrix, a XRD screening was carried out and compared to the precursor material, as reported in Fig. 3.

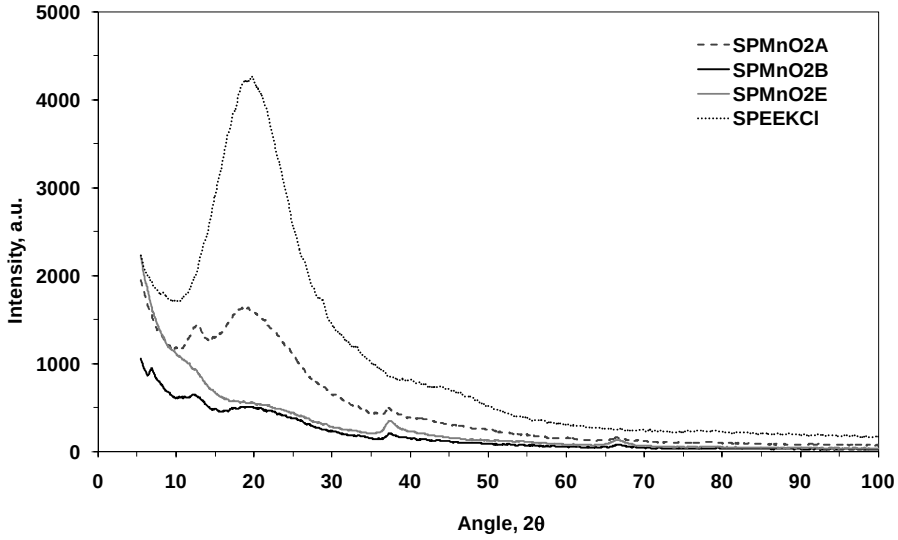

Figure 3: XRD profiles of precursor and prepared powders.

The precursor shows an amorphous structure typical of the functionalised polymer [8] centred at about 2θ=20 °, this profile is maintained in all the supported samples even if it is less pronounced with the increase of the manganese oxide content. All the other samples present three peaks (2θ=12 °, 37 ° and 66 °) related to the manganese oxide presence. The peak at 2θ=12 ° corresponds to the diffraction peak of layered manganese oxide of Barnesite type [10]. This peak intensity decreases when more strong reaction conditions are used (SPMnO2B and SPMnO2E), due to a probable different oxide structure [11]. In any case, the peaks related to the oxide profile are mainly attributable to an amorphous structure[10]. To better understand the influence of the reaction conditions on the morphology of the prepared compounds a TEM analysis was carried out on the SPMnO2A and SPMnO2E, obtained with mild and strong reaction conditions, respectively (Fig.4).

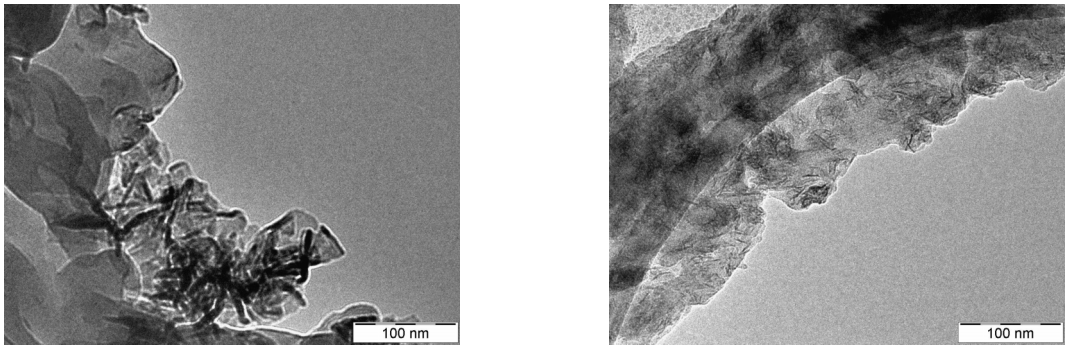

(a) (b)

Figure 4: TEM images of the samples a) SPMnO2A at 57kX of magnitude, b) SPMnO2E at 57kX of magnitude.

All the TEM images show a layered structure morphology, but the sample SPMnO2A reveals an higher tendency to curl and to grow into a tubular structure than sample SPMnO2E [11], in accordance with XRD profiles. The sample SPMnO2A, due to its pronounced lamellar structure, seems to be the most promising sample to store hydrogen. To evaluate its capability, gravimetric analyses at different temperatures and pressures were carried out on this material. In Fig.5a the hydrogen sorption-desorption cycles at 110 °C up to 40 bar are reported. The total H_2 sorption corresponds to the sum of the single steps obtained with 2-20 and 20-40 bar and this process is reversible. In Fig.5b the cycles from 2 bar up to 60 bar are shown, also in this case the reversibility is maintained even if a decrease of the H_2 sorption was found in the second cycle. This behaviour could be attributable to a possible structure change of the oxide due to the high pressure used in the measurement [11]

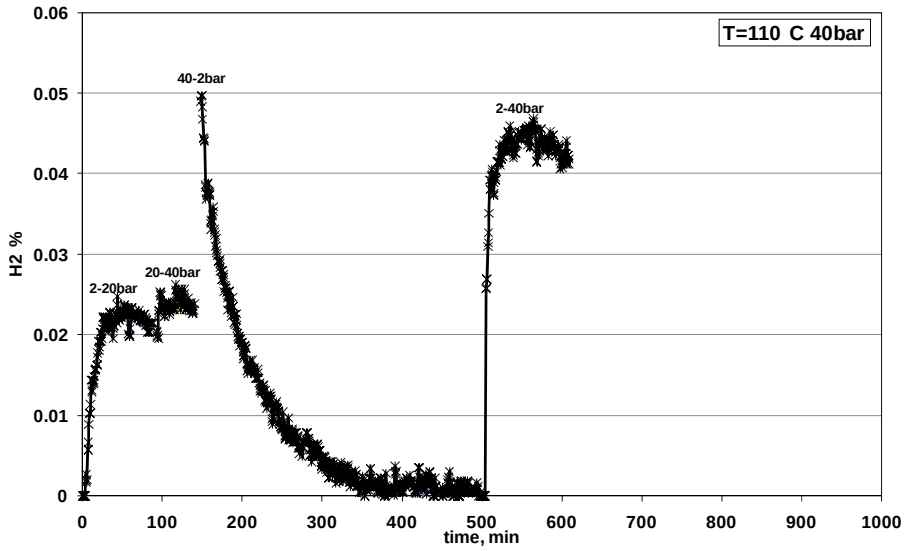

(a)

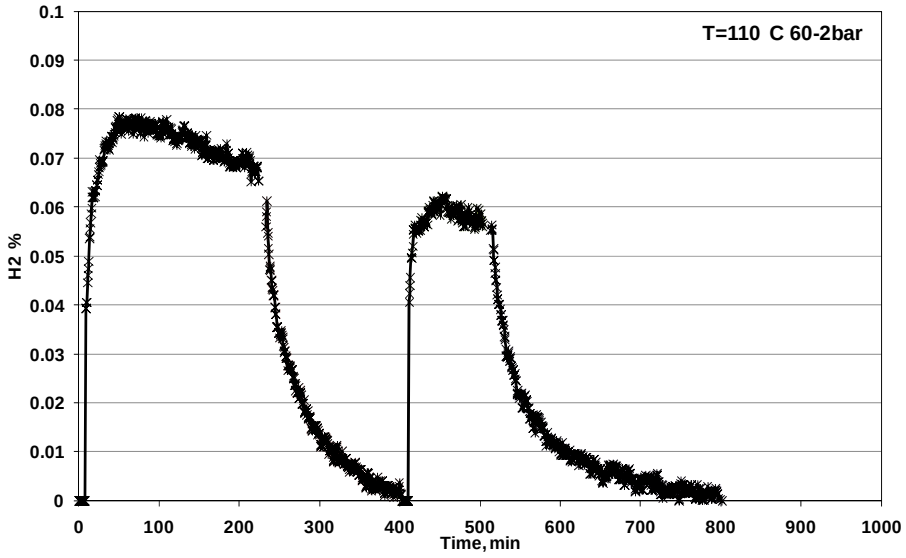

(b)

Figure 5: Hydrogen sorption-desorption cycles at 110 °C (a) up to 40 bar, (b) from 2 bar up to 60 bar.

To verify the behavior at low temperatures, tests at 50 °C and 32 °C were conducted, as reported in Fig. 6. At 50 °C the pressure increase up to 60 bar through the following steps: 2-10, 10-20, 20-40 and 40-60 bar. As it can be seen, also in this measurement, the total weight percentage of hydrogen sorption is the sum of each pressure step. In the last one, the sample was maintained for a long time (about 16 hours) at 60 bar to verify the sample stability. During this time, a slow and continuous increase of hydrogen sorption was observed

for about 10 hours and a total H_2 sorption of 0.24%wt/wt was reached. The same procedure was followed at 32 °C, in this case the H_2 sorption process starts at 20 bar and the total amount of H_2 stored is 0.06%wt/wt, due to the low temperature used in the measurement.

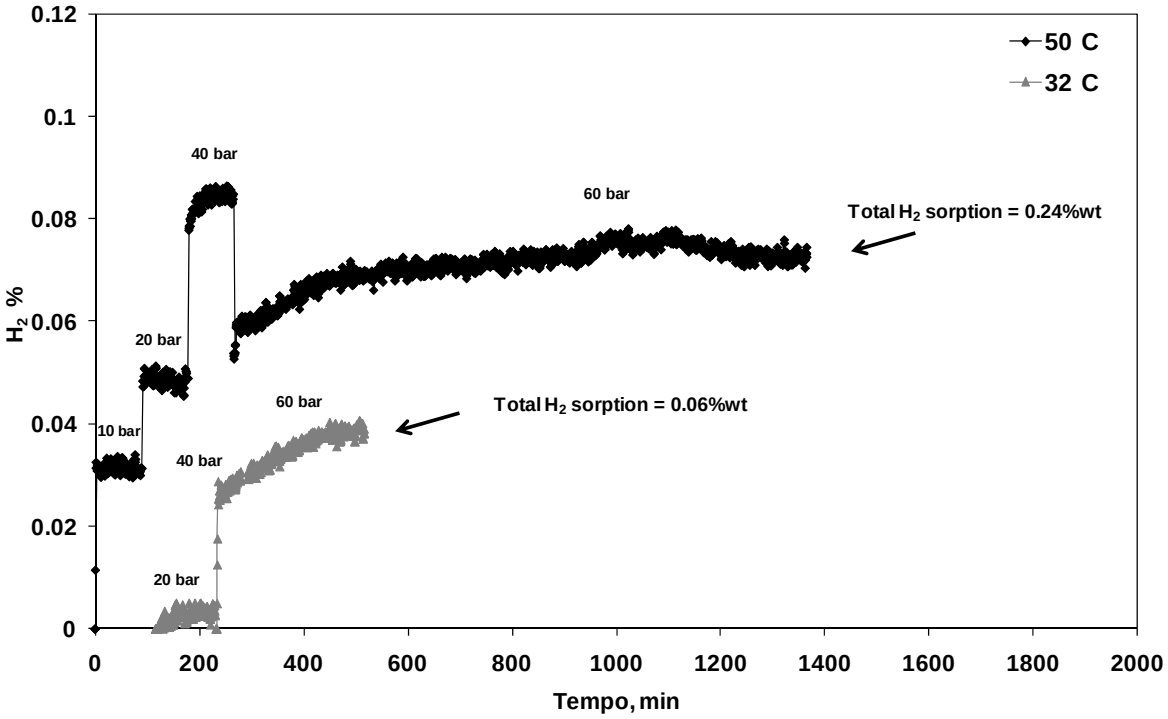

Figure 6: Hydrogen sorption cycles at 50 °C and 32 °C from 10 bar up to 60 bar.

A new material for hydrogen storage was developed starting from a functionalised PEEK containing chlorosulphonated groups acting as a support for manganese oxide. The influence of reaction conditions (time and reactants concentration) was evaluated by different chemical-physical characterisations. It was found that the polymer acts as a support of a layered manganese oxide dispersed on its surface, which amount increases by increasing the reaction time or reactants concentration. Mild reaction conditions produce a sample (SPMnO2A) with a higher acidity than the others (SPMnO2B and SPMnO2E) prepared by using strong reaction conditions. The SPMnO2A shows a similar SEM morphology of the precursor, on the contrary of other samples. The XRD profile present the typical peaks of the layered manganese oxide even if their intensity is higher when mild reaction conditions are used. The TEM images show a layered structure morphology, but the sample SPMnO2A reveals a higher tendency to curl and to grow into a tubular structure. For this reason, the sample SPMnO2A, seems to be the most promising sample to store hydrogen and gravimetric analyses on this sample were carried out. At 110 °C, it was found that the total H_2 sorption corresponds to the sum of the single steps obtained with 2-20 and 20-40 bar and this process is reversible. At 50 °C and 60bar a hydrogen sorption of 0.24%wt/wt was reached, while a value of 0.06%wt/wt was obtained at 32 °C.

Acknowledgments

The authors are grateful to Dr. Angelo Freni (CNR-ITAE) for the support in gravimetric measurements.

References

[1] A. Züttel, “Hydrogen storage and distribution systems”, Mitig Adapt Strat Glob Change, **12**, 343 (2007).

[2] W.R. Schmidt, Hydrogen storage in polymer-dispersed metal hydrides (PDMH), Proceedings of the 2001 DOE Hydrogen Program Review NREL/CP-570-30535.

[3] H. Fujii, T. Ichikawa, “Recent development on hydrogen storage materials composed of light elements”, Physica B, **383,** 45 (2006).

[4] J. Germain, J. Hradil, J.M.J. Fre´chet, F. Svec, “High Surface Area Nanoporous Polymers for Reversible Hydrogen Storage”, Chem. Mater., **18**, 4430 (2006).

[5] S.J. Cho, K. Choo, D.P. Kim, J.W. Kim, “H_2 sorption in HCl-treated polyaniline and polypyrrole”, Catal. Today, **120**, 336 (2007).

[6] B. Panella, L. Kossykh, U. D. Weglikowska, M. Hirsher, G. Zerbi, S. Roth, “Volumetric measurement of hydrogen storage in HCl-treated polyaniline and polypirrole”, Synthetic metals, **151**, 208 (2005).

[7] F. H. B. Lima, M. L. Calegaro, E. A. Ticianelli, “Electrocatalytic activity of manganese oxides prepared by thermal decomposition for oxygen reduction”, Electrochimica Acta, **52**, 3732 (2007).

[8] A. Carbone, R. Pedicini, G. Portale, A. Longo, L. D’Ilario, E. Passalacqua, “Sulphonated poly(ether ether ketone membranes for fuel cell application: Thermal and structural characterization”, Journal of Power Sources, **163,** 18 (2006).

[9] R. Pedicini, G. Squadrito, G. Giacoppo, A. Saccà and E. Passalacqua, “A Novel Polymeric Approach by Utilizing Functionalised Poly(ether ether ketone) for Hydrogen Storage Applications”, Extended abstract MRS Fall Meeting, Boston 2009.

[10] QingSu, Bingcai Pan, Bingjun Pan, Qingrui Zhang, Weiming Zhang, Lu Lv, Xiaoshu Wang, Jun Wu, Quanxing Zhang, Fabrication of polymer-supported nanosized hydrous manganese dioxide (HMO) for enhanced lead removal from waters“, Science oft he total Environment, 407 (2009), 5471-5477.

[11] Xun Wang and Yadong Li, Sinthesis and formation mechanism of manganese dioxide nanowires/nanoroads, Chem.Eur. J. 2003, 9, n °1.

National Strategies and Programs

Jörg Schindler

Abstract

The world faces an imminent transition to a postfossil era. The supply of crude oil has reached a plateau since 2005 and is expected to decline significantly in the coming decades. Natural gas, coal and nuclear energies will not be able to compensate this decline. The future of energy will have to be renewable. This will lead to a growing role of hydrogen as an energy carrier, especially in transport. National strategies and programs for hydrogen are driven by the motives of securing energy supply and providing clean fuel alternatives. The paper describes the past evolution and the present focus of these programs in Europe, North America and Asia.

Danish Partnership for Hydrogen and Fuel Cells

Aksel Mortensgaard, Danish Partnership for Hydrogen and Fuel Cells, Denmark

1 Danish Partnership for Hydrogen and Fuel Cells

A Danish national strategy for technological development within hydrogen and fuel cells identifies areas with development potential and provides guidelines for prioritization which can be used when formulating the various programmes for strategic research, development, and demonstration. The Danish national strategy proposed an organizational set-up based on comprehensive collaboration in executing a highly qualified, cross-disciplinary, and cross-institutional research, development and demonstration effort. In autumn 2007 this set-up became the Danish Partnership for Hydrogen and Fuel Cells. Participants in the Partnership comprise Danish key players from industry, research institutions, and authorities. Authorities as public funding providers participate with a status as observers. This enables efficient structuring of technological development and the necessary funding and optimum framework conditions can be discussed and defined. The Partnership enables all participants to make road maps and strategies, to define strategic directions and common goals, and to discuss and assess the extent to which the R, D &D activities meet the defined common goals for technical development. The Partnership also ensures international co-operation.

2 Hydrogen and Fuel Cell Technologies

Hydrogen and fuel cell technologies and products will improve the air we breathe, ensure secure and reliable energy supplies, reduce the emissions that cause climate change, and create economic growth and highly skilled jobs.

The potential applications for hydrogen and fuel cells are boundless from running our vehicles, heating and powering our homes, and generating electricity powering the grid to powering our cellular phones, laptops - and even children’s toys.

The electric power supply systems of the future will be characterized by a high proportion of renewable energy sources, and by decentralized, externally determined generation. In just over 20 years, Danish companies have pushed wind power from being a dream into a global multi-billion dollar industry. Denmark is in a strong position in terms of integrating more and more fluctuating and unpredictable energy sources such as wind power in the grid by hydrogen and fuel cells.

Hydrogen and fuel cells are not the only solution to overcome these challenges. However, they form an important part of the solution by offering very efficient and flexible production, conversion, storage, and use of energy. Fuel cells are potentially more simple and more quiet than alternative methods of electricity generation because they have no moving parts and they are less prone to unplanned outages.

3 A Strategic Direction for the Future

Denmark is a small player in an international context as there is a considerable focus on hydrogen and fuel cell technology development worldwide. This fact highlights the

importance of formulating a unified Danish approach to the development and utilization of Danish strengths and resources in this field. In June 2005 a Danish national strategy for research, development, and demonstration of hydrogen and fuel cell technologies was published.

The purpose of the strategy is to identify areas with development potentials and to provide guidelines for prioritization which can be used when formulating the various programmes for strategic research, development, and demonstration in the energy field. Danish activities in this area was based on the criterion that the initiatives should have a commercial potential beyond the domestic market and that the initiatives should be based on existing Danish competences.

The overall and long-term goal of the strategy is to ensure:

that Denmark develops and demonstrates effective and competitive technologies and systems that integrate hydrogen and fuel cells – primarily based on renewable energy sources – as an energy carrier in a clean, effective and reliable energy supply, and that Denmark takes a leading position in this field.

This large and complex task requires strong partnerships and a collaborative environment. It involves the private sector, public authorities and research, and educational institutions as well as regional development environments. It requires that their competencies can be coordinated and consistent technological solutions can be developed and demonstrated.

Table: Danish Focus Areas.

Production	**Area where funding is recommended**	**R&D**	**Demonstration**
	Small reformers (conventional fuel for hydrogen)	Development and integration into plants	Efficiency, reliability and price
	Electrolysis via reversible fuel cells	Improved understanding of processes; develop-ment of prototypes	Design and choice of materials
	Joint production of hydrogen-containing liquid fuel and hydrogen from biomass	Optimised production of pure hydrogen and hydrogen-containing liquid fuel	Efficiency, reliability and price
Storage	Metal hydrides and amines, nanoporous materials and light pressure containers	Lab.-scale optimisation, nanotechnology – new materials	Design and functionality, low price
Application: stationary, portable and transportation	Development of fuel cell technologies and system-integrated activities	Cell, stack and system development, system integration, improved efficiency, useful life, lower costs	Design, operation, reliability, useful life and price. Infrastruc- ture (distribution, filling stations, etc.)
Systems analyses, etc.	Socio-economic analyses, system and infrastructure analyses	Socio-economic and other analyses (life cycle, public acceptance, means, evaluations, etc.) Integration of new components	
	Safety, standards and environmental analyses	Analyses and evaluation of safety and standards (for both systems and components)	

4 Public-Private Partnership: A Danish Way to Success

The Danish organizational set-up is based on comprehensive collaboration in executing a highly qualified, cross-disciplinary and cross-institutional research, development and demonstration effort.

The main activities occur in the forum of dialogue. Here the key words are sharing of knowledge, integration and innovation through collaboration. Six different research, development, and demonstration activity lines are shown. The individual Steering Teams comprise key players (industry, research institutions, and authorities) involved in and responsible for activities in each activity line. Authorities participate as public funding providers. The task of the Steering Groups is to provide an overview of each project area, to make road maps and strategies to define strategic directions and common goals and to discuss and assess the extent to which the R&D activities meets the defined common goals for technical development.

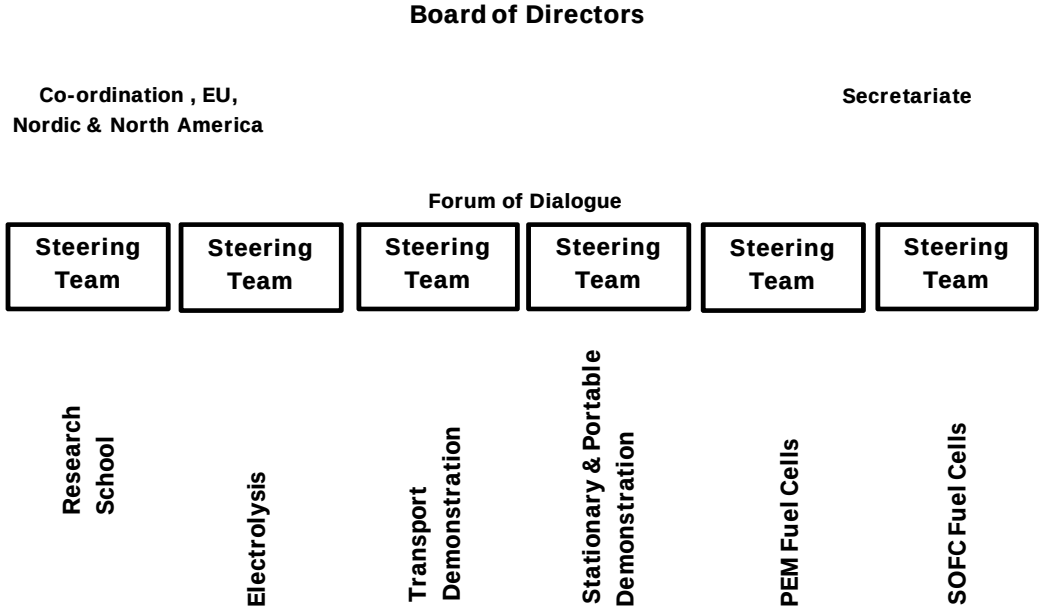

Figure: Organizational set-up.

A secretariat has been established to ensure:

- Active and professional communication and dissemination of information about hydrogen and fuel cells to all stakeholders in the Partnership and to society in general.
- Cooperation among the stakeholders of the Partnership.
- International co-operation with the European FCH-JU and other international players.

References

[1] Brintteknologier – Strategi for Forskning, Udvikling og Demonstration I, Danmark, Juni 2005

[2] Notat Vedrørende fem Partnerskaber, Oktober 2007, Handelshøjskolen i København.

Hydrogen Sweden's Strategy to Facilitate Regional Involvement in Hydrogen

Magnus Karlström, **Sven Wolf**, Hydrogen Sweden, Sweden

1 Introduction to Hydrogen Sweden

With a mission to facilitate the introduction of hydrogen as an energy carrier in Sweden, the non-profit Public-Private Partnership (PPP) of Hydrogen Sweden is applying an approach based on collaboration. Industry, universities, NGO's and local, regional and national government, are coming together to accelerate technology development and facilitate the evolution of early markets.

Inspired by the scientific theories of Innovation Systems, Hydrogen Sweden is designed as a Bridging Institution, acting as a coordinator and initiator that increase knowledge and motivation among different stakeholders. It is characterized by a balanced and pragmatic approach to hydrogen as an energy carrier, applying a long term perspective. Value is added through information activities, networking events, market and technology surveys, pre-studies and demonstration projects. Examples from the portfolio of co-operating hydrogen projects cover stationary, portable and transport applications. Hydrogen Sweden is also the Swedish coordinator in the Scandinavian Hydrogen Highway Partnership. The growing number of partners in Hydrogen Sweden recently passed 30 organisations, served by a hands-on secretariat of five employees.

2 Purpose

The serious challenge of reducing humanity's dependence on fossil fuels must be addressed with a range of activities. Among these, the research, development, demonstration and commercial introduction of new energy technologies is likely to play an important role. Hydrogen and Fuel Cell technologies are today considered to be one of the most promising new energy technologies, allowing for a more sustainable energy system with greater flexibility.

Hydrogen Sweden's purpose is to facilitate the introduction of hydrogen as an energy carrier in Sweden. The aim is to contribute to:

- Increased knowledge and awareness about the potential of hydrogen as an energy carrier
- More practical applications and demonstrations of hydrogen and fuel cell technologies
- Involving more actors with interests in the hydrogen area.
- Hydrogen being included to a larger extent in political strategies, regulations and legal framework as well as in research programmes.
- Economical growth and more working opportunities in the trade and industry related to hydrogen

3 Organisation

The Public-Private Partnership of Hydrogen Sweden is set up as a not for profit association with members among companies, public organizations or other associations. The members elect a Board for one year during the annual General Assembly. The Board members come from different parts of society, capturing different perspectives relevant to the introduction and promotion of hydrogen as an energy carrier in Sweden.

The operational part is the Secretariat and its Managing Director reports to the Board. Since the start, the Secretariat has grown from three to four and a half people. The team consists of the Managing Director, a Project Coordinator, a Senior Analyst, a Communications Manager and an Office Assistant.

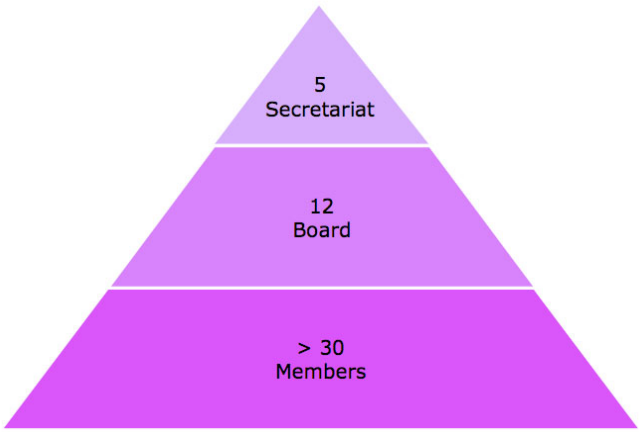

Figure 1: Organisation of Hydrogen Sweden.

4 Partnerships

Hydrogen Sweden is member of the following partnerships and organisations:

- European Hydrogen Association
- Scandinavian Hydrogen Highway Partnership

5 Approach

Hydrogen Sweden is applying an approach based on collaboration where industry, universities, NGO's and local, regional and national government, are coming together to accelerate technology development and facilitate the evolution of early markets. The activities are characterized by a balanced and pragmatic view of hydrogen as an energy carrier, applying a long term perspective. Synergies between hydrogen and other energy technologies are actively sought with the view to demonstrate and evaluate these synergies in practice.

6 Hydrogen Sweden Support to Swedish Regional and Community Actors

One major activity of Hydrogen Sweden is to support Swedish regional and community actors looking to set up successful hydrogen projects and networks.

Collaboration between regions and communities across Sweden and Europe is crucial as it dramatically can improve the cost effectiveness of the development process as well as increase its speed. In a European context, the European Regions' and Municipalities' Partnership on Hydrogen and Fuel Cells (HyRaMP), was launched in 2008. The question is now how regions and communities can act to get maximum value out of these engagements and how this may spear head the growth of the early markets for hydrogen and fuel cells.

Hydrogen Sweden's strategy to address the above mentioned issues and to facilitate the involvement and support of regional leaders and organizations will be explained in the presentation.

Examples from the regions of Västra Götaland and Skåne will be presented.

7 Quick Facts about Västra Götaland

At the western parts of Sweden lies the region of Västra Götaland.

- 1 .5 million inhabitants.
- 49 municipalities.
- 3 00 km long and 250 km wide.
- The largest city is Göteborg.
- The region has the largest port in Scandinavia.
- Sweden's leading region for industry and transportation

8 Quick Facts about Skåne

At the southernmost tip of Sweden lies Skåne. It is province, a county and a region. As a province it borders on its peers Halland, Småland and Blekinge, as well as Denmark, Germany, Poland and the Baltic States – albeit with some water between.

- million inhabitants.
- The largest city is Malmö.
- The largest private companies in Skåne are Posten AB, Tetra Laval and Skanska AB respectively.

Hydrogen and Fuel Cells news from the these regions will be summarized and also some examples of regional companies will be presented.

9 Conclusions and Learnings

Hydrogen Sweden's learnings how to involve regional actors are:

- Regional political support is important.
- The most powerful and quick way to gain acceptance has proven to be to establish collaboration with some of the big, well-known companies or authorities.
- Understanding regional companies concerns and drivers and how that relates to your own organization.
- By providing decision makers with information on what is going on in other companies, regions, or countries, in a way that gets them feeling that they are actually missing out on something important has proven efficient to increase their

motivation. Especially important is to inform about activities from countries close to region such as Norway and Denmark.

- To have a regional ambassadors that like what you are doing and then make sure they get the tools to help you.
- Seeking synergies with other regional supported technologies such as battery electric vehicles and biogas .

Canadian Hydrogen and Fuel Cell Programs

Nick Beck, Hydrogen, Fuel Cells and Transportation Energy, Natural Resources Canada, Canada

1 Introduction

Canada has been participating in the development of hydrogen and fuel cell technologies for more than two decades. Canada is the largest country per capita producer of hydrogen in the world, producing approximately 3 million tonnes annually. Canada is an international leader in the development of hydrogen and fuel cell technology.

Hydrogen and fuel cell technologies also represent a unique opportunity for Canada to reduce the environmental footprint from many sectors, such as, Transportation, which accounts for approximately 30% of total energy use and 25% of all greenhouse gas emissions in Canada. It is Canada's plan to move towards low carbon fuels, as well as other technologies, using electricity and hydrogen produced from renewable energy sources.

Along with government and academia, the hydrogen and fuel cell community in Canada is comprised of highly innovative smaller companies, which are investing heavily in R&D to further commercialize hydrogen and fuel cell technology. Although many of the companies are spread out across the country in cities such as, Calgary, AB; Toronto, ON; and Montreal, QC, Vancouver, BC, is said to have the largest cluster of hydrogen and fuel cell companies in the world.

As of today, Canada is operating a variety of hydrogen fuelled vehicles and fuelling stations, ranging from transit buses and automobiles, to forklifts and wheelchairs. In total there are 70 vehicles of different make and model operating on hydrogen in Canada. Canada is also operating 10 hydrogen re-fuelling stations across the country from Charlottetown, PEI to Whistler, BC.

2 Hydrogen & Fuel Cells | Research & Development – CanmetENERGY

Since the early 1980s, much advancement in Canadian hydrogen and fuel cell technology has been made. Current efforts in research and development (R&D) are continuing to advance this alternative energy option so that it is affordable and available to consumers.

Natural Resources Canada/CanmetENERGY/Hydrogen, Fuel Cells and Transportation Energy (HyFATE) group, has a long and successful history of partnerships with industry, academia, associations and other government organizations which support innovative research development and demonstrations in transportation technologies and fuels. Partners are actively sought and involved at an early stage of project development to ensure that the R&D supported will have a high likelihood of adoption by Canadian and international markets. All stakeholders benefit from these partnerships as projects and initiatives are co-funded and/or are supported by "in-kind" contributions.

Some examples of HyFATE's activities are:

- Managing RD&D transportation energy technology programs

- Advising on innovative energy technology R&D
- Conducting in-house hydrogen and fuel cell research
- Supporting safety work and the development of codes and standards, as well as training and certificate programs
- Coordinating workshops, seminars and information exchanges with public and private sector organizations
- Facilitating international student automotive engineering competitions such as Challenge X and ecoCAR
- Providing input into policies, developing national strategies and facilitating energy technology road maps
- Participating in federal committees and international groups and tasks such as the Canadian Hydrogen and Fuel Cell Committee, the International Energy Agency and the International Partnership for the Hydrogen Economy

3 Program Structure

Canada's program targets sustainable hydrogen production; hydrogen storage; fuel cells; and safety, codes and standards. Canada is also involved in several Demonstration projects.

3.1 Hydrogen production

Hydrogen's value as an energy carrier stems from the wide base of primary energy sources which can be employed to produce it. These include both renewable sources such as hydro, wind, solar and biomass, and non-renewable sources such as natural gas, coal and nuclear energy, as well as from waste streams.

Historically, Canada's main thrust of past investments has been electrolysis systems for hydrogen production from wind, hydrogen from low-value materials such as hydrogen sulphide and from coal or petroleum coke via the steam/iron process (a technology for centralized hydrogen production allowing easier carbon capture). Smaller program elements included purification and separation. Activities have steered away from technologies which are developed extensively in other countries and for which there was not a unique Canadian capability. Going forward, Canada's activities in the short term will focus almost exclusively on electrolytic hydrogen production integrated to renewable energy sources and the purification of waste hydrogen.

Highlights:

3.1.1 Development of advanced PEM water electrolyser

Market interest in PEM water electrolysis is quickly growing for backup power, renewable energy storage and onsite hydrogen generation applications. These markets require increased stack durability, lower total system cost, higher delivery pressures and hydrogen production rates up to 10 Nm^3/hr. This project is addressing technology needs for membrane durability improvements, bipolar plate manufacturing and coating, cost reductions and higher pressure stack design.

3.1.2 Materials for improved, durable electrocatalysts for hydrogen/oxygen alkaline electrolyzer systems

Alkaline electrolysis offers significant potential in two ways. First, it offers a method for large scale hydrogen production, which would expedite the transition to hydrogen. Second, if utilizing renewable electricity, alkaline electrolysis offers emissions free hydrogen production.

3.2 Hydrogen storage

Hydrogen storage is a key enabling technology for the deployment of fuel cell technologies in stationary, portable, and transportation applications. The challenge for all end-uses is reversible, lower cost, lighter weight, and higher-density hydrogen storage systems. For transportation, the overarching technical challenge for hydrogen storage is how to store the amount of hydrogen required for a conventional driving range (>300 miles) within the vehicular constraints of weight, volume, efficiency, safety, and cost. Durability over the performance lifetime of these systems must also be verified and validated, and acceptable refuelling times must be achieved.

Going forward, Canada will pursue the development and optimization of new hydrogen storage materials and systems. Gravimetric and volumetric densities, as well as cost, will be the key parameters addressed.

Highlights:

3.2.1 Materials for off-board hydrogen storage

Work is aimed at developing materials and technologies to store energy in a safe, solid hydride media. The stored energy can be used to power transportation, mobile and stationary fuel cell energy systems – as needed. These materials and technologies will improve Canada's ability to store excess/off-peak energy from the grid and from renewable energy technologies – particularly in remote community applications.

3.2.2 Development of lightweight hydrogen storage systems

Canada is working on enhancing hydrogen storage and generation for portable, long run time applications. A prototype developed offers hydrogen and fuel cell energy pack which can be utilised as a replacement for D-Cell battery packs in a variety of portable applications. The major benefit of this technology is that it has a higher energy density and can run continuously at a 5W steady state for a minimum of 26 hours, which is an improvement of almost 50% over the incumbent D-cell battery technology.

3.3 Fuel cells

Canada is working to improve fuel cell technologies. For transportation, small-scale stationary generation (e.g. back-up power), and portable devices, the focus is on proton exchange membrane (PEM) fuel cells, due to their low temperature operation and capability for fast start-up. For larger-scale distributed energy generation, the focus is on the high temperature solid oxide fuel cell (SOFC), which can directly use natural gas or other hydrocarbon fuels.

Highlights:

3.3.1 High temperature fuel cell cogeneration systems

The residual heat generated by a high temperature PEM fuel cell co-generation system can be channelled into a heat exchanger to produce domestic hot water. This CHP process reduces water heating costs, while also providing very efficient electricity generation. Co-generation systems present a viable option to reduce natural gas use and decrease air pollutants and CO^2 footprints.

3.3.2 Development of fuel cell humidifiers

Humidification is one of the key components in fuel cell systems, affecting performance, durability, size, cost and ultimately commercialization. This project is optimizing fuel cell humidifiers for better performance, reliability and integration with customers, in order to make systems ready for manufacturing and commercialization.

3.4 Codes, standards and safety

The successful global commercialization of hydrogen and fuel cells depends on internationally accepted codes and standards. These will help to increase the experience, knowledge and confidence of local, regional, and national officials in the use of hydrogen and fuel cell technology, and facilitate the development of smart regulations. R&D supports the development of performance-based, rather than product-specific, codes and standards. International collaboration in this area is essential.

Highlights:

3.4.1 ISO Technical Committee 197

Canada plays a leading role as chair of the ISO Technical Committee 197 (Hydrogen Technologies) and is a key contributor to the IEA Hydrogen Implementing Agreement Task 19. Task 19 participants have been working to identify the physical properties of hydrogen which impact the issue of safety.

3.4.2 Canadian Hydrogen Installation Code

Published by the Bureau de normalisation du Québec (BNQ) as a National Standard of Canada, the Canadian Hydrogen Installation Code (CHIC) [CAN/BNQ 1784-000] will help pave the way for a greater use of hydrogen as an energy carrier by guiding safe design and facilitating the approval process of hydrogen installations across Canada. This code has also been used as a guide for other countries and jurisdictions, to develop their own codes.

3.5 Demonstrations

Complementing the aforementioned R&D, HyFATE supports projects that demonstrate and deploy hydrogen and fuel cell technologies in Canada. These projects are building and evaluating fuelling options for a variety of on-road and off-road hydrogen-fuelled vehicles, as well as hydrogen infrastructure.

Highlights:

3.5.1 Hydrogen highway demonstration

By coordinating and promoting a network of demonstration projects, the BC Hydrogen Highway will advance commercialization of hydrogen fuel cell technologies for vehicles and fuelling systems as well as micro, portable and stationary power applications. It is also the background for the world's largest hybrid electric fuel cell bus fleet. These buses were a part of Canada's demonstration of sustainable transportation technologies for the 2010 Olympic and Paralympic Games. The BC Hydrogen Highway was also recognized by the Vancouver Olympic Committee's (VANOC) Sustainability Star program, a program that recognizes innovative environmental technology efforts in and surrounding the Vancouver 2010 Olympic and Paralympic Games.

3.5.2 Vancouver Fuel Cell Vehicle Program

The Vancouver Fuel Cell Vehicle Program (VFCVP) is a demonstration aimed to increase public awareness of hydrogen and fuel cell vehicles, and to test and evaluate the performance, durability and reliability of five Ford Focus fuel cell vehicles in Vancouver and Victoria, British Columbia.

The VFCVP is putting FCVs and hydrogen refueling systems to work in real-world applications to enable the evaluation and improvement of system performance. It is also helping facilitate international codes and standards development and other activities critical to preparing the market for a clean-energy future. The five Ford Focus vehicles will re-fuel at hydrogen fuelling stations located throughout B.C., such as the Victoria and Pacific Spirit Hydrogen Fuelling Stations.

3.5.3 Prince Edward Island Wind-Hydrogen Village

The Wind-Hydrogen Village project will develop and demonstrate a wind-hydrogen energy system to provide a reliable, grid-independent power source that is sufficient to electrify a small village and provide hydrogen fuel for vehicles.

Located on the North Cape of Prince Edward Island, the project will demonstrate, evaluate and refine hydrogen technologies while developing innovative and fully-operational wind-hydrogen control software and interface components, with potential applications both within Canada and abroad. There are two major operational components of the Wind-Hydrogen Village: village electrification; and hydrogen fuel to be used in vehicles for transportation in Charlottetown.

4 Summary

Canada continues to conduct research, development and demonstrations. Engineers and scientists will continue their work on developing, demonstrating and deploying hydrogen technologies that minimize environmental impact, increase economic growth and improve energy-efficiency.

The aforementioned achievements mentioned in this paper, illustrate the commitment Canada has made to become a global leader in the development of hydrogen technologies and infrastructure to benefit both the present and future generations.

References

[1] CanmetENERGY – http://canmetenergy-canmetenergie.nrcan.gc.ca

[2] Hydrogen and Fuel Cell Progress – www.h2fcprogress.collaboration.gc.ca

[3] Vancouver Fuel Cell Vehicle Program – www.vfcvp.ca

[4] BC's Hydrogen Highway – www.hydrogenhighway.ca

[5] Natural Resources Canada – www.nrcan.gc.ca

Hydrogen and Energy Utilities

Daniel Hustadt, Vattenfall Europe Innovation GmbH, Germany

Abstract

Renewable electricity generation plays one major role with the biggest share being wind energy. At the end of the year 2009 a wind power plant capacity of around 26 GW was installed in Germany. Several outlooks come to the conclusion that this capacity can be doubled in ten years (compare Figure 2). Additionally, the German government has set a target of 26 GW installed off-shore capacity in North and Baltic Sea until 2030.

At Vattenfall only a minor percentage of the electricity production comes from wind power today. This share will be increased up to 12% until 2030 following Vattenfall's strategy 'Making Electricity Clean'. This rapid development of wind power offers several opportunities but also means some challenges to Utilities.

1 Development of Wind Power

One challenge of electricity produced by wind turbines is the fluctuating generation of electricity. So the need for grid balancing and regulating power will increase, especially in the North where a large share of electricity from wind is produced.

Secondly situations where wind electricity production will exceed the actual demand or the transport capacities will occur more frequently since the regional demand will be almost stable in the near future.

Finally the installation of new conventional power plants in the north of Germany lead to an significant increase of capacity installed whereas demand and generation are separated locally from wind power production (demand centres in South of Germany, most of wind production capacity in the North).

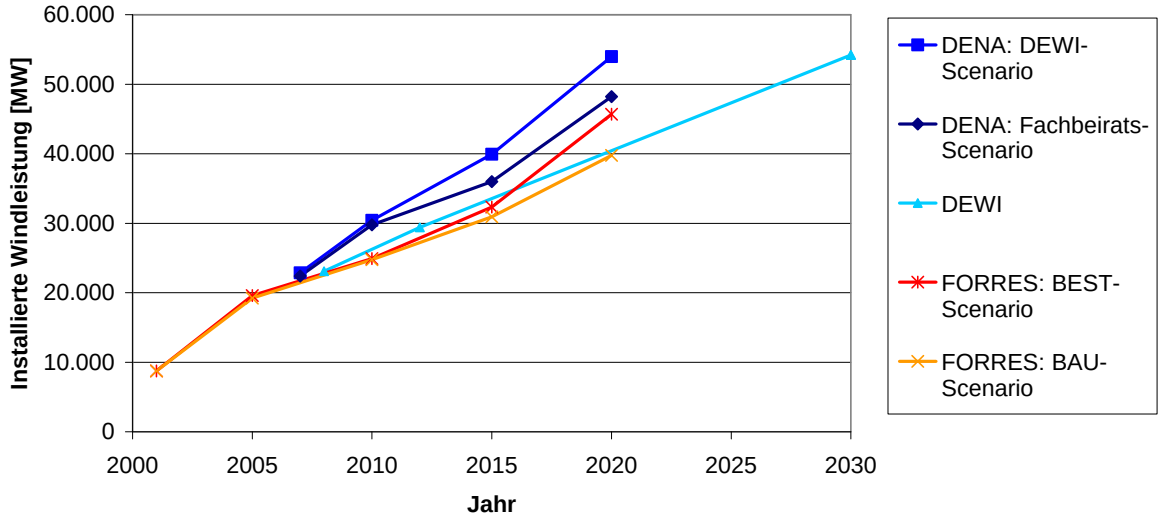

Figure 1: Prognosis of wind power development in Germany.

These high capacities in northern Germany need energy transport capacities to the south demand centres, balancing capacities and storage systems.

2 Consequences for Grid Operation

The classic requirement towards the transmission system operator (TSO) is to provide the grid and to balance it. This included stability of frequency, stability of voltage and the grid security (n-1 criteria). New challenges are the steadily increasing trading of energy, the feed in tariff (EEG) and the combined heat and power directive (KWK).

Challenge one is the system balance within the control area. The production from wind power has to be integrated which can be a tough task looking at the figures below. Table 1 shows the gradients of change of feed-in wind energy into the control area of Vattenfall transmission in 2007. The table shows how big deviations can be in one control area in Germany.

Table 1: Gradient of feed in change within control are Vattenfall Transmission 2007.

maximum feed-in	7.511 MW
minimal feed-in	2 MW
biggest increase over ¼ h	638 MW
biggest decrease over ¼ h	977 MW
biggest increase over 60 min	1.601 MW
biggest decrease over 60 min	1.618 MW
biggest difference between minimum and maximum a day	6.398 MW

Challenge two is the prognosis quality. Deviations between forecasted and actual feed-in of electricity can vary enormously as shown in Figure 1. For the control area of Vattenfall transmission alone deviations of 4000 MW between forecast and actual feed-in occurred during the storm “Emma” between February 29th and 3rd March 2008. So the requirements to meet the system stability criteria will be higher in future although forecast systems are good and are continuously improved. The need for balancing power will increase in future. Investments into the grid and the extension of it are necessary and economically the most reasonable choice. However the acceptance of newly constructed overland-lines is limited (“not in my backyard”) and so large grid extensions will be hard to realize in Germany.

Additional storage and balancing power capacities are desirable and hydrogen might play a role to offer these. When looking at the possibility of a re-conversion of stored hydrogen to electricity this might enable utilities to sell electricity on an exchange basis. The possibility to store energy in hydrogen helps to ensure the delivery of power in low wind phases and so to increase the reliability of the whole system – direct marketing of wind power might be easier with such systems and so an additional business opportunity for utilities might be enabled.

Compared to storing electricity in batteries (i.e. battery electric vehicles) storing energy in hydrogen offers a long term storage option. While battery electric cars will be connected and

disconnected to and from the grid quite unpredictably and the energy content which might be usable by utilities is limited hydrogen can be stored in large caverns for weeks and months. This long term storage option of hydrogen also represents a new business field for utilities.

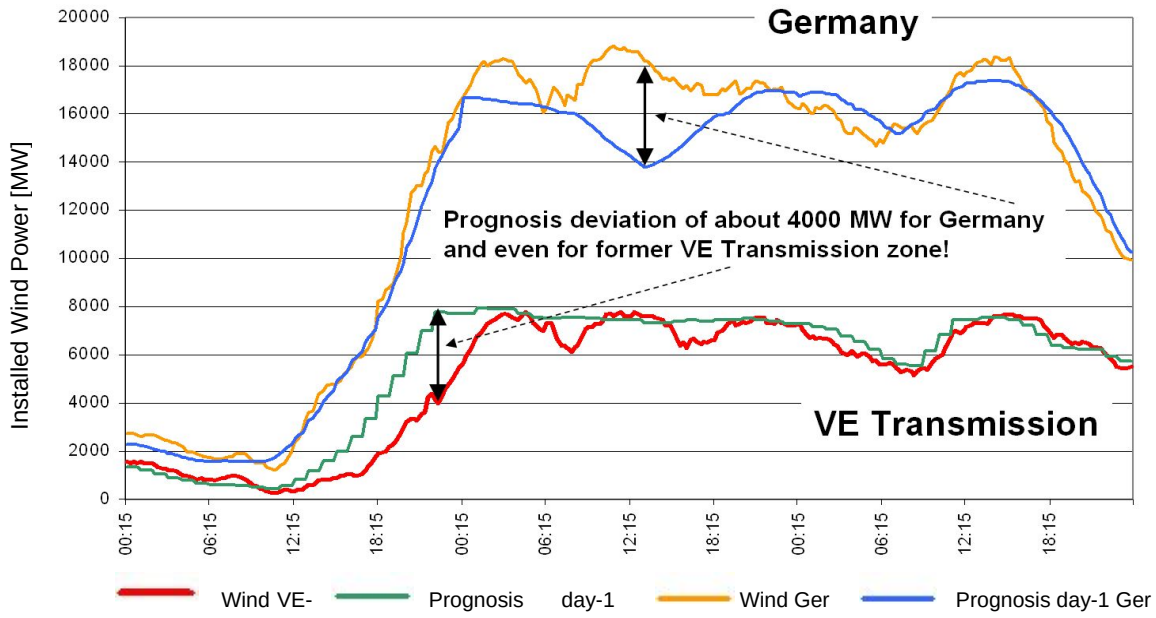

Figure 2: Prognosis deviations, example storm "Emma" Feb 29th - Mar 3rd 2008.

3 Options to Store Electricity from Wind

In Principle water pump storage, air pressure storage as well as hydrogen and battery storage systems are thinkable. Looking at different studies analyzing the “surplus” electricity amount which will be produced depending on the installed wind power capacity in the future one gets an impression of the order of magnitude. Looking at a 38 GW installed wind power-scenario the FHG-ISI scenario came up with 0.7 TWh of surplus electricity and even with 3.3 TWh in the 48 GW installed wind power scenario. For comparison: the installed water pump storage systems in Germany have an energy storage capacity of 0.21 TWh.

Additionally it is almost impossible to realize new big pump storage systems like Goldisthal in Germany particularly in northern Germany.

Compressed air storage systems have a low energy density and battery systems are large, costly and the life cycles are not proven yet.

Hydrogen produced from long proven electrolysis would convert wind electricity to another energy form comparable to water pump storage systems and make it storable. The production would be decoupled from the consumption.

Although proven for long time electrolysis and hydrogen as energy carrier also face challenges with the new requirements as using electrolysers for balancing, cost of the systems, transport and logistic for hydrogen as well as the build up of an relevant infrastructure.

In all hydrogen seems to be a storage option for electricity from wind. Once stored the hydrogen could be used for several purposes as for example in transport, chemical industry or electric re-conversion. In transport clean hydrogen enable CO_2-free transport and diversifies the resources demanded by transport means.

4 Hydrogen from Coal and Lignite

In the future also hydrogen production from coal and lignite might become a business field for utilities. The CCS technology will offer a CO_2-lean production method for hydrogen using the carbon gasification processes or the IGCC process. As these processes are only feasible in large scale commercial plants are not expected to be realized within the next 10 years. Until then the CCS technology has to be improved and significantly reduced in cost.

5 Business Opportunity Mobility

Stored hydrogen from renewable energies can offer a business opportunity with regard to mobility. In projects like CUTE and HyFleet:CUTE it has been already proven that hydrogen in public transport is an viable option to reduce green house gas, dust and noise emissions within cities. At the moment the h2mobility project, a consortium of major oil and gas companies, OEMs as well as utilities is working together on the realization of a nationwide network of hydrogen refuelling stations for cars in Germany. In a first step the business case for each company will be calculated and in a second the necessary infrastructure might be installed. All kinds of sources of hydrogen are analyzed - also hydrogen from renewables like wind or biomass. For utilities hydrogen from electricity is a new business field and could lead to a new segmenting on the field of fuels.

In Hamburg HafenCity the new hydrogen station HafenCity will follow the path of CUTE and HyFleet:CUTE. A new station with on-site electrolysis combined with trucked-in hydrogen will deliver enough hydrogen refuel 20 new fuel cell hybrid buses of Hochbahn when reaching the fleets' interim peak in 2013.

Russian R&D in Hydrogen and Fuel Cells

Malyshenko, S.P., Joint Institute for High Temperatures of Russian Academy of Sciences, Russia
Klimenko, A.V., **Reutov, B.F.**, Ministry for Education and Sciences of Russian Federation, Russia

1 Introduction

Russia has been developing and using hydrogen technologies in practice for many years, starting from the time of its first space program. Among its achievements are experimental liquid-hydrogen fuelled airplane-laboratory TU-155, which was tested back in 1986-1987, air and space hydrogen-fuelled engines, including an unparalleled engine RD-0120 with a forward thrust of 200 tf in each booster of “Buran-Energy” complex, experimental hypersonic ramjet engine (SCRAMJET) 58L that was successfully fly-tested with hypersonic flying laboratory (HFL) with Flight Mach number from 3 up to 7 , a fleet of demonstration taxi-cars fuelled by a mixture of gasoline and hydrogen which were successfully run in Kharkov in 80-ies, hydrogen forklifts, systems for liquid hydrogen production, storage and transportation, 250 kW AFC-based power generation units and many others which brought about R&D activities carried out at the end of the 20th century. The results of these works are presented in 8 volume collection of scientific papers entitled “Nuclear and hydrogen power and technologies” and in a number of monographs, published in 80-90-ies in the Russian language. In the nineties the hydrogen R&D program was considerably curtailed because of the political situation in Russia. At the beginning of the 21 century the Russian Ministry of Science and Education and Federal Agency for Science and Innovation (FASI) have re-initiated an R&D program in the field of hydrogen technologies by starting to fund R&D projects for power sector and transport. In 2008-2009 the Russian hydrogen program funded by federal budget comprises more than 40 research projects.

2 Policy and Legislation

By decree of the Russian president in May 2006, hydrogen energy technologies were given the status of critically important for further development of the national economy, which means that they are to be developed on a priority basis. The national programs through which research, development, and demonstration (RDD) projects were funded from 2002 to 2006 have been successfully completed. Since 2007, the projects aimed at development and deployment of hydrogen energy technologies, including projects related to fuel cells (FCs), are funded by the Russian government mainly through two national (or special federal) programs: (1) “R&D in the Priority Areas of the Russian Scientific and Technological Complex Development for 2007–2012” and (2) “National Technological Basis for 2007–2011.” The main objective of the first program is to accelerate research and development in the priority areas of science and engineering, while is the focus of the second program is to accelerate commercialization of innovative technologies and new products. Some H2-related

basic research is also funded through the programs of the Russia's Academy of Sciences and the Russian Foundation for Basic Research (RFBR).

3 Research & Development

Current directions of research and development in the field of hydrogen energy are determined by social and economic targets set by Energy Strategy of Russia for the period up to 2030 confirmed by the government in 2009. For example, increasing of the role of nuclear and coal fuelled thermal power stations and renewables in energy balance stimulates R&D in hydrogen accumulation of energy for load management and environmentally friendly hydrogen based technologies for autonomous power supply, also deep crude oil refining processes and increasing of quality of oil products requires R&D in large scale hydrogen production (up to 3-4 millions of tonnes in 2030) for oil industry.

In 2007-2009, over 60 organizations were involved in hydrogen projects implemented within the framework of the special federal program "R&D in the Priority Areas of the Russian Scientific and Technological Complex Development for 2007-2012 " Among the project coordinators are leading Russian research organizations: 8 federal scientific centres, 19 institutes of the Russian Academy of Sciences, 14 universities; as well as innovative SME, branch research institutes and design engineering departments. R&D carried out by them covers all aspects of hydrogen technologies.

4 Hydrogen Production Technologies

Within the framework of the Russian R&D program efficient compact units (including portable one) for catalytic conversion of hydrocarbons, PEM electrolysers operating under pressure of up to 13 MPa with productive capacity over 10 nm^3/h, stationary and on-board plasma-chemical converters for converting hydrocarbon fuels into syngas, hydrogen production units with systems of hydrothermal oxidation of Al and Mg-based solid materials , as well as some basic R&D in new catalysts (including nanostructured one) for thermochemical and electrochemical processes, of hydrogen production are being developed by Boreskov Institute of Catalysis, Russian Research Center "Kurchatov Institute", Joint Institute for High Temperatures, Frumkin Institute for Physical Chemistry and Electrochemistry, Moscow State University, Moscow Power Engineering Institute, Gubkin Oil and Gas University, Novosibirsk State University and others.

5 Hydrogen Storage Technologies

Hydrogen Storage Technologies are being studied and developed due to effort of more than 20 national research institutes and universities. New materials (including nanostructured and composite one) for reversible hydrogen storage systems and purification, hydrogen storage in non-equilibrium and regenerable systems, reversible solid storage systems integrated with stationary power generation units based on low temperature fuel cells with capacity of up to 5 kW(e) compact and safe metal hydride hydrogen sources for portable (mobile and transportable) power supply units, equipment and apparatus are being developed by Institute for Problems of Chemical Physics, Moscow State University, Joint Institute for High

Temperatures, Novosibirsk State University, Ural Institute for Physics of Metals, Moscow Power Engineering Institute, RRC “Kurchatov Institute” and others.

6 Fuel Cells

The efforts are also taken to develop fuel cells of various types for portable and stationary power units (AFC, PEMFC, SOFC, MCFC) for autonomous power supply with capacity of up to 100 kW. Portable AFC-based charging devices with gradient porous structures are in the deployment and commercialization stage; AFC-based power units of new generation as well as stationary and portable power units with PEMFC and SOFC with capacity from 5 to 100 kW, new catalysts (including nanostructured one) and MEA with reduced content of platinum from nanostructured ceramic ion-conducting materials, reversible PEM and solid oxide FCs of 0,5- 1 kW are being developed by Central Institute for Ship Electric Engineering and Technology, RRC “Kurchatov Institute”, “Aspect” Association, Independent Power Technology, Ural Electrochemical Plant, KVANT, Institute for Problems of Chemical Physics, Moscow Power Engineering Institute, All-Russian Institute of Experimental Physics, All-Russian Institute of Technical Physics, Institute of Physical and Power Engineering and others.

7 Hydrogen Powered Vehicles

Automobile “Lada-Antel-1” (based on an alkaline FC) and “Lada-Antel-2” (based on PEMFC) have been displayed at various motor shows. A few types of automobiles with ignition engines in which hydrogen-gasoline fuels are used have been designed and tested. A switch locomotive with FC-based engine is under development. Hydrogen Powered Vehicles Projects are implemented by AVTOVAZ, National Auto-Motor Institute, RSC “Energia”, Ural Electrochemical Plant, National Association of Hydrogen Energy, All-Russian Institute of Railway Technologies and others.

8 Hydrogen Combustion Power Technologies

Experimental high pressure hydrogen-oxygen steam generators with thermal power up to 25 MW have been developed and tested, model high temperature steam turbine units with these combustors of up to 5 MW capacity have been designed and tested by Joint Institute for High Temperatures and JSC “Chemical Automatics Design Bureau”.

9 Hydrogen Safety

The R&D is aimed at developing technologies, methods and means expected to provide for safety of hydrogen production and its use as a energy carrier. They cover experimental and theoretical study of combustion processes (including combustion under non-stationary conditions) and explosion of hydrogen-air mixtures under ambient conditions, in large closed volumes of various geometry (including accumulative one), in jets coming out of high-pressure containers and others, as well as development of inhibitors and stabilizers, systems of diagnostics, prevention and liquidation of fire and explosion hazardous situations, research in hydrogen safety codes and standards and their harmonization with international codes and standards. A unique equipment is used for carrying out these works; among them is a 13 m

diameter explosion camera, with designed capability for explosion resistance, equivalent to 1000 kg of TNT. Due to R&D carried out in 2007-2008 a new phenomenon of abnormal increase in pressure under non-stationary combustion of hydrogen – air mixtures and in the situation when explosion waves enter into accumulative volumes is discovered; new methods and means of control over the velocity of hydrogen flame spread, means to prevent combustion from turning into explosion, safety valves for reduction of pressure in high pressure containers and some other devices have been developed. Some new national hydrogen safety regulations have been drafted, including those for liquid hydrogen. The work on hydrogen safety is carried out by Joint Institute for High Temperatures, Research Center "Kurchatov Institute", JRC "Cryogenmash" and others.

10 Education

Within the framework of Ministry Education and Science's project on hydrogen education a number of scientific and education centre have been established for training specialists in hydrogen energy technologies, they are functioning on the basis of the leading Russian universities and research institutes (Moscow Power Engineering Institute, RRC Kurchatov Institute, Joint Institute for High Temperatures, Moscow High Technical University, Novosibirsk State University, Ioffe Physical-Technical Institute, Voronezh Polytechnical University, Moscow Institute of Physics and Technology, Tomsk Technical University, St. Petersburg State University). A few text books and method guides in hydrogen technologies and fuel cells for high school students have been published.

In Moscow Power Engineering Institute a new department specializing in "Electrochemical and Hydrogen Energy Technologies" has been established, where specialists and post-graduate students undergo training. For educating elementary school children a few colleges have been established, such colleges function under the auspice of Moscow Power Engineering Institute, Moscow Institute of Radio Technology, Electronics and Automatics (MIREA), Ioffe Physical-Technical Institute (St. Petersburg), Novosibirsk State University and others. MIREA prepared a few text-books for school children. A few "hydrogen clubs" are functioning at some schools, as well as scientific and education centre "Sokolinaya Gora" set up with assistance of Moscow State University and MIREA.

References

[1] Mazurenko S.N., Malyshenko S.P., Reutov B.F. Russian R&D in the field of hydrogen energy and technology. 16 World Hydrogen Energy Conference, Lyon, France, CD-ROM. 2006.

[2] Hydrogen Technologies. Innovation Developments Catalogue. Moscow. 2007.

[3] II International Conference „Hydrogen Storage Technologies". Abstracts. Moscow. 2009.

[4] II International forum „Hydrogen Technologies for developing countries". Proceedings. Moscow. 2008 (in Russ).

[5] Special Federal Program "R & D in the Priority Areas of the Russian Scientific and Technological Complex Development for 2007-2012". Rep. on results. 2008. FASI 2008 (in Russ).

German-Chinese H_2 & FC Activities in the Framework of the German-Chinese Sustainable Fuel Partnership (GCSFP)

Binggang Wang, **Ulrich Schüller**, Project Coordinator GCSFP
Jürgen Garche, FCBAT Ulm, Germany

1 Introduction

The sustained strong economic growth in the People's Republic of China is bringing about an increased demand for transport and mobility. The rapid increase in transport services is placing great demands on energy supply security, as well as on climate and environment protection.

In light of this situation, German and Chinese political and economic players have come together in the German Chinese Sustainable Fuel Partnership, based on intergovernmental agreement signed on December 1st 2003 by the German Federal Ministry of Transport, Building and Urban Development (BMVBS) and the Ministry for Science and Technology of the People's Republic of China (MOST).

The aim of this partnership is to develop alternative and sustainable concepts for energy supply and technology in the mobility sector, and to push ahead with their introduction.

By setting up pilot plants and constructing and operating fleets of vehicles, the project aims to demonstrate the utilisation of biofuels, synthetic fuels, hydrogen and electric mobility in the transport sector.

The activities of the GCSFP serve to exchange experiences and to economically develop new, sustainable technologies. The legal conditions (laws, regulations, guidelines) and the further development of standards and norms also have a role to play in this process, e.g.

- Strategic studies, e.g. "Strategy report on the development of fuels for road transport in the People's Republic of China" (see http://www.gcsfp.de/index.php?id=47).
- Workshops, e.g. the technical seminars "Hydrogen in mobile applications", "Biofuels and synthetic fuels" and "Electric mobility" in Germany and China, each with a comprehensive excursion programme.
- Conferences, e.g. "Clean Diesel Symposium" during the "Clean Vehicle Technology Exhibition and Conference" in Beijing
- Standardization projects, e.g. fuel standardization RIPP-Sinopec
- Demonstration projects, e.g. constructing and operating efficient taxi fleets, which are powered with synthetic fuel and fulfill particular requirements regarding emissions.

A very important role in the GCSFP program plays the mobility based on hydrogen and fuel cells. Deeper cooperation's in this field started with the Chinese-German H2&FC Workshop in Berlin (Germany), May 20th – 25th, 2007; (CD about this workshop is available at schuster@dena.de).

In the focus of that mutual H2&FC cooperation are the following projects:

1. Market introduction programs:

- Legal framework (regulations) for H2 vehicles
- Codes and Standards for H2 vehicles
- Test and measurement methods for H2&FCs (in preparation)

2. Basic research programs:

- Hydrogen storage materials
- Dynamic of PEFCs.

Besides these H2&FC projects there are also battery related projects in the framework of electro mobility:

- Study on Chinese and German Vehicle Battery Development
- Regulatory Frameworks for Electric Vehicles and Infrastructure in China and Europe/Germany
- Analysis and Comparison of Standards and Implementation Rules for the Application of Electric Vehicles and Vehicle Batteries
- Battery Safety Test Manual
- EV-Demonstration Project Rhein-Ruhr and Wuhan.

2 Analysis of the Legal Framework for a Hydrogen Infrastructure in China, as Prerequisite for a Harmonisation of the European/German and Chinese regulations

German partner: EnergieAgentur NRW, Düsseldorf
Chinese partner: Tsinghua University, Beijing
Project duration: Juli 2008 - Juni 2009.

2.1 Objectives:

The study is focused on the legal framework for a hydrogen infrastructure in China, Germany and Europe. Several laws, ordinances and standards were collected and scanned by lawyers in order to find out differences and similarities. The majority of the regulations come from the field of environmental, labour, health and safety law.

During the last time, China enacted several regulations concerning hydrogen and fuel cells, which shows the engagement in this field. Further standards focused on the technical details of hydrogen vehicles are in development and will be come into force soon.

2.2 Work programme:

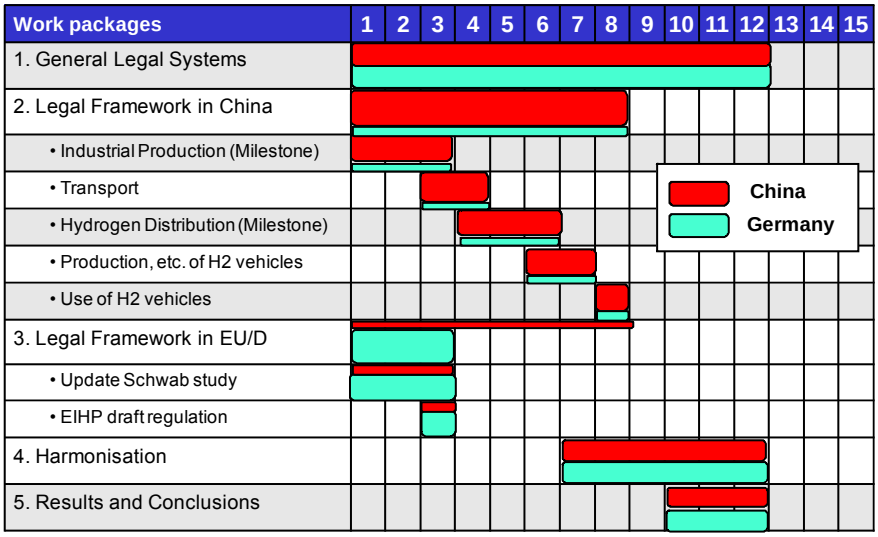

2.3 Conclusion

Many regulations in China, Germany and Europe are similar, especially in the field of environmental and labour law. Chinese law is partly stricter in regard of safety distances to special physical structures. The classification of hydrogen as dangerous substance is similar in China and D/EU. Also the classification as dangerous good with the respective packaging groups is comparable.

China has a great interest in pushing forward international cooperation and ex-change of technologies and experiences, which is mentioned in the Renewable Energy Program, of China. Due to the fact that China emphasises hydrogen technology and the development of fuel cells, significant administrative barriers to introduce a hydrogen infrastructure are not expected.

At the current situation (mid of 2009) urgent needs for action is not necessary to harmonize regulation for a hydrogen infrastructure on road traffic between China and D/EU. Latest regulations are very similar in Europe and China. It is recommended to pursue the adoption of new laws and standards in China and Germany/EU. Each field of infrastructure should be monitored.

The project partners recommend signing a political Memorandum of Understanding (MoU) to inform the other side about the regulations in early draft versions.

Until now UN-classification and UN-labelling of dangerous goods are identically. The trend to use international regulations is effect of the globalization. Other international regulations which have to be implemented will follow. Also for that reason China and Germany should enforce their engagement in the working parties of the United Nations Committees. The project partners recommend presenting consolidated positions in UN Working Party 29 for Global Technical Regulations (GTR) for hydrogen vehicles. Except the GTR for hydrogen vehicles there are no other UN Working Parties working along the infrastructure at the moment. It is recommended to initiate new Working Parties in other fields of the hydrogen infrastructure for road traffic.

3 Analysis of the Situation of Standards and Codes for Hydrogen and Fuel Cell Vehicles and Related Supply Infrastructures

German partner: Ludwig-Bölkow-Systemtechnik GmbH (LBST)

Chinese partner: China Automotive Technology & Research Center (CATARC)

Project duration: November 2008 - April 2010.

3.1 Objectives:

Goals of the study were to analyse the present situation of Standards and Codes In Europe/ Germany and in China, to identify the differences and commonalities in Standards and Codes and to develop joint conclusions and suggestions towards international standardisation bodies.

3.2 Work programme:

The work program of the study was agreed as follows:

1. WP 1. General relevance of Standards and Codes for H2&FC vehicles in China and Germany/EU
2. WP 2. Analysis and exchange of Standards and Codes for H2&FC vehicles in China

- 2.1. Transport of hydrogen on streets and rail;
- 2.2. Hydrogen Refuelling Stations (as and example: Shell station in Anting, Shanghai);
- 2.3. Approval and use of H2 vehicles

3. WP 3. Analysis and exchange of Standards and Codes for H2&FC vehicles in Germany/EU

- 3.1. Transport of hydrogen on streets and rail;
- 3.2. Hydrogen Refuelling Stations;
- 3.3. Approval and use of H2 vehicles

4. WP 4. Results and conclusions

- Differences Analysis {Gaps Analysis} (China/ D/ EU)
- Suggestion of agreed approach towards international standardisation bodies

3.3 Important results:

The most essential difference between China and Europe with regard to the relevance of standards is that standards in Europe are voluntary agreements between private organisations like industrial companies for the harmonization of requirements for technical interfaces, whereas in China mandatory standards exist, which are attributed regulatory characteristics. These regulatory characteristics in Europe can only be derived from regulations or directives, i.e. legal requirements. China seems to lack a framework or outline directive similar to the one existing in Europe. On the other hand, Europe as well as China certify road vehicles via a whole vehicle type approval process (as also does Japan) and not through a self-certification process like applied in the USA.

As the Chinese partner CATARC did not provide inputs on infrastructure-relevant issues nor participated in the analysis of differences in C&S between China and EU/D any

recommendations provided could only be drafted by the German side without harmonizing them with the Chinese partner in time.

3.4 Conclusions and recommendations:

Under the WTO's TBT Agreement signed by both China and the EU, it is agreed upon to avoid the proliferation of national standards that differ from one country to the next, it is recommended that countries be encouraged to bring their work to ISO/IEC and to contribute to the development of ISO and IEC International Standards and to use or adopt them as required.

4 Hydrogen Storage Materials - Development, Upscaling and Testing of Nanocomposite Materials for Hydrogen Storage

German partners:

- Karlsruhe Institute of Technology, Karlsruhe (Project leader)
- Fraunhofer-Institut für Fertigungstechnik und Angewandte Materialforschung, Dresden
- GKSS Forschungszentrum Geesthacht GmbH, Geesthacht
- Max-Planck-Institut für Kohlenforschung, Mülheim/Ruhr

Chinese partners:

- General Research Institute for Nonferrous Metals (GRINM), Beijing
- Nankai University, Tianjin

Project duration: October 2009 – March 2012

4.1 Objectives:

The goal of this study is the development, optimization and realization of a hydrogen sorption tank system for combination with a high temperature PEM fuel cell (HT-PEM FC) aiming at automotive applications, primarily.

In close collaboration between German and Chinese partners, suitable nanocomposite solid storage materials shall be developed further and an upscaling of the fabrication will be performed. The synthesized material will be tested on the kilogram scale in a prototype-level sorption tank system under realistic operation conditions.

4.2 Work programme:

1. WP 1 - (MPI):
   - Laboratory studies on Li-boranate-based mixtures with MgH2.
   - Investigation of intermediates and search for catalysts.
2. WP 2 - (FZK):
   - Upscale studies of boranate based mixtures of MgH2. Optimization of parameters.
   - Production of material for WP 3.
3. WP 3 - (FhG IFAM):
   - Design and construction of hydride storage tanks
   - Implementation in realistic tank test

- Environment and system integration with HT-PEM

4. WP 4 - (GKSS):

- Laboratory studies on Li-Ca-B-H and comparative screening of current H storage materials.

4.3 First results:

The work has started in the different WPs and first results have been achieved related to improved properties of nanocomposites made from borohydrides and Mg hydride and from amide based materials. Further investigations are under way. Moreover, experimental work focused on investigation of thermal properties of hydrides which were mixed with expanded natural graphite in order to improve the heat conduction properties. Therefore, cylindrical compacts were produced which show superior safety and heat conduction properties.

5 Experimental Study to the Dynamic Operation of PEMFC-Stacks

German partner: Zentrum für Sonnenenergie- und Wasserstoff- Forschung (ZSW), Ulm,
Chinese Partner: Dalian Institute of Chemical Physics (DICP), Dalian,
Project duration: October 2009 - September 2011

5.1 Objectives:

Lifetime of PEFC - Stacks with highly dynamic operation like in automotive applications is significantly shorter than the lifetime of comparable stationary Stacks caused by their high dynamic operation conditions.Therefore the project focus is to improve the lifetime of automotive PEMFC.

5.2 Work Programme:

ZSW

1. WP1 - Parameter definition and evaluation

- Definition of operation & measurement parameters; Evaluation/development of appropriate
- measurement methods & test benches and hardware for data logging

2. WP2 - Experiments

- Acquisition / development / construction and test of measurement methods and test benches;
- Manufacturing of short stacks with different GDL & flow field designs; Stack measurements with
- high dynamic operation including Start / Stop – procedures; Examination of selected operation
- states with neutron radiography

3. WP3 - Modeling

- Fluent Modelling of different flow field geometries

- Step 1: stationary 1-dimensional calculation, identification of critical areas; Step 2: dynamic
- calculation, identification of critical states; Step 3: implementation of Fluent PEM - Modul

4. WP4 - Validation

- Results of AP2 & AP3 → optimized flow field and GDL for dynamic operation will be constructed /
- elected and tested; Development of suitable operation strategies for dynamic operation; Construction and testing of a full sized Stack (≥ 20 cells) with optimized flow fields and GDLs.

DICP

1. WP1 - Measure the distributions of local current, temperature and voltage in a 300cm^2 cell in DICP; Compare the measurement results with those of 100 cm^2 cell from ZSW; Study the start/stop process.
2. WP2 - Investigate the fuel starvation behavior of a separated cell in a short stack in DICP; Change the cell parameters; Compare the test results with those of ZSW.
3. WP3 - Test the influence of different MEA structures (different catalyst, GDL and membranes) on the dynamic behaviour.
4. WP4 - Test the water distributions in different dynamic processes with a small DICP stack in Germany.

5.3 First results:

A test bench for high dynamic operation of PEFC Stacks is developed and currently under construction. A circuit board for locally resolved current density measurements under high dynamic operation is developed and currently under construction.

Acknowledgments

Thanks for support to

1. Legal Framework Project:

- Stefan GARCHE, EnergieAgentur NRW, Düsseldorf, garche@energieagentur.NRW.de
- Zongqiang MAO, Tsinghua University Beijing, maozq@tsinghua.edu.cn

2. Codes and Standards Project:

- Reinhold WURSTER, LBST Ottobrunn, wurster@lbst.de
- Yuntang HE, CATARC, heyuntang@catarc.ac.cn

3. Hydrogen Storage Material Project:

- Maximilian FICHTNER, KIT Karlsruhe, fichtner@kit.edu
- Shumao WANG; GRINM Beijing, wsm1963@sohu.com

4. Dynamic of PEMFCs Project:

- Günther SCHLUMBERGER, ZSW Ulm, guenther.schlumberger@zsw-bw.de
- Ming HOU, DICP Dalian, houming@dicp.ac.cn

Aims and First Assessments of the French Hydrogen Pathways Project HyFrance3

Alain Le Duigou, CEA/DEN/DANS/I-Tésé, France
Marie-Marguerite Quéméré, EDF R&D, Département EPI, France
Pierre Marion, **Pascal Houel,** IFP, France
Philippe Menanteau, CNRS LEPII, France
Laure Sinegre, Lionel Nadau, GdF Suez, Direction Recherche et Innovation, France
Aline Rastetter, ALPHEA, URODEV CENTER, France
Aude Cuni, Air Liquide, France
Philippe Mulard, TOTAL France
Loïc Antoine, ADEME, France
Thierry Alleau, AFH2, France

Abstract

The HyFrance Group was originally formed in France to support the European project HyWays, by providing (former projects HyFrance1 and HyFrance2) the French data and possible hydrogen pathways according to national specificities. HyFrance3 is a new project that focuses on the economic competitiveness of different steps of the hydrogen chain, from the production to end usage, at the time horizon of 2030 in France. The project is coordinated by CEA with the other partners being: ADEME (co-funding), AFH2, CNRS, IFP, Air Liquide, EdF, GdF Suez, TOTAL, ALPHEA. The project is divided into 4 sub-projects, that address present and future French hydrogen industrial markets for chemical & refinery uses, the analysis of the interplay between wind energy production and storage of hydrogen for different automotive requirements (refuelling stations, BtL plants, H_2/NG mix), massive hydrogen storage to balance various offer and demand characteristics, and the supply network (pipeline option competitiveness vs. trucked in supply) to distribute hydrogen in a French region for automotive applications. Technical and economical issues, as well as GHG emissions, are addressed.

Keyword: HyFrance, Hydrogen, Roadmap, Techno-economy, storage, wind energy, industrial applications, infrastructure

1 Introduction

HyFrance3 is a ADEME funded French project, involving ten partners in an national consortium, that consists of major players from a range of energy, scientific, research and engineering institutions together with SMEs: ADEME (partner and co-funding), AFH2, CNRS, IFP, Air Liquide, EdF, GdF Suez, TOTAL, ALPHEA and CEA (coordinator). These partners have already achieved a high level of international visibility, recognition and acceptance within the framework of the former projects HyFrance1 and HyFrance2 [1]. Those projects partners contributed, together with other partners such as BRGM, Renault, PSA, to work out

a French hydrogen energy roadmap, as a French application of the techno- and socio-economic methods and tools used in the European project HyWays [2] which aimed at developing a European hydrogen energy roadmap. As the aim of HyFrance is to identify the key issues, challenges, barriers and opportunities related to the development of hydrogen energy and its applications in France, HyFrance3 has been launched to focus on the economic competitiveness of different steps of the hydrogen value chain that had not been, or insufficiently, achieved in HyFrance1 and HyFrance2, from the production to end usage use, at the time horizon of 2030 in France.

This paper describes the topics addressed by this 18 months duration project that has been launched at the end of May 2009. The work is divided into 4 sub-projects, that cover both large scale systems (SP1, SP3, SP4) and a smaller scale one (SP2):

- SP1 : present and future French hydrogen industrial markets (merchant, captive and co-product), for chemical and refinery uses depending on different scenarios including the use of BtL,
- SP2 : technologies and costs of H_2 production from wind power for different transport requirements (refuelling stations, BtL plants, H_2/NG mix) with different grid configurations (isolated or connected wind power plants) and H_2 storage volumes,
- SP3 : relevance, dimensions and costs of centralized or decentralized hydrogen mass storage, to balance various offer and demand characteristics,
- SP4 : large scale infrastructure to satisfy massive demand vs. massive production or storage, by dimensioning the supply network (pipeline option competitiveness vs. trucked in supply) to distribute hydrogen in a French region for automotive applications.

Technical and economic issues, as well as GHG emissions, are addressed.

This national project aims also to pursue the French collective techno-economic expertise that emerged in the former HyFrance1 and HyFrance2 projects.

2 Present and Future French Hydrogen Industrial Markets

Similarly to the european and world markets, hydrogen in France is mainly produced for ammonia and refinery uses, both from fossil resources (captive and merchant supply) and as chemical processes co-product. In the short and medium term, given the prospects of an increasing hydrogen demand essentially for refinery use (desulfurisation, heavy crude oil processing, environmental requests), a progressive awareness of the limited fossil hydrocarbon reserves as well as increasingly stringent limitations of the emissions of greenhouse gases, low carbon content hydrogen production processes such as water electrolysis will appear relevant and long term candidate for hydrogen production. HyFrance3 aims to analyse the short and medium term hydrogen needs for a chemical and refinery use, up to 2030.

A study has been carried out, based upon literature data and a complete survey of the French producers and consumers. It appears that by-product hydrogen share exceeds 50% (including steel industry coke oven gas) of the total hydrogen production, with a significant ratio being burnt, while those quantities could be considered as potentially available to supply car fleets for instance, but for a transition phase only. Almost all hydrogen is produced and

consumed at the same location, and cross-border trade is negligible. In addition, emerging markets such as iron and steel industry could take benefit of a green hydrogen use, as foreseen for instance by the ULCOS (Ultra-Low CO_2 Steelmaking) project; this could represent very high supply requests, but rather in the long term. By and large, the French hydrogen industrial market should reasonably increase in the medium term. The CO_2 emissions associated to H_2 production are not very important (about 1 to 2% of the overall French emissions), but they could only be lowered either through expensive CO_2 capture and storage technologies (still to be demonstrated at a large scale) or by the use of nuclear or French electricity mix driven electrolysis.

As regards hydrogen needs for the refining industry, two petroleum scenarios are analysed. On the one hand, a "trend-setting" development scenario that perpetuate the current energy demand and technological progress foreseen together with an increase in bio-fuel use (10%, including a second generation allothermal bio-fuels ratio) hybridised cars and electrical vehicles (7.5% of the total number of cars in France). On the other hand, an "environmentally friendly" development scenario considers more ambitious hypothesis such as lower fuel consumptions (-20%), a strong increase in combined rail and road transport (20%), and 21% of cars without internal combustion engine: 15% electric vehicles (battery electric and hybrid), and 6% hydrogen fuel cell vehicles which corresponds to the HyWays "low" scenario for France in 2030. Calculations will use linear programming, to match the different fuels market demand with refinery scheme and crude oil supply, and therefore hydrogen requests, as a function of the scenarios and hypothesis chosen. Well-To-Weels BtL costs will be evaluated, taking into account the interplay with SP2 (above) when hydrogen is produced by electrolysis from wind energy. Overall CO_2 emissions will be estimated too.

3 Wind Energy Hydrogen Economics

Hydrogen production from wind energy often appears as a promising way to increase the renewable energy ratio in the energy mix, hydrogen being then developed as an electrical energy storage medium, as well as a very low CO_2 energy supply for a direct use in transports, together with an important energy security of energy supply. Different layouts may be considered: remote wind farms dedicated to hydrogen production on the one hand, and wind power systems connected to the grid, on the other hand, capable of providing a continuous electrolyser operation and possibly retailing electricity to the grid. Given the shape of hydrogen demand, different storage configurations may be necessary to guarantee continuous supply: irregular or regular requirements from refuelling stations, or continuous demand from a chemical process, for instance.

This topic aims at evaluating hydrogen production costs, given different types of demand, using wind power plants, electricity network, electrolysers, compressed hydrogen storage, and SOFC fuel cells to sell electricity to the grid. The simulation tool HOMER (NREL) is used to give the optimal techno-economic layout for each case, according to the components specifications and under the following economical assumptions: 3 MW wind systems, IHT S-556 electrolyser (760 Nm^3 H_2/h), 23 m^3 Air Liquide tube trailer storage (200 bar), 20 years lifetimes except for intermittently used electrolysers (10 years), and a 6% discount rate. The different cases considered are the supply of a hydrogen motorway service area in the south

of France (important H_2 demand peaks), of a Hythane bus fleet (continuous supply of a binary mixture of 20% Hydrogen and 80% natural gas), and of a 2000 barrels per day BtL station. Unlike the refuelling station and Hythane bus fleet cases, the last one does not require any hydrogen storage capacity, which is provided there by the biofuel plant, and then considers a supply "with the current".

The first simulations show a large hydrogen production cost range, depending on the very different characteristics of the demand. The refuelling station requires a 28 MW isolated wind farm and the most important storage capacity. Hydrogen production is then the most expensive, in some cases over 20€/kg, but can be lowered by an appropriate overall system of management. Hydrogen production cost is barely cheaper in the case of a 3 MW isolated wind farm capable of supplying a 100 buses fleet (12.5 kg/h) because of H_2 storage. It is much different with the BtL station that can be supplied without H_2 storage. An isolated 48 MW wind farm could supply roughly 7% of a 2000 barrels per day BtL station, at an average cost of 9 €/kg. All these costs can of course be noticeably lowered when the system is connected to the grid, the lowest range of 4-5 €/kg being reached for the BtL station with grid connection.

4 Hydrogen Mass Storage

The former project HyFrance2 promoted a French strategy for hydrogen production with CO_2-free or CO_2-reduced emissions, i.e. mainly steam methane reforming SMR (assuming the availability of cost-effective techniques for CO_2 capture and storage), conventional water electrolysis using the French electricity mix (90% from non-fossil resources) and regional biomass gasification (large resources available). Whatever may be the future hydrogen production methods, large scale use of hydrogen will require massive storage comparable to natural gas to balance supply and demand. This is specifically relevant for the production of renewable hydrogen from intermittent sources such as wind energy, as described above. But storage remains essential to connect large scale hydrogen continuous production, as cited above, with seasonal demands. The mass storage will interact with the hydrogen grid similar to the buffering capabilities in the current natural gas grid, and the locations could be very similar. But technical requirements and strategy may strongly differ: natural gas storage in France responds to both winter/summer stationary use fluctuations and strategic choices, whereas H_2 mass storage would be linked to seasonal demand changes related to the variations in automotive uses.

We evaluate hydrogen mass storage dimensioning and costs connected with an infrastructure network to be developed in a couple of French regions during the next decades (up to 2050), as described below. In the literature, four underground facilities are considered in which natural gas can be stored under pressure: depleted oil fields, aquifers, excavated rock mines, and salt caverns. Given the French geological layout, we consider the latter as the cheapest most convenient in principle. Thick salt deposits are located in the south and east of France, and salt caverns have the advantage of good performances in terms of filling and emptying (cycling), working volumes, reasonable depths and cushion gas needs. As said below, both south-east French administrative regions named Rhône-Alpes and PACA have been selected for this study. Hydrogen quantities to be stored have been evaluated, roughly

at a few tenth of thousands tons, as well as filling and emptying rates which may have a strong impact on the dimensioning. This fits on the one hand the demands in 2050 for personal cars and light duty vehicles with a hydrogen fuel cell or internal combustion engine, evaluated by two scenarios of the French project PROTEC H_2 (see below), and on the other hand a continuous hydrogen supply which considers a possible break (maintenance) for a whole month.

5 Hydrogen Infrastructure and Transport in a French Region

Currently, existing hydrogen production, storage and infrastructure is mostly used for the chemical and refining industries, and as said above, even if nearly 1600km of hydrogen pipelines in Europe have been identified, almost all hydrogen is produced and consumed on-site. In the future, hydrogen use will be spread all over the country, therefore a distribution infrastructure will be necessary. Its design and costs will be of a primary importance for the global use and acceptance of this energy carrier, case specific and strongly dependent on the scenarios of demand, essentially for transportation, delivery options and geographic locations (production, storage, refuelling stations).

Various projects such as HyWays and Roads2HyCom evaluated the technological developments and related costs of hydrogen infrastructure for transport and distribution. HyFrance3 aims to analyse the hydrogen infrastructure development in two French regions, selected on the basis of criteria such as industrial and research capacities, massive geological gas storage opportunities, and initiatives in hydrogen projects and demonstrations. South-East French administrative regions named Rhône-Alpes and PACA have been selected, which gather almost 20% of the French population. Deployment scenarios given by the recent French project PROTEC H_2 (calculated by the POLES code) have been selected to characterize hydrogen demands up to 2050: penetrations rates of 16% and 40% at that time horizon for passenger cars and light duty vehicles, together with somewhat lower penetration rate values, less than 2%, in 2030. The ECOTRANSHY code will be used to work out an economic model that can provide the main optimal features (trucks or pipelines? where? when?) of a hydrogen network originating from large-scale facilities (production and mass storage) and supplying a set of GPS-located delivery points with given demands (refuelling stations), at various time steps from 2010 to 2050. The approach has the advantage to mix in a unified framework economical issues (estimation of capital and operational expenditures), physical features pertaining to hydrogen (trucks characteristics, hydraulics of pipelines and compression stations), and geographical constraints (location of sources and consumptions). With regard to the supply, salt caverns mass storage locations inside the Rhône-Alpes and PACA regions will be considered at first, as well as long distances mass storage locations in the case of French regions lacking of geological mass storage capacities. Hydrogen transport between large scale production and geological mass storage facilities will be evaluated too.

6 Conclusion

This project aims to assess different steps of the hydrogen chain at the time horizon 2030 in France, from the production to the final use. Industrial markets (chemistry, refinery) should

reasonably increase in the medium term, mainly due to refinery use; steelmaking could represent very high supply requests, but rather in the long term. As regards hydrogen needs for the refining industry, two petroleum scenarios are analysed: a "trend-setting" one, and an "environmental" one that considers a 6% penetration rate of hydrogen fuel cell uses in vehicles in 2030. The wind energy hydrogen production first simulations show a large cost range: from 4-5 €/kg when the system is connected to the grid for a supply "with the current", up to over 20€/kg for an isolated refuelling station. As regards hydrogen massive underground storage, salt reservoirs located in the south and east of France will be considered; hydrogen quantities to be stored have been evaluated, roughly at a few tenth of thousands tons to balance supply and demand in the Rhône-Alpes and PACA regions. Those two French administrative regions have been selected to evaluate the 2 deployment scenarios given by the recent French project PROTEC H_2: penetrations rates of 16% and 40% at the time horizon 2050, together with somewhat lower penetration rate values, less than 2%, in 2030. ECOTRANSHY code will be used to work out an economic model that can provide the main optimal features of a hydrogen network originating from large-scale facilities to supply refuelling stations, at various time steps from 2010 to 2050. In addition to the technical and economic data that will be given, HyFrance3 offers, as a continuation of HyFrance1 and HyFrance2, the opportunity of a national debate on hydrogen by gathering the major French public and industrial research partners. Large scale analysis developed in HyFrance3 address practical topics that could lead to detailed developments in future projects, to evaluate for instance hydrogen scenarios that consider intermittent energy sources, massive production and hydrogen storage, and national transport and distribution infrastructures.

Acknowledgment

The project HyFrance3 is funded by the French ADEME, Agence de l'Environnement et de la Maîtrise de l'Énergie (Environment and Energy Management Agency), contract number 0874C0009.

References

[1] HyWays, the European Hydrogen Roadmap, Contract SES6-502596

[2] Towards a French Hydrogen Energy Roadmap: the HyFrance Project / J.M. Agator, S. Avril / WHEC 16 / 13-16 June 2006 – Lyon, France

[3] MANN (Margaret) & SPATH (Pamela), Life Cycle Assessment of Hydrogen Production via Natural Gas Steam Reforming, NREL/TP-570-27637, Revised February 2001

[4] Addressing the climate change challenge: the ULCOS breakthrough program - Tokyo, ISIJ 157th meeting, 30 March 2009 /Jean-Pierre Birat.

[5] IVY (Johanna), Summary of Electrolytic Hydrogen Production, Milestone Completion Report – NREL/MP-560-36734, September 2004

[6] Jean Andre (GdF Suez) and al. / ECOTRANSHY - Least-cost development of hydrogen transmission-distribution pipeline networks / WHEC 17 / 15-19 June 2008 – Brisbane, Australia

[7] Roads2HyCom Hydrogen & Fuel Cell Database (2007) (http://www.roads2hy.com/)

Financial Investments in Fuel Cells and Hydrogen Projects in Brazil

Maiana Brito de Matos, Universidade Estadual de Campinas (UNICAMP), Brazil
Newton Pimenta Neves Jr., **Ennio Peres da Silva**, **Cristiano Silva Pinto**, UNICAMP-SP, Brazil

Abstract

This work aims to identify, classify and account for the investments in hydrogen and fuel cells from 1999 to 2007 made by the public and private sectors in Brazil. Two methodologies were applied to obtain the data for this study. The Top-Down methodology was used to obtain the information from the sponsoring agencies, institutions and funds that promote science and technology in Brazil, such as *CNPq*, *FINEP*, *P&D ANEEL* and Regional Foundations for Research Support. The Bottom-Up methodology consisted in obtaining data directly from the research groups granted by those agencies. After accounting the total Brazilian investment in the period, this was compared with the investments made by the other BRIC countries (Russia, India and China). Next, BRIC countries investment was compared with those made by the European Union, Japan and the United States. The results show that in order to participate in the market share related to equipment and services for the hydrogen economy, Brazil needs to increase the efforts in research, development and innovation in the area. It will be also necessary to apply resources in other important research issues besides ethanol reforming, polymer electrolyte and solid oxide fuel cells, which are the current technologies supported by the Brazilian funding agencies. To achieve this, resources that are already available could be used more efficiently. Another important evidence is that the total annual investment made BRIC countries together is of the same order of magnitude as the investments made separately by the European Union, Japan and the United States.

Key words: Hydrogen, investments, fuel cell

1 Introduction

Brazil has two national programs for the development of the hydrogen economy; one articulated by the Ministry of Science Technology (MST) and another by the Ministry of Mines and Energy (MME). In 2002, the MST created the Brazilian Program for Fuel Cell Systems (PROCaC) and in 2004 MME created the roadmap for the introduction of the hydrogen economy in Brazil under the IPHE.

Several factors led the Brazilian government to organize actions about the use of hydrogen as an energy vector, namely: the concerns about climate change, the intensive use of fossil fuels, the dependence of imported oil from politically unstable countries, the importance of integrating renewable energy sources into the global energy matrix. Considering the efforts already made in the country under PROCaC, this study aims to evaluate comprehensively the investments in hydrogen and fuel cells in Brazil and compare them with those made by other countries, which can enable better strategic planning for the sector.

1.1 Methodologies: *Bottom-Up and Top-Down*

In this work, the Bottom-Up strategy was employed to obtain information directly from the research groups of universities or other institutions. On the other hand, the Top-Down methodology was employed to obtain information from the funding agencies of R&D projects, such as the National Council for Scientific and Technological Development (CNPq), Research and Projects Financing (FINEP), State Research Foundations (FAPs), National Energy Agency (ANEEL), National Petroleum Agency (ANP), etc. In this work, the consulted FAPs were FAPESP (São Paulo), FAPEMIG (Minas Gerais), FAPERJ (Rio de Janeiro), FAPERGS (Rio Grande do Sul), FAPESB (Bahia), FAPESC (Santa Catarina), and Fundação Araucária (Paraná). The choice of these FAPs was due to the great concentration of R&D groups working on hydrogen and fuel cell technologies in their respective states.

1.2 Total investments in hydrogen and fuel cells in Brazil

Table 1 presents a comparison between the total values obtained by both methodologies in each research field in Brazil from 1999 to 2007. There is a difference in values determined in each methodology, and this will be better explained later in this work. But the percentages in each of the areas were in good agreement.

Table 1: Investments in hydrogen and fuel cell technologies in Brazil from 1999 to 2007 according to the methodologies *Bottom-Up* and *Top-Down.*

	Investments *Bottom-Up*		Investments *Top-Down*	
Area	Million dollars	Percentage	Million dollars	Percentage
Hydrogen	16.9	41%	17.52	40%
Fuel Cell	18.06	44%	20.16	46%
Others Activities	6.17	15%	6.12	14%
TOTAL	41.13	100%	43.81	100%

The figure found in the methodology Top-Down (43.81 million U.S. dollars) was greater than that obtained in the Bottom-Up (41.13 million U.S. dollars). The calculated difference of 2.68 million dollars corresponds to 6%, which can be considered reasonable. But the difference in the number of projects between the methodologies reached 200, which is highly above the expectations. One possible explanation is that 43% of the R&D groups have not responded to the questionnaire; in addition, 54% of the respondents submitted incomplete answers. Another reason to be pointed out was the great difficulty in obtaining information from the funding agencies. The only exception was ANEEL, which has a database on its website containing all information related to R&D projects. In this case, only minor mistakes were found, related to the repetition of some projects in the database. Additionally, FAPESP may have supported a large number of small projects or accounted for scientific initiation scholarships, masters and doctoral projects. But, unfortunately, this could not be verified and revised.

1.3 Investments in hydrogen and fuel cell in the world

The major hydrogen programs in the world are carried out in the United States of America (U.S.), Japan and the European Union (EU). According to UNEP (2006), these countries account for about two thirds of the public investment in R&D of technologies related to hydrogen.

This work corroborates the findings of UNEP (2006), that the largest investors in hydrogen and fuel cells in the world are: the United States, Japan and the European Union. Although there are significant projects and investments in other countries, for instance Canada, Germany and Iceland, they are not presented here. Investments made by Russia, China and India have somewhat similar levels to those made by Brazil.

Table 2: Federal Investments in the Hydrogen Economy by BRIC countries: Brazil, Russia, India and China (amounts in millions U.S. dollars).

Year	Brazil *Top-Down (reference)*	Brazil *Top-Down* and *Bottom-Up*	Russia	India	China
1999	0.59	3.38	*na	na	na
2000	10.51	13.45	na	na	na
2001	1.15	4.09	na	na	24.07
2002	4.99	7.93	na	na	24.07
2003	5.52	8.45	na	na	24.07
2004	3.03	5.97	37.00	na	24.07
2005	5.29	8.23	30.00	18.97	24.07
2006	3.73	6.66	30.00	19.85	9.40
2007	9.00	11.94	30.00	18.89	
TOTAL	43.81	70.10	127.00	57.71	129.75
Annual Invest.	4.87	7.79	31.75	19.24	21.63
Total annual invest.		80.41			
%	***	10%	39%	24%	27%

na =not available

According to the data in Table 2, Brazil was the BRIC country which invested the least, accounting for 10% of the total annual investments made by BRICs.

The original intent was to obtain complete data from 1999 to 2007 in order to compare investments with those obtained in Brazil. However, in Table 2 and Table 3, one can observe

that there are some gaps due to the lack of information. So, it was chosen a similar period to make comparisons. Table 3 shows the period between 2001 and 2007 and includes data for all countries.

Table 3: Federal Investments in the Hydrogen Economy by BRICs, U.S., Japan and EU (millions U.S dollars).

Year	BRIC	U.S.	Japan	EU*
1999	3.38	Na	na	na
2000	13.45	na	79.66	na
2001	28.16	209.70	118.36	119.64
2002	32.00	240.70	165.00	109.45
2003	32.52	294.00	255.73	137.45
2004	67.04	298.50	310.58	159.09
2005	81.27	221.70	340.97	166.73
2006	65.91	232.46	288.18	154.00
2007	60.83	267.56	197.12	165.46
TOTAL	384.56	1.764.62	1.755.60	1.011.82
%	7.82%	35.89%	35.71%	20.58%
% U.S., JP & EU	***	38.94%	38.74%	22.33%

Total: BRIC, U.S., JP & EU	4,916.60
Total: U.S., JP & EU	4.532.04

In fact, Table 3 shows that BRIC investments over the period were modest, accounting for 7.82% of the total investments made by BRICs, U.S., Japan and the European Union. The total amount invested by BRICs is in the same order of magnitude of the annual investments made by the United States, Japan or the European Union, individually.

2 Conclusions and Suggestions

The lack of clear criteria to classify investments by the research institutions can be identified as one of the major problems in the development of this work, as well as the difficulties associated to the questionnaires that were not properly answered.

Despite the efforts, most of the funding agencies did not provide adequate information about the investments in the projects they were supporting. The exception was the R&D program supported by ANEEL that makes all information publicly available on its website.

Most of the Brazilian investments in fuel cells were aimed to PEMFC, with 56%, followed by SOFC with 37%. Regarding hydrogen projects (production, storage and distribution), ethanol reforming accounted for 95% of the amount invested, and the most significant share was allocated to the development of catalysts for reformation.

According to the data available for the period 1999-2007, the annual amount invested by BRIC countries corresponded to 80.41 million dollars, which was in the same order of magnitude of the annual public investment made by the United States, Japan or the European Union individually. However, it is also known that the private sector participation in these countries is substantial while in Brazil, nowadays, this participation can be considered low, at least in the hydrogen-related technologies.

Even without complete data for the period of interest, it was noted that the annual investment made by Brazil was the smallest among the BRIC countries. Despite the important achievements that have been communicated by the Brazilian research groups, this conclusion indicate that to improve its market share of equipment and services related to the Hydrogen Economy, Brazil will need to increase the efforts in research, development and innovation in several areas beyond ethanol reforming, proton exchange and solid oxide fuel cells. This can be achieved by employing new sources of funds and by making better use of the existing financial and personnel resources.

References

[1] CNPq **National Council for Scientific and Technological Development**. Available at: http://www.cnpq.br/cnpq/index.htm Access: nov 2008.

[2] *IEA International Energy Agency.* ***Hydrogen and Fuel Cells: Reviews of National R&D Programmes,*** **IEA/OECD**. 2004a, Paris.

[3] IPCC ***Intergovernmental Panel on Climate Change***. ***Evaluating the Costs of Mitigation of Greenhouse Gas Emissions by Sources and Removals by Sinks****. Second scientific assessment report. Working group III. Cambridge University Press*. Cambridge. 1996.

[4] P&D Aneel **Pesquisa e Desenvolvimento da Agência Nacional de Energia Elétrica**. **Banco de Dados Projetos**. Available at: <https://ped.aneel.gov.br/consultaPublica/consultarProjetos.asp>. Access: out 2008.

[5] UNEP ***United Nations Environment Programme***. ***The Hydrogen Economy: A non-technical review***. 2006. .Available at: http://www.unep.org/publications/search/pub_details_s.asp?ID=3771. Access: out 2008.

Policy and Action Programs for Hydrogen Energy

Kazuyuki Ochi, Coordinator for Industry-Academia-Government Collaboration, Industrial Promotion Section, Planning and Economics Division, Saijo City, Japan
Kotaro Itoh, Mayor of Saijo City, Japan
Hirohisa Uchida, School of Engineering, Tokai University, Japan

1 Introduction

In 1981, the then-largest scale solar power testing facility in the world was installed in Saijo city (Figure 1), and thus largely influenced the expansion of solar power systems in Japan. Since that time, upon making “a city full of warmth, vitality, and ideal amenities” the goal for Saijo, we have laid out a new earth environment friendly policy that puts new-energy and reduced-energy at the focus. Since 2001, with the support of the Ministry of Trade, Economy, and Industry, NEDO (The New Energy and Industrial Technology Development Organization), and Tokai University, we have been able to implement carbon-cutting initiatives as well as reduced-energy technology into the agricultural sphere. Also, using the MH (Metal Hydride) freezer System powered by hydrogen storage alloys and waste heat, we have developed a detailed method for delivering clean hydrogen energy to farms and fisheries in Saijo.

Figure 1: A solar system test facility of 1,000 kW with 22,000 solar panels.

From 2007, the cooling technique made possible through factory emissions and the MH of hydrogen storage alloys were applied to hydrogen strawberry cultivation and above-ground fisheries, both of which have been successful. The cultivation of strawberries all year-round is now possible due to hydrogen energy. Furthermore, compared with Freon-based cooling systems or oil heater-based temperature control systems in greenhouses, this MH cooling

technique is much more effective in cutting carbon emissions and cutting energy use levels. In this study, we shall detail potential applications of the MH of hydrogen storage alloys in both agriculture and fishery endeavours, as well as examples of how hydrogen energy is a clean energy source which acts kindly towards the environment while still aiding in food production technology.

Saijo city is blessed by a year-round temperate climate and a 5,000ha agricultural plain which is host to a multitude of crops produced, with a production value exceeding 15 billion yen (150 million dollars) annually.

The wide-open bay stretching to the north of Saijo is also blessed with natural resources, full of sea vegetation and sea creatures. The factories that stretch along this bay produce goods in value of 850 billion yen (8.5 billion dollars) annually, and the single most invaluable resource supporting these industries is water.

Within Saijo city, crystal clear underground water that is known as the “most delicious in Japan” springs forth naturally from myriad places, and is estimated to exceed 90,000 m^3 daily. It is named “uchinuki” water and is beloved by all citizens.

Aiming for the independence and success of local neighbourhoods, we have initiated a new, forward-thinking policy towards the global environment which we hope will be continued by generations to come.

2 Experiments

2.1 MH cold water production system (Figure 2)

Figure 2: MH cold water production system.

Aiming from the fact that hydrogen energy is clean and kind to the environment and establishing the merits of hydrogen as an unwavering secondary energy source with a fixed unit price, in 2001 we established an MH freezer [1] research plan using hydrogen storage

alloys where exothermic and endothermic heat reactions are used, and freezing is made by cyclic steps as defined in Figure 3.

The F-class MH freezer we established in December, 2002, had an output of approximately 11.6 kW/hr, and compared with a typical Freon-based refrigeration unit, it used 70% less power and less CO_2 emissions [2], thus proven to be more environment-friendly. In 2005, test plants were installed by the Ehime-based LLP “Tryout Ehime” for a C-class MH freezer with cold water production function with an output of approximately 2.3 kw/hr. Because the test plants actually manufactured a large amount of 5 °C water, they were converted for practical agricultural use in 2007, and experiments by Saijo city were begun.

2007 Condition and Performance of MH freezer with cold water production function

MH Water Cooling Device: Japan Steel Works, LTD.

Output: approx 2.3kw/hr(converted)

Type of Alloy: Low-heat use Titanium Alloy

Number of Alloy Tanks:

- High Temp Level (2 sets) (*Φ*: 210.7mm×L: 1,259×2set)
- Low Temp Level (2 sets) (*Φ*: 210.7mm×L: 1,099×2set)

Weight of Alloy Tanks:

- High Temp Level (20kg)
- Low Temp Level (18kg)

Alloy Weight:

- High Temp (36.0kg×2set)
- Low Temp (30.0kg×2set)

Energy Source:

- 420°C Metal Treatment Factory emissions (vapour),
- 95°C water made from that vapour,
- 20°C groundwater and purchased electrical power

Cycle Time (Please refer to Figure 3 for the definition.): 11 minutes as a base

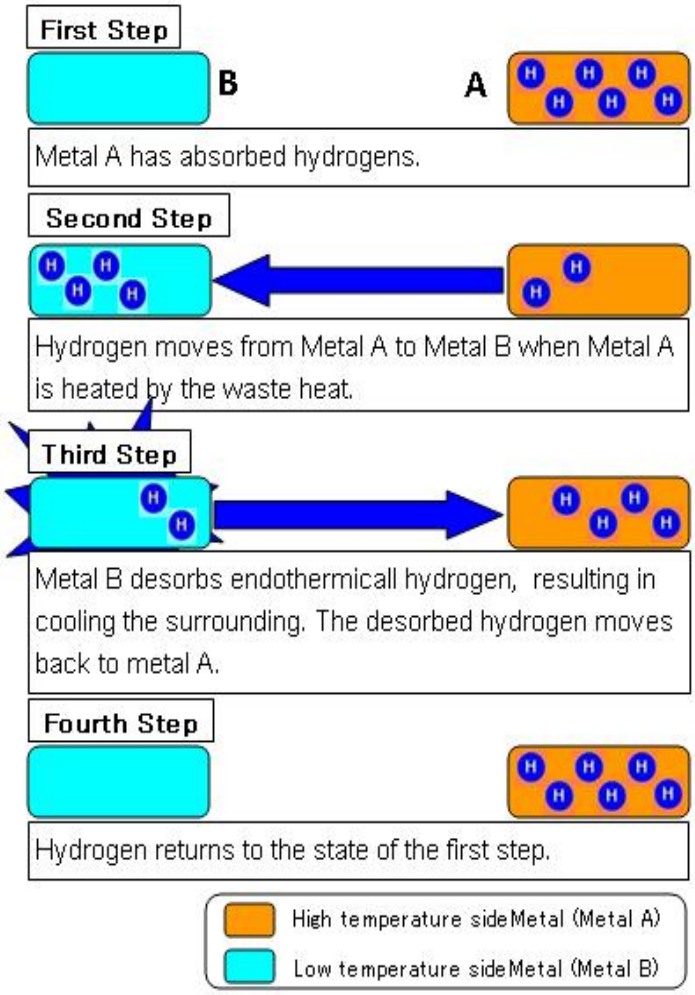

Figure 3: MH heat pump operation. One cycle is defined as completion of the above-mentioned 4 steps.

In the hydrogen strawberry cultivation experiment, the temperature of the water used for the greenhouse was a minimum of 0.98 °C, a maximum of 9.08 °C, and an average of 2.17 °C. From 2008, the area of the greenhouse was expanded to 97 m², and refrigerating units with the same cooling power as the MH Cold Water Production Systems were used in an

experiment. Each of the devices was shown to have the capability to produce 4.8 tons of 5 °C cool water per day.

In October 2009, while continuing the experiments at the 97 m² greenhouse, the construction of an agricultural greenhouse for the demonstration of daily-use practical purposes, measuring at 1,000 m², was completed to conform to the MH Cold Water Production System standards. Also, in February 2010, an above-ground fishery was also completed according to the MH Cold Water Production System standards.

The properties and conditions of the two newly-installed MH Cold Water Production System installations are detailed below.

2009 Condition and performance of MH Cold Water Production System

Per Installation:

- MH Cold Water Production Devices：Japan Steel Works, LTD.
- Types of Alloys: equal to the condition and the performance as in 2007.
- Number of Alloy Tanks： equal to the condition and the performance as in 2007.
- Weight of Alloy Tanks： equal to the condition and the performance as in 2007.
- Amount of Alloy： equal to the condition and the performance as in 2007.
- Source of Energy： The 200°C water vapour from the power unit of a chemical factory, the 95°C water reduced from it, 20°C ground water & purchased electrical power.
- Cycle Time： It is equal to expression Condition and the performance in 2007.

2.2 Hydrogen strawberry

The harvest of strawberries in Japan usually occurs from December until the following May, and from June to November, the temperature inside agricultural greenhouses exceeds 35 °C on many days, causing high-heat exposure problems. In Saijo as well, strawberries are considered to be a fruit difficult to produce, and properly controlling the heat environment in which they are grown is a crucial cultivation condition.

In 2007, connecting the MH Cold Water Production System with the 16 m^2 agricultural greenhouse, an environmentally low-cost and heat-environment controllable strawberry cultivation experiment facility was constructed, and an experiment was begun with 68 strawberry plants. In 2008, an MH Cold Water Production System was implemented in a larger greenhouse of 97 m², and approximately 660 strawberry plants were used in a study of early harvest techniques, harvest prolongation techniques, and heat-environment control techniques. In controlling the heat-environment, an expansion of the piping from 43.5 m to 283.5 m was necessary, and as a result, the heat of the water rose 150 % while being circulated through the piping. In 2009, a 1,000 m^2 daily-use practical purpose greenhouse was installed (Figure 4) and 6,200 strawberry plants were planted in late September.

Figure 4: Greenhouse of 1,000 square meters.

The necessary piping for heat-environment control was increased to 1,500 m.

2.3 Fish cultivation on Land

In order to increase food supply production via fisheries using the successes of the year-round strawberry cultivation experiments, a new MH Cold Water Production System was installed at 4 different locations using 5 ton tanks, and an above-ground fishery facility was born in September 2009. With the support of the Fisheries Research Agency and the Natural Center for Stock Enhancement, this above-ground fishery system was able to implement sustained water temperatures, and also installed a closed-circulation system [3] to enhance savings on the fishery's overall water waste. With the assistance of the School of Marine Science, Tokai University, we are continuing to farm "Satsuki Trout" with a success rate unheralded in the past.

2.4 Circulation of energy

The facilities established in 2009 have the MH Cold Water Production System at their core, and through it, the circulation of energy has become possible. (Figure 5) It is estimated that the approximate yearly carbon dioxide emission cut will be nearly 74 tons over all the facilities. Also, the MH Cold Water Production System offers a 89.9% energy reduction when compared with common Freon-based cooling systems [4].

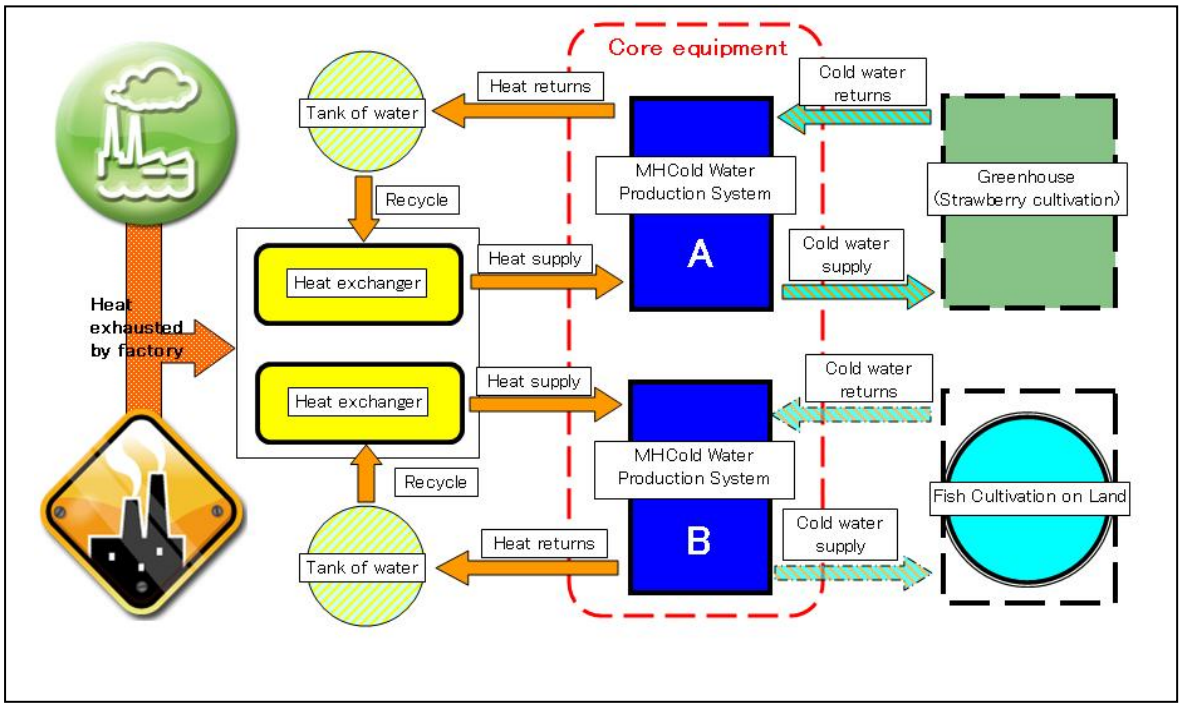

Figure 5: Energy cycles in Saijo city.

3 Results and Discussion

3.1 MH cold water production system

The specified temperature environment was able to be controlled regardless of the temperature change of the house for agriculture as a result of the temperature environment controls in the root sphere part beginning by booting up a system in May, 2009. Given a modification to the heat exchange efficiency of the system, the MH Cold Water Production System implemented in 2009 shows a 200 % increase in output production (4.0kw/h) when compared with the earlier 2007 model. Also, the predictability of the heat-environment control system was modified by an output control function as well as a water-temperature source gauge, and this allows the system to be used throughout the entire year. Furthermore, the space required to install the system was successfully reduced by 70 % to a small-scale model. The MH Cold Water Production System used for the fishery successfully offers an 8 % increase in output (4.3 kw/h) and a 36 % reduction in size from the agricultural greenhouse, as well as a 30.5 % reduction in manufacturing cost, bringing it down to 15 million yen (approx. $150,000).

3.2 Hydrogen strawberry

In 2007, due to the MH Cold Water Production System's heat-environment control, all of the strawberry plants were able to avoid heat damage in the summer months. Also, the start of the harvest became aligned with the harvest of strawberries force-flowered through the use of a Freon-based refrigeration system, and was estimated to accomplish an 85 % reduction in energy consumption. In 2009, the amount of strawberries harvested from the 6,200 plants

in the 1,000 m^2 greenhouse was an estimated 10kg per day. From here on, we will be aiming for a stable harvest amount even during Japanese mid-summer, during which in-house temperatures will exceed 40 °C.

3.3 Fish cultivation on land

On October 30th, 2009, 800 “Amago” Trout (*Oncorhynchus masou macrostomus*) minnows (approx. 18 cm long & 100 g in weight) were used to begin the fishery, and by late May, 2010, they are estimated to grow to 45cm long, 1kg “Satsuki Trout.” In each of the 4 tanks there are 200 fish. Three of the tanks are filled with man-made seawater, and the fourth tank is filled with fresh water, to be used for comparative purposes. The fish being bred in the man-made seawater tanks have reached 30cm in length and 250 g in weigh over a 3 month period, and are growing swiftly.

3.4 Development in the future

The MH Cold Water Production System is planned to be compartmentalized, allowing for a simpler construction, and for a reduction in installation costs.

Concerning Hydrogen Strawberries, we strive to successfully implement a year-round cultivation schedule and an increased prevalence of the strawberries. For the above-ground fishery project, we hope that the fruits of the MH Cold Water Production System can be further utilized in order to successfully breed “Satsuki Trout” well into the future.

All of the MH Cold Water Production Systems implanted after 2007 are examples of a new production form, in which facilities producing factory emissions and farms (including fisheries) become the pipeline for a physical cooperation in the construction of this form. In the example of a factory, in keeping with the human cultural tradition of the factory, factories will continue to function, yet their emissions will be yielded to farmers, who will in turn be able to use the emissions in producing agricultural goods, thus allowing them to cut back severely on their oil and electricity costs. This will allow for an overall reduction in the cost of production, and furthermore, it is expected to result in a massive reduction in carbon dioxide emissions. From this research, we are aiming to implement a low environmental load made possible through a locally active production model policy.

As the Japanese government is thoroughly endorsing environmental problem solutions such as the reduction of greenhouse gases [5], we are acting in accordance with this policy strengthening position. This study is a perfect match for the national policies being implemented and should thus be considering a leading model when grappling with environmental issues.

Acknowledgement

We are grateful to many organizations for support and indications:

- Ministry of Economy, Trade and Industry,
- Ministry of Agriculture, Forestry and Fisheries,
- Ehime Prefecture,
- New Energy and Industrial Technology Development Organization,
- Japan Foundation for Regional Vitalization,

- National Institute of Advanced Industrial Science and Technology in Shikoku,
- School of Engineering, and School of Marine Science and Technology of Tokai University,
- Center for Environment, Health and Field Science, Chiba University,
- Faculty of Agriculture, Ehine University,
- National Center for Stock Enhancement, Fisheries Research Agency,
- Kuraray CO., LTD.,
- TANIGUCHI HEAT TREATMENT CO.,LTD.,
- Saijo Industry and Information Center, for Support,
- LLP-TRYOUT Ehime and Itoh Engineer CO., LTD.

References

[1] H. Uchida, E. Akiba, S. Ono, K. Fukushima, K. Terao, T. Mashita, and K.Itoh, (Nov.2003) ”R&D of MH Freezer System as Eco Technology by Regional Consortium of Academic, Industrial and Governmental Sectors”, Proc.6th Int. Conf. New Energy System and Conversion (NESC2003), Busan, Korea, p.34-38.

[2] Saijo Industry & Information Centre for Support (Feb.2001), “The Advanced Type Hybrid Freezer System, Using Hydrogen Energy”, The Report on Research and Development of the Consortium, p.74.

[3] Yashima National Center for Stock Enhancement, Fisheries Research Agency (2004), “Development of Fish Breeding Technology for Use in a Closed-Circulation System”, http://fra-seika.fra.affrc.go.jp/~dbmngr/cgi-bin/search/search_detail.cgi?RESULT_ID=100&YEAR=2004.

[4] Saijo Industry & Information Centre for Support (Feb.2010) “A Large Amount of Cold and Hot Water Production System Experiment Using Natural Energy, Applied to Practical Use and Food Production”, The Report on the Model Project to Find Technology Seeds and Experiment in Social System for Low-Carbon Society, p.1-2,11-14.

[5] Ministry of the Environment (Oct. 2009), 2010, “The Priority Policy of Ministry of the Environment.”

IEA HIA: A Sustainable International Framework & Strategies for Collaborative RD&D in Hydrogen Energy

Mary-Rose de Valladares, IEA HIA, USA
Antonio Garcia-Conde, IEA HIA, Spain

The Hydrogen Implementing Agreement (HIA) of the International Energy Agency (IEA) is an autonomous organization within the framework of the Organisation for Economic Co-operation and Development (OECD). Its purpose is to develop and promote hydrogen as a clean, renewable energy source by facilitating international cooperation and information exchange for hydrogen research, development, and design (RD&D). This paper outlines the Agreement's mission, current research portfolio and accomplishments, ongoing collaborations, and plans for the future. The IEA HIA oral presentations will highlight results of current tasks. For more information, please see www.ieahia.org and the IEA HIA Strategic Plan for 2009-2014.

IEA-HIA tasks and activities encompass the full spectrum of research issues in hydrogen production, storage, conversion, safety, integrated systems and infrastructure, as well as analysis and outreach in support of its RD&D activities. Significant technical progress has been made in these areas as a result of IEA-HIA coordinated research. After completing its most recent term of operation on 30 June 2009, the Agreement began a new phase under the Strategic Plan for 2009-2014.[1] With 21 member countries, as well as the European Commission and the United Nations Industrial Development Organization (UNIDO), the Agreement has considerable organizational capacity which, coupled with its long-standing tradition of international collaboration, position it for continued success.

The HIA's capabilities have grown with each new member. Membership increased approximately 60% during the 2004-2009 term, and the role of industry will continue to grow in the next five years. Although there are no industry sponsors in the Implementing Agreement, significant industry participation has occurred and is occurring within the tasks. UNIDO's accession is of particular significance, as it extends the IEA HIA's outreach to the developing world and its vast opportunity for sustainable energy.

The IEA-HIA Vision is for a hydrogen future in which a clean, sustainable energy supply of global proportions plays a key role in all sectors of the economy. Contemplating a new phase of expansion and progress, the IEA-HIA Executive Committee adopted the 2009-2014 Mission Statement:

Accelerate hydrogen implementation and widespread utilization to optimize environmental protection, improve energy security and promote economic development internationally while establishing the HIA as a premier global resource for expertise in hydrogen.

[1] IEA HIA End of Term Report 2004-2009 / 2009-2014 Strategic Plan, March 2009.

1 Themes & Portfolios, 2009-2014: Overview

For the period 2009-2014, the IEA HIA has identified three major themes that stem from its mission and vision. These themes are at once goals and priorities. Each theme is associated with a set of portfolios that contain tasks and activities. The themes and portfolios are listed below:

- Collaborative RD&D that advances hydrogen science and technology, including four portfolios:
  - Hydrogen Production
  - Integrated Hydrogen Systems
  - Hydrogen Storage
  - Hydrogen Integration in Existing Infrastructure
- Analysis that Positions Hydrogen for technical progress and optimization, for market preparation and deployment, and for support in political decision-making, including three portfolios:
  - Technical
  - Market
  - Support for Political Decision-making
- Hydrogen Awareness, Understanding and Acceptance that fosters technology diffusion and commercialization, including three portfolios:
  - Information Dissemination
  - Safety
  - Outreach – Inform and engage critical subsets of HIA stakeholders

(See Figure 1: IEA HIA Strategic Framework 2009-2014*)*

2 Themes & Portfolios, 2009-2014: Descriptions

2.1 Theme 1: *Collaborative RD&D*

This RD&D is the IEA-HIA's core business. It is typically medium and long-term in scope and pre-competitive in nature. The IEA HIA's study *Hydrogen Production and Storage: Gaps and Priorities* examined near, mid and long-term research needs in hydrogen production and storage.[2] The 2009-2014 Strategic Plan will address many or all of the research needs identified by the study.

2.1.1 Production Portfolio

Progress has been made in new technologies for hydrogen Production. However, Hydrogen Production and Storage: Gaps and Priorities concluded that, overall, there are significant needs for improvement in increased plant efficiency, reduction of capital costs, and reliability and operating flexibility for all production processes.

With respect to near-term options, Electrolysis and natural gas reforming are proven technologies that can be used in the early phases of building a hydrogen infrastructure. *Task 24, Wind Energy and Hydrogen Integration*, is working to efficiently combine electrolysers (a

[2] Hydrogen Production and Storage: R&D Priorities and Gaps was published by the IEA in 2006.

constant input device) with variable output wind turbines for production of hydrogen as a transportation fuel and on-site conversion of hydrogen electricity for load-balancing. Small-scale natural gas reformers remain a subject of research; there are several demonstration cases but limited commercial availability. *Task 23, Small-Scale Reformers for On-Site Supply of Hydrogen*, is investigating both technical and marketing issues related to small scale reformers, including carbon capture and storage. Task 23 has recently been extended for another year.

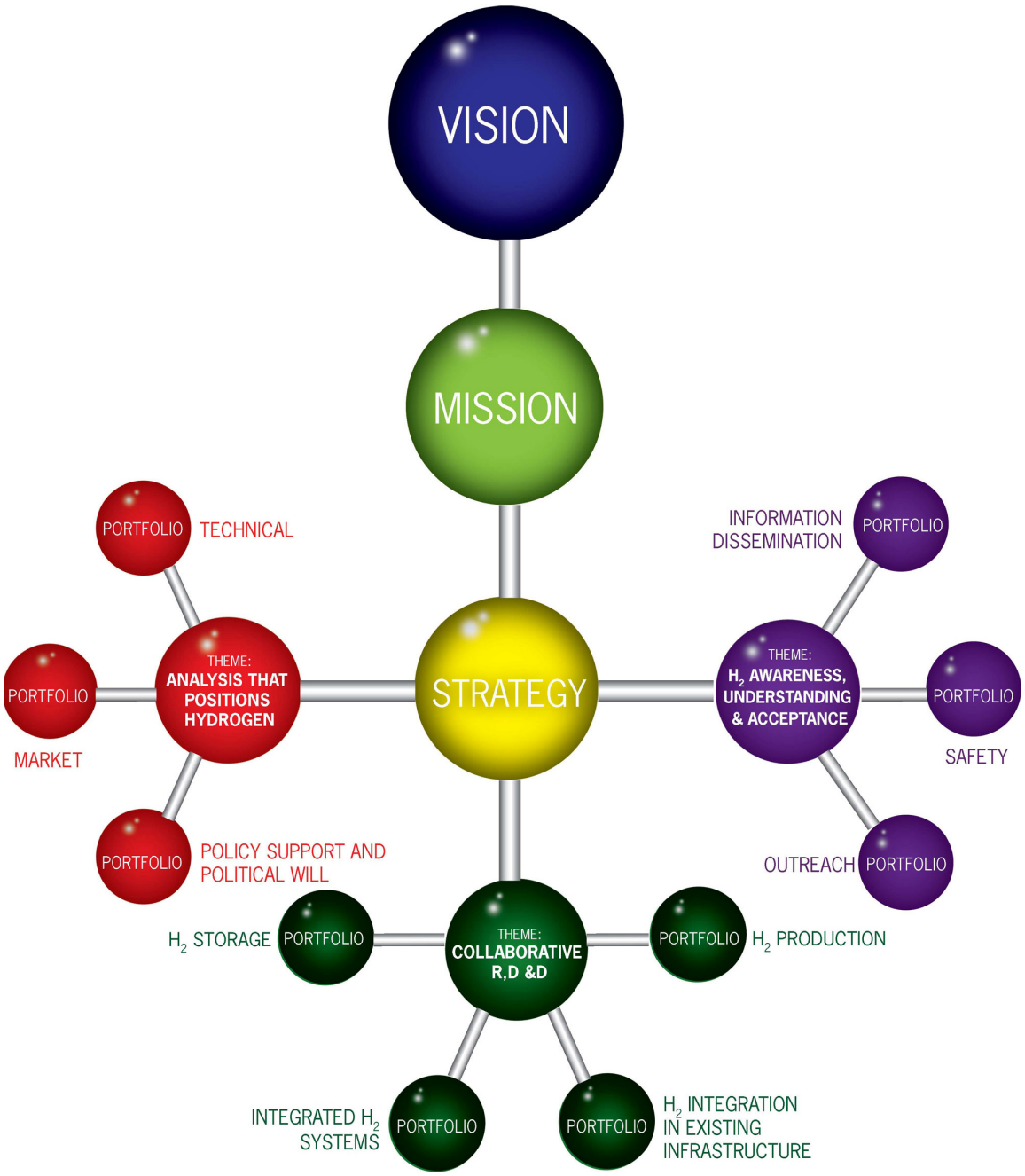

Figure 1: IEA HIA Strategic Framework 2009-2014.

Mid-term, central fossil-based production with CO_2 capture and storage could play a significant role. Research is needed on absorption and other types of separation processes as well as overall process layout and configuration. Biomass to hydrogen processes are also a mid-term option. More focus on feedstock preparation is needed. Logistics pose a challenge for this method and production appears economical only at large scale.

With respect to fossil energy carbon-containing materials, the potential for Carbon Capture and Sequestration (CCS) and pre-combustion decarbonization expand possibilities for sustainable use of these conventional resources. New efforts in this area during the 2009-2014 term may be gasification related. *Task 27, Near-Term Market Routes to Hydrogen by Co-Utilization of Biomass as a Renewable Energy Source with Fossil Fuels* addresses many of these issues.

Farther out on the time scale, basic and applied research is needed for both photoelectrolytic and biohydrogen production methods. Hydrogen production in Biological processes that entail the use of hydrogenases (enzymes) as well as genetically engineered organisms is characterized by low conversion efficiencies. Fundamental research is needed to understand the natural processes and genetic regulation involved in these reactions. It is anticipated that this work will continue through much or all of this term. *Task 21, BioHydrogen*, deals with these topics; this task is now under consideration for a three-year extension or succession by a new task. High temperature (>500ºC) production of hydrogen is also an important area of investigation for the mid and long term, focusing on materials development, high temperature membranes and heat exchangers, and High temperature electrolysis. *Task 25, High Temperature Hydrogen Production Processes*, examines solar and nuclear processes. This task was recently extended for another year.

Task 26, Advanced Materials for Waterphotolysis, is concentrating on advanced materials research related to photoelectrolytic water-splitting rather than continue at this time with design and development of photoelectrochemical (PEC) devices.

The need for continuing or additional advanced materials research was a recurring topic in the HIA's strategic assessment for 2009-2014. The need for research on catalysis was another recurring motif. Consequently, new basic and applied research activities in these areas are anticipated in this term.

As systems evolve for all types of hydrogen production methods, the HIA expects a heightened interest in applied technology research and development efforts on the componentry necessary for various hydrogen production methods.

2.1.2 Storage Portfolio

Both compressed gas and liquid hydrogen are commercially available today, but research continues to improve performance and reduce costs. R&D issues related to compressed gas include fracture mechanics, safety, compression energy, and volume. Important R&D issues for liquid hydrogen include: more efficient liquefaction, lower cost/better insulated containers, automated boil-off capture (e.g., via hydrides), re-liquefaction and volume.

For on-board hydrogen storage applications, research has focused on materials-based solid-state storage, which is currently in the development phase. The potential advantages of materials-based storage are lower volume, lower pressure (greater energy efficiency), and

higher purity of hydrogen output. Important materials storage R&D issues include: volume, weight, lower desorption temperatures, improved desorption kinetics, recharge time & pressure, heat management, cost, chemical and environmental reactivity, durability, container compatibility and optimization.

Task 22, Fundamental and Applied Hydrogen Storage Materials, is the largest hydrogen storage collaboration in the world. With over 50 projects to its credit, this task has recently been extended for another three years.

Later in this term, as storage systems meet technical targets, emphasis will shift to include R&D on componentry for all applications.

2.1.3 Integrated Systems Portfolio

Systems integration is an essential next step in collaborative hydrogen R&D. Systems integration brings component subsystems together, ensuring their efficient functioning.

Task 18, Integrated Systems Evaluation, has undertaken modeling and evaluation of a broad collection of hydrogen demonstration projects expressly for the purpose of analyzing and modeling their overall design and performance. In addition, Task 18 is the best resource for global information on all things hydrogen, including worldwide trends.

Market introduction and penetration of hydrogen technology require optimized, well-integrated systems. Therefore, as time goes on, the Agreement will focus increasing effort and attention on 1) the componentry, devices and sensors that comprise the systems; and 2) their engineering as integrated systems. This will likely translate into new activities and new tasks during the 2009-2014 term.

As an energy conversion device, the fuel cell is one of the most important hydrogen technologies, one in which the HIA has an abiding interest. As systems integration efforts advance, the HIA will certainly investigate fuel cell issues more closely, likely in cooperation with the IEA Advanced Fuel Cell Implementing Agreement.

2.1.4 Integration in Existing Infrastructure Portfolio

Future delivery of hydrogen requires the integration of hydrogen systems into the existing energy infrastructure. While that infrastructure services all sectors of the economy, the world's attention has focused first on the transport sector with its mass markets, followed by the stationary power sector. Expansion of the infrastructure will require coordination on many fronts: technology; finance and insurance; market mechanisms and policy instruments; construction and engineering; operation and maintenance; and codes and standards. While all these factors warrant attention, the HIA's focus is on RD&D issues and technical barriers—which requires research activities that interface with conventional resource chains (the grid, pipelines, trucking and other delivery systems). Likewise at issue are centralized and distributed hydrogen production, as well as mass storage.

A task on Infrastructure that will consider the hydrogen distribution network from production sites to end-users is being defined. The scope of this task is likely to feature modeling of pipelines (pumps and valves), as well as both gas and liquid mass storage above ground and underground storage in man-made and natural structures.

2.2 Theme 2: *Analysis that Positions Hydrogen*

In less than a decade, the avalanche of interest in hydrogen has been met by roadmaps and a wide array of analytic efforts on RD&D, infrastructure and market issues. Some fine analytic work on hydrogen is available today. However, a comprehensive analysis of global energy conditions that incorporates hydrogen in the world's energy future is a complex and challenging proposition, complicated by high levels of political, technical, environmental and economic uncertainty. There is, in effect, a hydrogen information gap that needs to be filled with coherent and balanced information, providing a clearer picture of hydrogen R&D needs and the future of hydrogen in the economy. Furthermore, the information needs to be appropriately packaged for specific audiences.

Therefore, the Agreement has reaffirmed its commitment to rigorous, independent analysis that supports collaborative R&D efforts and addresses the larger issue of the transition to hydrogen in the economy. This commitment amounts, in no uncertain terms, to an "Analytic Imperative." As the premier global resource for technical expertise in hydrogen energy, the IEA HIA is better positioned to offer balanced analysis on these questions than any other organization.

During the last term, the IEA HIA began the process of organizing for analysis that will address important questions about hydrogen demand, supply, and infrastructure. This process, spearheaded by the Executive Committee Analysis Group, is evolving into an Analysis Task whose definition is currently underway. The Executive Committee expects that development of analysis products will not only contribute to filling the information gap but also more firmly establish the HIA as the leading technical resource in hydrogen. The Agreement expects to cooperate closely on IEA analytic efforts such as the well-regarded Energy Technology Perspectives (ETP) and the World Energy Outlook (WEO) publications.

The Analysis theme contains three portfolios: technical, market and support for political decision-making. Collectively, these three portfolios will provide the analyses needed to provide relevant stakeholders and policy-makers with balanced information that stimulates RD&D, market adoption and widespread application of hydrogen.

2.2.1 Technical Portfolio

The technical portfolio comprises analysis intended, first and foremost, to promote advancement and optimization of the technology. This effort is also intended to ensure that the HIA provides a clear picture of evolving hydrogen RD&D needs.

There is a larger need to make a cross-cutting technical case for all hydrogen technologies, including production, storage, conversion (*e.g.* fuel cell) delivery and infrastructure. This effort will be based in the Analysis Task. The foundation for the effort is underway in the form of a literature review and gap analysis.

2.2.2 Market Portfolio

The market portfolio of analysis activities will deal expressly with issues of market preparation and deployment. These issues include the topic of market transformation that supports the deployment of innovative technology, bridging the early, and often fatal, stage of market introduction and the later stage of market penetration. The analytic market portfolio

effort will make the business case for hydrogen, positioning hydrogen for competitive advantage in the marketplace. This analysis will entail both supply and demand side assessments, including the non-energy sector. The supply side analysis will incorporate a market perspective. Techno-economic analysis with a market perspective will be performed on individual technologies.

2.2.3 Support for Political Decision-Making Portfolio

Recognizing that public policy will play a crucial role in development of hydrogen technology and its deployment in the marketplace, and that support for political decision-making is considered indispensable to a future with hydrogen energy, the Executive Committee approved the Support for Political Decision-Making Portfolio to undertake analysis that aligns investment in hydrogen technology with global public policy concerns (notably climate change and emissions reduction). Wherever appropriate, this analysis will utilize findings and conclusions from the Agreement's technical and market analyses. The results will be presented in position papers and briefs.

2.3 Theme 3: *Hydrogen Awareness, Understanding & Acceptance*

This theme complements the HIA's principal theme - Collaborative R&D, and its supporting theme - Analysis. It acknowledges that awareness, understanding and acceptance are requisite to technology diffusion and commercialization. It recognizes that the benefits of hydrogen must be articulated to stakeholders and decision makers. And it accepts a major role for the HIA in the communications process. Through this three-portfolio effort to foster technology diffusion and commercialization, the HIA expects to increase its visibility as the reference institute for hydrogen.

2.3.1 Information Dissemination Portfolio

The ultimate success of the "Analysis Imperative" depends upon effective information dissemination. This function targets key stakeholders in the science, energy and environmental communities, as well as the media, government and industry. The IEA is itself an important target audience, and the Agreement will also disseminate information beyond the borders of IEA member countries. UNIDO, a new IEA HIA member, is expected to both contribute to and benefit from information dissemination activities.

At the task level, Agreement Experts have produced over 1,000 HIA related publications/reports and 1,000 HIA related presentations during the 2004-2009 term. The trend toward increased production of information in publications/reports and presentations is expected to continue. As hydrogen progresses toward commercialization during the 2009-2014 term, the HIA newsletter (IEA HIA News) will evolve to focus more on hydrogen demonstrations and the hydrogen marketplace. The IEA HIA now develops and disseminates information via its Website, Annual Report, newsletter, and brochures in addition to its extensive technical reports and publications.

The Agreement's conference program facilitates preparation and delivery of abstracts, papers, exhibits, and related presentations. During the 2009-2014 term, the HIA expects to create new technology platforms and channels for information dissemination (e.g. Webinars and podcasts).

2.3.2 Safety Portfolio

Hydrogen safety and consumer comfort with hydrogen are vital ingredients for its acceptance. Hydrogen safety considerations cut across all HIA RD&D portfolios. *Task 19, Hydrogen Safety*, explicitly deals with safety through analysis, testing and the development of target information products. During this term, as safety information products become available, Task 19 plans to distribute them as broadly as possible. The Secretariat will participate directly in distribution and promotion of Task 19 safety products and will incorporate Task 19's safety findings into other Agreement communications whenever possible. Additional safety activities – one or more tasks – are projected for the new term. Precise topics will be defined as Task 19 nears its 2010 conclusion; the regulatory framework for codes and standards will likely be included.

2.3.3 Outreach Portfolio

This portfolio goes beyond information dissemination to both inform and engage a critical subset of IEA-HIA stakeholders and decision makers. Engagement may take several forms, including participation as an IEA-HIA Expert, a member, or possibly a sponsor. Engagement may also imply cooperation on a more limited timeframe or for a particular purpose.

To engage important target audiences, such as industry, government, and members of the renewable energy community, the Outreach Portfolio employs the full array of IEA-HIA information products and all available channels, including networking opportunities. Active participation of the Executive Committee Members, Operating Agents, and the Secretariat, who are well-positioned to carry out these activities in strategic situations around the world, is considered essential.

Many of the world's leading experts in hydrogen energy RD&D have partnered with the HIA since its inception. We are pleased to recognize their dedication and innovation with two new prizes: the IEA HIA Individual Prize and IEA HIA Project Prize.[3] The IEA HIA Individual Prize was created to celebrate hydrogen research and development distinguished by technical excellence and harmony in international cooperation that contributes to the understanding and advancement of basic and applied science.

The Agreement awarded its inaugural IEA HIA Individual Prize in June 2008 to Dr. Gary Sandrock. Although the Individual Prize was conceived as a single award, the Executive Committee decided that special circumstances warrant special measures: the late Dr. Tapan Kumar Bose, who passed away in 2008, was honored as the recipient of a IEA HIA Memorial Prize for lifetime achievement in hydrogen R&D. The first IEA HIA Project Prize will be awarded at the 2010 World Hydrogen Energy Conference, and the next Individual Prize may also be awarded in 2010.

3 Tasks, 2009-2014: Overview

Over the course of its thirty-two-year history, the IEA HIA has created a broad portfolio of twenty-seven (27) tasks, nine of which are operating presently, while others are still being

[3] The Executive Committee selects Individual Prize winners from nominations proposed by its members, and from members and Operating Agents in the case of the Project Prize.

defined. For each operational term of, the HIA's tasks correspond to its assessment of the hydrogen energy community's direction, priorities, and RD&D requirements.

The tables below review the tasks' accomplishments of the recent past (Figures 2-4), the Agreement's prospective schedule of tasks and Plan of Work (Figure 5), and Key Issues for the 2009-2014 term (Figure 6).

Figures 2-4 outline accomplishments of the twelve tasks operating during the 2004-2009 term, four of which are now complete. They reflect the Agreement's work for the last five years on pre-commercial collaborative RD&D on Hydrogen Production and Storage, and Assessment of the Market Environment.

Figure 2: Production RD&D Programs, 2004-2009.

Advancement of Science and Technology **via pre-commercial collaborative** Production RD&D **programs**	
Task	**Accomplishments, Benefits and Success Stories in Completed Term**
Task 15 Photobiological Production	**R&D Progress toward development of H_2 production by microalgae** • A novel, sustainable photobiological production of molecular hydrogen upon a reversible inactivation of the oxygen evolution in the green alga *Chlamydomonas reinhardtii* (Subtask A) • Identification of accessory genes and gene products necessary for the photoproduction of H_2 in *Chlamydomonas reinhardtii*. Finding that STA7 and starch metabolism play an important role in *C. reinhardtii* H_2 photoproduction. (Subtask A) • Identification and characterization of *tla1*, a novel gene involved in the regulation of the Chl antenna size in photosynthesis in *C. reinhardtii* (Subtask B) • The generation of 11.6 mol of H_2 per mol of glucose-6-phosphate using enzymes of the oxidative pentose phosphate cycle coupled to a hydrogenase purified from *Pyrococcus furiosus* (Subtask C) • The development of both smaller and larger Photobioreactors (Subtask D).
Task 16 Hydrogen from Carbon-Containing Materials	• **State of the Art reports for all three** Task 16 **subtasks**: **Subtask A** on the potential for cost reduction of large-scale processing from natural gas with pre-combustion de-carbonization of fossil energy; **Subtask B** on prospects for H_2 from biomass **from an industry perspective; and Subtask C on small-scale reformer technology** for distributed near to medium term H_2 supply. • **Substantial industry participation** on a challenging scope of work was an HIA first that serves as a benchmark for future industry participation
Task 20 Hydrogen from Waterphotolysis	• Development, acceptance and operation of two multi-year R&D PEC programs, one at the U.S. DOE and the other, called "NanoPEC" under EU 7th Framework Program • Pioneered Fe_2O_3 (Hematite) as very promising, abundant, low-cost and environmentally benign photoanode material. • Maturing PEC water-splitting tandem concepts • Photoelectrochemical (PEC) work on tungsten trioxide led to development of novel, highly sensitive, reliable and low-cost **pollution control sensors for auto industry**
Task 21 BioHydrogen	• Better genomic understanding of hydrogen-producing strict anaerobes • New assessment method for overall analysis of BioHydrogen (Subtask D) has been screened
Task 23	• Contributing to development of norms for small-scale reformers to

Advancement of Science and Technology **via pre-commercial collaborative** Production RD&D **programs**	
Small-Scale Reformers for On-Site Hydrogen Supply (SSR for Hydrogen)	harmonize industrialization. This effort, which includes carbon capture, is crucial to development of the hydrogen infrastructure and future distributed generation capability • Subtask 3 Market Studies stand to materially facilitate HIA analysis efforts • Fast-tracking the deployment process of market introduction and penetration of small-scale reformers for on-site hydrogen supply from multiple feedstocks, fossil and renewable
Task 24 Wind Energy and Hydrogen Integration	• Setting the stage for large-scale use of renewable wind energy for hydrogen production in the near future by addressing the entire wind to hydrogen production chain from technical, economical, social, environmental, market and legal perspectives • Exploring in detail possible applications for hydrogen, especially full wind & hydrogen integration by means of hydrogen storage and electrical conversion that balances the original wind energy production, allowing an approach to demand that closes the gap with conventional energies.
Task 25 High Temperature Production of Hydrogen	• Poised to elaborate world-wide knowledge on specific high temperature (>500ºC) processes (solar and nuclear) that will support production of massive quantities of zero-emission hydrogen • Producing **summary sheets** on high temperature processes in **general and detailed** versions
Task 26 ***NEW***	On track to create data base on advanced materials for waterphotolysis

Figure 3: Storage RD&D Programs, 2004-2009.

Advancement of Science and Technology **via pre-commercial collaborative** Storage RD&D **programs**	
Task	**Accomplishments, Benefits and Success Stories in Completed Term**
Task 17 Solid & Liquid State Storage	• Evolved into largest global R&D collaboration on hydrogen storage materials of its time, contributing to R&D, information dissemination and transfer of technology • Huge contribution to the literature with 900+ publications and presentations plus 17 patents
Task 22 Fundamental and Applied Hydrogen Storage Materials	• World's largest collaboration to-date on hydrogen storage materials R&D • Biannual week long Task 22 meetings serve as the ultimate global forum for expert cooperation on hydrogen storage R&D (emphasizing materials and the transportation sector), the grand challenge in hydrogen. As of December 2008 it produced 450+ publications/articles, 450+ presentations and 16 patents.

Figure 4: Assessment of Market Environment Programs, 2004-2009.

Assessment of Market Environment **including non-Energy Sector; and Analysis, Safety and Economics**	
Task 18 Integrated Systems Evaluation	World's best address for worldwide information and analysis on hydrogen and integrated systems • Database with 200+ National Documents • National Organizations database • National Projects database • State of the art analysis entitled Demonstration Project Evaluations - Used technical simulations that may be applied to other projects to replicate results - General conclusions in critical areas of system evaluations, data monitoring, modeling tools, system design, control systems and cost-benefit analysis • Synthesis, lessons learned and trend analysis relate to permitting, funding and technology performance • More than a dozen relevant case studies
Task 19 Hydrogen Safety	• Contribution to global understanding of H2safety through studies and databases laying foundation for codes and standards • Phase 1 laid theoretical groundwork for phase two testing program to evaluate the effects of equipment or system failures under a range of real life scenarios, environments& mitigation measures • Subtask A Activity 1 produced a Survey of Hydrogen Risk Methods in Phase 1 • Subtask A Activity 2 produced Comparative Risk Assessment Studies of Hydrogen and Hydrocarbon Fuelling Stations • Subtask A Activity 3 produced a Knowledge Gaps White Paper

Figure 5 sets forth a timeline for the Agreement's tasks and activities projecting through 2014. In summary, nine (9) tasks are presently active (December 2009); six (6) of the existing tasks are expected to be extended during the term; and seven (7) tasks are expected to be formed as successors to current tasks. Five (5) new tasks are forecast; significant progress has already been made in formulating new tasks (whether successors to existing tasks or new work).

Figure 5: IEA HIA Work Program Timeline, Current and Proposed/Future Tasks.

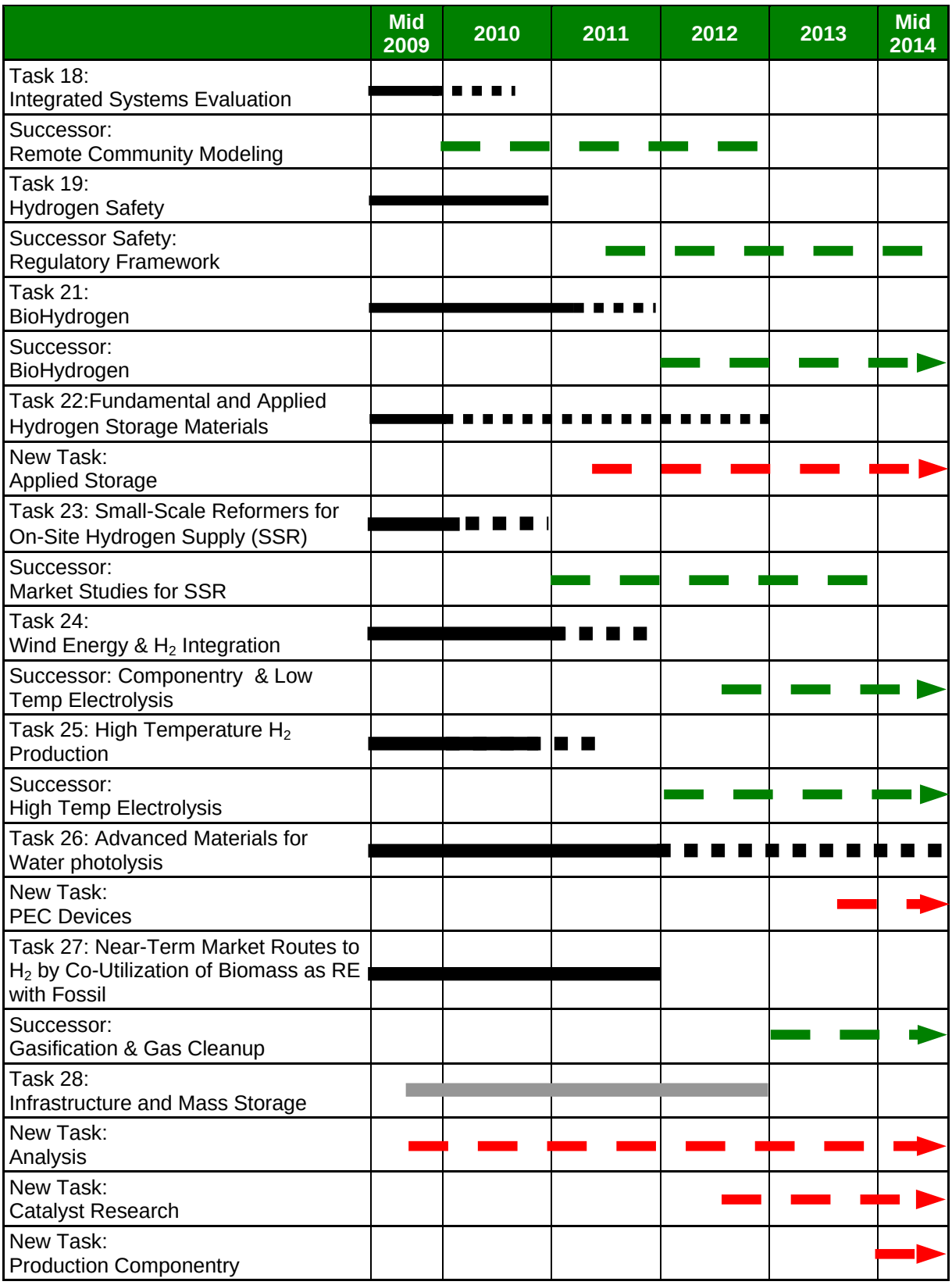

Key to Work Plan above:

- Solid black line = current task
- Solid grey line = task in definition
- Short dash broken line = task extension
- Long dash green black broken line = successor task
- Long dash red broken line = new task
- Arrow at end = means task is expected to continue after end of 2014 term

3.1 Work Program Table

Figure 6 is organized by theme & portfolio, and outlines the tasks' key issues & broad "approach." Tasks that have been proposed as potential additions to the Program of Work during the 2009-2014 term are featured in some portfolios' bottom sections. For context, you may refer to Figure 1: IEA HIA Strategic Framework 2009-2014

Figure 6: Plan of Work, 2009-2014.

	THEME & PORTFOLIO	KEY ISSUES	APPROACH In place 2009	APPROACH Proposed/Potential
FUNDAMENTAL		• Anaerobic use of bacterial dark fermentations and photosynthetic microbes; increased yields; biomimetics; biohydrogen acceptance • Advanced materials for photo-electrochemical (PEC) watersplitting • Advanced materials (catalysts) for other production methods • High temperature production from nuclear and solar • Electrolysis	• Task 21, BioHydrogen • Task 26, Advanced Materials for Waterphotolysis • Task 25, High Temperature Production	• Extend Task 21 past 2010 • Possible extension of Task 26 past 2011 • Task on catalyst research for other production methods • Possible extension of Task 25 • High temperature electrolysis activity
TECHNOLOGY	**RD&D** ***Production*** 	• Biofuels for reformers; CCS & emission handling • Gasification and gas clean-up • Design/development of photo-electrochemical (PEC) devices • Fully integrated wind and H_2 application • Co-gasification of biomass with fossil fuels; tradable intermediates	• Task 23, Small-Scale Reformers for On-Site Supply of Hydrogen • Task 24, Wind Energy and Hydrogen Integration • Task 27, Near-Market Routes to Hydrogen by Co-utilisation of Biomass as a Renewable Energy Source with Fossil Fuels	• Possible one year Task 23 extension past 2009 • Task on Purification/ separation, ICE for on-site reformers • Possible successor to Task 26 on development of PEC devices • Possible Task 24 extension • Follow-up activities/ successor task on low temperature electrolysis • Follow-on efforts TBD

Figure 6: Plan of Work, 2009-2014, *continued.*

	THEME & PORTFOLIO	KEY ISSUES	APPROACH In place 2009	APPROACH Proposed/Potential
FUNDAMENTAL	**RD&D** ***Storage*** H_2 STORAGE PORTFOLIO	• Reversible / regenerative H_2 storage media fulfilling int. targets • Fundamental & engineering understanding • Materials for stationary applications • Compression • Metal Embrittlement	• Task 22, Fundamental and Applied H_2 Storage Materials Development	• Task 22 seeking 2-3 year • Extension past 2009; there- • After, disposition of • activity TBD • Possible Task/activities on H_2 interactions with materials
TECHNOLOGY		• Applied Aspects of H_2 storage systems in vehicles: compressed gas, liquid and materials-based;		• New task examining • Technologies for H_2 storage: • Compressed gas, liquid and • Materials-based; Techno-economic analysis of alternatives. • Component task
	RD&D ***Integrated Systems*** PORTFOLIO INTEGRATED H_2 SYSTEMS	• All purpose information on H_2 integration • Harmonization of components for reformer systems; technology performance and cost; CCS & emission handling • Specifications for Integrated Systems	• Task 18, Integrated Systems Evaluation • Task 23, Small-Scale Reformers for On-Site Supply of Hydrogen • Task 24, Subtask B	• Possible continuation of • Current modeling and • Analysis of demonstration • systems • Possible one year extension of Task 23 • New Task H_2 Communities • Modeling and Design: islands, remote, and rural communities • Possible one year Task 23 extension past 2009
	RD&D *H_2 Integration in Existing Infrastructure*	• Geologic storage, pipelines, and "mass" storage	• In Definition: Infrastructure and Mass Storage Task	• TBD

Figure 6: Plan of Work, 2009-2014, *continued.*

	THEME & PORTFOLIO	KEY ISSUES	APPROACH In place 2009	APPROACH Proposed/Potential
CROSSCUTTING	 **Analyses that position H_2** *Technical* 	• "Where will the H_2 come from?" • What role will H_2 play? • Develop a balanced view • Competition in transport sector	• Analysis Group • Task 18 – H_2 Literature Review	• Analysis Task: Supply/Demand • Comprehensive report that includes CO_2 reduction based on introduction of H_2 technology • Proactive cooperation with IEA analytics • Part of proposed storage task: Techno-economic analysis of alternatives in automotive industry.
	Analyses that position H_2 *Market* 	• "Where will the H_2 come from?" • What role will H_2 play? • Include non-energy sector	• Analysis Group • Task 23, Subtask 3 Market Studies • Task 24, Subtask C and D, Business Concept Development • Task 27, Subtask D, Roadmap Development and Verification	• Analysis Task: Supply/Demand from a market perspective – a comprehensive report that includes CO_2 reduction market, cap & trade • Proactive cooperation with IEA analytics • Successor task on Market Studies for on-site reformer technology
	Analyses that position H_2 *Support for Political Decision-making* 	• Lack of information and clarity about the benefits of hydrogen (notably, CO_2 and pollution reduction) among stakeholders and decision makers whose influence is needed and useful for R&D, planning, demonstration and deployment		• Analysis Task: Briefs and position papers to address all issues, including CO_2 reduction, climate change

Figure 6: Plan of Work, 2009-2014, *continued.*

	THEME & PORTFOLIO	KEY ISSUES	APPROACH In place 2009	APPROACH Proposed/Potential
CROSSCUTTING	 **H_2 Awareness, Understanding and Acceptance** *Information Dissemination* 	• Broader and deeper information dissemination needed along with targeted dissemination.	• An element of the Outreach Program managed by Secretariat, it features: • IEA HIA Website • Annual Report • Conference strategy • Communication / Promotion materials • Public relations and media • Contributions to IEA events and • publications • Target audiences include: IEA member countries and IEA family • Gleneagles "+5" and potential H_2 members • Hydrogen community	• Increase information dissemination by continuing current activities and augmenting with: Enhanced conference strategy that features HIA seminars / workshops <200; and possible sponsorship of larger conference; webinars, possible pod-casts and other IT vehicles dissemination of safety products dissemination of analysis products cooperation with ETDE to expand market for information • Expand target audiences: Non-IEA member countries, developing world, and greater energy community
	H_2 Awareness, Understanding and Acceptance *Safety* 	• All aspects of hydrogen safety and consumer comfort with hydrogen	• Task 19	• Task 19 concludes in 2010. • High potential for multiple follow-up tasks in key areas. Definition of successor tasks to occur early in term. • Task 19 to complete information products and distribute with Secretariat support.
	H_2 Awareness, Understanding and Acceptance *Outreach*	• Inform and engage	• An element of the Outreach Program directed by ExCo and managed by the Secretariat.	• Inform and engage through information dissemination and targeted networking; build participation; influence stakeholders and decision makers. • **Potential Participants**: Members, experts, sponsors • **Stakeholders and Decision Makers**: IEA, IEA member countries; IEA non-member countries; Government & Industry; Hydrogen Community; Renewable Community

4 Conclusion and Final Remarks

The IEA HIA is in a period of growth and is well-positioned for continued success in its core business of collaborative RD&D, as well as analysis for technical optimization and market preparation, and hydrogen community outreach.

The Agreement is the world's premier global resource for technical expertise in hydrogen RD&D, offering its members a **Value Proposition** that facilitates world-class research and increases their impact. Members benefit from the Agreement's:

- **Neutral international profile:** The Agreement is a reliable, unbiased forum through which Members may access technical experts and achieve global reach to engage governments, academia, and industry.
- **Leveraged global resources:** Members may engage an established network of researchers and shared resources in the areas of science and technology, market analyses and outreach. The IEA-HIA Portfolio includes shorter term and long-term, pre-competitive activities. In all cases, intellectual property (IP) is treated with care.
- **Track record of success:** For 30+ years, IEA-HIA Tasks have facilitated collaborative research, and its membership continues to grow.

IEA HIA Experts who are presenting at the 2010 World Hydrogen Energy Conference will discuss the latest work of the Tasks, including recent results achieved since this paper's publication. Look for their 2009-2010 work in areas of renewed interest, such as hydrogen safety and market analysis, as well as their continuing advancements in hydrogen storage and production.

Epilogue

Since the November 2009 timeframe when this paper was prepared, the IEA HIA has marked several noteworthy milestones.

Four milestones are associated with the 2009-2014 Strategic Plan's Collaborative R,D&D theme. *Task 18 – Integrated Systems Evaluation*, part of the Integrated Systems Portfolio, was completed. *Task 21- BioHydrogen*, part of the H_2 Production Portfolio theme, was extended for a five year period (three years firm with an additional two year option). Task 28 – Large-Scale Hydrogen Delivery Infrastructure was approved as part of the Integration in Existing Infrastructure Portfolio. *Task 29 - Distributed and Community Hydrogen*, part of the Integrated Systems Portfolio, received preliminary approval.

With respect to the theme of Analysis that Positions Hydrogen, *Task 30 – Global Hydrogen Systems Analysis*, was approved.

The IEA HIA awarded its inaugural Project Prize 20 May during the Closing Ceremony of the World Hydrogen Technology Conference (WHEC) in Essen, Germany. Two Project Prizes were awarded. For Fundamental Research, the winner is Fundamental Safety Testing and Analysis of Hydrogen Storage Materials and Systems (H-25), a project of IEA HIA *Task 22 Fundamental and Applied Hydrogen Storage Materials Development*. For Technology Demonstration, the winner is ITHER (Infraestructura Tecnologica del Hidrogeno y Energias Renovables), a project of IEA HIA *Task 24 Wind Energy and Hydrogen Integration*.

Trends in Evaluation of Integrated Hydrogen Systems: IEA Hydrogen Task 18

Susan Schoenung, Longitude 122 West, Inc., USA
Mary Gillie, EA Technology, UK
Maria del Pilar Argumosa, National Institute of Aerospace Technology, Spain
Shannon Miles Halliday, Powertech Labs, Canada

Abstract

Under the auspices of the International Energy Agency's Hydrogen Implementing Agreement, Task 18, Evaluation of Integrated Hydrogen Systems, has been underway since the beginning of 2004. During this time, numerous hydrogen demonstration projects from participating countries have been evaluated for technical performance and lessons learned. As the work program has progressed, various trends have been discovered, based on the projects considered. Among the trends are types, sizes and complexity of projects; project lifetimes and successes; technical performance and maturity of subsystems; modeling tools; permitting and progress in safety standardization; funding mechanisms; early and niche market development; social acceptance and policy issues; and hydrogen and energy sources. In this paper the objectives and accomplishments of Task 18 are discussed, the project portfolio, consisting of both refueling stations for hydrogen-fueled vehicles and stationary power systems are described, and the trends are reviewed. Lessons learned are summarized.

1 Introduction

Fifteen countries have participated in Task 18, bringing demonstration projects for evaluation. Tables 1 and 2 list the projects, which have been assessed in this Task. These fall into two major categories: refueling stations and vehicles, and stationary systems for power production.

Table 1: Portfolio of refueling station and vehicle projects [1].

Project / location	Vehicle / power plant	Station description
ECTOS buses / Iceland	(3) Citaro fuel cell buses with Ballard fuel cells	Shell / alkaline electrolzer, compressed gas storage
Pacific Spirit Station / Canada	(5) Ford Focus fuel cell vehicles	BOC (Linde) / waste hydrogen, compressed gas storage
Malmo, Sweden	City buses / NG engine with mixed NG / H2 fuel	Public station, PEM electrolyzer, compressed gas storage, mix at pump
Energy station / Las Vegas	Converted truck / IC engine	Air products electrolyzer, compressed gas storage
EXPO 2008 / Zaragosa, Spain	1 full size and 2 midi-buses, H2 bikes	Public station; Compressed gas storage
HyNor, Norway	10 converted Prius hybrid ICE	Public station; compressed gas stored underground
HydroGEM, Netherlands	Factory vehicle / PEM fuel cell	On-site at ECN
Clean Energy Partnership / Germany	Numerous fuel cell and ICE	Two public stations in Berlin; liquid storage
H2 Truck / Denmark	1.2 kW fuel cell powered factory loading truck	On-site; replaceable hydrogen canisters
Fuel cell boat / Amsterdam	Commuter boat / PEM fuel cell engine	Shell / multipurpose station for hydrogen fueling

Table 2: Portfolio of stationary projects.

1.1 Project / location	Hydrogen source / Grid connection	Fuel cell description / application	Storage
Residential fuel cell project / Japan	Small reformers / local grid	PEM / home water heating	Gas
HyLink / Totara Valley, New Zealand	Wind electrolysis / none	PEM, Residential power and water heating	Low pressure gas in pipeline
IHAVU (Single family home) / Spain	PV electrolysis / grid back-up	2 kW PEM, household power with hydrogen energy storage	Gas / MH
Hawaii Power Park / Kahua Ranch, HI	Wind / PV electrolysis / local grid	5 kW Plug Power stationary fuel cell / ranch operations office	Gas
RES2H2 / Canary Islands, Spain	Wind electrolysis / none	PEM; integrated with desalination plant	Compressed Gas
Hydrogen Office	Wind electrolysis / local grid	20 kW PEM / building heat and power; fuel cell test facility	Gas
RES2H2 / Greece	Wind electrolysis / local grid	PEM, wind interface testing	Gas / MH
Lolland Hydrogen community / Denmark	Wind electrolysis / local grid back-up	2 kW IRD PEM, Residential CHP	Gas

2 Refueling Stations and Vehicle Trends

The refueling stations in the portfolio have matured from true demonstration systems in early 2004 to fully operational stations today. Some of the trends include:

- a move from lower pressure to higher pressure for both storage and dispensing
- a move from exclusively above ground storage to innovative underground storage
- prevalence of stations with public access from restricted access locations

Figure 1 shows the German station at Berlin Messedamm, which has been open to the public since 2004 [2]. Stations in Sweden, Norway, the US and Iceland are also publicly accessible.

Figure 1: Hydrogen station at Berlin Messedamm, Germany.

Figure 2 is a system diagram of the layout of the HyNor station at Porsgrunn, Norway [3]. Here the hydrogen is stored in underground submerged tanks. Underground storage of liquid hydrogen is used in some locations in Germany, but is still not permitted in the US.

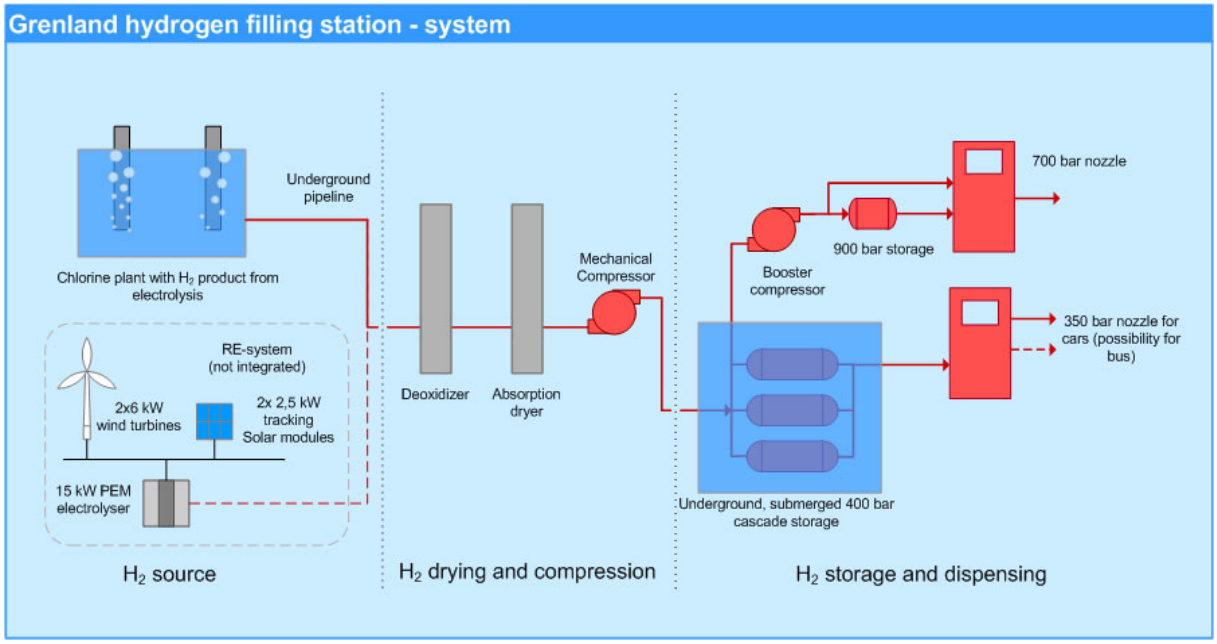

Figure 2: Grenland hydrogen filling station system diagram.

The move to on-board hydrogen storage pressure, from 350 to 700 bar has led to a significant increase in vehicle range. Other major trends in vehicle performance include better efficiency and longer life [4]. Figure 3 shows these trends the Honda FCX, while Figure 4 shows improvement in reliability for Daimler vehicles due to improved process control.

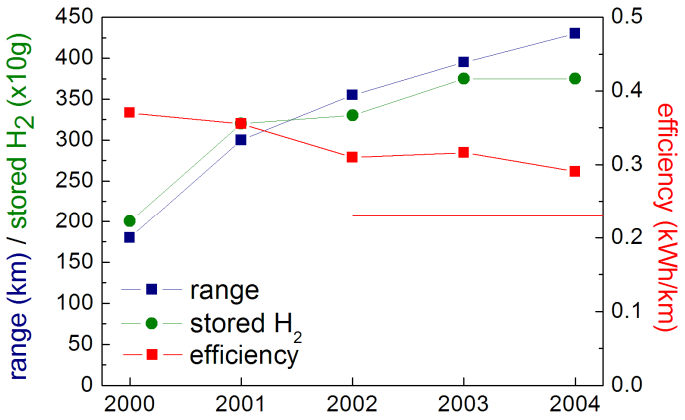

Figure 3: Trends in range, stored H_2 and performance.

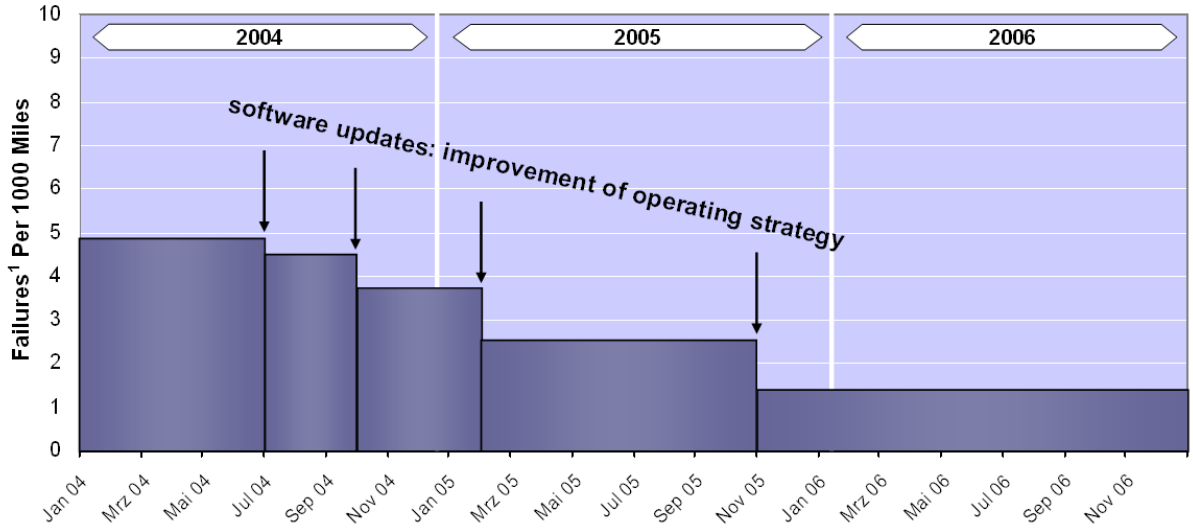

Figure 4: Vehicle reliability improvements (Source: Daimler).

The improved vehicle longevity is especially marked for the Canadian hydrogen highway project in British Columbia, to the extent that the demonstration Pacific Spirit Station, which is fueling seven different vehicle types, will remain open past its original plan to accommodate the vehicles [5]. With respect to buses, which were some of the first hydrogen vehicles on the road, more are in routine service (notably in California, Canada, London and Sweden) than simply in demonstration mode [6]. Sweden is moving toward mixtures of hydrogen and natural gas, while new hybrid (battery / fuel cell) buses are scheduled for placement in Hawaii in 2010 [7].

3 Stationary Systems

Stationary hydrogen systems, primarily for electric power production have predominated the Task 18 portfolio in the last few years. These tend to be somewhat small, individual, isolated projects focused on demonstrating subsystem performance, system integration and control optimization, more so than overall operation. As seen from the list in Table 2, the majority of projects combine renewable resources, primarily wind, with hydrogen production by electrolysis. Storage is mostly compressed gas, with some example of metal hydride storage, and electricity production using PEM fuel cells. A typical system diagram, for the Kahua Ranch power park demonstration in Hawaii, is shown in Figure 5 [8].

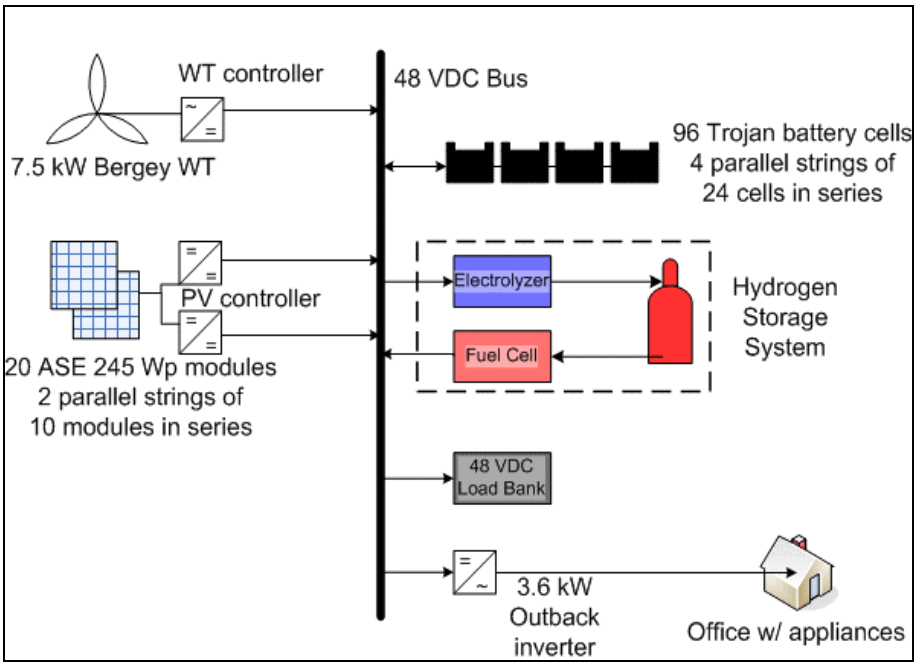

Figure 5: System diagram for Kahua Ranch system in Hawaii.

Several new trends in stationary systems are toward the use of mass-produced fuel cell systems for residences. In the Denmark community of Nakskov, combined heat and power units are being installed [9]. In Japan, several thousand homes have been outfitted with systems that provide power and hot water [10]. The Japanese system is shown in Figure 6.

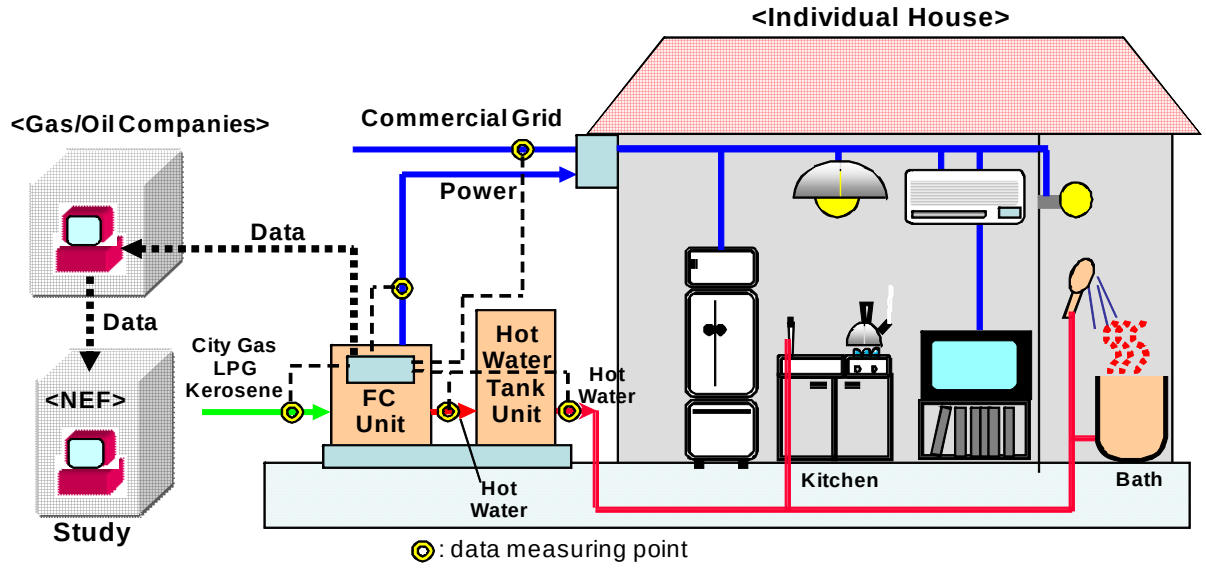

Figure 6: Domestic fuel cell system for power and water heating in Japan.

4 Project Technical Performance and Issues

The demonstration projects evaluated in this work have been primarily unique systems built from custom-made or first-of-a-kind components. While modeling and simulation have been performed, attempts to quantify operational performance, such as efficiency, has not been possible because of the intermittent and testing nature of the projects. In many cases, the hours of sustained operation have been limited, and hence the data sets are also limited. System and component failures have caused significant down time.

One area with recent extensive effort has been in the design and optimization of control systems. For both refueling stations and stationary power systems to be cost effective, not only must the subsystems be appropriately sized to be well matched, but the dynamic operation of all the various elements must also be optimized. In refueling stations, this is determined by the filling schedule of the cars or buses. In stationary systems, the operation depends not only on the schedule of the load, but also in some cases on the input energy from the wind or sun. Frequently the systems include batteries to control dispatch and charging the batteries becomes part of the equation. At the Kahua Ranch, a sophisticated control system has been refined, as shown in Figure 7. Similar design work has been done for the Italian hydrogen house, the HyLink project in New Zealand, and the IHAVU project in Spain.

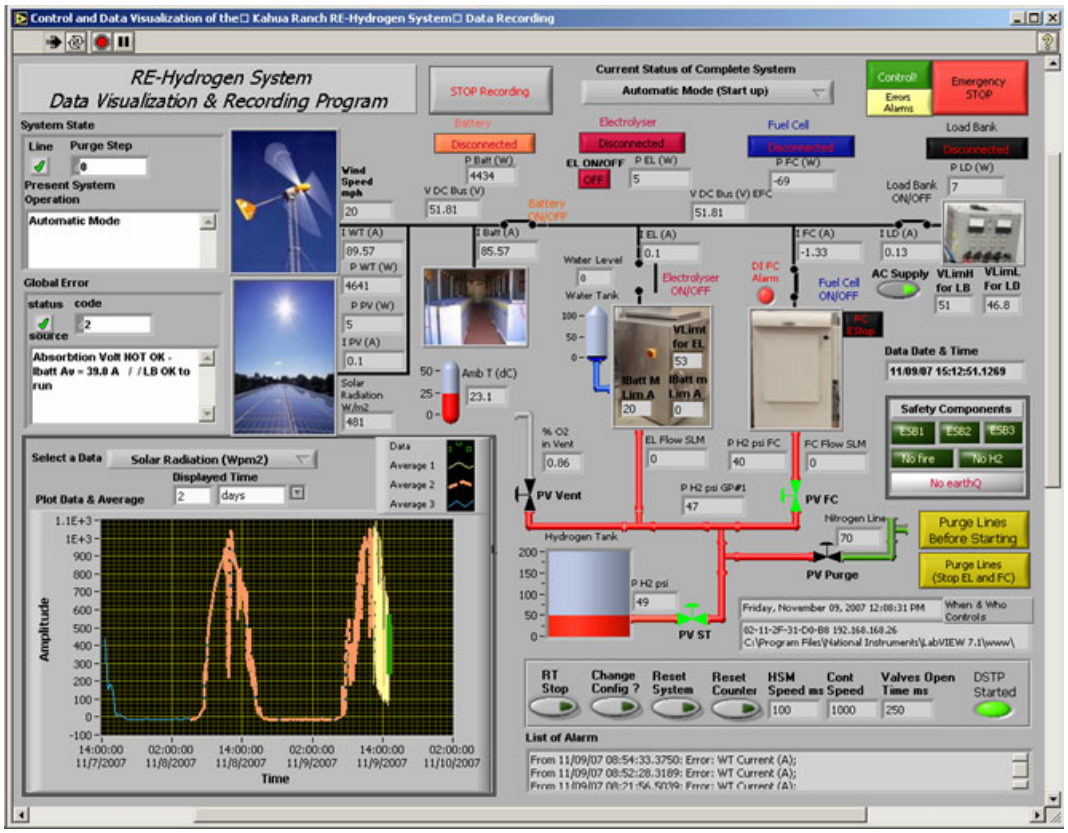

Figure 7: Control panel for Kahua Ranch project in Hawaii.

5 Social Benefits and Programmatic Issues

Throughout all of these projects, the communities involved have shown not only acceptance, but also a strong welcome for hydrogen and fuel cell technologies. The systems represent clean power and “green tech.” In remote locations, they can mean fuel price stability. A survey conducted by the Task 18 team found community pride in these systems and a source of jobs [11].

On the other hand, the projects have been plagued with discontinuities in government and private funding, leading to stops and starts in both planning and construction. Support for some projects to continue beyond the initial demonstration has been difficult to obtain. A funding survey by Task 18 members shows that industrial participation in the development of hydrogen leads to more success than government support alone, as indicated in Figure 8 [12].

Finally, permitting for system installation is still an issue, although major progress has been made since 2003, when every project was essentially acting alone to obtain permits. More recent projects have relied on established codes and processes as well as precedence

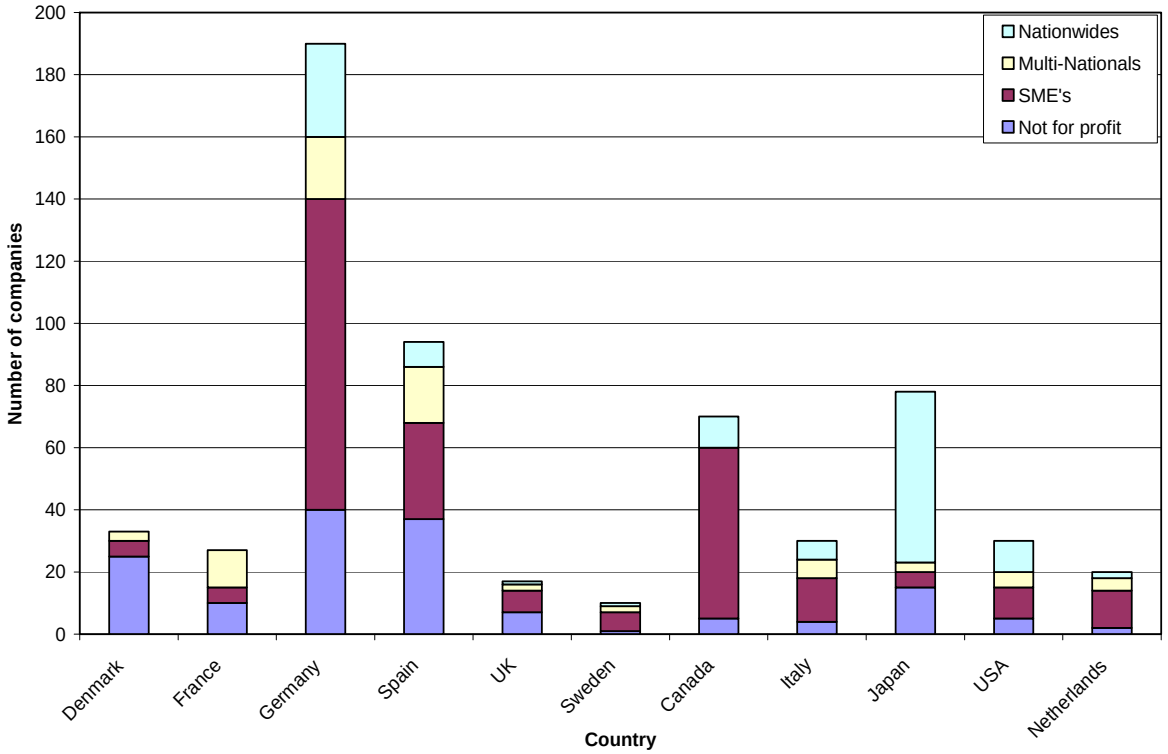

Figure 8: Hydrogen and fuel cell companies globally.

6 Conclusions

The work of Task 18 has illustrated some trends in hydrogen developments. Vehicles and refueling infrastructure are considerably more mature than stationary systems. A trend toward mass-produced systems for residences should aid in maturing such systems. The prevalence for using renewable resources for hydrogen production by electrolysis demands work on electrolyzers that can operate with time varying input. Control system design is of utmost importance. Ongoing funding to gather significant amounts of data are needed to optimize subsystem and system performance.

References

[1] Argumosa, “Evaluation of Hydrogen Demonstration Projects,” Subtask B Phase II report, 2010

[2] Clean Energy Partnership report “CEP Berlin 2009”

[3] Simonsen, “HyNor Station Grenland” case study; http://iea-hia-annex18.sharepointsite.net/public

[4] Hoevenaars and Weeda, “Trends in Hydrogen Vehicles,” ECN report, ECN-E--09-090, Sept 2009

[5] Olsen “Pacific Spirit Station,” case study; http://iea-hia-annex18.sharepointsite.net/public

[6] Gillie and Schoenung, “Trends in Hydrogen Projects,” EA Technology report No. 46080, Feb 2010

[7] Ewan and Farnsworth, “Hawaii Renewable Hydrogen Project,” NREL webinar, October 2009, www1.eere.energy.gov/.../pdfs/hawaii_renewable_hydrogen_program.pdf

[8] Lutz, et al, “The Hawaii Hydrogen Power Park Demonstration at Kahua Ranch,” Sandia report SAND-2010-0979P

[9] Jensen and Bech-Madsen, “Utilisation of Hydrogen and Fuel Cell Technology for Micro Combined Heat and Power Production,” 2007, www.bass.nu

[10] “Progress on the Large-scale Stationary Fuel Cell Demonstration Project in Japan,” NEDO Report, April, 2009

[11] Miles and Gillie, “Benefits and Barriers of the Development of Renewable/Hydrogen Systems in Remote and Island Communities,” Proc. HFC 2009, Vancouver, Canada

[12] Gillie and Platt, “Survey of Support Mechanisms for the Development and Demonstration of Hydrogen Systems,” EA Technology, Report no. 6250, September 2008

[13] Schoenung, et al, “Further Experiences in Permitting and Safety of Hydrogen Demonstration Systems,” Proc. NHA Conf, 2009, Columbia, South Carolina

IEA-HIA Activities on Small-Scale Reformers for On-Site Hydrogen Supply

Ingrid Schjølberg, Sintef Energy Research, Norway

Summary

Task 23 is a collaborative task on small scale reformers for on-site hydrogen supply under the IEA Hydrogen Implementing Agreement. Sixteen experts from nine member countries participate in this task, constituting a unique group of international gas suppliers, reformer technology suppliers and researchers. The task was kicked off in 2006 and is a continuation of previous activities. This paper describes the scope, goals and preliminary results for the task.

1 Introduction

Hydrogen production by on-site reforming is an important stepping stone towards the development of a hydrogen infrastructure for the transport sector. Today, on-site production units can be developed in any required size and capacity. It is important for vendors that norms for size, capacity and footprint exist to enable mass production and reduce costs. Therefore, a harmonization of the technology is essential.

Hydrogen by on-site production cannot be provided at a reasonable cost when including CO_2 capture and storage. However, choice of feedstock and improved energy efficiency can contribute to a reduction of emissions and thereby enable hydrogen production by small scale reforming. Task 23 performs studies on feedstock and possibilities for on-site hydrogen supply, based on suppliers operation experience, research and development activities supporting suppliers of on-site production units in future technology development.

Establishment of a market for hydrogen is a challenge as the number of cars and service stations is highly coupled and depending on a strong collaboration between car producers and gas suppliers. Task 23 constitutes a unique group of experts addressing the challenges of harmonization, emissions handling and market development. The experts represent international gas suppliers, technology suppliers and research institutes. This type of international collaboration across disciplines and industrial segments is essential to facilitate industrialization and hydrogen infrastructure development. A market guide based on results from Japan, Europe and California studies with respect to quality and quantity will facilitate the infrastructure development and produce a decision basis for end-user.

2 Harmonised Industrialisation

One of the main goals of Task 23 is to develop a harmonised framework for design of reformer units for on-site production. It is important for suppliers and end-users that norms and standards for size, footprint and capacity exist for hydrogen refuelling infrastructure to reduce costs. Six suppliers of which two are of the world's major suppliers of reformer technology participate in the work. The goal shall be reached through the development of

harmonized capacities, identification and application of relevant standards, regulations and codes.

Small scale reformer suppliers world wide have been identified and system data has been collected by use of a questionnaire, internet and Task 23 expertise. Available on-site reformers systems have been categorised into five different size ranges equivalent to those reported previously by NRELs study on state of the art of electrolytic hydrogen production [1].

The defined sizes are related to the number of hydrogen cars that can be served:

- Home: serves fuel needs of 1 – 5 cars with a hydrogen production rate of 200 to 1000 kg H_2/year (0.25 to 1.5 Nm^3/h)
- Small neighbourhood: serves fuel needs of 5 – 50 cars with a hydrogen production rate of 1000 to 10 000 kg H_2/year (1.5 to 15 Nm^3/h)
- Neighbourhood: serves fuel needs of 50 – 150 cars with a hydrogen production rate of 10 000 to 30 000 kg H_2/year (15 to 45 Nm^3/h)
- Small forecourt: serves fuel needs of 150 – 500 cars with a hydrogen production rate of 30 000 to 100 000 kg H_2/year (45 to 150 Nm^3/h)
- Forecourt: serves fuel needs of more than 500 cars with a hydrogen production rate larger than 100 000 kg H_2/year (larger than 150 Nm^3/h)

The study will result in recommendations for size, footprint and capacity.

3 Sustainability and Renewable Sources

A study is under development on the various fuel paths on when to convert a feedstock to hydrogen and when to use it directly. Available European [2] reports have been taken into account as well as Task 23 expertise.

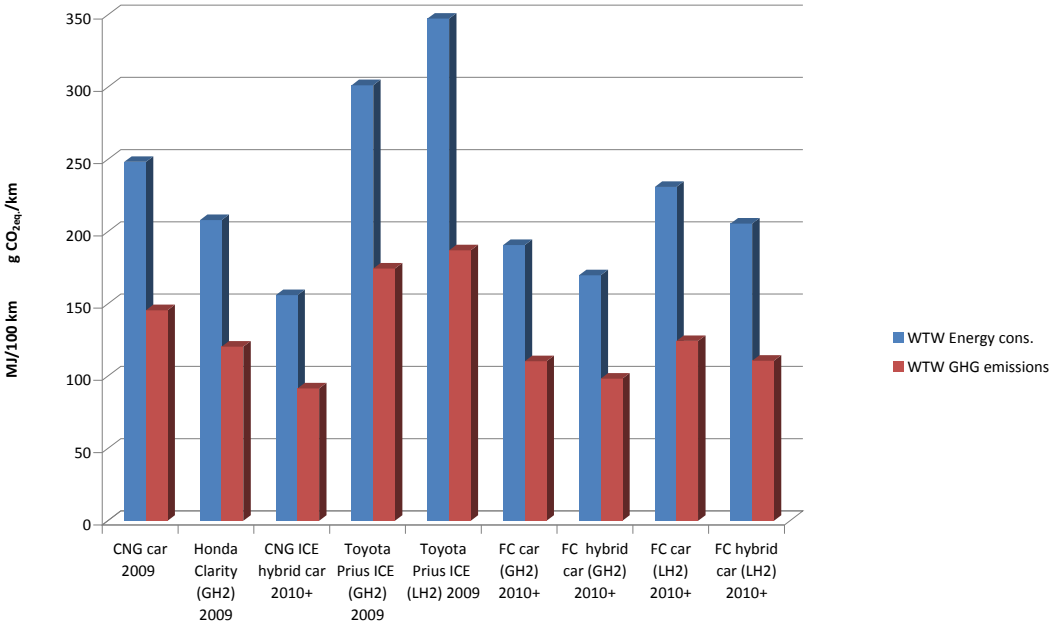

Figure 1: Fuel paths for CNG, hydrogen supplied by reforming.

Figure 1 shows an example of one of the fuel paths generated in the project. The figure shows a large variation in the WTW energy consumption. The energy consumption and emissions of the CNG ICE hybrid car (best available technology in 2010) is lower than for the fuel cell car. However, the fuel cell car is to be prefered compared to the CNG car (best available technology in 2009). This shows that small scale reforming can contribute to reduce emissions in an early market development. Various fuel paths will be presented in the final report of Task 23 in 2011.

Technology exists for small scale CO_2 capture. However, capturing CO_2 is an energy intensive business, unlike many other clean-up technologies (e.g. NOx, SOx) and in addition transportation costs and infrastructure for decentralized sources is required. The general consensus is that CCS at large point sources can be justified and hydrogen may be supplied from large plants with CCS.

4 Market Studies

Cheaper and more efficient small scale reformers, fewer and more compact components and growth in the hydrogen refuelling market will reduce the price of hydrogen. Three markets (US, Europe and Japan) has been evaluated and compared using existing studies based on medium and long term scenarios [3]-[5] as well as data supplied by the Task 23 experts. The parameters applied in the analysis are LHV, natural gas price, electricity price, process water consumption, plant capacity, efficiency, capital investment and operating costs. The goal of the analysis is to give an estimation of hydrogen supply cost, energy efficiency and CO_2 emission on WTT basis and substantiate the use of small-scale reformers in early market development.

5 IEA-HIA Task 23 current experts.

Country	Organization	Expert
Denmark	Haldor Topsoe	J.B.Hansen
Germany	Mahler AGS	R. Stauss
Japan	Tokyo Gas	I.Yasuda
Japan	Mitsubishi Kakoki Kaisha	A. Obuchi
Norway	Statoil	B.T. Børresen
Norway	Statoil	E.Ochoa-Fernández
Norway	SINTEF	I.Schjølberg
Netherlands	HyGear	D. Lieftink
Netherlands	ECN	E. van Dijk
Sweden	SGC	C.Nelsson
Sweden	Catator	F. Silversand
Italy	ENEA	E.Calo
Turkey	TÜBITAK	A.Ersoz
France	N-GHY	D.Grouset
France	N-GHY	P.Marty
France	GDF Suez	J.Saint-Just

Acknowledgement

Many thanks to the experts of IEA-HIA Task 23 who have contributed and worked on this topic since the task kick off in 2006. A special thanks to the subtask leaders in Task 23, Dr. Esther-Ochoa Fernandez (Statoil - Norway), Mr. Corfitz Nelsson (SGC-Sweden) and Dr. Isamu Yasuda (Tokyo Gas - Japan).

References

[1] J.Ivy (2004), Summary of Electrolytic Hydrogen Production, www.nrel.gov

[2] JRC, Concawe, EUCAR, Tank-to-wheels report, October 2008, www.ies.jrc.europa.eu

[3] www.hyways.de

[4] www.hyways-iphe.org

[5] www.jhfc.jp

Task 24: “Wind Energy and Hydrogen Integration”

Luis Correas, **Ismael Aso**, Foundation for the Development of New Hydrogen Technologies in Aragon, Spain

1 Purpose

The purpose of Task 24 is:

- Explore in detail all possible issues (technical, economic, social, environmental, market and legal) related to hydrogen production using electrolysis with wind energy.
- Explore in detail possible applications for hydrogen produced using electrolysis with wind energy, with special emphasis on wind and hydrogen integration by means of hydrogen storage and electrical conversion that balances the original wind energy production.

2 Framework

There is currently a broad interest in hydrogen production by means of renewable energy sources, as hydrogen is expected to be one of the main energy carriers in the near future. The IEA HIA has studied several possible renewable energy sources for hydrogen production. Within the current set of possibilities, water electrolysis by means of wind energy ranks high as a competitor to fossil fuel in terms of technical and economic feasibility.

Today, both water electrolysis and wind energy technologies are considered mature, although R&D efforts are still undertaken to enhance performance and cost savings in both technology fields. In principle, however, water electrolysis technologies were not conceived for such variable input conditions as those inherent to the nature of wind resources. Therefore, the current state of the art must be upgraded largely to avoid redundant power electronics. System integration improvements are expected to increase efficiency and reduce capital and O&M costs.

Although hydrogen applications are virtually unlimited, transportation and early markets in portable applications are expected to be near-term drivers for advancement of the hydrogen economy. At the same time, there is an interesting stationary application that arises related to wind energy and other renewable energies such as solar PV. Their inherent variable nature presents integration problems for market and grid operators. These conditions may retard their development in certain markets (e.g., wind energy in Denmark, Germany or Spain), where market penetration has already occurred. Storage systems can provide a solution to this problem by allowing wind energy to be stored closer to conventional energies, thereby increasing wind energy’s capability to follow demand, guarantee a desired amount of energy, offer a flat curve or a more smoothened curve, etc.

The fully integrated wind and hydrogen application connects wind technology with various hydrogen related technologies such as electrolyses (for production), hydrogen to electricity converters (for utilization), and storage systems.

If wind farms can be coupled to energy storage systems, wind energy will become available to offset the growth in network capacity. Furthermore, wind farms would become multi-purpose, decentralized producers of either electricity or hydrogen for fuel when the

automotive industry enters mass production of hydrogen-fuelled vehicles. In the short term, marginal but significant benefits can be obtained by improving dispatch ability and offering reserve power and grid services. In any case, the goal is to enhance the value of wind electricity itself.

Another important niche market will be off-grid systems relying solely on renewable energy sources. It makes sense to include these systems in the scope of this annex due to the inherent high cost of off-grid power systems; their role as an early adopter application; and the reality that most current operational wind/hydrogen applications are serving off-grid applications. Projects have been developed or proposed in various countries. These represent a good starting point for learning experience since they include very different stakeholders from every segment of the value chain, including research institutions, equipment manufacturers, and utilities.

3 Members

Two new participants joined during 2009: Statoilhydro (Norway) and Hydrogenics (Canada), both of them electrolyze companies, so nowadays the group in compound by 24 members listed in the table below:

Table 1: Actual Task 24 Members.

	EXPERT NAME	INSTITUTION NAME	Country
1	Luis Correas (Operagent Agent)	Aragon Hydrogen Foundation	Spain
2	Ismael Aso	Aragon Hydrogen Foundation	Spain
3	Rupert Gammon	Bryte Energy Ltd	England
4	Ken-ichiro OTA	Yokohama National University	Japan
5	Mila Rey	Gas Natural	Spain
6	Pablo Fontela	Endesa	Spain
7	Klaus Stolzenburg (Subtask C Leader)	PLANET GbR	Germany
8	Claus Jorgensen	RISO	Denmark
9	Ernest Burkhalter	IHT	Switzerland
10	Eli Varkaraki	CRES	Greece
11	Javier Pino	Seville University	Spain
12	Rafael Ben	Ariema	Spain
13	Aaron Hoskin (Subtask A Leader)	Natural Resources of Canada	Canada
14	Raquel Garde (Subtask D Leader)	CENER	Spain
15	Salvador Suarez	ITC	Spain
16	Kevin Harrison (Subtask B Leader)	NREL	USA
17	Allan Schroeder	RISO	Denmark
18	Sam Miyashita	NEDO	Japan
19	Dennis Krieg	Juelich	Germany
22	Stein Trygve Briskeby	StatoilHydro	Norway
24	Dirk Van den Heuvel	Hydrogenics	Canada

Task 24 is divided into four subtasks which are explain in more detail in points below.

Subtask A: State of the Art

Subtask Leader: Mr. Aaron Hoskin, Natural Resources of Canada

In this subtask, the goal is to conduct an in-depth review of the current state of the art in wind turbines, electrolysers, and and the power electronics which allow for system integration,. A detailed review of recent and on going wind-hydrogen installations will also be performed that includes the current state of the art as well as lessons learned relative to hydrogen production using wind energy and fully integrated wind energy & hydrogen technology.

Subtask B: Needed improvements & system integration. Technology development on main equipment and system integration concepts

Subtask Leader: Mr. Kevin Harrison , Natural Renewable Laboratory (USA)

In this part of the study, the scope is focused on the two main components for hydrogen production, the wind turbine and the electrolyses, as well as the intermediate connecting components. The in-depth analysis will research a future technical optima. The goal of this subtask is not to provide an enhanced design for either equipment but to develop proper specifications.

This subtask has to address the following issues:

- The dynamics
- Electrolyses durability under a very dynamic workload
- Development of specific wind turbines

Subtask C: Business concept development

Subtask Leader: Mr. Klaus Stolzenburg, PLANET GbR (Germany)

This subtask categorises wind-hydrogen systems with regard to their main purpose (such as electricity storage or vehicle fuel production) and plant size. It looks into the regulations on electricity and on alternative fuels in various countries to assess the possible opportunities and obstacles they may generate for hydrogen derived from wind energy.

Subtask C analyses countries by region with respect to the potential that they could provide for operating commercial wind-hydrogen systems in the future. Current and completed R&D and demonstration projects are introduced and examined with respect to costs and with regard to learnings made.

Subtask D: Applications. Emphasis on wind energy management

Subtask Leader: Ms. Raquel Garde, CENER (Spain)

In this subtask, near term applications for the hydrogen produced shall be studied, with a special emphasis on one of the main applications pointed out in subtask C. This application is wind energy management within the wind & hydrogen full integration concept. Given the noticeable synergy between hydrogen and wind energy regarding their integration for a further approach of renewable energy sources with inherent non continuous and random nature, it is considered appropriate to deal with this application in a separate subtask.

It is important to note that hydrogen used as an energy storage system to manage wind energy has many other competitor technologies which can be used in a wide power and energy range and can cover several energy functions.

In this subtask we are going to describe briefly the different energy storage systems that can compete with hydrogen in wind power management services. We will take into account the problems of the grid due to high penetration levels of wind power in order to analyse and

characterize the better use for hydrogen in this stationary application or other added value chains, compared to other technologies.

Finally, we will analyse in detail the components and performance of some demonstration projects listed below.

4 Activities and Results in 2009

4.1 Fourth Meeting

It was hold during the 15/17 th of April 2009 in Denver (USA) hosted by NREL (National Renewable Laboratory http://www.nrel.gov/) with the attendance of 11 members from 8 countries.

Figure 1: Attendees at fourth Meeting – NREL Facilities.

4.2 Fifth Meeting

The fifth meeting took place in Oldenburg (Germany) during 21-23 October, hosted by PLANET GbR (www.planet-energie.de) with attendance of fifteen members.

Figure 2: Attendees at Fifth Meeting – Oldenburg.

5 Case Wind-Hydrogen Project Studies

Main wind/hydrogen projects worldwide are being studied (Utsira (Norway), RES2H2 (Greece), Ramea and Prince Edward (Canada), Wind2H2 (USA), etc, and some results are shown below:

5.1 Sotavento Project (Spain)

This project was born thanks to a framework agreement between Gas Natural SDG and the Department of Innovation, Industry and Trade of the Xunta de Galicia for the development of renewable energy. In 2008 an agreement with the National Renewable Energy Center (CENER) was signed by Gas Natural to study, analyze and characterize the plant.

This facility is one of the largest global capacity where hydrogen is used in the energy management of a wind farm. Therefore, it could be used as a platform for the development of tests and studies in this type of facilities.

The facility uses the surplus electricity generated by the wind farm in an electrolyzer. This, from water and using electricity in four cells stacks, generates H_2 and O_2 (electrolysis).

The O_2, that is not going to be used in this process is released to the atmosphere and the H_2, produced at a rate of 60 Nm^3/h and a pressure of 10 bar, goes through a process of purification and drying to obtain a purity higher than 99.99%.

To increase storage capacity, the H_2 generated is compressed to 200 bar in two compressor groups supporting up to 61.8 Nm^3/h at 4 bar.

The storage system at 200 bar is composed by 7 blocks of 28 bottles each, with a maximum capacity of 1.725 Nm^3. These blocks are interconnected in two groups of H_2 storage, with the possibility of isolation of each group.

The storage H_2 can be used in a 55 kW engine in case of energy deficit. The compressed H_2 at 200 bar, is decompressed in a first stage to 14 bar and a second until the suction pressure of engine. The engine has a consumption of up to 70 Nm^3/h of H_2 at a pressure of 25-60 mbar H_2 and produces electricity to the wind farm grid.

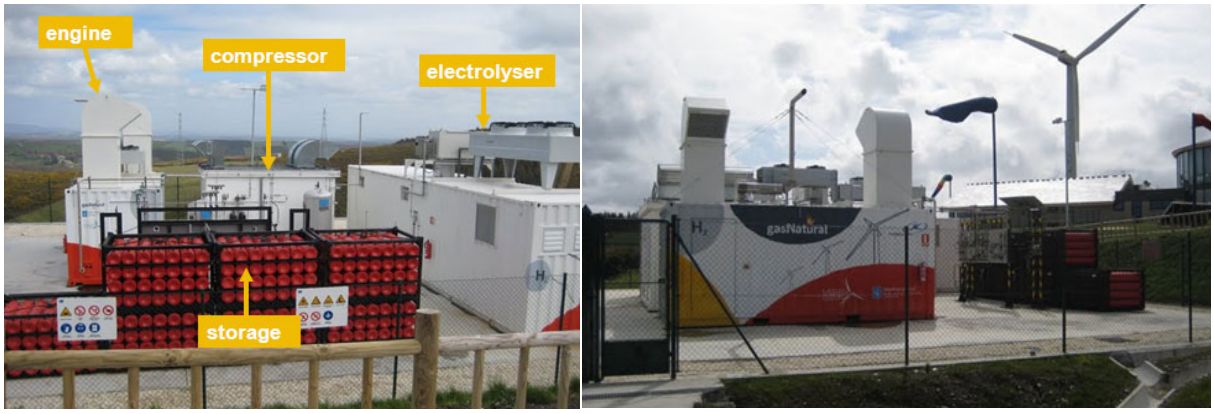

Figure 3: Pictures Sotavento project.

Some experimental results are shown below:

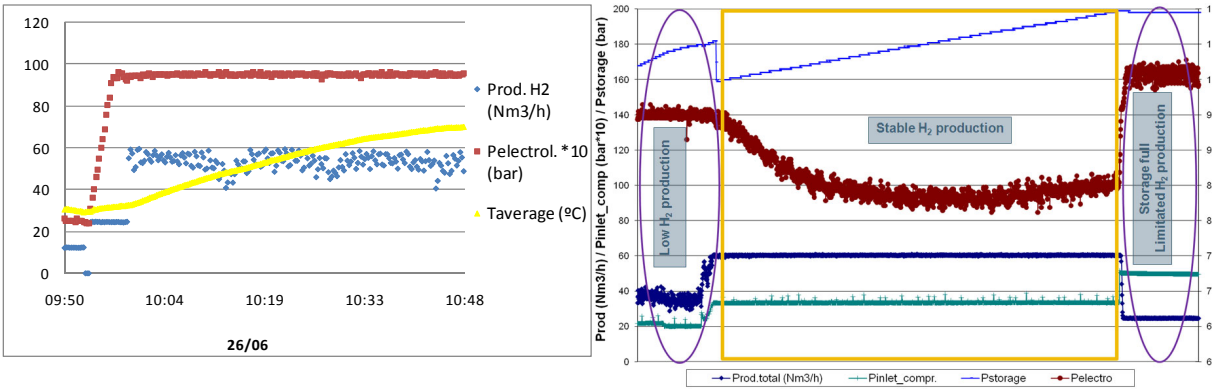

Figure 4: Left: Thermal electrolyser response, Right: Electrolyzer operation.

Lessons learned with the Project:

- Difficulties to obtain licenses because it doesn't exist legislation about this type of facilities.
- There isn't legislation about the sale price of the electricity produced by the engine.
- The control strategy of the equipments is not adequate to work with variable energy resources.
- The system is quite difficult to mode.
- Problems with the electronic power of the electrolyses.
- Harmonics generation

5.2 Hidrólica Project (Spain)

Promoted by Endesa, in Tahivilla wind park (Cadiz, Spain), main goals are:

- Energy optimization in wind farms
- Efficiency and exploitation improvements regarding primary energy
- Technical and commercial assessments of wind hydrogen systems
- Assessment of hydrogen storage and distribution systems
- Assessment of electricity production alternatives by means of H_2
- Technical and economic optimization of wind hydrogen plants
- Integration assessment of wind hydrogen systems in wind farms.

Main components are: PEM electrolyze 6 Nm^3/h, 5.5 Nm^3 hydrogen gas storage, and 12 kW fuel cell. Main lay is show below:

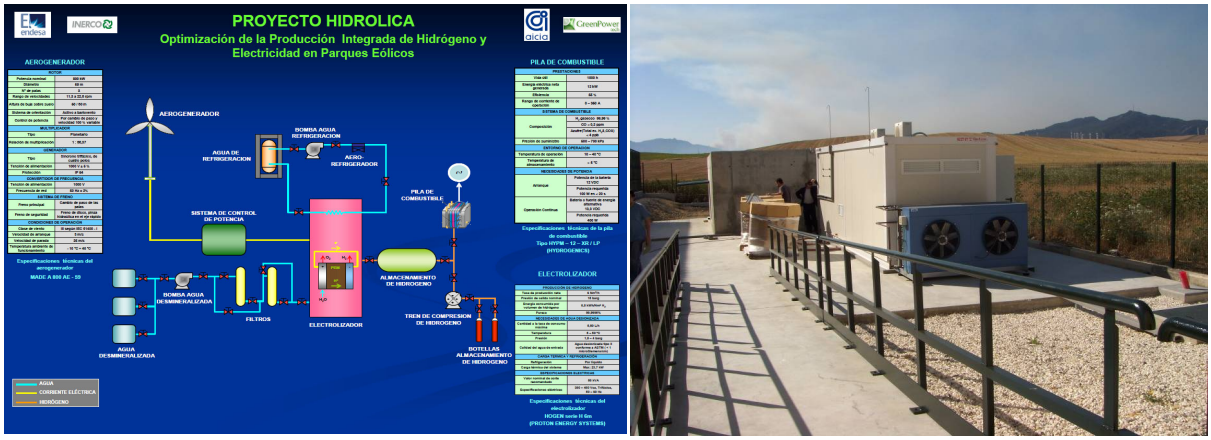

Figure 5: Left: Lay out Hidrolica Project, Right : equipment room.

Lessons learned with Hidrolica project:

- Converter (dc-ac fuel cell): Frequency transformer failure (3 moth delay due to high frequency transformer wrong design)
- Overall control system: Communication problems due to complexity in equipment
- High THD level in wind generator electrical power input
- Electrolyser : Deionised water feed pump failure (water leakage due to reversed draft)

Main conclusions are list below:

- A wind-hydrogen plant was tested and its viability demonstrated.
- Equipment time response has been quite good and more than enough to absorb wind farms variable output.
- Plant systems must be designed to keep a high efficiency working at all loads.
- Overall efficiency is around 14% which is too low (primary resource to electricity step is not considered). It is necessary to increase efficiency

5.3 ITHER Project (Spain)

The ***ITHER project, "Technology Infrastructure for Hydrogen and Renewable Energies***", promoted by the Foundation for the Development of New Hydrogen Technologies in Aragon, comprises a whole test and demonstration facility for photovoltaic, wind energy and hydrogen. This **4 M€** project developed during the last three years, has been completed in phase one in early 2008. Since December 2007 hydrogen from the sun is being produced.

The facilities display a complete picture of current PV and wind technology, consisting of a **635 kW wind farm** with three different turbines, a **100 kW grid connected photovoltaic** installation (three panel technologies, four different sun-tracking systems), and an isolated 2.7 kW photovoltaic application (1 kW concentrated PV, 1.7 photovoltaic roof with two advanced panel materials thin film and amorphous). The facility includes hydrogen production by a PEM and an alkaline electrolyser, storage (low pressure and high pressure) and fuel cells. Up to date, it is the only renewable-to-hydrogen project in the world that includes so many different technologies.

The hydrogen produced is used for mobile applications, for two end users: **20 hydrogen bikes**, and to feed a **hydrogen kart,** which take part in *FormulaZero* racing. *FormulaZero* (FZ) is an European racing that promotes a zero emissions karts championship based on fuel cell technology. The championship begins with a college edition, starting from bases and material support for teams (an 8 kW PEMFC). Different University teams (England, Holland, Belgium, USA and Spain) must conceive, design and manufacture a kart zero emission based on hydrogen and FC systems, testing their technological capabilities.

The ITHER project serves as showcase for renewable electricity and hydrogen production, for training and researching purposes at the Foundation, as well as for raising awareness on the future energy challenges. Recently, the Foundation for Hydrogen in Aragon and Swiss-based Company Industry Haute Technology signed an agreement to jointly develop wind-to-hydrogen solutions in the range of **MWs.**

Figure 6: ITHER Project: IHT Electrolyser 50 kW, FormulaZero Kart, Hydrogen Dispenser.

6 Next Steps 2010

During 2010, sixth meeting will take place in may in Denmark, hosted by Riso, and last meeting Phase I, will take place in October in Huesca (Spain), Final reports related to Subtasks will be completed and several diffusion activities worldwide will be realized to show results and lessons learned, related to wind/hydrogen initiatives

References

[1] Amitava Roy, SimonWatson, David Infield. “Comparison of electrical energy efficiency of atmospheric and high-pressure electrolysers. Int JJ Hydrogen Energy 2006: 1964-1979

[2] José Luis Bernal Agustin, Rodolfo Dufo, “ Hourly energy management for grid-connected wind-hydrogen system” Int JJ Hydrogen Energy 2008: 6401-6413

[3] J.Linnemann, R.Steinberger. “Realistic cost of wind-hydrogen vehicle fuel production . Int JJ Hydrogen Energy 2007: 1492-1499

[4] Olga Álvarez, Ismael Aso Aguarta “Determinación de la estrategia de producción de Hidrógeno en un parque eólico real. III Congreso nacional de Pilas de Combustible Septiembre 2008 Zaragoza (Spain)

[5] Claus Jorgensen, Stephanie Ropenus. “Production price of hydrogen from grid connected electrolysis in a power market with high wind penetration. . Int JJ Hydrogen Energy 2008: 5335-5344

[6] Genevieve Saur “Wind-to-Hydrogen Project: Electrolyzer Capital Cost Study. Technical Report NREL/TP-660-44103 December 2008.

[7] www.unizar.es/jlbernal www.unizar.es/rfufo

[8] Economical assessment of a wind-hydrogen energy system using WindHyGen® software, M. Aguado, E. Ayerbe, C. Azcárate, R. Blanco, R. Garde, F. Mallor, D. M. Rivas, International Journal of Hydrogen Energy, 34, 2009

IEA-HIA Task 25: High Temperature Processes for Hydrogen Production – Three Year Progress Review of the Project

F. le Naour, **S. Poitou**, **C. Mansilla**, CEA, France
C. Sattler, **M. Roeb**, **D. Graf**, DLR, Germany
G. Kolb, SNL, USA
A. Giaconia, **R. Liberatore**, **P. Tarquini**, ENEA, Italy
A. Meier, **D. Gstoehl**, PSI, Switzerland
R. Allen, University of Sheffield, UK
G. Karagiannakis, **C. Agrafiotis**, CPERI, Greece
R. Moliner, **I. Suelves**, CSIC, Spain
M. Gasik, **A. Lokkiluoto**, Aalto University Foundation, Finland
S.D. Ebbesen, RISOE DTU, Denmark
U. Vogt, EMPA, Switzerland
J. Hinkley, CSIRO, Australia

1 Introduction

Through the International Energy Agency organisation, CEA proposed to the Hydrogen Implement Agreement (HIA) Executive Committee that an expert group be set up to address the definition of the high temperature hydrogen production processes running either with a solar or a nuclear heat source. This project was accepted and referenced as Task No 25.

The purpose of Task 25 is to support production of massive quantities of hydrogen with zero-CO_2 emission through the use of high temperature processes (beyond 500°C) coupled with nuclear or solar heat sources. The overarching objective is to share existing worldwide knowledge on high temperature processes (HTPs) and further to develop expertise in global assessment of the HTPs that can be integrated in Hydrogen Production Road Mapping. The specific objectives are:

- To identify and classify HTPs and establish different and coherent criteria for successful application of each family of HTPs, based on a scientific/technological approach.
- To establish the state of the art and investigate the existing R&D, programs, projects on HTPs and other innovative ideas for massive production of hydrogen.

2 Task Description

2.1 Organisation

Task 25 was approved in late 2007 with a three year term of operation. This project is focused on innovative high temperature processes (HTPs) such as:

- Thermochemical cycles,
- High temperature steam electrolysis,
- Innovative direct water spitting.

More mature processes such as Steam Methane Reforming and Alkaline Electrolysis are only studied to compare them to HTPs in both technco-economic and yield terms.

Task 25 is split in four subtasks:

Subtask A: Scientific, technological review and analysis of the State of the Art of HTPs and assessment of mid to long-term HTPs deployment strategy.

Subtask B: Development of a methodology for the integration of HTPs.

Subtask C: Recommendations for HTPs deployment through demonstrators.

Subtask D: Coordination and links with other international organisations: dissemination of information.

Task 25 is led by an operating agent from CEA (French Atomic Energy Commission). The expert group is holding a meeting every semester and results from this group are presented every semester to the IEA/HIA Executive Committee by the Operating Agent.

2.2 Members

All members are recognised as experts in their field and are nominated by the representative of their respective country, belonging to the IEA/HIA executive Committee. The list of members presented below is not definitive and new members and/or new countries can always join this expert group.

Table 1: Members of the IEA/HIA task 25 project.

Australia: CSIRO: J. Hinkley	Italy: ENEA: A. Giaconia, P. Tarquini, R. Liberatore
Denmark: RISOE DTU: S. Ebbensen	Spain: Instituto de Carboquimica: R. Moliner, I. Suelves
Finland: Aalto University Foundation: M. Gasik, A. Lokkiluoto	Switzerland: PSI: A. Meier, D. Gstoehl, EMPA: U. Vogt
France: CEA: F. Le Naour, S. Poitou, C. Mansilla	UK: University of Sheffield: R. Allen
Germany: DLR : C. Sattler, M. Roeb, D. Graf	USA: Sandia National Lab : G. Kolb
Greece: APTL/CERTH: G. Karagiannakis, C. Agrafiotis	

3 Activities and Results

The scientific and technical achievements are described for each subtask below.

Subtask A - Scientific, Technological Review and Analysis of High Temperature Processes and State of the Art (Subtask Leader: C. Sattler, DLR):

A technical review of the different processes has been made through the results of the INNOHYP-CA project (European FP6). INNOHYP-CA established the state of the art in massive high temperature production of hydrogen by reviewing existing knowledge in Europe and worldwide. INNOHYP-CA provided a clear understanding of the basis for future European research.

The first aim of this subtask is to update and complete INNOHYP-CA results. For instance, apart from some international projects, INNOHYP-CA is mainly focused on European countries. The database has to be completed with other countries policies and national programs (e.g: South Africa, Korea, Japan, China).

The recent changes in the international policies concerning HTPs have led the group to discuss a strategy for supporting HTPs deployment through R&D studies. A report is in progress, in order to build recommendations for the future.

Subtask B - Development of a Methodological Approach to Integration of HTPs (Subtask Leader: A. Giaconia, ENEA):

The comparison between HTPs with very different levels of knowledge and maturity appears to be complex. The main challenge is to provide a good projection over a 20 year timescale.

Experts have shared the most recent research results on hydrogen production cost for various processes. A benchmark on cost investment of four simple fundamental components has been performed by three countries, in order to verify the homogeneity of the different methods.

This cross cost evaluation was encouraging. The differences between the results were easily explained by the choice of the material or the operating conditions (some methods are more open to exotic materials and flexible than others).

The next step was to define a global and common methodology for process assessment. A bibliographic study allowed discrimination between several methodologies and definition of the most accurate for our objective. The goal was to define and validate a tool for the multi-criteria assessment of hydrogen production processes, and then to perform an analysis on a couple of cases. The methodology had to take into account different viewpoints: economics, environment, multi-technology aspect, different states of development of the processes, data uncertainty, and incomparability of some of the criteria.

We chose an outranking method called Electre that was developed by the LAMSADE laboratory (Paris – Dauphine). We carried out a first multi-criteria evaluation based on processes and relevant criteria selected by the experts group. Fourteen processes and eight criteria were selected. The criteria ranking was based on two scenarios: one short-term scenario favouring economic and process feasibility and a long term scenario favouring environmental criteria. A sensitivity analysis was carried out, which permitted us to highlight

the impact of changing the input data and the methodology parameters on the result evolution. The interest of this methodology has been recognized by all the experts.

Subtask C - Establishment of Benchmarks, Recommendations for HTP R&D and Future Industrial Deployment (Subtask Leader: F. Le Naour, CEA)

This subtask only started in October 2009. Its goal is to determine demonstrators' needs within the next 10 years. Recommendations will be made about demonstrators, as a complement to the report on strategy (subtask A)

Subtask D - Coordination and Links with Other International Organizations; Dissemination of Information (Subtask Leader and Operating Agent: S. Poitou, CEA):

The objective of this subtask is the development of summary sheets describing every process using the same presentation format. This includes worldwide mapping and technical review of the high temperature process studies and development, database (relevant papers, books and websites).

Beside, an Internet site has been made to have a common documentation base: **https://www-prodh2-task25.cea.fr/.** This site is an exchange place between experts of the working group.

4 Conclusions

Through IEA, the initiative of this new group of experts appears to be an efficient way to promote High Temperature Hydrogen Production Processes with an original approach that allows deep collaboration in the same expert group of two major scientific communities working on energy: solar and nuclear.

At the end of the three year period, a one year extension period was approved by the Executive Committee.

This will enable the proposal of a new strategy to support longer term HTPs deployment, in particular concerning demonstrator needs. It will also lead to the definition of a successor task according to this strategy. This work will be completed by further investigation on the multi-criteria assessment methodology, in order to refine the first assumptions and to carry out new sensitivity analysis. The final goal is to highlight the impact of each parameter and the avenue worth investigating.

References

[1] A. Noglik, M. Roeb, T. Rzepczyk, J. Hinkley, C. Sattler, R. Pitz-Paal. Solar Thermochemical Generation of Hydrogen: Development of a Receiver Reactor for the Decomposition of Sulfuric Acid. J. of Solar Energy Engineering 131, Feb. 2009, 011003.1-7

[2] M. Lanchi, F. Laria, R. Liberatore, L. Marrelli, S. Sau, A. Spadoni, P. Tarquini. HI extraction by H3PO4 in the Sulfur–Iodine thermochemical water splitting cycle: Composition optimization of the HI/H2O/H3PO4/I2 biphasic quaternary system. International Journal of Hydrogen Energy, Volume 34, Issue 15, August 2009, Pages 6120-6128.

[3] J.L. Pinilla, R. Utrilla, M.J. Lázaro, I. Suelves, R. Moliner, J.M. Palacios. A novel rotary reactor configuration for simultaneous production of hydrogen and carbon nanofibers. Int J Hydrogen Energy, Volume 34, Issue 19, October 2009, Pages 8016-8022.

[4] D. Wiedenmann, A. Hauch, B. Grobéty, M. Mogensen, U.F. Vogt. Complementary techniques for solid oxide electrolysis cell characterisation at the micro- and nano-scale. International Journal of Hydrogen Energy, October 2009.

[5] D. Wiedenmann, U.F. Vogt, O. Patz, G. Schiller, WDX Studies on Ceramic Diffusion Barrier Layers of Metal Supported SOECs, Fuel Cells, special issue, Fuel Cells, 09, 2009, No. 6, 861-866

[6] D. Wiedenmann, A. Hauch, B. Grobéty, M. Mogensen, U. Vogt, Complementary techniques for solid oxide cell characterisation on micro- and nano-scale, (in press, Hydrogen and Energy)

[7] J. Leybros, T. Gilardi, A. Saturnin, C. Mansilla , P. Carles. Plant sizing and evaluation of hydrogen production costs from advanced processes coupled to a nuclear heat source. Part I: Sulphur-iodine cycle. International Journal of Hydrogen Energy (2009), Volume 35, Issue 3, February 2010, Pages 1008-1018.

[8] S. Haussener, D. Hirsch, C. Perkins, A. Weimer, A. Lewandowski, A. Steinfeld. Modeling of a multitube high-temperature solar thermochemical reactor for hydrogen production. ASME J. Solar Energy Eng. 131, 024503, 1-5 (2009).

[9] T. Melchior, N. Piatkowski, A. Steinfeld. H2 production by steam-quenching of Zn vapor in a hot-wall aerosol flow reactor. Chem. Eng. Sci. 64, 1095-1101 (2009).

[10] L. Schunk, W. Lipinski, A. Steinfeld. Heat transfer model of a solar receiver-reactor for the thermal dissociation of ZnO – Experimental validation at 10 kW and scale-up to 1 MW. Chem. Eng. J. 150, 502-508 (2009).

[11] R. Rivera-Tinco, C. Mansilla, C. Bouallou, F. Werkhoff, Hydrogen production by high temperature electrolysis coupled with EPR, SFR, or HTR: techno-economic study and coupling possibilites, Int. J. Nuclear Hydrogen Production and Applications, Vol. 1, No. 3, 2008.

[12] M.G. McKellar, J.E. OBrien, C.M. Stoots, J.S. Herring, Demonstration and System Analysis of High Temperature Steam Electrolysis for Large-Scale Hydrogen Production Using SOFCs, 8th EUROPEAN SOFC Forum, 2008, Lucerne

[13] Sigurvinsson J., Mansilla C., Lovera P., Werkoff F., Can high temperature steam electrolysis function with geothermal heat? Int. J. Hydrogen Energy 2007;32 (9):1174–82.

[14] W. Doenitz, R. Schmidberger, E. Steinheil, R. Streicher, “Hydrogen production by high temperature electrolysis of water vapour”, International Journal of Hydrogen Energy, Vol. 5, pp. 55-63, 1980.

[15] O’Brien, J. E., McKellar, M. G., Harvego, E. A., and Stoots, C. M., High-Temperature Electrolysis for Large-Scale Hydrogen and Syngas Production from Nuclear Energy – system Simulation and Economics, International Conference on Hydrogen Production, ICH2P-09, Oshawa, Canada, May 3-6, 2009.

[16] U.F. Vogt, J. Sfeir, J. Richter, C. Soltmann, P. Holtappels, B-site substituted lanthanum strontium ferrites as electrode materials for electrochemical applications, Pure Appl. Chem., Vol. 80, No. 11, pp. 2543–2552, 2008
S.H. Jensen, P.H. Larsen, M. Mogensen, Hydrogen and synthetic fuel production from renewable energy sources, Int. J. Hydrogen Energy 32 (2007) 3253-3257

[17] W. Doenitz, E. Erdle, “High temperature electrolysis of water vapour – Status of development and perspectives for application”, International Journal of Hydrogen Energy, Vol. 10, pp. 291-295, 1985.

[18] A. Hauch, S.D. Ebbesen, S.H. Jensen, M. Mogensen, Highly efficient high temperature electrolysis, J. Mater. Chem., 2008, 18, 2331-2340

[19] Meng Ni, Michael K.H. Leung, Dennis Y.C. Leung, Technological development of hydrogen production by solid oxide electrolyzer cell (SOEC), Int. J. of Hydrogen Energy 33 (2008) 2337-2354

[20] W. Dönitz, E. Erdle, R. Streicher, High temperature electrochemical technology for hydrogen production, chapter 3, Electrochemical Hydrogen Technologies, edited by Hartmut Wendt, Elsevier 1990

[21] E. Erdle, J. Gross, V. Meyringer, Possibilities for Hydrogen production by combination of a solar thermal central receiver system and high temperature electrolysis of steam, Solar thermal central receiver systems, Proceedings of third int. workshop, June 23-27, Konstanz, Springer-Verlag, Vol. 2, pp. 727-736, 1986

[22] G. Tsekouras, J. T.S. Irvine, (La,Sr)TiO3 perovskites as cathode for solid oxide electrolysis cell, International Workshop on High Temperature Electrolysis Limiting Factors, 2009 Karlsruhe

[23] T. Ishihara, T. Kannou, S. Hiura, N. Yamamoto, T. Yamada, Steam Electrolysis Cell Stack using LaGaO3-based Electrolyte, International Workshop on High Temperature Electrolysis Limiting Factors, 2009 Karlsruhe

[24] H. Matsumoto, T. Sakaia, S. Matsushitab, T. Ishihara, Intermediate-temperature steam electrolysis using proton-conducting perovskite, International Workshop on High Temperature Electrolysis Limiting Factors, 2009 Karlsruhe

Task 22 of IEA HIA – Fundamental and Applied Hydrogen Storage Materials Development

Bjørn C. Hauback, Institute for Energy Technology, Norway

During the last decade there has been a significant increased focus on hydrogen as the future energy carrier. The main reason is that a hydrogen economy may be an answer to the two major challenges facing the future global economy: climate changes and the security of energy supplies. The major components in the expected Hydrogen Economy involve production, storage and final use of hydrogen, e.g. in fuel cells. All parts in this chain are facing considerable technological challenges, in particular related to the key materials.

Hydrogen storage is a crucial step for providing a ready supply of hydrogen fuel to an end user, such as a car. Without effective storage systems, a Hydrogen Economy will be difficult to achieve. Hydrogen storage remains an undisputed problem for hydrogen- fuelled vehicles, and is considered by many to be the most technologically challenging aspect. During the years several countries have defined targets for hydrogen storage, for example US Department of Energy (DOE), NEDO in Japan and the European Commission in projects like NESSHY. These targets include a number of parameters important for practical hydrogen storage systems. One example is the targets given by US DOE. The most cited target for 2010 is 4.5 wt% hydrogen system gravimetric capacity for applications in vehicles. Compressed or liquid hydrogen will never meet these long-term goals for hydrogen storage. Main problems with liquid and compressed hydrogen storage are energy losses during liquefaction (30-40 %) and compression, volumetric and gravimetric densities (most severe for compressed hydrogen) and safety considerations. Thus the only potential long-term solution is hydrogen storage in solid materials in vehicles.

In spite of the significant achievements related to hydrogen storage in solid materials during the last years, further progress is still needed to fulfil the international goals, e.g. with respect to gravimetric and volumetric capacities, temperature and pressure for hydrogen release for mobile applications. Such research efforts will require new materials and solutions, and not simple, incremental improvements in current technologies. However, for stationary applications, there exist materials with acceptable properties. The gap between the present storage solutions and the storage system targets defined by US DOE is shown in figure 1. A solution requires collaboration optimizing competence and knowledge in different research groups worldwide. The International Energy Agency Hydrogen Implementation Agreement (IEA HIA) Task 22 “Fundamental and applied hydrogen storage materials development” is the largest international co-operative effort on hydrogen storage materials and by the end of 2009 with participation of 53 leading experts in the field from 18 countries including: Australia, Canada, Denmark, European Commission, France, Germany, Greece, Iceland, Italy, Japan, Korea, Lithuania, Norway, Netherlands, Sweden, Switzerland, United Kingdom and USA.

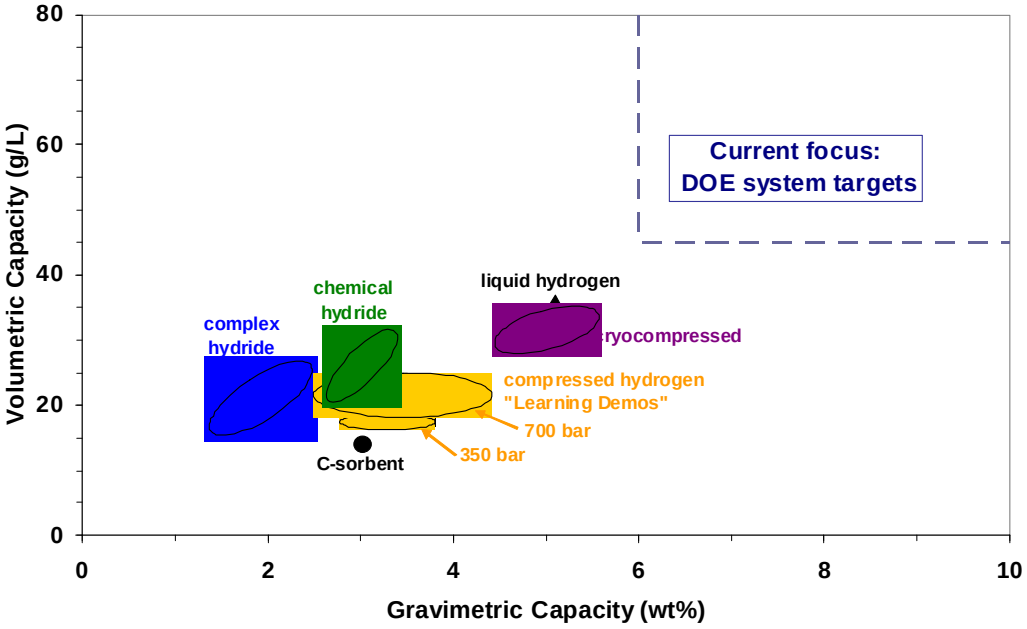

Figure 1: Volumetric hydrogen capacity (g/L) versus gravimetric capacity (wt%) for different hydrogen storage vehicle systems (Source: G. Sandrock, G. Thomas, U.S. DOE, 2008).

The major challenges related to materials for hydrogen storage can be summarized by:

- Gravimetric hydrogen density. A very few hydrogen storage materials reach a metal/hydrogen ratio higher than 2-3, and thus hydrogen storage materials fulfilling international goals should be based on light-weight elements.
- Thermodynamics. The release of hydrogen should take place at conditions (temperature and pressure) matching working conditions, for example for fuel cells.
- Reversibility. Important for on-board storage, but for off-board hydrogen regenerative hydrogen storage materials the hydrogen uptake should be a cheap and simple process.
- Kinetics. The use of catalysts is often important, but also use of nanoscale materials will improve the kinetics.

In addition, several other factors are of importance like availability of the elements and compounds, cost issues and safety.

Different classes of materials for hydrogen storage have been intensively studied during the last decades, the main groups of compounds are:

- Reversible metal hydrides
- Regenerative hydrogen storage materials (chemical hydrides)
- Nanoporous materials
- Rechargeable organic liquids and solids.

Figure 2: Participants at the Task 22 IEA HIA Experts Meeting in Jeju Island, Korea in April 2009.

Task 22 of IEA HIA addresses hydrogen storage in solid materials. The research efforts related to development of materials for use in vehicles will require *new* materials and solutions, and not simple, incremental improvements in current technologies. Phase 1 of Task 22 ended in December 2009 after 3 years and phase 2 has started for a new 3-years period.

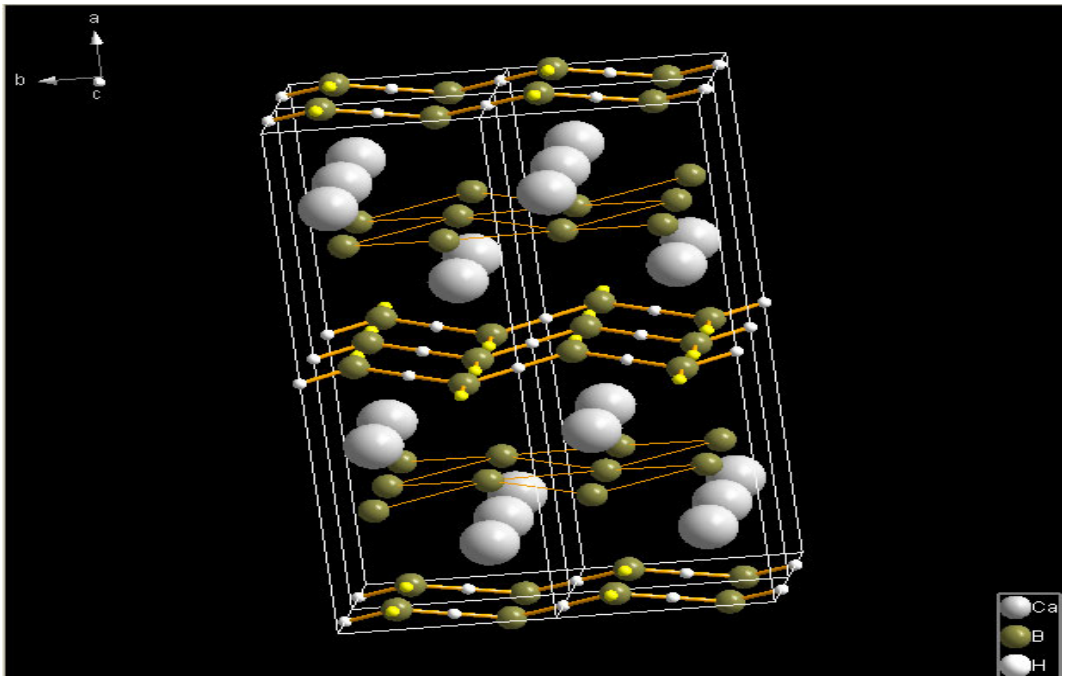

Figure 3: A promising hydrogen storage material: The intermediate phase of $Ca(BH_4)_2$ (source: Institute for Energy Technology).

The specific goals and objectives for research on hydrogen storage materials in Task 22 are:

1. Develop a reversible or regenerative hydrogen storage medium fulfilling international targets for hydrogen storage.
2. Develop the fundamental and engineering understanding of hydrogen storage by various hydrogen storage media that have the capability of meeting Target A.
3. Develop hydrogen storage materials and systems for use for mobile and stationary applications and also other potential energy related applications, for example in batteries.

The targets are not quantitative but instead refer to national and international targets. This gives more flexibility and will also include other relevant parameters than the conventional weigh percentage and hydrogen release temperatures.

The IEA Hydrogen Implementing Agreement's Collaboration on Hydrogen Safety

William Hoagland, Element One, Inc., USA

1 Introduction

In October 2004, the International Energy Agency Hydrogen Implementing Agreement (www.ieahia.org) initiated a task to collaborate on hydrogen safety. This Task 19 on hydrogen safety will be completed in October 2010, and a new proposed three-year task is under development. This task was intended to complement other cooperative efforts to help build the technology base around which codes and standards can be developed. In this way the new task on hydrogen safety will further goal of the IEA Hydrogen Implementing Agreement to accelerate the commercial introduction of hydrogen energy. This paper describes the task's specific scope and work plan, its results to date, and what future work is anticipated.

Hydrogen has been commonly used in a number of applications for the last one hundred years, and much experience has been gained from its production and use as an industrial chemical and in space programs, where it has become the fuel of choice because of its high energy-to-weight ratio. An understanding of hydrogen's physical properties is well established, but actual risks and hazards can only be determined within the context of real systems and operating experience. The existing lack of operating experience with hydrogen energy systems has been recognized as a significant barrier to their widespread adoption, and in recent years, several international efforts have been initiated to develop codes and standards to facilitate their introduction. Such codes and standards are usually developed through operating experience accumulated over time, but without long term experience, there is a natural tendency for such codes and standards to be unnecessarily restrictive.

The overall goal of the new IEA task on hydrogen safety is to develop data and other information that will facilitate the accelerated adoption of hydrogen systems. A well coordinated task on hydrogen safety directly supports the accomplishment of the Hydrogen Implementing Agreement's stated mission:

"…to accelerate hydrogen implementation and widespread utilization."

2 Description of the Collaborative Program

The specific objectives of the hydrogen safety task are to:

- develop testing methodologies around which collaborative testing programs can be conducted;
- collect information on the effects of component or system failures of hydrogen systems; and
- use the results obtained to develop targeted information packages for selected hydrogen energy stakeholder groups.

Three types of activities will be conducted under this subtask: 1) Risk Management, 2) Field Testing, and 3) Information Dissemination. They are described below.

During the first three years, the collaboration completed several products:

2.1 Risk Assessment Methodologies Survey

The Risk Assessment Methodologies Survey has been completed during the first three years of collaboration and is being updated to include additional information on:

1. Ignition probabilities;
2. Risk criteria; and
3. Consequence tools

2.2 Review and Analysis of Risk Assessment Studies

This report has been completed and has been posted on the Task 19 web site.

- **Knowledge Gaps White Paper**

  This report identified gaps in knowledge that added uncertainty to the risk analysis methodologies. This document has been posted on the Task 19 web site.

3 Risk Management Activities

Acceptability of new systems is traditionally measured against regulations, industry and company practices and the judgment of design and maintenance engineers. However, contemporary practice also incorporates systematic methods to balance risk measurement and risk criteria with costs. Management decisions are increasingly relying on Quantitative Risk Assessment (QRA) for managing the attainment of acceptable levels of safety, reliability and environmental protection in the most effective manner. QRA is being applied more frequently to individual projects and may be requested by regulators to assist in making acceptance and permitting decisions. It is a quantitative analysis methodology that can effectively fill in for the lack of operating experience for hydrogen systems in the pubic rather than industrial domain.

4 Survey Existing QRA Methodologies for Relevant Case Studies

Participants provided information on the methodologies for quantitative risk assessment of relevant case studies conducted in their countries. This information was analyzed to present the full variety of existing methodologies in relation to risk assessment of both complete systems and major components. The goal of this activity is to provide a thorough understanding of the composite scope of interest and capability of the international community in risk assessment and permit the individual participants to assess respective approaches. It also serves as a reference for international projects that require QRA.

5 Comparative Quantitative Risk Assessment of Hydrogen Energy Stations for Transportation and Power Applications with Existing Systems Using Conventional Fuels

It is appropriate that the reference for new hydrogen systems, like refueling stations or back-up power systems, be similar to facilities for related fuels like natural gas that have an

established safety record. This is a familiar reference point for the public, regulators and insurers who have a vested interest in safety. Acceptance of hydrogen systems will be more likely if the safety of hydrogen installations can be compared favorably or at par with an already familiar fuel technology. The participants also pooled data on such information as failure rates and other QRA input data will help generate a database for international reference.

6 Probabilistic Risk and Consequence Analysis Enhancement

Risk associated with unwanted hazardous events is a combination of two factors: the likelihood of the event and the seriousness of the event. There is a large accumulated body of knowledge on both the likelihood and severity of unwanted (accidental) events in conventional fuels such as gasoline, propane and natural gas (methane). The corresponding analyses for hydrogen have been highly dependent on the information and procedures for the latter conventional fuels. However, it is becoming increasingly apparent that dependency on data and models and modeling techniques derived from the conventional fuels can generate highly divergent evaluations of the behavior of hydrogen upon release and the consequences.

This effort is closely related to a testing program aimed at providing data on component and system failure rates. A lack of experience with hydrogen systems in consumer environments creates a corresponding lack of credible failure rate data for quantitative risk assessment. Both probability and consequence analyses as well as failure rate data for these systems use approaches that often lead to very conservative risk estimates. However, they also show a strong sensitivity to those modeling parameters and boundary conditions used when based on well-established conventional approaches. This emphasizes the need to base quantitative risk analyses for standardized hydrogen systems and consumer retail facilities on hydrogen-specific data and modeling techniques. This includes the real failure rate of key components installed in such systems with respect to their size and operating conditions as well as on scientifically and experimentally based data and methodologies for predicting consequences of failures of key components.

Based on these interests and concerns, we conduct two parallel sub-activities:

- Hazard identification and analysis and accident progress analysis
- Modeling of component failures

7 Testing Program to Evaluate the Effects of Equipment or System Failures under a Range of Real Life Scenarios, Environments and Mitigation Measures

For almost all risk analysis methodologies reference data is used for validating modeling and calculations of risk probabilities and/or consequences. With hydrogen being relatively new in large-scale use the question remains whether there exists sufficient validation data worldwide to perform calculations with the methodologies highlighted in risk management activities. These methodologies could point out the lack of data on hydrogen safety issues which makes it difficult to draw conclusions related to regulations (e.g. considering safety distances). Besides that, new applications and equipment have been suggested for hydrogen operating under more extreme conditions than applications and equipment used for

conventional fuels. The safety features for these new applications and equipment should be tested and analyzed. This will also lead to the identification of new accident scenarios addressed under the risk management effort.

The testing program will focus on both testing and experimental data, i.e., testing data as collected by checking the performance of applications and equipment and experimental data as collected by experiments with hydrogen release, ignition, fire, explosions and preventive and protective measures. In other words, testing data is more equipment specific, whereas experimental data is more hydrogen specific. Experimental data in particular will give new insight in controlling the size of hazardous areas. Reducing the size of the hazardous area will result in less stringent mitigating measures.

The main effort under the testing task was to create a Hydrogen Testing and Experimental Database (HyTEX) and populate it with all available data. This database will include other existing databases either by linking or direct inclusion. This database has been launched and is currently undergoing beta testing. As such it is only available to participants of Task 19.

Another activity of the Experimental and Testing subtask is that the results of the risk management efforts will be linked to the testing program. Lack of data arising from analyzing methodologies in the risk management activity can be compared to the existing data. If data is not available this could give rise to new recommendations on testing and experimental programs, if yet not already covered by ongoing or planned testing projects. Other activities may be undertaken based on the specific experience and interest of the Participants.

8 Development of Targeted Information Packages for Stakeholder Groups

The development of a homogenous worldwide infrastructure will be necessary before hydrogen energy can achieve widespread utilization and public acceptance. Safety concerns caused by the lack of real operating experience (and the cost of their mitigation) are major inhibitors to the accelerated development of such infrastructure. As information is collected during the testing program, a beneficial impact can only be achieved if it is conveyed to those stakeholders who will participate in the development of the new infrastructure.

The goal of the information dissemination activity will be to use the results obtained in the testing and evaluation program to develop targeted information packages for stakeholder groups (permitting officials, insurance providers, system developers, and early adopters of these new products and systems). This activity is more advanced in some countries compared to others that could benefit from the experiences gained in the infrastructure development process.

9 More Information

More information about the IEA and this task may be found by contacting the operating agent, William Hoagland at william@hoagland.us , or from the following web sites:

www.iea.org

www.ieahia.org

www.ieah2safety.com

An Overview of IEA Annex 19, Subtask B: Experimental Data Bases Relevant to Hydrogen Safety Standards Development

W. G. Houf, **R. W. Schefer**, **J. Keller**, Sandia National Laboratories, Livermore, USA
C. Blake, National Renewable Energy Laboratory, USA
B. Hoagland, Element One, Inc., USA
W. Pitts, National Institute of Standards and Technology, USA
M. Royle, Health and Safety Laboratory, UK
S. Ruban, **S. Jallais**, Air Liquide, France
A. Bengaouer, Commissariat à l'Energie Atomique, France
L. Shirvill, **T. Gautier**, Shell Global Solutions UK, Shell Technology Centre, UK
J. Suzuki, Japan Automobile Research Institute, Japan
D. Willoughby, Health and Safety Laboratory, UK

1 Introduction

The International Energy Agency (IEA) Annex 19 on Hydrogen Safety was established in 2004 to facilitate the hydrogen safety codes and standards development process. Organizationally, Annex 19 is divided into three subtasks: Risk Management (Subtask A), the Testing and Experimental Program (Subtask B), and Targeted Information Packages for Stakeholder Groups (Subtask C). In the present paper we summarize the current status and results of Subtask B, the Testing and Experimental Program. A key element in this program is the identification and development of experimental databases that are relevant to accident scenarios in real systems. Such databases are integral to a better understanding of the consequences of such accidents as well as to the validation of models developed to predict the risks and hazards associated with the accidents. A number of research groups are active in this program and include groups from Europe, Canada, Japan, and the United States. In this paper, an overview of each group's effort, the methodology and the current status of databases in the various areas are provided. Further links to details of the work, links to relevant references and information on the availability of databases are provided. Finally, an evaluation of current data gaps is given by the authors to provide greater insight into future research needs and directions.

2 United States Contribution to Experimental Data Relevant to Hydrogen Safety Standards Development

2.1 Sandia National Laboratories*

Sandia's work on hydrogen safety supports the Safety, Codes, and Standards element of the U.S. Department of Energy's Hydrogen Fuel Cells and Infrastructure Technology Program. The goal of the work is to provide the necessary experimental data and analysis to provide a sound technical basis for the development of hydrogen safety, codes, and standards.

Initial experimental work at Sandia began in 2002 and focused on quantifying the hazards associated with unintended releases of hydrogen from high-pressure gaseous sources. Experiments were performed with SRI International at their Corral Hollow test site near Livermore California to measure the flame length and radiative heat flux from large-scale hydrogen jet flames [1, 2]. This data was used to develop a predictive capability for large-scale hydrogen jet flame thermal radiation based on experimentally verified correlations and engineering models [3]. In 2007, a set of large-scale experimental tests were performed to characterize the effectiveness of barrier walls to mitigate hydrogen jet flame hazard [4]. A total of 4 different barrier configurations were evaluated using high-speed video and other suitable transducers to characterize the flame wall interactions. A second set of barrier experiments was performed in 2008 to study the effect of the ignition delay time (the time between the beginning of the release and ignition) on the amount of ignition overpressure generated [5, 6].

In addition to investigating high-momentum choked-flow releases of hydrogen, Sandia has also experimentally investigated the slow-leak regime where buoyancy can significantly affect the concentration decay and trajectory of an unignited hydrogen leak [7, 8]. Laboratory scale experiments have been performed where Planar Laser Rayleigh Scattering (PLRS) was used to measure the instantaneous concentration field in vertical and horizontal buoyant hydrogen jets. Particle Image Velocimetry (PIV) was also used to characterize the velocity. This database provides a good test for the validation of models for unintended releases of hydrogen where the effects of buoyancy are important.

Laboratory scale experiments have also been performed to study the lean ignition limits of hydrogen/air mixtures in turbulent jets using a non-intrusive laser ignition source [9]. As part of these experiments Planar Laser Rayleigh Scattering was used to measure the instantaneous hydrogen concentration field in the jet and this data was correlated with observations of ignition and jet light-up.

In many unintended gaseous hydrogen releases where ignition has occurred, the ignition source is well known (for example a nearby open flame, or an electrical spark). However, for a large number of reported incidents the ignition source has not been identified. These events are often referred to as auto-ignition events. Two of the most likely ignition sources for these events include shock heating of the resulting hydrogen/air mixture and ignition due to

---

* Sandia is a multiprogram laboratory operated by Sandia Corporation, a Lockheed Martin Company, for the United States Department of Energy's National Nuclear Security Administration under Contract DE-AC04-94-AL85000.

electrostatically charged particles. In collaboration with Dryer [10] of Princeton University Sandia has implemented a combined experimental and modeling program to identify the potential role of shock heating as an auto-ignition source. In addition, Sandia has worked with SRI International to experimentally study electrically charged particles as a source of auto-ignition [11].

Testing and modeling have also recently been performed to investigate gaseous releases from hydrogen fuel-cell vehicles in tunnels. A series of half-scale experiments has recently been completed at the SRI Corral Hollow facility to measure hydrogen concentration and ignition delay overpressure in a tunnel resulting from the release produced by activation of the simulated PRD (pressure release device) on a scaled model of a gaseous hydrogen vehicle [12].

References

[1] Schefer, R.W., Houf, W.G., Bourne, B., and Colton, J., “Spatial and Radiative Properties of an Open-Flame Hydrogen Plume,” International Journal of Hydrogen Energy, Vol. 31, 1332-1340, August 2006.

[2] Schefer, R.W., Houf, W.G., Williams, T.C., Bourne, B., and Colton, J., “Characterization of High-Pressure, Under-Expanded Hydrogen-Jet Flames,” International Journal of Hydrogen Energy, Vol. 32, 2081–2093, August 2007.

[3] Houf, W.G., and Schefer, R.W., “Predicting Radiative Heat Fluxes and Flammability Envelopes from Unintended Releases of Hydrogen,” Int. Jour. of Hydrogen Energy, Vol. 32, 136-151, January 2007.

[4] Schefer, R.W., Groethe, M., Houf, W.G. and Evans, G., “Experimental Evaluation of Barrier Walls for Risk Reduction of Unintended Hydrogen Releases,” Int. Jour. of Hydrogen Energy, Vol. 34, 1590-1606, February 2009a.

[5] Schefer, R.W., Merilo, E.G., Groethe, M.A., Houf, W.G., “Experimental Investigation of Hydrogen Jet Fire Mitigation by Barrier Walls,” 3rd Int. Conf. on Hydrogen Safety, Ajaccio, Corsica, September 16-19, 2009b.

[6] Merilo, E.G., Groethe, M.A., “FY08 Report on Experimental Investigation of Hydrogen Jet Fire Hazard Mitigation my Barrier Walls,” SRI International (Project 17861) Final Report Prepared for Sandia National Laboratories, December, 2008.

[7] Schefer, R.W., Houf, W.G., Williams, T.C., “Investigation of Small-Scale Unintended Releases of Hydrogen: Buoyancy Effects,” Int. Jour. of Hydrogen Energy, Vol. 33, 4702-4712, September 2008a.

[8] Schefer, R.W., Houf, W.G., Williams, T.C., “Investigation of Small-Scale Unintended Releases of Hydrogen: Momentum-dominated Regime,” Vol. 33, 6373-6384, November 2008b.

[9] Schefer, R.W., Evans, G.H., Zhang, J., Ruggles, A.J., Greif, R., “Ignitability Limits for Combustion of Unintended Hydrogen Releases: Experimental and Theoretical Results,” 3rd Int. Conf. on Hydrogen Safety, Ajaccio, Corsica, September 16-19, 2009c.

[10] Dryer, F.L., Chaos, M., Zhao, Z., Stein, J.N., Alpert, J.Y., Homer, C.J., “Spontaneous Ignition of Pressurized Releases of Hydrogen and Natural Gas Into Air,” Combustion Science and Technology, Vol. 179, 663-694, 2007.

[11] Merilo, E.G., “FY09 Report on Experimental Investigation of Static Charge as a Source of Spontaneous Ignition of Hydrogen Jet Fires,” SRI International (Project PYD-19086) Final Report prepared for Sandia National Laboratories, December 2009.

[12] Houf, W.G., Evans, G.H., James, S.C., “Simulation of Hydrogen Releases from Fuel-Cell Vehicles in Tunnels,” 18th World Hydrogen Energy Conference, Essen, Germany, May 16-21, 2010.

2.2 National Renewable Energy Laboratory

The United States Department of Energy’s National Renewable Energy Laboratory (NREL) in Golden, Colorado has supported the International Energy Agency (IEA) Annex 19 for several years through the Hydrogen Safety, Codes and Standards Program research activities. NREL, in collaboration with Sandia National Labs and other national laboratories, is responsible for the implementation of a national agenda for hydrogen codes and standards [1].

The collection and dissemination of research, development, and demonstration data for the purposes of the development of codes and standards is included in the objectives of the national agenda. As a result, hydrogen safety information and data have been collected to create a Hydrogen Safety Bibliographic Database [2] that is available to the general public through NRELs web site [3]. In addition to the bibliographic database, NREL also participates in several learning demonstrations through which operational and safety data is collected and disseminated [3].

The bibliographic database is currently comprised of 748 hydrogen safety-related references. The content is reviewed for accuracy and updated on a yearly basis. The web-based database includes a “suggested additions” feature which allows users to recommend additions to the database which are not present. A major highlight of NRELs collaboration with the IEA Annex 19 tasks is the effort to parallel the data resources contained in the HySafe Database for hydrogen safety information. In 2008, a complete review of each database was conducted to ensure that all information was concurrent in each database. Regular updates are provided to the Annex 19 members. As a result, the bibliographic database also appears as a resource in the IEA Task 19 HyTex Database.

Hydrogen safety information is also collected and disseminated through three learning demonstration projects:

- Hydrogen Fuel Cell Vehicle and Infrastructure Learning Demonstration [4]
- Hydrogen Fuel Cell Bus Evaluations [5]
- Early Fuel Cell Market Demonstrations (Forklift Operations) [6]

These projects involve gathering extensive data, including safety information, from the systems and components under real-world conditions, analyzing these detailed data, and then comparing results to technical targets. While the raw data are protected by NREL, analysis results are aggregated into public results called composite data products. These public results show the status and progress of the technology and include safety-related information. Regular updates are provided by NREL to the Annex 19 members where the information can be used as a resource to contribute to the understanding of the risks and hazards associated with the use of hydrogen.

References

[1] Blake, C.W., A National Agenda for Hydrogen Codes and Standards, Proceedings of the International Symposium of Materials Issues and a Hydrogen Economy, Richmond, VA, USA, November 12-15, 2007.

[2] Hydrogen Safety Bibliographic Database, http://nrelpubs.nrel.gov/Webtop/ws/hsdb/www/hydrogen/SearchForm, accessed 2.10.2010.

[3] NREL Technology Validation Program, http://www.nrel.gov/hydrogen/proj_tech_validation.html, accessed 2.10.2010.

[4] Hydrogen Fuel Cell Vehicle and Infrastructure Learning Demonstration, http://www.nrel.gov/hydrogen/proj_learning_demo.html, accessed 2.10.2010.

[5] Hydrogen Fuel Cell Bus Evaluations, http://www.nrel.gov/hydrogen/proj_fc_bus_eval.html, accessed 2.10.2010.

[6] Early Fuel Cell Market Demonstrations, http://www.nrel.gov/hydrogen/proj_fc_market_demo.html, accessed 2.10.2010.

2.3 National Institute of Standards and Technology (NIST) Testing and Experimental Program for Hydrogen Fire Safety

NIST has a research program designed to provide experimental data, understanding, and model validation to support code development for the safe utilization of hydrogen in enclosed spaces. Current efforts are focused on hydrogen-fueled vehicles parked inside residential garages, but the results are applicable to other types of systems, e.g., residential fuel cells for power generation.

Efforts are focused on two particular problems: 1) the mixing and combustion behavior of hydrogen in enclosed spaces as the result of an unintended release and 2) the development of an experimental system for testing hydrogen sensors which incorporates potential interferents. The research is a coordinated effort involving in-house research, academic research grants, and contractor experimentation.

2.3.1 Mixing and combustion behavior of unintended releases of hydrogen

A series of experiments designed to characterize the mixing behavior of hydrogen within and subsequent removal from a typical residential garage following unintended releases has been carried out at NIST using helium as a surrogate. A study of the mixing behavior of helium within an idealized ¼-scale two-car residential garage was designed to provide reference data for validating mixing models and an improved understanding of the mixing and loss processes. The tests involved scaled releases of helium equivalent to 5 kg of hydrogen over one or four hour periods into an enclosure with a vent(s) on the front face. Vent areas were scaled to provide air exchange rates with the surroundings typical of actual garages in the United States. Additional parameters varied include the helium release location (near the floor and ceiling in the center and near the floor in the rear), vent configuration and size (two single vents with different areas located at the center of the face and a face with two vents located near the floor and ceiling). Results have been reported at a

recent symposium and will appear shortly as a NIST Technical Note incorporating electronic files of the experimental measurements.

A continuing series of measurements involves the release of helium into a real-scale garage attached to an environmental test house at NIST. The focus of these measurements is the mixing behavior of the surrogate gas within the garage, the role of ambient weather conditions on the mixing within and removal of the helium from the garage, and characterizing the penetration of helium into the attached structure.

NIST contracted with Southwest Research Institute to perform a series of experiments in which hydrogen was released into a full-scale two car garage at a rate corresponding to 5 kg/hour. These tests were designed to characterize the mixing behavior of hydrogen in a real-scale garage exposed to the elements and the combustion behavior following ignition after the build up of hydrogen. Hydrogen concentrations during the releases were tracked using a series of eight sensors spanning heights from the floor to the ceiling. When hydrogen volume fractions at a position near the ceiling reached specified levels ranging from 8% to 29%, the mixtures were ignited. The subsequent combustion behavior was characterized using a combination of high-speed pressure probes, thermocouples, and visible and infrared videography. Twenty-five tests were done with 19 involving an empty garage and 6 with a vehicle parked inside the garage. The results of this investigation will be released shortly by NIST as a Government Contractors Report. Additional analysis of the findings is being performed by NIST researchers.

NIST awarded research grants to two university research groups to investigate the mixing and combustion behavior of hydrogen escaping from a pin-hole opening and the potential for catalytic surfaces to ignite hydrogen/air mixtures. The findings of the former study have been incorporated into a draft standard prepared by the Society of Automotive Engineers.

2.3.2 Hydrogen sensor characterization and testing

NIST has a long history of testing smoke detectors. This expertise has been utilized to develop a facility for performance testing of hydrogen sensors known as the Hydrogen Detector Environment Evaluator (HyDEE). This facility is based on a small, low-speed temperature-controlled wind tunnel with an air flow to which known concentrations of hydrogen and a variety of other gases and vapors can be added. The response of a sensor is determined when exposed to known hydrogen concentrations in the presence of a range of additional gases and vapors representing nuisance and obfuscating or sensor-poisoning substances. Testing is underway to characterize the behaviors of a variety of types of sensors to a wide range of conditions in the HyDEE. The ultimate goal is to identify a range of ambient conditions appropriate for standards testing of hydrogen sensors.

References

[1] Photograph of Hy-SEF Facility.Yang, J.C., “A Thermodynamic Analysis of Refilling of a Hydrogen Tank,” International Journal of Hydrogen Energy 34, 6712-6721 (2009).

[2] Yang, J.C., “Material-Based Hydrogen Storage,” International Journal of Hydrogen Energy 33, 4424-4426 (2008).

[3] Yang, J.C. and Huber, M.L., “Analysis of Thermodynamic Processes Involving Hydrogen,” International Journal of Hydrogen Energy 33, 4413-4418 (2008).

[4] Linteris, G. and Babushok, V.I., “Promotion of Hydrogen-Air Ignition by Iron-Containing Compounds,” Proceedings of the Combustion Institute 32, 2535-2542 (2009).

[5] Yang, J.C., “Hydrogen Fire Safety Research Activities at NIST,” 4th Fire Science and Engineering Conference, Beijing, China, October 2007.

[6] Pitts, W.M.; Prasad, K., Yang, J.C., and Fernandez, M.G., “Experimental Characterization and Modeling of Helium Dispersion in a ¼-Scale Two-Car Residential Garage,” 3rd International Conference on Hydrogen Safety, Ajaccio, Corsica, France (September 2009).

[7] Prasad, K., Pitts, W.M., and Yang, J.C., “A Numerical Study of Hydrogen or Helium Release and Mixing in Partially Confined Spaces,” National Hydrogen Association Meeting, Columbia, SC, March 2009.

[8] Marsh, N. and Cleary, T.G., “Towards a Test Method for Hydrogen Sensor Performance,” National Hydrogen Association Meeting, Sacramento, CA, March 2008.

[9] Marsh, N. and Cleary T.G., “Preliminary Performance Assessment of Commercially-Available Hydrogen Sensors,” Proceedings of the International Symposium on Materials Issues in a Hydrogen Economy, Richmond, VA, November 2007.

[10] Prasad, K., Bryner, N., Cleary, T.G., Hamins, A., Marsh, N., Pitts, W.M., and Yang, J.C., “Numerical Simulation of Hydrogen Leakage and Mixing in Large Confined Spaces,” National Hydrogen Association Meeting, Sacramento, CA, March 2008.

[11] Butler, M. S., Moran, C.W., Sunderland, P.B. and Axelbaum, R.L., “Limits for Hydrogen Leaks That Can Support Stable Flames,” International Journal of Hydrogen Energy 34, 5174-5182 (2009).

3 United Kingdom Contribution to Experimental Data Relevant to Hydrogen Safety Standards Development

Over the past eight years, work conducted in the United Kingdom has contributed greatly to the body of experimental data relevant to hydrogen safety. At the 2002 WHEC in Montreal, Shell presented a paper on Safety Considerations in Retailing Hydrogen [1]. Although industry knew how to handle hydrogen safely in an industrial setting, retailing hydrogen for fuel-cell vehicle applications presented new challenges due to the very high storage pressures involved and the close proximity of the public.

Much of the experimental work in the UK has been conducted at the Health & Safety Laboratory, Buxton (HSL), and funded by the Health & Safety Executive (HSE) and Shell.

When stored as a high pressure gas, the hazards associated with jet releases from accidental leaks must be considered and these were the first to be studied experimentally. The early work was limited to release pressures of up to 15 MPa, and data on the characteristics of both ignited [2] and unignited [3] jet releases were reported.

In 2004 Shell initiated a major study on the explosion hazards posed by hydrogen leaks, co-funded by HSE, ExxonMobil, and BP. Explosion experiments were conducted in environments replicating those found on retail stations, and included both 'worst case' pre-mixed hydrogen-air clouds and high-pressure (up to 40 MPa) jet releases of hydrogen. The results provide comprehensive data sets of measured overpressures that can be used to test and validate explosion models necessary for hazard assessments [4][5][6].

Although the early work described above was focused on retailing hydrogen for vehicle application, more recent work has specifically addressed installation permitting for hydrogen and fuel-cell stationary applications in the European project HyPer [7]. Experimental data has been reported on the consequences of jet releases [8] and the efficacy of barriers in reducing separation distances [9].

There is anecdotal evidence that leaks of high-pressure hydrogen often spontaneously ignite. This is important because a spontaneously igniting leak will always result in a jet fire rather than accumulate and possibly result in an explosion. The HSL have reviewed this phenomenon [10] and it is the subject of ongoing study.

Other ongoing studies to address knowledge gaps are: hydrogen venting and liquid hydrogen hazards. Vents are an essential part of the safety system on hydrogen installations and they must be located to minimize the hazards posed by emergency venting. The HSL have produced a critique of the literature on this subject [11] and experiments are in progress to quantify the hazards of both un-ignited and ignited vents. Liquefied hydrogen is one of the options for transporting and storing hydrogen in bulk. The HSL have published a position paper on this subject [12]; there is a dearth of data and plans are in place for experiments to address this.

Hydrogen may also be transported and used in a mixture with natural gas. Experimental data has been generated in the UK on the hazards posed by mixtures of hydrogen and natural gas as part of the European project Naturalhy. This project studied many aspects including explosions in congested regions [13], and in vented confined explosions [14].

References

[1] Cracknell, R.F., Alcock, J.L., Rowson, J.J., Shirvill, L.C., and Ungut, A., Safety Considerations in Retailing Hydrogen, 14th World Hydrogen Energy Conference, Montreal, Canada, 2002.

[2] Shirvill, L.C., Roberts, P., Butler, T.A., Roberts, T.A., and Royle, M., Characterization of the Hazards from Jet Releases of Hydrogen, International Conference on Hydrogen Safety, Pisa, Italy, 7-10 September 2005.

[3] Shirvill, L.C., Roberts, P., Butler, T.A., Roberts, T.A., and Royle, M., Dispersion of Hydrogen from High-pressure Sources, Hazards XIX Symposium, I. Chem. E. Symposium Series No. 151, Manchester, 28 -30 March, 2006.

[4] Shirvill, L.C., Roberts, T.A., Designing for Safe Operations: Understanding the hazards posed by high-pressure leaks from hydrogen refuelling systems, USA National Hydrogen Association Annual Conference, Long Beach, California, USA, March 12-16 2006.

[5] Shirvill, L.C., Royle. M., and Roberts, T.A., Hydrogen Releases Ignited in a Simulated Vehicle Refuelling Environment, 2nd International Conference on Hydrogen Safety, San Sebastian, Spain, 11-13 September 2007.

[6] Shirvill, L.C., and Royle. M., Designing for Safe Operations: Understanding the hazards posed by high-pressure leaks from hydrogen refuelling systems (Part 2), USA National Hydrogen Association Annual Conference, Sacramento, California, USA, March 31 – April 3, 2008.

[7] Pritchard, D.K., Royle, M., and Willoughby, D., Installation Permitting Guidance for Hydrogen and Fuel Cell Stationary Applications: UK Version, HSE Research Report RR715, 2009. http://www.hse.gov.uk/research/rrhtm/rr715.htm

[8] Royle, M., and Willoughby, D.B., Consequences of Catastrophic Releases of Ignited and Unignited Hydrogen Jet Releases, 3rd International Conference on Hydrogen Safety, Ajaccio, Corsica, September 16-19 2009.

[9] Willoughby, D.B., and Royle, M.,The Interaction of Hydrogen Jet Releases with Walls and Barriers, 3rd International Conference on Hydrogen Safety, Ajaccio, Corsica, September 16-19 2009.

[10] Gummer, J., and Hawksworth, S., Spontaneous Ignition of Hydrogen, HSE Research Report RR615, 2008. http://www.hse.gov.uk/research/rrpdf/rr615.pdf

[11] Astbury, G., R., Venting of Low Pressure Hydrogen Gas – A Critique of the Literature, Trans IChemE, Part B, Process Safety and Environmental Protection, 2007, 85(B4):289-304.

[12] Pritchard, D.K., and Rattigan, W.M., Hazards of Liquid Hydrogen: Position Paper, HSE Research Report RR769, January 2010.

[13] http://www.hse.gov.uk/research/rrpdf/rr769.pdf

[14] Royle, M., Shirvill, L.C., and Roberts, T.A., Vapour Cloud Explosions from Ignition of Methane/Hydrogen /Air Mixture in a Congested Region, 2nd International Conference on Hydrogen Safety, San Sebastian, Spain, 11-13 September 2007.

[15] Lowesmith, B.J., Mumby, C., Hankinson, G., and Puttock, J., Vented Confined Explosions Involving Methane/Hydrogen Mixtures, 3rd International Conference on Hydrogen Safety, Ajaccio, Corsica, September 16-19 2009.

4 France Contribution to Experimental Data Relevant to Hydrogen Safety Standards Development

Work on hydrogen energy safety was initiated in France in 1999 with a project on mechanical and thermal resistance of high pressure composite hydrogen cylinders for use in road vehicles (Figure 1A). This work was funded by the European Commission and handled by CEA (Commissariat à l'Energie Atomique), INERIS and Air Liquide [Chaineaux et al., 2000].

During the same period, INERIS (National Institute of Industrial Environment and Risks) performed experimental work funded by the French Ministry of Environment. Instrumented atmospheric dispersion experiments of massive spillage of liquid H2 were performed [Proust et al., 2000]. The overpressures and flame velocity generated by stoichiometric quiescent volume explosion were also studied (Figure 1B).

Moreover, in the framework of another French ministry project, INERIS has setup large-scale fully instrumented experiments to study the formation of flammable clouds resulting from a finite duration release of hydrogen (Figure 1C) in a quiescent room (80 m^3 chamber) [Lacome et al., 2007]. The experimental results show that for the subsonic jet, stratification appears at the top. A diffusion phase follows this stratification and, for all the tested cases the concentration became homogeneous after four hours.

In 2005, the ANR (French National Research Agency) was founded. The National Action Plan on Hydrogen and Fuel Cells Program (PANACHE) has supported 4 safety related projects: DRIVE, HYDROMEL, HYPE and DIMITRHY. These projects will be detailed in the following paragraphs.

The project DRIVE (Experimental Data for the Evaluation of hydrogen Risks onboard vehicles, the Validation of numerical tools and the Edition of guidelines) was managed by INERIS with CEA, PSA and IRPHE as partners. It investigated experimentally different types of leaks and the dispersion of hydrogen either inside the vehicle or outside the vehicle in the most critical situation when the vehicle is parked in an enclosed space such as a private garage. The build-up mechanisms of an explosive atmosphere, including the effects of confinement and ventilation mixture were studied in detail in the CEA Garage installation (Figure 1D) [Gupta et al., 2007; Cariteau et al.. 2009]. Tests of deflagration in simulated car motor area were performed by INERIS in order to define maximum tolerable explosive volumes for various leakage environments. Experimental work was also performed by INERIS on jet flames providing data on hydrogen flame length and on hydrogen flame radiation for some severe scenarios [Proust et al., 2009]. The ignition potential of some electrical and mechanical components and the leak potential of aged fittings were also assessed by INERIS. Impinging jet dispersion of classical obstacles (cylinder, sphere…) is also investigated by IRPHE in sonic and subsonic regimes [Dubois et al., 2009].

The Hydromel project is focused on safety aspects related to addition of hydrogen in natural gas transportation network. The consortium is coordinated by INERIS with CEA, Air Liquide, GDF-SUEZ, Icare (CNRS Orléans), LCD (CNRS Poitiers) as partners. The phenomenological program was dedicated to determine specific combustion properties of H2 / NG: ignition delays, laminar flame velocities (Figure 1E), flame acceleration patterns (Icare – Yahyahoui et al., 2009), detonation cell sizes, deflagration to detonation lengths (LCD-Sorin et al., 2009), and flame radiation parameters (Studer et al., 2009b).

The HYPE project (PSA, CEA and Air Liquide) is focused on high pressure composite cylinder behavior in fire. Cylinder durability experiments of unprotected cylinders in classical liquid hydrocarbons pool fires are performed by INERIS. Moreover, specific highly instrumented experiments to understand heat transfer to the cylinder have also been included in the program.

The DIMITRHY (Data and instrumentation for hydrogen risk mitigation in public applications of fuel cell systems) (CEA, INERIS, AIR LIQUIDE, PSA, HELION, IRPHE) project follows on from the DRIVE project. The work program is mainly focused on mitigation strategies for the formation of explosive atmosphere by ventilation (natural and forced) and for the reduction of explosion consequences by reducing the confinement of the explosion through optimal vent sizing. Dispersion and explosion experiments will be performed by CEA and INERIS. Moreover, advanced modeling will also be used to orient and analyze the experimental work.

The project H2E (Hydrogen Horizon Energy) led by AIR LIQUIDE and funded by OSEO has been launched mid-2009. The risk and safety part of the project (in collaboration with CEA, INERIS, and LCD) will be presented in details in a specific article.

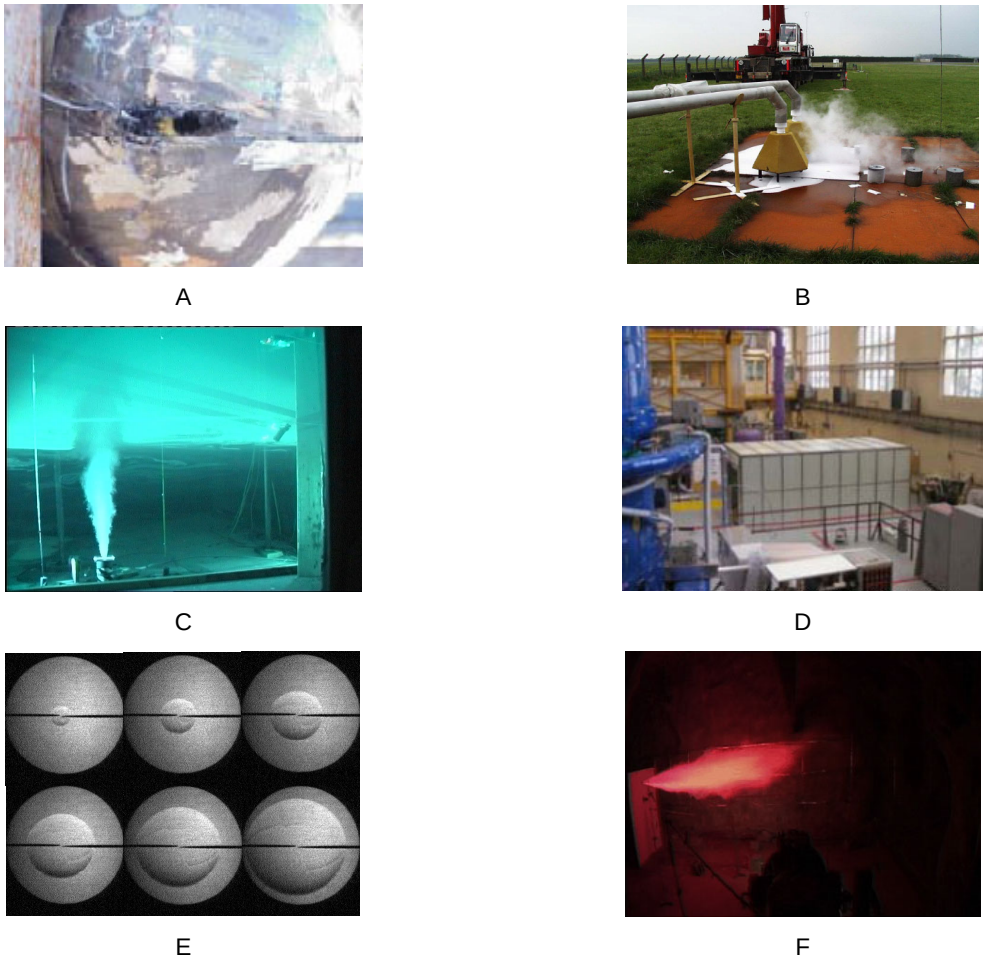

Figure 1: Photos representative of the projects.

References

[1] Benteboula S., Bengaouer A., Cariteau B., Comparison of two simplified models predictions with experimental measurements for gas release within an enclosure, ICHS3, 2009.

[2] Cariteau B., Brinster J., Studer E. Tkatschenko I, Jonquet G., Experimental results on the dispersion of buoyant gas in a full scale garage from a complex source, ICHS3, 2009.

[3] Cariteau B., Brinster, J., Tkatschenlo, I., Experiments on the distribution of concentration due to buoyant gas low flow rate releases in an enclosure, ICHS3, 2009.

[4] Chaineaux J., Devillers C., Serre-Combe P., Sûreté des dispositifs de stockage de l'hydrogène sous haute pression equipant des véhicules routiers, Contrat n°13461-97-11 F1ED ISP F, Rapport Final, Décembre 2000.

[5] Gupta S., Brinster J., Studer, E., Tkatschenko, I., Hydrogen related risks within a private garage: concentration measurements in a realistic full scale experimental facility, International Journal of Hydrogen Energy, 34, 5902 – 5911, 2009.

[6] Lacome, J.M., Dagba, Y., Jamois, D., Perette, L., Proust, C., Large-scale hydrogen release in an isothermal confined area, ICHS2, 2007.

[7] Proust, C., Chelhaoui, S., Joly, C., Process of the formation and explosion of hydrogen air cloud following an extensive spillage of liquid hydrogen, presented at the 5th Annual Conference of the National Hydrogen Association, Washington, USA, March 2000.

[8] Studer, E., Kudriakov, S., Jallais, S., Blanchetière, V., Hébrard, J., Benchmark exercises related to the safety analysis of h2/gn mixtures transportation by pipelines, ICHS3, 2009a.

[9] Studer, E., Jamois, D., Jallais, S., Leroy, G., Hebrard, J., Blanchetière, V., Properties of large-scale methane/hydrogen jet fires, International Journal of Hydrogen Energy, Vol. 34, 9611 – 9619, 2009b.

[10] Sorin, R., Bozier, O., Zitoun, R., Desbordes, D., Deflagration to Detonation Transition in Binary Fuel H2/CH4 with Air Mixtures, ICDERS, 2009.

[11] Yahyahoui, M., Coudoro, K., Djebaili-Chaumeix, N., Paillard, C.E., Experimental and Modelling Study of Hydrogen/Methane/Air mixtures in a Spherical Bomb, 6th Mediterranean Combustion Symposium, Porticcio, Corsica, June 7-11, 2009.

5 Japan Contribution to Experimental Data Relevant to Hydrogen Safety Standards Development

5.1 Fire safety evaluations of vehicles equipped with hydrogen fuel cylinders: Comparison with gasoline and CNG vehicles

To verify the fire safety of compressed hydrogen vehicles, fire tests have been conducted on vehicles that use compressed hydrogen, compressed natural gas (CNG), and gasoline as fuels. The vehicle fire evaluations compared temperatures around the vehicles and the cylinders, the internal pressure of the cylinders, the radiation heat fluxes around the vehicles, the sound pressure levels when the pressure release device (PRD) was activated, and the damage to the vehicles and surrounding flammable objects. Results of the tests indicate that vehicles equipped with compressed hydrogen gas cylinders are not more dangerous than CNG or gasoline vehicles in the event of a vehicle fire [1].

5.2 Hy-SEF: Hydrogen and Fuel Cell Vehicle Safety Evaluation Facility

A new comprehensive facility was constructed for the evaluation of hydrogen and fuel cell vehicle safety at the Japan Automobile Institute by METI and NEDO [2]. The new facility includes an explosion resistant indoor vehicle fire test building with sufficient strength to

withstand an explosion of a high pressure hydrogen tank of 260 litre capacity and 70 MPa pressure. The facility has an exhaust gas cleaning system and enough space to observe vehicle fire flames of not only hydrogen but also other conventional fuels, such as gasoline or CNG. The building is 18 m in diameter, 16 m high, and the walls are made of 1.2 m thick reinforce concrete covered on the inside with steel plate. The following experimental testing program performed in the facility is summarized below. The program verifies the validity of the fuel leakage standard [3] for the collision of hydrogen vehicle.

5.3 Dispersion and ignition behavior of leaks from a hydrogen-fueled vehicle

To verify the fuel leakage standard hydrogen was leaked from the under floor of a vehicle at a flow rate exceeding 131 NL/min, which is the allowable hydrogen leakage rate from the collision of a compressed hydrogen fuelled vehicle in Japan. The resulting distribution of the hydrogen concentration in the engine compartment and the dispersion of hydrogen after stoppage of the leak were investigated. In addition, ignition tests were also conducted and the effects on the surroundings (mainly for people) were investigated to verify the safety of the allowable leakage rate. The tests demonstrated that if hydrogen leaks from the under floor of a vehicle at a flow rate of 1000 NL/min and is ignited in the engine compartment, people around the vehicle will not be seriously injured. Therefore, a flow rate of 131 NL/min, the allowable fuel leak rate for the collision of compressed hydrogen fuelled vehicles, assures a sufficient level of safety [4].

Figure 2: Photograph of Hy-SEF Facility.

5.4 Gaps in the experimental data base and future plans to fill these gaps

Some fire safety knowledge gaps related to hydrogen-fueled vehicles have been identified and are discussed below. These knowledge gaps are currently being investigated in research projects commissioned by NEDO.

When a jet flame is formed by fire activation of the PRD on a hydrogen-fueled vehicle, it is not known whether it is better for first responders to extinguish the flame or to continue to cool the hydrogen containers with water cannon without extinguishing the flame. The risk of

rupture of the compressed hydrogen containers must be suppressed and testing methods need to be developed to insure this. In addition, the risk of fire spread to vehicles parked adjacent to the hydrogen-fueled vehicle is unknown and needs to be investigated. The combustion behavior of the hydrogen gas and surrounding materials is unknown for the case where a hydrogen-fueled vehicle is parked in an enclosure and leaked hydrogen gas penetrates into surrounding porous materials such as the walls and ceiling.

References

[1] Fire Safety Evaluation of a Vehicle Equipped with Hydrogen Fuel Cylinders: Comparison with Gasoline and CNG Vehicles, SAE Transactions, Journal of Passenger Cars Mechanical Systems, 2006-01-0129, (http://www.sae.org/technical/papers/).

[2] The new Facility for Hydrogen and Fuel Cell Vehicle Safety Evaluation, International Journal of Hydrogen Energy, Volume 32, Issue 13, Pages 2105-2606, September 2007, (http://www.sciencedirect.com/).

[3] Attachment 100, Technical Standard of the Safety Regulations for Road Vehicles in Japan (http://oica.net/wp-content/uploads/attachment100.pdf).

[4] Diffusion and Ignition Behaviour on the Assumption of Hydrogen Leakage from a Hydrogen-fuelled Vehicle, SAE Transactions, Volume 116 Journal of Passenger Cars-Mechanical Systems, 2007-01-0428 and (http://www.sae.org/technical/papers/).

Renewable Hydrogen Production

Alan C. Lloyd, Ed Pike, and Anil Baral

Abstract

The need for renewable energy in an environmentally constrained world leads us to examine the potential role of hydrogen produced from renewable sources. Rationales for renewable hydrogen include climate, local air quality, and sustainability goals. Hydrogen can be produced from a variety of current and potential new future renewable resources for applications including transportation and electricity generation. We also examine the effectivenss of a number of policies that have been implemented or adopted. These policies range from specific standards for renewable hydrogen production to broader policies to increase renewable energy or reduce GHG more broadly.

Hydrogen Production as Part of Sustainable Use of Energy in Wastewater Treatment Plants

Emanuel Grün, **Burkhard Teichgräber**, Emschergenossenschaft, Germany

1 Introduction

In its current World Energy Outlook forecast dating from November 2009, the International Energy Agency (iea) warned against a pronounced increase of the worldwide energy consumption until 2030 unless there happened profound changes in global energy utilisation. According to their calculations, about $ 10,000 billion must be invested around the world in low-carbon technologies and in energy efficiency during the next 20 years.

Thus, Germany too is facing the immense challenge posed by global climate changes, although contrary to the worldwide development this country has a decreasing energy consumption tendency and thus anticipates some of future developments. The challenge can only be met by energy politics which are open to new technologies and market-orientated.

In Germany, energy supply has for decades been based on a well-balanced energy mix. In recent years, there has been a pro-rata change from fossil fuels towards regenerative forms of energy. Sustainable technologies such as wind power and solar energy have particularly been promoted. Other energy carriers bound to play a major role in the 21st Century are hydrogen and fuel cells, which are likely to contribute greatly to climate protection in the future.

The Renewable Energy Law (EEG) has given a new boost to energy generation from wind, water, sun, biomass and geothermal sources. By now, 15% of the electric energy consumed in Germany already stem from regenerative sources [1]. The wind power industry aims at covering approx. 25% of the entire energy consumption by 2020. This necessitates finding a way to deal with the surplus production of electricity on days with strong winds. A reasonable solution may be hybrid power plants which in case of excess capacity produce and store hydrogen.

Prior to the market launch and commercialisation of hydrogen and fuel cells, however, the pertaining hydrogen infrastructure must be established.

Hydrogen as storage medium of electricity is very versatile and utilisable for stationary or mobile applications. It offers solutions for the acceptance of volatile energy surpluses from solar power and wind power and provides a considerably larger vehicle operation range than electro-mobility. Hydrogen supplied from regenerative sources is thus a viable contribution to expanding the spectrum of energy carriers available for individual traffic.

Germany consumes about 30% of its primary energy in the traffic sector. Hydrogen and fuel cells may be playing a major role in traffic by 2050. More than 70% of passenger cars and commercial vehicles could be running with hydrogen-fuel cell technologies [2]. The crucial limiting factor is the distribution degree of hydrogen vehicles and the nationwide availability of hydrogen.

Industrial hydrogen is available in Germany in large amounts, for instance as synthetic gas from coal upgrading. Per year, 19 billion Nm^3 are produced or generated as by-product [3], with 3.9 billion in North Rhine-Westphalia alone [4]. This land also sports a 240 km long hydrogen pipeline, which in future might be further expanded to serve as the spine of the overall hydrogen infrastructure. However, the energetic use of hydrogen must be inseparably connected with its production on the basis of regenerative energies.

The general principle of raw material utilisation also applies to sewage sludge. Reserves, resources, and availability as a high-quality product must be considered here. Generally, the availability of this raw material is guaranteed as long as there are human beings, but the upgrading of the sludge will allow for higher levels of value creation.

Water management not only supplies a regenerative energy source – sewage sludge from wastewater treatment –, but also major potentials for the introduction of a hydrogen-based energy infrastructure. Particularly suited are the wastewater treatment plants, which offer themselves as energy supplier for stationary and mobile demands because of their favourable location characteristics. There are approx. 10,500 wastewater treatment plants, predominantly in urban areas, which makes for an excellent connection infrastructure. This network of wastewater treatment plants might provide the starting point for a nationwide local hydrogen infrastructure in Germany.

2 Energy at Wastewater Treatment Plants

Wastewater treatment plants (WWTPs) are both suppliers and consumers of energy. The energy consumption at WWTPs is high and makes for a major percentage of the operation costs. As the processes of wastewater and sludge treatment are very energy-intensive, energy saving and on-site energy production play a crucial role in the operation of wastewater treatment plants. In recent years, Emschergenossenschaft and Lippeverband managed to lower the energy consumption at their WWTPs and to raise the on-site energy production.

One crucial factor of on-site energy production at WWTPs is the utilisation of digester gas in combined heat and power plants (CHPs), a technology which is an established method of internal energy production. Utilising the digester gas through heat-power-coupling in CHPs allows for high energy efficiency degrees, with the mechanical efficiency degree amounting to 30%-35%, the thermal efficiency degree to 50% [5].

In 2006, the production of electric energy in digester gas CHPs in WWTPs in Germany amounted to about 0.94 TWh [6]. At modern WWTPs, the ratio of self-supply with electric energy is approx. 50%-70% (depending on the process technology used). Through co-fermentation – the co-treatment of bio-waste in the fermenters at the WWTPs –, the biogas production and thus the potential of upgraded gas or hydrogen can be increased significantly.

For autonomous combustion, the digested sewage sludge must be dewatered to a degree of at least 45% of dry solids or mixed with other energy carriers (coal fines, shredder fluff); it will then supply further energy, which can be used to cover the demand mentioned above.

In order to reduce the energy demand for wastewater treatment, Emschergenossenschaft and Lippeverband use methods such as area-wide energy benchmarking, energy studies, and load management.

Due to these loops consisting of regular reporting, analysis and measure deduction, which now are run routinely, and the resulting technical measures, recent years have seen a continuous improvement of the energetic situation at the WWTPS of Emschergenossenschaft and Lippeverband. In the long run, it will be possible to cover the energy demand of the WWTPS with sewage sludge utilisation from internal sources [7]. Emschergenossenschaft and Lippeverband strive together for this goal at their respective WWTPs.

3 Production of Green Hydrogen at Wastewater Treatment Plants

The generation of hydrogen at WWTPs is an additional factor of energy production and consumption there. The digester gas which is produced during the anaerobic sewage sludge stabilisation in fermenters is available as renewable resource for hydrogen production, with electrolytic production being a further option. Both ways are described below.

3.1 Hydrogen from biogas through gas reformation

For the production of hydrogen, the biogas is converted in a catalyser at 900° C with addition of steam, analogous to the industrial steam reformation of natural gas. This production path is climate-neutral, as biogas is a renewable energy source.

Being the biggest operator of wastewater treatment plants, the Emschergenossenschaft decided early to test and further develop the processing of digester gas into biomethane and hydrogen in the „EuWaK“ demonstration project at the WWTP in Bottrop („EuWaK” standing for “Erdgas und Wasserstoff aus Kläranlagen“ = “Natural gas and hydrogen from wastewater treatment plants”). The EuWaK project was realised with funding of the federal land of North Rhine-Westphalia and the European Union.

The success of the project depends on a marked problem-solving competence of everybody involved, with interdisciplinary co-operation or „trans-disciplinarity“ being particularly demanded.

The project partners of the Emschergenossenschaft for project development and project realisation are the engineering company Tuttahs & Meyer, the FIW research institute for water and waste management at the RWTH Aachen, the consulting engineers Redlich and Partners, as well as the city of Bottrop. In the pilot project, the digester gas is first converted into biomethane, a component current of which is discharged and supplied at a natural gas filling station to in-house vehicles running with natural gas. In the second step, the remaining biomethane is converted into hydrogen in a steam reformer. The maximum digester gas input currently is 120 Nm^3/h, which is equivalent to a dimension of about 10% of the entire digester gas amount. The capacity of the biogas processing amounts to 72 Nm^3/h, that of the hydrogen processing to ca. 100 Nm^3/h. The generated hydrogen is led via a pipeline to a nearby school centre, where electric energy and heat for the energy supply of the schools are produced in a CHP. In this way, the project succeeded in demonstrating the complete local hydrogen infrastructure from the renewable energy source sewage sludge to the

hydrogen consumer for the first time. A further target of the project is the stable production of high-quality hydrogen, the plan being to supply not only the natural gas filling station, but to provide a hydrogen filling station with hydrogen immediately from the sewage sludge production. Further details of the project will be explained in the report on „Green Hydrogen and Natural Gas from Digester Gas of Wastewater Treatment Plants“.

3.2 Hydrogen from water through electrolysis

Hydrogen can be produced through electrolysis run in a regenerative way (wind power, photo-voltaics, etc.) The oxygen produced at the same time can be used in the wastewater treatment process. This method is employed at the WWTP at Barth in Mecklenburg-Western Pomerania, with the produced hydrogen being used to fuel a fuel cell bus [8].

4 Hydrogen Infrastructure and Wastewater Treatment Plants

The hydrogen production at WWTPs plays a role particularly in building up the hydrogen infrastructure. WWTPs are the first de-central production locations and can supply local vehicle fleets and serve as junctions in the filling station network to be built. The intermediate step of biomethane generation is a bridging technology towards hydrogen and established the WWTPs as filling station locations.

Because of the complex technology and the necessary digester gas amounts, current estimations regard only large WWTPs with a capacity of 100,000 PE onwards as suitable for hydrogen production. In Germany, there are 237 WWTPs of this size. The hydrogen potential of the digester gas on these WWTPs is estimated to be about 260 million m³, which corresponds to ca. 1% of the total hydrogen production in Germany. Another source calculated the hydrogen production potential from the digester gas of all German WWTPs to be 1.65 billion m³ per year [9].

If this hydrogen amount were completely used as fuel, a mileage of 6.2 billion km/a could be achieved. Compared to the total mileage of all passenger cars of 525 billion km/a, this makes for a ratio of 1.2% [9].

The biogas production from the anaerobic sewage sludge treatment at the WWTPs of Emschergenossenschaft and Lippeverband amounts to ca. 45 m Nm³/a, which could be reformed into ca. 60 m Nm³/a of hydrogen. Depending on the frame conditions, ca. 17,000 passenger cars could be supplied with hydrogen.

Even if only a part of this biogas were used for hydrogen production, this part would suffice to satisfy the foreseeable demand for hydrogen-fuelled vehicles in the surrounding area relevant for the refuelling. In the next 15-20 years, the hydrogen supply of vehicles could stem from the potential of the biogas from WWTPs. If a significant market penetration with hydrogen-fuelled vehicles is achieved, it will be necessary to utilise other hydrogen sources.

If only „green hydrogen“ is used, that is hydrogen from regenerative sources, hydrogen-fuelled vehicles can be classified as „zero emission vehicles“. This potential is fulfilled with hydrogen from WWTPs.

The local hydrogen production at WWTPs has one advantage: in case of direct utilisation at the WWTP (filling station), there is no need for an extensive infrastructure to distribute the hydrogen. This allows for the early building of filling stations at the WWTPs which need

neither infrastructure nor distribution logistics. For WWTP owners, hydrogen production as fuel is interesting because mobile utilisation makes for a higher price level than stationary usage. The prerequisite, however, is that the discharged energy of the digester gas can be replaced by regenerative energy sources.

5 Conclusion

In the energy supply of the future, hydrogen will play a major role, provided that the production is based on regenerative energy sources. For the owners of wastewater treatment plants, the hydrogen technology opens up interesting perspectives. Compared with the entire hydrogen amount produced in Germany, the potential of hydrogen production from digester gas must be regarded as low; still, WWTPs will be able play quite a significant role in the building up of the hydrogen infrastructure, particularly during the extension of the filling station network.

References

[1] BMU, Erneuerbare Energien in Zahlen. Berlin, Juni 2009

[2] BMVBS, Bundesministerium für Verkehr, Bau und Stadtentwicklung (2009): GermanHy - Woher kommt der Wasserstoff in Deutschland bis 2050? August 2009

[3] Geitmann, S. : Wasserstoff & Brennstoffzellen - die Technik von morgen. Hydrogeit Verlag, Kremmen.

[4] Grube, T. et al., Perspektiven für den Ausbau der Wasserstoffinfrastruktur am Beispiel NRW. Chemie Ingenieur Technik 2009, 81, No. 5, S. 591-598.

[5] Steinmetz, H., Ansätze für energieoptimierte Kläranlagen. In: Stuttgarter Berichte zur Siedlungswasserwirtschaft. Bd. 191: Innovative Konzepte für Kläranlagen; Oldenbourg Industrieverlag GmbH, 2007

[6] Schröder, M., Realisierung von Energiepotenzialen der deutschen Wasserwirtschaft - DBU geförderte Studie der DWA. DWA-Energietage 20.-22. Oktober 2008 in Fulda.

[7] Kroiss, H., Svardal, K., Energiebedarf von Abwasserreinigungsanlagen. Öwaw 11-12/2009, S. 170

[8] Haas et al., Das Wasserstoff-Sauerstoff-Projekt in Barth. ATV-DVWK- Tagung „Neue Energiekonzepte auf Kläranlagen unter Einbeziehung der Wasserstofftechnologie“. 13. November 2003, Köln.

[9] Schröder, M., Produktionsunternehmen Kläranlagen. KA - Wasserwirtschaft, Abwasser, Abfall 2002 (49) Nr. 10

[10] BMU, Stand der Abwasserbeseitigung in der Bundesrepublik Deutschland. Berlin, Dezember 2002

Regional Hydrogen Roadmap – Project Development Framework for the Sahara Wind Project

Khalid Benhamou, Sahara Wind Inc. Morocco
Abdelaziz Arbaoui, Al Akhawayn University, Morocco
Sidi Mohamed Ould Mustapha, Faculté des Sciences et Techniques de l'Université de Nouakchott, Morocco

Summary

The trade winds that blow along the Atlantic coast from Morocco to Senegal represent one of the the largest and most productive wind potentials available on earth. Because of the erratic nature of winds however, wind electricity cannot be integrated locally on any significant scale, unless mechanisms are developed for storing these intermittent renewable energies. Developing distributed wind energy solutions feeding into smaller electricity markets are essential for solving energy access issues and enabling the development of a local, viable renewable energy industry. These may be critical to address the region's economic challenges currently under pressure from Sub-Saharan migrant populations. Wind-electrolysis for the production of hydrogen can be used in grid stabilization, as power storage, fuel or chemical feedstock in specific industries. The objective of the NATO SfP 'Sahara Trade Winds to Hydrogen' project is to support the region's universities through an applied research framework in partnership with industries where electrolysis applications are relevant. By powering two university campuses in Morocco and Mauritania with small grid connected wind turbines and 30 kW electrolyzers generating hydrogen for power back-up as part of "green campus concepts" we demonstrated that wind-electrolysis for the production of hydrogen could absorb larger quantities of cheap generated wind electricity in order to maximize renewable energy uptakes within the regions weaker grid infrastructures. Creating synergies with local industries to tap into a widely available renewable energy source opens new possibilities for end users such as utilities or mining industries when processing raw minerals, whose exports generates key incomes in regions most exposed to desertification and climate change issue. Initiated by Sahara Wind Inc. a company from the private sector, along with the Al Akhawayn University, the École Nationale Supérieure des Arts et Métiers ENSAM of Meknès and the University of Nouakchott this project is funded under the NATO Science for Peace and security collaborative programs. Being associated to the larger scale Sahara Wind Project, this initial NATO funded Project serves as the foundation of an ambitious program aimed at tackling energy scarcity and sustainable development objectives through industrial synergies utilizing hydrogen energy technologies. This combination takes advantage of the significant breakthroughs expected to happen in the near future regarding hydrogen technologies when associated with larger sources of renewable energies. The reliance on the ability of public bodies such as universities, public utilities and other institutions to concretize dynamic partnerships with the local industry and the private sector was key to the success of this program.

Keywords: trade winds, intermittent storage, grid stability, high wind penetration, energy access, capacity building, industrial synergies, small wind turbines, electrolyzers, fuel cells, hydrogen.

1 Introduction

Wind-electrolysis offers great possibilities for absorbing large quantities of cheap wind generated electricity to produce hydrogen as a valuable fuel resource or chemical feedstock, while maximizing the renewable energy uptake of the weak grid infrastructures of the trade winds coastlines of Morocco and Mauritania. Wind-electrolysis for hydrogen production can be used for grid stabilization, power restitution/backup and as fuel or feedstock for specific uses in remote locations.

The equipping of wind-hydrogen laboratories in both Morocco and Mauritania enabled us to utilize the full length of the NATO Science for Peace SfP-982620 project (36 months) to carry out an exhaustive wind resource assessment program, in both countries in partnership with the region's telecom operators. Since mobile phone coverage is widely distributed and generally made available before access to electricity, the main advantage of this technology is that it relies on a series of repeaters consisting of high mast tower infrastructures. The availability of high mast towers located on regular distances provides an ideal platform within which a wind measurement program can be conducted. The regularity of the telecommunication networks provide a good distribution setting enabling wind energy potentials of a region to be exhaustively mapped with a high level of accuracy and at much lower costs than any other on-site wind measurement programs.

Accuracy and certification of wind measurements represent in our case a capital, generating added value for all teams involved in this program. Hence, choices of wind monitoring equipments have focused on the use of certified, calibrated instruments, rather than lower instruments costs. The access to mast tower infrastructures for wind measurements enabled us to focus our strategy on the reliability of the measurements carried out in this project as the quality of the data collected can already be used by financial institutions for funding wind project developments in the region. Our equipment deployment strategy relied on the selection of calibrated wind measurement instruments that have been installed on several heights of the telecom mast infrastructures.

Since the objective of our project is to reinforce the link between industry and academia, working with the telecom companies in our program was an important first step in engaging end users. This activity, initiated in Mauritania by the University of Nouakchott and Sahara Wind inc. proved to be essential for duplicating collaboration protocols in Morocco, as Mauritania telecom (Mauritel) is in part a subsidiary of Maroc telecom which operates the largest mast tower infrastructure network in Morocco as well. Hence, the wind monitoring program could be extended to Morocco thereafter enabling us to dispose of a complete measurement protocol funded by the NATO Science for Peace and Security programme on a region covering a distance of several thousand Kilometers.

The collaborative environment among institutions in Mauritania being more conducive due to the smaller communities and markets sizes have prompted us to rely on the high level of

flexibility and availability of local operators to start this applied research partnership in a joint sharing of assets with local academic institutions in Morocco as well.

The availability of high mast towers located over regular distances provided an ideal platform within which our wind measurement program could be conducted at minimal costs. Through this approach the wind energy potentials of the region could be exhaustively mapped with a high level of accuracy enabling us simulate the amount of renewable hydrogen which could be generated through wind-electrolysis over a very large area. This enabled us to go beyond weaker grid limitations for accessing the value of wind energy as we are integrating this renewable energy potential into the simultaneous production of electricity and hydrogen in a synergetic context.

Hence, we were able to identify specific industrial applications which could make use of hydrogen related processes such as the mining industries which along with the respective utilities of Morocco and Mauritania are the region's main electricity consumers.

Since this region is located on the edge of one of the largest electricity grids (that of the EU), its large renewable energy potential could be used to produce significant amounts of cheap wind energy that could ultimately end up supplying larger electricity markets. This however, will require an effect of scale. Developing initial mechanisms to progressively firm these intermittent energy sources locally is an imperative first step as this lies on the critical path of major alternative, sustainable energy developments. The role of hydrogen in such case may be quite relevant as it applies to small distributed applications such as the telecoms, or access to clean water for instance that will be up scaled to larger industrial operations which will ultimately be part of a much larger renewable energy supply network infrastructure.

The Sahara Wind Project which has a capacity of 5 GW of wind energy connected to a High Voltage Direct Current infrastructure to disserve both North African and European electricity markets aims precisely at satisfying these objectives. The phasing of the Sahara Wind Project through our collaboration with the region's main industries is thereby significantly enhanced. As an upstream project development activity for its Sahara Wind Project, the NATO 'Sahara Trade Winds to Hydrogen' Project coordinated by Sahara Wind Inc. -a company from the private sector- aims at getting local scientific communities, industries and end user groups to participate in an applied research program with the objective of developing exploitable energy systems capable of integrating the region's widely available renewable energies. This NATO Science for Peace SfP-982620 project enabled applied research platforms to be deployed within the main research and educational centers of Morocco and Mauritania. Around these, adequate training and capacity building programs with subsequent pilot projects deployed within the region's industries (and NATO SfP-982620 project partners) will enable the integration of intermittent sources of renewable energies in the weaker grid infrastructure of the Saharan/Sahel region.

The region can make use of its qualified pool of university professors, engineers and scientists who lacked to a greater extent appropriately equipped research and training infrastructures. The NATO SfP-982620 Project aimed precisely at addressing this issue in providing wind- electrolysis hardware within an integrated energy strategy to support a long term vision.

Support for co-development of wind-electrolyzer test benches have been provided by manufacturers to the extent that University Campuses will be fed by small wind turbines stabilized by electrolyzers and as part of their respective “green campus concepts”. An industrial engineering program for building small wind turbines enabling engineering students to better address the operation and maintenance of these systems, when deployed either around their campuses, or in remote sites.

In order to make hydrogen technologies more accessible to a younger generation of future scientists and engineers the electrolysis equipment (in the 30 kW range) has been integrated as a practical energy storage feature of a green university campus. Its direct association to renewables and the integration of more accessible small wind turbine technologies into such clean energy system will familiarize students with hydrogen technologies introduced on a scale that is more functional and somewhat larger then laboratory devices.

Morocco disposes of a larger scientific community then Mauritania, however many of the country's challenges in rural electrification are effectively not being addressed by academia, but rather by utilities or agencies that do not conduct research programs. Through this NATO funded project, Morocco and Mauritania’s educational institutions initiated a comprehensive applied research program aimed at developing the access to renewable energy through the production hydrogen through a end-use synergetic approach, and integrated within the country’s main industries.

As natural gas reforming processes represents today a large majority of the world’s hydrogen production, emitting over 6 tons of CO_2 per ton of hydrogen in the process, the production of hydrogen through wind-electrolysis is carbon free as this process can be duplicated over a very large scale in Morocco and Mauritania’s trade wind regions. In generating both electricity and hydrogen without CO_2 emissions, significant environmental and energy security concerns are being effectively addressed. Indeed, as natural gas supply disruptions to NATO countries have recently highlighted, the dependency on a single source of energy relying on fixed infrastructures which required hefty investments is a highly sensitive matter. Taping into such natural gas resources to produce hydrogen, would strain these issues even further making the hydrogen economy hardly conceivable. Thus, the need to diversify away from natural gas supplies, whose demand is likely to rise even further, is of paramount importance to the collective energy security of NATO member and partner countries alike (including gas producing countries) as well as for the future of a hydrogen economy. Demonstrating its sustainability based on the renewable energy potentials of the trade winds is therefore a key pre-requisite.

Using wind-electrolysis over such a large scale provides a paradigm shift as it highlights the role of a vast renewable energy source -the trade winds – which can be used to generate simultaneously electricity and hydrogen on a significant scale. At the same time, intermittency, grid stability and power transmission issues are sidestepped because on-site hydrogen production facilitates the access to wind electricity, as hydrogen becomes both an energy storage medium and a valuable feedstock used locally in the mine processing industries.

2 Conclusion

Since electricity cannot be stored, integrating wind energy systems locally is essential as it reinforces local ownership of the wind resource while supporting income earning and energy intensive industries on a regional basis. Using the power of the elements such as wind and sea water as feedstock to supply an industry such as mine processing in the region will enable wind energy to be accessed and a clean, sustainable, value added mineral processing industry to be established locally. This bottom up capacity building will lead to the development of large scale renewable energy networks linking energy markets with adequate resources from the trade winds such as the Sahara Wind Project. This project development approach can be essential to the collective energy security of NATO member and partner countries alike, as it would reinforce the perspectives of a hydrogen economy, address environmental security concerns and enable a maximization of the mineral resource outputs that can be drawn from inside the Sahara Desert.

Hydrogen Energy Research and Collaboration in Australia

Andrew Dicks*, Queensland University of Technology, Brisbane, Australia

1 Background

Interest in Hydrogen Energy within Australia can be traced back to at least the 1930s when a Councillor Kemp in Brisbane considered converting vehicles to run on hydrogen generated from Queensland's plentiful supply of high grade coal. The state government ordered the construction of a high pressure plant but this was never built as the end of WWII signalled a return to relatively cheap oil and petrol. In 1962 opportunities in hydrogen were re-introduced by Professor John M O'Bockris, a former academic from Flinders University, South Australia. A leading authority in electrolytic hydrogen, Bockris influenced many Australians including the late Sir Mark Oliphant, Barbara Hardy AO and Dr Sukhvinder Badwal of the Commonwealth Scientific and Industrial Research Organisation, CSIRO. Dr Badwal was instrumental in setting up Ceramic Fuel Cells Ltd. as a spin-out from CSIRO in 1992. The 1960s also saw the start of work on alternative fuels, including hydrogen, for internal combustion engines led by Professor Harry C. Watson and colleagues from the University of Melbourne. During the last three decades of the 20th century, research within Australian universities and CSIRO on hydrogen energy and related technologies continued in a fragmented fashion.

In 2003 a National Hydrogen Study was carried out on behalf of the Department of Industry Tourism and Resources and with this a conference was held in Broome that proved to be something of a turning point for hydrogen energy in Australia. In response to renewed interest, a bid for hosting the 2008 World Hydrogen Energy Conference was presented to the IAHE in 2004 by the Australian Institute of Energy, and subsequently the 17th WHEC was held in Brisbane in June 2008. Also, stimulated by the National Hydrogen Study of 2003, the CSIRO set about bringing together various research players in the hydrogen energy space to create a critical mass of expertise. As a result of this, by end of 2006 a research cluster had become established known as the National Hydrogen Materials Alliance (NHMA). Interest has been maintained nationally and in 2009 a new Australian Association for Hydrogen Energy was established to serve as the peak body representing national interests in hydrogen and fuel cells liaising with various appropriate international bodies.

2 National Hydrogen Materials Alliance (NHMA)

The National Hydrogen Materials Alliance (NHMA) has been a cluster of twelve research groups from Australian universities and included the Australian Nuclear Science and Technology Organization (ANSTO), brought together by the CSIRO in 2006 to provide a framework for collaboration. The aim of the alliance was to tackle the major challenges in materials, in moving towards a hydrogen economy. These are associated with the safe and

* Corresponding author, email: andrew.dicks@qut.edu.au

economical production of clean renewable hydrogen, solid state storage of hydrogen especially for transport applications, and efficient cost-effective fuel cell systems for conversion of the chemical energy in hydrogen into electrical energy. A cash contribution from CSIRO of almost $3AUD million over a period of 2.5 years has leveraged in-kind contributions from all of the partners to provide some $10AUD million of investment in research. The alliance project partners contributed to a matrix of eight projects. One stream of projects was concerned with materials for hydrogen storage, based on light metals (lithium and magnesium), carbons and porous materials. The second stream was devoted to materials aspects of hydrogen production and utilisation. The projects on hydrogen production included one devoted to developing catalysts for the decomposition of hydrocarbons, a project on the integration of renewable energy sources (PV and wind) with electrolysers, and a project on the direct splitting of water with photocatalysts. A final project was concerned with materials for solid oxide fuel cells.

3 Research Outcomes of the NHMA

3.1 Hydrogen generation

In the near term it is widely held that hydrogen will be produced most economically from hydrocarbon fuels such as natural gas. Two significant developments in this area have been made by alliance researchers. The first is the synthesis of highly active catalyst based on supported nickel with addition of a Pt metal for steam reforming and partial oxidation. This has been demonstrated in a compact microchannel reactor, at significantly lower temperatures (650° C or below) than normally encountered. It may find application for solar reforming. The second is the development of metal/metal oxide catalysts for generation of pure hydrogen from natural gas without the need for complex processing. In this case, doped iron/iron oxide and tungsten/tungsten oxide have been found to work well [1]. In addition to the investigation of the new catalyst materials, progress has been made in developing a catalytic gasification process for dealing with solid fuels such as biomass.

Ultimately hydrogen will need to be generated from sustainable energy sources, either by electrolysis of water or directly to split water into its component hydrogen and oxygen by a direct photocatalytic process. Research in the alliance has focused on coupling photovoltaic panels or wind turbines directly with electrolysers in a highly efficient manner without the need of expensive DC-DC converter or maximum power point tracker technology [2]. In this context computer models have been developed for a proton exchange membrane electrolyser that can also function as a fuel cell. This unitized regenerative fuel cell model has been validated against experimental data in an internationally leading study [3].

Direct water splitting has been tackled by researchers in four institutions and has led to the development of testing protocols that are to be published in peer reviewed articles. World class facilities have been set up in Queensland to measure the effectiveness of photocatalysts for water splitting. Various photocatalyst materials have been evaluated including titania (TiO_2) and its variants such as $CaTiO_3$ [4], mesoporous iron oxide films, two multi-component systems - ZnO-ZnS composite system, and dye-sensitised polymeric spheres. Gradual improvements have been made in efficiency and cost reduction has been addressed. Through collaboration and exchanging of samples, the role of TiO_2 in water

splitting catalysts has been addressed by several research groups and a better understanding of the science of the materials has emerged.

3.2 Hydrogen storage materials

The development of materials for hydrogen storage is critically dependent on having access to reliable methods of measuring hydrogen uptake. For this reason, the researchers at Griffith University have constructed a variable volume manometric analyser, which will allow groups around the country to have access to a definitive unique world-class facility, enabling users to benchmark their research against other international groups. The analyser is the first phase of what is intended to be a National Hydrogen Materials Reference Facility**.**

Whilst some work was carried out on the storage of hydrogen in materials based on lithium [5], a much larger collaborative effort across seven universities has been devoted to magnesium materials. The R&D investigated cast materials as well as ball milled materials, including nanocomposites. The materials included $NaBH_4$-MgH_2, cast Mg-10%Ni alloys, Mg-$Ti_{0.4}Cr_{0.15}Mn_{0.15}V_{0.3}$, Mg-SiC-Ni, and Mg with various carbon additives. The main outcome from the research on Mg materials is that the kinetics of hydrogen desorption/absorption as well the amount of hydrogen stored in the alloys are highly dependent on the additives [6,7,8,9]. Theoretical modeling also proved to be useful in this work [10.11].

Hydrogen storage in carbon continues to be a controversial area of research. Microporous carbons prepared by a “one step” process and doped with transition metals all had high surface areas (>2000 m^2g^{-1}) and reasonable hydrogen storage capacities at low temperatures [12,13]. Doping of mesoporous carbons with nickel was found to increases storage capacity and in the case of multiwalled carbon nanotubes, storage capacity can also be improved by irradiation with gamma rays or microwaves, or by increasing defects by using high energy ball milling. Much higher storage capacities are however exhibited by carbon aerogels, with values of over 5 wt.% at 77K, depending on the method of activation.

From the work in the storage stream, it can be concluded that magnesium alloys continue to provide good prospects as practical hydrogen storage materials. It is too early to say whether porous materials or carbons are likely to fare any better, and further work would be worth pursuing in metal organic framework materials and in some classes of carbon materials, on the grounds that they may be more cost effective than magnesium alloys.

3.3 Hydrogen utilisation

One of the best ways of directly utilizing hydrogen is to convert the chemical energy in the hydrogen directly into electricity in a fuel cell. Fuel cell research is a very active field internationally and the project within the alliance has focused on one small area where maximum impact could be possible. This has concerned identifying new materials for solid oxide fuel cells (SOFCs) that can operate at much lower temperatures than the conventional natural gas fuelled systems. Lower temperature SOFCs are potentially more robust than the conventional high temperature SOFCs. Researchers at the University of Queensland have discovered 3 new materials systems in the La_2O_3-WO_3 system that with appropriate doping can produce a range of new ionic conductors that are comparable to the state-of-the-art Yttria Stabilised Zirconia (YSZ) [14]. This is a significant scientific advance that has opened new systems for consideration as ionic conductors. Tests have also shown that new ceramic

electronic conductors based on the TiO_2-Nb_2O_5-Cr_2O_3 system may also be useful as catalysts for the partial oxidation or steam reforming of methane that could be used internally within an SOFC. Again this is a significant advance that could be applied to SOFC developments world-wide.

It has become clear that the strategic support from CSIRO has resulted in the establishment of a critical mass of researchers covering a wide range of interests in hydrogen energy throughout Australia. By bringing the various groups together, the NHMA has achieved some clear technical advances in materials for hydrogen storage, catalysts for hydrogen generation, photocatalysts and in new materials for solid oxide fuel cells. More than 33 peer reviewed papers and over 30 conference papers have been published describing the outcomes of the NHMA, which has served to train 13 PhD students and several masters and undergraduate students.

4 Activities after the NHMA

Towards the end of 2008 the Department of Resources, Energy and Tourism (DRET) published a *National Hydrogen Technology Roadmap* that had been developed for the Council of Australian Governments (COAG). This presents a vision for hydrogen and fuel cells in Australia that: “By 2020 Australia is effectively exploiting emerging hydrogen and fuel cell market and supply chain opportunities, locally and globally” The Roadmap also identifies the potential role of Australian governments, industry and researchers and recommends strategies in the possible development of a hydrogen economy. A companion *Australian Hydrogen Activity 2008* complements the Roadmap by outlining Australian research projects related to hydrogen and fuel cells. Copies of both the roadmap and activity report can be obtained from the DRET and online at www.ret.gov.au/energy.

One of the recommendations of the *National Hydrogen Technology Roadmap* was to set up “an appropriately-funded and well-managed, industry-led national body for coordinated sector representation and promotion of the interests of hydrogen and fuel cell-related industry and professionals.” This recommendation has led to the formation of the Australian Association for Hydrogen Energy (AAHE), a non-profit company limited by guarantee and registered in 2009 for “the benefit of the Australian public, to advance the knowledge and understanding of production, storage, transport, safety, distribution and end use of hydrogen energy.” It is intended that the AAHE will also provide a forum for the dissemination of research results now that the NHMA has run its course. The new association will therefore be running workshops and seminars, and an annual national conference, as well as providing a source of information on hydrogen and fuel cell activities within Australia. The AAHE will also represent Australia at the international level, interfacing with organisations such as the International Energy Agency, Hydrogen Implementing Agreement, the Partnership for Advancing the Transition to Hydrogen, and the International Partnership for Hydrogen in the Economy.

More details of the Australian Association for Hydrogen Energy can be found at www.hydrogenaustralia.com.

References

[1] Sim, A.; Smith, A.J.; Cant, N.W.; Trimm, D.L.; 'Improved Steam-Iron Process', 17th World Hydrogen Energy Conference, 15-19 June 2008, Queensland, Australia

[2] Clarke, R.E., Giddey, S., Ciacchi, F.T., Badwal, S.P.S. (CSIRO Energy Technology), Paul, B., Andrews, J., 2009, "Direct coupling of an electrolyser integrated to a solar PV system for hydrogen generation", International Journal of Hydrogen Energy, 34, 2531-2542.

[3] A. Doddathimmaiah, J. Andrews, Theory, modelling and performance measurement of unitised regenerative fuel cells. International Journal of Hydrogen Energy, Volume 34, Issue 19, October 2009, Pages 8157-8170

[4] T Bak, T Burg, J Nowotny, PJ Blennerhassett, Electrical Conductivity and Thermoelectric Power of CaTiO3 at n-p Transition" Adv.Appl.Ceram., 106 (2007) 101-104

[5] J F Mao, X B Yu, Z P Guo, H K Liu, Z Wu , J Ni "Improvement of the LiAlH4-NaBH4 system for reversible hydrogen storage" J. Phys. Chem. C, 113 (2009) 10813

[6] A. Ranjbar, Z.P. Guo, X.B. Yu, D.Wexler, A. Calka, C.J. Kim, H.K. Liu,"Hydrogen storage properties of MgH2–SiC composites" Mater. Chem. and Phys., 114 (1) (2009) 168-172.

[7] J. F. Mao, X. B. Yu, Z. P. Guo, H. K. Liu, Z. Wu, J. Ni "Enhanced hydrogen storage performances of NaBH4-MgH2 system" J. Alloy Compd. 479 (2009) 619.

[8] H.B. Lu, C.K. Poh, L.C. Zhang, Z.P. Guo, X.B. Yu, H.K. Liu "Dehydrogenation characteristics of Ti- and Ni/Ti-catalyzed Mg hydrides" J. Alloy Compd. 481 (2009) 152.

[9] X. B. Yu, Y. H. Guo, Z. X. Yang, Z. P. Guo, H. K. Liu, S. X. Dou "Synthesis of catalyzed magnesium hydride with low absorption/desorption temperature", Scripta Materialia 61 (2009) 469–472.

[10] Gould, T., Gray, E., Dobson, J.F. "van der Waals dispersion power laws for cleavage, exfoliation and stretching in multi-scale, layered systems", Phys. Rev. B 79, 113402, (2009)

[11] Dobson, J.F., Gould, T., Klich, I. "Dispersion interaction between crossed conducting wires", John F. Dobson, Phys. Rev. A 80, 012506, (2009)

[12] H.Y. Tian, C.E. Buckley, S. Mulè, M. Paskevicius, B.B. Dhal."Preparation, microstructure and hydrogen sorption properties of nanoporous carbon aerogels under ambient drying." Nanotechnology, 19 (2008) 475605 1 - 7.

[13] H.Y. Tian, C.E. Buckley, S.B. Wang, M.F. Zhou"Enhanced hydrogen storage capacity in carbon aerogels treated with KOH.". Carbon, 47 (2009) 2128 – 2130.

[14] A Lashtabeg, J Bradley, A Dicks, G Auchterloni, J Drennan. Structural and conductivity studies of Y10_xLaxW2O21, Journal of Solid State Chemistry 183 (2010) 1095–1101

Energetic, Exergetic, Thermoeconomic and Environmental Analysis of Various Systems for the Cogeneration of Biogas Produced by an Urban Wastewater Treatment Plant UWTP. (1)

J.J. Coble, Industrial Engineering Department, Nebrija University, Spain
A. Contreras, Chemistry Department, Industrial Engineering College, Spain

Abstract

General awareness that the world's energy resources are limited has meant that it is increasingly important to examine energy-saving devices and fuels more closely, in order to use our limited available resources in a more sustainable manner. With this in mind, we studied biogas from a UWTP, because it is a renewable fuel with a neutral contribution to CO_2 emissions. We compared two technologies for using biogas as an energy source: cogeneration using either motor-generators or phosphoric acid fuel cells. The comparison was made from the energetic, exergetic, thermo-economic and environmental points of view, internalizing all the costs involved in each case. We used data supplied by the UWTP at the City of Madrid Plant Nursery, which uses motor-generators, and the UWTPs in Portland, Oregon, and in Red Hook, New York, which use a phosphoric acid fuel cell. The joint work carried out has been divided into three parts for publication purposes, and we present here the first of these, which refers to the energy analysis.

Keywords: Cogeneration, UWTP, motor-generators, fuel cell, energy analysis.

1 Introduction

Wastewater treatment plants require large quantities of both electricity and heat in order to function properly. Cogeneration systems are ideally suited to these requirements, as they enable two or more useable energies (such as heat, electricity, industrial cold, etc.), to be employed simultaneously, using a single primary source. By using residual heat produced during the electricity generation process, this type of system improves the efficiency of fuel consumption [1].

Not all cogeneration systems perform and behave in the same way on site. It is therefore essential to compare systems in order to choose the most appropriate one. However, comparison would be incomplete if it were done solely in energetic terms. We therefore propose a methodology that involves not only energetic, but also exergetic, thermo-economic and environmental comparisons, as each of these on its own will not provide an adequate assessment of the system studies. This has been proven with the use of phosphoric acid fuel cells.

2 The Cogeneration Systems that Were Compared

As mentioned above, the cogeneration systems that were compared were motor-generators with subsequent heat recovery in a boiler, against cogeneration in phosphoric acid fuel cells. In both cases, the fuel employed was the biogas produced by the wastewater treatment plant in the study.

Motor-generation with heat recovery is a cogeneration system that uses an internal combustion engine connected to an electrical power generator and with a waste heat boiler that uses the waste heat from the process to heat up water. These systems are in widespread use because of their cost-efficiency, mobility and performance. However, with these systems, it is important to check the effective advantage of using internal combustion, as well as the real operating and maintenance costs [2].

Phosphoric acid fuel cells systems are cogeneration devices that do not function like a heater, but instead like an electro-chemical device, and their performance is not limited by their Carnot performance. The efficiency of these devices can be far superior to that of motor-generators. They are the ideal systems for stationary applications using cogeneration, due to the high temperature of the electrolytic medium (120-200 ºC) [3].

The results on the energy features of these two cogeneration systems - motor-generators, and phosphoric acid fuel cells - are presented in this study.

3 Biogas

The amount of biogas that may be produced during the anaerobic digestion process can be estimated by relating it to the chemical oxygen demand (COD) of the water or mud to be treated, providing an estimated value of 0.35 m3 CH4/kg CDO eliminated. The importance of its value as fuel is reflected in its large lowest calorific output: around 6000 kcal/STPm3 for a biogas with a composition o f 70% CH4 and 30% CO2.

Table 1 shows the average volumetric composition of the biogas that was studied, in which the presence of ammonia can be seen to be practically insignificant. It has therefore not been taken into account in the subsequent stoichiometric calculations.

Table 1: Average volumetric composition of the studied biogas, in %.

VOLUMETRIC COMPOSITION OF THE BIOGAS (In %).			
$\%CH_4$	$\%CO_2$	$\%H_2S$	$\%NH_3$
65.32%	34.67%	< 0.003%	< 0.0001%

The apparent molecular weight of the biogas can be calculated on the basis of the above data and the molecular weight of each species, as can its apparent density, which has values of 32.61 kg/kmol and 1.14 kg/STPm^3, respectively.

Calculating the highest and lowest calorific output level of the biogas is fundamental in order to find out its energy content, either per cubic metre (measured under normal conditions), or per kilogramme, so as to measure its potential for use as energy. Using the appropriate calculation correlations, therefore, we obtained the results show in Table 2.

Table 2: Approximate highest and lowest calorific output of the biogas per $STPm^3$ or per Kg.

APPROXIMATE HIGHEST AND LOWEST CALORIFIC OUTPUT ($kJ/STPm^3$, $kcal/STPm^3$, kJ/kg y kcal/kg)
P.C.S. = 25984.36 $kJ/STPm^3$ = 6236.25 $kcal/STPm^3$
P.C.I. = 23344.90 $kJ/STPm^3$ = 5602.78 $kcal/STPm^3$
P.C.S. = 22640.40 kJ/kg = 5433.70 kcal/kg
P.C.I. = 20340.60 kJ/kg = 4881.74 kcal/kg

From the results obtained, we were able to see the potential for use as energy of the biogas produced at the UWTP. The basic energy parameters for the operation of the WTP are as follows:

$$\eta = \frac{\text{ELECTRIC ENERGY PRODUCED}}{\text{ELECTRIC ENERGY CONSUMED}} = \frac{5.720.000\ kWh}{19.843.000\ kWh} = 28{,}82\%$$

$$\frac{\text{ELECTRIC ENERGY CONSUMED}}{\text{per head}} = \frac{19.843.000\ kWh}{451.643\ \text{per head}} = 43{,}93\ kWh/\text{per head}$$

$$\frac{Biogas_{PRODUCED}}{\text{per head}} = \frac{3.984.000\ STPm^3}{451.643\ \text{per head}} = 8{,}821\ STPm^3/\text{per head}$$

$$\frac{\text{ELECTRIC ENERGY PRODUCED}}{\text{per head}} = \frac{5.720.000\ kWh}{451.643\ \text{per head}} = 12{,}66\ kWh/\text{per head}$$

4 Energy Comparison of Both Systems

In this study, we defined new ratios that make it easier to compare the two cogeneration systems studied.

The ratios were defined as follows:

- FPE (EOF) is the electric output factor, which is obtained by dividing the electicity produce dby teh biogas consumed.
- FPT (TOF) is the thermal output factor, which is obtained by dividing the thermal energy produced by the biogas consumed.
- CII (ICI) is the cost of installation in terms of the electrical kilowats installed, which is obtained by dividing the cost of the installation by the electical kilowats installed.
- CIP (ICP) is the cost of installation in terms of electrical kilowats produced, which is obtained by dividing the cost of the installation by the electical kilowats produced.

4.1 The cogeneration system using motor-generators

With the motor-generators, we had to calculate and analyse the system on the basis of the balance of mass and energy for reactive systems. We used the following equations for this purpose:

$$\frac{\dot{Q}_{VC}}{\dot{n}_C} - \frac{\dot{W}_{VC}}{\dot{n}_C} = \sum_P n_P \left(\bar{h}_f^o + \Delta\bar{h}\right)_P - \sum_R n_R \left(\bar{h}_f^o + \Delta\bar{h}\right)_R \quad (1)$$

$$\Delta\bar{h} = \bar{h}\,(T, P) - \bar{h}\,(T_{ref}\,, P_{ref}) \quad (2)$$

By applying these to the control volume selected for the motor-generator system, and taking into account the principal factor of excess air (n) used for combustion, we were able to obtain the results with the EES programme [4]. If we take the results that refer to 50% of excess air as a standard working measurement in motor-generators using biogas, and taking into account the financial costs of the cogeneration system shown in Table 3, the results are as follows:

Table 3: Basic parameters and installation and operational costs for the Municipal Plant Nursery UWTP's biogas cogeneration system.

COSTS OF THE COGENERATION SYSTEM USING MOTOR-GENERATORS	
Power (3 motor-generators, 455 kW each)	1,365 kW
Investment/kW	1,502.53 €/kW
Lifespan	20 years
Cost of investment	**2,050,953.45 €**
Annual operating costs	
Fuel	93,878.1 €
General operation and maintenance	20,000 €
Labour	54,000 €
Total cost (investment and first year of operation)	**2,218,831.55 €**

$$\mathbf{EOF} = \frac{\text{ELECTRIC ENERGY PRODUCED}}{\mathbf{Biogas_{CONSUMED}}} = \frac{\mathbf{5.720.000\ kWh}}{\mathbf{3.984.000\ STPm^3}} = \mathbf{1{,}435\ kWh/STPm^3\ Biogas}$$

$$\mathbf{TOF} = \frac{\text{THERMAL ENERGY PRODUCED}}{\mathbf{Biogas_{CONSUMED}}} = \frac{\mathbf{9.533.333{,}33\ kWh}}{\mathbf{3.984.000\ STPm^3}} = \mathbf{2{,}392\ kWh/STPm^3\ Biogas}$$

$$\mathbf{ICI} = \frac{\mathbf{System\ cost}}{\mathbf{kWe\ \ installed}} = \mathbf{1.502{,}53\ euros/kWe_{\ INSTALLED}}$$

$$\mathbf{ICP} = \frac{\mathbf{System\ cost}}{\mathbf{kWhe\ \ produced}} = \frac{\mathbf{2.050.953{,}45\ euros}}{\mathbf{5.720.000\ kWhe}} = \mathbf{0{,}3585\ euros/kWhe_{PRODUCED}}$$

4.2 The cogeneration system using phosphoric acid fuel cells

In this case, it was necessary to use the data from a Pure Cell ™ Model 200 (200kW) phosphoric acid fuel cell, fed with reformed biogas [5, 6]. The differences in compositon of the two biogases have been adjusted by modifying the input flow. The results obtained for calorific power, electrical power, emissions, etc., once these modifications had been made, are shown in Table 4.

Table 4: Electrical and calorific performance of the phosphoric acid fuel cell, based on the data from the PureCell™ Model 200 (200 kW).

TEST	TEST CONDITIONS	INPUT GAS FLOW (STP m^3/s)	INPUT CALORIFIC POWER (kW)	ELECTRICAL OUTPUT		CALORIFIC OUTPUT	
				ELECTRICITY (kWe)	EFFICIENCY (%)	HEAT (kWt)	EFFICIENCY (%)
1	200 kW required output	0.02366	524.88	193.1	36.79%	297.17	56.62%
2		0.02363	524.30	193.1	36.83%	294.24	56.12%
3		0.02360	523.71	193	36.85%	303.73	58.00%
AVERAGE VALUE		**0.02363**	**524.30**	**193.1**	**36.83%**	**315.95**	**60.26%**
4	150 kW required output	0.0180	399.74	152.3	38.10%	209.54	52.42%
5		0.0178	396.23	152.2	38.41%	202.21	51.04%
6		0.0179	398.57	152.3	38.21%	204.82	51.39%
AVERAGE VALUE		**0.01795**	**398.28**	**152.3**	**38.24%**	**205.23**	**51.53%**
7	100 kW required output	0.01198	265.87	101.5	38.18%	137.127	51.58%
8		0.01257	279.03	101.5	36.38%	151.194	54.19%
9		0.01221	270.91	101.5	37.47%	134.782	49.75%
AVERAGE VALUE		**0.01225**	**271.93**	**101.5**	**37.32%**	**140.644**	**51.72%**

The results for the parameters used in our comparison are as follows:

$$\mathbf{EOF} = \frac{\text{ELECTRIC ENERGY PRODUCED}}{\mathbf{Biogas_{CONSUMED}}} = \frac{\mathbf{5.867.400\ kWhe}}{\mathbf{2.496.256{,}4\ STPm^3}} = \mathbf{2{,}35\ kWh/STPm^3\ Biogas}$$

$$\mathbf{TOF} = \frac{\text{THERMAL ENERGY PRODUCED}}{\mathbf{Biogas_{CONSUMED}}} = \frac{\mathbf{9.533.333{,}33\ kWh}}{\mathbf{2.496.256{,}4\ STPm^3}} = \mathbf{3{,}82\ kWh/STPm^3\ Biogas}$$

$$\mathbf{ICI} = \frac{\mathbf{System\ cost}}{\mathbf{kWe\ \ installed}} = \mathbf{4.300\ euros/kWe_{\ INSTALLED}}$$

$$\mathbf{ICP} = \frac{\mathbf{System\ cost}}{\mathbf{kWhe\ \ produced}} = \frac{\mathbf{6.020.000\ euros}}{\mathbf{5.867.400\ kWhe}} = \mathbf{1{,}026\ euros/kWhe_{PRODUCED}}$$

It can be seen that FPE (EOF) is 61% greater in the fuel cell than in the motor-generator, and the FPT (TOF), is also 63% higher in the fuel cell. The set-up costs and one year of operation of this system are shown in Table 5.

Table 5: Basic parameters and installation and operating costs of the biogas cogeneration system using fuel cells.

COST OF THE COGENERATION SYSTEM USING FUEL CELLS	
Power (7 fuel cells, 200 kW each)	1,400 kW
Investment/kW	4,300 €/kW
Lifespan	20 years
Cost of investment	**6,020,000 €**
Annual operating costs	
Fuel	93,878.1 €
General operation and maintenance	12,512 €
Labour	54,000 €
Total cost (investment and first year of operation)	**6,180,390.1 €**

5 Conclusions

The energy analysis of the cogeneration systems studied has made it clear that the use of motor-generators is better suited in terms of installation costs and the first year of operation than phosphoric acid fuel cells. However, as we have already mentioned, this analysis alone is not enough to provide a realistic idea of each of the systems studied. It is therefore necessary to proceed with the energy, thermo-economic and environmental analyses, in order to get a precise idea of the behaviour of both these systems.

References

[1] Abusoglu. M. Kanoglu. Exergetic and thermo-economic analyses of diesel engine powered cogeneration: Part 1 – Formulations. Applied Thermal Engineering (2009). 29.(23). 234.241.

[2] G. Bidini. U. Desideri. S. Saetta. P.P. Bocchini. Internal combustion engine combined heat and power plants: case study of the University of Perugia Power Plant. Applied Thermal Engineering (1998). 18. 401-412.

[3] PureCellTM Model 200 power solution. www.utcpower.com.

[4] EES (Engineering Equation Solver). F-Chart Software. www.fchart.com.

[5] Greenhouse Gas Technology Center Southern Research Institute. EPA & New York State Energy Research and Development Authority (2004). “Environmental Technology Verification Report: Electric Power and Heat Generation Using UTC Fuel Cells´ PC25C Power Plant and Anaerobic Digester Gas”.

[6] Ott G. Sanger D. Tooze D. Hydrogen Fuel Cells: A solution for utilizing Waste Methane at Columbia Boulevard Wastewater Treatment Plant. Final Technical Report. Climate Change Fuel Cell Program (2000). City of Portland. Oregon.

Environmental Impact of Hydrogen Technologies

Ibrahim Dincer and T. Nejat Veziroglu

Abstract

This chapter discusses the role of hydrogen technologies as a potential solution for current and future environmental problems, and to provide a better environment and sustainable development. It also assesses the hydrogen production methods for sustainable hydrogen production by evaluating their greenhouse gas emissions and air pollutants. Two case studies are presented to discuss the environmental impact and energy utilization aspects, and to highlight the importance of the topic and show that these can help achieve a better environment and sustainability.

Atmospheric Consequences of the Perspective Use of Hydrogen in the European Transport Sector in 2050

C. Richter, **M. Schultz**, **S. Schröder**, Forschungszentrum Jülich, Jülich, Germany

1 Introduction

Hydrogen is the second most abundant oxidizable trace gas in the atmosphere. In the troposphere, the lowest part of the atmosphere reaching from the surface to about 10km height, hydrogen influences the concentration of the hydroxyl radical OH. This radical is the main oxidizing agent in the atmosphere and its concentration determines the lifetime (and thus the radiative forcing influence) of the greenhouse gas methane and it controls regional pollution levels downwind from emission sources. The concentration of OH is determined by a complex interplay of different chemical reactions of various air pollutants such as the mainly man made trace gases nitrogen oxides NO_x, carbon monoxide CO and the mainly biogenic volatile organic compounds VOCs.

Despite of this importance as an indirect greenhouse gas the tropospheric cycle of hydrogen is quite uncertain. Figure 1 shows the different source and sink terms and uncertainties following the review paper [1] for present day conditions. Future wide-spread use of hydrogen as energy carrier could lead to significant perturbations in the global atmospheric hydrogen budget and therefore influence the methane and air pollutant removal rate.

To assess the impact of a possibly emerging hydrogen economy on the atmospheric composition, not only the likely rise in hydrogen emissions has to be considered. Accompanying changes in NO_x and CO emissions due to enhanced needs for power generation on the one hand and reduced air pollution from the combustion of fossil fuels on the other hand must be treated as well. This is particularly important for the transition period where the economy of scale suggests that the required hydrogen will largely be produced by coal gasification and gas reforming.

The large-scale introduction of hydrogen as energy carrier necessitates the build-up of new infrastructures for production, transport, storage and distribution. Considering the costs of this build-up and the accompanying research and development expenses, in the beginning only highly developed countries can afford the introduction of H_2 into the energy sector. The largest potential for hydrogen use is generally seen in the sector of mobile applications, in particular as propellant in passenger cars, busses and light-duty freight vehicles [2]. In order to realistically assess the potential consequences of increased hydrogen use on the environment, plausible emission scenarios have to be developed based on realistic assumptions about the evolution of a hydrogen network and the technologies that will be applied in the hydrogen production and distribution chain (e.g. Hyways, 2006). In the paper at hand European traffic emission scenarios have been developed to assess the potential changes in atmospheric composition over the next decades. Simulations of the global atmospheric hydrogen budget were done with the global atmospheric chemistry and transport model ECHAM5-MOZ [3, 4].

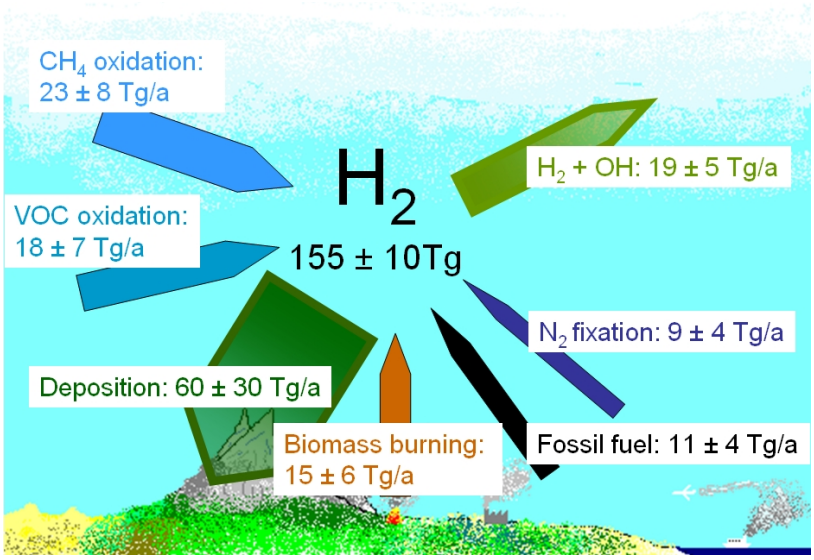

Figure 1: Tropospheric mass, sources, and sinks of H_2 at present.

A reference simulation was made for the years 2001-2008 to test the capability of the model to simulate global hydrogen concentrations and their observed seasonal cycle. The results were compared with available measurements of hydrogen and other trace gases as shown in Figure 2. At the left hand side time series of monthly means at Mace Head in Ireland are shown, at the right hand side the latitudinal gradient of annual means of the year 2003 is shown. The model (red squares) agrees with the observations within the measurement uncertainty, which is dominated by uncertainties in the instrument calibration [5]. The modeled hydrogen budget terms lie within the error margins given in [1]. ECHAM5-MOZ therefore can be said to be suitable for modelling the global hydrogen cycle.

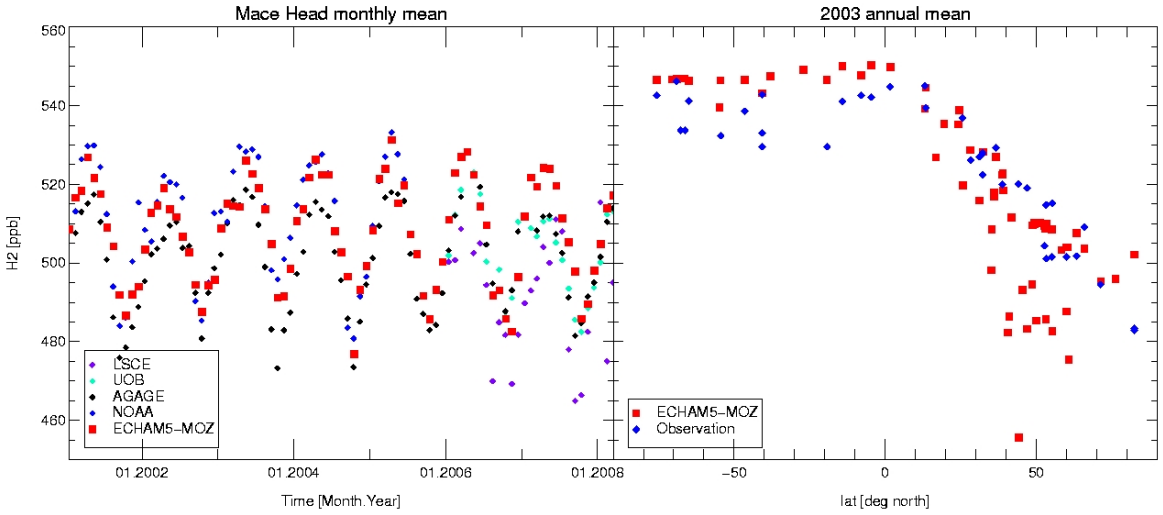

Figure 2: Observation vs. model hydrogen concentrations.

Two emission scenarios were developed based on the European HyWays project [1] and using extrapolated projections from the European Commission report "European Energy and

Transport -Trends to 2030" [6, 7]. The first is a business as usual (BAU) scenario, with fossil fuels remaining the main energy carrier till 2050. For simplicity we assume that no technological development takes place to reduce the average NO_x, CO and VOC emissions of the vehicle fleet. This scenario is compared to a hydrogen scenario (HY) where 50% of the traffic sector fossil fuel use in 2050 is replaced with hydrogen fuel cell cars which are free of air pollutant emissions. As a consequence, traffic emissions of trace gases other than hydrogen are half that of the BAU scenario. Conversely, country specific power plant emissions are scaled up to accommodate for the increased energy needs to produce the hydrogen. This scaling assumes that the primary energy mix will remain similar for each country. The potential fraction of “carbon-free” (i.e. wind, solar or nuclear) energy use for hydrogen production is taken into account. A high estimate of a 10% loss rate of hydrogen in the production, distribution and storage chain is used. This quite pessimistic (worst case) assumption was chosen to see a clear effect in the global hydrogen distribution. It should be noted however, that optimistic assumptions predict loss rates as low as 2% to be achievable [8] and leakage rates of about 3% can probably be assumed as realistic [9].

The European and global emissions of CO, H_2 and NO_x in the year 2000 are summarized in table 1 together with the emissions derived from the BAU and HY scenarios. The baseline emissions were taken from the RETRO inventory [10-13]. Transport (tra) and power generation (pow) are stated separately.

Table 1: Emissions of CO, H_2 and NO_x in the traffic and power generation section and in total given for the year 2000 RETRO inventory and the two year 2050 scenarios.

	CO [Tg/yr]			**H2 [Tg/yr]**			**NOx [Tg/yr]**		
	tra	pow	total	tra	pow	total	tra	pow	total
RETRO World	192	2,2	1026	5,8	0,1	29	31,8	26,7	132,0
RETRO 'EU'	22	0,3	39	0,66	0,01	1,13	6,7	3,6	15,9
BAU 'EU'	46	0,3	63	1,38	0,01	1,85	13,3	3,6	22,5
HY 'EU'	23	0,6	40	15,2	0,02	15,7	6,7	6,9	19,2

Compared to the year 2000 the transport emissions of all species in Europe will roughly double in the BAU scenario. The power generation emissions stay the same. In the HY scenario the traffic emissions of CO and NO_x nearly stay the same, but the power generation emissions of these species will rise by a factor of about two. The hydrogen transport emissions (all emissions of the hydrogen production, distribution and storage chain are attributed to this sector) will rise by a factor of 23 and will make up more than half of the today total global hydrogen emissions. Thus the European transport emissions will play an important role in the global hydrogen budget. This is also demonstrated in figure 3, where exemplarily the August monthly mean global hydrogen surface concentrations of the BAU (left side) and the HY scenario (right side) are shown. Although the additional H_2 emissions only take place in Europe, the surface concentration is elevated on the whole globe. As the amounts of NO_x and CO emissions do not change drastically the changes in the concentration patterns of this species remain locally in Europe. The highest changes (up to +20% and -15%) of the OH concentration also take place locally in Europe, accompanying

the NO_x and CO changes. In the “remote” regions away from Europe the elevated hydrogen lowers the OH concentration by about 1-3%.

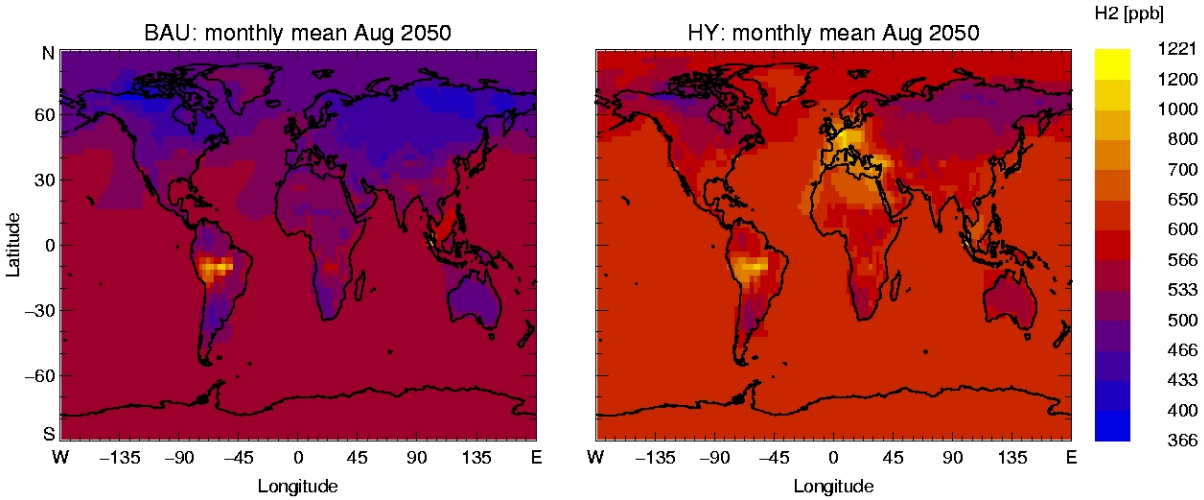

Figure 3: August monthly mean hydrogen surface concentration of the BAU and the HY scenario.

References

[1] D. H. Ehhalt and F. Rohrer. The tropospheric cycle of H_2: a critical review. Tellus B, 61(3):500{535, 2009.

[2] European Commission. HyWays - The European Hydrogen Roadmap. Luxembourg, 2008.

[3] E. Roeckner, G. Buml, L. Bonaventura, R. Brokopf, M. Esch, M. Giorgetta, S. Hagemann, I. Kirchner, L. Kornblueh, E. Manzini, A. Rhodin, U. Schlese, U. Schulzweida, and A. Tompkins. The atmospheric general circulation model ECHAM5, part I. Technical Report 349, Max Planck Institute for Meteorology, 2003.

[4] L.W. Horowitz, S. Walters, D.L. Mauzerall, L.K. Emmons, P.J. Rasch, C. Granier, X. Tie, J.-F. Lamarque, M.G. Schultz, G.S. Tyndall, J.J. Orlando, and G.P. Brasseur. A global simulation of tropospheric ozone and related tracers: Description and evaluation of MOZART, version 2. Journal of Geophysical Research, 108(D24):4784, 2003.

[5] A. Jordan. Calibration of Atmospheric Hydrogen. In: Proceedings of the 14th WMO/IAEA Meeting of Experts on Carbon Dioxide, Other Greenhouse Gases, and Related Tracer Measurement Techniques, Helsinki, Sept. 2007. WMO-GAW Report, 186. WMO-GAW, Helsinki. pp. 21-25, 2009.

[6] L. Mantzos, P. Capros, N. Kouvaritakis, and M. ZekaPaschou. European energy and transport trends to 2030, 2003.

[7] P. Capros, L. Mantzos, V. Papandreou, and N. Tasios. European Energy and Transport Trends to 2030 - Update 2007. European Communities, 2008.

[8] T. Feck. Wasserstoff-Emissionen und ihre Auswirkungen auf den arktischen Ozonverlust. Forschungszentrum Jülich GmbH, Zentralbibliothek, Verlag, 2009.

[9] M.G. Schultz, T. Diehl, G.P. Brasseur, and W. Zittel. Air pollution and climate-forcing impacts of a global hydrogen economy. Science, 302(5645):624{627, 2003.

[10] T. Pulles, M. van het Bolscher, R. Brand, and A. Visschedijk. Assessment of global emissions from fuel combustion in the final decades of the 20th century - application of the emission inventory model TEAM. TNO Built Environment and Geoscience, 2007-A-R0132/B, 2007.

[11] Ø. Endresen, E. Sørgård, J.K. Sundet, S.B. Dalsøren, I.S.A. Isaksen, T.F. Berglen, and G. Gravir. Emission from international sea transportation and environmental impact. J. Geophys. Res., 108(17), 2003.

[12] V. Grewe, M. Dameris, C. Fichter, and R. Sausen. Impact of aircraft nox emissions. part 1: Interactively coupled climate-chemistry simulations and sensitivities to climate-chemistry feedback, lightning and model resolution. Meteorologische Zeitschrift, 11(3):177-186, 2002.

[13] M.G. Schultz, A. Heil, J.J. Hoelzemann, A. Spessa, K. Thonicke, J.G. Goldammer, A.C. Held, J.M.C. Pereira, and M. van het Bolscher. Global wildland fire emissions from 1960 to 2000. Global Biogeochem. Cycles, 22, 2008.

Economics and Synergies of Electrolytic and Thermochemical Methods of Environmentally Benign Hydrogen Production

G. F. Naterer, University of Ontario Institute of Technology, Canada

Abstract

Most of the world's hydrogen (about 97%) is currently derived from fossil fuels. For reduction of greenhouse gases, improvement of urban air quality, and energy security, among other reasons, carbon-free sources of hydrogen production are crucial to hydrogen becoming a significant energy carrier. Nuclear hydrogen production is a promising carbon-free alternative for large-scale, low-cost production of hydrogen in the future. Two nuclear technologies, applied in tandem, have a promising potential to generate hydrogen economically without leading to greenhouse gas emissions: 1) electrolysis and 2) thermochemical decomposition of water. This paper will investigate their unique complementary roles and economics of producing hydrogen, from a Canadian perspective. Together they can serve a unique potential for both de-centralized hydrogen needs in periods of low-demand electricity, and centralized base-load production from a nuclear station. Hydrogen production has a significantly higher thermal efficiency, but electrolysis can take advantage of low electricity prices during off-peak hours. By effectively linking these systems, water-based production of hydrogen can become more competitive against the predominant existing technology, SMR (steam-methane reforming).

1 Introduction

This paper examines the synergistic roles of electrolysis and thermochemical water decomposition, which together can provide a lower-cost sustainable supply of hydrogen than current technologies. In particular, thermochemical water decomposition, driven by nuclear heat with a copper-chlorine (Cu-Cl) cycle, splits water into hydrogen and oxygen through intermediate copper and chlorine compounds (Serban, Lewis, Basco; [1, 2], Naterer et al. [3 - 5]). Unlike other sustainable energy resources (e.g., solar, wind), nuclear heat used in this thermochemical cycle enables large-scale direct production of hydrogen. A Cu-Cl plant could be eventually linked with nuclear reactors to achieve higher efficiencies of hydrogen production than any other conventional technology. Recent advances in a hybrid Cu-Cl cycle linked with Canada's nuclear reactors were presented by Suppiah et al. [6].

Much effort internationally is being focused on the Sulfur-Iodine (S-I) cycle and its variations, as well as High-Temperature Electrolysis (HTE) for nuclear-based hydrogen production. The copper-chlorine (Cu-Cl) cycle offers a number of advantages over the S-I cycle, including lower operating temperatures, capability of utilizing low-grade waste heat from nuclear reactors and lower-cost materials. This paper examines the additional benefits of integrating electrolysis and thermochemical hydrogen production, due to their unique advantages of de-centralized off-peak and centralized base-load production, respectively, to reduce costs and

become more competitive against the predominant existing technology, SMR (steam-methane reforming).

2 Hydrogen Costs by Electrolysis

A case study of distributed hydrogen production by electrolysis was examined by Miller [7, 8] for hydrogen vehicles supplied by neighbourhood fueling stations. Costs were reported in 2002 US dollars, assuming a 15%/year return on investment and a 10-year amortization, which is approximately equivalent to an annual capital charge of 20%. A production cost of $300 /kW for the electrolysis cells was assumed, along with storage costs of $800,000 /tonne of hydrogen via tube storage.

The parameters of the case study are 600,000 vehicles that are fueled by hydrogen produced from a medium sized nuclear reactor (700 MW), which requires about 56 kWh per kilogram of hydrogen from electrolysis. The energy content of hydrogen is about three times higher than gasoline, weight for weight, and the conversion efficiency of a fuel cell versus ICE is about 2 to 2.5 times better. This implies an overall hydrogen to gasoline weight ratio of about 6 to 7.5. A typical fill-up scenario for a gasoline vehicle is 40 L (30 kg), equivalent to 3 kg of hydrogen, stored in 700-atmosphere aluminum carbon-fibre reinforced cylinders, occupying about 80 L. Given this fuel requirement and number of vehicles, the required supply of hydrogen can be determined, after which the continuous electrolysis supply becomes known. If off-peak electricity is used instead for electrolysis, then a threshold price is established, wherein hydrogen is only produced below the threshold. When this threshold price is lowered, more capacity of electrolysis is needed to produce a given quantity of hydrogen over a shorter duration. Also, more storage capacity is needed, due to longer periods without generation of hydrogen.

For a given threshold price, a larger electrolysis capacity implies less storage is needed to meet peak demand, but there is more expensive capacity of installed units and higher hydrogen cost. Conversely, less installation capacity requires more storage hours and higher storage costs. This again indicates an optimum exists at a particular electrolysis installation capacity, above which the price becomes excessive, per kg of hydrogen produced.

3 Hydrogen Costs with the Copper-Chlorine (Cu-Cl) Cycle

The Cu-Cl thermochemical cycle uses a series of reactions to achieve the overall splitting of water into hydrogen and oxygen. The chemical reactions form a closed internal loop that re-cycles all chemicals on a continuous basis, without emitting any greenhouse gases externally to the atmosphere.

Recent studies at the Argonne National Laboratory [9] quoted an approximate capital cost of $124M for a Cu-Cl plant that produces 125 tonnes/day of hydrogen. Using the power law for the capital cost of a chemical plant that varies with size raised to about the 0.66 power, to scale down the plant capacity to 10 tonnes/day, the capital cost becomes about $29M. This represents a future cost in 2015, when the current status of Cu-Cl technology can be scaled up to a pilot plant capacity. For consistency with past reported data for electrolysis [7, 8], the capital cost will be discounted back in time to account for 3% inflationary price changes over a decade. Multiplying the resulting capital cost by 20% for the annual capital charge, dividing

by the plant size (in tonnes per day), times 142 GJ /tonne and 365 days per year, yields a contribution of $7.7 /GJ for the capital portion of the hydrogen cost.

The cost of energy input for the thermochemical plant is heat from nuclear or other sources. Consider the following two approaches for this cost estimation. The first option uses natural gas for the high-temperature heat requirement of the Cu-Cl cycle, consuming about 40% of the net cycle heat input. Then using the previously quoted natural gas cost of 5$ /GJ, dividing by the cycle efficiency of 43%, multiplying by the high-grade heat portion, and finally adding the previously quoted distribution fee for natural gas, yields an energy cost of about 6.3$ /GJ. In practice, utilizing waste heat can raise the cycle's efficiency, and improving the internal re-cycling of heat can further reduce the high-grade heat requirement, both of which would lead to lower energy costs.

Unlike de-centralized electrolysis without distribution costs (hydrogen is generated locally at fueling stations), hydrogen needs to be transported from a centralized Cu-Cl plant to the fueling stations. Costs of truck transportation operating with compressed gas by tube trailer are about 4.6$ /GJ, for distances of about 16 km. Herein lies a key synergy between off-peak electrolysis and thermochemical production of hydrogen. The trucking costs rise with distance from the Cu-Cl plant, so thermochemical production is competitive in the vicinity of large cities, but de-centralized electrolysis (without transportation costs) has lower costs farther away in surrounding towns. In this way, electrolysis and thermochemical production have synergistic roles with each other, similarly to centralized base-load electricity with nuclear power, together with de-centralized supply from wind or solar power.

Alternatively, hydrogen can be distributed within a city by pipeline. However, these costs become higher and pipelines only become competitive when the demand grows to large capacities. The pipeline option can eventually carry much higher capacities of hydrogen at no additional cost. So there is an inversely proportional decrease in unit cost for higher capacities of hydrogen. Similar economic tradeoffs exist between electrolysis and thermochemical production with pipeline transportation. Shorter pipelines are needed between fueling stations in cities, whereas de-centralized electrolysis becomes more economically attractive in surrounding towns, since more expensive piping networks of hydrogen raise the costs of hydrogen.

4 Results and Discussion

This section will present results to demonstrate the synergistic roles of off-peak electrolysis and thermochemical production of hydrogen. The different methods have a unique potential to serve both de-centralized needs in off-peak hours, and centralized base-load production from a nuclear station, respectively. Thermochemical methods have significantly higher thermal efficiency, but electrolysis can take advantage of low electricity prices during off-peak hours, as well as intermittent and de-centralized supplies of electricity like wind, solar or tidal power. By effectively linking these systems, water-based production of hydrogen can become more competitive against the predominant existing technology, SMR (steam-methane reforming).

Figure 1 shows that thermochemical production becomes more competitive at larger capacities of hydrogen production. Below capacities of between about 10-20 tonnes/day,

electrolysis from off-peak electricity has a lower unit cost of hydrogen production, although the advantage reverses at higher capacities. Furthermore, electrolysis costs have taken advantage of off-peak electricity, so an analogous benefit could be realized with a Cu-Cl cycle linked with SCWR. For example, a certain base-load production of hydrogen can be maintained with SCWR, but a bypass heat exchanger could re-direct steam from the power turbine to the Cu-Cl plant during off-peak periods of low electricity demand. Discounting the energy cost by an equivalent amount as the off-peak electrolysis, a further potential cost reduction of $2.8 /GJ is illustrated in Figure 1. The legend shows ">$2.8 /GJ" because further discounts can be realized at a lower price threshold of off-peak electricity, although the corresponding storage costs rise. Various uncertainties, idealizations and simplified underlying assumptions have been used in this cost analysis, so the results are intended more to provide qualitative trends, rather than precise costs. A key result is the predicted cross-over point between electrolysis and thermochemical production, at about 10-20 tonnes/day. The emerging hydrogen economy will have many needs for both lower and higher capacities, so electrolysis and thermochemical methods will remain complementary to each other.

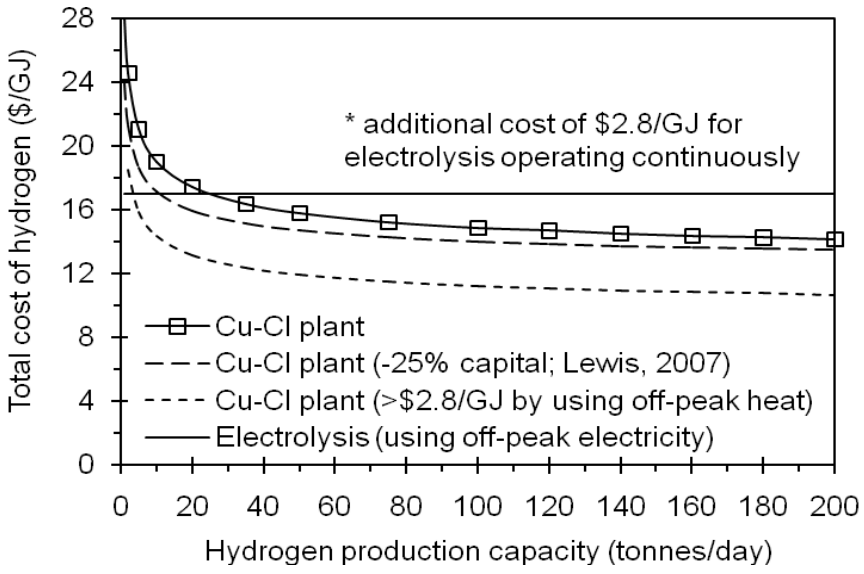

Figure 1: Comparison between electrolysis and thermochemical production methods.

5 Conclusions

This paper has examined the potential of electrolysis and thermochemical hydrogen production to serve both de-centralized needs with production during off-peak hours, and centralized base-load production from a nuclear station, respectively. Thermochemical methods have significantly higher thermal efficiency, but electrolysis can take advantage of low electricity prices during off-peak hours, local use of byproducts of heat and oxygen, as well as intermittent and de-centralized supplies of electricity like wind, solar or tidal power. By

effectively linking these systems, production of hydrogen from nuclear and/or renewable energy can become more competitive against the predominant existing technology, SMR.

Acknowledgements

Support of this research from Atomic Energy of Canada Limited, Ontario Research Fund and the Natural Sciences and Research Council of Canada (NSERC) is gratefully acknowledged.

References

[1] Serban, M., Lewis, M., Basco, J., “Kinetic Study of the Hydrogen and Oxygen Production Reactions in the Copper-Chloride Thermochemical Cycle”, AIChE 2004 Spring National Meeting, New Orleans, LA, April 25-29, 2004

[2] Lewis, M. A., Masin, J. G., Vilim, R. B., Serban, M., “Development of the Low Temperature Cu-Cl Thermochemical Cycle”, International Congress on Advances in Nuclear Power Plants, May 15 - 19, 2005, Seoul, Korea

[3] Naterer, G. F., Gabriel, K., Wang, Z., Daggupati, V., Gravelsins, “Thermochemical Hydrogen Production with a Copper-Chlorine Cycle, I: Oxygen Release from Copper Oxychloride Decomposition” (in press), International Journal of Hydrogen Energy, 2008

[4] Naterer, G. F., Daggupati, V., Marin, G., Gabriel, K., Wang, Z., “Thermochemical Hydrogen Production with a Copper-Chlorine Cycle, II: Flashing and Drying of Aqueous Cupric Chloride" (in press), International Journal of Hydrogen Energy, 2008

[5] Wang, Z., Naterer, G. F., Gabriel, K., “Multiphase Reactor Scale-up for Cu-Cl Thermochemical Hydrogen Production” (in press), International Journal of Hydrogen Energy, 2008

[6] Suppiah, S., Li., J., Sadhankar, R., Kutchcoskie, K. J., “Study of the Hybrid Cu-Cl Cycle for Nuclear Hydrogen Production”, Proceedings of the EIC Climate Change Technology Conference, pp. 231 – 238, Ottawa, Ontario, 2006

[7] Miller, A. J., Duffey, R. B., “Sustainable and Economic Hydrogen Co-generation from Nuclear Energy in Competitive Power Markets”, International Energy Workshop, Laxenburg, Austria, June 24 – 26, 2003

[8] Miller, A. I., “Electrochemical Production of Hydrogen by Nuclear Energy”, Nuclear Production of Hydrogen - Technologies and Perspectives for Global Deployment, Chapter 4, American Nuclear Society, La Grange Park, Illinois, 2004

[9] Lewis, M. A., “Recent Advances in Cu-Cl Cycle Research and Development”, ORF Nuclear Hydrogen Workshop, Oshawa, Ontario, Canada, December 20, 2007

Impact of H_2 Emissions of a Global Hydrogen Economy on the Stratosphere

Jens-Uwe Grooß, **Thomas Feck**, **Bärbel Vogel**, **Martin Riese**, Forschungszentrum Jülich GmbH, Germany

"Green" hydrogen is seen as a major element of the future energy supply to reduce greenhouse gas emissions substantially. However, due to the possible interactions of hydrogen (H_2) with other atmospheric constituents there is a need to analyse the implications of additional atmospheric H_2 that could result from hydrogen leakage of a global hydrogen infrastructure. Emissions of molecular H_2 can occur along the whole hydrogen process chain which increases the tropospheric H_2 burden. The impact of these emissions is inverstigated.

Figure 1 is a sketch that clarifies the path way and impact of hydrogen in the stratosphere. The air follows the Brewer-Dobson circulation in which air enters the stratosphere through the tropical tropopause, ascends then to the upper stratosphere and finally descends in polar latitudes within a typical transport time frame of 4 to 8 years.

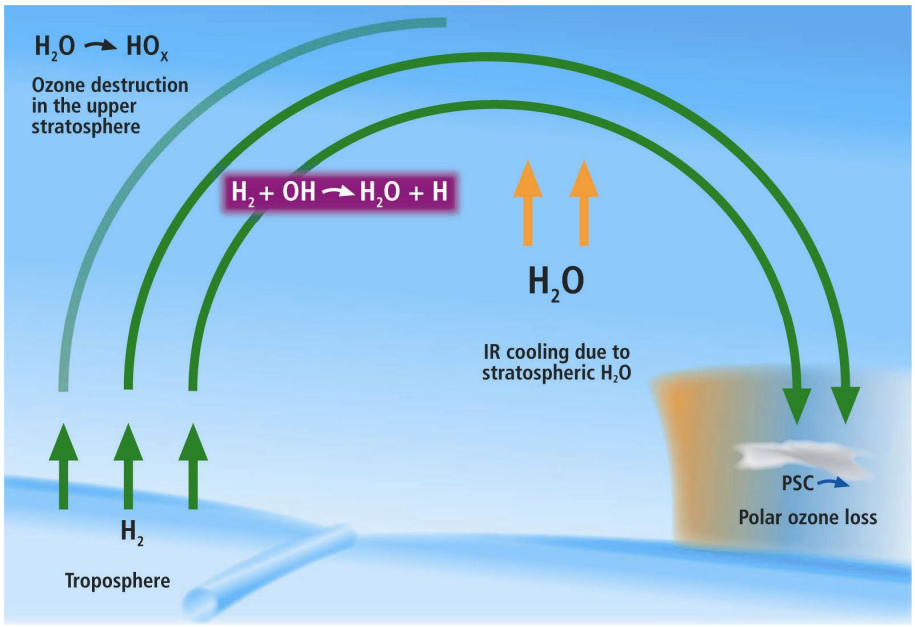

Figure 1: Impact of H_2 in the stratosphere.

Along this pathway, hydrogen is oxidised to form water vapour. As stratospheric air is typically very dry, any additional hydrogen release results in an increase of stratospheric water vapour. The impact on ozone is three-fold:

1. an increased production of HO_x radicals OH and HO_2 from H_2O that contribute to gas-phase ozone depletion

2. an increased heterogeneous reactivity of polar stratospheric particles (liquid sulfate aerosol and Polar Stratospheric Clouds, PSCs) responsible for chlorine activation and subsequent ozone loss
3. an increased infrared cooling of the stratosphere due to rising infrared emissions leading to an enhanced presence of PSCs

While (1) can be neglected, the effects (2) and (3) are important and may lead to additional polar ozone depletion. Hence a global hydrogen economy could potentially provoke polar ozone loss and could lead to a substantial delay of the current projected recovery of the stratospheric ozone layer.

In 2003, Tromp et al. published a simulation study indicating a significant reduction of stratospheric ozone due to emissions by leakages of a potential future H_2 economy, mainly by effect (2) and (3) mentioned above. This study was heavily criticised because of unrealistically high estimation of the overall hydrogen emission rate (20%) and because of inconsistencies of model parameters [1-3].

Investigations of the complete process chain and estimates of future trends in hydrogen technologies show that the expected loss rates of 2% and below are technically feasible [4, 5] For comparison, current emissions of natural gas are estimated to be between 0.5 and 1.8% throughout the production chain [6-8].

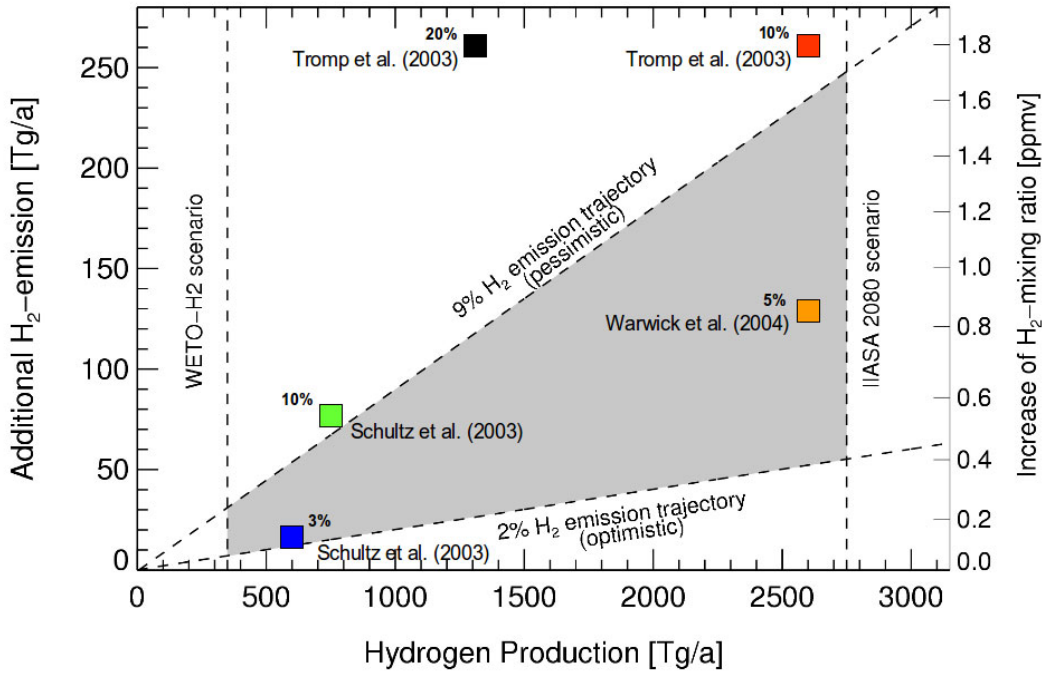

Figure 2: Projected hydrogen production and emissions.

Figure 2 shows the range of projected hydrogen production rates bracketed by the WETO-H_2 and the IIASA-2080 scenarios [9, 10]. Corresponding emissions by leakages are shown on the ordinate. The realistic range is indicated by the grey shaded area. Also shown are the assumptions made in the earlier studies by Tromp et al. [11], Warwick et al. [12], and Schultz

et al. [13]. The second ordinate shows the corresponding estimated tropospheric hydrogen increase. For the atmosphere, only the hydrogen emissions and not the global production rates are relevant.

As the impact of additional hydrogen emissions is rather small, we used methods designed such that the resulting effect would not be hidden within the natural variability.

Simulations of the Chemical Lagrangian Model of the Stratosphere (CLaMS) [14] were used to investigate the impact of H_2 emissions on the stratosphere. First, the H_2 oxidation and the corresponding water vapour increase along the Brewer-Dobson circulation is simulated in a box model mode of CLaMS. The results of these simulations were used to analyse the impact of possible H_2 emissions on stratospheric polar ozone in two complementary methods.

The first method is an estimation utilizing the fact that a tight linear correlation between derived chemical ozone loss and temperature-threshold based proxies V_{psc} and V_{ACl} has been found [15-17]. We investigated how these two proxies would change with increasing water vapour and with decreasing temperatures. This change was then translated into additional ozone depletion. From this analysis it was found that the largest effect of additional hydrogen emissions would occur for the coldest stratospheric Arctic winters. The complementary second method was to run a set of simulations with the full 3-dimensional Chemical Transport Model (CTM) CLaMS [14, 18] on the identical meteorology with the exception that the water vapour was varied corresponding to the hydrogen emission assumptions [19].

Even under extreme assumptions, i.e. a replacement of 90% of the current global fossil primary energy input replaced by hydrogen, a leakage rate of approximately 10% of the product gas into the atmosphere, and no reductions of current stratospheric CFC levels (that should decrease due to the regulations of the Montreal Protocol), the results of both methods show only very moderate increase of polar stratospheric ozone depletion due to the additional hydrogen emissions. Hence the risk of a substantial damage to the stratospheric ozone layer due to hydrogen emissions of a hydrogen economy is very low compared to the positive climate implications that would evolve from the avoidance of greenhouse gas emissions.

References

[1] Jaffe, S.: Hydrogen report is full of hot air, The Scientist, 17, 2003.

[2] Kammen, D. M. and Lipman, T. E.: Assessing the Future Hydrogen Economy, Science, 302, 226–229, 2003.

[3] Prather, J. M.: An Environmental Experiment with H2?, Science, 302, 581–582, 2003.

[4] Feck, T.: Wasserstoff-Emissionen und ihre Auswirkungen auf den arktischen Ozonverlust, Risikoanalyse einer globalen Wassterstoffwirtschaft, Schriften des Forschungszentrums Jülich, Energy & Environment, Vol. 51, ISBN 978 – 3 – 89336 - 593-7, 2009.

[5] Bond, S.W., M. K. Vollmer, M. Steinbacher, S. Reimann, and B. Buchmann, H2 in the atmosphere – an integration from the exhaust pipe to a remote alpine site ,

Geophysical Research Abstracts, Vol. 11, EGU2009-1813, EGU General Assembly, 2009.

[6] Dedikov, J. V., Akopova, G. S., Gladkaja, N. G., Piotrovskij, A. S., Markellov, V. A., Salichov, S. S., Kaesler, H., Ramm, A., von Blumencronb, A. M., and Lelieveld, J.: Estimating methane releases from natural gas production and transmission in Russia, Atmospheric Environment, 33, 3291–3299, 1999.

[7] Oonk, J. and Vosbeek, M.: Methane emissions due to oil and natural gas operations in the Netherlands, TNO-MEP, Apeldoorn (The Netherlands), TNO report no. R95/168, 1995.

[8] Zittel,W.: Untersuchungen zum Kenntnisstand über Methanemissionen beim Export von Erdgas aus Russland nach Deutschland, available at http://www.lbst.de, 1997.

[9] EC: World Energy Technology Outlook 2050 - WETO-H2. European Commission, DG Research, Luxembourg, 2006.

[10] Baretto, L., Makihira, A. und Riahi, K.: The hydrogen economy in the 21st century: a sustainable development scenario, International Journal of Hydrogen Energy, Vol. 28:S. 267–284, 2003.

[11] Tromp, T. K., Shia, R.-L., Allen, M., Eiler, J. M., and Yung, Y. L.: Potential Environmental Impact of a Hydrogen Economy on the Stratosphere, Science, 300, 1740–1742, 2003.

[12] Warwick, N., Bekki, S., Nisbet, E., and Pyle, J. A.: Impact of a hydrogen economy on the stratosphere and troposphere studied in a 2D model, Geophys. Res. Lett., 31, 2004.

[13] Schultz, M. G., Diehl, T., Brasseur, G. P., and Zittel, W.: Air Pollution and Climate-Forcing Impacts of a Global Hydrogen Economy, Science, 302, 624–627, 2003.

[14] McKenna, D. S., Grooß, J.-U., Günther, G., Konopka, P., Müller, R., Carver, G., and Sasano, Y.: A new Chemical Lagrangian Model of the Stratosphere (CLaMS): 2. Formulation of chemistry scheme and initialization, J. Geophys. Res., 107, 4256, doi:10.1029/2000JD000113, 2002.

[15] Rex, M., Salawitch, R. J., von der Gathen, P., Harris, N. R., Chipperfield, M. P., and Naujokat, B.: Arctic ozone loss and climate change, Geophys. Res. Lett., 31, 2004.

[16] Drdla, K. and Müller, R.: Temperature thresholds for polar stratospheric ozone loss, Atmos. Chem. Phys., in preparation, 2010.

[17] Tilmes, S., Müller, R., and Salawitch, R.: The Sensitivity of Polar Ozone Depletion to Proposed Geoengineering Schemes, Science, 320, 1201–1204, 2008.

[18] Grooß, J.-U. and Müller, R.: Simulation of ozone loss in Arctic winter 2004/2005, Geophys. Res. Lett., 34, doi:10.1029/2006GL028901, 2007.

[19] Vogel, B., Feck, T., and Grooß, J.-U.: Impact of stratospheric water vapor increase on polar ozone loss, J. Geophys. Res., submitted, 2010.

[20] Drdla, K.: Temperature thresholds for polar stratospheric ozone loss, AGU Fall 2005 Meeting, A31D-03, 2005.

[21] Feck, T., Grooß, J.-U., and Riese, M.: Sensitivity of Arctic ozone loss to stratospheric H2O, Geophys. Res. Lett., 35, doi:10.1029/2007GL031334, 2008.

1. **Einsatz von multispektralen Satellitenbilddaten in der Wasserhaushalts- und Stoffstrommodellierung – dargestellt am Beispiel des Rureinzugsgebietes**
von C. Montzka (2008), XX, 238 Seiten
ISBN: 978-3-89336-508-1

2. **Ozone Production in the Atmosphere Simulation Chamber SAPHIR**
by C. A. Richter (2008), XIV, 147 pages
ISBN: 978-3-89336-513-5

3. **Entwicklung neuer Schutz- und Kontaktierungsschichten für Hochtemperatur-Brennstoffzellen**
von T. Kiefer (2008), 138 Seiten
ISBN: 978-3-89336-514-2

4. **Optimierung der Reflektivität keramischer Wärmedämmschichten aus Yttrium-teilstabilisiertem Zirkoniumdioxid für den Einsatz auf metallischen Komponenten in Gasturbinen**
von A. Stuke (2008), X, 201 Seiten
ISBN: 978-3-89336-515-9

5. **Lichtstreuende Oberflächen, Schichten und Schichtsysteme zur Verbesserung der Lichteinkopplung in Silizium-Dünnschichtsolarzellen**
von M. Berginski (2008), XV, 171 Seiten
ISBN: 978-3-89336-516-6

6. **Politikszenarien für den Klimaschutz IV – Szenarien bis 2030**
hrsg.von P. Markewitz, F. Chr. Matthes (2008), 376 Seiten
ISBN 978-3-89336-518-0

7. **Untersuchungen zum Verschmutzungsverhalten rheinischer Braunkohlen in Kohledampferzeugern**
von A. Schlüter (2008), 164 Seiten
ISBN 978-3-89336-524-1

8. **Inorganic Microporous Membranes for Gas Separation in Fossil Fuel Power Plants**
by G. van der Donk (2008), VI, 120 pages
ISBN: 978-3-89336-525-8

9. **Sinterung von Zirkoniumdioxid-Elektrolyten im Mehrlagenverbund der oxidkeramischen Brennstoffzelle (SOFC)**
von R. Mücke (2008), VI, 165 Seiten
ISBN: 978-3-89336-529-6

10. **Safety Considerations on Liquid Hydrogen**
by K. Verfondern (2008), VIII, 167 pages
ISBN: 978-3-89336-530-2

11. **Kerosinreformierung für Luftfahrtanwendungen**
    von R. C. Samsun (2008), VII, 218 Seiten
    ISBN: 978-3-89336-531-9

12. **Der 4. Deutsche Wasserstoff Congress 2008 – Tagungsband**
    hrsg. von D. Stolten, B. Emonts, Th. Grube (2008), 269 Seiten
    ISBN: 978-3-89336-533-3

13. **Organic matter in Late Devonian sediments as an indicator for environmental changes**
    by M. Kloppisch (2008), XII, 188 pages
    ISBN: 978-3-89336-534-0

14. **Entschwefelung von Mitteldestillaten für die Anwendung in mobilen Brennstoffzellen-Systemen**
    von J. Latz (2008), XII, 215 Seiten
    ISBN: 978-3-89336-535-7

15. **RED-IMPACT**
    Impact of Partitioning, Transmutation and Waste Reduction Technologies on the Final Nuclear Waste Disposal
    SYNTHESIS REPORT
    ed. by W. von Lensa, R. Nabbi, M. Rossbach (2008), 178 pages
    ISBN 978-3-89336-538-8

16. **Ferritic Steel Interconnectors and their Interactions with Ni Base Anodes in Solid Oxide Fuel Cells (SOFC)**
    by J. H. Froitzheim (2008), 169 pages
    ISBN: 978-3-89336-540-1

17. **Integrated Modelling of Nutrients in Selected River Basins of Turkey**
    Results of a bilateral German-Turkish Research Project
    project coord. M. Karpuzcu, F. Wendland (2008), XVI, 183 pages
    ISBN: 978-3-89336-541-8

18. **Isotopengeochemische Studien zur klimatischen Ausprägung der Jüngeren Dryas in terrestrischen Archiven Eurasiens**
    von J. Parplies (2008), XI, 155 Seiten, Anh.
    ISBN: 978-3-89336-542-5

19. **Untersuchungen zur Klimavariabilität auf dem Tibetischen Plateau - Ein Beitrag auf der Basis stabiler Kohlenstoff- und Sauerstoffisotope in Jahrringen von Bäumen waldgrenznaher Standorte**
    von J. Griessinger (2008), XIII, 172 Seiten
    ISBN: 978-3-89336-544-9

20. **Neutron-Irradiation + Helium Hardening & Embrittlement Modeling of 9%Cr-Steels in an Engineering Perspective (HELENA)**
by R. Chaouadi (2008), VIII, 139 pages
ISBN: 978-3-89336-545-6

21. **in Bearbeitung**

22. **Verbundvorhaben APAWAGS (AOEV und Wassergenerierung) – Teilprojekt: Brennstoffreformierung – Schlussbericht**
von R. Peters, R. C. Samsun, J. Pasel, Z. Porš, D. Stolten (2008), VI, 106 Seiten
ISBN: 978-3-89336-547-0

23. **FREEVAL**
Evaluation of a Fire Radiative Power Product derived from Meteosat 8/9 and Identification of Operational User Needs
Final Report
project coord. M. Schultz, M. Wooster (2008), 139 pages
ISBN: 978-3-89336-549-4

24. **Untersuchungen zum Alkaliverhalten unter Oxycoal-Bedingungen**
von C. Weber (2008), VII, 143, XII Seiten
ISBN: 978-3-89336-551-7

25. **Grundlegende Untersuchungen zur Freisetzung von Spurstoffen, Heißgaschemie, Korrosionsbeständigkeit keramischer Werkstoffe und Alkalirückhaltung in der Druckkohlenstaubfeuerung**
von M. Müller (2008), 207 Seiten
ISBN: 978-3-89336-552-4

26. **Analytik von ozoninduzierten phenolischen Sekundärmetaboliten in *Nicotiana tabacum* L. cv Bel W3 mittels LC-MS**
von I. Koch (2008), III, V, 153 Seiten
ISBN 978-3-89336-553-1

27. **IEF-3 Report 2009. Grundlagenforschung für die Anwendung**
(2009), ca. 230 Seiten
ISBN: 978-3-89336-554-8

28. **Influence of Composition and Processing in the Oxidation Behavior of MCrAlY-Coatings for TBC Applications**
by J. Toscano (2009), 168 pages
ISBN: 978-3-89336-556-2

29. **Modellgestützte Analyse signifikanter Phosphorbelastungen in hessischen Oberflächengewässern aus diffusen und punktuellen Quellen**
von B. Tetzlaff (2009), 149 Seiten
ISBN: 978-3-89336-557-9

30. **Nickelreaktivlot / Oxidkeramik – Fügungen als elektrisch isolierende Dichtungskonzepte für Hochtemperatur-Brennstoffzellen-Stacks**
von S. Zügner (2009), 136 Seiten
ISBN: 978-3-89336-558-6

31. **Langzeitbeobachtung der Dosisbelastung der Bevölkerung in radioaktiv kontaminierten Gebieten Weißrusslands – Korma-Studie**
von H. Dederichs, J. Pillath, B. Heuel-Fabianek, P. Hill, R. Lennartz (2009), Getr. Pag.
ISBN: 978-3-89336-532-3

32. **Herstellung von Hochtemperatur-Brennstoffzellen über physikalische Gasphasenabscheidung**
von N. Jordán Escalona (2009), 148 Seiten
ISBN: 978-3-89336-532-3

33. **Real-time Digital Control of Plasma Position and Shape on the TEXTOR Tokamak**
by M. Mitri (2009), IV, 128 pages
ISBN: 978-3-89336-567-8

34. **Freisetzung und Einbindung von Alkalimetallverbindungen in kohlebefeuerten Kombikraftwerken**
von M. Müller (2009), 155 Seiten
ISBN: 978-3-89336-568-5

35. **Kosten von Brennstoffzellensystemen auf Massenbasis in Abhängigkeit von der Absatzmenge**
von J. Werhahn (2009), 242 Seiten
ISBN: 978-3-89336-569-2

36. **Einfluss von Reoxidationszyklen auf die Betriebsfestigkeit von anodengestützten Festoxid-Brennstoffzellen**
von M. Ettler (2009), 138 Seiten
ISBN: 978-3-89336-570-8

37. **Großflächige Plasmaabscheidung von mikrokristallinem Silizium für mikromorphe Dünnschichtsolarmodule**
von T. Kilper (2009), XVII, 154 Seiten
ISBN: 978-3-89336-572-2

38. **Generalized detailed balance theory of solar cells**
by T. Kirchartz (2009), IV, 198 pages
ISBN: 978-3-89336-573-9

39. **The Influence of the Dynamic Ergodic Divertor on the Radial Electric Field at the Tokamak TEXTOR**
von J. W. Coenen (2009), xii, 122, XXVI pages
ISBN: 978-3-89336-574-6

40. **Sicherheitstechnik im Wandel Nuklearer Systeme**
von K. Nünighoff (2009), viii, 215 Seiten
ISBN: 978-3-89336-578-4

41. **Pulvermetallurgie hochporöser NiTi-Legierungen für Implanat- und Dämpfungsanwendungen**
von M. Köhl (2009), XVII, 199 Seiten
ISBN: 978-3-89336-580-7

42. **Einfluss der Bondcoatzusammensetzung und Herstellungsparameter auf die Lebensdauer von Wärmedämmschichten bei zyklischer Temperaturbelastung**
von M. Subanovic (2009), 188, VI Seiten
ISBN: 978-3-89336-582-1

43. **Oxygen Permeation and Thermo-Chemical Stability of Oxygen Permeation Membrane Materials for the Oxyfuel Process**
by A. J. Ellett (2009), 176 pages
ISBN: 978-3-89336-581-4

44. **Korrosion von polykristallinem Aluminiumoxid (PCA) durch Metalljodidschmelzen sowie deren Benetzungseigenschaften**
von S. C. Fischer (2009), 148 Seiten
ISBN: 978-3-89336-584-5

45. **IEF-3 Report 2009. Basic Research for Applications**
(2009), 217 Seiten
ISBN: 978-3-89336-585-2

46. **Verbundvorhaben ELBASYS (Elektrische Basissysteme in einem CFK-Rumpf) - Teilprojekt: Brennstoffzellenabgase zur Tankinertisierung - Schlussbericht**
von R. Peters, J. Latz, J. Pasel, R. C. Samsun, D. Stolten
(2009), xi, 202 Seiten
ISBN: 978-3-89336-587-6

47. **Aging of ^{14}C-labeled Atrazine Residues in Soil: Location, Characterization and Biological Accessibility**
by N. D. Jablonowski (2009), IX, 104 pages
ISBN: 978-3-89336-588-3

48. **Entwicklung eines energetischen Sanierungsmodells für den europäischen Wohngebäudesektor unter dem Aspekt der Erstellung von Szenarien für Energie- und CO_2 - Einsparpotenziale bis 2030**
von P. Hansen (2009), XXII, 281 Seiten
ISBN: 978-3-89336-590-6

49. **Reduktion der Chromfreisetzung aus metallischen Interkonnektoren für Hochtemperaturbrennstofzellen durch Schutzschichtsysteme**
von R. Trebbels (2009), iii, 135 Seiten
ISBN: 978-3-89336-591-3

50. **Bruchmechanische Untersuchung von Metall / Keramik-Verbundsystemen für die Anwendung in der Hochtemperaturbrennstoffzelle**
von B. Kuhn (2009), 118 Seiten
ISBN: 978-3-89336-592-0

51. **Wasserstoff-Emissionen und ihre Auswirkungen auf den arktischen Ozonverlust**
Risikoanalyse einer globalen Wasserstoffwirtschaft
von T. Feck (2009), 180 Seiten
ISBN: 978-3-89336-593-7

52. **Development of a new Online Method for Compound Specific Measurements of Organic Aerosols**
by T. Hohaus (2009), 156 pages
ISBN: 978-3-89336-596-8

53. **Entwicklung einer FPGA basierten Ansteuerungselektronik für Justageeinheiten im Michelson Interferometer**
von H. Nöldgen (2009), 121 Seiten
ISBN: 978-3-89336-599-9

54. **Observation – and model – based study of the extratropical UT/LS**
by A. Kunz (2010), xii, 120, xii pages
ISBN: 978-3-89336-603-3

55. **Herstellung polykristalliner Szintillatoren für die Positronen-Emissions-Tomographie (PET)**
von S. K. Karim (2010), VIII, 154 Seiten
ISBN: 978-3-89336-610-1

56. **Kombination eines Gebäudekondensators mit H2-Rekombinatorelementen in Leichwasserreaktoren**
von S. Kelm (2010), vii, 119 Seiten
ISBN: 978-3-89336-611-8

57. **Plant Leaf Motion Estimation Using A 5D Affine Optical Flow Model**
by T. Schuchert (2010), X, 143 pages
ISBN: 978-3-89336-613-2

58. **Tracer-tracer relations as a tool for research on polar ozone loss**
by R. Müller (2010), 116 pages
ISBN: 978-3-89336-614-9

59. **Sorption of polycyclic aromatic hydrocarbon (PAH) to Yangtze River sediments and their components**
by J. Zhang (2010), X, 109 pages
ISBN: 978-3-89336-616-3

60. **Weltweite Innovationen bei der Entwicklung von CCS-Technologien und Möglichkeiten der Nutzung und des Recyclings von CO_2**
Studie im Auftrag des BMWi
von W. Kuckshinrichs et al. (2010), X, 139 Seiten
ISBN: 978-3-89336-617-0

61. **Herstellung und Charakterisierung von sauerstoffionenleitenden Dünnschichtmembranstrukturen**
von M. Betz (2010), XII, 112 Seiten
ISBN: 978-3-89336-618-7

62. **Politikszenarien für den Klimaschutz V – auf dem Weg zum Strukturwandel, Treibhausgas-Emissionsszenarien bis zum Jahr 2030**
hrsg. von P. Hansen, F. Chr. Matthes (2010), 276 Seiten
ISBN: 978-3-89336-619-4

63. **Charakterisierung Biogener Sekundärer Organischer Aerosole mit Statistischen Methoden**
von C. Spindler (2010), iv, 163 Seiten
ISBN: 978-3-89336-622-4

64. **Stabile Algorithmen für die Magnetotomographie an Brennstoffzellen**
von M. Wannert (2010), ix, 119 Seiten
ISBN: 978-3-89336-623-1

65. **Sauerstofftransport und Degradationsverhalten von Hochtemperatur-membranen für CO2-freie Kraftwerke**
von D. Schlehuber (2010), VII, 139 Seiten
ISBN: 978-3-89336-630-9

66. **Entwicklung und Herstellung von foliengegossenen, anodengestützten Festoxidbrennstoffzellen**
von W. Schafbauer (2010), VI, 164 Seiten
ISBN: 978-3-89336-631-6

67. **Disposal strategy of proton irradiated mercury from high power spallation sources**
by S. Chiriki (2010), xiv, 124 pages
ISBN: 978-3-89336-632-3

68. **Oxides with polyatomic anions considered as new electrolyte materials for solid oxide fuel cells (SOFCs)**
by O. H. Bin Hassan (2010), vii, 121 pages
ISBN: 978-3-89336-633-0

69. **Von der Komponente zum Stack: Entwicklung und Auslegung von HT-PEFC-Stacks der 5 kW-Klasse**
von A. Bendzulla (2010), IX, 203 Seiten
ISBN: 978-3-89336-634-7

70. **Satellitengestützte Schwerewellenmessungen in der Atmosphäre und Perspektiven einer zukünftigen ESA Mission (PREMIER)**
von S. Höfer (2010), 81 Seiten
ISBN: 978-3-89336-637-8

71. **Untersuchungen der Verhältnisse stabiler Kohlenstoffisotope in atmosphärisch relevanten VOC in Simulations- und Feldexperimenten**
von H. Spahn (2010), IV, 210 Seiten
ISBN: 978-3-89336-638-5

72. **Entwicklung und Charakterisierung eines metallischen Substrats für nanostrukturierte keramische Gastrennmembranen**
von K. Brands (2010), vii, 137 Seiten
ISBN: 978-3-89336-640-8

73. **Hybridisierung und Regelung eines mobilen Direktmethanol-Brennstoff-zellen-Systems**
von J. Chr. Wilhelm (2010), 220 Seiten
ISBN: 978-3-89336-642-2

74. **Charakterisierung perowskitischer Hochtemperaturmembranen zur Sauerstoffbereitstellung für fossil gefeuerte Kraftwerksprozesse**
von S.A. Möbius (2010) III, 208 Seiten
ISBN: 978-3-89336-643-9

75. **Characterization of natural porous media by NMR and MRI techniques: High and low magnetic field studies for estimation of hydraulic properties**
by L.-R. Stingaciu (2010), 96 pages
ISBN: 978-3-89336-645-3

76. **Hydrological Characterization of a Forest Soil Using Electrical Resistivity Tomography**
by Chr. Oberdörster (2010), XXI, 151 pages
ISBN: 978-3-89336-647-7

77. **Ableitung von atomarem Sauerstoff und Wasserstoff aus Satellitendaten und deren Abhängigkeit vom solaren Zyklus**
von C. Lehmann (2010), 127 Seiten
ISBN: 978-3-89336-649-1

78. **18th World Hydrogen Energy Conference 2010 – WHEC2010 Proceedings**
Speeches and Plenary Talks
ed. by D. Stolten, B. Emonts (2010)
ISBN: 978-3-89336-658-3

78-1. **18th World Hydrogen Energy Conference 2010 – WHEC2010 Proceedings**
Parallel Sessions Book 1:
Fuel Cell Basics / Fuel Infrastructures
ed. by D. Stolten, T. Grube (2010), ca. 460 pages
ISBN: 978-3-89336-651-4

78-2. **18th World Hydrogen Energy Conference 2010 – WHEC2010 Proceedings**
Parallel Sessions Book 2:
Hydrogen Production Technologies – Part 1
ed. by D. Stolten, T. Grube (2010), ca. 400 pages
ISBN: 978-3-89336-652-1

78-3. **18th World Hydrogen Energy Conference 2010 – WHEC2010 Proceedings**
Parallel Sessions Book 3:
Hydrogen Production Technologies – Part 2
ed. by D. Stolten, T. Grube (2010), ca. 640 pages
ISBN: 978-3-89336-653-8

78-4. **18th World Hydrogen Energy Conference 2010 – WHEC2010 Proceedings**
Parallel Sessions Book 4:
Storage Systems / Policy Perspectives, Initiatives and Cooperations
ed. by D. Stolten, T. Grube (2010), ca. 500 pages
ISBN: 978-3-89336-654-5

78-5. **18th World Hydrogen Energy Conference 2010 – WHEC2010 Proceedings**
Parallel Sessions Book 5:
Stategic Analysis / Safety Issues / Existing and Emerging Markets
ed. by D. Stolten, T. Grube (2010), ca. 530 pages
ISBN: 978-3-89336-655-2

78-6. **18th World Hydrogen Energy Conference 2010 – WHEC2010 Proceedings**
Parallel Sessions Book 6:
Stationary Applications / Transportation Applications
ed. by D. Stolten, T. Grube (2010), ca. 330 pages
ISBN: 978-3-89336-656-9

Schriften des Forschungszentrums Jülich
Reihe Energie & Umwelt / Energy & Environment

78 Set (7 Bände)

18th World Hydrogen Energy Conference 2010 – WHEC2010 Proceedings
eb. by D. Stolten, T. Grube, B. Emonts (2010)
ISBN: 978-3-89336-657-6

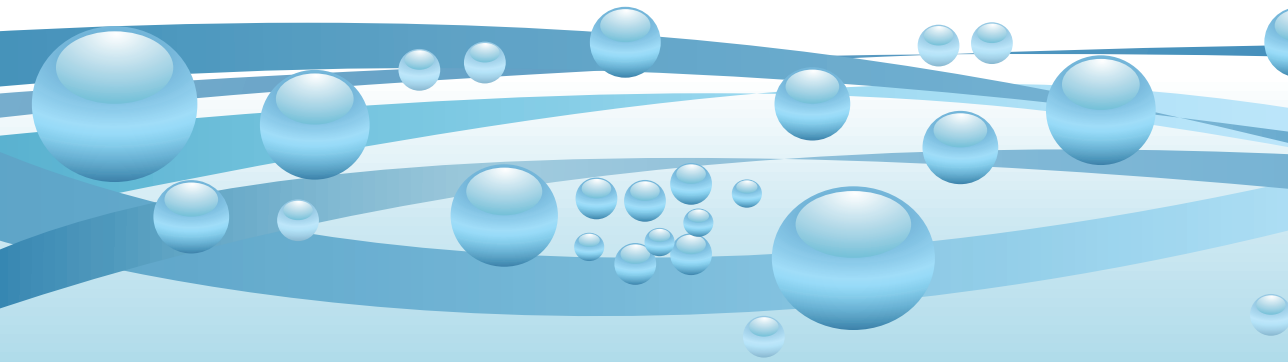

Energy & Environment
Volume 78-4 Book 4

Vol. 78	ISBN 978-3-89336-658-3
Vol. 78-1 Book 1:	ISBN 978-3-89336-651-4
Vol. 78-2 Book 2:	ISBN 978-3-89336-652-1
Vol. 78-3 Book 3:	ISBN 978-3-89336-653-8
Vol. 78-4 Book 4:	**ISBN 978-3-89336-654-5**
Vol. 78-5 Book 5:	ISBN 978-3-89336-655-2
Vol. 78-6 Book 6:	ISBN 978-3-89336-656-9
Vol. 78 Set (complete book series):	ISBN 978-3-89336-657-6

JÜLICH
FORSCHUNGSZENTRUM